P.O.Box 2345, Beijing 100023,China
Fax: +86-10-85381893
E-mail: wjg@wjgnet.com www.wjgnet.com

World J Gastroenterol 2003;9(8):1635-1645
World Journal of Gastroenterology
 ISSN 1007-9327

• REVIEW •

Current status of severe acute respiratory syndrome in China

Qing-He Nie, Xin-Dong Luo, Jian-Zhong Zhang, Qin Su

Qing-He Nie, Xin-Dong Luo, The Chinese PLA Center of Diagnosis and Treatment for Infectious Diseases, Tangdu Hospital, Fourth Military Medical University, Xi' an 710038, Shaanxi Province, China
Jian-Zhong Zhang, Department of Pathology, Bei jing 306 Hospital, Beijing 100101, China
Qin Su, Department of Pathology, Tangdu Hospital, Fourth Military Medical University, Xi' an, 710038, Shaanxi Province, China
Correspondence to: Dr. Qing-He Nie, The Chinese PLA Center of Diagnosis and Treatment for Infectious Diseases, Tangdu Hospital, Fourth Military Medical University, Xi' an 710038, Shaanxi Province, China. nieqinghe@hotmail.com
Telephone: +86-29-3377452 **Fax:** +86-29-3537377
Received: 2003-06-30 **Accepted:** 2003-07-06

Abstract

Severe acute respiratory syndrome (SARS), also called infectious atypical pneumonia, is an emerging infectious disease caused by a novel variant of coronavirus (SARS-associated coronavirus, SARS-CoV). It is mainly characterized by pulmonary infection with a high infectivity and fatality. SARS is swept across almost all the continents of the globe, and has currently involved 33 countries and regions, including the mainland China, Hong Kong, Taiwan, North America and Europe. On June 30, 2003, an acumulative total reached 8450 cases with 810 deaths. SARS epidemic was very rampant in March, April and May 2003 in the mainland of China and Hong Kong. Chinese scientists and healthcare workers cooperated closely with other scientists from all over the world to fight the disease. On April 16, 2003, World Health Organization (WHO) formally declared that SARS-CoV was an etiological agent of SARS. Currently, there is no specific and effective therapy and prevention method for SARS. The main treatments include corticosteroid therapy, anti-viral agents, anti-infection, mechanical ventilation and isolation. This disease can be prevented and controlled, and it is also curable. Under the endeavor of the Chinese Government, medical staffs and other related professionals, SARS has been under control in China, and Chinese scientists have also made a great contribution to SARS research. Other studies in developing new detection assays and therapies, and discovering new drugs and vaccines are in progress. In this paper, we briefly review the current status of SARS in China.

Nie QH, Luo XD, Zhang JZ, Su Q. Current status of severe acute respiratory syndrome in China. *World J Gastroenterol* 2003; 9 (8): 1635-1645

http://www.wjgnet.com/1007-9327/9/1635.asp

INTRODUCTION

On November 16, 2002, the first case of SARS patient was found in Foshan city, Guangdong Province, China[1]. Severe acute respiratory syndrome (SARS) is different from ordinary pneumonias caused by bacteria, other viruses, chlamydia and mycoplasma. The disease starts with an abrupt onset of fever, progresses swiftly, and is subjected to acute respiratory failure. Furthermore, it results in multiple organ dysfunctions with a higher infectivity and fatality. The main clinical manifestations of the patient are high fever, non-productive cough, myalgia and dyspnea. The patient has no response to any antibacterial therapy. At the beginning, the experts in Guangdong Province believed that it might be caused by a novel virus infection, and designated it as "atypical pneumonia" based on its clinical manifestations. On April 8, 2003, the State Council of the People' s Republic of China classified this illness as a legal infectious disease, and named it as infectious atypical pneumonia according to its higher infectivity, quick transmission and high mortality. The same kind of patients was found in Hong Kong and Vietnam at the end of February[2,3]. Dr. Carlo Urbani, an Italian epidemiologist working at the Hanoi Office of the World Health Organization (WHO), first reported to WHO and named this disease as severe acute respiratory syndrome. Later, Dr. Urbani caught the disease himself and died on March 29, 2003. In memory of Dr. Urbani' s great contributions in fighting against this disease, WHO formally designated this disease with unknown causes as SARS on April 16, 2003[4]. Ksiazek and his colleagues proposed that their first isolate be named the Urbani strain of SARS-associated coronavirus (SARS-CoV)[4,5].

On March 12, 2003, WHO issued a global alert of SARS outbreak, and called upon 11 laboratories (including the Institute of Virology, Center of Disease Control and Prevention, China, and Guangdong Center of Disease Control and Prevention, China) in 9 countries to join a collaborative multi-center research project on SARS. Chinese medical and health care workers have been keeping abreast of the advances in SARS research, and have achieved a number of success while fighting against SARS. In this paper, we briefly reviewed the current status of SARS research in China.

EPIDEMIOLOGY

General situation

During the period from November 16, 2002 to April 16, 2003, 13 cities had reports of SARS cases in Guangdong Province, China. Among the 13 reported cases of SARS, 3 were cooks, 3 officers, 2 farmers, 2 retired persons, 2 workers, and 1 businessman. Their age ranged from 18 to 84 years, the majority (77 %) was between 30-50 years. No evidence of mutual transmission was found between the reported cases[6]. The first case of SARS in Guangzhou was found on January 2, 2003. The epidemic broke out and reached the peak early in February, and then the incidence started to decline. As to age distribution of the patients, most patients were between 20-50 years. The patients were present in all the 13 counties and cities, but concentrated in 7-city areas, accounting for 95 % of the total cases, in which 28.7 % of the patients were healthcare workers. Of the 36 deaths, their age ranged from 5 to 89 years, and half of them were older than 60 years. Some of the deaths (38.9 %) were complicated with underlying diseases, including hypertension, diabetes, heart disease, and pulmonary emphysema. There was also a clustering trend: more than 2 patients were found in 42 families, 277 cases of healthcare workers were from 28 hospitals and institutes[7]. The incidence in Beijing had a similar feature to Guangdong (Table 1)[8]. Till June 30, 2003, an acumulative total reached 8 450 cases with 810 deaths. In the mainland of China, there were 5 327 cases

Table 1 History of SARS contact and incubation period in 80 cases

	Male (*n*, %)	Female (*n*, %)	Age (year)	Contact history	Incubation period (d)
Total	28 (35 %)	52 (65 %)	31.6±10.1	72 / 80(90 %)	7.6±4.3
Healthcare worker	13 (24.5 %)	40 (7.5 %)	30.8±8.4	49 / 53(92.5 %)	7.8±4.5
Non-healthcare worker	15 (55.6%)	12(44.4%)	36.4±12.1	23 / 27(85.2 %)	7.7±3.1

of SARS in which 348 patients died, and 1 755 cases with 298 deaths and 681 cases with 84 deaths occurred in Hong Kong and Taiwan, respectively. The national case reports showed that SARS patients were distributed in almost all professions, and healthcare workers with the infection accounted for 20-30 % at the early stage of SARS epidemic. There was no difference between both sexes in the incidence. SARS patients were found in every age group, and predominant in 20-49 years group (about 80 % of cases). The mortality in senile patients was significantly higher than that in young patients[9,10].

A professor from Zhongshan University in Guangzhou suffering from SARS stayed at Jinghua Grand Hotel, and a 28-year-old resident in Hong Kong got infected there, leading to SARS outbreak in the Prince Wales Hospital. However, a study made by Medical College of Zhongshan University indicated that at least 3 sources contributed to the outbreak early in March, that is to say, the source of SARS outbreak in Hong Kong was more than one. The mainland of China reported for the first time that no new case was found on June 2, 2003. No confirmed, suspected cases and deaths occurred for the first time on June 19, 2003 in China. Xiaotangshan Hospital, a speciality SARS hospital in Beijing, was then closed, demonstrating that a decisive victory has been won in fighting against SARS in China.

Infectious source

Currently, the known patient with SARS is the only infectious source. In the primary stage, symptoms are more obvious and it has high infectivity, while in the recovery stage, its infectivity is lost. Not all the cases have the same infectivity. Highly contagious cases are those who deliver a large amount of viruses for a long time, especially with severe cough, or those who undergo an endotracheal intubation with a splashing of droplets. Few cases with very strong infectiousness are called "super-spreader", who usually are the first cases or the first cluster of SARS patients during the outbreak. Usually, the early cases of SARS have a high infectivity and a strong pathogenicity, which would decrease later with progression of the epidemic. It is still unclear that why some individuals exposed to the patient did not contract SARS. Does occult infection of SARS exist? If yes, what role it plays in transmission and what is its epidemiologic significance? All these need to be further studied.

The initial results of epidemiologic surveys showed that the first reported cases or the first cluster of SARS were cook and market purchasers in some cities of Guangdong Province. A certain number of the sporadic cases did not have a contact history of SARS patients, from which we could deduce that there might be some other route of transmission and animal-mediated route of transmission may play a role in pathogenesis. Sources of infection may include some species of animals and the detail is unclear.

From May 23, 2003, scientists in Hong Kong and Shenzhen have collaborated in search for the origins of SARS. On the basis of population epidemic investigations, researchers have been on the track of animals infected with SARS viruses and have targeted at the wild mammal animals in their study. They have confirmed the kinship relations between these animals and human SARS viruses based on an evolutionary analysis of the SARS virus genes of different genera. It seems that they have observed the origin of the human SARS viruses based on these findings. By nearly a month of painstaking efforts, researchers have isolated 3 SARS specimens from 6 Paguma larvata. The fully genetic sequencing of one specimen showed that the SARS viruses in Paguma larvata bore 99 % homology with the SARS viruses in the human body. A further genetic analysis confirmed that SARS viruses in animals were the precursors of the SARS viruses in humans. The testing and analysis of the SARS antibody were performed in 10 people who were engaged in wild animal businesses, among them, 5 people had a positive response, indicating that the SARS viruses in wild animals may infect those who have close contacts with them. These findings have provided important evidences for further investigation of the origins of SARS viruses in humans, and their associated chains, and will lay a foundation for the future development of SARS vaccines and treatment serum. Currently, there is no strong evidence that demonstrates SARS is transmitted through animals or insects.

Route of transmission

Airborne droplets from the patient are the main route of transmission. It is not clear whether there are other transmission routes, personal touch by hands, playthings contaminated by the secretions from the patient' s respiratory tract. Close contact refers to the direct touch of the patient' s secretions and body fluid during treatment and nursing of the patients. The transmission scope is closely correlated with the environment of the ward, course of treatment, patient' s condition, time of exposure and personal protection of healthcare workers and visitors. Improper protection increases the risk of infection. Rubbing nose and eyes with the contaminated hands may also be a route of the transmission. Sexual transmission of SARS has not been confirmed, but close contact during sexual intercourse may increase the chance to get infected.

Lin *et al*[11] from the Institute of Preventive Medicine, University of Taiwan, also believed that only when respiratory symptoms appeared did the patient have infectivity. As for the route of transmission they have made the following two conclusions. The first is that the special shell antigen of SARS-CoV might come from chromosome 6q in human tissues (MCH/HLA). Once the virus enters human body, the invader is wrapped by the special tissue antigens in some individual hosts, so that the virus loses its capacity to infect other persons. Clinically, this strong tissue antigen might relate to severe leukopenia or lymphopenia in SARS patients. Once the disease progresses to respiratory distress, the lungs would try to dissolve the mucus produced by acute inflammation, by activating the body defense system to secrete proteolytic enzymes for the mucus dissolution. Meanwhile, the enzymes would also dissolve the tissue antigens of the shell, and make the virus resume its infectivity to other individuals. This clear-cut route of transmission is characterized by SARS-CoV. It has been proposed that SARS be liable to transmit among the family members because of the same type of HLA. The second is that different strains of bacteria in the sewage are able to produce proteolytic enzymes and dissolve the shell protein of SARS-CoV, and promote its infectivity to others. This mechanism might explain why SARS outbreak occurred in Amoy Garden, as well as in sporadic individuals who had been

to the epidemic regions, without direct contact with the patients. This virus can enter the human body via any part of mucosa, including respiratory tract, oral cavity, and genital tract. Owing to the higher concentration of proteolytic enzymes in the lung, SARS patients have a strong infectivity even at the early stage of the disease. Although the above hypotheses could explain some phenomena in SARS epidemiology, they need to be further confirmed.

Susceptible population

The ordinary population is very susceptible to SARS, the healthcare workers who have close contacts to the patients during the treatment and nursing, are the high-risk group. Anyone who has a history of close contact to the patients is a high-risk individual, and may exist the occult infection. In view of professions, healthcare workers are the most easily infected persons. Compared with other infectious diseases, the rate of SARS infection was very high in medical professionals, accounting for 20-30 % in some areas. It might be due to the insufficient protective measures in the early epidemic stage of SARS. But in Beijing, the rate of infection was relatively low in healthcare workers both at hospitals and at CDC. It is suggested that personal protection plays an important role in prevention of SARS among the healthcare workers. In order to protect the doctors and nurses, the Chinese Government has taken almost all the necessary preventive measures to strengthen sterilization and ventilation in the wards and to forestall medical staffs to be overworked. This is why the incidence of SARS has been kept at a lower level in the healthcare workers.

Distribution characteristics in epidemic areas

There are four kinds of SARS epidemic situation in China: (1) Epidemic area of SARS (in Zhujiang Delta of Guangdong Province, China, there was no direct relationship among the primary cases in different cities). (2) Imported SARS cases, which caused local spreading (as in Shanxi Province and Beijing, etc.). (3) Imported SARS cases, which did not cause local spreading (as in Hunan Province and Sichuan Province, etc.), and (4) no SARS cases reported.

Epidemiological statistical analysis and prediction

How will the SARS epidemic situation develop? How to control SARS effectively? Are there any scientific ways to predict the SARS epidemic situation? According to the current actual SARS epidemic situation in the world, the Center of Geosystem Science and the Key Laboratory of Geodynamics of the Chinese Academy of Sciences have studied the relationship between SARS epidemic situation and its development based on their accumulated experience for years, established the systemic dynamics model of SARS contagion, and calculated the relationship between the control of SARS epidemic situation and its development in detail. The results were identical with the current actual SARS situation in the world, and the model could predict the SARS epidemic situation. The successful establishment of this model is important to evaluate and predict SARS epidemic situations. The task group of "SARS Epidemic Trend and Control System" in Xi' an Jiaotong University made use of computers to make computing simulation with the data and theories by using the statistical methods and parameters confirmed in the epidemic transmission, and then composed the software by modifications and got the predicting cuve to meet the actual demand. They finally put forward the epidemic patterns and trend of SARS. The predicted number of increasing cases of SARS was basically identical with that publicized by the Ministry of Public Health every day.

According to the data of the diagnosed, suspected and dead cases of SARS in the world, the task group of mathematical epidemiology in the University of Science and Technology of China has established the epidemic spatial statistical model of SARS, and predicted on June 10, 2003, that the number of SARS inpatients in Beijing would be decreased below 60[12].

There are so many problems which need to be further studied. For example, our understanding of the source of SARS infection remains on the conditions of SARS patients, and little is known about its effect on sub-clinical SARS patients and animals, as well as the blood transmission and fecal-mouth transmission ,except for the short distance transmission of droplets from respiratory tract and transmission by close contacts. The reason why the incidence rate is high in young people and low in children and elderly people is not clear. What are the influence factors of the superior infectors?

ETIOLOGY

At the beginning of the study conducted by the Chinese scientists, chlamydia-like and coronavirus-like granules were found by electron microscopy in the dead bodies of SARS patients in Guangdong Province, China. Though chlamydia was thought to be the possible pathogen of SARS, it could not be confirmed in foreign laboratories due to the limited specimens for assay. Furthermore, there was not much possibility that chlamydia was the pathogen of SARS according to the clinical manifestations and therapeutic efficacy of SARS patients. Thus it might be due to the secondary infection. After the outbreak of SARS in Hong Kong, researchers isolated the avian influenza virus from a symptomatic child in Hong Kong, which was soon excluded to be the pathogen of SARS. Not long after, paramyxovirus was found in many SARS patients, but not in all the SARS patients in the further studies. However, all these findings could not be further confirmed.

The Pei Weishi Research Group of Hong Kong incubated the blood and tissue samples from SARS patients in cell lines which are not usually used to culture and isolate viruses. The genes of infected tissues were randomly screened in order to find the DNA fragments which could provide useful clues. On March 17, 2003, the cultured tissues isolated from two SARS patients could kill the cell line which is usually used to culture hepatitis A virus. In order to find the relationship between it and SARS, we observed the different reactions occurred when serum in the early and recovery stages was used to culture the tissues. Antibody reaction occurred in the former, while it did not occur in the latter. It was obvious that there was something in the culture, which was related to SARS. Nicols is the first who has found and isolated coronavirus in the tissue samples by electron microscopy. In the following days, three foreign laboratories including that in Hong Kong have confirmed almost at the same time that the pathogen of SARS is a novel kind of coronavirus.

On March 23, 2003, the Institute of Microbiology and Epidemiology, Academy of Military Medical Sciences of China, successfully isolated coronavirus from the pulmonary tissues of SARS patients and established its animal model. Based on the model, the pathogen was isolated by cell culture of samples from pulmonary tissues of the dead bodies and nasopharyngeal swabs. Coronavirus granules were found by electron microscopy in the pathological cells and their culture supernatant. The results of SARS patient serum detected by immunofluorescence staining showed that the isolated virus was closely related to SARS virus, which could induce infection of SARS in mice. The coronavirus-like granules were also found in the pulmonary tissues of mice. The cDNA fragments were amplified with RT-PCR, respectively from the pulmonary tissues of SARS dead bodies, the infected mice, and the infected

cell culture isolations. The whole genome of coronavirus was sequenced at 11pm, on April 15,2003. The sequence had 60 % homogeneity with the known coronavirus, and was about 30 000 bp long, which was identical with the results reported in Canada and USA, suggesting that it is a novel kind of coronavirus closely related with the epidemic of SARS, and may be the major pathogen of SARS.

Hong Kong University has found that some gene fragments have different sequences by comparing "6 SARS samples" from different regions (2 from Hong Kong, 2 from Guangzhou, China, 1 from Canada and 1 from USA), indicating that the "6 viruses" are different members of one family. However, it is not quite sure which one is their "mother". The inclination of the researchers is that one of the two samples from Hong Kong was similar with the two samples from Canada and USA respectively, the other one from Hong Kong was similar with the two from Guangdong, China. Further study is needed to clarify whether the members of such a family exist or they are deprived of a variety of SARS viruses.

Shanghai Institute of Life Science, Chinese Academy of Sciences, has successfully cloned the 6 main protein genes of S, M, N, E, RNA polymerase and proteinase (3CL), and found the expression samples of proteins E, N, and 3CL in the experiment of expression, isolation and purification of the important protein genes. The expression samples passed the drug virtual screening. This achievement is of great importance in the study of biological functions of SARS virus and in seeking after the vaccines and drugs against SARS virus.

The survival time of SARS virus in different conditions varies greatly. It can survive for a long time in 3 human discharges (sputum, feces, and urine) and in blood at 24 ℃, for 5 days in sputum and feces, for 10 days in urine, and for 15 days in blood, respectively. In the indoor condition, it can survive for 3 days on the surface of filter paper, cotton, wood block, soil, metal, plastic, glass, etc. SARS virus is sensitive to temperature. Its survival rate decreases with increasing temperature. It can survive for 4 days in the culture condition without serum at 37 ℃, and can be inactivated at 56 ℃ for 90 minutes, at 75 ℃ for 30 minutes, respectively.

PATHOLOGY

Macroscopically, the pulmonary tissue is swollen and extensively consolidated. The surface blood vessels are dilated and hyperemic, dot or sheet necrosis and hemorrhagic infarct can be found. Thrombi are formed in the pulmonary artery, and wine liquid flows out from the cut section.

Light microscopy

Chronic inflammatory cell infiltration can be found in trachea and bronchioles, and some necrosis tissues and a few inflammatory cells in the duct and some shed mucous epithelia. The pathology in the lung shows severe acute interstitial exudation, pulmonary interstitial and alveolar septum capillaries are severely dilated and congested, and there is a medium amount of lymphocytes, macrophages and polymorphonuclear white cells infiltrated. Some red blood cells are exudated into the alveolar septum and cavity. Pale and red fluids are exudated in most alveolar cavities, and hyaline membrane is formed in about 20-30 % alveolar cavities, but no inflammatory cells infiltrate into alveolar cavities, and focal compensatory emphysema can be seen. Diffuse alveolar epithelial cell injuries are manifested as pyknosis of chromatin to mass in alveolar epithelial cells which are distributed along the karyotheca, apoptosis of alveolar epithelial cells, vacuolar changes of nuclei in some alveolar epithelial cells. The necrosis in pulmonary tissue is not obvious and the phenomenon of lymphocytes attacking alveolar epithelial cells is not found. Regional proliferation is very active in the H type alveolar epithelial cells. Under light microscopy, some virus inclusion bodies-like structures can be observed in alveolar intraepithelial cells. The surface of pleura is smooth, subpleura stroma is edematous and loose, capillaries are dilated and congested with lymphocytes infiltrated.

Many superficial and deep lymph nodes show extensive or large regional hemorrhage and necrosis which are significant in the subcapsular region. Cell proliferation is obvious around the necrosis tissues and the phenomenon of red blood cells phagocytosed by macrophages . Hemosiderin is deposited in the cytoplasm. The lymphocyte infiltration is decreased , the lymphoid follicle structure can hardly be seen. The vascular and splenic sinusoids are greatly dilated and congested, the white pulp is decreased . Extensive and fused hemorrhage and necrosis as well as cell reactive hyperplasia are easily found.

Vacuolation can be found in a few cardiac myocytes, there are interstitial infiltration of a few lymphocytes and mild vascular dilation. The structure of hepatic lobule remains integrated. Mildly mixed hepatocellular fatty degeneration and mildly hydropic degeneration can be seen in the lobules, focal hemorrhagic inflammation and apoptotic body can be occasionally found. Liver sinusoid is dilated and congested, mild reactive hyperplasia occurs in Kupffer cells, and infiltration of lymphocytes is observed. Bilateral adrenal gland also shows focal hemorrhagic inflammation and lymphocyte infiltration which are obvious in the medulla. The structure of glomerulus is almost normal, the capillaries are dilated and congested, but no hyaline thrombus and fibrinoid necrosis can be found. Renal tubular epithelial cells are swollen, with few protein casts and tubular necrosis, there are focal hemorrhage and interstitial lymphocyte infiltration[8]. The structure of the walls of stomach and intestinal tract remains its integrity with a few lymphocytes infiltrated in the lamina propria mucosae and submucosa. Vasodilatation and congestion can also be seen. The intestinal tract shows segmental hemorrhage, and the rest changes are the same as in the stomach.

Transmission electron microscopy

The structure of pulmonary tissue remains very well, intracellular mitochondria and endoplasmic reticulum in alveolar epithelial cells and some endothelial cells of capillaries are swollen, the matrix is very loose, degranules can be found in some rough endoplasmic reticula. Chromatin in the nucleus is changed into mass shape and is not well distributed and is accumulated under the nuclear membrane. Type I alveolar epithelial cells show proliferation which is characterized by increased number, abundant chromatin, intracytoplasmic lamellar bodies, widened interspace of capillaries in the alveolar septum and increased pinocytosis vesicles in the endothelial cells. It is observed that there are many virus-like particles in most of the type II alveolar epithelial cells, bronchioles epithelial cells and intracytoplasma of some endothelial cells of capillaries in the alveolar septum which has an envelope with halation or in the shape of garland and is about 100-150 μm in size with low density in the centre, and these kinds of virus-like particles can also be seen in the dilated endoplasmic reticulum. In addition, chlamydia-like inclusion bodies at different stages which have reticular bodies, midbodies and elementary bodies can be seen in very few alveolar epithelial cells and endothelial cells. In the edema fluid of alveolar cavity, virus-like particles can be found. Proliferation of macrophages in which virus-like particles can also be found is mainly seen in the alveolar septum and alveolar cavity[19].

Many virus-like particles can be found in a few cardiac myocytes which are the same as in the lung tissues. Mild swelling of mitochondrion and endoplasmic reticulum is found in the hepatocytes, and lipid droplet with moderate electron

density is also found, and chlamydia-like inclusion bodies at different stages are seen in the cytoplasm. Some renal tubular epithelial cells show swelling and no villi, virus-like and chlamydia-like particles are also found in them. The injured immune organs mainly include the spleen, lymph nodes and bone marrow. Deposited plasma protein can be seen in the central arteries of splenic corpuscle, massive necrosis can be found in the white medulla and marginal sinus lymph tissues. Some remaining lymphocytes are at the apoptotic state. Blood vessels in the lymph nodes are severely dilated and congested, and lymphoid nodules are atrophied and disappeared, a lot of monocytes are found in the lymphatic sinus, the lymph tissue shows focal necrosis and lymphocytes show apoptosis. Hematopoietic area of myeloid tissue is decreased, granulocyte and macrophage systems are relatively inhibited, polychromatophil erythroblasts show little focal proliferation[20,21].

Tissues around the venules and the vascular walls of lung, heart, liver, kidneys, adrenal gland and striated muscles show swelling, and there are monocytes, lymphocytes, plasmocytes and neutrophilic granulocytes infiltrated.

After the nude mouse is inoculated with SARS virus, and onset of SARS occurs. The main lesions are found in the lung and liver, the alveolar cavity is microscopically very narrow even atelectatic, the alveolar septum is widened, bronchioles epithelial cells are shed. Swollen hepatocytes show hydropic degeneration and vacuolation and some hepatocyes show pyknosis and necrosis. And other anomalies include myocardial hyperemia and increased multinuclear giant cells in the spleen.

In the culture medium of Vero E6 cells infected with SARS virus, virus particles can be found under electron microscope with negative staining which is in the shape of ball with coronally arrayed processes, the end of the process is also a round shape and there is a wide interspace between processes. The diameter of the virus is about 80-120 μm. The viruses detected from the culture medium of cells infected with viruses from Beijing and Guangdong are similar.

PATHOGENESIS

The mechanism of the injury caused by SARS virus is unknown. It is suspected that there are auto-antibodies developed after the infection of SARS virus which induces the autoimmunity reaction, and the current studies cannot explain it.

The reasons why T cells of SARS patients are quickly declined in a short time after the onset of SARS are probable as following: (1) SARS virus directly attacks T cells and causes them splitting and to be destructed quickly which results in the sharp decrease of the count of T cells. (2) After the infection of SARS, SARS virus has no effect on the immune system and results in the abnormal distribution and leads to the decrease of T cells in the peripheral blood. (3) SARS virus, or its productions or its components act as a super-antigen and polyclonally activate T cells and lead the activated T cells to death and decrease of T cells in the peripheral blood.

CLINICAL MANIFESTATIONS

The analysis of the blood samples of SARS patients has shown that the latent period of SARS is at least 4 days and the longest is 17 days. This is related to the load of virus and individuality. The one who has been infected but without symptoms has no infectivity, no such cases have been reported so far.

After the patient is infected with SARS, he will have a high fever and dry cough without the symptoms of influenza such as nasal mucus, pharyngalgia, spitting white or yellow sputum. But sometimes there is some blood in the sputum, and the patient will feel short of breath, and even develop ARDS. Generally, the count of white blood cells will increase when a patient has a fever, but it is normal or below it when the SARS patient has a fever. The most prominent phenomenon is that the X-ray characteristics are not disassociated with its clinical situations. The patient with common pneumonia usually has very severe clinical manifestations and then the changes in the X-ray films can be found. But the X-ray films of SARS patients have very significant changes when the patient of SARS is not very severe, which show floccule shadows and have the trend of quick development[29-31].

The symptoms of SARS include high fever (more than 38 ℃), dry cough, shortness of breath, headache, anorexia, malaise, skin eruption and diarrhea without the common symptoms of influenza such as nasal mucus, pharyngalgia, spitting white or yellow sputum. But sometimes there is some blood in the sputum and the patient will feel short of breath, and even develop ARDS. About 7 % patients of SARS need artificial breathing. The clinical manifestations in different areas in China are shown in Table 2.

The manifestations of chest radiograph of SARS include patchy consolidation or reticular consolidation. Some patients' conditions develop very fast, large patchy consolidation is shown in the chest film and multiple lobes or bilateral lung are involved. The absorbance of the patchy consolidation is very slow. The sites and scope of pulmonary lesions in SARS patients are shown in Table 3.

Table 2 Clinical manifestations in different areas of China

	Fever (%)	Dry cough (%)	Shortness of breath (%)	Chest pain (%)	Bloody sputum (%)	Diarrhea (%)	Headache (%)	Muscle pain (%)	Inertia (%)
Guangzhou[22]	100	72.2	31.2	1.9	11.5	24.2	25.8		24.6
Guangzhou[23]	97.7	81.2	20	22.3		22.3	63.5	41.2	74.1
Guangzhou[24]	100	92		22	13	24	61	60	92
Beijing[25]	97.8	68.9	53.3		9.8	26.7		26.7	60
Beijing[26]	100	87.8	12.2						
Henan[27]	100	67	29	17		17		50	83
Hongkong[28]	100	62	20			10	20	54	

Table 3 Sites and scope of pulmonary lesions in SARS patients

	Superior lung field	Medial lung field	Inferior lung field	Hilum of lung	Multiple lobes	Total
Pachy-lung markings, small shadow	3(2.5)	5(4.2)	10(8.5)	2(1.7)	0(0)	20(16.9)
Unilateral inflammation	8(6.8)	11(9.3)	16(13.6)	0(0)	0(0)	35(29.7)
Bilateral inflammation	3(2.5)	7(5.9)	15(12.7)	0(0)	37(31.4)	62(52.5)
Total	14(11.9)	23(19.5)	41(34.7)	2(1.7)	37(31.4)	117(99.2)

The count of white blood cells of SARS patients is normal or below it, and CD4+ and CD8+ T lymphocytes are also decreased, but all these will be in the normal range after patients are fully recovered.

LABORATORY EXAMINATION

Theoretically, there are three ways to diagnose SARS: cell culture, RT-PCR and detection of antibody. All these ways are mature, so progress in the detecting techniques can be achieved in the work of prevention and cure of SARS easier than that in the study of vaccines and drugs. But cell culture and detection of antibody have no effect at the early stage of clinical diagnosis. Cell culture needs very high requirements of laboratory conditions and experienced operators, it takes a long time to isolate viruses or bacteria, and its positive rate is low. The time of the generation of antibody against SARS virus in the body is at least 10 days, and the time of the generation of IgG is at least 15-20 days. The antibody has interactions with the *in vivo* immune system, the mechanism of the generation of antibody is not clear. Whether all SARS patients have antibody after 3 weeks of infection needs to be further studied. RT-PCR is the simple and easy diagnostic method of SARS at the early stage[33-35]. Although there are many kinds of RT-PCR kits in China, it needs further improvement for its clinical use. It is needed to explore how to get the best virus nucleic acid and the best sampling time. Till today, the diagnosis still depends on the epidemiology and clinical symptoms, no methods have been found to be effective in the prevention and cure of SARS. The natural immunity adhesive function of red blood cells in two SARS cases in China was detected, and it was found that its adhesive function was lowered with aggravation of SARS. It is thought that it may be a good index indicating the degrees of the conditions of SARS patients.

Laboratory examinations, points for attention and evaluation of data

The Ministry of Public Health of PRC proposed the precautions on June 7, 2003 for guidance in practice and applications of tests supposed to be of diagnostic value for SARS.

Virus isolation by cell culture The method is used to isolate SARS virus from human respiratory secretion, blood, urine, stool and autopsy tissue samples. The positive result is considered as a reliable evidence for the presence of replicating SARS virus, and for the diagnosis of the disease or a virus-carrier status in combination with the clinical symptoms. The test must be performed by specialists in a BSL-3 laboratory. Thus, it is difficult at present to be widely used. Another weak point is that this assay is laborious and time-consuming, thereby not suitable for the quick diagnosis. Usually, the positive rate of this assay is not high, and the negative result cannot be regarded as a reliable evidence to exclude SARS. For these reasons, it is not a routine examination in clinical laboratories of most medical centers.

Detection of viral nucleic acid by polymerase-chain reaction following reverse transcription (RT-PCR) The procedure can be used for detection of SARS virus from human respiratory secretion, blood, serum, urine, stool and autopsy tissue samples. It is a quick and convenient method.

Up to date, it is not clear what time is best for sampling and what samples are optimal for the assay. Its sensitivity remains to be improved. The possibility of false negativity is considerably high. In addition, inappropriately handling of the samples often leads to laboratory pollution by the viral nucleic acids and false negative results. When the virus is detected in different samples from the same individual, or the amplification product is demonstrated repeatedly in the same sample, the positivity is established, meaning that the sample contains nucleic acids of SARS virus. For the clinically suspected patients, the positive reaction is a diagnostic parameter for SARS. For apparently healthy individuals, the positive result is a reliable evidence for the establishment of their virus-carrier status. Apparently, a negative reaction cannot be regarded as an evidence to exclude SARS or the suspected either.

Immunofluorescence test and enzyme-linked immunosorbent assay (ELISA) for antibodies to SARS virus The procedures are used to demonstrate specific SARS virus antibody from the serum. The antibody is detectable in a majority of samples from asymptomatically infected individuals and SARS patients for about 10 days, or even later for some cases, after being infected or onset of the disease.

The assays are used mainly for verification of the clinical diagnosis and for epidemiological surveys. A positive reaction obtained using sera from the convalescent suspected patients, or a four-time increase in its titer during recovery compared to that in the acute stage can be regarded as a diagnostic parameter for SARS. Occurrence of the antibody is also found in healthy individuals, reflecting the past infection of SARS virus. As for the replicating virus and its nucleic acids as described above, the antibody is not always detectable in SARS patients. A negative result, therefore, cannot be regarded as a reliable evidence to exclude the possibility of SARS.

Laboratory approaches for assays of SARS in China

A chip covering genomic sequences of all the reported coronaviruses, including SARS virus, was prepared and the detection has been established based on the microarray, as declared by Benyuan-Zhengyang Gene Technology Company Limited, China and its partner organizations in May 2003. The genotyping, conducted based on this system and similar assays, may be useful for determination of pathogenic factors and monitoring of mutations in the genomes of these viruses from different geographic areas, possibly providing some clues to the origin of SARS virus. Moreover, this system and database were designed to be an open platform, allowing the online processing and analysis of data by customers through Internet. In addition, the online exchange and management of detection data from all registered customers can provide an opportunity for the related administrations to obtain statistic information about the disease epidemics on time[37].

The virus-collecting facility, prepared by a group in Wu Jianxiong Laboratory, Dongnan University allows collection and concentration of viral particles from air, claiming to be able to process 30 liters of air per minute. According to the manufacturer, its collection efficiency can be as high as 90 %, as tested using protein particles and the inactivated viral particles. It can be used for sampling from air and viral particle concentration. In combination with PCR, the device may be applied for the detection of SARS virus contamination of the air, providing timely and dynamic data of the viral load.

A preliminary observation was made on dynamic changes of circulating T cells and serum immunoglobulin contents in 124 SARS patients by the Beijing Group of the National Emergent and Technological Action on SARS Prevention and Treatment. A marked decrease was found for all subsets of T lymphocytes examined, including those expressing CD3, CD4 and CD8, with their cell counts reduced to about one third of those of healthy individuals. This shows that the immune functions of SARS patients are severely impaired. The counts of CD4- and CD8-positive T cells were found to decrease quickly at the same time, the change was more pronounced during the period between the 10^{th} day and the 14^{th} day. This is in accordance with the disease course for most cases, its levels going up gradually two weeks after the onset with the recovery

of the patients. It appears reasonable to consider T cells to be involved in the pathogenesis of SARS.

Another apparatus, invented by Gene Company Limited and the Molecular Medical Diagnosis Center in Hong Kong based on the fast DNA hybridization, was claimed to allow the detection of SARS-associated coronavirus in patients' samples and identification of the mutated viruses within 15 minutes. Rong-An Tan, the technical spokesman of the diagnosis center, declared that the system could be used to detect SARS-associated virus from blood, saliva and secretion samples. According to him, the times requested for the detection range from 1 to 15 minutes, with 5 or 6 mutated viruses demonstrated as conducted in Guangzhou, Taiwan and Hong Kong for separate cases.

A seroassay for circulating antibody to SARS virus, namely immuno-chromatography test (ICT), is now being established in Taiwan University Hospital. As claimed by the laboratory, it is possible to determine the diagnosis of SARS at the 7th or 8th day by this assay, much earlier than RT-PCR that cannot show the positive result till the 21st day after the disease onset. The project, currently, is reported to arrive at the ultimate stage of sensitivity assessment. ICT is hoped to be an assay faster than RT-PCR by 13 days[27].

Dalian Institute of Chemistry and Physics, the Chinese Academy of Sciences, recently claimed to have established an early detection system for the virus-induced respiratory diseases with fever based on a controlled micro-current chip. They have finished the preparation of the chip and established the system. Currently, the system is under the evaluation using 9 primer pairs for the amplification following RT, with the SARS virus and parainfluenza virus RNA samples as the templates and a negative control, respectively. The system is characterized by its early detection of viral RNA even if the target sequence contained in samples is minimal in quantity. The controlled micro-current chip is also known as a chip laboratory, which is greatly different from the ordinary gene chips regarding their principles, preparation and applications. It is characterized by high-throughout and large-scale integration. Several fundamental units, involving sample preparation, biological and chemical reactions, isolation and detection, are integrated onto a single chip as small as several cm, being able to finish different reactions and to characterize their minimal-amount products[39].

Recently, artificial virus-like particles were prepared, with the SARS coronavirus nucleic acid enveloped within liposome, by a group in the Laboratory of Clinical Chemistry, Beijing Hospital under the Ministry of Public Health. The reagent may prompt technical improvement, standardization and quality control of the RT-PCR for SARS, as the kits currently available are not stable enough and require further clinical verification. The virus-like particles have been characterized by two properties: safety (non-infectious) and stability. This is of application value for the quality control of RT-PCR for SARS virus in clinical laboratories of medical centers, as well as for evaluation of new diagnostic reagents for the disease[40].

DIAGNOSIS AND DIFFERENTIAL DIAGNOSIS

Criteria for clinical diagnosis of SARS proposed by Ministry of Public Health of PRC

Epidemiological history The history evidences indicative for SARS include close contact with the patient, individuals from an infected group, having infectivity to others, and a tourist back, or a resident moving away from the epidemic regions two weeks before onset of the disease where there are SARS patients reported and the secondary infection has taken place.

Symptoms and signs The onset of the disease is acute. Fever is the first symptom, with the body temperature above 38 ℃ for most cases and chilling as one of the complaints occasionally. Headache, joint pain, fatigue and diarrhea may also be the complaints. Usually respiratory catarrh symptom is not evident. Coughing may be the manifestation, mostly a dry cough with very little sputum. Occasionally, little blood is present in the sputum. Chest distress is common, with the quick respiration, short ness of breath and even breathing difficulty in unfavorable cases. Signs of the lung disorder are usually not obvious, with some moist rales heard or pulmonary consolidation found in some cases. In a small number of the patients, fever is not the first symptom. This is particularly true for those cases operated recently or having some accompanying diseases.

Laboratory tests Usually, the count of peripheral blood leukocytes is not increased, or even decreased. The count of lymphocytes decreases in most cases examined.

Chest roentgenological examination There are various degrees of pulmonary infiltration, with many small pieces of lungs involved or in a meshwork pattern. In the fast progressing cases, massive shadows are present frequently, with multiple or bilateral lobes involved. Their resolution is usually slow. Occurrence and resolution of the roentgenological changes are not necessarily in accordance with the related symptoms and signs. For the cases not showing the changes, reexamination should be performed one or two days later.

Response to antibiotics Treatment with various antibiotics is not effective.

Diagnotic criteria For suspected cases: With positive findings in the epidemiological history + symptoms and signs + laboratory tests, or the epidemiological history + symptoms and signs + laboratory tests, or the symptoms and signs + laboratory tests + X-ray examination.

For cases with a clinical diagnosis of SARS: With positive findings in the epidemiological history + symptoms and signs + X-ray examination , or more, or the symptoms and signs + X-ray examination + no response to antibiotics , or the history + symptoms and signs + laboratory tests + X-ray examination.

For cases under medical observation: With findings in the symptoms and signs + laboratory tests.

For severe cases of SARS: SARS cases with one of the following findings: (1) a breathing difficulty, with respiratory rate exceeding 30 times per minute; (2) hypoxemia even during O_2 inhalation at 3-5 L/min, with PaO_2 below 70 mmHg and SpO_2 below 93 %, or having acute lung injury (ALI) or acute respiratory distress syndrome (ARDS); (3) multiple-lobe lesions involving more than one third of the lungs in area, or enlargement of the pulmonary lesion by more than 50 % within 48 hours as shown by chest roentgenograms; (4) shock or multiple organ dysfunction syndrome (MODS); (5) with a severe accompanying disease or a complicating infection, or with the age exceeding 50 years.

Differential diagnosis

Attention should be paid to the exclusion of other diseases or clinical syndromes such as infection of the upper respiratory tract, influenza, bacterial or fungous pneumonia, pulmonary infection complicating AIDS, legionnaires disease, pulmonary tuberculosis, epidemic hemorrhagic fever, pulmonary neoplasms, non-infectious interstitial pulmonary diseases, pulmonary edema, atelectasis, pulmonary embolism, pulmonary eosinophilic pneumonia and pulmonary vasculitis.

TREATMENT

Patients under the medical observation should receive treatment and observation in the appointed isolation ward or hospital, or under isolation observation in their homes. For the later case, the patients should live in a well-ventilated room and avoid

any close contact with other family members. They should be still under the observation of the disease-control department with their body temperature measured every day during the period. The patients, whose conditions are found to progress and to meet the criteria for SARS or the suspected during the observation, should be sent immediately to the appointed hospital by the special vehicles for isolation and treatment.

The key procedures of prevention and treatment of SARS are early detection, report, isolation and early treatment.

Treatment protocol for SARS and its suspected cases recommended by Chinese Center for Disease Control and Prevention (China CDC)

General therapy The general treatment includes adequate rest and supplement of nutrients such as fluid and vitamins, avoidance of intense and vigorous coughing. The patient' s condition should be observed intensively, since the onset of SARS within 14 days probably belongs to the progressive period in the majority of patients. Regular reexamination of chest x-rays and the functions of heart, liver and kidney are also necessary. The interval for the reinspection of chest x-rays in early phase of SARS should not be more than 3 days. SpO_2 should be checked daily.

Expectant treatment (1) Antipyretic analgesics should be used for patients with fever more than 38.5 ℃ and systemic prominent soreness. For the patients with hyperpyrexia, cooling measures should be applied such as ice compress and sponge bath with alcohol. (2) Antibechic and expectorant should be given when the patients suffer from cough and expectoration. (3) Corresponding measures should be taken when dysfunctions of multiple organs such as heart, liver and kidney take place. (4) Persistent oxygen inhalation by nasal tube should be applied early to the patients with obvious tachypnea and mild hypoxemia. (5) Aspirin medication should be avoided in children for fear of resulting in Reye syndrome.

Antibacterial treatment It is recommended to use antibiotics such as macrolides, fluoroquinolones, β-lactams and tetracyclines early in the course of SARS. Vancomycin or norvancomycin should be chosen as the preferable therapy when the infection caused by antimicrobial-resistant cocci is evidenced either clinically or experimentally.

Glucocorticoid therapy The following indications for the use of corticosteroids are proposed: Patients with severe toxic reaction and persistent high fever, and those with rapid deterioration of the chest film by increased infiltration progressing to a critical condition. The drug should be given regularly with the doses matching the actual condition of the disease and should be used with caution in children.

Selective therapy Selective therapy includes the use of antiviral agents, immunopotentiators and Chinese herbs.

Treatment of critical cases (1) Intensive care and monitoring should be applied to the patients with severe dyspnea or those who meet the criteria of a critical case. (2) Noninvasive and positive pressure ventilation is recommended for those with SaO_2 less than 93% while the oxygen inspiration is at 3-5 L/min and breath rate $\geqslant$ 30/min, in which CPAP with nasal mask is preferable. Routine level of inspiratory positive airway pressure should be set at 4-10 cmH_2O. Selection of adequate breathing masks, and persistent use of noninvasive ventilation that is interrupted no more than 30 min including hora decubitus till the disease remission are required. (3) For patients with severe dyspnea and hypoxemia, SaO_2 < 90 % or oxygenation index < 200 mmHg at 5 $L \cdot min^{-1}$ of oxygen inhalation, failure to tolerate or respond to noninvasive ventilation should be promptly followed by invasive ventilation after intubation. (4) Timely therapeutic measures should be taken once shock or MODS takes place in SARS patients and consultations of relevant experts are indicated when the treatment is limited by professional skill or poor medical equipments.

Standard treatment protocol for SARS (suspected and probable) in adult patients in Hong Kong[41]

Antibacterial treatment Levofloxacin 500 mg is given once daily intravenously or orally, or clarithromycin 500 mg is given twice daily orally plus co-amoxiclav (amoxicillin and clavulanic acid) 375 mg three times daily orally if patient is younger than 18 years, or pregnant, or suspected to have tuberculosis.

Ribavirin and methylprednisolone Combination treatment with ribavirin and methylprednisolone is given when the patient has extensive or bilateral chest radiographic involvement, or persistent chest radiographic involvement and persistent high fever for 2 days, or clinical and chest radiographic or laboratory findings suggestive of worsening, or oxygen saturation < 95 % in room air.

Standard corticosteroid regimen for 21 days Methylprednisolone 1 mg/kg is given every 8 h (3 mg/kg daily) intravenously for 5 days, then methylprednisolone 1 mg/kg is given every 12 h (2 mg/kg daily) intravenously for 5 days, followed by prednisolone 0.5 mg/kg twice daily (1 mg/kg daily) orally for 5 days, prednisolone 0.5 mg/kg daily orally for 3 days, prednisolone 0.25 mg/kg daily orally for 3 days, withdrawal of drugs.

Ribavirin regimen for 10-14 days Ribavirin 400 mg is given every 8 h (1 200 mg daily) intravenously for at least 3 days (or until condition becomes stable), followed by ribavirin 1 200 mg twice daily (2 400 mg daily) orally.

Pulsed methylprednisolone Pulsed methylprednisolone is given if clinical condition, chest radiograph, or oxygen saturation worsen (at least two of these), and lymphopenia persists, followed by methylprednisolone 500 mg twice daily intravenously for 2 days, and then standard corticosteroid regimen.

Ventilation

Non-invasive ventilation or mechanical ventilation should be considered if oxygen saturation < 96 % while O_2 > 6 L per min or if the patient complains of increasing shortness of breath.

Indications for intubation: (1) Failure to respond to non-invasive ventilation, SaO_2 less than 93 % while oxygen inspiration with facial/nasal mask at 5 L/min and progressive deterioration on chest radiography. (2) Failure to tolerate noninvasive ventilation while with severe dyspnea and hypoxemia. (3) With serious toxic reaction and rapid deteriorating conditions[42-46].

One of the important principles that should be noted in mechanical ventilation is the permission of hypercapnia that is usually performed when there are extensive pulmonary consolidation, poor compliance, and possible pneumothorax. In this way, the tidal volume and oxygen supply per minute could be reduced at the moment. SaO_2<90 % and positive end expiratory pressure (PEEP) at 10-15 cmH_2O may prevent atrophy of pulmonary alveoli and improve oxygen supply.

Academician Zhong Nanshan has recently emphasized 4 important therapies for SARS, including paying attention to fever and myalgia at the acute onset with a combination of traditional Chinese and Western medicine, prompt medication with large-dose of corticosteroids to prevent development of pulmonary fibrosis, timely application of nasal (facial) mask ventilation to improve the supply of oxygen, preventing alveolar collapse thus reducing the need for intubation and timely treatment of complications (especially super infections).

Therapeutic approaches in research

The SARS therapy with convalescent sera was firstly proposed

and used for himself by Dr. Su-Chun Jiang. Later, It was also used for the critically ill patients by Hong Kong scholars and achieved some beneficial effects[48]. However, detailed information about it has not been available.

Theoretically, the therapy is specific, but ineffective when used before severe and irreversible pathological changes take place. On the other hand, it should be screened for the pathogens that are probably transmitted via blood such as HBV, HCV and HIV in patients before the sera are used. Meanwhile, more attention should be paid to the possibility of serum sickness reaction[49, 50]. Other drugs such as protease inhibitors[51] and pulmoalveolar surfactant[52] have been under research and development.

Immunomodulators or immunopotentiators such as thymosin or thymopeptide and glutamine dipeptides have been proposed to be used in the treatment of SARS, though the current evaluation of these approaches remains absent. The therapy is based on the finding that the number of peripheral blood T lymphocytes, especially subgroups of CD4+ and CD8+, is significantly decreased in acute phase of SARS patients, suggesting that impairment of cellular immunity does occur in the early stage of SARS.

The therapies described above are the components of the whole treatment protocol for SARS. Their effectiveness and safety have not been systemically evaluated by prospective, randomized and controlled clinical trials. Therefore, it is hard to conclude which is better. SARS, a disease coming all of a sudden, is highly contagious. The researchers working in the first line of anti-SARS battle are engaged in clinical therapeutic activities. Meanwhile, they are also facing the risk to be infected. Under the circumstances, it is more difficult to perform a well and strictly designed clinical trial, and further more, plenty of concrete problems such as ethnics, research time, and lack of investigators and experimental control may also exist. Therefore it is difficult to make sure the effectiveness and safety of different therapies used in the coming months and years, if well designed trials are not performed. Notwithstanding these difficulties and problems, a reasonably designed clinical trial for SARS therapy remains to be very necessary[53].

Development of new anti-SARS drugs in China

Sivelestat sodium is the first newly developed anti-SARS drug in China that has been approved to enter clinical trials on May, 19, 2003, by State Food and Drug Administration of China. It is also the first one that has been approved to be tested in clinical trial since the rapid ratification program for anti-SARS drugs came into operation. It is an injection of chemical medicine used mainly to prevent and alleviate acute lung injury induced by PMN elastase via a mechanism of inhibiting systemic inflammatory response, with an attempt to improve pulmonary function, shorten the period of ventilation, decrease ventilator-related lung injury and other complications.

On May 21, 2003, the researchers in the Fourth Military Medical University discovered 3 polypeptides that exhibit prominent inhibitory effects on SARS virus *in vitro*, which may lay a solid foundation for the development of new polypeptide-type anti-SARS drugs. They found that a corona-like ring existed in the periphery of SARS virus and there were 4 constitutive proteins within this structure, in which the protein S plays a central role in the virus replication and invasion to human cells. These polypeptides were observed to be able to prevent coronavirus from invading the cells. Currently, these polypeptides have acquired the identification from Institute for Viral Disease Control and Prevention of China CDC. On May 15, State Intellectual Property Office of China has accepted the patent application for these findings.

A research group in the Second Military Medical University currently developed a kind of suspension containing porcine pulmoalveolar surfactant for SARS therapy, which has been approved to enter clinical trial by State Food and Drug Administration of China. It has been demonstrated by the animal study that its primary actions are to reduce pulmoalveolar surface tension, improve pulmonary ventilation and gas exchange, as well as prevent the formation of atelectasis and pulmonary edema. Furthermore, the safety, simplicity, sufferingless of this therapy make it possible to be applied in county or even in rural hospitals[54].

National Center for Drug Screening and Shanghai Institute of Materia Medica have received a considerable variety of pharmaceutical compounds, totally more than 4 000 samples, from more than 50 institutes of drug research in more than 20 domestic provinces and municipalities, as well as from that in USA and South Korea for screening new anti-SARS drugs. Co-operations among National Center for Drug Screening, Shanghai Institute of Materia Medica, Shanghai Municipal Center for Disease Control and Prevention and Academy of Military Medical Sciences have made more than 400 samples screened, in which 3 compounds, namely ZZ-I natural unity compound, an empirical prescription of Chinese medicine "Jieduwan" (detoxicating pill) and 5-hydroxytryptamine receptor antagonist DDDC-AS-001, were found to be the most powerful agents in anti-SARS efficiency among those currently screened all over the world.

TRADITIONAL CHINESE MEDICINE

The clinical characteristics of SARS are mainly manifested as prominent symptoms due to noxious heat and pathogenic dampness in most cases, which may lead to the rapid exhaustion of yin-qi and body fluids, and severe complications. Accordingly, the preventive strategy against SARS is to clear away the lung heat and toxic substances, to remove the pathogenic dampnes' s by aromatics and to supplement qi and promote the production of body fluids.

Prevention and treatment protocol for SARS and suspected cases by State Administration of Traditional Chinese Medicine of China

In order to improve the curative effects on the basis of recommended treatment protocol for SARS or suspected cases and discharge criteria by Ministry of Public Health, the following therapeutic approaches of the traditional Chinese medicine are proposed to be used in the anti-SARS treatment. It is recommended that the therapeutic principles of traditional Chinese medicine, namely diagnosis and treatment based on an overall analysis of the illness and the patient' s condition, should be performed in the treatment of SARS and suspected cases. Meanwhile, the treatment protocols should be adjusted as the patient' s condition changes.

In the early phase, the SARS patients are characterized by the impairment of pulmonary function due to noxious heat and stagnation of damp-heat, which are symptomatically categorized into 3 types of pulmonary impairment due to noxious heat, stagnation of damp heat and exterior cold and interior heat with dampness. For the cases manifested as pulmonary impairment due to noxious heat, it is suitable to promote pulmonary function by eliminating toxic heat via activating superficial channels and choosing a modified prescription of Yinqiao Powder plus Maxing Shigan Decoction. For the patients displaying stagnation of damp-heat, it is recommended to disperse the pathogenic factor out of the body by a revised recipe of Sanren Decoction plus Shengjiang Powder. When the condition is dominated by more dampness and less heat in these cases, Huopu Xialing Decoction should be adopted. For those with a manifestation of exterior cold

and interior heat, the therapeutic strategy is to clear the interior heat and ventilate the lung to get rid of toxic heat, which can be achieved by a modified prescription of Maxing Shigan Decoction plus Shengjiang Powder.

In the metaphase of SARS, the manifestations of the patients are displayed as the invasion of lung by epidemic pathogenic factors, abundant heat both in exterior and interior, accumulation of noxious heat, obstruction of Shaoyang by pathogenic factors and excessive epidemic pathogenic factors both in exterior and interior. For these patients, it is suitable to clear away heat and toxic materials, expell the lung heat and suppress the pathogenic factors with Qingfei Jiedu Decoction. A modified prescription of Ganlu Xiaodu Pill can exert the function of clearing away heat and toxic materials, eliminating dampness and keeping away filthiness, which is favorable for those with accumulated toxic heat. For patients with obstruction of Shaoyang by toxic heat, the therapeutic principles are to clear away the toxic heat at Shaoyang channel and to remove the damp-heat and a modified recipe of Haoqin Qidan Decoction should be adopted. For the patients with predominating toxic heat, pathogenic heat should be removed from blood and excessive heat should be purged. For this purpose, a modified recipe of Qiwen Baidu Decoction should be used.

In the critical phase, SARS cases are manifested as excessive accumulation of toxic heat with impaired body resistance, consumption of both qi and yin, and loss of consciousness and collapse. Accordingly, they are divided into accumulation of phlegm damp-heat blocking pulmonary vessels, stagnation of excessive pathogenic heat with deficiency of both qi and yin, excessive damp-heat weakening body resistance and blockage of breath. For the accumulation of phlegm toxic damp-heat blocking pulmonary vessels, it is helpful to invigorate qi for detoxication, eliminate phlegm for dispersing toxic damp-heat and remove blood heat for activating the channels. To achieve this purpose, Huoxie Xiefei Decoction should be used. For the patients with pulmonary stagnation of damp-heat with deficiency of both qi and yin, it is beneficial to clear away heat and promote diuresis, and to invigorate qi and nourish yin. Under the circumstances, Yifei Huazhuo Decoction is indicated. For the patients with hyperpyrexia weakening body resistance and blockage of breath, the preferable choice is to invigorate qi for restoring the vitality, dredge channels for promoting resuscitation, and choose Shenfu Decoction for getting the therapeutical purpose.

In the recovery phase, the symptoms of deficiency of both qi and yin, and deficiency of the lung and spleen, and the stagnant damp-heat are noted as the primary characteristics of SARS cases. For the former, it is recommended to nourish qi and yin, dispel pathogenic dampness to activate the channels, and to choose a modified prescription of Lishi Qinshu Yiqi Decoction. For the latter, it is reasonable to nourish qi and invigorate the spleen, which can be achieved by a modified prescription of Shenglin Baishu Powder plus Gegen Qinlian Decoction.

PROBLEMS AND COGITATION[55-57]

(1) The SARS cases reported in domestic medical literatures are all diagnosed on the basis of clinical experience without pathogenic evidences. (2) It is not worthwhile to advocate that the same contents are repeatedly reported by several papers or the same paper are repeatedly published by different journals. (3) Researches are lack of creative and constructive results or even simply repeat what have been performed overseas. (4) Most of the papers published are empty in contents with no substantive conclusions. Besides, some clinical reports are published by different journals. (5) The reasons why such inferior papers have been published are the insufficient collection of data and a lack of experience. (6) The achievements of SARS related research are exaggerated sometimes in certain domestic media, which mislead the public and should be prohibited. (7) Co-operations and communications in SARS research are seldom carried out among domestic research institutes, which deeply impressed the author when he was working in Beijing Xiaotangshan Hospital.

REFERENCES

1 **WHO**. Cumulative number of reported cases of severe acute respiratory syndrome (SARS). March 31, 2003 (http://www.who.int/csr/sarsarchive/2003-03-31/en)
2 **WHO**. Weekly epidemiological record. 14 March 2003, 78th year / 14 March 2003. http://www.who.int/wer/pdf/2003/wer7811.pdf
3 **Berned Sebastian Kamps,** Kamps-Hoffmann. 1. Timeline. SARS Reference (First Edition). May 8,2003.http://sarsreference.com/index.htm
4 **Reilley B**, Van Herp M, Sermand D, Dentico N. SARS and Carlo Urbani. *N Engl J Med* 2003; **348**: 1951-1952
5 **WHO**. Coronavirus never before seen in humans is the cause of SARS. 16 April 2003. http://www.who.int/csr/sarsarchive/2003-04-16/en/
6 **Luo HM**, Yu HJ, Ni DX, Yin WW, Gao LD, Mo JJ, Yang WZ, Yan JY, Liang Gd, Zeng G, Li LM. Etiology of infectious SARS and live survey. *Zhonghua Liuxing Bingxue Zazhi* 2003; **24**: 336-339
7 **He JF**, Peng GW, Zheng HZ, Luo HM, Liang WJ, Li LH, Guo RL, Deng ZH. An epidemiological study on the index cases of sever acute respiratory syndrome occurred in different cities among Guangdong province. *Zhonghua Liuxing Bingxue Zazhi* 2003; **24**: 347-349
8 **Lu HY**, Huo N, Xu XY, Wang GF, Li JP, Wang GQ, Li HC, Wang J, Nie LG. The epidemiologic characteristics of 80 patients with sever acute respiratory syndrome (SARS). *Beijing Daxue Xuebao (Yixueban)* 2003; **35S**: 8-11
9 **Wang M**, Du L, Zhou RH, Di B, Liu YF, Qing PZ, Wu XW, Chen XS, Qiu JC, Li ZR. Study on the epidemiology and measeures for control on severe acute respiratory syndrome in Guangzhou city. *Zhonghua Liuxing Bingxue Zazhi* 2003; **24**: 353-355
10 **Liu ZJ**, Sheng Z, He X, Huang RG, Teng RM, Ning F, Li XM, Ding LX, Lin CY. An epidemiological analysis on a input SARS case. *Zhonghua Liuxing Bingxue Zazhi* 2003; **4**: 358-359
11 **Zhonghua yixuehui**, Zhonghua yufang yixuehui, Zhonghua yiyuan guanli xuehui. Summary of academic seminar between two shores on control SARS. *Zhonghua Yixue Zazhi* 2003; **83**: 708-712
12 **Liu B**. Establishment of model of SARS space statistics in University of Science and Technology of China. http://www.gmd.com.cn/gmw/defaulta.htm, 2003.06.16
13 **Hong T**, Wang JW, Sun YL, Duan SM, Chen LB, Qu JG, Ni AP, Liang GD, Ren LL, Yang RQ, Guo F, Zhou WM, Chen J, Li DX, Xu WB, Xu H, Guo YJ, Dai SL, Bi SL, Dong XP, Ruan L. Chlamydia- like and coronavirus-like agents found in dead cases of atypical pneumonia by electron microscopy. *Zhonghua Yixue Zazhi* 2003; **83**: 632-636
14 **Zhu QY**, Qin ED, Wang CE. The isolation and identification of a novel coronavirus from patient of severe acute respiratory syndrome. *Zhongguo Gongcheng Shengwu Zazhi* 2003; **23**: 106-112
15 **Fan BC**, Jiang T, Yu M, Deng YQ, Peng WM, Chang GH, Shi BY, Liu BH, Yang BA, Zhu QY, Qing ED. Determination and analysis of 3' untranslated regions of 4 strains of SARS coronavirus isolated in China. *Zhongguo Shengwu Huaxue Yu Fenzi Shengwu Xuebao* 2003; **19**: 273-277
16 http://www.washprofile.org/chinese/sars-pathogen-042503.cfm 2003.04.25
17 **Ding YQ**. Preliminary discussion of etiology and pathogenesis of acute respiratory syndrome. *Jiefangjun Yixue Zazhi* 2003; **28**: 475-476
18 **Zhao JM**, Zhou GD, Sun YL, Wang SS, Yang JF, Mao YL, Pan D, Mao PY, Cheng Y, Wang YD, Xin SJ, Zhou XZ, Lu JY, Li L, Chen JM. Pathological and etiological findings in a dead case of sever acute respiratory syndrome of China. *Jiefangjun Yixue Zazhi* 2003; **28**: 379-382

19 **Wang CE**, Qin ED, Gan YH, Li YC, Wu XH, Cao JT, Yu M, Shi BY, Yan G, Li JF, Zhu QY. Pathological observation on suckling mice and vero E6 cells inoculated with SARS samples. *Jiefangjun Yixue Zazhi* 2003; **28**: 383-384

20 **Lai HW**, Lai RQ, Yang CH, Feng XD, Wang ZC. Pathology and ultrastructure in one infectious SARS case. *Jiefangjun Yixue Zazhi* 2003; **28S**: S34-S35

21 **Ji XL**, Tong Y, Shen MS. Mechanisms of lung injury in severe acute respiratory syndrome (SARS):histopathological analysis. *Zhonghua Weishengwuxue He Mianyixue Zazhi* 2003; **23**: 321-324

22 **Zhang FC**, Yin ZB, Tang XP, Min X. Liu JX, Chen YQ, Wang J, Chen WL, Chen WS, Jia WD, Lei CL. Clinical analysis of 260 cases with severe acute respiratory syndrome in Guangzhou areas. *Zhonghua Chuanranbing Zazhi* 2003; **21**: 84-86

23 **Peng J**, Hou JL, Guo YB, Feng XR, Chen JJ, Liu DL, Zhu YF, Jiang RL, Chen YP. Clinical characteristics of the severe acute respiratory syndrome in Guangzhou. *Zhonghua Chuanranbing Zazhi* 2003; **21**: 89-92

24 **Zhao ZW**, Zhang FC, Xu M, Huang K, Zhong WN, Cai WP, Yin ZB, Huang SD, Deng ZT, Wei M. Clinical analysis of 190 cases outbreak with atypical pneumonia in Guangzhou in spring. *Zhonghua Yixue Zazhi* 2003; **83**: 713-718

25 **Huo N**, Lu HY, Xu XY, Wang GF, Li HC,Wang GQ, Li JP, Wang J, Nie LG, Gao XM, Zhao ZD, Li J, Li YH, Zhuang H. Clinical characteristics and outcome of 45 early stage patients with SARS. *Beijing Daxue Xuebao (Yixueban)* 2003; **35S**: 19-22

26 **Gao ZC**, Zhu JH, Sun Y, Ding XL, Ma JS, Cui YX, Du XK, Gao T, He QY. Clinical investigation of nosocomial severe acute respiratory syndrome. *Zhongguo Weizhongbing Jijiu Yixue* 2003; **15**: 332-335

27 **Hu DS**, Zhang WD, Xi YL, Wen HW, Song LP, Wang WM, Dai LP, Yang WJ, Zhang MX, Kang QZ, Qiao HL, Xue LX, Duan GC, Dong ZM, Zheng YL. Epidemiological study on the outbreak of severe acute respiratory syndrome in Henan, China. *Zhengzhou Daxue Xuabao* 2003; **38**: 342-3344

28 **Chan-Yeung M**, Yu WC. Outbreak of severe acute respiratory syndrome in Hongkong special administrative region: case report. *BMJ* 2003; **326**: 850-852

29 **Ma W**, Chen GF, Li TS, Gao L, Han TZ, Liu DC. Analysis of chest x-ray manifestations in 118 patient with severe acute respiratory syndrome. *Zhongguo Weizhongbing Jijiu Yixue* 2003; **15**: 338-342

30 **Wang RG**, Sun HY, Song LY, Song W, Cui H, Li BS, Wang GF, Xu XY, Li N, Nie LG, Na J. Plain radiograph and CT features of 112 patients with SARS in acute stage. *Beijing Daxue Xuebao (Yixue ban)* 2003; **35**: 29-33

31 **Ma J**, Li N, Que CL,Li HC, Nie LG, Wang GF. Dynamic observation of the features of chest radiograph in SARS. *Beijing Daxue Xuebao(yixue ban)* 2003; **35**: 38-40

32 **Li TS**, Qiu ZF, Han Y, Zhang HW, Wamg Z, Liu ZY, Fan HW, Lv W, Yu Y, Wang HL, Zhang HY, Xie J, Zhou BD, Ma XJ, Ni AP, Wang AX, Deng GH. The alterations of T cell subjects in acute respiratory syndrome during acute phase. *Zhonghua Jianyan Yixue Zazhi* 2003; **26**: 297-299

33 **Wang Y**, Ma WL, Song YB, Xiao WW, Zhang B, Huang H, Wang HM, Ma XD, Zheng WL. Gene sequence analysis of SARS-associated coronavirus by nested RT-PCR. *Diyi Junyi Daxue Xuabao* 2003; **23**: 421-423

34 **Yang J**, Wang HZ, Chen JJ, Hou JL. Clinical detection of polymerase gene of SARS-associated coronavirus. *Diyi Junyi Daxue Xuabao* 2003; **23**: 424-427

35 **Wu XW**, Chen G, Di B, Yin AH, He YS, Wang M, Zhou XY, He LJ, Luo K, Du L. Establishment of fluorescent PCR method for detection of SARS coronavirus and the clinical trial. *Zhonghua Jianyan Yixue Zazhi* 2003; **26**: 300-301

36 **Wang HB**, Mao YL, Jiu LC, Jia L, Ma HB, Cui EB. The changes of red cell nature-immune-adhesion function in two patients with atypical pneumonia at different stages. *Zhongguo Yixue Jianyan Zazhi* 2003; **4**: 85-86

37 **Li B**. Researchers in China have developed the chip of the whole genome of SARS virus. http://www.xinhua.org/ 2003.05.08 19: 10:36

38 Taiwan University invented the way of ICT which can quickly confirm whether someone is infected with SARS. http://www.sars.ac.cn/show.php?id=5222

39 **Liu B**. Micorflow control chip can detect SARS virus. *Science and technology daily* 2003.06.16

40 **China has cloned SARS-like virus particle**. Jian kang bao,http://www.jkb.com.cn 2003.06.17

41 **Fisher DA**, Lim TK, Lim YT, Singh KS, Tambyah PA. Atypical presentations of SARS. *Lancet* 2003; **361**: 1740

42 **So LK**, Lau AC, Yam LY, Cheung TM, Poon E, Yung RW, Yuen KY. Development of a standard treatment protocol for severe acute respiratory syndrome. *Lancet* 2003; **361**: 1615-1617

43 **Lapinsky SE**, Hawryluck L. ICU management of severe acute respiratory syndrome. *Intensive Care Med* 2003; **29:** 870-875

44 **Allegra L**, Blasi F. Problems and perspectives in the treatment of respiratory infections caused by atypical pathogens. *Pulm Pharmacol Ther* 2001; **14**: 21-27

45 **Atabai K**, Matthay MA. The pulmonary physician in critical care. 5: Acute lung injury and the acute respiratory distress syndrome: definitions and epidemiology. *Thorax* 2002; **57**: 452-458

46 **The Acute Respiratory Distress Syndrome Network**. Ventilation with lower tidal volumes as compared with traditional tidal volumes for acute lung injury and the acute respiratory distress syndrome. *N Engl J Med* 2000; **342**: 1301-1308

47 **Zhong NS**. Status of diagnosis and treatment of SARS. *Zhongguo Yixue Luntanbao* 2003.4.29

48 **Jiang SC**, Wei H, Wang Y. Prevention and cure of hospital infection due to severe respiratory syndrome. *Zhonghua Yixue Zazhi* 2003; **13**: 401-404

49 **Wong VWS**, Dai D, Wu AKL, Sung JJY.Treatment of severe acute respiratory syndrome with convalescent plasma. H K MJ. http://www.hkmj.org.hk/hkmj/update/SARS/cr1606.htm

50 **WHO Recommendations on SARS and Blood Safety**. http://www.who.int/csr/sars/guidelines/ bloodsafety/en/

51 **Anand K**, Ziebuhr J, Wadhwani P, Mesters JR, Hilgenfeld R. Coronavirus main proteinase (3CLpro) Structure: Basis for Design of Anti-SARS Drugs. *Science* 2003; **300**: 1763-1767

52 **Moller JC**, Schaible T, Roll C, Schiffmann JH, Bindl L, Schrod L, Reiss I, Kohl M, Demirakca S, Hentschel R, Paul T, Vierzig A, Groneck P, Von Seefeld H, Schumacher H, Gortner L. Treatment with bovine surfactant in severe acute respiratory distress syndrome in children: a randomized multicenter study. *Intensive Care Med* 2003; **29**: 437-446

53 **Zhao RTG**. General situation of the treatment of SARS and problems needed to solve.Jian kang bao,http://www.jkb.com.cn. 2003-05-23

54 **Xiao X**, Yuan MD. http://www.xinhua.org, 2003-06-20 15:49:01

55 **Zhang JZ**. Severe acute respiratory syndrome and its lesions in digestive system. *World J Gastroenterol* 2003; **9**: 1135-1138

56 **Nie QH**, Luo XD, Hui WL. Advances in clinical diagnosis and treatment of severe acute respiratory syndrome. *World J Gastroenterol* 2003; **9**: 1139-1143

57 **Nie QH**, Luo XD, Hui WL. An emerging infectious disease: severe acute respiratory syndrome. *Shijie Huaren Xiaohua ZaZhi* 2003; **11**: 881-887

Edited by Wang XL

P.O.Box 2345, Beijing 100023,China
Fax: +86-10-85381893
E-mail: wjg@wjgnet.com www.wjgnet.com

World J Gastroenterol 2003;9(8):1646-1656
World Journal of Gastroenterology
 ISSN 1007-9327

• REVIEW •

Progress in searching for susceptibility gene for inflammatory bowel disease by positional cloning

Chang-Qing Zheng, Gang-Zheng Hu, Zhao-Shu Zeng, Lian-Jie Lin, Gin-Ge Gu

Chang-Qing Zheng, Gang-Zheng Hu, Lian-Jie Lin, Gin-Ge Gu, Department of Gastroenterology, the Second Affiliated Clinical College of China Medical University, Shenyang 110001, Liaoning Province, China
Zhao-Shu Zeng, Department of Serology, College of Forensic Medicine, China Medical University, Shenyang 110001, Liaoning Province, China
Correspondence to: Professor Chang-Qing Zheng, Department of Internal Medicine, the Second Affiliated Clinical College of China Medical University, Shenyang 110001, Liaoning Province, China. zhengchangqing88@163.com
Telephone: +86-24-83956682 **Fax:** +86-24-83956682
Received: 2003-03-03 **Accepted:** 2003-04-11

Abstract

Inflammatory bowel disease (IBD) includes two clinical subtypes: Crohn disease (CD) and ulcerative colitis (UC). The general prevalence is about 1.0-2.0 % in Western countries. It is predominantly regarded as a multifactorial disorder involving environmental factors and polygenic defects. The view was confirmed by a lot of evidences from clinical attributions and animal models, especially from epidemiological investigations. So the etiological study of IBD has been focused on searching for susceptibility genes by positional cloning, which consists of two steps: linkage analysis and association analysis. Linkage analysis has been an important method of searching for susceptibility genes to polygenic diseases as well as single-gene disorders. IBD, as a polygenic disease, has been widely investigated by linkage analysis for susceptibility gene since 1996. The paper reviewed 38 articles, which covered almost all original researches in relation to IBD and linkage analysis. So far, several loci, such as 16q, 12q, 6p and 3p, have been identified by the studies. The most striking is 16q12 (IBD1), which linked only with CD not UC in the majority of studies. Association analysis, as one essential step for positional cloning, is usually carried out by genotyping candidate genes selected by means of linkage analysis or other methods, for figuring out the frequencies of alleles and comparing the frequencies between IBD group and healthy control group to identify the specific allele. It has been established that IBD is implicated in immune disorder. So the studies were centered on the genes of NOD2/CARD15, HLA-II, cytokine, cytokine receptor and adhesion molecule. This paper reviewed 14 original articles on association between NOD2 and IBD that have been published since 2001. All results, with the exception of one report from a Japanese group, provide evidences that the three kinds of variants of NOD2 are susceptibility factors for IBD. This article also comprehensively analyzed 18 original researches of HLA gene polymorphism in IBD. We found extensive discrepancy among the conclusions and a novel hypothesis was put forward to explain the discordance. Most studies published recently on association between IBD and cytokine gene polymorphism were reviewed.

Zheng CQ, Hu GZ, Zeng ZS, Lin LJ, Gu GG. Progress in searching for susceptibility gene for inflammatory bowel disease by positional cloning. *World J Gastroenterol* 2003; 9(8): 1646-1656
http://www.wjgnet.com/1007-9327/9/1646.asp

INTRODUCTION

Inflammatory bowel disease (IBD) is composed of two clinical subtypes: Crohn disease (CD) and ulcerative colitis (UC). Its general prevalence is 0.1-0.2 % in Western countries[1]. There has been no epidemiological investigation of large scale for the prevalence or incidence of IBD in China so far, despite the facts that UC is common in China and CD has been more frequently diagnosed by clinical physicians in recent years[2]. The pathogenesis of IBD has not been clearly identified. Today, the most generally accepted pathogenesis of IBD is that IBD is resulted from abnormal immune response to enteric bacteria in individuals with susceptibility due to genetically polygenic defects. Therefore, investigators have searched human genome for the loci of susceptibility genes by linkage analysis and have achieved great success. On the other hand, association analysis, as one of the essential steps for positional cloning, was carried out by many investigators to identify the specific allele. It has established that IBD is implicated in immune disorder. Biochemical substances involved in immunoregulation are very rich and the corresponding genes are widely distributed in genome. Genome-wide linkage analysis has suggested multiple candidate regions in several chromosomes for IBD, therefore, considerable numbers of candidate genes should be selected for association analysis. In recent years, these studies were centered on the genes of NOD2/CARD15, HLA-II, cytokine, cytokine receptor and adhesion molecule. These studies were summarized in this review.

IBD IS A MULTIFACTORIAL DISEASE

There have been a number of hypotheses about the pathogenesis of IBD, but neither environmental factors, such as habit of diet and behavior, infection of microorganisms and contact of chemical or physical pathogenic agents, nor single-gene genetic disorder alone can fully explain its complex phenotypes. Thereby, it is thought to be a multifactorial disease. The view was supported by a larger amount of evidences from clinical attributions and animal models, especially epidemiologic investigations and linkage analyses.

Persuasive evidences of genetic contribution to IBD[3-12]

A. The first-degree relatives of affected individuals show about 20-50-fold increased risk of developing the disease compared with the general population for CD, and 10-20-fold increased risks for UC. Moreover, the affected siblings frequently present at similar ages and concordance rates reach up to 80 % for disease site, behavior and presence of extraintestinal manifestation. B. Twin studies have shown that the concordance rate of CD is about 20-44 % for monozygotic twins, and 3.8-6.5 % for dizygotic twins; the concordance rate of UC is about 6-16 % and 3 % respectively[6,7]. C. There are significant ethnic differences in disease frequency. For instance, the prevalence in Ashkenazi Jews is much higher than that in other races, even though they share similar living environment in the same community[8,9]. D. All genome-scanning linkage analyses detected some linkage loci, certain of which were subsequently confirmed by replication studies only involving certain

chromosomes; NOD2 was consistently identified as the susceptibility gene for CD in recent years. E. Simulation studies on animal models have showed that transgenic mice or gene-knockout mice are subject to colitis similar to human IBD, and that spontaneous colitis or hapten-induced colitis manifests fairly different in different strains of mice[10-12].

Evidence of environmental contribution

A. The concordance rate of IBD for monozygotic twins is much less than 100 %. The identical genotype with different phenotypes means that environmental factors take part in the pathogenesis of the disease[6,7]. B. Intestinal bacteria are suggested as the main environmental contributions demonstrated by many evidences: antibiotic therapy can usually induce temporary remission for most IBD cases[13], diversion of faeces stream can make distal improvement in patients with CD[14], some studies suggested that certain strains of intestinal bacteria were associated with IBD[15,16], colonization with normal enteric bacterial flora was required for the occurrence of disease in animals with CD irrespective of the underlying defect[10-12]. C. smoking is likely to be associated with the progress of IBD[17,18]. D. Migrant epidemiological studies demonstrated that population of identical ethnic background, when lived in different communities, showed discordant incidence[8,9,19,20].

IBD is not a disorder of simple mendelian inheritance[3,21-25]

Genetic disease of classic Mendelian model, which consists of Mendelian dominant and recessive genetic disorders, is a phenotype of single-gene defect and called single-gene disorder. IBD has previously been interpreted as genetic disease of Mendelian recessive model. But segregation analyses offered counter-evidence that IBD followed the principle of Mendelian inheritance. Parents of most IBD probands were healthy, frequency of siblings or children of the patients was much less than 50 %, the decline in frequency of affected second-degree relatives compared with first-degree relatives was greater than that predicted by autosomal dominant inheritance, in which the frequency was expected to decrease by 1/2 with each step. Incidence of IBD in children of affected spouses was sharply less than 100 % and a similar proportion of affected siblings and children of affected probands was inconsistent with autosomal recessive inheritance. Linkage analysis has detected several linkage loci that are distributed on a number of chromosomes.

LINKAGE ANALYSIS

It is very difficult to find the biochemical substances, which express qualitative difference between patients and healthy population by means of classical functional cloning. So linkage analysis, as the first step of positional cloning, may serve as a unique and practicable substitution for the time being. Figuring out genetic distance between marked loci and susceptibility gene by means of pedigree investigation and genotyping, then defining the approximate position of susceptibility gene in genomic map are the essential courses of linkage analysis. The dramatic progress of human genome project, which has located nearly 10 000 marker loci in genomic map, has greatly boosted positional cloning for complex genetic diseases. Epidemiological studies have identified striking genetic contributions to the etiology of IBD, but so far, studies with traditional biochemical methods have not yet identified the products with quantitative defects. Many investigators have turned to linkage analysis and have achieved great success. The important data from 38 original researches, which covered almost all articles in relation to IBD and linkage analysis that have been published since 1996, are listed in Table 1[26-63], and some aspects were reviewed as follows.

The common course of linkage analysis for IBD is: collecting families with affected sibling pairs (ASP) or affected relative pairs (ARP) $\geqslant$2 by strict ascertainment, genotyping of genome-wide or certain chromosomes according to microsatellite polymorphisms, figuring out multi-point maximal non-parametric LOD score (MLOD) and two-point LOD score by means of statistical software, inferring genetic distances of susceptibility genes to marker loci and locations in physical genome map, offering candidate genes for association analysis. The majority of investigations found certain suggestive linkage loci with various LOD score, but when defined according to different LOD thresholds, the locations or number of linkage loci were variable. In view of the traits of statistical software and quantity of subjects in most studies, we only displayed the results with MLOD $\geqslant$2.0 or 3.0, represented by ± and +. The chromosomes, on which the linkage loci strongly supported (MLOD$\geqslant$3.0) by at least one of 8 linkage analyses of genome-wide scanning located, include chromosomes 1, 3, 5, 6, 7, 12, 14, 16, 18 and 19, as well as chromosomes 4, 10, 17 and x with suggestive evidence (2.0$\leqslant$MLOD<3.0). Although there was striking discrepancy among the genome-wide scans in respect of linkage loci, almost all studies detected more than 3 linkage loci. This shows that the pathogenesis of IBD is involved in multiple genes and manifests obvious genetic heterogeneity. Several loci were supported by relative more studies, such as 16q, 12q, 6p, and 3p. Because Hugot *et al*[26] and Satsangi *et al*[27] detected strong linkage evidences for chromosomes 16, 12, 6, 3 and 7 in 1996, subsequent studies mainly focused on these chromosomes. It can be seen from Table 1 that more evidences were offered for these loci, with the exception of 16q, simply because these loci were investigated by more studies. Some loci supported by certain genome-wide scans, such as 14q, 5q, 19p, likely to harbor susceptibility genes, were less investigated.

Stratification studies demonstrated significant variances as to the degree and loci of linkage between families with severe IBD and those with only slight IBD, male patients and female patients, Jewish people and non-Jewish people, as well as between UC and CD. Some investigators examined families with CD patients only; others examined families with UC patients only, but most studies detected both families and those with mixed patients and compared the differences of linkage loci between the two groups. As shown in Table 1, there were some differences between UC and CD. The most striking is 16q12 (IBD1), which linked only with CD not UC in the majority of studies. This shows that CD and UC have some common susceptibility genes, as well as certain individual susceptibility genes. Three studies[32,47,48] found that certain loci linked only with the families with early onset of CD. All subjects examined by the studies listed in Table 1 included Caucasian or Jewish patients from Europe, Australia and northern America, but no Mongolian patients. Three studies[28,29,42] demonstrated significant differences between Jewish patients and non-Jewish patients. In respect of nationality of patients, it seems there are no remarkable differences among American, English, German, Australian, Canadian, Italian, Dutch and Belgian. But Paavola *et al*[40] examined chromosomes 1, 3, 7, 12, 14 and 16 in Finnish patients and did not find linkage loci. Fisher *et al*[33] found that some loci on chromosomes 6p, 1, 14 and 18 linked only with IBD of male sufferer. These results confirm the extensive genetic heterogeneity of IBD.

Linkage analysis is intended as an essential tactic to offer candidate genes for association analysis. We should focus our attention on the linkage loci containing some candidate genes, products of which have been suggested as pathogenic factors by other methods, as well as confirmed by subsequent replication studies. The loci meeting these conditions were briefly reviewed here.

Table 1 Data of linkage analysis

Ref	Author	Year	Subject	Scope	Linkage loci for IBD	Linkage loci for CD	Linkage loci for UC
R26	Hugot JP	1996	Caucasian CD	Autosome		16q(IBD1)+	
R27	Satsangi J	1996	Northern european IBD	Autosome	7+, 12+, 3±	7±, 12±, 3±	7+
R28	Cho JH	1998	American IBD[a]	Genome	(3q+,1p±)(non-Jewish), (3q±,4q±)[e]	16±	––
R29	Ma Y	1999	American CD[a]	Genome		14q±, 17q±[e], 5q±[e]	
R30	Hampe J	1999	European IBD[b]	Genome	1±, 6±, X±	10±, 12±, 16±	4±, X±
R31	Duerr RH	2000	American CD[a]	Genome		14q+	
R32	Rioux JD	2000	Canadian IBD	Genome	19p+, 5q+, 3p±, 6p±	5q+[f], 19p+	19p±
R33	Fisher SA	2002	European IBD	Genome	(6p+,1+,14+,18+)(male)	6p+(male)	6p+(male)
R34	Brant SR	1998	American CD[a]	3,7,12,16		16q(IBD1)±	
R35	Rioux JD	1998	Toronto IBD	3,7,12,16	– –	––	––
R36	Curran ME	1998	European IBD[b]	12,16	– –	12q±	––
R37	Annese V	1999	Italian IBD	3,6,7,12,16	16q±	16q±	16q±
R38	Vermeire S	2000	Belgian CD	3,7,12,16		––	
R39	Dechairo B	2001	European IBD	3,6,7,	6p+	––	––
R40	Paavola P	2001	Finnish IBD	1,3,7,12,14,16	– –	––	––
R41	Gavanaugh J	2001	IBD[c]	12,16	16q+	16q+	––
R42	Ohmen JD	1996	American IBD[a]	16	– –	16q±[e]	––
R43	Parkes M	1996	English IBD	16	– –	16q±	––
R44	CavanaughJA	1998	Australian CD	16		16q+(IBD1)	
R45	Mirza MM	1998	Northern european UC	16			16q±(IBD1)
R46	Porabosco P	2000	Italian IBD	16	16q+	16q+	16q+
R47	Brant SR	2000	American CD	16		16q+[f], 16q±	
R48	Akollar PN	2001	Jewish CD	16		16q+[f]	
R49	Van Heel DA	2002	European CD	16		––	
R50	Zouali H	2001	European CD	16		16q+	
R51	Hampe J	2002	European IBD	16	16p±	16q+, 16p±	––
R52	Satsangi J	1996	European IBD	6(MHC-II)	– –	––	6p(MHC-II)+
R53	Silverber MS	1999	Canadian CD	6		6p(MHC-II)±	
R54	Hampe J	1999	Northern european IBD[b]	6	6p+	6p+	6p+
R55	Yang H	1999	American CD	6		6p(MHC)+	
R56	Duerr RH	1998	Northern american IBD	12	12q±	––	––
R57	Yang H	1999	American IBD	12	– –	12q±	––
R58	Lesage S	2000	Northern european CD[d]	12		––	
R59	Parkes M	2000	American IBD	12	12q+	––	12q+
R60	Hampe J	2001	Northern european IBD[b]	3	– –	––	––
R61	Duerr RH	2002	American IBD	3	3p+	––	––
R62	Rioux JD	2001	American CD	5q		5q+	
R63	Vermeire S	2001	Belgian CD	X		Xq±	

Note: CD, CD-only family; UC, UC-only family; IBD=UC+CD+mixed family; +, convincing linkage (LOD≥3.0); ±, suggestive linkage (3.0>LOD≥2.0); —, no suggestive linkage (LOD<2.0); [a], including Jewish; [b], family from English, German and Dutch; [c], family from Northern American, European and Australian; [d], family from French and Belgian; [e], linkage only for Jewish; [f], linkage only for IBD with early onset.

Chromosome 16 As shown in Table 1, 14 out of 25 related studies found linkage loci for CD with MLOD more than 2.0 on the chromosome, additionally, some loci with suggestive score (MLOD between 1.0 and 2.0) were detected. Only 3 studies found linkage loci with UC, furthermore, 2 of them also detected linkage with CD, and the other one merely examined UC families. It can be inferred from these studies that chromosome 16 contains susceptibility gene for CD rather than UC. Chromosome 16 is comparatively short, with 98 Mb of physical length, 130.8 cm of genetic distance, and has been spaced by about 200 microsatellite markers[64]. The linkage loci suggested by the studies in Table 1 were distributed in most part of chromosome 16 (for instance, D16S409-419[26], D16S748-764[28], D16S411[42,43], D16S3136[50]), but only pericentromeric region on 16q was the most consistent linkage region. The important candidate genes in the region are NOD2, CD11integrins, CD19, Sialophorin, IL-4 receptor gene etc. NOD2 gene has been established as susceptibility gene to CD. It remains unanswered if there are other susceptibility genes in the chromosome. Hampe *et al*[51] examined additional regions with high-density experiment using 39 microsatellite markers and found three-peak logarithm of odds (LOD) scores of 2.7, 3.2, and 3.1 on proximal 16p, proximal 16q, and central 16q, respectively. Taking account of the differences of suggestive markers, it is probable that there are other susceptibility genes for CD in the chromosome.

Chromosome 12 Six out of 19 studies found suggestive linkage loci in the chromosome, 4 of them for CD, and one for UC. Though the studies with suggestive MLOD are rare, several studies found linkage loci with slightly suggestive significance (MLOD between 1.0 and 2.0) with IBD, especially with UC. This may result from the fact that the sample sizes in most studies were not large enough; furthermore, they were predominantly consisted of CD families. Parkes *et al*[59] examined 581 affected relative pairs, of which 252 were from CD-only families, 138 from UC-only families, and 191 from mixed families (the sample size was much larger than that in most of other studies, especially for UC), and found that MLOD at certain marker on chromosome 12 was 5.26 for all IBD, 3.91 for UC and 1.66 for CD. In summary, it is probable that

Table 2 Data of association analysis for NOD2

Ref year author	Subject	Main conclusion
R65, 2001	Europe CD, UC	A. Find P241S, R432R, R675W, G881R, IVS8-133delAinSCT, 980fs etc.31 variants
Hugot, JP		B. R675W, G881R, 980fs with CD, not with UC
		C. CD-GRR 3.0 at SHEM, 38.0 at HOM, 44.0 at CHEM
R66, 2001	American CD	A. 3020insC with CD
Ogura Y		B. CD-GRR 1.5 at SHEM, 17.6 at HOM
R67, 2001	German, English CD	A. 3020insC with CD, not with UC
Hampe J	UC	B. CD-GRR 2.6 at SHEM, 42.1 at HOM
R68, 2002	Europe CD, UC	A. Find 67 sequence variants, 9 of which gene frequency >5 %
Lesage S		B. R702W, G908R, 3020insC with CD, not with UC
		C. Support gene-dosage effect
R69, 2002	Europe CD, UC	A. R702W, G908R, 3020insC with CD, especially ileum CD, not with UC
Cuthbert AP		B. P628S linkage disequilibrium with the other three mutations
		C. CD-GRR 3.0 at SHEM, >22.0 at HOM or at CHEM
		D. Mutation frequency: familial CD > sporadic CD
R70, 2002	Dutch CD	A. 3020insC with CD, G2722C not with CD
Murillo L		B. No association with clinical phenotype
R71, 2002	German, Norwegian	A. R675W, G881R, 980fs with CD
Hampe J	CD	B. Especially with ileum CD
R72, 2002	Canadian CD	A. R702W, G908R, 1007fs with CD, especially ileum CD
Vermeire S		B. No difference between familial CD and sporadic CD
R73, 2002	German UC, CD	A. 3020insC with CD, not with UC
Radlmayr M		B. Association with fistula, fibrostenosis, ileocecum resection
R74, 2002	Japanese CD, UC	A. R675W, G881R, 3020insC not with CD or UC
Inoue N		
R75, 2002	Europe CD	A. R675W, G881R, 3020insC with CD
Vermeire S		B. Not with effect of Infliximb
R76, 2002	American CD	A. R702W, G908R, 1007fs with CD
Abreu MT		B. With fibrostenosis
R77, 2002	English CD	A. R702W, G908R, 1007fs with CD, especially ileum CD
Ahmad T		B. 3020insC with early onset of CD
		C. CD-GRR 2.4 at SHEM, 9.8 at HOM, 29.3 at CHEM
R49, 2002	Europe CD	A. R702W, 1007fs with CD, linkage disequilibrium with P628S
Van heel DA		B. Support gene-dosage effect

Note: CD=Crohn disease; UC=ulcerative colitis; CD-GRR=CD-genotype relative risk; SHEM=simple heterogeneous mutation; HOM= Homozygous mutation; CHEM=complex heterogeneous mutation; *P* value is uniformly set at $\leqslant$0.05; Nomenclatures were not uniform among the studies, R675W=R702W, G881R=G908R, 1007fs=980fs=3020insC.

chromosome 12 contains susceptibility genes both for CD and UC, but with only weak contributions. The most consistent microsatellite markers lay in 12q13, which is also called IBD2. The main candidate genes in the region are IFN-γ, natural resistance associated macrophage protein (MRAMP2), vitamin D receptor genes etc.

Chromosome 6 Eight out of 14 studies found linkage loci in the chromosome. There was no remarkable difference between CD and UC in terms of the number of suggestive studies or LOD score in most studies. This shows that common susceptibility genes for both CD and UC are probably located in chromosome 6. Linkage markers of most studies were distributed in 6p13, which was called IBD3 in some studies. The important candidate susceptibility genes in the region include HLA-A, HLA-B, HLA-C, HLA-E, HLA-F, HLA-G, MIC-A, MIC-B, HLA-DR, HLA-DP, HLA-DQ, HLA-DM, LMP-2, LMP-7, transporterin antigen processing (TAP)-1, TAP-2, TNF-α, TNF-β, (LT-α), heat shock proteins (HSP), complement C4, C2 genes etc.

Chromosome 3 Four out of 16 related studies found linkage loci with LOD score more than 2.0. It should be noticed that the LOD scores in 4 studies for all IBD were always higher than that for CD or UC alone and no LOD score for CD or UC alone reached 2.0 in all related studies. It may be partly due to the fact that the sample sizes were much smaller after stratifications and could not reach the threshold of statistical significance. It is very likely that there are some common susceptibility genes for CD and UC, but they probably confer slight genetic contribution to IBD, since some studies found linkage loci in the chromosome only with weakly suggestive LOD score[30,39,60]. The considerable linkage region was proximal 3p. The principal candidate genes in the region include CCR2, CCR5, IL-4RA, IL-5RA, lactotransferrin, IFN-α A2, cathelicidin antimicrobial peptide genes etc.

Chromosome 5q It was confirmed by only 3 studies involved in the chromosome. The linkage loci were located in 5q32-35, which happened to be in the region of cytokine-rich cluster and was called IBD5 in some studies. The main candidate genes are IL-3, IL-4, IL-5, IL-13, CSF-2 genes etc. The cytokines have been accepted as playing important roles in initiating IBD. So further investigations are needed.

14q11(IBD4) and 19p13 They were suggested as linkage loci in some studies. 14q11 contains the immunoloregulation members TCR-α/δ gene and 19p13 contains ICAM1, C3, TBXA2 and LTB4H genes.

ASSOCIATION ANALYSIS

Association analysis, as an essential step for positional cloning, was usually carried out by genotyping candidate genes selected by means of linkage analysis or other methods, for figuring out the frequencies of alleles and comparing the frequencies

Table 3 Data of association analysis for HLA

Ref	Year	Author	Subject	Region	Association with CD	Association with UC
R83	1995	Duerr RH	American UC	HLA-DR2		DRB1*1601-
R84	1995	Nakajima A	Japanese CD	DR, DQ, DP	(DRB1*0405,0410,DQA1*03,DQB1 *0401,0402)+, (DQA1*0102,DRB1* 1501,1302,DQB1*0602) -	
R85	1996	Reishagen M	German CD	DRB1, DQA1, DQB1	DRB1*07+, DRB1*03-	
R86	1996	Hesresbach D	French CD	HLA-I, HLA-II, TAP	DRB1*1302+, DRB1*04+[c]	
R52	1996	Satsangi J	Europe IBD	DRB, DQB		DRB1*103+, DRB1*12+
R87	1996	Danze PM	French CD	DRB1, DQB1	(DQB1*0501, DRB1*07, 01)+ (DQB1*0602 / 0603, DRB1*03)-	
R88	1996	Heresbach D	French UC	HLA-II, TAP		DRB1*03-
R89	1997	Bouma G	Dutch IBD	HLA-DR		DRB1*15+, DRB1*13-
R90	1998	Fernandez AM	Spanish UC	DRB1		DRB1*1501+, DRB1*
R91	1998	Cariappa A	American CD	DRB, DQB, DPB	Haplotype DRB3*0301 / DRB1*1302+	1502(severe)+
R92	1999	Bouma G	Dutch UC	DR, TNF-α, LT-α		DRB1*0103+, DRB1*15(female)+
R93	1999	Yoshitake S	Japanese IBD	DQ, DR, DP	DQB1*0402+, DRB1*1502-	(DRB1*1502,DRB5*0102, DQA1*0103,DQB1*06011, DPA1*0201,DPB1*0901)+, (DRB4*0101,DQA1*0302) -
R94	1999	Stokkers PC	Meta-analysis	DR, DQ, TNF-α	(DR7,DRB3*0301,DQ4)+, (DR2,DR3)-	(DR2, DR9, DRB1*0103)+, DR4 -
R95	1999	Hirv K	Estonians UC	DR, DQ, TNF-α		DRB1*1501+
R96	2001	Seki SS	Japanese UC	HLA-I, HLA-II		(MICA-TM-STR6, B52, DR2)+
R97	2002	Lantermann A	IBD[a]	DPA1	DPA1*02021(German)+	
R98	2002	Orchard TR	Europe IBD	HLA-B, DR, TNF-α	Uveitis with (B*27,B*58,DRB1*0103)	
R77	2002	Ahmad T	CD[b]	HLA-I, HLA-II TNF-α, LT-α, HSP70	(DRB1*0701,CW*0802)+, DRB1*0103(fistula)+, DRB1*1501-	

Note: UC= Ulcerative colitis; CD= Crohn disease; IBD= UC+CD; [a], German, South Africa and South Korea IBD; [b], white people CD; [c], DRB1*04 is only associated with CD with no effect to cortexin; *P* value is uniformly set at $\leqslant$0.05; +, Positive association; -, Negative association.

between IBD group and healthy control group to identify the specific allele. It has established that IBD is implicated in immune disorders. So studies have been centered on genes of NOD2/CARD15, HLA-II, cytokine, cytokine receptor and adhesion molecule.

NOD2/CARD15 mutations

Identification of NOD2 as susceptibility gene for IBD is supported by linkage analysis, association analysis and immunological function analysis. In this review, crucial information from 14 original studies on the relationship between IBD and NOD2 mutations are listed in Table 2[49, 65-77] and were comprehensively analyzed as follows. NOD1 is an intracellular protein composed of a N-terminal caspase recruitment domain (CARD), a centrally located nucleotide binding domain (NBD), and a leucine rich repeat (LRR) domain at its C-terminus which could activate nuclear factor κB (NFκB) and also promote apoptosis[78]. NOD2 was identified by searching the public database for genes encoding similar proteins to NOD1. The gene happens to be located on chromosome 16q12, a domain called IBD1 supported by most linkage analysis. NOD2 has one more CARD at its N-terminal than NOD1. It is expressed primarily in monocytes and following stimulation by bacterial lipopolysaccharide (LPS), which occurs at LRR domain, activates NF-κB.

So far, approximately one hundred sequence variants have been detected in NOD2 gene, most of which were rare mutations, and located in LRR domain. Lesage *et al* discovered 67 sequence variants in the gene, 9 out of them with gene frequencies more than 5 %. This demonstrates that NOD2 gene has high polymorphism. Of these alleles, P268S, R702W, G908R and 1007fs are consistently confirmed to be the genetic susceptibility factors to IBD. Gene frequency of P268S in general population was about 20-28 %, a little higher than other three variants. While it was remarkably higher in CD patients, transmission disequilibrium test (TDT) suggested that this was very likely to be the result of transmission disequilibrium with other three variants, but not the independent susceptibility factor to CD. R702W, G908R and 1007fs are widely considered as independent susceptibility factors. 1007fs allele frequency was different among all reports: about 1.6-3.3 % in control population and 6.6-23.7 % in CD patients. All the studies, with the exception of a report from Japanese group, strongly support the association of 1007fs with CD. Allele frequency of R702W was slightly higher than that of 1007fs, and was significantly higher in CD patients than in control population. Allele frequency of G908R was about 1.5 % and has been suggested as an independent susceptibility factor to CD, but the statistical values in some reports did not reach significant level. This may be due to its lower gene frequency. The CD-genotype relative risk of the three mutations was about 3.0 for simple heterozygote mutation, and more than 20.0 for homozygote mutation or compound heterozygote mutation. This supports the fact that mutations in NOD2 gene show a gene-dosage effect and somewhat recessive trait. Five studies, in which subjects included UC patients, did not find any persuasive evidences that the three mutations were associated with UC. It' s worthy to point out that association of the three mutations with CD was not confirmed in study by the Japanese group. The discordance is usually explained by the view that CD is a genetic disease with high locus heterogeneity or allele heterogeneity among patients from different races or different geographic territories. With respect to the association of three mutations with clinical phenotypes, most reports suggested 3 mutations were only associated with ileum CD and certain reports found they were associated with fibrostenosis, fistula or effect of medicine.

How can the mutations of NOD2 initiate CD[65,66,79-82]? Some

studies have provided evidences that NOD2 is an intracellular receptor for bacterial pathogenic agents, and expresses only in monocytes. LRR of NOD2, after being activated by lipopolysaccharide (LPS), can trigger NF-κB signal pathway, which promotes the expression of certain proinflammatory cytokines. LRR can also promote apoptosis. So it is the most likely mechanism that the mutations in NOD2 either raise sensitivity of monocyte to bacterial pathogenic agents, with the result of overexpression of certain proinflammatory cytokines, or cause deficiency of apoptosis, leading to monocyte accumulation in intestinal mucosa and chronicity of the course. There are some questions about the relation between mutations in LRR and activity of NF-κB. Though high activity of NF-κB is always found in monocytes in lamina propria of intestinal mucosa from CD patients, it descends in cells with frame-shift mutation in LRR *in vitro* when stimulated by LPS. Functional study by Hugot *et al* demonstrated that expression of a NOD2 mutant form lacking the entire LRR region results in enhanced NF-κB activity, whereas the frame-shift mutation causing a truncated protein missing the final 33 amino results in low NF-κB activity. The potential explanation may be that the truncated protein leads to elevated NF-κB when stimulated by an untested bacterial LPS and that the frame-shift mutation may have a differential effect on caspase 9 induced apoptosis. To understand the mechanism how mutations in NOD2 confer susceptibility to CD, more functional analyses should be ingeniously performed. Identification of NOD2 was a great achievement in the history of exploring genetic susceptible factor for IBD. Detecting of the mutations may well have some clinical benefits for the prediction of onset risk, classification of disease, individualization of therapy and future gene therapy, but it should not be used as a tool for diagnosis since there is about 6-9 % overall allele frequency of the three single nucleotide polymorphisms (SNPs) in general population.

HLA gene polymorphisms

HLA gene is composed of three regions: HLA-I, HLA-II and HLA-III. HLA-I mainly includes HLA-A, HLA-B and HLA-C, and HLA-II mainly contains HLA-DR, HLA-DQ, HLA-DP. The primary immunity relative genes in HLA-III region are TNF-α, TNF-β, (LT-α), complement 2 (C2), complement 4(C4). Genes in the regions are highly polymorphic. HLA-II is expressed primarily in macrophages, dendritic cells and thymic epithelial cells, playing important parts in presenting exogenous antigen. Immunologic studies have shown strong evidences that IBD is closely associated with disturbance of Th lymphocyte subclass, and that the major environmental factor inducing immune disorder is intestinal bacterial flora. T lymphocytes accept enteric antigens presented by microphages, so it is naturally viewed that sequence variants of HLA-II are likely to cause disorder of antigen presenting and result in imbalance of Th lymphocyte subclass. HLA genes located in IBD3 (6p13) were identified by linkage analysis, it is sensible to select HLA gene as candidate gene for association analysis. This review collected 18 studies published since 1995 and listed the main results in Table 3[52,77,87-98]. Most studies published before 1995 usually typed HLA by examining serum HLA antigen through immunologic assay. The studies shown in Table 3 tried to identify HLA alleles by using reliable and precise molecular biological techniques, such as specific sequence primer polymerase chain reaction (PCR-SSP), specific sequence oligonucleotide probe assay (PCR-SSO) and gene sequencing.

It could be summarized from Table 3 that polymorphisms positively or negatively associated with UC or CD are mainly located in DRB1 or DQB1, which are the key regions to determine the polymorphism of peptide-binding cleft. The sequence variants in the regions could change the affinity for distinct antigen peptides. According to serum typing, results from more than two studies suggest that UC is positively associated with DR2, DR9 and negatively associated with DR4, and that CD is positively associated with DR7, DQ4, negatively with DR2, DR3. Further genotypings by molecular biological technique found that only DRB1*0103, DRB1*1501 and DRB1*1502 were associated with UC in more than two studies. Other variants in the regions have not been confirmed to be positively or negatively associated with UC or CD. Many investigators studied the association between polymorphism and clinical phenotype (p-ANCA, sex, extent, age of onset, site of disease, effect of certain medicine, complication, certain extraintestinal symptoms), but their conclusions were not consistent. The heterogeneity was obvious between UC and CD in respect of association with polymorphisms of HLA-II genes. The alleles associated with UC or CD were not associated with the others. On the contrary, DR2, positively associated with UC in some reports, was negatively associated with CD in other reports.

Stokkers *et al*[94] carried out a meta-analysis involving 29 pieces of related reports published from 1980 to 1999 (there were some overlaps between those and reports listed in Table 2). Taking a wider view of all these studies, we discovered a remarkable characteristic: the vast majority of studies discovered certain positively or negatively associated alleles, but all the suggested alleles showed significant discrepancy (there were always both evidences and counterevidences of the association as to any of the alleles among the studies). The contradiction cannot be explained by race heterogeneity because there are discrepancies both in white people and yellow people. It cannot be convinced that sequence variants in HLA-II gene are not associated with IBD and positive results are due to confusions either from linkage disequilibrium or from coincidences resulted from high polymorphisms. In view of the functional property of HLA-II and the widespread contradictions in association analysis, we consider that polymorphism in the regions, to some extent, plays a role in initiating IBD, but the involved alleles differ between different communities (in view of geographic situation, climatic condition and dietary culture) and even between individuals in the same community. The constituent characteristics (sort, ratio, total amount and time order of all antigens) of antigen compound (all kinds of antigens) derived from intestine in one community are distinct from that in an other community. The antigen presenting cells (APC) containing certain HLA-II allele, only when disposing and presenting the antigen compound with matching constituent characteristic, can cause pathologic response. There are different predominant antigen compound in different communities, so the predominantly matching alleles implicated in IBD might be different among communities, and therefore no particular or unchanged antigen and HLA-II allele can take part in pathologic lesions in all IBD. Nevertheless, some of them may play a more dominant role in one community than in another community.

Cytokine, cytokine receptor and adhesion molecule polymorphisms

IL-1β, excreted mainly by microphages, up-regulates the expression of HLA-II, adhesion molecule and IFN-γ in an autocrine manner. It can also, through paracrine, promote activity of Th lymphocyte and play an important part in triggering immune response. IBD is regarded as the result of imbalance of Th lymphocyte subclass, thereby, IL-1β, IL-1β receptor (IL-1R), IL-1 receptor antagonist (IL-1RA), balance of IL-1β/IL-1RA may be associated with IBD. Up to date, many investigators have tried to explore association between IBD and gene polymorphism, but studies in recent years did not

find any positive results[99-101]. Nemetz *et al* found that IL-1β-511*2 allele was associated with the overexpression of IL-1β and descent of bone mineral density[102], and that IL-1β(+3953,-511) allele is associated with pathological course and patient' s condition[103]. Mwantembe *et al*[104] examined the polymorphism of IL-1β, IL-1R and IL-1RA genes by *TaqI, Pst I* and VNTR and discovered IL-1R (*TaqI-*) allele frequency was significantly higher in white patients than that in white healthy controls and Negro patients, whereas IL-1R (*Pst I-)* allele frequency was higher in Negro patients than those in white patients. IL-1β and IL-1RA genes were not located in the region which was strongly supported by linkage analysis.

TNF-α is suggested as a pathogenic factor for IBD because its concentration is usually increased in intestinal mucosa of IBD patients, and therapy of anti-TNF-α antibody Infliximb has shown satisfactory effects on refractory IBD. The gene is located in IBD3 (6p13) which is supported by linkage analysis. Most studies in recent years discovered certain alleles were associated with IBD. Van Heel *et al*[105] found (-857C) TNF-α allele was associated with IBD. Sashio *et al*[106] found TNF-α (-308G/A, -238 G/A) allele was associated with UC. Mitchell *et al*[107] found that TNF-α (-308G/A) was associated with sclerosis cholangitis. Koss *et al*[108] found that different haplotypes of TNF-α gene were associated with the expression of TNF-α. Louis *et al*[109] discovered (-308) TNF-α was associated with certain clinical phenotypes of CD. Negoro *et al*[110] discovered (-1031C, -803A, -857T) TNF-α was associated with CD. These results show that sequence variants of TNF-α gene, especially (-308G/A) may take part in the pathogenesis of IBD by enhancing the expression of TNF-α and promoting activity and proliferation of Th lymphocytes.

IL-4, expressed mainly in Th2 lymphocytes, plays an important role in regulating the balance of Th lymphocyte subclasses and induces differentiation and proliferation of B lymphocytes or microphages, thereby it is regarded as a principal factor in initiating UC. IL-4 and IL-4 receptor (IL-4R) gene are separately located in 5q31-33 (IBD5) and 16q12 (IBD1) which are supported by linkage analyses. Klein *et al* [111] and Aithal *et al*[112] found that certain alleles of the genes were associated with CD. Peng *et al* examined IL-4 polymorphisms in Chinese people and found IL-4-RP2 allele frequency was obviously higher in UC patients than in healthy control, whereas RP1 allele frequency was higher in healthy control than in UC patients[99].

IL-10, mainly excreted by Th3 or Th2 lymphocytes, can suppress the expression of IL-12 and TNF-α in natural killer cells or microphages, restrain activity or proliferation of Th1 lymphocytes. The functional deficiency of IL-10 may be an important maintenance factor for chronicity of IBD. The fact that IL-10 gene knockout mice are subject to colitis similar to human IBD is a persuasive evidence. But studies in recent years did not discover any allele was associated with IBD (allele IL-10 (-627, -1117, -1082, -592, -819) etc.)[101,107,113,114]. Koss *et al*[108] found IL-10 (-1082G/A) allele was associated with the down-regulation of IL-10 expression.

ICAM-1 plays an important role in regulating the homing of lymphocytes. Overexpression of ICAM-1 and significant lymphocyte infiltration have been found in intestinal mucosa of IBD patients. ICAM-1 gene is located in 19p13, which is supported by some linkage analysis. Yang *et al*[115,116] found that R241 allele was associated only with ANCA-positive UC. Contrarily, Braun *et al*[117] reported that ICAM-1 R241 allele and R/G241 heterogeneous mutation were much more frequent in UC patients than in healthy control irrespective of ANCA-positive or ANCA-negative.

Other investigators examined E-selection, L-selection, CCR2, CCR5, IL-6, NRAMP1 and IFN-r genes and found they had no association with IBD[95,118-121].

PROBLEMS AND PERSPECTIVES

Taking a wide view of these studies, we could find extensive discrepancies, which are usually interpreted by the view that IBD is a genetic disease with widespread heterogeneity[122]. It means that the complicated clinical phenotypes of IBD are determined by interaction of multiple genes with environmental factors. Single gene contributes little to IBD, and only polygenic defects with corresponding conformation underlie the complicated phenotypes of IBD. One phenotype may be determined by more than one conformation models of polygenic defects. Nevertheless, we should take into account of other aspects to resolve the discordant results in linkage analyses. A. Entrance criteria and clinical classifications of subjects must be controled more strictly and uniformly, since a minor mistake may influence the outcomes[123,124]. B. The microsatellite markers used by different investigators were not uniform, some investigators selected high-density markers, and others used somehow lower density markers. This could result in discrepancy conclusion. C. The sizes of sample were different among the studies, ranging from about 100 patients to more than 600 patients. Stratification studies performed using small sample sizes may cause false-negative error. Cavanaugh *et al*[41] carried out an international multicenter study, which involved 613 families from 12 study centers. By pooling of data sets, which were acquired from 12 independent centers using the same statistical method, despite the lack of convincing evidence for linkage based on data from individual center, they discovered unequivocal linkage for IBD on chromosome 16 (MLOD 5.79). D. The principle of linkage analysis is based on the view that crossing over in meiosis I is random and physical distance on chromosomes is necessarily in accord with genetic distance. The findings that significant association was found, but no linkage was suggested for the same subject group and the same loci demonstrated somehow theoretical disability of linkage analysis[49,125,126]. E. Other molecular biological mechanisms such as epigenetics may also play a role in initiating IBD[127]. In addition, if IBD is thought as a genetic disorder like familial adenomatous polyposis (certain mutations were inherited from parents, then somatic mutations were accumulated in certain cells such as macrophages or epithelial cells in intestinal mucosa or lymphoid tissue), all phenomena observed so far would not produce counterevidence. Today, linkage analysis has shed lights on genetic diseases such as diabetes mellitus, hypertension, asthma, Alzheimer' s disease and arteriosclerosis, as well as single-gene disorders. As for IBD, we have identified several linkage loci, which harbor a number of important candidate genes pending further confirmation by association analysis and functional analysis.

At present, about 30 candidate genes have been investigated by means of association analysis, and the majority of them either have no association with IBD or have not been confirmed by replication studies. With respect to HLA gene, though the majority of investigations discovered certain positively or negatively associated alleles, all the suggested alleles showed significant discrepancy. The three mutations in NOD2 gene have been consistently confirmed to be the independent susceptibility factors for CD in all-14 original studies except for one from a Japanese group, but how the variants can cause CD remains to be answered. Taking a wide view of all reports, which reached statistic significance, we discovered that frequencies of any alleles ever suggested by association analysis did not manifest a great absolute difference between patients and healthy controls. For instance, only about 20 % CD patients carried at least one of the three alleles of NOD2, whereas about 4-7 % healthy population also carried one of them. This shows that no allele ever studied demonstrates high specifity and sensitivity of the association with IBD and other

alleles need to be explored. It should be noted that the results of most studies, irrespective of positive or negative, did not absolutely ascertain the involvement of genes as susceptibility genes to IBD, since these could be confounded by a number of factors such as type I error or type II error caused by linkage disequilibrium or coincidence. In addition, there are many sequence variants in most genes, some of them are rare mutations and can only be properly analyzed in study of very large samples. Most investigators only detected variants in certain regions of the genes, instead of sequencing of whole gene of these alleles, therefore these results cannot represent the whole genes. The associations of some alleles with clinical phenotype of IBD have been detected by stratification study in many studies, but studies on the associations with the expression of cytokines involving the regulation of Th lymphocytes, were far less and more studies need to be carried out. The biochemical substances, which were ever suggested to be pathogenic factors for IBD, are of great variety, so it' s important to select proper candidate genes for association analysis. Since 1996, nearly 40 linkage analyses have identified several linkage loci in different chromosomes, such as IBD1, IBD2, IBD3, IBD4, and IBD5. Therefore, the genes located in such loci, and their products widely established as pathogenic factors for IBD, should be preferentially selected as candidate genes. Association analysis is an important method for unraveling the pathogenesis of IBD at gene level and will contribute tremendously to the understanding of IBD in the near future.

REFERENCES

1 **Probert CS**, Jayanthi V, Rampton DS, Mayberry JF. Epidemiology of inflammatory bowel disease in different ethnic and religious groups: limitations and aetiological clues. *Int J Colorectal Dis* 1996; **11**: 25-28

2 Z**heng JJ**. Incidence of inflammatory bowel disease in: Zheng JJ, Chu XQ, eds. Inflammatory bowel disease: basis and clinic. Beijing: *Science Press* 2001: 36-36

3 **Binder V**. Genetic epidemiology in inflammatory bowel disease. *Dig Dis* 1998; **16**: 351-355

4 **Heresbach D**, Gulwani-Akolkar B, Lesser M, Akolkar PN, Lin XY, Heresbach-Le Berre N, Bretagne JF, Katz S, Silver J. Anticipation in Crohn's disease may be influenced by gender and ethnicity of the transmitting parent. *Am J Gastroenterol* 1998; **93**: 2368-2372

5 **Satsangi J**, Grootscholten C, Holt H, Jewell DP. Clinical patterns of familial inflammatory bowel disease. *Gut* 1996; **38**: 738-741

6 **Tysk C,** Lindberg E, Jarnerot G, Floderus-Myrhed B. Ulcerative colitis and Crohn's disease in an unselected population of monozygotic and dizygotic Twins. A study of heritability and the inflence of smoking. *Gut* 1988; **29**: 990-996

7 **Thompson NP**, Driscoll R, Pounder RE, Wakefield AJ. Genetics versus environment in inflammatory bowel disease: result of a British twin Study. *BMJ* 1996; **312**: 95-96

8 **Roth MP,** Petersen GM, McElree C, Vadheim CM, Panish JF, Rotter JI. Familial empiric risk estimates of inflammatory bowel disease in Ashkenazi Jews. *Gastroenterology* 1989; **96**: 1016-1020

9 **Jayanthi V**, Probert CS, Pinder D, Wicks AC, Mayberry JF. Epidemiology of Crohn's disease in Indian migrants and the indigenous population in Leicestershire. *Q J Med* 1992; **82**: 125-138

10 **Blumberg RS**, Saubermann LJ, Strober W. Animal models of mucosal inflammation and their relation to human inflammatory bowel disease. *Curr Opin Immunol* 1999; **11**: 648-656

11 **Kosiewicz MM**, Nast CC, Krishnan A, Rivera-Nieves J, Moskaluk CA, Matsumoto S, Kozaiwa K, Cominelli F. Th1-type responses mediate spontaneous ileitis in a novel murine model of Crohn's disease. *J Clin Invest* 2001; **107**: 695-702

12 **Wirtz S**, Neurath MF. Animal models of intestinsl inflammation: new insight into the molecular pathogenesis and immunotherapy of inflammatory bowel disease. *Int J Colorectal Dis* 2000; **15**: 144-160

13 **Mckay DM**. Intestinal inflammation and the gut microflora. *Can J Gastroenterol* 1999; **13**: 509-516

14 **Shanahan F**. Probiotics and inflammatory bowel disease: is there a scientific rationale? *Inflamm Bowel Dis* 2000; **6**: 107-115

15 **Masseret E**, Boudeau J, Colombel JF, Neut C, Desreumaux P, Joly B, Cortot A, Darfeuille-Michaud A. Genetically related Escherichia coli strains associated with Crohn's disease. *Gut* 2001; **48**: 320-325

16 **Sutton CL,** Kim J, Yamane A, Dalwadi H, Wei B, Landers C, Targan SR, Braun J. Identification of a novel bacterial sequence associated with Crohn's disease. *Gastroenterology* 2000; **119**: 23-31

17 **Cosnes J,** Beaugerie L, Carbonnel F, Gendre JP. Smoking cessation and the course of Crohn's disease: an intervention study. *Gastroenterology* 2001; **120**: 1093-1099

18 **Tysk C,** Jarnerot G. Has smoking changed the epidemiology of ulcerative colitis? *Scand J Gastroenterol* 1992; **27**: 508-512

19 **Feehally J,** Burden AC, Mayberry JF, Probert CS, Roshan M, Samanta AK, Woods KL. Disease variations in Asians in Leicester. *Q J Med* 1993; **86**: 263-269

20 **Jayanthi V**, Probert CS, Pollock DJ, Baithun SI, Rampton DS, Mayberry JF. Low incidence of ulcerative colitis and proctitis in Bangladeshi migrants in Britain. *Digestion* 1992; **52**: 34-42

21 **Lander ES**, Schork NJ. Genetic dissection of complex traits. *Science* 1994; **265**: 2037-2048

22 **Karban A,** Eliakim R, Brant SR. Genetics of inflammatory bowel disease. *Isr Med Assoc J* 2002; **4**: 798-802

23 **Laharie D,** Debeugny S, Peeters M, Van Gossum A, Gower-Rousseau C, Belaiche J, Fiasse R, Dupas JL, Lerebours E, Piotte S, Cortot A, Vermeire S, Grandbastien B, Colombel JF. Inflammatory bowel disease in spouses and their offspring. *Gastroenterology* 2001; **120**: 816-819

24 **Orholm M**, Iselius L, Sorensen TI, Munkholm P, Langholz E, Binder V. Investigation of inheritance of chronic inflammatory bowel disease by complex segregation analysis. *BMJ* 1993; **306**: 20-24

25 **Kuster w**, Pascoe L, Purrmann J, Funk S, Majewski F, Pascoe L, Purrmann J. The genetics of Crohn disease: complex segregation analysis of a family study with 265 patients with Crohn disease and 5,387 relatives. *Am J Med Genet* 1989; **32**: 105-108

26 **Hugot JP**, Laurent-Puig P, Gower-Rousseau C, Olson JM, Lee JC, Beaugerie L, Naom I, Dupas JL, Van Gossum A, Orholm M, Bonaiti-Pellie C, Weissenbach J, Mathew CG, Lennard-Jones JE, Cortot A, Colombel JF, Thomas G. Mapping of a susceptibility locus for Crohn's disease on chromosome 16. *Nature* 1996; **379**: 821-823

27 **Satsangi J**, Parkes M, Louis E, Hashimoto L, Kato N, Welsh K, Terwilliger JD, Lathrop GM, Bell JI, Jewell DP. Two-stage genome-wide search in inflammatory bowel disease provides evidence for susceptibility loci on chromosomes 3, 7 and 12. *Nat Genet* 1996; **14**: 199-202

28 **Cho JH**, Nicolae DL, Gold LH, Fields CT, LaBuda MC, Rohal PM, Pickles MR, Qin L, Fu Y, Mann JS, Kirschner BS, Jabs EW, Weber J, Hanauer SB, Bayless TM, Brant SR. Identification of novel susceptibility loci for inflammatory bowel disease on chromosomes 1p, 3q, and 4q: evidence for epistasis between 1p and inflammatory bowel disease1. *Proc Natl Acad Sci U S A* 1998; **95**: 7502-7507

29 **Ma Y,** Ohmen JD, Li Z, Bentley LG, McElree C, Pressman S, Targan SR, Fischel-Ghodsian N, Rotter JI, Yang H. A genome-wide search identifies potential new susceptibility loci for Crohn's disease. *Inflamm Bowel Dis* 1999; **5**: 271-278

30 **Hampe J**, Schreiber S, Shaw SH, Lau KF, Bridger S, Macpherson AJ, Cardon LR, Sakul H, Harris TJ, Buckler A, Hall J, Stokkers P, van Deventer SJ, Nurnberg P, Mirza MM, Lee JC, Lennard-Jones JE, Mathew CG, Curran ME. A genomewide analysis provides evidence for novel linkages in inflammatory bowel disease in a large European cohort. *Am J Hum Genet* 1999; **64**: 808-816

31 **Duerr RH**, Barmada MM, Zhang L, Pfutzer R, Weeks DE. High-density genome scan in Crohn disease shows confirmed linkage to chromosome 14q11-12. *Am J Hum Genet* 2000; **66**: 1857-1862

32 **Rioux JD**, Silverberg MS, Daly MJ, Steinhart AH, McLeod RS, Griffiths AM, Green T, Brettin TS, Stone V, Bull SB, Bitton A, Williams CN, Greenberg GR, Cohen Z, Lander ES, Hudson TJ, Siminovitch KA. Genomewide search in Canadian families with inflammatory bowel disease reveals two novel susceptibility loci. *Am J Hum Genet* 2000; **66**: 1863-1870

33 **Fisher SA**, Hampe J, Macpherson AJ, Forbes A, Lennard-Jones JE, Schreiber S, Curran ME, Mathew CG, Lewis CM. Sex stratification of an inflammatory bowel disease genome search shows Male-specific linkage to the HLA region of chromosome 6. *Eur J Hum Genet* 2002; **10**: 259-265

34 **Brant SR,** Fu Y, Fields CT, Baltazar R, Ravenhill G, Pickles MR, Rohal PM, Mann J, Kirschner BS, Jabs EW, Bayless TM, Hanauer SB, Cho JH. American families with Crohn's disease have strong evidence for linkage to chromosome 16 but not chromosome 12. *Gastroenterology* 1998; **115**: 1056-1061

35 **Rioux JD**, Daly MJ, Green T, Stone V, Lander ES, Hudson TJ, Steinhart AH, Bull S, Cohen Z, Greenberg G, Griffiths A, McLeod R, Silverberg M, Williams CN, Siminovitch KA. Absence of linkage between inflammatory bowel disease and selected loci on chromosomes 3, 7, 12, and 16. *Gastroenterology* 1998; **115**: 1062-1065

36 **Curran ME**, Lau KF, Hampe J, Schreiber S, Bridger S, Macpherson AJ, Cardon LR, Sakul H, Harris TJ, Stokkers P, Van Deventer SJ, Mirza M, Raedler A, Kruis W, Meckler U, Theuer D, Herrmann T, Gionchetti P, Lee J, Mathew C, Lennard-Jones J. Genetic analysis of inflammatory bowel disease in a large European cohort supports linkage to chromosomes 12 and 16. *Gastroenterology* 1998; **115**: 1066-1071

37 **Annese V**, Latiano A, Bovio P, Forabosco P, Piepoli A, Lombardi G, Andreoli A, Astegiano M, Gionchetti P, Riegler G, Sturniolo GC, Clementi M, Rappaport E, Fortina P, Devoto M, Gasparini P, Andriulli A. Genetic analysis in Italian families with inflammatory bowel disease supports linkage to the IBD1 locus-a GISC study. *Eur J Hum Genet* 1999; **7**: 567-573

38 **Vermeire S**, Peeters M, Vlietinck R, Parkes M, Satsangi J, Jewell D, Rutgeerts P. Exclusion of linkage of Crohn's disease to previously reported regions on chromosomes 12, 7, and 3 in the Belgian population indicates genetic heterogeneity. *In Flamm Bowel Dis* 2000; **6**: 165-170

39 **Dechairo B**, Dimon C, van Heel D, Mackay I, Edwards M, Scambler P, Jewell D, Cardon L, Lench N, Carey A. Replication and extension studies of inflammatory bowel disease susceptibility regions confirm linkage to chromosome 6p (inflammatory bowel disease3). *Eur J Hum Genet* 2001; **9**: 627-633

40 **Paavola P,** Helio T, Kiuru M, Halme L, Turunen U, Terwilliger J, Karvonen AL, Julkunen R, Niemela S, Nurmi H, Farkkila M, Kontula K. Genetic analysis in Finnish families with inflammatory bowel disease supports linkage to chromosome 3p21.*Eur J Hum Genet* 2001; **9**: 328-334

41 **Cavanaugh J**. The IBD International Genetics Consortium. International collaboration provides convincing linkage replication in complex disease through analysis of a large pooled data set: Crohn disease and chromosome 16. *Am J Hum Genet* 2001; **68**: 1165-1171

42 **Ohmen JD**, Yang HY, Yamamoto KK, Zhao HY, Ma Y, Bentley LG, Huang Z, Gerwehr S, Pressman S, McElree C, Targan S, Rotter JI, Fischel-Ghodsian N. Susceptibility locus for inflammatory bowel disease on chromosome 16 has a role in Crohn's disease, but not in ulcerative colitis. *Hum Mol Genet* 1996; **5**: 1679-1683

43 **Parkes M,** Satsangi J, Lathrop GM, Bell JI, Jewell DP. Susceptibility loci in inflammatory bowel disease. *Lancet* 1996; **348**: 1588

44 **Cavanaugh JA**, Callen DF, Wilson SR, Stanford PM, Sraml ME, Gorska M, Crawford J, Whitmore SA, Shlegel C, Foote S, Kohonen-Corish M, Pavli P. Analysis of Australian Crohn's disease pedigrees refines the localization for susceptibility to inflammatory bowel disease on chromosome 16. *Ann Hum Genet* 1998; **62**: 291-298

45 **Mirza MM**, Lee J, Teare D, Hugot JP, Laurent-Puig P, Colombel JF, Hodgson SV, Thomas G, Easton DF, Lennard-Jones JE, Mathew CG. Evidence of linkage of the inflammatory bowel disease susceptibility locus on chromosome 16 (IBD1) to ulcerative colitis. *J Med Genet* 1998; **35**: 218-221

46 **Forabosco P**, Collins A, Latiano A, Annese V, Clementi M, Andriulli A, Fortina P, Devoto M, Morton NE. Combined segregation and linkage analysis of inflammatory bowel disease in the IBD1 region using severity to characterise Crohn's disease and ulcerative colitis. On behalf of the GISC. *Eur J Hum Genet* 2000; **8**: 846-852

47 **Brant SR**, Panhuysen CI, Bailey-Wilson JE, Rohal PM, Lee S, Mann J, Ravenhill G, Kirschner BS, Hanauer SB, Cho JH, Bayless TM. Linkage heterogeneity for the IBD1 locus in Crohn's disease pedigrees by disease onset and severity. *Gastroenterology* 2000; **119**: 1483-1490

48 **Akolkar PN,** Gulwani-Akolkar B, Lin XY, Zhou Z, Daly M, Katz S, Levine J, Present D, Gelb B, Desnick R, Mayer L, Silver J. The IBD1 locus for susceptibility to Crohn's disease has a greater impact in Ashkenazi Jews with early onset disease. *Am J Gastroenterol* 2001; **96**: 1127-1132

49 **Van Heel DA,** McGovern DP, Cardon LR, Dechairo BM, Lench NJ, Carey AH, Jewell DP. Fine mapping of the IBD1 locus did not identify Crohn disease-associated NOD2 variants: Implications for complex disease genetics. *Am J Med Genet* 2002; **111**: 253-259

50 **Zouali H**, Chamaillard M, Lesage S, Cezard JP, Colombel JF, Belaiche J, Almer S, Tysk C, Montague S, Gassull M, Christensen S, Finkel Y, Gower-Rousseau C, Modigliani R, Macry J, Selinger-Leneman H, Thomas G, Hugot JP. Genetic refinement and physical mapping of a chromosome 16q candidate region for inflammatory bowel disease. *Eur J Hum Genet* 2001; **9**: 731-742

51 **Hampe J**, Frenzel H, Mirza MM, Croucher PJ, Cuthbert A, Mascheretti S, Huse K, Platzer M, Bridger S, Meyer B, Nurnberg P, Stokkers P, Krawczak M, Mathew CG, Curran M, Schreiber S. Evidence for a NOD2-independent susceptibility locus for inflammatory bowel disease on chromosome 16p. *Proc Natl Acad Sci U S A* 2002; **99**: 321-326

52 **Satsangi J,** Welsh KI, Bunce M, Julier C, Farrant JM, Bell JI, Jewell DP. Contribution of genes of the major histocompatibility complex to susceptibility and disease phenotype in inflammatory bowel disease. *Lancet* 1996; **347**: 1212-1217

53 **Silverberg MS**. Evidence for linkage between Crohn disease and a locus near the major histocompatibility complex on chromosome 6 in a Canadian inflammatory bowel disease population. *Gastroenterology* 1999; **116**: A.820

54 **Hampe J,** Shaw SH, Saiz R, Leysens N, Lantermann A, Mascheretti S, Lynch NJ, MacPherson AJ, Bridger S, van Deventer S, Stokkers P, Morin P, Mirza MM, Forbes A, Lennard-Jones JE, Mathew CG, Curran ME, Schreiber S. Linkage of inflammatory bowel disease to human chromosome 6p. *Am J Hum Genet* 1999; **65**: 1647-1655

55 **Yang H,** Plevy SE, Taylor K, Tyan D, Fischel-Ghodsian N, McElree C, Targan SR, Rotter JI. Linkage of Crohn's disease to the major histocompatibility complex region is detected by multiple non-parametric analyses. *Gut* 1999; **44**: 519-526

56 **Duerr RH**, Barmada MM, Zhang L, Davis S, Preston RA, Chensny LJ, Brown JL, Ehrlich GD, Weeks DE, Aston CE. Linkage and association between inflammatory bowel disease and a locus on chromosome 12. *Am J Hum Genet* 1998; **63**: 95-100

57 **Yang H**, Ohmen JD, Ma Y, Bentley LG, Targan SR, Fischel-Ghodsian N, Rotter JI. Additional evidence of linkage between Crohn's disease and a putative locus on chromosome 12. *Genet Med* 1999; **1**: 194-198

58 **Lesage S**, Zouali H, Colombel JF, Belaiche J, Cezard JP, Tysk C, Almer S, Gassull M, Binder V, Chamaillard M, Le Gall I, Thomas G, Hugot JP. Genetic analyses of chromosome 12 loci in Crohn's disease. *Gut* 2000; **47**: 787-791

59 **Parkes M**, Barmada MM, Satsangi J, Weeks DE, Jewell DP, Duerr RH. The IBD2 locus shows linkage heterogeneity between ulcerative colitis and Crohn disease. *Am J Hum Genet* 2000; **67**: 1605-1610

60 **Hampe J,** Lynch NJ, Daniels S, Bridger S, Macpherson AJ, Stokkers P, Forbes A, Lennard-Jones JE, Mathew CG, Curran ME, Schreiber S. Fine mapping of the chromosome 3p susceptibility locus in inflammatory bowel disease. *Gut* 2001; **48**: 191-197

61 **Duerr RH,** Barmada MM, Zhang L. Evidence for an inflammatory bowel disease locus on chromosome 3p26: linkage, transmission / disequilibrium and partitioning of linkage. *Hum Mol Genet* 2002; **11**: 2599-2606

62 **Rioux JD**, Daly MJ, Silverberg MS, Lindblad K, Steinhart H, Cohen Z, Delmonte T, Kocher K, Miller K, Guschwan S, Kulbokas EJ, O'Leary S, Winchester E, Dewar K, Green T, Stone V, Chow C, Cohen A, Langelier D, Lapointe G, Gaudet D, Faith J, Branco N, Bull SB, McLeod RS, Griffiths AM, Bitton A, Greenberg GR, Lander ES, Siminovitch KA, Hudson TJ. Genetic variation in the 5q31 cytokine gene cluster confers susceptibility to Crohn disease. *Nat Genet* 2001; **29**: 223-228

63 **Vermeire S**, Satsangi J, Peeters M, Parkes M, Jewell DP, Vlietinck R, Rutgeerts P. Evidence for inflammatory bowel disease of a susceptibility locus on the X chromosome. *Gastroenterology* 2001; **120**: 834-840

64 **Dib C,** Faure S, Fizames C, Samson D, Drouot N, Vignal A, Millasseau P, Marc S, Hazan J, Seboun E, Lathrop M, Gyapay G, Morissette J, Weissenbach J. A comprehensive genetic map of the human genome based on 5,264 microsatellites. *Nature* 1996; **380**: 152-154

65 **Hugot JP**, Chamaillard M, Zouali H, Lesage S, Cezard JP, Belaiche J, Almer S, Tysk C, O'Morain CA, Gassull M, Binder V, Finkel Y, Cortot A, Modigliani R, Laurent-Puig P, Gower-Rousseau C, Macry J, Colombel JF, Sahbatou M, Thomas G. Association of NOD2 leucine-rich repeat variants with susceptibility to Crohn's disease. *Nature* 2001; **411**: 599-603

66 **Ogura Y**, Bonen DK, Inohara N, Nicolae DL, Chen FF, Ramos R, Britton H, Moran T, Karaliuskas R, Duerr RH, Achkar JP, Brant SR, Bayless TM, Kirschner BS, Hanauer SB, Nunez G, Cho JH. A frameshift mutation in NOD2 associated with susceptibility to Crohn's disease. *Nature* 2001; **411**: 603-606

67 **Hampe J**, Cuthbert A, Croucher PJ, Mirza MM, Mascheretti S, Fisher S,Frenzel H, King K, Hasselmeyer A, MacPherson AJ, Bridger S, van Deventer S, Forbes A, Nikolaus S, Lennard-Jones JE, Foelsch UR, Krawczak M, Lewis C, Schreiber S, Mathew CG. Association between insertion mutation in NOD2 gene and Crohn's disease in German and British populations. *Lancet* 2001; **357**: 1902-1904

68 **Lesage S**, Zouali H, Cezard JP, Colombel JF, Belaiche J, Almer S, Tysk C, O'Morain C, Gassull M, Binder V, Finkel Y, Modigliani R, Gower-Rousseau C, Macry J, Merlin F, Chamaillard M, Jannot AS, Thomas G, Hugot JP. EPWG-IBD Group; EPIMAD Group; GETAID Group. CARD15/NOD2 mutational analysis and genotype-phenotype correlation in 612 patients with inflammatory bowel disease. *Am J Hum Genet* 2002; **70**: 845-857

69 **Cuthbert AP,** Fisher SA, Mirza MM, King K, Hampe J, Croucher PJ, Mascheretti S, Sanderson J, Forbes A, Mansfield J, Schreiber S, Lewis CM, Mathew CG. The contribution of NOD2 gene mutations to the risk and site of disease in inflammatory bowel disease. *Gastroenterology* 2002; **122**: 867-874

70 **Murillo L,** Crusius JB, van Bodegraven AA, Alizadeh BZ, Pena AS. CARD15 gene and the classification of Crohn's disease. *Immunogenetics* 2002; **54**: 59-61

71 **Hampe J,** Grebe J, Nikolaus S, Solberg C, Croucher PJ, Mascheretti S, Jahnsen J, Moum B, Klump B, Krawczak M, Mirza MM, Foelsch UR, Vatn M, Schreiber S. Association of NOD2 (CARD 15) genotype with clinical course of Crohn's disease: a cohort study. *Lancet* 2002; **359**: 1661-1665

72 **Vermeire S,** Wild G, Kocher K, Cousineau J, Dufresne L, Bitton A, Langelier D, Pare P, Lapointe G, Cohen A, Daly MJ, Rioux JD. CARD15 genetic variation in a Quebec population: prevalence, genotype-phenotype relationship, and haplotype structure. *Am J Hum Genet* 2002; **71**: 74-83

73 **Radlmayr M,** Torok HP, Martin K, Folwaczny C. The c-insertion mutation of the NOD2 gene is associated with fistulizing and fibrostenotic phenotypes in Crohn's disease. *Gastroenterology* 2002; **122**: 2091-2092

74 **Inoue N**, Tamura K, Kinouchi Y, Fukuda Y, Takahashi S, Ogura Y, Inohara N, Nunez G, Kishi Y, Koike Y, Shimosegawa T, Shimoyama T, Hibi T. Lack of common NOD2 variants in Japanese patients with Crohn's disease. *Gastroenterology* 2002; **123**: 86-91

75 **Vermeire S**, Louis E, Rutgeerts P, De Vos M, Van Gossum A, Belaiche J, Pescatore P, Fiasse R, Pelckmans P, Vlietinck R, Merlin F, Zouali H, Thomas G, Colombel JF, Hugot JP. Belgian Group of Infliximab Expanded Access Program and Fondation Jean Dausset CEPH, Paris, France. NOD2/CARD15 does not influence response to infliximab in Crohn's disease. *Gastroenterology* 2002; **123**: 106-111

76 **Abreu MT,** Taylor KD, Lin YC, Hang T, Gaiennie J, Landers CJ, Vasiliauskas EA, Kam LY, Rojany M, Papadakis KA, Rotter JI, Targan SR, Yang H. Mutations in NOD2 are associated with fibrostenosing disease in patients with Crohn's disease. *Gastroenterology* 2002; **123**: 679-688

77 **Ahmad T,** Armuzzi A, Bunce M, Mulcahy-Hawes K, Marshall SE, Orchard TR,Crawshaw J, Large O, de Silva A, Cook JT, Barnardo M, Cullen S, Welsh KI, Jewell DP. The molecular classification of the clinical manifestations of Crohn's disease. *Gastroenterology* 2002; **122**: 854-866

78 **Inohara N**, Koseki T, del Peso L, Hu Y, Yee C, Chen S, Carrio R, Merino J, Liu D, Ni J, Nunez G. Nod1, an Apaf-1-like activator of caspase-9 and nuclear factor-kappaB. *J Biol Chem* 1999; **274**: 14560-14567

79 **Ogura Y,** Inohara N, Benito A, Chen FF, Yamaoka S, Nunez G. Nod2, a Nod1/Apaf-1 family member that is restricted to monocytes and activates NF-Kb. *J Bio Chem* 2001; **276**: 4812-4818

80 **Inohara N**, Ogura Y, Chen FF, Muto A, Nunez G. Hunan Nod1 confers responsiveness to bacterial lipopolysaccharides. *J Bio Chem* 2001; **276**: 2551-2554

81 **Schreiber S**, Nikolaus S, Hampe J. Activation of nuclear factor kappa B in inflammatory bowel disease. *Gut* 1998; **42**: 477-484

82 **Zareie M,** Singh PK, Irvine EJ, Sherman PM, McKay DM, Perdue MH. Monocyte/macrophage activation by normal bacteria and bacterial products: implications for altered epithelial function in Crohn's disease. *Am J Pathol* 2001; **158**: 1101-1109

83 **Duerr RH**, Neigut DA. Molecularly defined HLA-DR2 alleles in ulcerative colitis and an antineutrophil cytoplasmic antibody-positive subgroup. *Gastroenterology* 1995; **108**: 423-427

84 **Nakajima A,** Matsuhashi N, Kodama T, Yazaki Y, Takazoe M, Kimura A. HLA-linked susceptibility and resistance genes in Crohn's disease. *Gastroenterology* 1995; **109**: 1462-1467

85 **Reinshagen M,** Loeliger C, Kuehnl P, Weiss U, Manfras BJ, Adler G, Boehm BO. HLA class II gene frequencies in Crohn's disease: a population based analysis in Germany. *Gut* 1996; **38**: 538-542

86 **Hesresbach D**, Alizadeh M, Bretagne JF, Gautier A, Quillivic F, Lemarchand B, Gosselin M, Genetet B, Semana G. Investigation of the association of major histocompatibility complex genes, including HLA class I, class II and TAP genes, with clinical forms of Crohn's disease. *Eur J Immunogenet* 1996; **23**: 141-151

87 **Danze PM,** Colombel JF, Jacquot S, Loste MN, Heresbach D, Ategbo S, Khamassi S, Perichon B, Semana G, Charron D, Cezard JP. Association of HLA class II genes with susceptibility to Crohn's disease. *Gut* 1996; **39**: 69-72

88 **Heresbach D,** Alizadeh M, Reumaux D, Colombel JF, Delamaire M, Danze PM, Gosselin M, Genetet B, Bretagne JF, Semana G. Are HLA-DR or TAP genes genetic markers of severity in ulcerative colitis? *J Autoimmun* 1996; **9**: 777-784

89 **Bouma G,** Oudkerk Pool M, Crusius JB, Schreuder GM, Hellemans HP, Meijer BU, Kostense PJ, Giphart MJ, Meuwissen SG, Pena AS. Evidence for genetic heterogeneity in inflammatory bowel disease (IBD); HLA genes in the predisposition to suffer from ulcerative colitis (UC) and Crohn's disease (CD). *Clin Exp Immunol* 1997; **109**: 175-179

90 **Fernandez Arquero M**, Lopez Nava G, De la Concha EG, Figueredo MA, Santa Cruz S, Dumitru CG, Diaz Rubio M, Garcia Paredes J. HLA-DR2 gene and Spanish patients with ulcerative colitis. *Rev Esp Enferm Dig* 1998; **90**: 243-249

91 **Cariappa A,** Sands B, Forcione D, Finkelstein D, Podolsky DK, Pillai S. Analysis of MHC class II DP, DQ and DR alleles in Crohn's disease. *Gut* 1998; **43**: 210-215

92 **Bouma G**, Crusius JB, Garcia-Gonzalez MA, Meijer BU, Hellemans HP, Hakvoort RJ, Schreuder GM, Kostense PJ, Meuwissen SG, Pena AS. Genetic markers in clinically well defined patients with ulcerative colitis (UC). *Clin Exp Immunol* 1999; **115**: 294-300

93 **Yoshitake S,** Kimura A, Okada M, Yao T, Sasazuki T. HLA class II alleles in Japanese patients with inflammatory bowel disease. *Tissue Antigens* 1999; **53**: 350-358

94 **Stokkers PC,** Reitsma PH, Tytgat GN, van Deventer SJ. HLA-DR and -DQ phenotypes in inflammatory bowel disease: a meta-analysis. *Gut* 1999; **45**: 395-401

95 **Hirv K,** Seyfarth M, Uibo R, Kull K, Salupere R, Latza U, Rink L. Polymorphisms in tumor necrosis factor and adhesion molecule genes in patients with inflammatory bowel disease: associations with HLA-DR and -DQ alleles and subclinical markers. *Scand J Gastroenterol* 1999; **34**: 1025-1032

96 **Seki SS,** Sugimura K, Ota M, Matsuzawa J, Katsuyama Y, Ishizuka K, Mochizuki T, Suzuki K, Yoneyama O, Mizuki N, Honma T, Inoko H, Asakura H. Stratification analysis of MICA

triplet repeat polymorphisms and HLA antigens associated with ulcerative colitis in Japanese. *Tissue Antigens* 2001; **58**: 71-76

97 **Lantermann A**, Hampe J, Kim WH, Winter TA, Kidd M, Nagy M, Folsch UR, Schreiber S. Investigation of HLA-DPA1 genotypes as predictors of inflammatory bowel disease in the German, South African, and South Korean populations. *Int J Colorectal Dis* 2002; **17**: 238-244

98 **Orchard TR**, Chua CN, Ahmad T, Cheng H, Welsh KI, Jewell DP. Uveitis and erythema nodosum in inflammatory bowel disease: clinical features and the role of HLA genes. *Gastroenterology* 2002; **123**: 714-718

99 **Peng Z,** Hu P, Cui Y, Li C. Interleukin (IL)-1beta, IL-1 receptor antagonist and IL-4 gene polymorphisms in ulcerative colitis in the Chinese. *Zhonghua Neike Zazhi* 2002; **41**: 248-251

100 **Craggs A**, West S, Curtis A, Welfare M, Hudson M, Donaldson P, Mansfield J. Absence of a genetic association between IL-1RN and IL-1B gene polymorphisms in ulcerative colitis and Crohn disease in multiple populations from northeast England. *Scand J Gastroenterol* 2001; **36**: 1173-1178

101 **Donaldson PT**, Norris S, Constantini PK, Bernal W, Harrison P, Williams R. The interleukin-1 and interleukin-10 gene polymorphisms in primary sclerosing cholangitis: no associations with disease susceptibility / resistance. *J Hepatol* 2000; **32**: 882-886

102 **Nemetz A**, Toth M, Garcia-Gonzalez MA, Zagoni T, Feher J, Pena AS, Tulassay Z. Allelic variation at the interleukin 1beta gene is associated with decreased bone mass in patients with inflammatory bowel diseases. *Gut* 2001; **49**: 644-649

103 **Nemetz A**, Nosti-Escanilla MP, Molnar T, Kope A, Kovacs A, Feher J, Tulassay Z, Nagy F, Garcia-Gonzalez MA, Pena AS. IL1B gene polymorphisms influence the course and severity of inflammatory bowel disease. *Immunogenetics* 1999; **49**: 527-531

104 **Mwantembe O,** Gaillard MC, Barkhuizen M, Pillay V, Berry SD, Dewar JB, Song E. Ethnic differences in allelic associations of the interleukin-1 gene cluster in South African patients with inflammatory bowel disease (IBD) and in control individuals. *Immunogenetics* 2001; **52**: 249-254

105 **van Heel DA**, Udalova IA, De Silva AP, McGovern DP, Kinouchi Y, Hull J, Lench NJ, Cardon LR, Carey AH, Jewell DP, Kwiatkowski D. Inflammatory bowel disease is associated with a TNF polymorphism that affects an interaction between the OCT1 and NF-kappa B transcription factors. *Hum Mol Genet* 2002; **11**: 1281-1289

106 **Sashio H,** Tamura K, Ito R, Yamamoto Y, Bamba H, Kosaka T, Fukui S, Sawada K, Fukuda Y, Tamura K, Satomi M, Shimoyama T, Furuyama J. Polymorphisms of the TNF gene and the TNF receptor superfamily member 1B gene are associated with susceptibility to ulcerative colitis and Crohn's disease, respectively. *Immunogenetics* 2002; **53**: 1020-1027

107 **Mitchell SA,** Grove J, Spurkland A, Boberg KM, Fleming KA, Day CP, Schrumpf E, Chapman RW. European Study Group of Primary Sclerosing Cholangitis. Association of the tumor necrosis factor alpha -308 but not the interleukin 10 -627 promoter polymorphism with genetic susceptibility to primary sclerosing cholangitis. *Gut* 2001; **49**: 288-294

108 **Koss K,** Satsangi J, Welsh KI, Jewell DP. Cytokine (TNF alpha, LT alpha and IL-10) polymorphisms in inflammatory bowel diseases and normal controls: differential effects on production and allele frequencies. *Genes Immun* 2000; **1**: 185-190

109 **Louis E,** Peeters M, Franchimont D, Seidel L, Fontaine F, Demolin G, Croes F, Dupont P, Davin L, Omri S, Rutgeerts P, Belaiche J. Tumour necrosis factor (TNF) gene polymorphism in Crohn's disease (CD): influence on disease behaviour? *Clin Exp Immunol* 2000; **119**: 64-68

110 **Negoro K,** Kinouchi Y, Hiwatashi N, Takahashi S, Takagi S, Satoh J, Shimosegawa T, Toyota T. Crohn'disease is associated with novel polymorphisms in the 5'-flanking region of the tumor necrosis factor gene. *Gastroenterology* 1999; **117**: 1062-1068

111 **Klein W,** Tromm A, Griga T, Fricke H, Folwaczny C, Hocke M, Eitner K, Marx M, Duerig N, Epplen JT. Interleukin-4 and interleukin-4 receptor gene polymorphisms in inflammatory bowel diseases. *Genes Immun* 2001; **2**: 287-289

112 **Aithal GP,** Day CP, Leathart J, Daly AK, Hudson M. Association of single nucleotide polymorphisms in the interleukin-4 gene and interleukin-4 receptor gene with Crohn's disease in a British population. *Genes Immun* 2001; **2**: 44-47

113 **Aithal GP**, Craggs A, Day CP, Welfare M, Daly AK, Mansfield JC, Hudson M. Role of polymorphisms in the interleukin-10 gene in determining disease susceptibility and phenotype in inflammatory bowel disease. *Dig Dis Sci* 2001; **46**: 1520-1525

114 **Klein W,** Tromm A, Griga T, Fricke H, Folwaczny C, Hocke M, Eitner K, Marx M, Runte M, Epplen JT. The IL-10 gene is not involved in the predisposition to inflammatory bowel disease. *Electrophoresis* 2000; **21**: 3578-3582

115 **Yang H**. Analysis of ICAM-1 gene polymorphism in immunologic subsets of inflammatory bowel disease. *Exp Clin Immunogenet* 1997; **14**: 214-225

116 **Yang H,** Vora DK, Targan SR, Toyoda H, Beaudet AL, Rotter JI. Intercellular adhesion molecule 1 gene associations with immunologic subsets of inflammatory bowel disease. *Gastroenterology* 1995; **109**: 440-448

117 **Braun C,** Zahn R, Martin K, Albert E, Folwaczny C. Polymorphisms of the ICAM-1 gene are associated with inflammatory bowel disease, regardless of the p-ANCA status. *Clin Immunol* 2001; **101**: 357-360

118 **Klein W,** Tromm A, Griga T, Fricke H, Folwaczny C, Hocke M, Eitner K, Marx M, Epplen JT. The polymorphism at position -174 of the IL-6 gene is not associated with inflammatory bowel disease. *Eur J Gastroenterol Hepatol* 2001; **13**: 45-47

119 **Koss K**, Satsangi J, Welsh KI, Jewell DP. Is interleukin-6 important in inflammatory bowel disease? *Genes Immun* 2000; **1**: 207-212

120 **Stokkers PC,** de Heer K, Leegwater AC, Reitsma PH, Tytgat GN, van Deventer SJ. Inflammatory bowel disease and the genes for the natural resistance-associated macrophage protein-1 and the interferon-gamma receptor 1. *Int J Colorectal Dis* 1999; **14**: 13-17

121 **Hampe J,** Hermann B, Bridger S, MacPherson AJ, Mathew CG, Schreiber S. The interferon-gamma gene as a positional and functional candidate gene for inflammatory bowel disease. *Int J Colorectal Dis* 1998; **13**: 260-263

122 **Xia B,** Crusius JBA, Meuwissen SGM, Pea AS. Inflammatory bowel disease: definition, epidemiology, etiologic aspects, and immunogenetic studies. *World J Gastroenterol* 1998; **4**: 446-458

123 **Silverberg MS,** Daly MJ, Moskovitz DN, Rioux JD, McLeod RS, Cohen Z, Greenberg GR, Hudson TJ, Siminovitch KA, Steinhart AH. Diagnostic misclassification reduces the ability to detect linkage in inflammatory bowel disease genetic studies. *Gut* 2001; **49**: 773-776

124 **Ghosh S**. Linking genotype with phenotype in inflammatory bowel disease-Will we ever have reagent standard patients? *Dis Markers* 2000; **16**: 167-171

125 **Hampe J**, Wienker T, Nurnberg P, Schreiber S. Mapping genes for polygenic disorders: consideration for study design in the complex trait of inflammatory bowel disease. *Hum Hered* 2000; **50**: 91-101

126 **Schreiber S**. Genetics of inflammayory bowel disease: a puzzle with contradictions? *Gut* 2000; **47**: 746–747

127 **Petronis A**, Petroniene R. Epigenetics of inflammatory bowel disease. *Gut* 2000; **47**: 302-306

Edited by Yuan HJ and Wang XL

P.O.Box 2345, Beijing 100023,China
Fax: +86-10-85381893
E-mail: wjg@wjgnet.com www.wjgnet.com

World J Gastroenterol 2003;9(8):1657-1661
World Journal of Gastroenterology
 ISSN 1007-9327

• REVIEW •

RNA interference: Antiviral weapon and beyond

Quan-Chu Wang, Qing-He Nie, Zhi-Hua Feng

Quan-Chu Wang, Qing-He Nie, Zhi-Hua Feng, The Center of Diagnosis and Treatment for Infectious Diseases of Chinese PLA, Tangdu Hospital, Fourth Military Medical University, Xi' an 710038, Shaanxi Province, China
Correspondence to: Qing-He Nie, The Center of Diagnosis and Treatment for Infectious Diseases of Chinese PLA, Tangdu Hospital, Fourth Military Medical University, Xi' an 710038, Shaanxi Province, China. nieqinghe@hotmail.com
Telephone: +86-29-3377452 **Fax:** +86-29-3377452
Received: 2003-04-04 **Accepted:** 2003-05-11

Abstract

RNA interference (RNAi) is a remarkable type of gene regulation based on sequence-specific targeting and degradation of RNA. The term encompasses related pathways found in a broad range of eukaryotic organisms, including fungi, plants, and animals. RNA interference is part of a sophisticated network of interconnected pathways for cellular defense, RNA surveillance, and development and it may become a powerful tool to manipulate gene expression experimentally. RNAi technology is currently being evaluated not only as an extremely powerful instrument for functional genomic analyses, but also as a potentially useful method to develop specific dsRNA based gene-silencing therapeutics. Several laboratories have been interested in using RNAi to control viral infection and many reports in *Nature* and in *Cell* show that short interfering (si) RNAs can inhibit infection by HIV-1, polio and hepatitis C viruses in a sequence-specific manner. RNA-based strategies for gene inhibition in mammalian cells have recently been described, which offer the promise of antiviral therapy.

Wang QC, Nie QH, Feng ZH. RNA interference: Antiviral weapon and beyond. *World J Gastroenterol* 2003; 9(8): 1657-1661
http://www.wjgnet.com/1007-9327/9/1657.asp

INTRODUCTION

RNA, long upstaged by its more glamorous sibling, DNA, is turning out to have star qualities of its own. *Science* hails the electrifying discoveries of RNA interference as 2002's breakthrough of the year. RNA interference, also named RNA silencing or post transcriptional gene silencing (PTGS), is a phenomenon in which small double-stranded RNA molecules induce sequence-specific degradation of homologous single-stranded RNA[1]. RNAi activity plays a role in host-cell protection from viruses and transposons in plants and insects. From a practical perspective, RNAi can therefore be used to target gene expression and has been proved to be a very powerful technique to knock down specific genes to evaluate their physiological roles in *Caenorhabditis elegans*, *Drosophila melanogaster*, and humans[2-5].

Previous reports have show that RNAi has following important characteristics[7-11]. (1) RNAi can be induced through transfection or microinjection of long double-stranded RNA. In plants and invertebrates, the double-stranded RNA is cleaved into 19- to 23-nt RNA fragments known as small interfering RNAs (siRNA). siRNAs are double-stranded RNA (dsRNA) molecules with characteristic 2-nucleotide over hanging 3' ends. They act as intermediates in the RNA interference (RNAi) pathway, which is thought to protect cells from harmful transposons and highly repetitive sequences by targeting their RNA transcripts for endonucleolytic cleavage and subsequent exonucleolytic degradation. siRNA-directed RNA degradation is central to the antiviral response in plants, where it represents a potent form of sequence-based immunity. Only RNA molecules <30 bases in length can be used to exclusively induce RNAi in mammalian cells because longer molecules also activate the nonspecific double-stranded RNA-dependent response. (2) RNAi has amplification activity and different durations. In plants and nematodes, RNAi activity is long-term and disseminates throughout the organism via an uncharacterized amplification mechanism. In mammalian cells, amplification activity seems absent, and interference activity is transient, lasting for only 3-5 days. More recently, DNA expression vectors have been developed to express hairpin or duplex siRNA, which employ the type III class of RNA polymerase promoters to drive the expression of siRNA molecules. In addition, stable cell lines containing siRNA expression plasmids have been produced to induce RNAi over longer durations. (3) RNAi can be induced locally and then spread throughout the organism in plants, and this aspect of the process likely reflects its role in viral defense.

The power of siRNAs springs from the cellular biochemistry of the RNAi pathway. Like antisense oligonucleotides, siRNAs use sequence complementarity to target an mRNA for destruction. Unlike the antisense pathway, the RNAi pathway couples the specificity of an RNA guide to the stability and efficiency of a multiple-turnover protein enzyme. The ability to manipulate RNA interference thus sets the stage for realizing a wide variety of practical applications of biotechnology ranging from molecular farming to possibly even gene therapy in animals. Gitlin *et al*[12] showed that RNAi drastically reduced polio infection in HeLa cells. While analysing the antiviral effects of siRNA over a course of viral infection, they found that siRNA-resistant viruses turned out to carry silent base-pair mismatches in the siRNA complementary sequences. The authors argued, therefore, that if RNAi was to be used for therapeutic reasons, siRNA needed to be designed against highly conserved parts of the viral genome. Adelman et *al*[13] demonstrated that dsRNA-mediated interference also could act as a viral defense mechanism in mosquito cells. These observations are consistent with RNA interference as the mechanism of resistance to DEN-2 in transformed mosquito cells. Kay *et al*[14] went beyond the *in vitro* systems and genetically engineered mice that expressed siRNA against hepatitis C RNA to show that this technique also worked well *in vivo* to prevent viral replication. After this bumper crop of promising results, it remains to be seen how close we are to RNAi-mediated antiviral therapy. Because siRNA taps into natural gene-silencing pathways, a new form of intracellular immunization against viral infection might be just around the corner.

INTERFERING HCV

HCV genome is a single-stranded RNA that functions as both a messenger RNA and a replication template, making it an

attractive target for the study of RNA interference[15-21]. Previous results from Izumi RE' s laboratory[22] identified a small (60 nt) RNA from the yeast S. cerevisiae that specifically inhibited internal ribosome entry site (IRES)-mediated translation programmed by poliovirus (PV) and hepatitis C virus (HCV) 5' -untranslated region (5' UTR). The yeast inhibitor RNA (called RNAi) was found to efficiently compete with viral 5' UTR for binding to several cellular polypeptides that presumably play important roles in IRES-mediated translation. RNA interference offers further hope that a novel approach to silencing troublesome genes will become a valuable disease-fighting tool. But the therapy must leap many hurdles before it can be safely applied to humans. The power of small RNAs to shut down specific gene activities has now been brought to bear on an animal model of hepatitis. Mice infused with a siRNA against a cell death receptor recovered their liver function after experimentally induced injury. The work of Song *et al*[23] suggests that one type of entirely natural nucleic acid, small interfering RNAs (siRNAs), may hold promise as a therapeutic agent even without further engineering. These investigators provided the first *in vivo* evidence that infusion of siRNAs into an animal could alleviate disease, in this case hepatitis. Assembly of a siRNA strand into an RISC seemed to protect it from rapid degradation, the normal fate of small single-stranded RNA in cells. With this durability in mind, Song *et al*. set out to test whether direct infusion of siRNAs into mice might protect them from fulminant hepatitis. Both mice and humans with this disease suffered severe hepatic failure complicated with consequent encephalopathy, cerebral edema, metabolic imbalance and organ collapse. Infusing a solution of siRNA into a mouse' s tail, in massive amount, equivalent to half the animal' s blood volume protected it against hepatitis. And in animals that were already ailing, RNAi shut down the inflammation enough to allow the liver to recover. Despite the traumatic delivery method, the mice didn' t appear to suffer side effects. They gave mice injections of siRNA designed to shut down a gene called Fas, when over-activated during inflammatory response, it induced liver cells to self-destruct. The next day, the animals were given an antibody that sent Fas into hyperdrive. Control mice died of acute liver failure within a few days, but 82 % of the siRNA-treated mice remained free from serious disease and survived. About 80 % and 90 % of their liver cells incorporated the siRNA. Furthermore, the RNA molecules functioned for 10 days before fading completely after 3 weeks, lasting roughly three times longer than in previous studies. Another set of animals faced a different challenge: injections of cells with ConA, which compelled the immune system to attack the liver and produced the scarring seen in viral hepatitis. Animals infused with siRNA developed no liver damage. Silencing Fas expression with RNAi holds some therapeutic promise to prevent liver injury by protecting hepatocytes from cytotoxicity. In addition, biologists have agreeed that the best strategy would be to aim siRNA directly at hepatitis B or C viruses, but that would require a different siRNA than the one used by Song' s team. Evidences from several laboratories suggest that, in petri dishes, siRNA can stop hepatitis C from replicating. McCaffrey *et al*[24] showed that transgene expression could be suppressed in adult mice by synthetic small interfering RNAs and small-hairpin RNAs transcribed *in vivo* from DNA templates. They also showed the therapeutic potential of this technique by demonstrating effective targeting of a sequence from hepatitis C virus by RNA interference *in vivo*. Wilson *et al*[25] found RNA interference blocked gene expression and RNA synthesis from hepatitis C replicons propagated in human liver cells. Double-stranded small interfering RNA (siRNA) molecules designed to target the HCV genome were introduced through electroporation into a human hepatoma cell line (Huh-7) that contained an HCV subgenomic replicon. Two siRNA dramatically reduced virus-specific protein expression and RNA synthesis to levels that were 90 % less than those seen in cells treated with negative control siRNA. These same siRNA protected naive Huh-7 cells from challenge with HCV replicon RNA. Treatment of cells with synthetic siRNA was effective for more than 72 h, but the duration of RNA interference could be extended beyond 3 weeks through stable expression of complementary strands of the interfering RNA by using a bicistronic expression vector. These results suggest that a gene-therapeutic approach with siRNA can ultimately be used to treat HCV.

The utility of siRNA as a therapy against HCV infection will depend on the development of efficient delivery systems that induce long-lasting RNAi activity[26]. HCV is an attractive target for its localization in the liver, an organ that can be readily targeted by nucleic acid molecules and viral vectors. In future, chemically modified synthetic siRNA, with improved resistance to nucleases coupled with enhanced duration of RNAi, may become a possibility for therapeutic applications. On the other hand, gene therapy offers another possibility to express siRNA that targets HCV in a patient' s liver. Based on the above experiments, the use of siRNA as a treatment for HCV infections has great potential for use alone or in combination with conventional IFN/ribavirin therapy as means to decrease virus loads and eventually clear the persistent viruses from its host[27]. As therapeutic agents, siRNAs have enticing properties. Their actions appear to be short-lived in mammals, they are sequence specific and natural, cellular products and may therefore not produce toxic metabolites. Nonetheless, caveats for clinical use remain. Delivering siRNAs to the appropriate cells is a major challenge. siRNAs have thus far only been administered intravenously to mice by ' hydrodynamic transfection' , the rapid infusion of siRNA in a volume one-tenth the mass of the animal. Furthermore, the liver seems to be particularly receptive to exogenous RNA. Better delivery methods-such as formulation of siRNAs with compounds that promote transit across cell membranes-are clearly required before siRNAs can be used in therapy, especially to suppress gene expression in tissues other than in the liver. Nonetheless, the results of Song *et al*[23] have revealed the power of siRNAs in a disease model.

FACILITATING FUNCTIONAL GENOMICS

Until recently, RNA interference has been viewed primarily as a thorn in the side of plant molecular geneticists, limiting expression of transgenes and interfering with a number of applications that require consistent, high-level transgene expression. With our present understanding of the process, however, it is clear that RNA interference has enormous potential for engineering control of gene expression, as well as for a tool in functional genomics. It can be experimentally induced with high efficiency and targeted to a single specific gene or to a family of related genes. Likewise, dsRNA-induced TGS (transcriptional gene silencing) may have similar potential to control gene expression. Unwanted RNA interference, on the other hand, can be alleviated using viral suppressor technology or mutants impaired in silencing[28-30].

Genome-sequencing projects have provided tremendous amount of information about the genetic make-up of an organism. One way for finding out what genes do is to inactivate them, and to study the effects, in ' model' organisms. Kamath *et al*[4] used double-stranded RNAs to rapidly and transiently inactivate 16 757 of the worm' s predicted protein-coding genes. Meanwhile, Ashrafi and co-workers[31] have analysed these genes specifically to see if they had a role in regulating body fat. Together, their work has set a new standard

for systematic, genome-wide genetic studies. RNAi-based loss-of-function screens like these are tremendously powerful. Yet they have some disadvantages compared with classical genetic screening. For instance, some genes are more difficult to target by RNAi than others. And there are many non-coding RNAs, which are not translated into proteins. It remains to be seen if they are susceptible to RNAi. But there are still a vast number of protein-coding genes, from many different organisms, to study in detailed RNAi-based functional analyses, and this will keep the army of cell and molecular biologists busy for some time. Soon it will be possible to carry out RNAi-based screens in animal and human cells, using short synthetic double-stranded RNAs or plasmid- or virus-based DNA molecules that encode hairpin RNAs[32-34]. With the development of phenotypic read-outs based on cell biology, the hunt will begin.

SILENCING HIV-1

RNA interference represents an exciting new technology that may have therapeutic applications in the treatment of viral infections such as HCV and HIV. RNA interference is also found in HIV. Previous reports have shown that siRNA directed against the HIV genome can effectively inhibit virus production in cell-culture systems[35-38]. In addition, RNAi activity directed toward the major HIV receptor protein, CD4, led to decreased entry of HIV into cells[39-41]. However, replication of HIV occurred through an integrated DNA genome. Does it mean that RNAi is ineffective in clearing the virus? By targeting several regions of the HIV-1 genome, Jacque *et al*[42] showed that siRNA mediated viral genome degradation and caused downregulation of viral gene expression and they proved that RNAi worked even when the viral genome was contained within the nucleoprotein complex. They also showed that intracellularly made siRNA (transcribed from a plasmid) worked well, providing possible ways for delivering gene-therapy agents against HIV. To assess the effects of RNAi on HIV-1 infection, Novina *et al*[43] targeted both cellular and viral RNAs. The HeLa-derived cell line Magi-CCR5 (which expresses human CD4, and the chemokine receptors CCR5 and CXCR4) was transfected with short interfering RNA specific for the gene of interest and then infected with HIV-1. Cells transfected with siRNA specific for CD4 expressed CD4 mRNA at a level eight times lower than control cells, which led to a four-fold reduction in HIV-1 entry. Therefore, siRNA-directed silencing of CD4 specifically inhibited HIV entry and hence replication. Next, the viral structural protein Gag was targeted by transfecting cells with siRNA specific for the p24 component of this polyprotein. p24-siRNA-transfected cells showed a four-fold decrease in viral protein compared with controls, implying that viral amplification was inhibited by this approach. The authors also carried out transfection assays on human T cells, to assess the effect of RNAi on viral infectivity in a more physiological context. H9 cells were transfected with siRNA against green fluorescent protein (GFP) and were infected with an HIV-1 strain in which the *nef* gene was replaced with GFP. Again, silencing of viral gene expression occurred, resulting in reduced GFP and HIV-1 protein expression. These and other recent studies[44-46] show that siRNA can inhibit viral replication at several stages of infection, including very early stages, when viruses are most vulnerable. Infection can also be blocked by targeting either viral genes or host genes that are involved in the viral life cycle. It has been shown that siRNA directed against HIV-1 has the potential to be useful treatments. This study extended work by Lee *et al*[47,48] who used a vector-based RNAi strategy to silence an HIV-1 gene, and established that siRNA technology could be used to suppress multiple steps of the HIV-1 life cycle. They described a mammalian Pol III promoter system capable of expressing functional double-stranded siRNA following transfection into human cells. In the case of the 293 cells cotransfected with the HIV-1 pNL4-3 proviral DNA and the siRNA-producing constructs, they were able to achieve up to 4 logs of inhibition of expression from the HIV-1 DNA. Martinez *et al*[49] found that suppression of chemokine receptor expression by RNA interference could inhibit HIV-1 replication. Their results demonstrate that RNAi may be used to block HIV entry and replication through the blockade of cellular gene expression. Park *et al*[50] showed that HIV-1 replication was totally suppressed in a sequence-specific manner by six long dsRNAs containing the HIV-1 gag and env genes in HIV-1-infected cells. Especially, E2 dsRNA containing the major CD4-binding domain sequence of gp120, dramatically inhibited the expression of the HIV-1 p24 antigen in PBMCs for a relatively long time. Coburn *et al*[51] demonstrated that siRNA duplexes targeted against the essential Tat and Rev regulatory proteins encoded by HIV-1 could specifically block Tat and Rev expression and function. More importantly, they showed that these same siRNAs could effectively inhibit HIV-1 gene expression and replication in cell cultures, including those of human T-cell lines and primary lymphocytes. These results demonstrate the utility of RNAi for modulating the HIV replication cycle and provide the evidence that genomic HIV-1 RNA, existing within a nucleoprotein reverse-transcription complex, is amenable to siRNA-mediated degradation.

But does it actually work as an antiviral weapon? More recent studies have suggested that it does, at least in cells in culture dishes. Gitlin *et al*[12] reported that specific siRNA administered to human cells from the outside, like a drug, could enter them and protect them against infection by the rapidly multiplying poliovirus. Jacque *et al*[42], meanwhile, reported similar results in their studies with the AIDS virus HIV-1. These authors further demonstrated that if the siRNA were expressed from inside cells, rather than simply administered from the outside, the cells became largely immune to subsequent HIV-1 is infection. These results are exciting, and suggest that RNAi perfectly suitable to many antiviral applications. But one important factor is that not all viral RNA sequences are equally accessible to siRNA. Some sequences might be buried within secondary structures or within highly folded regions in target RNAs, whereas others might come form tight complexes with proteins that obscure their recognition. Optimal targets must be chosen by trial and error. Another issue is that viruses often produce mutated progeny molecules. Some of these naturally help the viruses escape immune surveillance or inhibition by drugs, but they might also prevent recognition by siRNA. To overcome this obstacle, one might need to target viral RNA sequences that are conserved and normally invariant between different strains, or to simultaneously target several viral sequences. Finally, the problem of how to deliver siRNA to cells needs to be addressed. They can certainly be delivered efficiently to cells in culture, but methods must be improved before RNAi can be used in animals, let alone patients.

FUTURE DIRECTIONS

The field of RNAi is moving at an impressive pace and generating exciting results that are clearly associated with RNA interference, transgene silencing and transposon mobilization[52-55]. Possible links to X-chromosome inactivation, imprinting and interferon response have also been suggested, but not yet firmly established. RNAi also has a considerable economic potential, especially in agriculture. A better understanding of PTGS should allow a more efficient response to viral infection and the development of transgene/host associations that can override silencing to allow the expression of interested proteins. Now that early mouse embryos are known to be susceptible to

RNAi, it will be critical to determine whether this technique can also be applied to tissue culture[56-60]. The possible repercussions of RNAi in mammals are potentially far-reaching in the fight against certain diseases such as cancer or virus/ parasite infection, as well as for the analysis of more fundamental problems in neurobiology and cell and developmental biology. In the next ten years, RNAi will probably be regarded as one of the major breakthroughs of the 2000s. A new report has shown that incubating a target mRNA with *Drosophila* embryonic extracts and the cognate dsRNA *in vitro* leads to its degradation in a process that recapitulates many of the features of RNA interference *in vivo* (including sequence specificity, length dependence and amplification). This important study has paved the way for a biochemical analysis of RNA interference. In relation to RNA interference in mammals, it is important to note that in contrast to the sequence-specific RNAi effect observed in mouse embryos, this new study has shown that incubation of an mRNA with rabbit reticulocyte lysates and dsRNA induces nonspecific mRNA degradation, one possible reason for this difference could be that the interferon response present in rabbit reticulocyte lysate is not functional in early mouse embryos[61-65].

Although antiviral RNAi technology has not yet been optimized, the phenomenon does appear to be both general and effective. In 1988, the concept of "intracellular immunization" was proposed, whereby one could express within cells inhibitory molecules (usually proteins) that could protect these cells from specific viral infections in the future[66-75]. The promise of intracellular immunization now appears to be closer to reality - although amazingly, through the use of small RNAs rather than peptides or proteins. The potential of using RNAi activity for the treatment of viral diseases and cancer has aroused a great deal of interests in the scientific community. Many laboratories have reported the use of RNAi activity in cultured cells infected with HIV, human papillomavirus, and polio or containing a variety of cancer genes. The clinical applications of RNA is just around the corner.

REFERENCES

1 **Zamore PD**. Ancient pathways programmed by small RNAs. *Science* 2002; **296**: 1265-1269
2 **Williams RW**, Rubin GM. ARGONAUTE1 is required for efficient RNA interference in Drosophila embryos. *Proc Natl Acad Sci U S A* 2002; **99**: 6889-6894
3 **Ge Q**, McManus MT, Nguyen T, Shen CH, Sharp PA, Eisen HN, Chen J. RNA interference of influenza virus production by directly targeting mRNA for degradation and indirectly inhibiting all viral RNA transcription. *Proc Natl Acad Sci U S A* 2003; **100**: 2718-2723
4 **Kamath RS**, Fraser AG, Dong Y, Poulin G, Durbin R, Gotta M, Kanapin A, Le Bot N, Moreno S, Sohrmann M, Welchman DP, Zipperlen P, Ahringer J. Systematic functional analysis of the Caenorhabditis elegans genome using RNAi. *Nature* 2003; **421**: 231-237
5 **Schwarz DS**, Hutvagner G, Haley B, Zamore PD. Evidence that siRNAs function as guides, not primers, in the Drosophila and human RNAi pathways. *Mol Cell* 2002; **10**: 537-548
6 **Pantaleo V,** Rubino L, Russo M. Replication of Carnation Italian ringspot virus defective interfering RNA in Saccharomyces cerevisiae. *J Virol* 2003; **77**: 2116-2123
7 **Dennis C**. Small RNAs: the genome's guiding hand? *Nature* 2002; **420**: 732
8 **Jia Q,** Sun R. Inhibition of gammaherpesvirus replication by RNA interference. *J Virol* 2003; **77**: 3301-3306
9 **Van Wezel R**, Liu H, Wu Z, Stanley J, Hong Y. Contribution of the zinc finger to zinc and DNA binding by a suppressor of post-transcriptional gene silencing. *J Virol* 2003; **77**: 696-700
10 **Qu F**, Ren T, Morris TJ. The coat protein of turnip crinkle virus suppresses posttranscriptional gene silencing at an early initiation step. *J Virol* 2003; **77**: 511-522
11 **Ray D**, White KA. An internally located RNA hairpin enhances replication of Tomato bushy stunt virus RNAs. *J Virol* 2003; **77**: 245-257
12 **Gitlin L**, Karelsky S, Andino R. Short interfering RNA confers intracellular antiviral immunity in human cells. *Nature* 2002; **418**: 430-434
13 **Adelman ZN**, Sanchez-Vargas I, Travanty EA, Carlson JO, Beaty BJ, Blair CD, Olson KE. RNA sicencing of dengue virus type 2 replication in transformed C6/36 mosquito cells transcribing an inverted-repeat RNA derived from the virus genome. *J Virol* 2002; **76**: 12925-12933
14 **McCaffrey AP**, Kay MA. A story of mice and men. *Gene Ther* 2002; **9**: 1563
15 **Gong GZ**, Lai LY, Jiang YF, He Y, Su XS. HCV replication in PBMC and its influence on interferon therapy. *World J Gastroenterol* 2003; **9**: 291-294
16 **Yan FM**, Chen AS, Hao F, Zhao XP, Gu CH, Zhao LB, Yang DL, Hao LJ. Hepatitis C virus may infect extrahepatic tissues in patients with hepatitis C. *World J Gastroenterol* 2000; **6**: 805-811
17 **Yu YC**, Mao Q, Gu CH, Li QF, Wang YM. Activity of HDV ribozymes to trans-cleave HCV RNA. *World J Gastroenterol* 2002; **8**: 694-698
18 **Song ZQ**, Hao F, Min F, Ma QY, Liu GD. Hepatitis C virus infection of human hepatoma cell line 7721 *in vitro*. *World J Gastroenterol* 2001; **7**: 685-689
19 **Dai YM,** Shou ZP, Ni CR, Wang NJ, Zhang SP. Localization of HCV RNA and capsid protein in human hepatocellular carcinoma. *World J Gastroenterol* 2000; **6**: 136-137
20 **Cheng JL**, Liu BL, Zhang Y, Tong WB, Yan Z, Feng BF. Hepatitis C virus in human B lymphocytes transformed by Epstein-Barr virus in vitro by in situ reverse transcriptase-polymerase chain reaction. *World J Gastroenterol* 2001; **7**: 370-375
21 **Meier V**, Mihm S, Wietzke Braun P, Ramadori G. HCV-RNA positivity in peripheral blood mononuclear cells of patients with chronic HCV infection: does it really mean viral replication? *World J Gastroenterol* 2001; **7**: 228-234
22 **Izumi RE**, Valdez B, Banerjee R, Srivastava M, Dasgupta A. Nucleolin stimulates viral internal ribosome entry site-mediated translation. *Virus Res* 2001; **76**: 17-29
23 **Song E,** Lee SK, Wang J, Ince N, Ouyang N, Min J, Chen J, Shankar P, Lieberman J. RNA interference targeting Fas protects mice from fulminant hepatitis. *Nat Med* 2003; **9**: 347-351
24 **McCaffrey AP,** Meuse L, Pham TT, Conklin DS, Hannon GJ, Kay MA. RNA interference in adult mice. *Nature* 2002; **418**: 38-39
25 **Wilson JA**, Jayasena S, Khvorova A, Sabatinos S, Rodrigue-Gervais IG, Arya S, Sarangi F, Harris-Brandts M, Beaulieu S, Richardson CD. RNA interference blocks gene expression and RNA synthesis from hepatitis C replicons propagated in human liver cells. *Proc Natl Acad Sci U S A* 2003; **100**: 2783-2788
26 **Randall G**, Grakoui A, Rice CM. Clearance of replicating hepatitis C virus replicon RNAs in cell culture by small interfering RNAs. *Proc Natl Acad Sci U S A* 2003; **100**: 235-240
27 **Zamore PD**, Aronin N. siRNAs knock down hepatitis. *Nat Med* 2003; **9**: 266-267
28 **Pomerantz RJ.** RNA interference meets HIV-1: will silence be golden? *Nat Med* 2002; **8**: 659-660
29 **Mallory AC**, Parks G, Endres MW, Baulcombe D, Bowman LH, Pruss GJ, Vance VB. The amplicon-plus system for high-level expression of transgenes in plants. *Nat Biotechnol* 2002; **20**: 622-625
30 **Caplen NJ,** Zheng Z, Falgout B, Morgan RA. Inhibition of viral gene expression and replication in mosquito cells by dsRNA-triggered RNA interference. *Mol Ther* 2002; **6**: 243-251
31 **Ashrafi K,** Chang FY, Watts JL, Fraser AG, Kamath RS, Ahringer J, Ruvkun G. Genome-wide RNAi analysis of Caenorhabditis elegans fat regulatory genes. *Nature* 2003; **421**: 268-272
32 **Miyagishi M**, Taira K. U6 promoter-driven siRNA with four uridine 3' overhangs efficiently suppress targeted gene expression in mammalian cells. *Nat Biotechnol* 2002; **20**: 497-500
33 **Nicholson RH**, Nicholson AW. Molecular characterization of a mouse cDNA encoding Dicer, a ribonuclease III ortholog involved in RNA interference. *Mamm Genome* 2002; **13**: 67-73
34 **Adelman ZN**, Blair CD, Carlson JO, Beaty BJ, Olson KE. Sindbis virus-induced silencing of dengue viruses in mosquitoes. *Insect Mol Biol* 2001; **10**: 265-273

35 **Hu WY,** Myers CP, Kilzer JM, Pfaff SL, Bushman FD. Inhibition of retroviral pathogenesis by RNA interference. *Curr Biol* 2002; **12**: 1301-1311

36 **Dector MA**, Romero P, Lopez S, Arias CF. Rotavirus gene silencing by small interfering RNAs. *EMBO Rep* 2002; **3**: 1175-1180

37 **Surabhi RM**, Gaynor RB. RNA interference directed against viral and cellular targets inhibits human immunodeficiency Virus Type 1 replication. *J Virol* 2002; **76**: 12963-12973

38 **Martinez de Alba AE**, Flores R, Hernandez C. Two chloroplastic viroids induce the accumulation of small RNAs associated with posttranscriptional gene silencing. *J Virol* 2002; 76: 13094-13096

39 **Park WS**, Miyano-Kurosaki N, Hayafune M, Nakajima E, Matsuzaki T, Shimada F, Takaku H. Prevention of HIV-1 infection in human peripheral blood mononuclear cells by specific RNA interference. *Nucleic Acids Res* 2002; **30**: 4830-4835

40 **Kitabwalla M**, Ruprecht RM. RNA interference-a new weapon against HIV and beyond. *N Engl J Med* 2002; **347**: 1364-1367

41 **Capodici J**, Kariko K, Weissman D. Inhibition of HIV-1 infection by small interfering RNA-mediated RNAinterference. *J Immunol* 2002; **169**: 5196-5201

42 **Jacque JM,** Triques K, Stevenson M. Modulation of HIV-1 replication by RNA interference. *Nature* 2002; **418**: 435-438

43 **Novina CD**, Murray MF, Dykxhoorn DM, Beresford PJ, Riess J, Lee SK, Collman RG, Lieberman J, Shankar P, Sharp PA. siRNA-directed inhibition of HIV-1 infection.*Nat Med* 2002; **8**: 681-686

44 **Wojtkowiak A**, Siek A, Alejska M, Jarmolowski A, Szweykowska-Kulinska Z, Figlerowicz M. RNAi and viral vectors as useful tools in the functional genomics of plants. Construction of BMV-based vectors for RNA delivery into plant cells. *Cell Mol Biol Lett* 2002; **7**: 511-522

45 **Xia H,** Mao Q, Paulson HL, Davidson BL. siRNA-mediated gene silencing *in vitro* and *in vivo*. *Nat Biotechnol* 2002; **20**: 1006-1010

46 **Rhodes A**, James W. Inhibition of heterologous strains of HIV by antisense RNA. *AIDS* 1991; **5**: 145-151

47 **Lee NS**, Dohjima T, Bauer G, Li H, Li MJ, Ehsani A, Salvaterra P, Rossi J. Expression of small interfering RNAs targeted against HIV-1 rev transcripts in human cells. *Nat Biotecrnol* 2002; **20**: 500-505

48 **Song E**, Lee SK, Wang J, Ince N, Ouyang N, Min J, Chen J, Shankar P, Lieberman J. RNA interference targeting Fas protects mice from fulminant hepatitis. *Nat Med* 2003; **9**: 347-351

49 **Martinez MA**, Clotet B, Este JA. RNA interference of HIV replication. *Trends Immunol* 2002; **23**: 559-561

50 **Park WS**, Miyano-Kurosaki N, Hayafune M, Nakajima E, Matsuzaki T, Shimada F, Takaku H. Prevention of HIV-1 infection in human peripheral blood mononuclear cells by specific RNA interference. *Nucleic Acids Res* 2002; **30**: 4830-4835

51 **Coburn GA**, Cullen BR. Potent and specific inhibition of human immunodeficiency virus type 1 replication by RNA interference. *J Virol* 2002; **76**: 9225-9231

52 **Couzin J**. RNA interference. Mini RNA molecules shield mouse liver from hepatitis. *Science* 2003; **299**: 995

53 **Jia Q,** Sun R. Inhibition of gammaherpesvirus replication by RNA interference. *J Virol* 2003; **77**: 3301-3306

54 **Agami R**. RNAi and related mechanisms and their potential use for therapy. *Curr Opin Chem Biol* 2002; **6**: 829-834

55 **Lin SL**, Ying SY. D-RNAi (messenger RNA-antisense DNA interference) as a novel defense system against cancer and viral infections. *Curr Cancer Drug Targets* 2001; **1**: 241-247

56 **Di Serio F**, Schob H, Iglesias A, Tarina C, Bouldoires E, Meins F Jr. Sense- and antisense-mediated gene silencing in tobacco is inhibited by the same viral suppressors and is associated with accumulation of small RNAs. *Proc Natl Acad Sci U S A* 2001; **98**: 6506-6510

57 **Vaucheret H**, Fagard M. Transcriptional gene silencing in plants: targets, inducers and regulators. *Trends Genet* 2001; **17**: 29-35

58 **Blair CD**, Adelman ZN, Olson KE. Molecular strategies for interrupting arthropod-borne virus transmission by mosquitoes. *Clin Microbiol Rev* 2000; **13**: 651-661

59 **Morel JB,** Vaucheret H. Post-transcriptional gene silencing mutants. *Plant Mol Biol* 2000; **43**: 275-284

60 **Hammond SM**, Bernstein E, Beach D, Hannon GJ. An RNA-directed nuclease mediates post-transcriptional gene silencing in Drosophila cells. *Nature* 2000; **404**: 293-296

61 **Yamamoto T**, Omoto S, Mizuguchi M, Mizukami H, Okuyama H, Okada N, Saksena NK, Brisibe EA, Otake K, Fuji YR. Double-stranded nef RNA interferes with human immunodeficiency virus type 1 replication. *Microbiol Immunol* 2002; **46**: 809-817

62 **Couzin J**. Breakthrough of the year. Small RNAs make big splash. *Science* 2002; **298**: 2296-2297

63 **Brummelkamp TR**, Bernards R, Agami R. Stable suppression of tumorigenicity by virus-mediated RNA interference. *Cancer Cell* 2002; **2**: 243-247

64 **Olson KE,** Adelman ZN, Travanty EA, Sanchez-Vargas I, Beaty BJ, Blair CD. Developing arbovirus resistance in mosquitoes. *Insect Biochem Mol Biol* 2002; **32**: 1333-1343

65 **Jiang M**, Milner J. Selective silencing of viral gene expression in HPV-positive human cervical carcinoma cells treated with siRNA, a primer of RNA interference. *Oncogene* 2002; **21**: 6041-6048

66 **Hao CQ**, Feng ZH, Zhou YX, Nie QH, Li JG, Jia ZS, Liang XS, Xie YM, Cao YZ, Kang WZ. Construction,package and identification of replication-deficient recombinant adenovirus expression vector of HCV C. *Shijie Huaren Xiaohua Zazhi* 2003; **11**: 144-147

67 **Jia ZS**, Chen L, Hao CQ, Feng ZH, Li JG, Wang JP, Cao YZ, Zhou YX. Intracellular immunization by hammerhead ribozyme against HCV. *Shijie Huaren Xiaohua Zazhi* 2003; **11**: 148-150

68 **Cheng YQ**, Nie QH, Zhou YX, Huang XF, Luo H, Yang HG. Ultrastructure characteristics of HCV infected human trophoblast cells in culture. *Shijie Huaren Xiaohua Zazhi* 2003; **11**: 151-156

69 **Liang XS**, Lian JQ, Zhou YX, Nie QH, Hao CQ. Inhibitory effect of IRES specific inhibitor RNA on HCV IRES mediated protein translation. *Shijie Huaren Xiaohua Zazhi* 2003; **11**: 157-160

70 **Sun L**, Zhou YX, Hao CQ, Feng ZH, Zhao J, Hu PZ, Fu Y, Ma FC, Chang JQ, Wang JP, Nie QH. Effect of DNA vaccine on anti-HCV infection in mice with subcutaneous inoculating tumor. *Shijie Huaren Xiaohua Zazhi* 2003; **11**: 165-168

71 **Sun Y**, Cheng RX, Feng DY, Ouyang XM, Zheng H. Effect of HCV NS3 on proliferation and phosphorylation of MAPK in human hepatocytes. *Shijie Huaren Xiaohua Zazhi* 2003; **11**: 173-177

72 **Zhang L**, Zhao GZ, Li Y, Shi LL. Dynamic changes of HVR1 quasispecies in chronic hepatitis C after IFN therapy. *Shijie Huaren Xiaohua Zazhi* 2003; **11**: 182-184

73 **Li L**, Cheng J, Li F, Wang JJ, Zhang J, Wu Q, Han P, Chen GF, Ji D, Li K. Clinical and pathological characteristics of steatohepatitis in patients with chronic hepatitis C virus infection. *Shijie Huaren Xiaohua Zazhi* 2002; **10**: 1009-1013

74 **Zhang J**, Cheng J, Li L, Liu AB, Wu Q, Li K, Dong J, Wang L, Lu YY. Apolipoprotein A I and A II in the patients infected with hepatitis C virus. *Shijie Huaren Xiaohua Zazhi* 2002; **10**: 1014-1017

75 **Cheng J**, Ren JY, Li L, Lu ZM, Li K, Hong Y, Lu YY, Wang G, Liu Y, Zhang LX, Chen JM. Liver steatosis of transgenic mice expressing hepatitis C virus structural proteins. *Shijie Huaren Xiaohua Zazhi* 2002; **10**: 1022-1026

Edited by Yuan HT and Wang XL

P.O.Box 2345, Beijing 100023,China
Fax: +86-10-85381893
E-mail: wjg@wjgnet.com www.wjgnet.com

World J Gastroenterol 2003;9(8):1662-1666
World Journal of Gastroenterology
 ISSN 1007-9327

• GASTRIC CANCER •

Growth, invasion, metastasis, differentiation, angiogenesis and apoptosis of gastric cancer regulated by expression of PTEN encoding products

Hua-Chuan Zheng, Yi-Ling Li, Jin-Min Sun, Xue-Fei Yang, Xiao-Han Li, Wei-Guo Jiang, Yin-Chang Zhang, Yan Xin

Hua-Chuan Zheng, Jin-Min Sun, Xue-Fei Yang, Yin-Chang Zhang, Yan Xin, Lab. 4, Cancer Institute, The First Affiliated Hospital of China Medical University, Shenyang 110001, Liaoning Province, China
Yi-Ling Li, Department of Digestive Diseases, The First Affiliated Hospital of China Medical University, Shenyang 110001, Liaoning Province, China
Xiao-Han Li, Wei-Guo Jiang, Department of Pathology, The Second Affiliated Hospital of China Medical University, Shenyang 110004, Liaoning Province, China
Correspondence to: Hua-Chuan Zheng, Lab. 4, Cancer Institute, The First Affiliated Hospital of China Medical University, Shenyang 110001, Liaoning Province, China. zheng_huachuan@hotmail.com
Telephone: +86-24-23256666 Ext 6351 **Fax:** +86-24-23253443
Received: 2003-03-05 **Accepted:** 2003-03-29

Abstract

AIM: To investigate expression of PTEN in gastric cancer and to explore its roles in tumorigenesis and progression of gastric cancer.

METHODS: Formalin-fixed and paraffin-embedded tissues of adjacent non-tumor mucosa and primary foci from 113 cases of gastric cancers were studied for the expression of PTEN and Caspase-3 and microvessel density (MVD) by streptavidin-peroxidase (S-P) immunohistochemistry with antibodies against PTEN, Caspase-3, and CD34. The relationship between PTEN and Caspase 3 expression and clinicopathological parameters of tumors was compared.

RESULTS: Primary gastric cancer cells expressed PTEN less frequently than adjacent epithelial cells of primary foci (54.9 % *vs* 89.4 %; P=0.000, χ^2=33.474). PTEN expression was significantly associated with invasive depth (P=0.003, rs=0.274), metastasis (P=0.036, rs=0.197), growth pattern (P=0.008, rs=0.282), Lauren's classification (P=0.000, rs=0.345), and histological classification (P=0.005, rs=0.262) of tumors, but not with tumor size (P=0.639, rs=0.045), Borrmann's classification (P=0.544, rs=0.070) or TNM staging (P=0.172, rs=0.129). PTEN expression was negatively correlated with MDV in primary gastric cancer (P=0.020, F=5.558). Primary gastric cancer cells showed less frequent immunoreactivity to Caspase-3 than adjacent epithelial cells of primary foci (32.7 % *vs* 50.4 %; P=0.007,χ^2=7.286). Caspase-3 expression was dependent of PTEN expression in primary gastric cancer cells (P=0.000, χ^2=15.266).

CONCLUSION: Down-regulated expression of PTEN plays an important role in tumorigenesis, progression, growth, differentiation and angiogenesis of gastric cancer. Low expression of PTEN can decrease expression of Caspase-3 to disorder apoptosis of tumor cells, which might explain the molecular mechanisms of PTEN contributions to tumorigenesis and progression of gastric cancer.

Zheng HC, Li YL, Sun JM, Yang XF, Li XH, Jiang WG, Zhang YC, Xin Y. Growth, invasion, metastasis, differentiation, angiogenesis and apoptosis of gastric cancer regulated by expression of PTEN encoding products. *World J Gastroenterol* 2003; 9(8): 1662-1666
http://www.wjgnet.com/1007-9327/9/1662.asp

INTRODUCTION

Human suppressor gene, PTEN/MMAC1/TEP1 (phosphatase and tensin homology deleted from chromosome ten/mutated in multiple advanced cancer 1/TGF-β-regulated and epithelial cell enriched phosphatase 1), located on chromosome 10q23. 3 encodes a dual specific protein- phospholipid phosphatase that is involved in regulation of a variety of signal transduction pathways[1]. PTEN inhibits shc' s (src-homology collagen) phosphorylation following epidermal growth factor (EGF) stimulation and therefore blocks the activation of the Ras/MAP-kinase (MAPK) pathway[2]. Another mechanism that involves the protein phosphatase activity of PTEN is dephosphorylation and inactivation of focal adhesion kinase (FAK), thus playing a crucial role of PTEN in the interaction between extracellular matrix and cytoskeleton[3,4]. Besides its function as the protein phosphase, PTEN acts as a phospholipid phosphatase with phosphatidylinosiol 3,4,5-triphosphate (PIP_3) as a substrate[5-7]. Recently, many studies have shown that there are several putative mechanisms relating to tumor suppression as follows: inhibiting cell invasion and metastasis by dephosphorylating FAK, inhibiting cell apoptosis and increasing cell growth by dephosphorylating PIP_3, restraining cell differentiation by inhibiting MAPK signal pathway[5,8,9]. Mutation or abnormal expression of PTEN protein occurs commonly in multiple tumors and significantly correlates with tumorigenesis and progression of different malignancies[10-20]. It was reportedly suggested that deletion or mutation of PTEN could enhance the expression of vascular epithelial growth factor (VEGF) and matrix metalloproteinases (MMPs), which in turn closely correlated with tumor angiogenesis and metastasis[10-14]. Jones *et al*.[15] found that activation of PTEN signal pathway could reduce expression of Caspase-3, resulting in inhibition of cellular apoptosis.

Gastric cancer is one of the commonest malignancies in China, and even in the world. In patients with gastric cancer, the natural disease process consists of carcinogenesis, metastasis and eventual death. However, the molecular aspects of carcinogenesis and progression of gastric cancer remain elusive[16-18]. In the current study, we evaluated the expression of PTEN in adjacent epithelial cells, primary gastric cancer cells and intented to find if there was any correlation between its expression and clinicopathological features and microvessel density (MVD) of gastric cancer, as well as between PTEN and Caspase-3 expression in primary foci in order to clarify its role in tumorigenesis and progression of gastric cancer.

MATERIALS AND METHODS

Patients

One hundred and thirteen cases of surgically resected specimens of gastric cancer were collected from the Second Affiliated Hospital of China Medical University from Sept, 1997 to Feb, 2001, including 83 men and 30 women. Their age ranged from 26 to 83 years, with the mean age of 57.1 years. Among them, 38 tumors were accompanied by lymph node or organ metastasis. None of the patients had received radiotherapy or chemotherapy before operation.

Preparation of tissue samples

Adjacent mucosa and primary lesions of each case were fixed in 4 % formaldehyde solution, embedded in paraffin, incised into 4 μm sections and mounted on poly-lysine-coated slides. These sections were stained by hematoxylin-and-eosin method to confirm their histological diagnosis and other microscopic characteristics.

Evaluation of clinicopathological parameters

Clinical staging for each gastric carcinoma was evaluated according to the TNM system. Gross appearance of the tumors was described according to the Borrmann' s classification. Histomorphological architecture of the tumor samples was expressed on the basis of Lauren' s and Nakamura' s classifications. Growth patterns of gastric cancer were classified in the light of Zhang' s classification. Tumor diameter, invasive depth and metastasis were determined as well.

Immunohistochemistry

Representative and consecutive sections were studied with streptavidin-peroxidase immunohistochemistry (S-P kit from Zhongshan Biotech., China). Anti-PTEN, anti-CD34 and anti-Caspase-3 antibodies were purchased from Antibody Dignostica (USA), Zhongshan (China), and DAKO (Japan), respectively. All procedures were implemented according to the product recommendation. For negative controls, sections were processed as above but treated with PBS (0.01 mol/L, pH7.4) instead of primary antibodies.

Evaluation of PTEN and Caspase-3 immunostaining

The immunoreactivity to PTEN and Caspase-3 was localized in the cytoplasm. From 5 randomly selected representative fields of each section, two independent observers counted one hundred cells. According to the proportion of positive ones in counted cells, the degree of immunostaining was graded as follows: negative(-), ≤5 %; weakly positive (+), 5-25 %; moderately positive (++), 25-50 %; and strongly positive (+++), ≥50 %.

Microvessel density counting

Modified Weidner' s method was used to calculate MVD by anti-CD34 immunohistochemistry, which was described as follows. Microvessels in sclerotic areas within tumor, where microvessels were sparse and immediately adjacent areas of unaffected gastric tissue were considered as hot points in vessel counts. Observers selected five such areas and counted individual microvessels in a 400×field (i.e. 40×objective lens and 10×ocular lens, 0.1885 mm^2 per field). Any brown staining endothelial cell or endothelial cell cluster that was clearly separated from adjacent microvessel, tumor cells, and other connective tissue elements was considered as a single, countable microvessel. They must agree on what constituted a single microvessel.

Statistical analysis

Statistical evaluation was performed using chi-square test to compare the rates between different groups, using Spearman test to analyze the rank data, and using the one-way ANOVA to differentiate the means of different groups. $P<0.05$ was considered as statistically significant. SPSS 10.0 software was employed to analyze all data.

RESULTS

PTEN expression in adjacent epithelial cells and cancer cells of primary gastric cancer

Figures 1-3 show that PTEN was positively expressed in the nuclei of adjacent epithelial cells, lymphocytes and cancer cells of primary foci of gastric cancer. In this study, epithelial cells and cancer cells were immunostained for PTEN protein in 89.4 % and 54.9 % of the tumors, respectively. There was a significant difference between them ($P<0.05$) (Table 1).

Table 1 PTEN expression in adjacent epithelial cells and cancer cells of primary gastric cancer

Groups	*n*	PTEN expression				
		-	+	++	+++	PR(%)
Adjacent epithelial cells	113	12	10	23	68	89.4
Primary cancer cells	113	51	13	11	38	54.9[a]

Notes: PR: positive rate, [a]$P=0.000$ ($\chi^2=33.474$, Pearson' R=0.385).

Table 2 Relationship between expression of PTEN in primary foci and clinicopathological features of gastric cancer

Clinicopathological features	*n*	PTEN expression					*rs*	*P* value
		-	+	++	+++	PR(%)		
Tumor size							0.045	0.639
<4 cm	47	20	6	4	17	57.4		
≥4 cm	66	31	7	7	21	53.0		
Borrmann's Classification							0.070	0.544
I/II	28	12	3	3	10	57.1		
III/IV	59	30	5	6	18	49.2		
Invasive depth							0.274	0.003
Above submucosa	26	7	4	2	13	73.1		
Muscularis propria	34	14	2	4	14	58.8		
Below subserosa	53	30	7	5	11	56.6		
Metastasis							0.197	0.036
Negative	76	28	10	8	29	62.7		
Positive	38	23	3	3	9	39.5		
TNM staging							0.129	0.172
O	18	7	4	1	6	61.1		
I	28	11	2	2	13	60.7		
II	40	19	3	5	13	52.5		
III	17	7	3	3	4	58.8		
IV	10	7	1	0	2	30.0		
Growth pattern							0.282	0.008
Mass	23	8	2	2	11	65.2		
Nest	30	12	3	4	11	60.0		
Diffuse	34	22	3	3	6	35.3		
Lauren's Classification							0.345	0.000
Intestinal type	36	8	2	6	20	77.8		
Diffuse type	57	32	10	3	12	43.9		
Mixed type	20	11	1	2	6	45.0		
Histological classification							0.262	0.005
Differentiated	53	18	3	8	24	66.0		
Undifferentiated	60	33	10	3	14	45.0		

Notes: PR: positive rate.

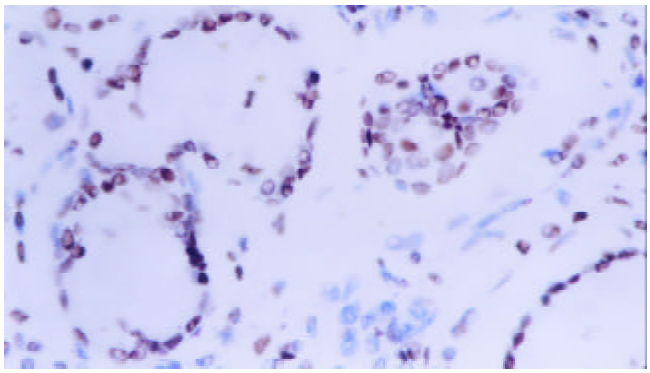

Figure 1 PTEN was immunostained in cell nuclear. It was strongly expressed in gastric epithelial cells (+++) (S-P, ×400).

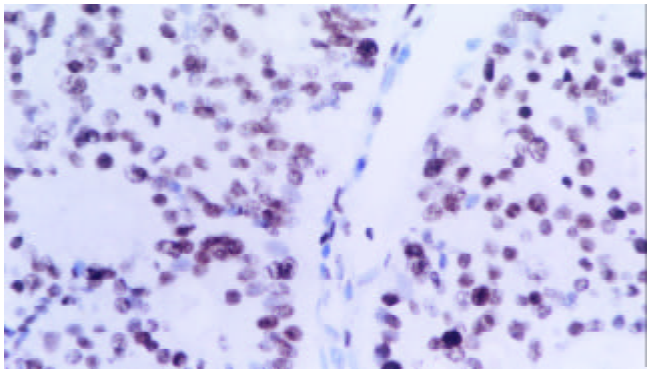

Figure 2 PTEN was strongly expressed in gastric well-differentiated adenocarcinoma (+++) (S-P, ×400).

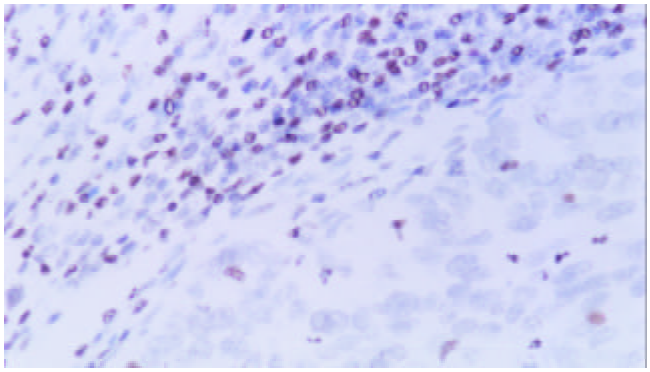

Figure 3 PTEN was negatively expressed in poorly-differentiated adenocarcinoma cells (-) and tumor infiltrated lymphocytes showed strong expression of PTEN (+++) (S-P, ×400).

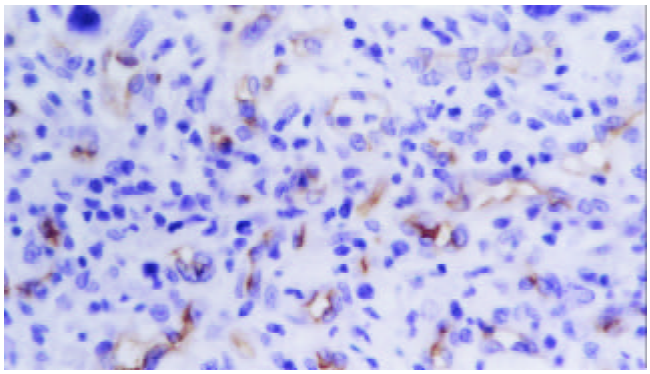

Figure 4 CD34 was located in cytoplasm and cellular membrane of vascular endothelial cells (S-P, ×400).

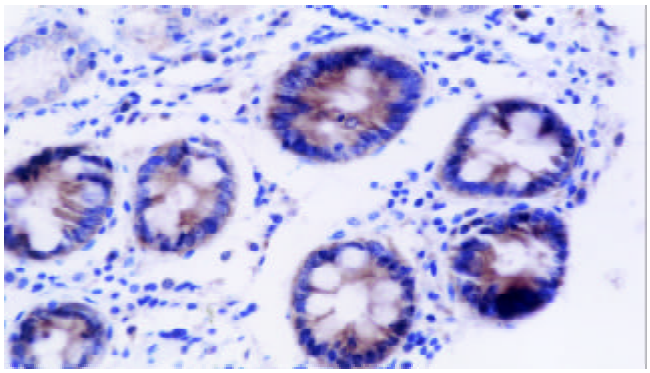

Figure 5 Caspase-3 was distributed in cytoplasm. Caspase-3 was strongly expressed in gastric epithelial cells (+++) (S-P,×400).

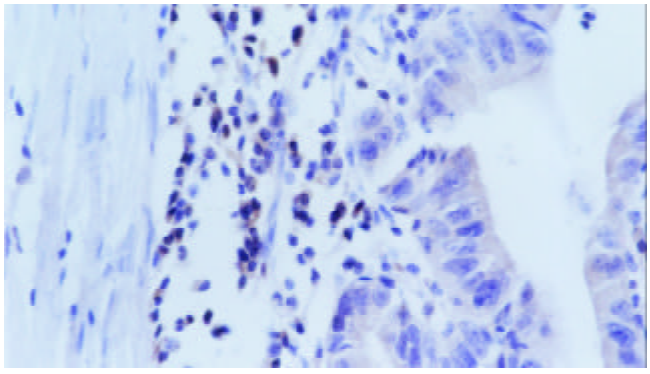

Figure 6 Caspase-3 was positively expressed in well-differentiated adenocarcinoma of stomach (++), and strongly in tumor infiltrated lymphocytes (+++) (S-P, ×400).

Correlation between PTEN expression in primary cancer cells and clinicopathological features of gastric cancer

PTEN expression in primary cancer cells was significantly associated with invasive depth, metastasis, growth pattern, Lauren's Classification, and histological classification of gastric cancer ($P<0.05$). There was no close correlation between PTEN expression and tumor size, Borrmann's Classification or TNM staging ($P>0.05$). One ANOVA analysis showed PTEN expression was negatively correlated with MDV in primary gastric cancer ($P<0.05$) (Tables 2-3, Figure 4).

Table 3 Relationship between expression of PTEN expression and MVD in primary gastric cancer

PTEN expression	*n*	MVD (mean± standard error)	*F* value	*P* value
-	51	52.53±25.47	5.558	0.020
+~+++	62	41.84±22.69		
Total	113	46.67±24.47		

Table 4 Relationship between expression of PTEN and Caspase-3 in primary gastric cancer cells

PTEN expression	*n*	Caspase-3 expression		
		-	+~+++	PR(%)
-	51	44	7	13.7[a]
+~+++	62	32	30	48.4
Total	113	76	37	32.7

Notes: PR: positive rate. [a]$P=0.000$ ($\chi^2=15.266$, Pearson's R=0.368).

Relationship between PTEN and Caspase-3 expression in primary gastric cancer cells

Figures 5-6 showed positive immunostaining of Caspase-3 in

the cytoplasm of adjacent epithelial cells, infiltrating lymphocytes, and cancer cells of primary gastric cancer. Cancer cells showed less frequent immunoreactivity to Caspase-3 than adjacent epithelial cells (32.7 % *vs* 50.4 %; $P<0.05$). Moreover, Caspase-3 expression was dependent of PTEN expression in primary gastric cancer cells ($P<0.05$) (Table 4).

DISCUSSION

Deletion or down-regulation of tumor suppressing genes plays an important role in the multiple steps of tumorigenesis and progression of gastric cancer. PTEN, a tumor-suppressing gene, makes a great contribution to cellular differentiation, reproduction and apoptosis, as well as cellular adhesion and mobility[8,9]. Some studies showed down-regulation of PTEN protein expression was due to genetic changes such as mutation, loss of heterozygosity, hypermethylation in gastric cancer, prostate cancer and breast cancer[19-21]. Our results showed that expression of PTEN decreased in primary gastric cancer cells, compared with that in adjacent epithelial cells. This revealed that genetic changes of PTEN gene could play an important role in malignant transition of gastric epithelial cells.

Low expression of PTEN gene product was involved in clinicopathological stage and metastasis of various malignancies. We found that the positive rate of PTEN was lower in gastric cancer with metastasis than that without metastasis. Additionally, the positive rate of PTEN expression tended to decrease with increase of invasive depth. These results were similar to other kinds of tumors[22-29]. Mass-type gastric cancer showed more expression of PTEN than nest-type one, the latter more than diffuse-type one, demonstrating that PTEN expression was implicated in the growth pattern of gastric cancer. These results suggest that deletion or reduced expression of PTEN protein probably facilitates the invasive and metastatic ability of gastric cancer cells. Several studies revealed that PTEN could enhance mobility and metastasis of tumor cells by regulating MMPs and VEGF[10-14]. There was another report that PTEN dephosphorylated FAK so as to be involved in cellular adhesion[30]. Deletion or reduced expression of PTEN could result in decreased cellular adhesion, increased synthesis of MMPs and VEGF, which subsequently contributed to invasion and angiogenesis of tumor tissues. These biological effects possibly underlay the prelude of invasion and metastasis of tumor. Our results revealed that reduced expression of PTEN was implicated in progression of gastric cancer probably by decreased cellular adhesion, increased cellular mobility and angiogenesis, and could act as an objective and effective marker to reflect the pathobiological behaviors of gastric cancer.

In addition, undifferentiated carcinomas showed the lower expression of PTEN than differentiated ones, suggesting that down-regulated expression of PTEN was closely associated with differentiation of gastric cancer. Diffuse-type gastric cancer showed fewer expression of PTEN than intestinal-type one. It supported that there were different tumorigenetic pathways between diffuse- and intestinal-type gastric cancer. Diffuse-type gastric cancer, the main part of which was undifferentiated, showed diffusely invasive growth pattern. It was possible that down-regulation of PTEN expression could influence the function of cellular skeleton, mobility and adhesion of cancer cells.

Angiogenesis was necessary for tumor growth, invasion and metastasis, and tumor-host interaction induced several sorts of tumor angiogenetic factors such as VEGF and MMPs to stimulate the intratumoral and peritumoral neovascularization[31,32]. In this study, we found that mean MVD was negatively related to PTEN expression in primary gastric cancer. Huang *et al.*[12] found that inhibition of endogenous endothelial PTEN by adenovirus-mediated over-expression of a dominant negative PTEN mutant in cultured endothelial cells potently enhanced a variety of VEGF-mediated cellular responses by PIP_3-kinase signaling, including cell survival, mitogenesis, and migration. In contrast, these effects of VEGF were significantly inhibited by over-expression of wild-type PTEN. Moreover, overexpression of wild-type PTEN modulated endothelial tube formation *in vitro* and vascular sprouting in an *ex vivo* model of angiogenesis. On the other hand, decreased and loss of expression of wild-type PTEN would facilitate MMPs expression which played an important role in angiogenic processes, including proliferation of endothelial cells, breakdown of the extracellular matrix and endothelial cell migration[33]. These *in vivo and in vitro* observations suggested that down-regulated expression of PTEN in gastric cancer increased angiogenesis by up-regulating VEGF and MMPs.

Some investigators found that PTEN could promote cell apoptosis, which in turn inhibited tumor growth[34]. Additionally Caspase-3 played an important role in apoptosis as an effector. Krajewska *et al.*[35] delineated for the first time some of the *in vivo* patterns of Caspase-3 expression in human tissues. Their observation that Caspase-3 was detectable in almost all types of cell implied its role in the regulation of cell life and death in a variety of types of cells as a proteinase. Our finding showed that Caspase-3 was less frequently expressed in gastric cancer cells than in adjacent epithelial cells. In addition, our study showed that expression of PTEN was positively correlated with expression of Caspase-3 in primary gastric cancer cells. Schwartzbauer *et al.*[36] found increased PTEN expression by recombinant adenovirus in cultured neonatal rat primary cardiomyocytes caused cardiomyocyte apoptosis as evidenced by increased caspase-3 activity and cleaved poly (A) DP-ribose polymerase. Furthermore, several studies suggested PTEN could enhance Fas/FasL-mediated or cytochrome-c-mediated apoptosis, whose apoptotic pathway evoked Caspase-3[34,37]. Consequently, we could infer that low expression of PTEN could decrease expression of Caspase-3 to make tumor cells apoptosis dysfunction, which underlay the theoretic basis of contribution of PTEN to tumorigenesis and progression of gastric cancer.

In conclusion, expression of PTEN and Caspase-3 is down-regulated in tumorigenesis of gastric cancer. Decreased expression of PTEN is implicated in progression of gastric cancer by decreased cell adhesion and increased angiogenesis and cell mobility. Moreover, low expression of PTEN can reduce expression of Caspase-3 to make tumor cells apoptosis disorder, which forms molecular mechanisms of PTEN contribution to tumorigenesis and progression of gastric cancer. However, a further study is necessary to directly clarify regulatory roles of PTEN and MMP-7 expression in angiogenesis of gastric cancer.

REFERENCES

1 **Steck PA,** Pershouse MA, Jasser SA, Yung WK, Lin H, Ligon AH, Langford LA, Baumgard ML, Hattier T, Davis T, Frye C, Hu R, Swedlund B, Teng DH, Tavtigian SV. Identification of a candidate tumour suppressor gene, MMAC1, at chromosome 10q23.3 that is mutated in multiple advanced cancers. *Nat Genet* 1997; **15**: 356-362

2 **Gu J**, Tamura M, Yamada KM. Tumor suppressor PTEN inhibits integrin- and growth factor-mediated mitogen-activated protein (MAP) kinase signaling pathways. *J Cell Biol* 1998; **143**: 1375-1383

3 **Tamura M**, Gu J, Takino T, Yamada KM. Tumor suppressor PTEN inhibition of cell invasion, migration, and growth: differential involvement of focal adhesion kinase and p130Cas. *Cancer Res* 1999; **59**: 442-449

4 **Tamura M**, Gu J, Tran H, Yamada KM. PTEN gene and integrin signaling in cancer. *J Natl Cancer Inst* 1999; **91**: 1820-1828

5 **Maehama T**, Dixon JE. The tumor suppressor, PTEN / MMAC1,

dephosphorylates the lipid second messenger, phosphatidylinositol 3, 4, 5-trisphosphate. *J Biol Chen* 1998; **273**: 13375-13378

6 **Hopkin K**. A surprising function for the PTEN tumor suppressor. *Science* 1998; **282**: 1027-1030

7 **Cantley LC**, Neel BG. New insight into tumor suppression: PTEN suppresses tumor formation by restraining the phosphoinositide 3-kinase / AKT pathway. *Proc Natl Acad Sci USA* 1999; **96**: 4240-4245

8 **Besson A**, Robbins SM, Yong VW. PTEN / MMAC1 / TEP1 in signal transduction and tumorigenesis. *Eur J Biochem* 1999; **263**: 605-611

9 **Waite KA**, Eng C. Protean PTEN: form and function. *Am J Hum Genet* 2002; **70**: 829-844

10 **Koul D**, Parthasarathy R, Shen R, Davies MA, Jasser SA, Chintala SK, Rao JS, Sun Y, Benvenisite EN, Liu TJ, Yung WK. Suppression of matrix metalloproteinase-2 gene expression and invasion in human glioma cells by MMAC / PTEN. *Oncogene* 2001; **20**: 6669-6678

11 **Tsugawa K**, Jones MK, Sugimachi K, Sarfeh IJ, Tarnawski AS. Biological role of phosphatase pten in cancer and tissue injury healing. *Front Biosci* 2002; **7**: E245-251

12 **Huang J**, Kontos CD. PTEN modulates vascular endothelial growth factor-mediated signaling and angiogenic effects. *J Biol Chem* 2002; **277**: 10760-10766

13 **Byzova TV**, Goldman CK, Pampori N, Thomas KA, Bett A, Shattil SJ, Plow EF. A mechanism for modulation of cellular responses to VEGF: activation of the integrins. *Mol Cell* 2000; **6**: 851-860

14 **Jiang BH**, Zheng JZ, Aoki M, Vogt PK. Phosphatidylinositol 3-kinase signaling mediates angiogenesis and expression of vascular endothelial growth factor in endothelial cells. *Proc Natl Acad Sci USA* 2000; **97**: 1749-1753

15 **Jones RG**, Elford AR, Parsons MJ, Wu L, Krawczyk CM, Yeh WC, Hakem R, Rottapel R, Woodgett JR, Ohashi PS. CD28-dependent activation of protein kinase B / Akt blocks Fas-mediated apoptosis by preventing death-inducing signaling complex assembly. *J Exp Med* 2002; **196**: 335-348

16 **Parkin DM**. Global cancer statistics in the year 2000. *Lancet Oncol* 2001; **2**: 533-543

17 **Chen XY**, van Der Hulst RW, Shi Y, Xiao SD, Tytgat GN, Ten Kate FJ. Comparison of precancerous conditions: atrophy and intestinal metaplasia in *Helicobacter pylori* gastritis among Chinese and dutch patients. *J Clin Pathol* 2001; **54**: 367-370

18 **Xin Y**, Li XL, Wang YP, Zhang SM, Zheng HC, Wu DY, Zhang YC. Relationship between phenotypes of cell-function differentiation and pathobiological behavior of gastric carcinomas. *World J Gastroenterol* 2001; **7**: 53-59

19 **Kondo K,** Yao M, Kobayashi K, Ota S, Yoshida M, Kaneko S, Baba M, Sakai N, Kishida T, Kawakami S, Uemura H, Nagashima Y, Nakatani Y, Hosaka M. PTEN / MMAC1 / TEP1 mutations in human primary renal-cell carcinomas and renal carcinoma cell lines. *Int J Cancer* 2001; **91**: 219-224

20 **Wang DS**, Rieger-Christ K, Latini JM, Moinzadeh A, Stoffel J, Pezza JA, Saini K, Libertino JA, Summerhayes IC. Molecular analysis of PTEN and MXI1 in primary bladder carcinoma. *Int J Cancer* 2000; **88**: 620-625

21 **Salvesen HB**, MacDonald N, Ryan A, Jacobs IJ, Lynch ED, Akslen LA, Das S. PTEN methylation is associated with advanced stage and microsatellite instability in endometrial carcinoma. *Int J Cancer* 2001; **91**: 22-26

22 **Lee JI**, Soria JC, Hassan KA, El-Naggar AK, Tang X, Liu DD, Hong WK, Mao L. Loss of PTEN expression as a prognostic marker for tongue cancer. *Arch Otolaryngol Head Neck Surg* 2001; **127**: 1441-1445

23 **Verma RS**, Manikal M, Conte RA, Godec CJ. Chromosomal basis of adenocarcinoma of the prostate. *Cancer Invest* 1999; **17**: 441-447

24 **McMenamin ME**, Soung P, Perera S, Kaplan I, Loda M, Sellers WR. Loss of PTEN expression in paraffin-embedded primary prostate cancer correlates with high gleason score and advanced stage. *Cancer Res* 1999; **59**: 4291-4296

25 **Rustia** A, Wierzbicki V, Marrocco L, Tossini A, Zamponi C, Lista F. Is exon 5 of the PTEN / MMAC1 gene a prognostic marker in anaplastic glioma? *Neurosurg Rev* 2001; **24**: 97-102

26 **Nozaki M**, Tada M, Kobayashi H, Zhang CL, Sawamura Y, Abe H, Ishii N, Van Meir EG. Roles of the functional loss of p53 and other genes in astrocytoma tumorigenesis and progression. *Neurooncol* 1999; **1**: 124-137

27 **Minaguchi T**, Yoshikawa H, Oda K, Ishino T, Yasugi T, Onda T, Nakagawa S, Matsumoto K, Kawana K, Taketani Y. PTEN mutation located only outside exons 5, 6, and 7 is an independent predictor of favorable survival in endometrial carcinomas. *Clin Cancer Res* 2001; **7**: 2636-2642

28 **Tada K**, Shiraishi S, Kamiryo T, Nakamura H, Hirano H, Kuratsu J, Kochi M, Saya H, Ushio Y. Analysis of loss of heterozygosity on chromosome 10 in patients with malignant astrocytic tumors: correlation with patient age and survival. *J Neurosurg* 2001; **95**: 651-659

29 **Mills GB**, Lu Y, Kohn EC. Linking molecular therapeutics to molecular diagnostics: inhibition of the FRAP / RAFT / TOR component of the PI3K pathway preferentially blocks PTEN mutant cells *in vitro* and *in vivo*. *Proc Natl Acad Sci USA* 2001; **98**: 10031-10033

30 **Maehama T**, Taylor GS, Dixon JE. PTEN and myotubularin: novel phosphoinositide phosphatases. *Annu Rev Biochem* 2001; **70**: 247-279

31 **Kim TS**, Kim YB. Correlation between expression of matrix metalloproteinas-2 (MMP-2), and matrix metalloproteinase-9 (MMP-9) and angiogenesis in colorectal adenocarcinoma. *J Korean Med Sci* 1999; **14**: 263-270

32 **Giatromanolaki A**, Koukourakis MI, Stathopoulos GP, Kapsoritakis A, Paspatis G, Kakolyris S, Sivridis E, Georgoulias V, Harris AL, Gatter KC. Angiogenic interactions of vascular endothelial growth factor of thymidine phosphorylase, and of p53 protein expression in locally advanced gastric cancer. *Oncol Res* 2000; **12**: 33-41

33 **Cox G**, O'Byrne KJ. Matrix metalloproteinases and cancer. *Anticancer Res* 2001; **21**: 4207-4219

34 **Carson JP**, Kulik G, Weber MJ. Antiapoptotic signaling in LNCaP prostate cancer cells: a survival signaling pathway independent of phosphatidylinositol 3'-kinase and Akt / protein kinase B. *Cancer Res* 1999; **59**: 1449-1453

35 **Krajewska M**, Wang HG, Krajewski S, Zapata JM, Shabaik A, Gascoyne R, Reed JC. Immunohistochemical analysis of *in vivo* patterns of expression of CPP32 (Caspase-3), a cell death protease. *Cancer Res* 1997; **57**: 1605-1613

36 **Schwartzbauer G**, Robbins J. The tumor suppressor gene PTEN can regulate cardiac hypertrophy and survival. *J Biol Chem* 2001; **276**: 35786-357893

37 **Wick W**, Furnari FB, Naumann U, Cavenee WK, Weller M. PTEN gene transfer in human malignant glioma: sensitization to irradiation and CD95L-induced apoptosis. *Oncogene* 1999; **18**: 3936-3943

Edited by Xu XQ

P.O.Box 2345, Beijing 100023,China
Fax: +86-10-85381893
E-mail: wjg@wjgnet.com www.wjgnet.com

World J Gastroenterol 2003;9(8):1667-1674
World Journal of Gastroenterology
 ISSN 1007-9327

• LIVER CANCER •

Characterization of focal hepatic lesions with contrast-enhanced C-cube gray scale ultrasonography

Wen-Ping Wang, Hong Ding, Qing Qi, Feng Mao, Zhi-Zhang Xu, Masatoshi Kudo

Wen-Ping Wang, Hong Ding, Qing Qi, Feng Mao, Zhi-Zhang Xu, Department of Ultrasound, Zhongshan Hospital of Fudan University, 180 Fenglin Road, Shanghai, 200032, China
Masatoshi Kudo, Department of Gastroenterology and Hepatology, School of Medicine, Kinki University, 377-2, Ohno-Higashi, Osaka-Sayama, 589-8511, Japan
Correspondence to: Dr. Hong Ding, Department of Ultrasound, Zhongshan Hospital of Fudan University, 180 Fenglin Road, Shanghai, 200032, China. hongding3@hotmail.com
Telephone: +86-21-64041990 Ext 2474 **Fax:** +86-21-64220319
Received: 2003-04-02 **Accepted:** 2003-05-19

Abstract

AIM: To characterize enhancement patterns of focal hepatic lesions using C-cube gray scale sonography with a microbubble contrast agent and to evaluate its usefulness in differential diagnosis of hepatic lesions.

METHODS: Fifty-four patients with 58 focal hepatic lesions were examined with Levovist-enhanced C-cube gray scale sonography. The final diagnosis of hepatic lesions was 29 primary liver cancers, 4 metastases, 8 hemangiomas, 12 focal nodular hyperplasias, 2 inflammatory pseudotumors of the liver and 3 angiomyolipomas. The initiation time of enhancement in various lesions and enhancement duration after administration of contrast agent were compared. Vascular findings in lesions were classified as peripheral enhancement, homogenous enhancement, mosaic enhancement and no enhancement depending on microbubble signals in the lesion relative to the liver parenchyma.

RESULTS: The initiation time of enhancement in hemangioma (48±12 s) was significantly later compared to other lesions ($P<0.05$). The enhancement duration of malignancies (69±33 s in primary liver cancer, 61±23 s in metastasis) was significantly shorter compared to benign lesions ($P<0.05$). Intranodular enhancement appearing at arterial phase and decreasing at portal venous phase was considered characteristic for malignancy. Intranodular enhancement did not appear earlier than the liver parenchyma, and peripheral enhancement pattern was regarded as positive findings for hemangioma. Intranodular enhancement appeared in the arterial phase, and homogenous enhancement pattern sustained in the whole portal venous phase were regarded as positive findings for focal nodular hyperplasia. No microbubble signals appeared in two inflammatory pseudotumors of the liver.

CONCLUSION: C-cube gray scale sonography can demonstrate dynamic intranodular enhancement in various focal hepatic lesions. The information provided by this methodology may be useful in the differential diagnosis of hepatic lesions.

Wang WP, Ding H, Qi Q, Mao F, Xu ZZ, Kudo M. Characterization of focal hepatic lesions with contrast-enhanced C-cube gray scale ultrasonography. *World J Gastroenterol* 2003; 9(8): 1667-1674
http://www.wjgnet.com/1007-9327/9/1667.asp

INTRODUCTION

Color Doppler ultrasonography (US) is the most widely used imaging modality in screening detection of hepatic tumors and differential diagnosis of malignancies based on tumor vascularity. Unfortunately, conventional Doppler US does not provide satisfactory results in the evaluation of tumor vascularity because of limitations such as a lack of sensitivity to slow flow and deeply located flow, inevitable motion artifacts from either respiratory or cardiac activity, and poor showing of tumor stain.

Over the past decade, great efforts have been made to improve both ultrasound instruments and echo-enhancing agents to demonstrate tumor flow more sensitively with non-invasive modalities. Harmonic imaging is a newly developed technique used with microbubble contrast agents that interact with the imaging process. The microbubbles reflect ultrasonic echoes with a low acoustic power, additionally, they resonant and emit multiple frequencies when acoustic power is sufficiently elevated[1]. Second harmonic imaging, which transmits sonographic pulses at one frequency and then selectively receives echoes at twice that frequency, has been shown to be excellent in eliminating clutter noises and displaying the slower blood flow in smaller vessels when compared to conventional Doppler US[2-5].

However, the intensity of second harmonic frequency of some microbubble contrast agents (e.g., Levovist) is lower than that of fundamental ones[1, 6]. In addition to second harmonics, the microbubbles emit multiple frequencies such as subharmonic, ultraharmonic, etc. Recently, a commercially available C-cube gray scale US (C^3-Mode™, Esaote Biomedica, Genoa, Italy) technique uses comparative digital decorrelation and a digital adaptive band pass filtering process, providing a combination of gray scale, Doppler and contrast signals. It utilizes the signal coming from the microbubbles with not only the second harmonics, but also the fundamental, sub- and ultra-harmonics from the contrast agent. Therefore, this new technique might be able to provide increased sensitivity in demonstrating slow blood flow in focal liver lesions with good spatial resolution in comparison to contrast-enhanced conventional US or second harmonic imaging.

The purpose of this study was to characterize enhancement patterns in focal hepatic lesions with contrast-enhanced C-cube gray scale US.

MATERIALS AND METHODS

Subjects

Between October 2001 and March 2002, 54 patients with clinically and histopathologically diagnosed hepatic tumors who were referred for hepatic color Doppler US were examined with C-cube gray scale US in combination with a microbubble contrast agent. All the patients gave fully informed consent for the study that had received approval from our institutional review board.

The patients consisted of 31 men and 23 women aged between 20-68 years (mean, 47 years). Contrast-enhanced C-cube gray scale US was performed 2-3 days before treatment. In patients with multiple lesions, the largest one was selected for contrast

study except 4 patients with different types of hepatic lesions. Therefore, a total of 58 hepatic lesions were studied with contrast agents. They were 29 cases of primary liver cancer (PLC) (hepatocellular carcinoma, HCC, 27; cholangiocarcinoma, 2), 8 of hemangiomas, 12 of focal nodular hyperplasias (FNH), 2 of inflammatory pseudotumors of the liver (IPT), 3 of angiomyolipomas, and 4 of metastases (gastric cancer, 1; breast cancer, 2; nasopharyngeal carcinoma, 1). Histopathological diagnosis was obtained by surgical resection or US-guided percutaneous biopsy in all the 33 malignancies, 3 hemangiomas, 7 FNHs, 2 IPTs and 3 angiomyolipomas. Other 5 hemangiomas and 5 FNHs were diagnosed according to the typical imaging findings on contrast-enhanced computed tomography (CT), magnetic resonance imaging, as well as clinical follow-up which showed no change of lesion size for more than one year.

The maximal diameters of the 58 hepatic lesions measured on conventional US were as follows: PLC, 1.1-8.2 cm (mean, 3.3 cm); metastasis, 2.2-3.5 cm (mean, 2.8 cm); hemangioma, 1.0-8.0 cm (mean, 5.5 cm); FNH, 1.1-7.3 cm (mean, 4.5 cm); angiomyolipoma, 2.4-7.3 cm (mean, 6.3 cm) and IPT, 1.7-4.1 cm (mean, 2.9 cm).

Contrast agent

The contrast agent was Levovist (Schering AG, Berlin, Germany), which is a suspension of monosaccharide microparticles (galactose) in sterile water. Microbubbles were stabilized in the microparticle suspension with an average diameter of 1.3 μm, which could traverse the pulmonary capillary bed and enhance the signal of blood. Before US examination, the agent was prepared with 5 mL of water by shaking vigorously for 5-10 s. After standing for 2 min for equilibration, a total of 2.5 g Levovist (6 mL 400 mg/mL concentration) was injected manually through a 20-gauge canula placed in an antecubital vein at a speed of 1 mL/s and flushed by an additional 5 mL of normal saline.

Imaging

Contrast-enhanced C-cube gray scale US was performed with a commercially available US system, Technos DU6 US system (Esaote Biomedica, Genoa, Italy), equipped with C^3-Mode™ technology. A convex-arrayed wide band transducer CA 421 was used at a frequency of 2-5 MHz. There were two states in contrast examination: LOW state and C^3-Mode state. At the LOW state, the system transmitted pulses at a low acoustic power with a mechanical index of 0.2-0.4 that theoretically would not destroy microbubbles. At C^3-Mode state, the system transmitted pulses at a high acoustic power with a mechanical index of 1.0-1.4 to destroy microbubbles in the scanning plane. We could transfer from the LOW state to the C^3-Mode state by simply pressing a keyboard button to obtain signals of microbubble collapse, and the system automatically returned to the LOW state then.

Conventional US was performed on all lesions before contrast-enhanced study started. An ideal plane was selected for clearly showing the lesion and the surrounding liver parenchyma. Following administration of Levovist, we monitored the same scanning plane using LOW state and obtained a series of C^3-Mode images by pressing the key button manually for 7-8 minutes. During 15-120 s after injection of Levovist, we obtained C^3-Mode images of high mechanical index every 5-10 s. After that (121-480 s after injection of Levovist), we obtained C^3-Mode images every 20-30 s. During the entire scanning procedure, we held the transducer and unfroze it during the same stage of the patient's respiration to maintain the same scanning plane. The time delay between the initiation of contrast injection and the time at which the C^3-Mode image obtained was automatically recorded on the US system.

Analysis

All US images were recorded on digital videotapes and still images were stored digitally on a hard disk in the US system. Videotapes and still images were reviewed by two authors who were unaware of the findings on other imaging modalities and the final diagnosis of the lesions.

The time of occurrence of microbubble signals in the lesion and in surrounding liver parenchyma after administration of Levovist (injection-enhancement delay time), and subsequent time of microbubble signals decreased in the lesion on C^3-Mode images (injection-decrease delay time) were carefully recorded. Enhancement decrease in a lesion was defined as the echogenicity lower in the lesion than that in the same-depth of surrounding liver parenchyma. In this way, we calculated enhancement duration of various lesions.

The entire procedure of contrast-enhanced C-cube gray scale US was classified into three phases. As vascular transit time of blood through the liver was associated with liver diseases, such as hepatic cirrhosis[7-9], we modified the scheme that Kim *et al*[10] used on dynamic CT. Arterial phase prior to the enhancement appeared in the liver parenchyma, approximately 15-50 s after administration of Levovist, and portal venous phase appeared 51-120 s after administration of Levovist, and delayed phase appeared 121 s after administration of Levovist.

Based on the enhancement of microbubble signals in the lesion relative to the surrounding liver parenchyma, vascular findings in lesions on C^3-Mode images in the arterial phase were classified as peripheral enhancement (continuous or discontinuous ring enhancement occurred in the periphery of the lesion), homogenous enhancement (enhancement occurred in the whole lesion), mosaic enhancement (enhancement occurred in some area of the lesion), and no enhancement (no microbubble signal occurred in the lesion while enhancement in the liver parenchyma occurred). All the enhancement patterns including peripheral, homogenous and mosaic enhancements were defined as positive enhancement, namely positive detection of intranodular vascularity.

All the data were normal distribution and homogeneity of variance after tested. The data were analyzed using SAS (SAS 6.04 for windows). Continuous variables were compared by means of independent *t*-test. Categorical data were analyzed with chi square test. A P value <0.05 was considered to be significant.

RESULTS

The detection rate of intranodular vascularity was 96.6 % (56/58) on C-cube gray scale US with administration of Levovist. All PLCs, metastases, hemangiomas, FNHs, and angiomyolipomas presented positive enhancement. No microbubble signals appeared in the lesions of IPT, resulting in a vascular defect when liver parenchymal perfusion was observed on C-cube gray scale US.

The initiation time of microbubble enhancement in various lesions and in the surrounding liver parenchyma after administration of Levovist, as well as enhancement duration of various lesions are listed in Table 1. Except hemangioma, all other lesions enhanced earlier than the liver parenchyma. The initiation time of enhancement in hemangioma (48±12 s after administration of Levovist) was significantly later when compared to other lesions ($P<0.05$). The enhancement in HCC (Figure 1), cholangiocarcinoma (Figure 2), and metastasis (Figure 3) decreased more rapidly when compared to benign liver lesions. The enhancement duration of malignancies (69±33 s in PLC, 59±22 s in metastasis, respectively) was significantly shorter when compared to benign liver lesions ($P<0.05$).

If the intranodular enhancement appeared at arterial phase

and enhancement decreased at portal venous phase in a lesion was considered characteristic for malignancy, the sensitivity, specificity and positive predictive values for contrast-enhanced C-cube gray scale US to differentiate malignancies from benign liver lesions were 90.9 % (30/33), 92.0 % (23/25), and 93.8 % (30/32), respectively.

Vascular findings in all lesions at the arterial phase on contrast-enhanced C-cube gray scale US are shown in Table 2. Peripheral enhancement was detected in 50.0 % (2/4) of metastases and 87.5 % (7/8) of hemangiomas, homogenous enhancement in 55.2 % (16/29) of PLCs, 100 % (12/12) of FNHs, and mosaic enhancement in 41.4 % (12/29) of PLCs, and 66.7 % (2/3) of angiomyolipomas.

With respect to the enhancement patterns on contrast-enhanced C-cube gray scale US, no specific enhancement pattern was found among malignancies. For benign liver lesions, however, the enhancement patterns were specific. After administration of Levovist, hemangioma enhanced later than the liver parenchyma, and peripheral enhancement was obtained in most hemangiomas (Figure 4). All FNHs enhanced earlier than the liver parenchyma and presented homogenous enhancement (Figure 5). Most angiomyolipomas enhanced early and showed mosaic enhancement pattern (Figure 6).

If the intranodular enhancement did not appear earlier than the surrounding liver parenchyma after administration of Levovist, and the peripheral enhancement patterns were regarded as positive findings for hemangioma, the sensitivity, specificity and positive predictive values were 87.5 % (7/8), 94.0 % (47/50) and 70.0 % (7/10), respectively.

If the intranodular enhancement appeared in the arterial phase, and the homogenous enhancement pattern sustained in the whole portal venous phase were regarded as positive findings for FNH, the sensitivity, specificity and positive predictive values were 100 % (12/12), 95.7 % (44/46) and 85.7 % (12/14), respectively.

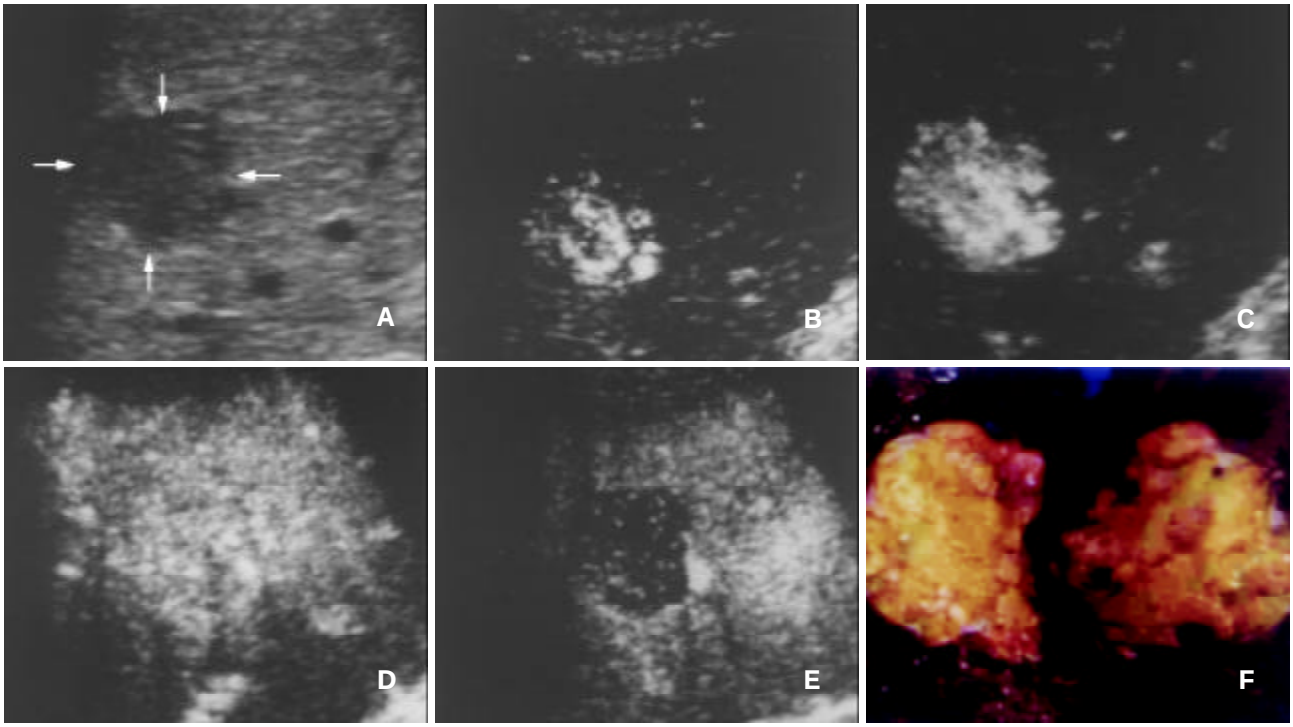

Figure 1 A 47-year-old man with hepatocellular carcinoma. A. Intercostal precontrast conventional sonography exhibits a hypoechogenic lesion (arrows) of 2.7 cm in diameter. B-E. Contrast-enhanced C-cube gray scale sonography at 23 s (B), 28 s (C) and 43 s (D) after injection of Levovist shows that intranodular signals enhance gradually and earlier than the liver parenchyma, and enhancement decreases rapidly in the portal venous phase (110 s, E). This suggests hypervascularity of hepatocellular carcinoma with an early enhancement and early wash-out of contrast. F. Gross specimen of the resected tumor exhibits a gray fish-like profile and suggests the typical appearance of hepatocellular carcinoma.

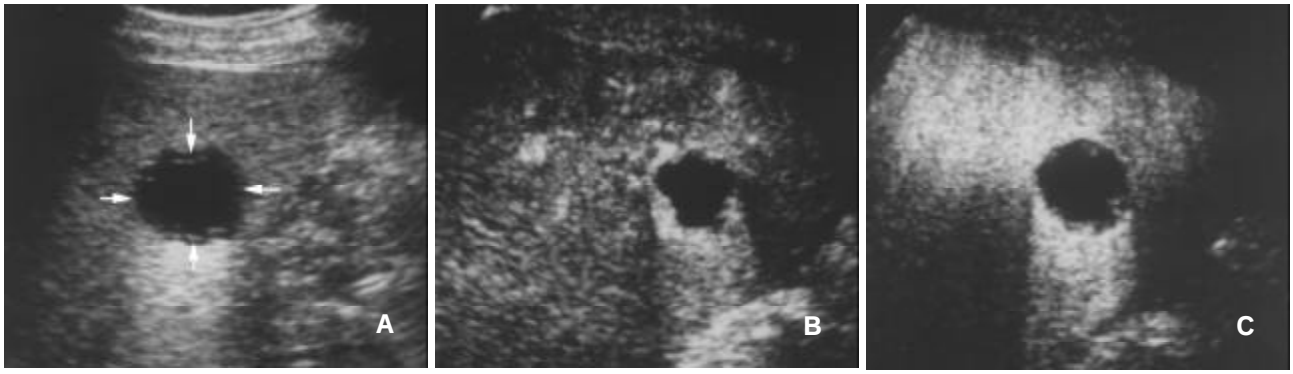

Figure 2 A 48-year-old man with metastasis of nasopharyngeal carcinoma. A. Intercostal section of precontrast conventional sonography exhibits a hypoechogenic lesion (arrows) with a diameter of 3.5 cm. B. Contrast-enhanced C-cube gray scale sonography at 24 s after injection of Levovist shows that peripheral enhancement appears at the same time with the liver parenchyma. C. Intranodular enhancement decreases at 107 s in the portal venous phase, earlier than that in the liver parenchyma.

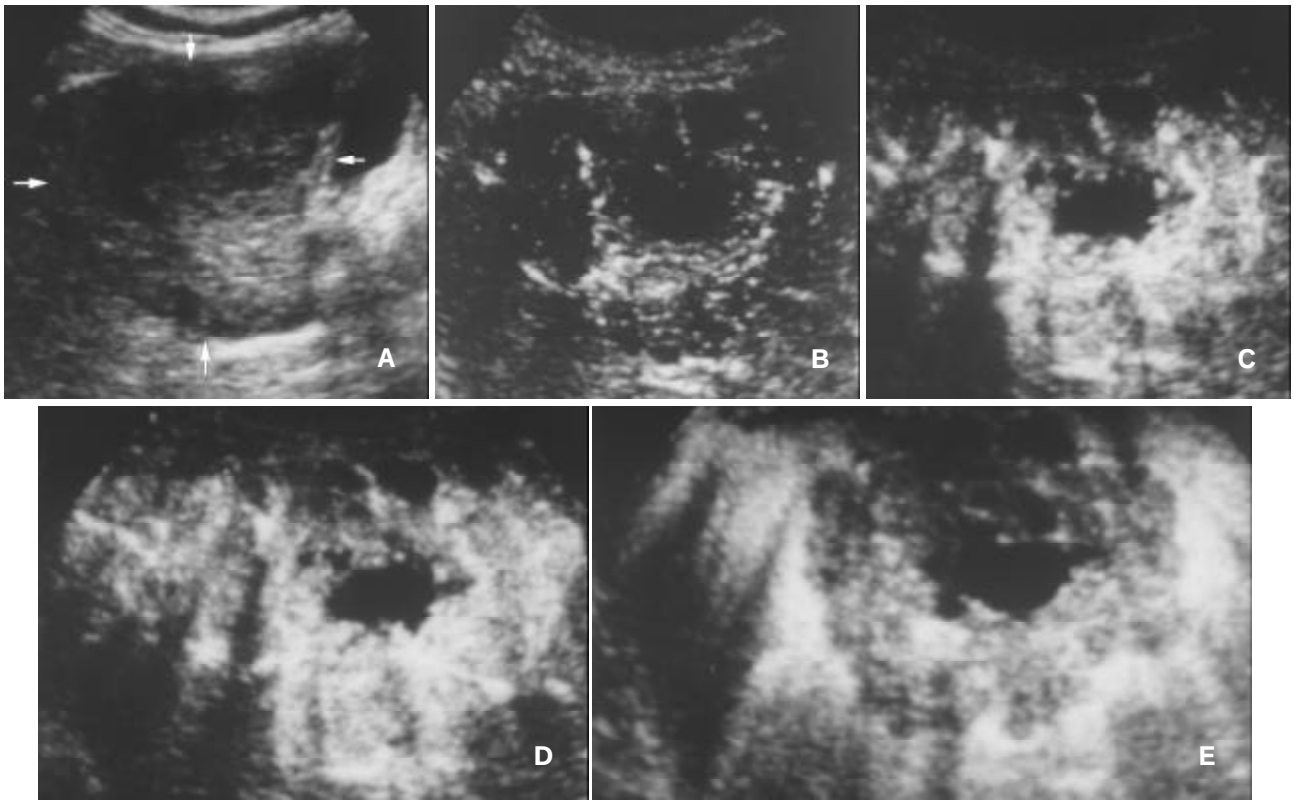

Figure 3 A 62-year-old woman with cholangiocarcinoma. A. Subcostal section of precontrast conventional sonography shows a hypoechogenic lesion (arrows) in segment V of the liver with a diameter of 8.0 cm. B-E. Contrast-enhanced C-cube gray scale sonography at 16 s (B), 20 s (C) and 25 s (D) after injection of Levovist shows that intranodular signals enhance gradually and earlier than the liver parenchyma, and enhancement decreases rapidly in the portal venous phase (78 s, E). Histopathology of US-guided percutaneous biopsy reveals cholangiocarcinoma of the liver.

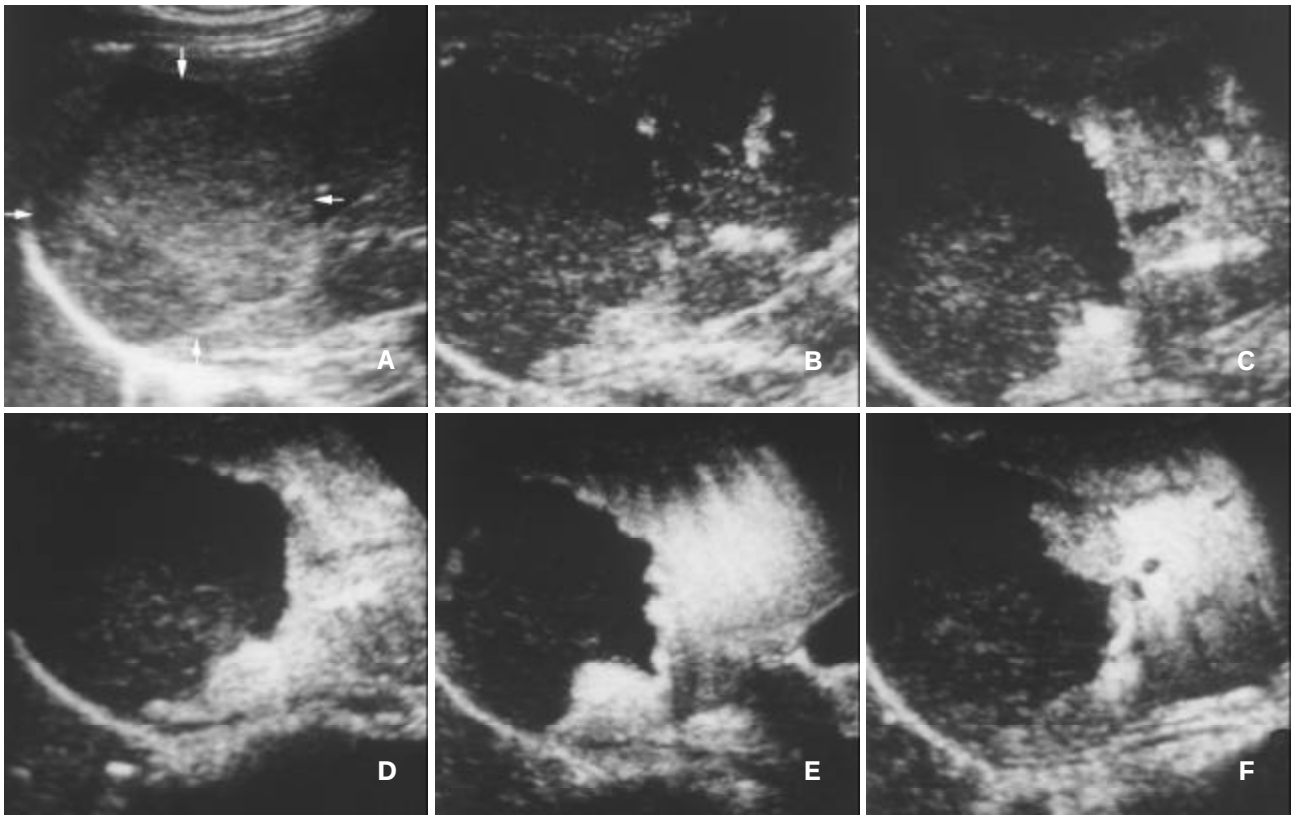

Figure 4 A 45-year-old female with hemangioma. A. Intercostal section of precontrast conventional sonography exhibits a hypoechogenic lesion (arrows) of 6.5 cm in diameter. B. Contrast-enhanced C-cube gray scale sonography at 23 s (B) after injection of Levovist shows that no microbubble signal appears in the lesion while enhancement in the liver parenchyma begins. C-F. C-cube gray scale sonography demonstrates gradual peripheral enhancement at 32 s (C), 47 s (D), 113 s (E) and 370 s (F) with a long enhancement duration.

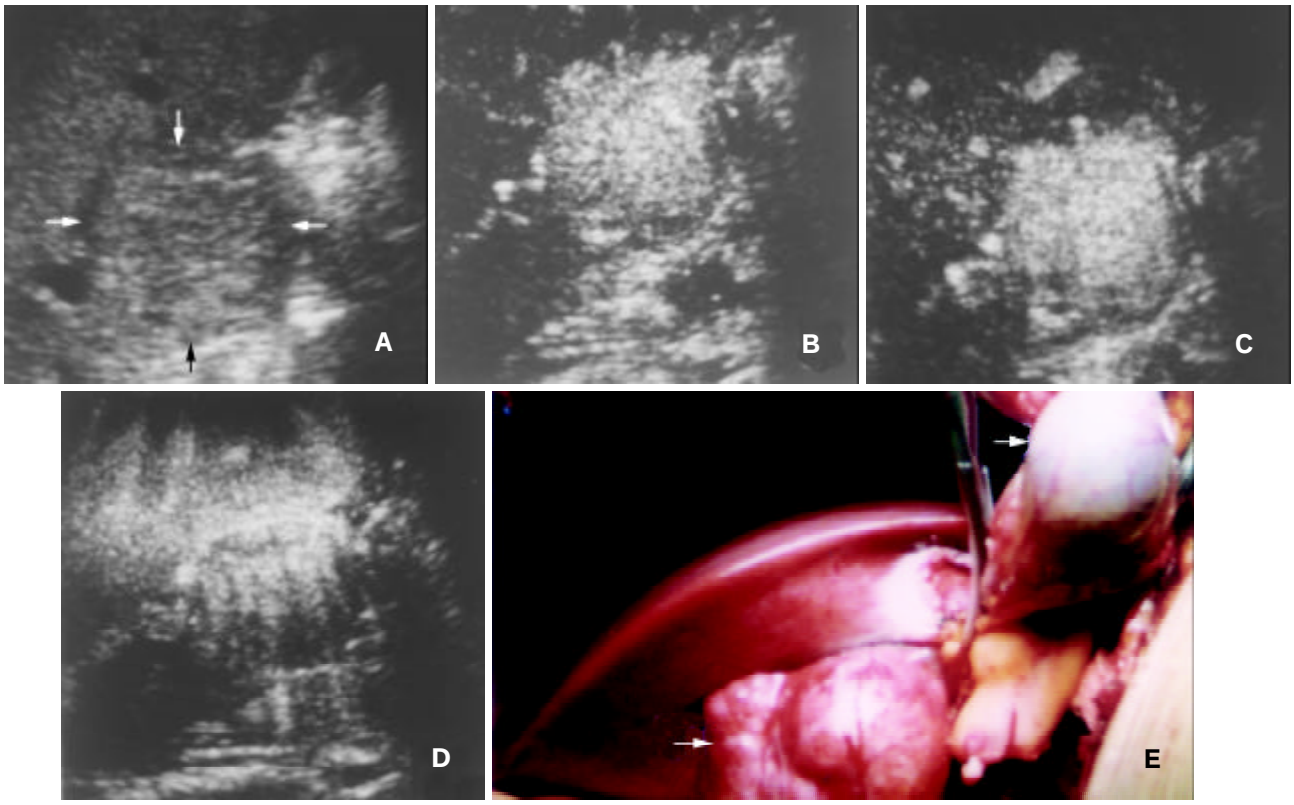

Figure 5 A 29-year-old man with focal nodular hyperplasia. A. Intercostal section of precontrast conventional sonography exhibits an isoechoic lesion (arrows) in segment V of the liver with a diameter of 4.8 cm. B-D. Contrast-enhanced C-cube gray scale sonography at 49 s (B) and 60 s (C) after injection of Levovist shows that intranodular signals enhance earlier than the liver parenchyma, and enhancement sustains in the portal venous phase until the delayed phase (140 s, D), suggestive of slow wash-out of contrast in the lesion. E. Appearance of the lesion and its surrounding organs in laparotomy. The lesion (arrow) protrudes from the liver with a smooth capsule while the gallbladder (arrowhead) is lifted with hemostatic forceps. Histopathology of the tumor revealed focal nodular hyperplasia.

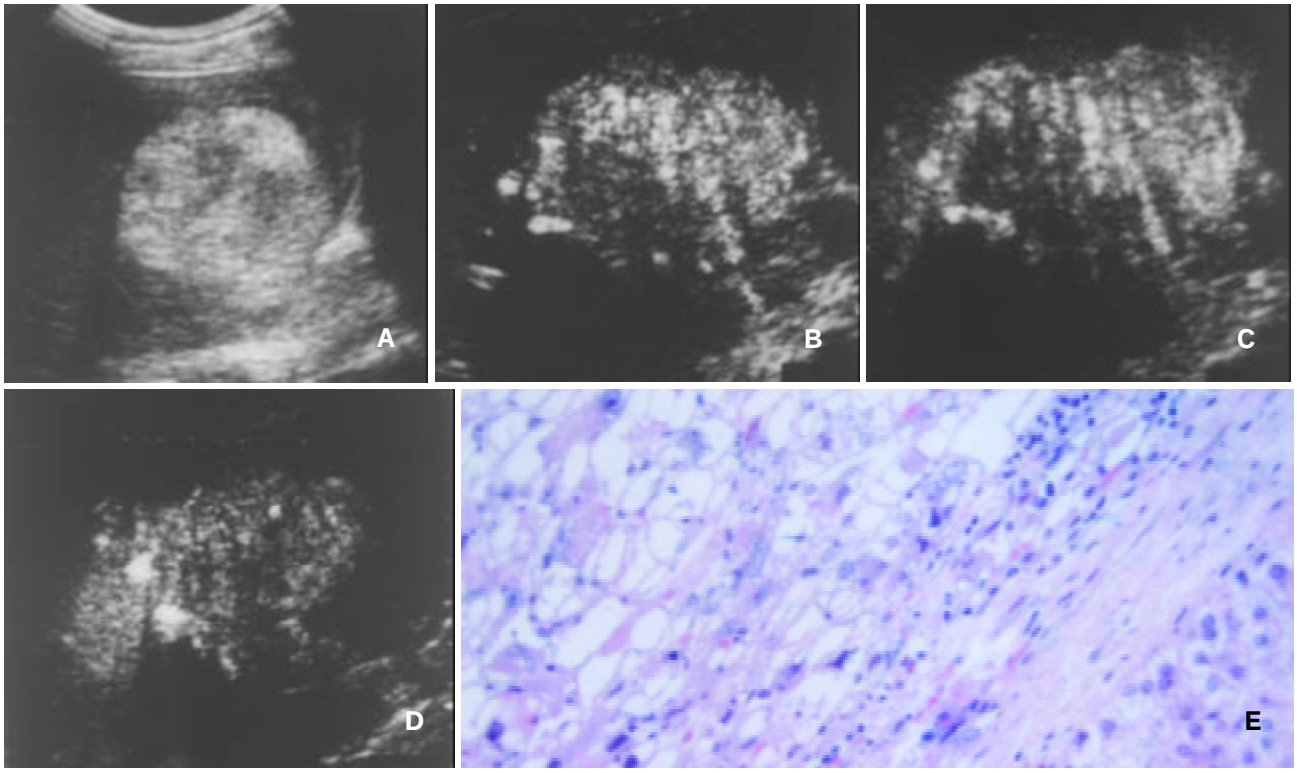

Figure 6 A 51-year-old female with angiomyolipoma. A. Subcostal section of precontrast conventional sonography exhibits a hyperechogenic lesion of 7.3 cm in diameter. B-D. Contrast-enhanced C-cube gray scale sonography at 54 s (B) and 110 s (C) after injection of Levovist shows that intranodular signals enhance earlier than the liver parenchyma with an inhomogenous enhancement pattern, and enhancement decreases in the delayed phase (206 s, D). E. Photomicrography shows defuse sheets of adipocytes and muscle cells adjacent to the noncirrhotic liver tissue, presenting a typical appearance of angiomyolipoma (HE 400).

Table 1 Hemodynamics of focal hepatic lesions on contrast-enhanced C-cube gray scale ultrasonography

Types of lesion	No. of lesions	Injection-enhancement delay time (mean±SD) (s)			Enhancement duration (mean±SD) (s)	
		Liver	Lesion	*P* Value	Lesion	*P* Value
Primary liver cancer	29	33±10	23±6	<0.05	69±33[b]	–
Metastasis	4	26±7	26±11	<0.05	59±22[c]	–
Hemangioma	8	36±8	48±12[a]	–	221±47	<0.05
Focal nodular hyperplasia	12	29±9	20±6	<0.05	196±96	<0.05
Angiomyolipoma	3	37±12	26±6	<0.05	177±90	<0.05

[a]The injection-enhancement delay time after administration of Levovist in hemangioma was significantly longer than that in other types of lesions ($P<0.05$). [b]The enhancement duration in primary liver cancer was significantly shorter than that in benign lesions ($P<0.05$). [c]The enhancement duration in metastasis was significantly shorter than that in benign lesions ($P<0.05$).

Table 2 Enhancement patterns of focal liver lesions in the arterial phase on contrast-enhanced C-cube gray scale ultrasonography

Enhancement patterns	Peripheral	Homogenous	Mosaic	Negative	Total
Primary liver cancer	1	16	12	0	29
Metastasis	2	0	2	0	4
Hemangioma	7	0	1	0	8
Focal nodular hyperplasia	0	12	0	0	12
Angiomyolipoma	0	1	2	0	3
Inflammatory pseudotumor	0	0	0	2	2
Total	10	29	17	2	58

Note: Values are number of lesions.

DISCUSSION

The characterization of focal liver lesions depends closely on their specific intranodular hemodynamics[11-14]. Various imaging modalities have been studied for demonstrating the typical vasculature of focal liver lesions. Contrast-enhanced US may be especially promising for depicting intranodular vascularity not only because of its easy performance, but also because of its particular advantages of providing dynamic flow information on a tomographic plane basis[4, 15, 16].

Levovist is the most widely used microbubble contrast agent for intravenous administration in the clinical setting. The backscatter signals caused by vibration or disruption of the microbubbles are received and used for image formation. Interval delay imaging or intermittent harmonic imaging[4, 16-19], which transmits an ultrasound beam with a flexible interval, destroys most of the microbubbles in a region of interest with high acoustic power, and permits refreshment of microbubbles in the scanning plane during the low acoustic power period due to fresh blood inflow. C-cube gray scale US is a newly available technique using interval delay scanning to destroy microbubbles in the scanning plane. With the help of the low acoustic power image on LOW state, we could obtain intranodular capillary flow signals on the same sonographic scanning plane. Moreover, a series of C^3-Mode images with microbubbles collapse provide dynamic information of enhancement patterns of focal liver lesions. Therefore, we could continuously observe the lesion of interest from the arterial phase to the delayed phase. The detailed enhancement process of each lesion could be obtained just as a single-level dynamic CT study[20]. In the present study, positive enhancement was detected in all focal liver lesions except for two IPT with complete necrosis. No false negative nodule was found on contrast-enhanced C-cube gray scale US.

The blood of normal liver is supplied both by the portal vein and by the hepatic artery, whereas the blood of most neoplastic tumors of the liver are supplied by the hepatic artery. The typical vascular patterns of PLC are high velocity signals on color Doppler US[21, 22], and high attenuation at the early phase and low attenuation at the portal venous phase relative to the liver parenchyma on dynamic CT[23]. In this study, the injection-enhancement delay time of PLC was shorter than that of the liver parenchyma after administration of Levovist, presenting an early enhancement at the arterial phase. As the portal venous phase arrived, the concentration of microbubbles in the hepatic artery decreased. We recorded the injection-decrease delay time of various focal liver lesions and found that the injection-decrease delay time of PLC was relatively shorter compared to benign liver lesions. The difference of enhancement duration between PLC and benign liver lesions was statistically significant ($P<0.05$). The hemodynamics of PLC was that, namely, it enhanced early in the arterial phase and washed out rapidly in the portal venous phase. These findings were highly corresponding to the appearance of PLC on contrast-enhanced dynamic CT[23-25].

As to intranodular enhancement patterns of PLC in the arterial phase, homogenous or mosaic enhancements were found in most lesions of PLC (96.7 %, 28/29), which were also found in other focal liver lesions.

Similarly, 4 liver matestases enhanced early in the arterial phase and the enhancement decreased rapidly in the portal venous phase, resulting in a shorter enhancement duration compared to benign liver lesions ($P<0.05$). This was probably due to their hemodynamics of mainly arterial blood supply. The enhancement patterns of metastases were peripheral or mosaic enhancements, which were also nonspecific and found in other liver lesions. Further study may be needed to clarify this results.

Hemangioma is usually rich in vessels with a sluggish blood circulation. After administration of a contrast agent, the enhancement of most hemangiomas on helical CT was a peripheral puddle pattern in the arterial phase and cotton wool sign in post vascular phase[25, 26]. On contrast-enhanced C-cube gray scale US, similarly, the injection-enhancement delay time of hemangioma was significantly longer compared to other types of focal liver lesions (Table 1). As the arterial phase ended, the

enhancement in hemangioma sustained and lasted over a long period. With respect to the enhancement patterns, peripheral enhancement was shown in most hemangiomas (87.5 %, 7/8). Since microbubbles were destroyed when they were imaged by ultrasound beam, intratumoral enhancement could not be obtained with C-cube gray scale US using 5-10 s interval transmission in relatively large hemangioma. Based upon our preliminary experience, we supposed that at least one minute of interval transmission would be needed to image the microbubbles in the center of hemangioma. The specific characteristics of hemangioma after administration of Levovist was that, in short, it enhanced slowly and mainly at the periphery of the lesion with a long period of enhancement.

Except hemangioma, other benign liver lesions including 12 FNHs and 3 angiomyolipomas demonstrated positive enhancement on contrast-enhanced C-cube gray scale US, presenting their hypervascular characteristics. These lesions enhanced early in the arterial phase and positive enhancement lasted over a long period until the delayed phase. Their enhancement duration was relatively longer compared to hepatic malignancies (P<0.05).

FNH is not a neoplasm but a hyperplastic response of liver parenchyma to the presence of a preexisting vascular malformation. FNH is a hypervascular lesion bypassing the portal venous system and exhibiting a varying degree of arteriovenous shunting[27]. On contrast-enhanced C-cube gray scale US, all FNH lesions showed early enhancement and appeared homogenously. In the portal venous and delayed phase, the intranodular enhancement was somewhat greater than that in the same-depth of surrounding liver parenchyma (Figure 5). The enhancement pattern of FNH seemed to be exclusively caused by arterial vascularization in the lesion, an absent capillary bed, and a vascular volume in excess of that of the normal liver[27-29].

Hepatic angiomyolipoma is a rare benign mesenchymal tumor, composed of a varying heterogenous mixture of three tissue components: blood vessels, smooth muscle and adipose cells. Most angiomyolipoma markedly enhanced with curved vessels in the arterial phase, and remained enhancement in the portal venous phase on spiral CT[30]. Its appearance on contrast-enhanced C-cube gray scale US was corresponding to that on helical CT. It enhanced inhomogenously because of the presence of the multiple ingredients within the lesion.

Contrast-enhanced C-cube gray scale US images microbubbles intermittently with a high mechanical index. This technique allows the detection of blood in the capillary bed, where the flow velocity is too low to be detected with Doppler US flow techniques. On the other hand, however, tumor vessel cannot be shown real-timely. It is because the microbubbles in small vessels (i.e. tumor vessels) cannot be detected with a low mechanical index on the LOW state, and real time C^3-Mode state with a high mechanical index breaks microbubbles when they are imaged. This is one limitation of C-cube gray scale US.

In conclusion, C-cube gray scale US with administration of Levovist can demonstrate dynamic intranodular enhancement in various focal hepatic lesions. The information provided by this methodology may be useful in the differential diagnosis of hepatic lesions on the basis of demonstrating characteristic appearances of various hepatic lesions. Additional study with a greater number of cases is in progress to gather additional data to support and replenish these results.

REFERENCES

1 **Calliada F**, Campani R, Bottinelli O, Bozzini A, Sommaruga MG. Ultrasound contrast agents basic principles. *Eur J Radiol* 1998; **27**(Suppl): S157-S160

2 **Kono Y**, Moriyasu F, Mine Y, Nada T, Kamiyama N, Suginoshita Y, Matsumura T, Kobayashi K, Chiba T. Gray-scale second harmonic imaging of the liver with galactose-based microbubbles. *Invest Radiol* 1997; **32**: 120-125

3 **Choi BI**, Kim TK, Han JK, Kim AY, Seong CK, Park SJ. Vascularity of hepatocellular carcinoma: assessment with contrast-enhanced second-harmonic versus conventional power Doppler US. *Radiology* 2000; **214**: 381-386

4 **Wilson SR**, Burns PN, Muradali D, Wilson JA, Lai X. Harmonic hepatic US with microbubble contrast agent: initial experience showing improved characterization of hemangioma, hepatocellular carcinoma, and metastasis. *Radiology* 2000; **215**: 153-161

5 **Maresca G**, Summaria V, Colagrande C, Manfredi R, Calliada F. New prospects for ultrasound contrast agents. *Eur J Radiol* 1998; **27**(Suppl): S171-S178

6 **Hosoki T**, Mitomo M, Chor S, Miyahara N, Ohtani M, Morimoto K. Visualization of tumor vessels in hepatocellular carcinoma. Power Doppler compared with color Doppler and angiography. *Acta Radiol* 1997; **38**: 422-427

7 **Blomley MJ**, Albrecht T, Cosgrove DO, Jayaram V, Eckersley RJ, Patel N, Taylor-Robinson S, Bauer A, Schlief R. Liver vascular transit time analyzed with dynamic hepatic venography with bolus injections of an US contrast agent: early experience in seven patients with metastases. *Radiology* 1998; **209**: 862-866

8 **Albrecht T**, Blomley MJ, Cosgrove DO, Taylor-Robinson SD, Jayaram V, Eckersley R, Urbank A, Butler-Barnes J, Patel N. Non-invasive diagnosis of hepatic cirrhosis by transit-time analysis of an ultrasound contrast agent. *Lancet* 1999; **353**: 1579-1583

9 **Bang N**, Nielsen MB, Rasmussen AN, Osterhammel PA, Pedersen JF. Hepatic vein transit time of an ultrasound contrast agent: simplified procedure using pulse inversion imaging. *Br J Radiol* 2001; **74**: 752-755

10 **Kim T**, Murakami T, Takahashi S, Tsuda K, Tomoda K, Narumi Y, Oi H, Sakon M, Nakamura H. Optimal phases of dynamic CT for detecting hepatocellular carcinoma: evaluation of unenhanced and triple-phase images. *Abdom Imaging* 1999; **24**: 473-480

11 **Kudo M**. Morphological diagnosis of hepatocellular carcinoma: special emphasis on intranodular hemodynamic imaging. *Hepatogastroenterology* 1998; **45**(Suppl 3): 1226-1231

12 **Koito K**, Namieno T, Morita K. Differential diagnosis of small hepatocellular carcinoma and adenomatous hyperplasia with power Doppler sonography. *AJR Am J Roentgenol* 1998; **170**: 157-161

13 **Brancatelli G**, Federle MP, Grazioli L, Blachar A, Peterson MS, Thaete L. Focal nodular hyperplasia: CT findings with emphasis on multiphasic helical CT in 78 patients. *Radiology* 2001; **219**: 61-68

14 **Kudo M**. Imaging diagnosis of hepatocellular carcinoma and premalignant / borderline lesions. *Semin Liver Dis* 1999; **19**: 297-309

15 **Kim TK**, Choi BI, Han JK, Hong HS, Park SH, Moon SG. Hepatic tumors: contrast agent-enhancement patterns with pulse-inversion harmonic US. *Radiology* 2000; **216**: 411-417

16 **Ding H**, Kudo M, Onda H, Suetomi Y, Minami Y, Maekawa K. Hepatocellular carcinoma: depiction of tumor parenchymal flow with intermittent harmonic power Doppler US during the early arterial phase in dual-display mode. *Radiology* 2001; **220**: 349-356

17 **Heckemann RA**, Cosgrove DO, Blomley MJ, Eckersley RJ, Harvey CJ, Mine Y. Liver lesions: intermittent second-harmonic gray-scale US can increase conspicuity with microbubble contrast material - early experience. *Radiology* 2000; **216**: 592-596

18 **Ding H**, Kudo M, Onda H, Suetomi Y, Minami Y, Maekawa K. Contrast-enhanced subtraction harmonic sonography for evaluating treatment response in patients with hepatocellular carcinoma. *AJR Am J Roentgenol* 2001; **176**: 661-666

19 **Hancock J**, Dittrich H, Jewitt DE, Monaghan MJ. Evaluation of myocardial, hepatic, and renal perfusion in a variety of clinical conditions using an intravenous ultrasound contrast agent (Optison) and second harmonic imaging. *Heart* 1999; **81**: 636-641

20 **Ueda K**, Matsui O, Kawamori Y, Nakanuma Y, Kadoya M, Yoshikawa J, Gabata T, Nonomura A, Takashima T. Hypervascular hepatocellular carcinoma: evaluation of hemodynamics with dynamic CT during hepatic arteriography. *Radiology* 1998; **206**: 161-166

21 **Gaiani S**, Casali A, Serra C, Piscaglia F, Gramantieri L, Volpe L, Siringo S, Bolondi L. Assessment of vascular patterns of small liver mass lesions: value and limitation of the different Doppler ultrasound modalities. *Am J Gastroenterol* 2000; **95**: 3537-3546

22 **Taylor KJ**, Ramos I, Carter D, Morse SS, Snower D, Fortune K. Correlation of Doppler US tumor signals with neovascular morphologic features. *Radiology* 1988; **166**(Pt 1): 57-62

23 **Lee HM**, Lu DS, Krasny RM, Busuttil R, Kadell B, Lucas J. Hepatic lesion characterization in cirrhosis: significance of arterial hypervascularity on dual-phase helical CT. *AJR Am J Roentgenol* 1997; **169**: 125-130

24 **Van Hoe LV**, Baert AL, Gryspeerdt S, Vandenbosh G, Nevens F, Van Steenbergen W, Marchal G. Dual-phase helical CT of the liver: value of an early-phase acquisition in the differential diagnosis of noncystic focal lesions. *AJR Am J Roentgenol* 1997; **168**: 1185-1192

25 **Nino-Murcia M**, Olcott EW, Jeffrey RB Jr, Lamm RL, Beaulieu CF, Jain KA. Focal liver lesions: pattern-based classification scheme for enhancement at arterial phase CT. *Radiology* 2000; **215**: 746-751

26 **Gryspeerdt S**, Van Hoe L, Marchal G, Baert AL. Evaluation of hepatic perfusion disorders with double-phase spiral CT. *Radio Graphics* 1997; **17**: 337-348

27 **Uggowitzer M**, Kugler C, Groll R, Mischinger HJ, Stacher R, Fickert P, Weiglein A. Sonographic evaluation of focal nodular hyperplasias (FNH) of the liver with a transpulmonary galactose-based contrast agent (Levovist). *Br J Radiol* 1998; **71**: 1026-1032

28 **Ruppert-Kohlmayr AJ**, Uggowitzer MM, Kugler C, Zebedin D, Schaffler G, Ruppert GS. Focal nodular hyperplasia and hepatocellular adenoma of the liver: differentiation with multiphasic helical CT. *AJR Am J Roentgenol* 2001; **176**: 1493-1498

29 **Miyayama S**, Matsui O, Ueda K, Kifune K, Yamashiro M, Yamamoto T, Komatsu T, Kumano T. Hemodynamics of small hepatic focal nodular hyperplasia: evaluation with single-level dynamic CT during hepatic arteriography. *AJR Am J Roentgenol* 2000; **174**: 1567-1569

30 **Yan F**, Zeng M, Zhou K, Shi W, Zheng W, Da R, Fan J, Ji Y. Hepatic angiomyolipoma: various appearances on two-phase contrast scanning of spiral CT. *Eur J Radiol* 2002; **41**: 12-18

Edited by Zhang JZ

P.O.Box 2345, Beijing 100023,China
Fax: +86-10-85381893
E-mail: wjg@wjgnet.com www.wjgnet.com

World J Gastroenterol 2003;9(8):1675-1678
World Journal of Gastroenterology
 ISSN 1007-9327

• LIVER CANCER •

Study on the possibility of insulin as a carrier of IUdR for hepatocellular carcinoma-targeted therapy

Xiao-Hong Ou, An-Ren Kuang, Xian Peng, Yu-Guo Zhong

Xiao-Hong Ou, An-Ren Kuang, Department of Nuclear Medicine, West China Hospital of Sichuan University, Sichuan Province, China
Xian Peng, Yu-Guo Zhong, Department of Pharmaceutical, Sichuan University, Sichuan Province, China
Supported by The National Natural Science Foundation of China, Grant No 30270415
Correspondence to: An-Ren Kuang, Department of Nuclear Medicine, West China Hospital of Sichuan University, Chengdu, China. ouxiaohong2002@xinhuanet.com
Telephone: +86-28-85422696 **Fax:** +86-28-85422696
Received: 2003-01-04 **Accepted:** 2003-02-17

Abstract

AIM: To evaluate the possibility of using insulin as a carrier for carcinoma-targeted therapy mediated by receptor, and to investigate the expression of insulin receptor in human hepatocellular carcinoma and the receptor binding characteristics of insulin-IUdR (iododeoxyuridine).

METHODS: IUdR was covalently conjugated to insulin. Receptor binding assays of ^{125}I-insulin to human hepatocellular carcinoma and its adjacent tissue were performed. Competitive displacements of ^{125}I-insulin by insulin and insulin-IUdR to bind to insulin receptor were respectively carried out. Statistical comparisons between the means were made with paired t-test at a confidence level of 95 %.

RESULTS: The data indicated that there were high- and low- affinity binding sites for ^{125}I-insulin on both hepatocellular carcinoma and its adjacent tissue. Hepatocellular carcinoma had a significantly higher Bmax for high affinity binding site than its adjacent liver tissue (P<0.05, t=2.275). Insulin-IUdR competed as effectively as insulin with ^{125}I-insulin for binding to insulin receptor. Values of $IC_{50}1$, $C_{50}2$, KI1 and KI2 for insulin-IUdR were 11.50±2.83 nmol·L^{-1}, 19.35±5.11 nmol·L^{-1}, 11.26±2.65 nmol·L^{-1} and 19.30±5.02 nmol·L^{-1} respectively, and for insulin were 5.01±1.24 nmol·L^{-1},17.75±4.86 nmol·L^{-1}, 4.85±1.12 nmol·L^{-1} and 17.69±4.81 nmol·L^{-1}, respectively. Values of $IC_{50}1$ and KI1 for insulin-IUdR were significantly higher than that for insulin (P<0.01, t=4.537 and 4.813).

CONCLUSION: It is possible to use insulin as a carrier for carcinoma-targeted therapy mediated by receptor.

Ou XH, Kuang AR, Peng X,Zhong YG. Study on the possibility of insulin as a carrier of IUdR for hepatocellular carcinoma-targeted therapy. *World J Gastroenterol* 2003; 9(8): 1675-1678
http://www.wjgnet.com/1007-9327/9/1675.asp

INTRODUCTION

Hepatocellular carcinoma is one of the most common cancers with highly uneven geographic distribution and its treatment by conventional methods is still difficult. In recent years receptor-based radiopharmaceuticals have been used for localization diagnosis and therapy of certain tumors[1-5]. Insulin may be a convenient carrier for anticancer drugs or radionuclides in targeted therapy of carcinoma, because several studies have shown there is an increased expression of insulin receptor on a variety of malignant tumor cells[6-11]. Moreover, insulin is internalized by cells possessing insulin receptor and reported in the cell nuclei subsequent to endocytosis[12-14].

S-iodo-z-deoxyuridine (IUdR), a thymidine analog, can be incorporated into the DNA of cells in the S phase. ^{125}I-IUdR has been successfully applied for the treatment of bladder cancer and hepatic metastases[15-18]. Short-range Auger electrons emitted by ^{125}I-IUdR can cause DNA double-strand broken and deliver a lethal radiation dose to the cell when it is incorporated into DNA. But when killing malignant cells, ^{125}I-IUdR also brings damage to normal tissues, such as the bone marrow, the small intestine and the large intestine. To reduce the damage, we presented a strategy for IUdR targeting delivery to hepatocellular carcinoma which exploited the efficiency and specificity of internalization afforded by the process of receptor-mediated endocytosis. IUdR was primarily used in this investigation, because it had the identical chemical and biological properties with ^{125}I-IUdR. The expression of insulin receptor in human hepatocellular carcinoma and the receptor binding characteristics of insulin-IUdR conjugate were investigated.

MATERIALS AND METHODS

Preparation of cell membrane

Hepatocellular carcinoma and its adjacent liver tissue specimens were obtained from six patients at surgery whose diagnosis was confirmed by histopathology and immediately frozen at -70 ℃ for further use. Cell membrane fractions were prepared according to established techniques[19]. Tissues were cut into pieces, put into Tris-HCL buffer (pH 7.5) and homogenized. The cell membrane fractions purified by centrifugation in a discontinuity sucrose density gradient were stored at -70 ℃. The protein concentration was determined according to Lowrry method[20].

Radioiodination of insulin

Porcine insulin was radioiodinated with the Ch-T method and purified by polyacrylamide gel electrophoresis. The radiochemical purity of ^{125}I-insulin was measured by TLC (thin layer chromatogray).

Preparation of insulin-IUdR

Insulin-IUdR was kindly synthesized by Department of Pharmaceutical, Sichuan University. Briefly, both IUdR (1.2 g) and succinic anhydride (1.5 g) were dissolved in 25 ml of pyridrine and the mixture was stirred at 70-80 ℃ for 24 hours. The solvents were evaporated under vacuum and the residue was crystallized from isopropanol.

Conjugation of IUdR-succinin to insulin was done as follows: IUdR-succinin (50 mg), EDC (100 mg) and HOBt (50 mg) were dissolved in 3 ml phosphate-buffered saline (pH=8.9) and mixed with 1 ml phosphate-buffered saline (pH=8.9) containing 25 mg insulin. The mixture was stirred at

4 ℃ for 48 hours. The precipitation was removed by filtration and pH of the solvent was adjusted to 5.5 with 0.5 mol· L^{-1} HCl. The reaction mixture was kept at 4 ℃ overnight. Thereafter, white solid precipitation was collected with filter and purified by polyacrylamine agarose gel electrophoresis. The solvents were evaporated under vacuum.

Isolated insulin-IUdR was analyzed by analytical HPLC (Beckman) with 4×200 mm ODS column. The mobile phase was 27 % (v/v) acetonitrile and 73 % 0.1 mol· L^{-1} NaH_2PO_4 (pH=0.3) at a flow rate of 0.5 ml· min^{-1}.

SDS-polyacrylamine gel electrophoresis (SDS-PAGE) was performed in 15 % polyacrylamine gel to calculate the molecular weight of insulin-IUdR.

Saturation binding assay

Cell membrane fractions (80 μg protein) of hepatocellular carcinoma or its adjacent liver tissue were incubated for 20 hours at 4 ℃ with binding buffer (NaCl 118 mmol· L^{-1} $CaCl_2$ 1.3 mmol· L^{-1} KCl 5 mmol· L^{-1} $MgSO_4$ 1.2 mmol· L^{-1} KH_2PO_4 1.2 mmol· L^{-1} pH 7.5) containing increasing concentration (5×10^3-5×10^5 cpm) of ^{125}I-insulin. The free ligands were removed by centrifugation at 2 000×g for 10 minutes after addition of 0.1 ml 0.3 % bovine γ-globulin and 0.8 mL 15.8 % PEG. Radioactivity of the membrane pellets was determined in a gamma counter for one minute as the total binding. The nonspecific binding was estimated by incubating membrane with ^{125}I-insulin in the presence of 4.3 nmol unlabeled insulin. Specific binding was obtained by subtracting nonspecific binding from total binding.

Competition binding assay

Cell membrane fractions (80 μg protein) were incubated with 5 nmol ^{125}I-insulin in the presence of increasing concentrations (10^{-12}-10^{-7} mol/L) of the unlabeled insulin or insulin-IUdR. After incubated for 20 hours at 4 ℃, the unbound ligands were removed as saturation binding assay. Radioactivity of the membrane pellets was determined in a gamma counter for one lmin as the total binding. The nonspecific binding was estimated by incubating membrane with ^{125}I-insulin in the presence of 4.3 nmol unlabeled insulin.

Statistical analysis

Binding data were calculated on a computer with receptor binding analysis software. Values are presented as means ±SD. Statistical comparisons between the means were made with paired *t*-test at a confidence level of 95 %.

RESULTS

Radioiodination of insulin

The radiochemical purity of ^{125}I-insulin was 98 % and remained over 95 % after 14 days stored at -20 ℃.

Analysis of insulin-IUdR

The recovery of insulin-IUdR was about 76.3 %. HPLC showed that isolated insulin-IUdR (retention time 13.91 min) yield was about 98 % (shown in Figure 1). The other 2 % was the insulin (8.81 min) and IUdR (3.87 min).

The calculated molecular weight of insulin-IUdR was 7179Da according to its relative position to the molecular weight marker in the SDS-PAGE pattern.

Saturation binding assay

For cell membrane of hepatocellular carcinoma and its adjacent tissue, as concentration of the radioligand increased, binding amount went up and then plateaued rapidly (Figure 2). The Scatchard plot corresponding to the saturation binding curve had a slightly curvilinear shape (Figure 3). Curvilinear Scatchard plots were characteristic of insulin binding in many other systems and had been attributed to interaction of ligand with two or more classes of sites that exhibited different affinities. Using the RBA software, the Scatchard plot of hepatocellular carcinoma could be resolved in a component with Kd=2.20 nmol· L^{-1} (Bmax=0.36 nmol/L) and another component with Kd=18.8 nmol· L^{-1} (Bmax=1.58 nmol· L^{-1}) by the computer. And that of adjacent tissue could be resolved in a component with Kd=2.21 nmol· L^{-1} (Bmax=0.33 nmol· L^{-1}) and another component with Kd=17.89 nmol· L^{-1} (Bmax=1.09 nmol· L^{-1}). Remarkably higher Bmax of high affinity insulin binding sites was identified in hepatocellular carcinoma (P<0.05).

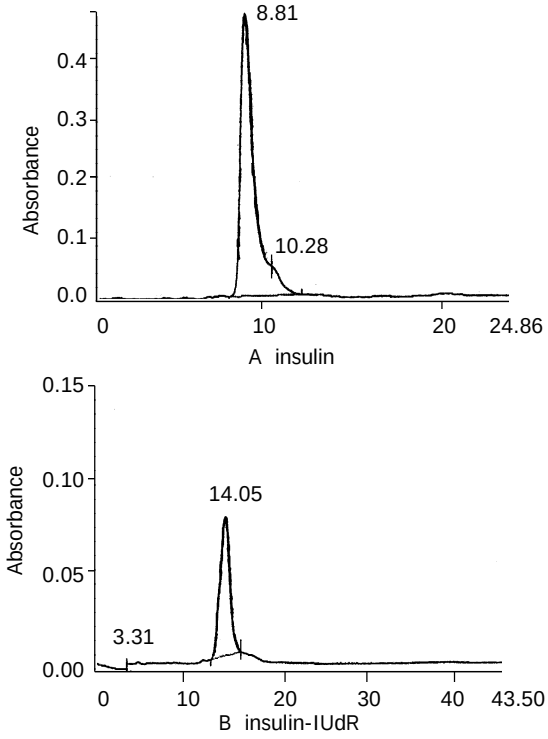

Figure 1 Insulin and insulin-IUdR analysis by HPLC. Retention time of insulin was 8.81 minutes (A); Retention time of insulin-IUdR was 13.91 minutes (B).

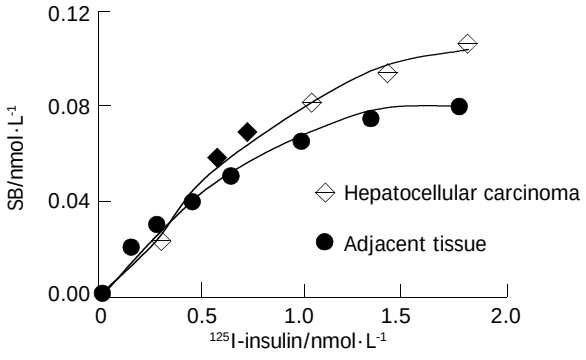

Figure 2 Saturation binding curves of ^{125}I-insulin in hepatocellular carcinoma and its adjacent tissue.

Competition binding assay

Competition displacement assays compared the ability of insulin-IUdR and unlabeled insulin to compete with ^{125}I-insulin for binding to insulin receptor in hepatocellulor carcinoma (Figure 4). The conjugate competed as effectively as insulin for binding to the insulin receptor in a dose-dependent manner. IUdR had no effect on ^{125}I-insulin binding (data not shown). Values of IC_{50} and KI for insulin-IUdR and insulin are shown

in Table 2. Although there were increased $IC_{50}1$ and KI1, the data showed that most of the receptor-binding activity of insulin-IUdR remained.

Table 1 Values of Bmax and Kd of ^{125}I-insulin binding to insulin receptor in hepatocellular carcinoma and its adjacent liver tissue (mean ±SD for six identical experiments)

	High affinity sites		Low affinity sites	
	Bmax (nmol·L^{-1})	Kd (nmol·L^{-1})	Bmax (nmol·L^{-1})	Kd (nmol·L^{-1})
Hepatocellular carcinoma	1.58±0.16[a]	2.20±0.66	0.36±0.11	18.80±7.85
Adjacent liver tissue	1.09±0.51	2.21±0.72	0.33±0.74	17.89±7.87

[a]P<0.05 *vs* adjacent liver tissue. Bmax was the maximal amount of ligand bound; Kd was the dissociation constant of the binding site for the ligand.

Table 2 Values of IC_{50} and KI for insulin-IUdR and insulin competing with ^{125}I-insulin for binding to insulin receptor on hepatocellular carcinoma (mean ±SD for four identical experiments)

	High affinity sites		Low affinity sites	
	IC_{50} (nmol·L^{-1})	KI (nmol·L^{-1})	IC_{50} (nmol·L^{-1})	KI (nmol·L^{-1})
Insulin-IUdR	11.50±2.83[b]	11.26±2.65[b]	19.35±5.11	19.30±5.02
Insulin	5.01±1.24	4.85±1.12	17.75±4.86	17.69±4.81

[b]P<0.01 *vs* insulin. IC_{50} was the concentration of competing ligand to displace radioligand binding by 50 %; KI was the dissociation constant of competing ligand.

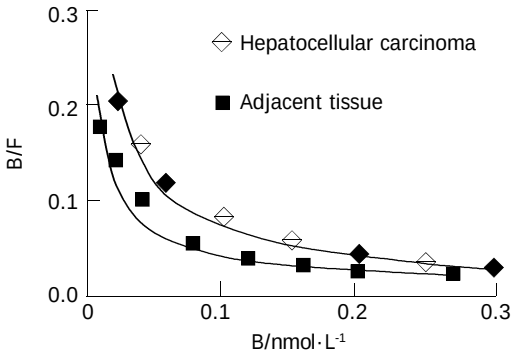

Figure 3 The Scatchard plot corresponding to the saturation binding.

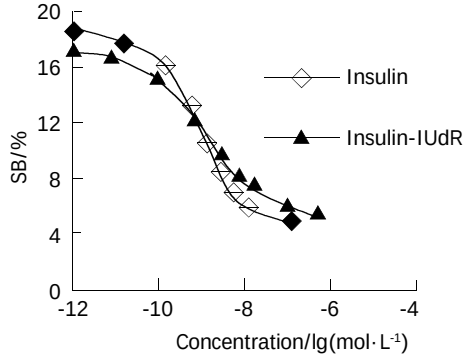

Figure 4 Competitive binding curves of ^{125}I-insulin against insulin-IUdR or insulin.

DISCUSSION

In recent years, there have been several studies on target delivery of specific gene to living cells mediated by insulin receptor. For example, Ivanova *et al* introduced a foreign DNA into early mouse and rabbit embryos by using insulin as a carrier[21], and Alexder carried out transfection of H-11 murine epithelial mammary cells as well as murine and sheep mammary glands using insulin-containing constructs that deliver DNA by receptor-mediated endocytosis[22]. Sosenkranz *et al* synthesized a soluble construct consisting of a plasmid carrying the gene of SV40 large T-antigen and an insulin-poly-L-lysine conjugate which is able to selectively transfect PLC/PRF/S human hepatoma cells possessing insulin receptors[23]. Moreover, Zhang *et al* measured the levels of luciferase gene expression in human or rat glioma cells after targeting the PIL-encapsulated plasmid DNA via human insulin receptor, the human epidermal growth factor receptor, or rat transferrin receptor. The highest levels of gene expression were obtained after targeting the insulin receptor, and this may derive from the nuclear targeting properties of this receptor system[24].

In the present study, we presented a procedure for tumor treatment which combined the targeted transportation function afforded by insulin receptor mediating endocytosis with radiotoxicity of ^{125}I-IUdR to cells at the S phase. IUdR is usually administrated by local infusion or intratumor injection. Systemic therapy is not indicated because of potential severity of undesirable side effects. Insulin used as a carrier might offer an advantage in this aspect. Firstly, most of ^{125}I-IUdR is directly delivered into the liver by insulin. Thereby, other actively dividing normal tissue can efficiently avoid being damaged. Secondly, because of overexpression of insulin receptor in tumor cells, there will be very little conjugate entering normal liver cells. At last, Auger electron' s range is about 10 nm, it is hardly harmful to cells until it is incorporated in the DNA of cells. Since IUdR can only be incorporated in the DNA of cells at the S phase[25], non-dividing tissues possessing insulin receptor will not be injured.

We found that hepatocellular carcinoma bound more ^{125}I-insulin than its adjacent liver tissue. Amir kurtaran has successfully applied ^{123}I-insulin for *in vivo* scintigraphy in the diagnosis of hepatocellular carcinoma[26]. Kuang Anren reported that ^{131}I-insulin was localized within H22 hepatoma in mice, and cleared rapidly from the rest of the body[27]. Schars reported that insulin receptor might play a role in the regulation of hepatocellular carcinoma[28]. Our finding was consistent with theirs. The results demonstrated that escalated binding site for ^{125}I-insulin was expressed in hepatocellular carcinoma. The Bmax values indicated that the increased binding of ^{125}I-insulin in hepatocellular carcinoma was due to an apparent increase in high affinity insulin receptor rather than an increase in low affinity insulin receptor. Our studies also showed that high affinity insulin receptor, constituting 87.72 % of insulin receptor on cell surface of hepatocellular carcinoma, predominated over low affinity insulin receptor. These observations indicated that more IUdR covalently linked to insulin could be transferred to the carcinoma through mediation of the overexpressed high affinity insulin receptor.

It has also been verified in *in vitro* studies that insulin-IUdR is capable of binding specifically to insulin receptor in human hepatocellular carcinoma with high affinity. Chakrabarti *et al* conjugated ^{125}I-IUdR with T101 antibody via polylysine, but the conjugate remained only 68 % immunoactivity[29]. The conjugate used was prepared by covalently linking IUdR to insulin via succine. This complex has an advantage over the conjugate linked via poly-L-lysine[30] or albumin[31] or other large molecules. Both succine and IUdR are small molecules. The small size of the complex may result in less interference in insulin binding to its receptor or other cellular proteins and may permit this complex to be processed intracellularly in a manner more identical to that of unlabelled insulin.

Why insulin-IUdR has an increased IC_{50} and KI for high affinity insulin receptor but not for low affinity receptor is unclear. It is possible that the functional sites of structural microheterogeneity in the two receptors have different sensitivity to the structural change of ligand. Competition binding assays showed that insulin-IUdR still maintained the greater part of affinity for insulin receptor. Therefore, it is not necessary to administer insulin-IUdR in a micromolar range, which may result in glucopenia.

SDS-polyacrylamine agarose gel electrophoresis showed the molecular weight of insulin-IUdR was 7 179 Da, which was equal to the total weight of one molecule of insulin (M_r=5 800 Da) and three molecules of IUdR (M_r=454 Da). It might be concluded that the ratio of insulin molarity to the IUdR is 1:3. On the basis of this molar ratio, it is calculated that for administration 100-300 MBq ^{125}I-IUdR, about 10^{-9}mol insulin was required. Administration of such a low dose of insulin in therapy would not result in glucopenia.

In summary, hepatocellular carcinoma overexpressing insulin receptor and insulin-IUdR conjugate can specifically bind to insulin receptor. This new conjugate holds promise for therapy of hepatocellular carcinoma, but further investigation into transportation of IUdR and its interactions with tumor cells during subsequent intracellular processing would be a desirable prerequisite.

REFERENCES

1 **Menda Y**, Kahn D. Somatostatin receptor imaging of non-small cell lung cancer with 99mTc depreotide. *Semin Nucl Med* 2002;**32**: 92-96

2 **Virgolini** I, Traub T, Novotny C, Leimer M, Fuger B, Li SR, Patri P, Pangerl T,Angelberger P, Raderer M, Andreae F, Kurtaran A, Dudczak R. New trends in peptide receptor radioligands. *Q J Nucl Med* 2001; **45:** 153-159

3 **Rao PS**, Thakur ML, Pallela V, Patti R, Reddy K, Li H, Sharma S, Pham HL, Diggles L, Minami C, Marcus CS. 99mTc labeled VIP analog: evaluation for imaging colorectal cancer. *Nucl Med Biol* 2001; **28**: 445-450

4 **Thakur ML**, Marcus CS, Saeed S, Pallela V, Minami C, Diggles L, Le Pham H, Ahdoot R, Kalinowski EA. 99mTc-labeled vasoactive intestinal peptide analog for rapid localization of tumors in humans. *J Nucl Med* 2000; **41**: 107-110

5 **Heppeler A**, Froidevaux S, Eberle AN, Maecke HR. Receptor targeting for tumor localisation and therapy with radiopeptides. *Curr Med Chem* 2000; **7**: 971-994

6 **Kalli KR**, Falowo OI, Bale LK, Zschunke MA, Roche PC, Conover CA. Functional insulin receptors on human epithelial ovarian carcinoma cells:implications for IGF-II mitogenic signaling. *Endocrinology* 2002; **143**: 3259-3267

7 **Vella V**, Sciacca L, Pandini G, Mineo R, Squatrito S, Vigneri R, Belfiore A. The IGF system in thyroid cancer: new concepts. *Mol Pathol* 2001; **54**: 121-124

8 **Maune S**, Gorogh T. Detection of overexpression of insulin receptor gene in laryngeal carcinoma cells by using differential display method. *Laryngorhinootologie* 2000; **79**: 438-441

9 **Spector SA**, Olson ET, Gumbs AA, Friess H, Buchler MW, Seymour NE. Human insulin receptor and insulin signaling proteins in hepatic disease. *J Surg Res* 1999; **83**: 32-35

10 **Frittitta L**, Vigneri R, Stampfer MR, Goldfine ID. Insulin receptor overexpression in 184B5 human mamary epithelial cells induces a ligand-dependent transformed phenotype. *J Cell Biochem* 1995; **57**: 666-669

11 **Freund GG**, Kulas DT, Way BA, Mooney RA. Functional insuln and insulin-like growth factor-1 receptors are preferentially expressed in multiple myeloma cell lines as compared to B-lymphoblastoid cell lines. *Cancer Res* 1994; **54**: 3179-3185

12 **Shah N**, Zhang S, Harada S, Smith RM, Jarett L. Electron microscopic visualization of insulin translocation into the cytoplasm and nuclei of intact H35 hepatoma cells using covalently linked nanogold-insulin. *Endocrinology* 1995; **136**: 2825-2835

13 **Harada S**, Smith RM, Smith JA, Jarett L. Inhibition of insulin-degrading enzyme increases translocation of insulin to the nucleus in H35 rat hepatoma cells: evidence of a cytosolic pathway. *Endocrinology* 1993; **132**: 2293-2298

14 **Harada S**, Loten EG, Smith RM, Jarett L. Nonreceptor mediated nuclear accumulation of insulin in H35 rat hepatoma cells. *J Cell Physiol* 1992; **153**: 607-613

15 **Chiou RK**, Dalrymple GV, Baranowska-Kortylewicz J, Holdeman KP, Schneiderman MH, Harrison KA, Taylor RJ. Tumor localization and systemic absorption of intravesical instillation of radio-iodinated iododeoxyuridine in patients with bladder cancer. *J Urol* 1999; **162**: 58-62

16 **Morgan RJ Jr**, Newman EM, Doroshow JH, McGonigle K, Margolin K, Raschko J, Chow W, Somlo G, Leong L, Tetef M, Shibata S, Hamasaki V, Carroll M, Vasilev S, Akman S, Coluzzi P, Wagman L, Longmate J, Paz B, Yen Y, Klevecz R. Phase I trial of intraperitoneal iododeoxyuridine with and without intravenous high-dose folinic acid in the treatment of advanced malignancies primarily confined to the peritoneal cavity: flow cytometric and pharmacokinetic analysis. *Cancer Res* 1998; **58**: 2793-2800

17 **Sondak VK**, Robertson JM, Sussman JJ, Saran PA, Chang AE, Lawrence TS. Preoperative idoxuridine and radiation for large soft tissue sarcomas: clinical results with five-year follow-up. *Ann Surg Oncol* 1998; **5**: 106-112

18 **Daghighian F**, Humm JL, Macapinlac HA, Zhang J, Izzo J, Finn R, Kemeny N, Larson SM. Pharmacokinetics and dosimetry of iodine-125-IUdR in the treatment of colorectal cancer metastatic to liver. *J Nucl Med* 1996; **37**(Suppl 4): 29s-32s

19 **Yan XQ**, Cheng ML, Liu BW, Lan TH. Study on binding assay of insulin receptor in liver cell membrane. *Zhonghua Heyixue Zazhi* 1986; **6**: 91-93

20 **Cheng YQ**. Shengwu huaxue shiyan fangfa he jishu.1. Beijing: *Science Press* 2002: 164-166

21 **Ivanova MM**, Rosenkranz AA, Smirnova OA, Nikitin VA, Sobolev AS, Landa V, Naroditsky BS, Ernst LK. Receptor-mediated transport of foreign DNA into preimplantation mammalian embryos. *Mol Reprod Dev* 1999; **54**: 112-120

22 **Sobolev AS**, Rosenkranz AA, Smirnova OA, Nikitin VA, Neugodova GL, Naroditsky BS, Shilov IN, Shatski IN, Ernst LK. Receptor mediated transfection of murine and ovine mammary glands *in vivo*. *J Biol Chem* 1998; **273**: 7928-7933

23 **Rosenkranz AA**, Yachmenev SV, Jans DA, Serebryakova NV, Murav'ev VI, Peters R, Sobolev AS. Receptor-mediated endocytosis and nuclear transport of a transfecting DNA construct. *Exp Cell Res* 1992; **199**: 323-329

24 **Zhang Y**, Boado RJ, Pardridge WM. Marked enhancement in gene expression by targeting the human insulin receptor. *J Gene Med* 2003; **5**: 157-163

25 **Toyohara J**, Hayashi A, Sato M, Tanaka H, Haraguchi K, Yoshimura Y, Yonekura Y, Fujibayashi Y. Rationale of 5-^{125}I-iodo-4'-thio-2'-deoxyuridine as a potential iodinated proliferation marker. *J Nucl Med* 2002; **43**: 1218-1226

26 **Kurtaran A**, Li SR, Raderer M, Leimer M, Muller C, Pidlich J, Neuhold N, Hubsch P, Angelberger P, Scheithauer W, Virgolini I. Technetium-99m-galactosyl- neoglycoal bumin combined with iodine-123Tyr (A14) insulin visualized human hepatocellular carcinomas. *J Nucl Med* 1995; **36**: 1875-1881

27 **Kuang AR**, Zhou LY, Liang ZL, Tan TZ, Wang CJ. Evaluation of hepatoma targeting ability with radioiodiated insulin in H22 bearing mice. *Zhonghua Heyixue Zazhi* 1999; **19**: 179-180

28 **Scharf JG**, Dombrowski F, Ramadori G. The IGF axis and hepatocarcinogenesis. *Mol Pathol* 2001; **54**: 138-144

29 **Chakrabarti MC**, Paik CH, Carrasquillo JA. Preparation and *in vitro* studies of [125I]IUDR-T101 antibody conjugate. *Cancer Biother Radiopharm* 1999; **14**: 91-98

30 **Wagner E**, Ogris M, Zauner W. Polylysine-based transfection systems utilizing receptor-mediated delivery. *Adv Drug Deliv Rev* 1998; **30**: 97-113

31 **Huckett B**, Ariatti M, Hawtrey AO. Evidence for targeted gene transfer by receptor-mediated endocytosis. Stable expression following insulin-directed entry of NEO into HepG2 cells. *Biochem Pharmacol* 1990; **40**: 253-263

Edited by Xu XQ and Zhu LH

P.O.Box 2345, Beijing 100023,China
Fax: +86-10-85381893
E-mail: wjg@wjgnet.com www.wjgnet.com

World J Gastroenterol 2003;9(8):1679-1682
World Journal of Gastroenterology
 ISSN 1007-9327

• LIVER CANCER •

Assessment of hepatic VX2 tumors of rabbits with second harmonic imaging under high and low acoustic pressures

Wen-Hua Du, Wei-Xiao Yang, Xiang Wang, Xiu-Qin Xiong, Yi Zhou, Tao Li

Wen-Hua Du, Wei-Xiao Yang, Xiang Wang, Xiu-Qin Xiong, Yi Zhou, Tao Li, Department of Ultrasonography, Daping Hospital and Research Institute of Surgery, the Third Military Medical University, Chongqing 400042, China
Supported by the National Natural Science Foundation of China, No. 30070227
Correspondence to: Wen-Hua Du, Department of Ultrasonography, Daping Hospital and Research Institute of Surgery, the Third Military Medical University, Chongqing 400042, China. duwenhua001@163.com
Telephone: +86-23-68757441
Received: 2002-10-08 **Accepted:** 2003-02-11

Abstract

AIM: To investigate the possible clinical application value of second harmonic imaging under low acoustic pressure.

METHODS: Six New Zealand rabbits, averaging 2.7±0.4 kg, were selected and operated upon to construct hepatic VX2 tumor carrier model. Hepatic VX2 tumors were imaged with B mode Ultrasonography (US), and second harmonic imaging (SHI) under high mechanic index (1.6) and low mechanic index (0.1). Echo agent was intravenously injected through ear vein at a dose of 0.01 mL/kg under B mode US and high MI SHI, and 0.05 mL/kg under low MI SHI, and then the venous channel was cleaned with sterilized saline. All the images were recorded by magnetic optics (MO), and they were analyzed further by at least two independent experienced sonographers.

RESULTS: Totally 6 hypoechoic and 3 hyperechoic lesions were found in the six carrier rabbits with a mean size about 2.1±0.4 under B mode ultrasound, they were oval or round in shape with a clear outline or a hypoechoic halo at the margin of the lesions. Contrast agent could not change the echogenicity of the lesions under B mode US and SHI under high acoustic pressure. However, it could greatly increase the real time visualization sensitivity of the lesions with SHI under low acoustic pressure.

CONCLUSION: Our results suggest that contrast enhanced SHI with low MI and a bubble non-destructive method would be much more helpful than conventional SHI in our future clinical applications.

Du WH, Yang WX, Wang X, Xiong XQ, Zhou Y, Li T. Assessment of hepatic VX2 tumors of rabbits with second harmonic imaging under high and low acoustic pressures. *World J Gastroenterol* 2003; 9(8): 1679-1682
http://www.wjgnet.com/1007-9327/9/1679.asp

INTRODUCTION

Second harmonic imaging (SHI) technique has been shown more valuable than conventional B mode ultrasonography (US). SHI involves transmitting at frequency *f* and receiving at frequency *2f*, and the contrast enhanced echoes can therefore be obtained at second harmonic frequency because of the non-linear motion of the gas bubbles when destroyed by high acoustic pressures[1,2]. However, the use of second harmonic technique under high acoustic pressure (mechanical indexes 0.6-1.2) does not usually provide ideal images because of the short duration of enhancement and no quantitative evaluation and other technical difficulties. To avoid this, new dedicated software operating at low acoustic pressure (mechanical index <0.4) has been demonstrated to produce significant harmonic answer together with a real time imaging based on the maintenance of microbubbles. Only very small amount of microbubbles would allow the evaluation of blood flow volume and blood flow in normal and pathologic tissues. Liver image has been recently proven to be the first area where microbubbles manifest similarly to that of computed tomography or magnetic resonance imaging contrast media. In particular, this technique, applied to the evaluation of perfusional pattern of hepatic mass lesions, provides a significant contribution to their detection and characteristics. In this study, we aimed to find out the features of these two ultrasonographic methods in the depiction of hepatic metastasis.

MATERIALS AND METHODS

Preparation of animal models

Six New Zealand rabbits weighing 2.6-3.2 kg, average 2.7±0.4 kg, were anaesthetized by Sumianxin (a product of the Changchun Argo-Pastoral University) at 0.2 mL/kg through intramuscular injection. Hairs over the abdominal region were moulted by 8 % sodium sulfide, then the region was cleaned by saline water. Median incision right beneath the metasternum was made to expose the right lobe of liver. A tunnel about 3 cm deep at the lobe was constructed with an ophthalmic nipper. Viable VX2 tumor masses about 2-3 mm^3 were implanted into the tunnel, locally stanched and then each layer of the abdominal wall was sutured accordingly. 2 or 3 weeks later, these rabbits were ready for use. VX2 tumor is a kind of skin squamous cancer induced by Shope virus, viable VX2 tumor could be transplanted and underwent passages in the New Zealand rabbits, and therefore was used as mimicking metastatic hepatic tumor models.

Preparation of echo contrast agent

Self made echo contrast agent was made from 5 % (g/L) human albumin and 40 % (g/L) Dextran at a ratio of 1:3 (v/v), the mixture was then undergone electromechanical sonication (Sonication machine JY92-2D was manufactured by Ninbo Xinzhi Research Institute) for 90 seconds under mechanical energy of 280 W. During the sonication process, perfluropropane gas was mixed into the mixture. Microbubbles manufactured in this way were counted by a Coulter counter, at a concentration of 1.6×10^9 bubbles/L averaging 4.3±2.1 μm.

Equipment

A transducer S8 connected to HP-5500 ultrasound system was used, second harmonic imaging was transmitted at frequency 3MHz receiving at frequency 6 MHz, conventional mechanic index was tuned to 1.6, while low mechanic index was tuned

to 0.1. During the whole process of experiment, the image depth, compensation and TGC should be kept constant.

Methods

Hepatic VX2 tumors were imaged with conventional B mode US, and second harmonic imaging (SHI) under conventional mechanic index (1.6) and low mechanic index (0.1). An intravenous bolus echo agent was injected through ear vein at a dose of 0.01 mL/kg under conventional B mode US and high acoustic pressure SHI, and 0.05 mL/kg under low acoustic pressure SHI, and then the venous channel was cleaned with sterilized saline. All the images were recorded real-timely by magnetic optics (MO), and they were analyzed further by at least two independent but experienced sonographers.

RESULTS

Features of VX2 tumor under conventional and harmonic B mode US

A total of 6 hypoechoic and 3 hyperechoic lesions were found in the six carrier rabbits with a mean size of 2.1±0.4 cm under conventional B mode ultrasound, no hyperechoic or iso echoic lesions were found. They were oval or round in shape with a clear outline or a hypoechoic halo at the margin of the lesions. Contrast images under conventional B mode US also showed no improvement at all (Figure 1).

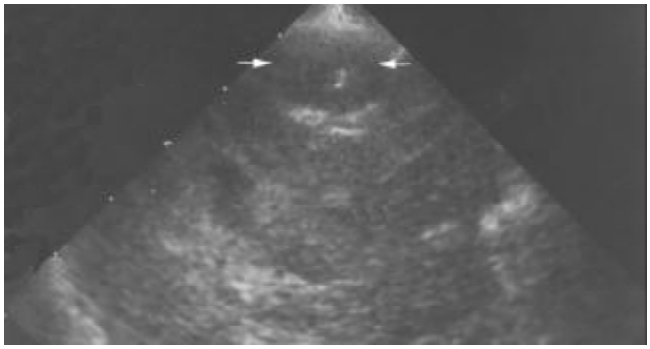

Figure 1 Image of VX2 tumor lesion under conventional B mode US. Arrow indicated the VX2 tumor lesion at the anterior part of the right lobe. It was oval and hypoechoic with a small hyperechoic scar at the center of the lesion.

VX2 tumor lesions assessed by SHI under high and low acoustic pressures

SHI under high acoustic pressure (Mechanic index 1.6) could reveal a short duration enhancement of the hepatic arteries and tumor lesions at the early phase, and an enhancement of the liver parenchyma and a decreased echo at the later phase. A pronounced arterial enhancement was also found at one side of the lesion, which might be considered as the nutrient artery of the tumor. In addition, branches of the afferent artery were seen at the same time. Interestingly, a branch vessel was also found coming from the same artery going to the other side of the lesion as shown in Figure 2a. The whole process of contrast enhanced SHI under high acoustic pressure lasted only for a few seconds.

Visualization by second harmonic imaging under low acoustic pressure was quite different from that by SHI under low acoustic pressure. The echogenicity of liver parenchyma and hepatic VX2 tumor lesions was extremely low, and no structures were observable at first. About five seconds after injection of contrast agent, image of the inferior vena cava could be observed. Again about fifteen seconds later, the contrast agent could be observed within the tumor lesion, as time went by, the afferent artery and its branches of the lesion could gradually and clearly be visualized. A suspicious branch artery was also observed going to the other side of the lesion near the afferent vessels, as what we observed by second harmonic imaging under high acoustic pressure (Figure 2b). As the contrast agent accumulated in the lesion, VX2 tumor appeared as a hyperechoic contour and even satellite lesions could also be observable just beside the original lesion (Figure 3). About 40 seconds later, arteries in the liver parenchyma gradually appeared markedly, and about 20 to 30 seconds afterwards the portal venous system could be visualized. At this stage, the tumor lesion was revealed as hypoechoic. During the last stage period, about 2 minutes after injection of contrast agent, the echogenicity of the liver parenchyma became hyperechoic, while the tumor lesion and its satellite lesion became typically hypoechoic. The whole process of visualization by second harmonic imaging under low acoustic pressure lasted for almost four minutes.

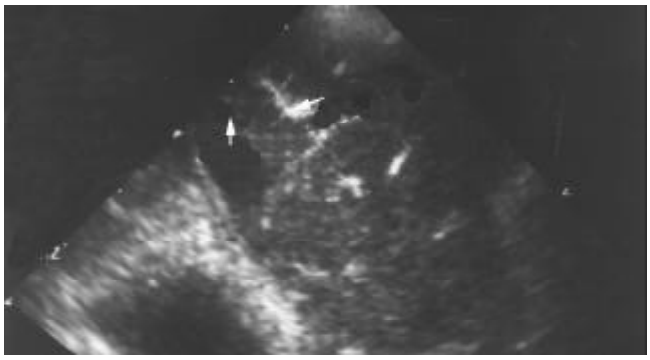

Figure 2a Image of VX2 tumor lesion under high MI second harmonic imaging. Arrow indicated the nutrient artery of same VX2 tumor lesion, and the suspicious artery of a satellite lesion.

Figure 2b Contrast enhanced second harmonic image under low MI revealed the enhancement of nutrient arteries of VX2 tumor lesion and the nutritive artery of satellite lesion.

Figure 3 Image of second harmonic under low MI. It showed the clear tumor and its satellite lesion.

DISCUSSION

The accurate recognition or exclusion of focal liver lesions was a primary objective of diagnostic imaging in patients who were suspected to have a tumor, and the detection of tumor lesions should include their number, location and size. Detection of small liver lesions may be difficult when the acoustic properties of the lesions were similar to those of the surrounding liver parenchyma[3]. The overall accuracy of US imaging in the detection of liver lesions has been shown to range from 53-77 %, but the sensitivity of milimeter nodules has been found to be as low as 20 %[4-6]. US contrast agents were originally developed and used to overcome some of the shortage of US in the assessment of lesional and parenchymal microcirculation by increasing the linear backscattering from the microvascular blood pool. The latest generation of US contrast agents prepared from perflurocarbon gases has been shown to be highly effective in enhancing Doppler signals within the macrovasculature and the microvasculature for several minutes following an intravenous bolus injection[7-9]. However, US contrast agents do not enhance the tumor lesion or parenchyma microvasculature on the fundamental gray-scale image, since the echoes from the tissues are too strong compared to the small volume of microbubbles in the microcirculation[10]. Thus these agents do not significantly improve the detectability of liver lesions when used in association with fundamental imaging, as what we have found in this study. It is necessary to take advantage of their nonlinear characteristics and selectively detect their emission of harmonics in order to increase the US sensitivity to contrast.

A dramatic improvement of contrast enhanced US was the discovery that the bursting of air-based microbubbles caused by high mechanic acoustic pressure US generated large quantities of harmonic frequencies (non-linear response). By decreasing the fundamental frequency, the contrast between highly vascularized lesions containing microbubbles and poorly vascularized tissues were increased[11-14]. Therefore, both macrovasculature and microvasculature of the liver tumor lesions could be well visualized. Some significant limitations about this technique have also been found. Due to the need of breaking air based microbubbles in order to achieve harmonics, the scans have to be started only 2-3 minutes following contrast agent bolus injection, and thus would miss completely the arterial and early portal phases. Furthermore, since all malignancies appear as hypoechoic and all benign tumors isoechoic in late phase[15], discrimination between hepatocellular carcinoma and metastasis, hemangiomas and focal nodular hyperplasia cannot be achieved. In our experiment, although contrast enhanced second harmonic imaging under high acoustic pressure could reveal an increased visualization of the tumor lesions and its surrounding liver parenchymal arteries, the major defect of this method was the short duration of visualization. A suitable method for the detection of hypervascular and hypovascular focal liver lesions should be a bubble non-destruction method with very low MI and high sensitivity for harmonics, allowing continuous real-time imaging of the whole liver and the visualization at the arterial, portal, and late phase during the same examination period with a single contrast agent administration only[16-21]. Furthermore, it should allow us to carry out perfusion and reperfusion studies following the planned bubble destruction and characterization of either hyper- or hypovascular lesions simultaneously[21-25]. We herewith reported our experimental results using this new technique, using a low MI SHI, a nearly complete cancellation of signals from stationary tissues was achieved. Prior to the injection of self-made albumin contrast agent, only high amplitude signals were visualized, such as large vessel walls and the diaphragm. After albumin contrast agent injection, a true subtraction effect was obtained due to the high level harmonic signals coming from the bubbles and the dynamic threshold suppressing low amplitude signals moving toward the transducer. In all rabbits, the whole vasculatures could be observed and studied, including an arterial phase about 15-40 seconds, an early portal phase about 40 to 50 seconds, and a complete portal phase about one and a half minutes. This result is in agreement with what has been described by Solbiati, and this "portal phase" is suggested to be "hepatic sinusoidal phases"[26-31]. The scans could be performed to study the changes of enhancement in these areas by moving the transducer throughout the liver visualizing not only the vascular phases in real time, but also any peculiar region of interest. Using this technique of second harmonic imaging under low acoustic pressure, we could therefore achieve the best visualization of macrocirculation and microcirculation simultaneously. Most interestingly, some satellite lesions, which were not found by high MI SHI, were now clearly revealed by low MI SHI as shown in Figures 2b and 3. It can be concluded that contrast enhanced ultrasonography with second harmonic imaging under low acoustic pressure is currently more sensitive than that with second harmonic imaging under high acoustic pressure in the detection of metastatic lesions as VX2 tumors. This study suggests that this new technique of low MI and microbubble non-destructive method would be much more helpful in our future clinical applications.

REFERENCES

1 **Choi BI,** Kim TK, Han JK, Kim AY, Seong CK, Park SJ. Vascularity of hepatocellular carcinoma: assessment with contrast-enhanced second-harmonic versus conventional power Doppler US. *Radiology* 2000; **214**: 381-386

2 **Kono Y,** Moriyasu F, Nada T, Suginoshita Y, Matsumura T, Toda Y, Nakamura T, Chiba T. Ultrasonographic arterial portography with second harmonic imaging: evaluation of hepatic parenchymal enhancement with portal venous flow. *J Ultrasound Med* 1999; **18**: 395-402

3 **Sirlin CB,** Girard MS, Baker KG, Steinbach GC, Deiranieh LH, Mattrey RF. Effect of acquisition rate on liver and portal vein enhancement with microbubble contrast. *Ultrasound Med Biol* 1999; **25**: 331-338

4 **Tanaka S,** Kitamura T, Ohshima A, Umeda K, Okuda S, Ohtani T, Tatsuta M, Yamamoto K. Diagnostic accuracy of ultrasonography for hepatocellular carcinoma. *Cancer* 1986; **58**: 344-347

5 **Tanaka S,** Kitamura T, Nakanishi K, Okuda S, Kojima J, Fujimoto I. Recent advances in ultrasonographic diagnosis of hepatocellular carcinoma. *Cancer* 1989; **63**: 1313-1317

6 **Tanaka S,** Kitamura T, Imaoka S, Sasaki Y, Taniguchi H, Ishiguro S. Hepatocellular carcinoma: sonographic and histologic correlation. *Am J Roentgenol* 1983; **140**: 701-707

7 **Harvey CJ,** Blomley MJ, Eckersley RJ, Cosgrove DO, Patel N, Heckemann RA, Butler-Barnes J. Hepatic malignancies: Improved detection with pulse-inversion US in late phase of enhancement with SHU508A-early experience. *Radiology* 2000; **216**: 903-908

8 **Carter R,** Hemingway D, Cooke TG, Pickard R, Poon FW, MacKillop JA, McArdle CS. A prospective study of six methods for detection of hepatic colorectal metastases. *Ann Royal Coll Surg Eng* 1996; **78**: 27-30

9 **Forsberg F,** Liu JB, Merton DA, Rawool NM, Goldberg BB. Parenchymal enhancement and tumor visualization using a new sonographic contrast agent. *J Ultrasound Med* 1995; **14**: 949-957

10 **Girard MS,** Sirlin CB, Baker KG, Hall LA, Mattrey RF. Liver tumor detection with ultrasound contrast: a blinded prospective study in rabbits. *Acad Radiol* 1998; **5**(Suppl 1): S189-191

11 **Mattrey RF,** Wrigley R, Steinbach GC, Schutt EG, Evitts DP. Gas emulsions as ultrasound contrast agents: preliminary results in rabbits and dogs. *Invest Radiol* 1994; **29**(Suppl 2): S139-S141

12 **Girard MS,** Kono Y, Sirlin CB, Baker KG, Deiranieh LH, Mattrey RF. B-mode enhancement of the liver with microbubble contrast agent: a blinded study in rabbits with VX2 tumors. *Acad Radiol* 2001; **8**: 734-740

13 **Porter TR,** Xie F. Visually discernible myocardial echocardiographic contrast after intravenous injection of solicated dextrose albumin microbubbles containing high molecular weight, less soluble gases. *J Am Coll Cardiol* 1995; **25**: 509-515
14 **Kim TK,** Han JK, Kim AY, Choi BI. Limitations of characterization of hepatic hemangiomas using a sonographic contrast agent (Levovist) and power Doppler ultrasonography. *J Ultrasound Med* 1999; **18**: 737-743
15 **Koito K,** Namieno T, Morita K. Differential diagnosis of small hepatocellular carcinoma and adenomatous hyperplasia with power Doppler sonography. *Am J Roentgenol* 1998; **170**: 157-161
16 **Gaiani S,** Casali A, Serra C, Piscaglia F, Gramantieri L, Volpe L, Siringo S, Bolondi L. Assessment of vascular patterns of small liver mass lesions: value and limitation of the different Doppler ultrasound modalities. *Am J Gastroenterol* 2000; **95**: 3537-3546
17 **Kim TK,** Choi BI, Han JK, Hong HS, Park SH, Moon SG. Hepatic tumors: contrast agent-enhancement patterns with pulse-inversion harmonic US. *Radiology* 2000; **216**: 411-417
18 **Choi BI,** Kim TK, Han JK, Chung JW, Park JH, Han MC. Power versus conventional color Doppler sonography: comparison in the depiction of vasculature in liver tumors. *Radiology* 1996, **200**: 55-58
19 **Bartolozzi C,** Lencioni R, Ricci P, Paolicchi A, Rossi P, Passariello R. Hepatocellular carcinoma treatment with percutaneous ethanol injection: evaluation with contrast-enhanced color Doppler US. *Radiology* 1998; **209**: 387-393
20 **Seidel G,** Vidal-Langwasser M, Algermissen C, Gerriets T, Kaps M. The influence of doppler system settings on the clearance kinetics of different ultrasound contrast agents. *Eur J Ultrasound* 1999; **9**: 167-175
21 **Cosgrove D.** Ultrasound contrast enhancement of tumors. *Clin Radiol* 1996; **51**(Suppl 1): 44-49
22 **Gaiani S,** Volpe L, Piscaglia F, Bolondi L. Vascularity of liver tumours and recent advances in Doppler ultrasound. *J Hepatol* 2001; **34**: 474-482
23 **Leen E,** McArdle CS. Ultrasound contrast agents in liver imaging. *Clin Radiol* 1996; **51**(Suppl 1): 35-39
24 **Cosgrove D**. Microbubble enhancement of tumour neovascularity. *Eur Radiol* 1999; **9**(Suppl 3): S413-414
25 **Strobel D,** Krodel U, Martus P, Hahn EG, Becker D. Clinical evaluation of contrast enhanced color Doppler sonography in the differential diagnosis of liver tumors. *J Clin Ultrasound* 2000; **28**:1-13
26 **Hosten N,** Puls R, Bechstein WO, Felix R. Focal liver lesions: Doppler ultrasound. *Eur Radiol* 1999; **9**: 428-435
27 **Leen E.** The role of contrast-enhanced ultrasound in the characterisation of focal liver lesions. *Eur Radiol* 2001; **11**(Suppl 3): E27-34
28 **Ramnarine KV,** Kyriakopoulou K, Gordon P, McDicken NW, McArdle CS, Leen E. Improved characterization of focal liver tumors: dynamic power Doppler imaging using NC100100 echo-enhancer. *Eur J Ultrasound* 2000; **11**: 95-104
29 **Solbiati L,** Tonolini M, Cova L, Goldberg SN. The role of contrast-enhanced ultrasound in the detection of focal liver lesions. *Eur Radiol* 2001; **11**(Suppl 3): E15-26
30 **Catalano O,** Esposito M, Lobianco R, Cusati B, Altei F, Siani A. Hepatocellular carcinoma treated with chemoembolization: assessment with contrast-enhanced doppler ultrasonography. *Cardiovasc Intervent Radiol* 1999; **22**: 486-492
31 **Blomley M,** Albrecht T, Cosgrove D, Jayaram V, Butler-Barnes J, Echersley R. Stimulated acoustic emission in liver parenchyma with Levovist. *Lancet* 1998; **351**: 568

Edited by Wu XN and Wang XL

P.O.Box 2345, Beijing 100023,China
Fax: +86-10-85381893
E-mail: wjg@wjgnet.com www.wjgnet.com

World J Gastroenterol 2003;9(8):1683-1688
World Journal of Gastroenterology
 ISSN 1007-9327

• LIVER CANCER •

Peroxisome proliferator-activated receptor gamma ligands inhibit cell growth and induce apoptosis in human liver cancer BEL-7402 cells

Ming-Yi Li, Hua Deng, Jia-Ming Zhao, Dong Dai, Xiao-Yu Tan

Ming-Yi Li, Dong Dai, Xiao-Yu Tan, Department of General Surgery, Affiliated Hospital of Guangdong Medical College, Zhangjiang 524001, Guangdong Province, China
Hua Deng, Department of Biochemistry and Molecular Biology, Beijing Institute for Cancer Research, Da Hong-Luo Chang Street, Beijing 100034, China
Jia-Ming Zhao, Central Experiment, Affiliated Hospital of Guangdong Medical College, Zhangjiang 524001, Guangdong Province, China
Correspondence to: Ming-Yi Li, Department of General Surgery, Affiliated Hospital of Guangdong Medical College, Zhangjiang 524001, Guangdong Province, China. zjmyli@sohu.com
Telephone: +86-759-2387613
Received: 2002-11-06 **Accepted:** 2003-01-28

Abstract

AIM: To investigate the characteristics of PPAR gamma ligands induced apoptosis in liver cancer cells.

METHODS: The effects of ligands for each of the PPAR gamma ligands on DNA synthesis and cell viability were examined in BEL-7402 liver cancer cells. Apoptosis was characterized by Hochest33258 staining, DNA fragmentation, TUNEL and ELISA, and cell cycle kinetics by FACS. Modulation of apoptosis related caspases expression by PPAR gamma ligands was examined by Western blot.

RESULTS: PPARgamma ligands, 15-deoxy-^{12,14}-prostaglandin J2 (15d-PGJ2) and troglitazone (TGZ), suppressed DNA synthesis of BEL-7402 cells. Both 15d-PGJ2 and TGZ induced BEL-7402 cell death in a dose dependent manner, which was associated with an increase in fragmented DNA and TUNEL-positive cells. At concentrations of 10 and 30 μM, 15d-PGJ_2 or troglitazone increased the proportion of cells with G_0/G_1 phase DNA content and decreased those with S phase DNA content. There was no significant change in the proportion of cells with G_2/M DNA content. The activities of Caspases-3, -6, -7 and -9 were increased by 15d-PGJ2 and TGZ treatment, while the activity of Caspase 8 had not significantly changed.

CONCLUSION: The present results suggest the potential usefulness of PPAR gamma ligands for chemoprevention and treatment of liver cancers.

Li MY, Deng H, Zhao JM, Dai D, Tan XY. Peroxisome proliferator-activated receptor gamma ligands inhibit cell growth and induce apoptosis in human liver cancer BEL-7402 cells. *World J Gastroenterol* 2003; 9(8): 1683-1688
http://www.wjgnet.com/1007-9327/9/1683.asp

INTRODUCTION

Peroxisome proliferator-activated receptors (PPARs) are members of the nuclear hormone receptor family. Three distinct PPARs, termed PPAR-α, PPAR-β and PPAR-γ, have been identified. PPAR-α is abundant in primary hepatocytes, where it regulates the expression of proteins involved in fatty acid metabolism. PPAR-β is the most widely distributed subtype and is often expressed at high levels. PPAR-γ is predominantly seen in adipose tissue, where it plays a critical role in regulating adipocyte differentiation. The ability of PPAR-γ to regulate cell differentiation and proliferation has inspired a number of researchers to explore the use of PPAR-γ agonists as chemotherapeutic agents[1-7]. PPAR-γ is highly expressed in human lipocarcinomas and various other human tumors including breast, lung, colon, prostate, bladder and gastric cancer[8-13]. Furthermore, prostaglandin 15d-PGJ_2 and/or troglitazone induce apoptosis and growth inhibition of human breast, lung, colon, prostate, bladder, gastric and thyroid carcinoma cells *in vitro*.

In support of the *in vitro* data, there are now many reported examples of tumor growth suppression/arrest in tumor-bearing rodent models treated with PPAR-γ agonist therapies. For example, troglitazone treatment of nude mice implanted with papillary thyroid tumors reduced tumor growth and prevented distant metastasis. Both estrogen receptor positive (MCF-7) and negative (MDA-MB-231) breast cancer cell lines undergo cell cycle arrest when treated with15d-PGJ_2 or troglitazone and similar effects are observed in rodent breast cancer *in vivo* models[14-18]. PPAR-γ ligands have been shown to inhibit growth and induce terminal differentiation of liposarcoma cells, and to inhibit growth and induce apoptosis of breast cancer cells, prostatic carcinoma, and lung cancer cells.

In the field of gastroenterology, many investigators have focused on the role of PPAR-γ in colon cancer, since PPAR-γ is highly expressed in human colon and colon tumors. The effects of PPAR-γ on colon cancer are still unclear and controversial[19-25], since PPAR-γ ligands have been reported both to promote the development and to reduce the growth rate of colon tumors. PPAR-γ ligands also inhibit the growth of human gastric carcinoma cells through induction of apoptosis[25]. However, the effects of PPAR-γ ligands on growth of human liver cancer cells have not been examined. In this study, we investigated the effects of PPAR-γ ligands 15d-PGJ_2 and troglitazone on growth of human liver cancer BEL-7402 cells and whether 15d-PGJ_2 and troglitazone affected the cell cycle, apoptosis, and Caspases activity of BEL-7402 cells.

MATERIALS AND METHODS

Cell line and reagents

Human liver cancer cell line BEL-7402 was provided by the American Type Culture Collection. Cells were grown in RPMI-1640 medium supplemented with 15 % new born bovine serum, penicillin G (100 kU/L) and kanamycin (0.1 g/L) at 37 ℃ in a 5 % CO_2-95 % air atmosphere. Anti-Caspases-3, -6, -7, -8 and -9 antibodies were obtained from Sigma Chemical Co. 15-deoxy-$\Delta^{12,14}$-prostaglandin J_2 (15d-PGJ_2) and troglitazone were

obtained from Cayman Chemical Co. All other chemicals were purchased from Sigma Chemical Co (St Louis, MO, USA).

Determination of cell proliferation rate

BEL-7402 cells (1×10^5) were seeded in 24 well plates and cultured for 24 h. The cultures were divided into three groups: the first group (control) was cultured in the RPMI1640 medium, the second group was cultured in the continuous presence of 20 μM 15-deoxy-$\triangle^{12,14}$-prostaglandin J_2 (15d-PGJ_2), the third was cultured in the continuous presence of 20 μM troglitazone. Cells were then harvested every 24 h by trypsinization and cell numbers were counted with a hemocytometer, three cultures were used for experiments at each time point.

[^{3}H] thymidine incorporation

Subconfluent cells were cultured in 24-well plates and incubated for 24 h with 5uCi of [^{3}H] thymidine. The cells were then washed 3 times with HBSS, lysed with 1M NaOH, and lysate was counted by liquid scintillation.

Hoechst 33258 staining

Cells were fixed with 4 % formaldehyde in phosphate buffered saline (PBS) for 10 min, stained by Hoechst33258 (10 mg/L) for one hour, and subjected to fluorescence microscopy. After treated with 15d-PGJ_2 or troglitazone, the morphologic changes including reduction in volume, nuclear chromatin condensation were observed.

Electron microscopy (EM)

Control BEL-7402 cells or those treated with 15-deoxy-$\triangle^{12,14}$-prostaglandin J_2 (15d-PGJ_2) or troglitazone for 48 h and that remained attached to the surface of the culture dishes were gently washed with serum-free medium, and then fixed with 2.5 % glutaraldehyde in 0.1 M sodium cacodylate buffer. These cells were scraped from the surface of the dishes and pelleted by spinning for 5 min at 10 000×g. The cells were osmicated with 1 % osmium tetroxide, then block was stained, dehydrated in graded ethanol, infiltrated with propylene oxide, and embedded with EMBED overnight and cured in a 60 ℃ oven for 48 h. Silver sections were cut with an Ultracut E microtome, collected on a formvar and carbon-coated grid, stained with uranyl acetate and Reynold's lead citrate, and viewed under a JEOL100 CX electron microscope.

Ladder detection assay

After induction of apoptosis, cells (7×10^6/sample, both attached and detached cells) were lyzed with 150 μl hypotonic lysis buffer (edetic acid 10 mM, 0.5 % Triton X-100, Tris-HCl, ph7.4) for 15 min on ice and were precipitated with 2.5 % polyethylene glycol and NaCl 1 M for 15 min at 4 ℃. After centrifugation at 16 000×g for 10 min at room temperature, the supernatant was incubated in the presence of proteinase K (0.3 g/L) at 37 ℃ for one hour and precipitated with isopropanol at -20 ℃. After centrifugation, each pellet was dissolved in 10 μl of Tris-EDTA (pH 7.6) and electrophoresed on a 1.5 % agarose gel containing ethidium bromide. Ladder formation of oligonucleosomal DNA was detected under ultraviolet light.

Detection of apoptotic DNA fragmentation

BEL-7402 cells were grown in 96-well culture plates. The cells were incubated with various doses of 15d-PGJ_2 and troglitazone for 6 h. Apoptotic DNA fragmentation was determined using a commercially available enzyme-linked immunosorbent assay (ELISA) kit from Roche Co. This assay was based on a quantitative sandwich enzyme-immunoassay directed against cytoplasmic histone-associated DNA fragments. Briefly, the cells were incubated in 200 μl of lysis buffer provided in the kit, the lysates were centrifuged, and 20 μl of the supernatant containing cytoplasmic histone-associated DNA fragments was reacted overnight at 4 ℃ in streptavidin-coated microtitrator wells with 80 μl of the immunoreagent mixture containing biotinylated anti-histone antibody and peroxidase-conjugated anti-DNA antibody. After washed, the immunocomplex-bound peroxidase was probed with 2,2' -azino-di[3-ethylbenzthiazoline sulfonate] for spectrophotometric detection at 405 nm.

TUENL assay

TUNEL assay was performed using the apoptosis detection system. Cells were fixed by 4 % paraformaldehyde in PBS overnight at 4 ℃. The samples were washed three times with PBS and permeabilized by 0.2 % Triton X-100 in PBS for 15 min on ice. After washed twice, cells were equilibrated at room temperature for 15 to 30 min in equilibration buffer(potassium cacodylate 200 mM, dithiothreitol 0.2 mM, bovine serum albumin 0.25 g/L, and cobalt chloride 2.5 mM in Tris-HCl 25 mM, pH 6.6) and then incubated in the presence of fluorescein-12-dUTP 5 μM, dATP 10 μM, edetic acid 100 μM, and terminal deoxynucleotidyl transferase at 37 ℃ for 1.5 h in the dark. The tailing reaction was terminated by 2×standard saline citrate (SSC). The samples were washed three times with PBS and analyzed by fluorescence microscopy. At least 1000 cells were counted, and the percentage of TUNEL-positive cells was determined.

Flow cytometry

For DNA content analysis, cells were treated with different concentrations of 15-deoxy-$\triangle^{12,14}$-prostaglandin J_2 (15d-PGJ_2) and troglitazone for 24 h. 1×10^6 cells were harvested, pelleted and washed with phosphate-buffered saline (PBS), and resuspended in PBS containing 20 mg/L PI and 1 g/L ribonuclease A. 10^6 fixed cells were examined under each experimental condition by flow cytometry, and percentage of degraded DNA was determined by the number of cells displaying subdiploid (sub-G_1). DNA divided by the total number of cells was examined. Cell cycle analysis was performed under the same experimental conditions and distributions were determined using the CellFit program. All measurements were carried out under the same instrumental settings.

Western blot analysis

The cells were lysed in lysis buffer [hepes 25 mM, 1.5 % Triton X-100, 1 % sodium deoxycholate, 0.1 %SDS, NaCl 0.5 M, edetic acid 5 mM, NaF 50 mM, sodium vanadate 0.1 mM, phenylmethylsulfonyl fluoride (PMSF) 1 mM, and leupeptin 0.1 g/L, pH7.8] at 4 ℃ with sonication. The lysates were centrifuged at 15 000 g for 15 min and the concentration of the protein in each lysate was determined with Coomassie brilliant blue G-250. Loading buffer (Tris-HCl 42 mM, 10 % glycerol, 2.3 % SDS, 5 % 2-mercaptoethanol and 0.002 % bromophenol blue) was then added to each lysate, which was subsequently boiled for 3 min and then electrophoresed on a SDS-polyacrylamide gel. Proteins were transferred to nitrocellulose and incubated sequentially with anti-Caspases-3, -6, -7, -8 and -9 antibodies and then with peroxidase-conjugated secondary antibodies in the second reaction. Detection was performed with enhanced chemiluminescence reagent. The results on Western blot analysis represented the average of three individual experiments.

Statistical analysis

Data were presented as the mean ± standard error of the mean, unless otherwise indicated. Multiple comparisons were examined for significant differences using analysis of variance, followed by individual comparisons with the Bonferroni post-test. Comparisons between two groups were made with the Student's *t* test. A $P<0.05$ was considered significant.

RESULTS

Effects of 15d-PGJ$_2$ and troglitazone on proliferation and cell cycle

Cells were cultured in the presence or absence of 15d-PGJ$_2$ or troglitazone and cell numbers were determined over three days. In the absence of 15d-PGJ$_2$ or troglitazone, the number of control cells doubled approximately every 24 h in RPMI 1640 medium supplemented with 10 % fetal calf serum. By contrast, in the continuous presence of 20 μM 15d-PGJ$_2$ or troglitazone' the growth of BEL-7402 cells was significantly inhibited (Figure 1A). We next examined by [^{3}H]-thymidine incorporation whether 15d-PGJ$_2$ or troglitazone affected DNA synthesis of BEL-7402 cells. Cells were treated with various doses of 15d-PGJ$_2$ or troglitazone (10, 20, 30 μM). The results showed that 15d-PGJ$_2$ or troglitazone significantly and dose-dependently inhibited [^{3}H]-thymidine incorporation into BEL-7402 cells (Figures 1B, 1C). Table 1 indicates the effects of 15d-PGJ$_2$ or troglitazone on the cell cycle distribution of BEL-7402 cells. 15d-PGJ$_2$ or troglitazone at 10 μM induced limited or no change in the cell cycle distribution of cells. At concentrations of 20 and 30 μM, 15d-PGJ$_2$ or troglitazone increased the proportion of cells with G_0/G_1 phase DNA content and decreased those with S phase DNA content. There was no significant change in the proportion of cells with G_2/M DNA content.

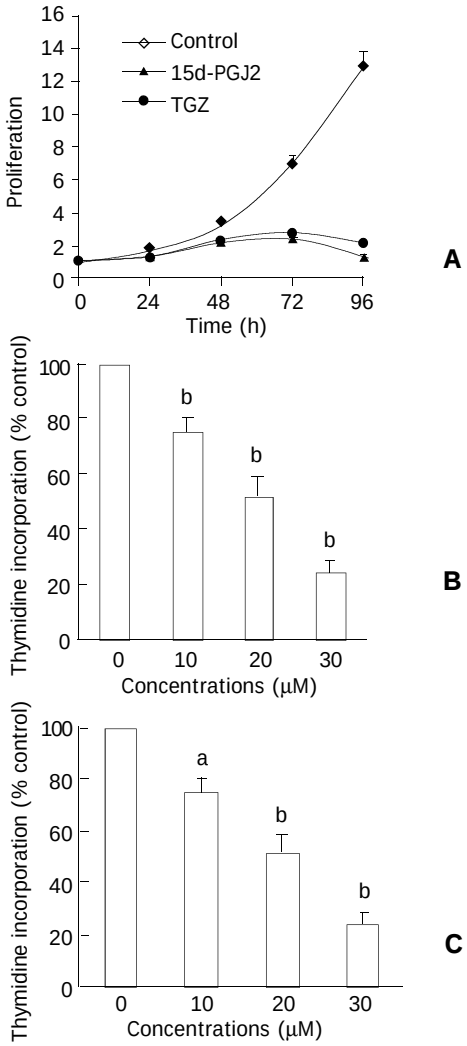

Figure 1 Concentration and time effect of 15d-PGJ2 or TGZ on growth of BEL-7402 cells. (A) BEL-7402 cells were incubated with 20 μM 15d-PGJ2 or TGZ for 12, 24, 48, 72, 96 h. (B) BEL-7402 cells were incubated with various concentrations of 15d-PGJ2 for 48 h; (C) BEL-7402 cells were incubated with various concentrations of TGZ for 48 h. The value was represented as mean ±SEM (n=3). [a]P<0.05 and [b]P<0.01 versus corresponding control group.

Effect of 15d-PGJ$_2$ or troglitazone on induction of apoptosis in BEL-7402 cells

Morphological changes 15d-PGJ$_2$ or troglitazone treatment of BEL-7402 cells altered their morphology and induced DNA strand breaks in a manner consistent with apoptosis. That the changes were indeed induced by apoptosis and not necrosis was confirmed by EM and Hoechst 33258 staining. 15d-PGJ$_2$ or troglitazone-treated cells showed compacted nuclear chromatin with fine granular masses marginated against the nuclear enveloped and condensed cytoplasm, the nuclear outline was convoluted and the organelles were preserved.

TUNEL assay To determine whether 15d-PGJ$_2$ or troglitazone has a capacity to induce apoptosis in BEL-7402 cells, exponentially growing cells were exposed to various concentrations of 15d-PGJ$_2$ or troglitazone. TUNEL assay was performed. 15d-PGJ$_2$ or troglitazone dramatically increased the number of TUNEL-positive cells in a dose-dependent manner.

DNA fragments Agarose gel electrophoresis exhibited DNA ladder formation in BEL-7402 cells after exposed to different concentrations of 15d-PGJ$_2$ or troglitazone for 48 h. Compared with control, the DNA laddering was more clearly observed by the treatment with 15d-PGJ$_2$ or troglitazone. ELISA assay also showed that 15d-PGJ$_2$ or troglitazone induced DNA fragment in a dose-dependent manner (Figure 2).

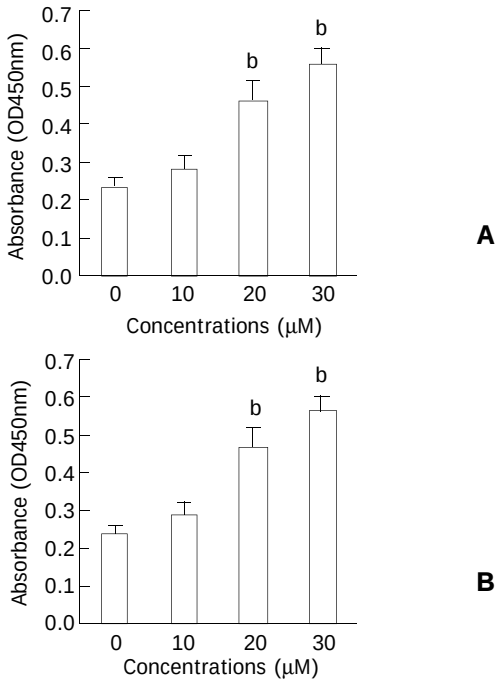

Figure 2 DNA fragmentation by ELISA assay, as measured by absorbance (OD 450 values). Culture of BEL-7402 cells for 48 h in the presence of 15d-PGJ2 / TGZ resulted in dose dependent DNA fragmentation. A) 15d-PGJ2; B) TGZ. [b]P<0.01 compared to respective control. The value was represented as mean ± SEM (n=3).

Flow cytometry In order to determine the effect of 15d-PGJ$_2$ or troglitazone on apoptosis in BEL-7402 cells, cells were exposed to 15d-PGJ$_2$ or troglitazone for 48 h, apoptotic damage of DNA was detected according to the sub-G_1 peak on a flow cytometer. Cells in sub-G_1 phase were increased from 2.1±0.3 % to 55.8±4.7 % or 50.0±4.1 % after 15d-PGJ$_2$ or troglitazone treatment (Table1).

Effect of 15d-PGJ$_2$ or troglitazone on the activities of Caspase-3, -6, -7, -8 and -9

In order to elucidate the pathway leading to apoptosis, we

examined the activation of Caspases-3, -6, -7, -8 and -9, which were reported to initiate apoptosis upon various stimuli. BEL-7402 cells treated with15d-PGJ_2 or troglitazone for 24 h were analyzed for the enzymatic activity by Western blot. The results showed that Caspases-3, -6, -7, -8 and -9 were activited after 15d-PGJ_2 or troglitazone treatment in BEL-7402 cells, while the activity of Caspase 8 had not significantly changed (Figure 3).

Table 1 Effect of 15d-PGJ2 and TGZ on cell cycle distribution and apoptosis in BEL-7402 cells

Treatment (μm)	%Cell cycle distribution			%apoptosis
	G_0/G_1	S	G_2/M	
Control	49.7±1.5	34.8±2.1	15.5±1.1	2.1±0.3
15d-PGJ2				
10	50.5±2.6	34.2±1.7	15.3±0.5	13.9±1.1[b]
20	64.8±2.9[b]	19.5±1.5[b]	15.7±0.2	33.5±2.3[b]
30	71.6±4.2[b]	14.1±0.6[b]	14.4±1.3	55.8±4.7[b]
TGZ				
10	54.2±2.1	29.4±1.3	16.6±0.9	10.3±1.1[b]
20	61.5±3.1[b]	28.2±1.7[b]	14.9±1.7	25.5±1.8[b]
30	68.9±4.8[b]	14.2±0.8[b]	16.9±1.4	50.0±4.1[b]

Cell cycle distribution was determined after 24 h of treatment in one group and apoptosis was determined after 48 h of treatment in the other group. The tabulated percentages were an average calculated on the results of three separate experiments. The value was represented as mean±SEM (n=3). [b]P<0.01 versus corresponding control group.

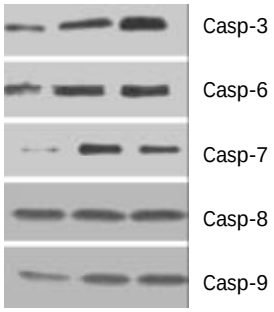

Figure 3 Western blot analysis of the activities of Caspases-3, -6, -7, -8 and –9 in human liver cancer cell line BEL-7402 cells: lane 1: control, lane 2: 30 μM TGZ treated BEL-7402 cells; lane 3: 30 μM 15d-PGJ2 treated BEL-7402 cells.

DISCUSSION

Several members of the family of nuclear hormone receptors (NHR) play crucial roles in the control of cellular homeostasis, and administration of their cognate ligands has successfully been used in cancer treatment[26-33]. The nuclear receptor superfamily includes members such as the estrogen, thyroid and glucocorticoid receptors as well as the subfamily of peroxisome proliferator-activated receptors. The PPAR family comprises PPAR-α, PPAR-β and PPAR-γ. The PPARs bind as heterodimers with retinoic-x acid receptor (RXR) to a subset of DR-1 elements, peroxisome proliferator response elements and have been shown to regulate expression of genes involved in the transport, metabolism and storage of fatty acids. Transcriptional activation of the PPAR-RXR heterodimers is enhanced upon binding of a large variety of ligands including saturated and unsaturated fatty acids, arachidonic acid derivatives and a wide range of synthetic drugs with different subtype specificities.

For the last 10 years, administration of peroxisome proliferators, PPAR-α agonists, has been known to induce hepatocarcinogenesis in rodents. However, cancer development is probably induced by mechanisms secondary to PPAR-α transcriptional activation. A role in growth regulation for the two remaining PPAR subtypes has also been suggested. Whichever, upregulaties PPAR-β expression has been associated with colon cancer and activation of PPAR-β stimulates post-confluent proliferation of pre-adipocytes. Opposite effects on cell proliferation are mediated by activation of PPAR-γ. PPAR-γ agonists could be promising therapeutic or chemopreventive agents in oncology, since they can induce apoptosis or differentiation in several tumors, by acting as inhibitors of malignancy progression. PPAR-γ activation inhibits the growth of several tumors as shown by *in intro* and *in vivo* studies performed on liposarcoma, breast cancer and leukemia. However, conflicting evidence exists on the role of PPAR-γ activation in colon cancer, where different studies have shown that PPAR-γ activation promotes tumor development or, in contrast, protects against colon cancer, depending on the cell model[34-42]. In the present study, in order to examine the effects of PPAR-γ ligands 15d-PGJ_2 or troglitazone on the BEL-7402 cell growth, we employed cell counting and [^{3}H]-thymidine incorporation assay. The results showed 15d-PGJ_2 or troglitazone significantly and concentration-dependently inhibited the growth of BEL-7402 cells. To examine whether growth inhibition of BEL-7402 cells by 15d-PGJ_2 or troglitazonem was a result of cell cycle arrest, BEL-7402 cells treated with either vehicle or 15d-PGJ_2/troglitazone were analyzed by FACScan. BEL-7402 cells treated with 15d-PGJ_2 and troglitazone exhibited decreased fractions of S phase cells from 34.8±2.1 % in controls to14.4±1.3 % and 16.9±1.4 %, respectively, resulting in a remarkable increase in accumulation if cells at G_1 phase, increased from a control level of 49.7±1.5 % to 71.6±1.5 % and 68.9±4.8 %. Therefore, the inhibitory effect of 15d-PGJ_2 or troglitazone on growth of BEL-7402 cells may thus be due in part to PPAR-γ-mediated G_1 cell cycle arrest. Similar findings of G_1 cell cycle arrest by PPAR-γ ligands have been reported for colon cancer cells and prostate cancer cells. Several reports suggested that PPAR-γ ligands affected cell cycle-related genes and proteins. Others demonstrated that PPAR-γ activation caused G_1 cell cycle arrest of fibroblasts and SV40-transformed adipogenic HIB1B cells, and that this arrest was strongly associated with loss of E2F/DP DNA binding through modulation of phosphorylation by phosphatase 2A[43-47].

Previous studies have shown that PPAR-γ activation generally promotes apoptosis and/or differentiation in several normal and tumor cells such as human breast cancer cells, human gastric cancer cells, human non-small cell lung carcinoma, human glioblastoma cells, macrophages, endothelial cells and liposarcoma. In the present study, to determine the underlying mechanisms of the growth inhibitory effect of PPAR-γ ligands, we investigated whether 15d-PGJ_2 or troglitazone acted by inducing apoptosis of liver cancer BEL-7402 cells. We performed DNA fragments and morphological changes assay EM or Hoechst 33258. The results showed that 15d-PGJ_2 or troglitazone induced apoptosis in a dose-dependent manner, indicating that growth inhibition of BEL-7402 by PPAR-γ ligands was, in part, associated with apoptosis.

Recent evidence indicates that increased expression and activation of some Caspase zymogens in tumor cells can lead to efficient inhibition of tumor cell growth, invasion and metastasis and tumor regression[48-56]. Such a Caspase-dependent cessation of tumor cell proliferation and dissemination is accomplished via an active process of tumor cells death collectively named as apoptosis. It has been demonstrated that a high level of activity of effector Caspases-3, -6, -7 and -8, in tumor cells plays a decisive role in their commitment to apoptosis[57-66]. To-date studies on zymogens of the effector

Caspases in primary human tumors showed an increased expression of procasp-3 and -6 in breast carcinoma, pancreatic carcinoma and non-small cell lung carcinoma compared to normal tissue and benign or premalignant lesions. This suggests that tumor cells of some epithelial neoplasms may acquire an increased apoptotic potential during progression at the levels of primary tumor. The zymogens of casp-3 and -7 in tumor cells can be activated by the initiator Caspases, such as casp-8 and casp-9, and by the aspartyl-specific serine proteinase granzyme B upon its perforin-assisted entry into the cytoplasm of tumor cells. Procasp-6 can be activated by casp-3 while the generated casp-6 can activate in turn the zymogen of casp-3. In the present study, in order to elucidate the pathway leading to apoptosis, we examined activation of Caspases-3, -6, -7, -8 and -9, which have been reported to initiate apoptosis upon various stimuli. BEL-7402 cells treated with15d-PGJ_2 or troglitazone for 24 h were analyzed for the enzymatic activity by Western blot. The results showed that Caspases-3, -6, -7, -8 and -9 were activited after 15d-PGJ_2 or troglitazone treatment in BEL-7402 cells, while the activity of Caspase 8 had not significantly changed, indicating that activation of Caspases plays an important role in the apoptosis induced by 15d-PGJ_2 or troglitazone.

In conclusion, the present results, together with reports by other investigators, suggest a potential usefulness of PPAR gamma ligands for chemoprevention and treatment of liver cancers. Further basic as well as clinical studies are required to develop new strategies to fight liver cancers using PPAR gamma ligands.

REFERENCES

1 **Mangelsdorf DJ**, Thummel C, Beato M, Herrlich P, Schutz G, Umesono K, Blumberg B, Kastner P, Mark M, Chambon P. The nuclear receptor superfamily: the second decade. *Cell* 1995; **83**: 835-839

2 **Spiegelman BM,** Flier JS. Adipogenesis and obesity: rounding out the big picture. *Cell* 1996; **87**: 377-389

3 **Sarraf P**, Mueller E, Jones D, King FJ, DeAngelo DJ, Partridge JB, Holden SA, Chen LB, Singer S, Fletcher C, Spiegelman BM. Differentiation and reversal of malignant changes in colon cancer through PPARgamma. *Nat Med* 1998; **4**: 1046–1052

4 **Mueller E,** Sarraf P, Tontonoz P, Evans RM, Martin KJ, Zhang M, Fletcher C, Singer S, Spiegelman BM. Terminal differentiation of human breast cancer through PPAR gamma. *Mol Cell* 1998; **1**: 465-470

5 **Kubota T,** Koshizuka K, Williamson EA, Asou H, Said JW, Holden S, Miyoshi I, Koeffler HP. Ligand for peroxisome proliferator-activated receptor gamma (troglitazone) has potent antitumor effect against human prostate cancer both *in vitro* and *in vivo*. *Cancer Res* 1998; **58**: 3344–3352

6 **Takahashi N,** Okumura T, Motomura W, Fujimoto Y, Kawabata I, Kohgo Y. Activation of PPARgamma inhibits cell growth and induces apoptosis in human gastric cancer cells. *FEBS Lett* 1999; **455**: 135-139

7 **Chinetti G,** Griglio S, Antonucci M. Activation of proliferator-activated receptors alpha and gamma induces apoptosis of human monocyte-derived macrophages. *J Biol Chem* 1998; **273**: 25573–25580

8 **Vamecq J**, Latruffe N. Medical significance of peroxisome proliferator-activated receptors. *Lancet* 1999; **354**: 141-148

9 **Tontonoz P**, Hu E, Spiegelman BM. Stimulation of adipogenesis in fibroblasts by PPAR gamma 2, a lipid-activated transcription factor. *Cell* 1994; **79**: 1147–1156

10 **Forman BM**, Tontonoz P, Chen J, Brun RP, Spiegelman BM, Evans RM. 15-Deoxy-delta 12, 14-prostaglandin J2 is a ligand for the adipocyte determination factor PPAR gamma. *Cell* 1995; **83**: 803–812

11 **Kliewer SA**, Lenhard JM, Willson TM, Patel I, Morris DC. A prostaglandin J2 metabolite binds peroxisome proliferator-activated receptor gamma and promotes adipocyte differentiation. *Cell* 1995; **83**: 813–819

12 **Mansen A**, Guardiola-Diaz H, Rafter J. Expression of the peroxisome proliferator-activated receptor (PPAR) in the mouse colonic mucosa. *Biochem Biophys Res Commun* 1996; **222**: 844–851

13 **Fajas L**, Auboeuf D, Raspe E, Schoonjans K, Lefebvre AM, Saladin R, Najib J, Laville M, Fruchart JC, Deeb S, Vidal-Puig A, Flier J, Briggs MR, Staels B, Vidal H, Auwerx J. The organization, promoter analysis, and expression of the human PPARgamma gene. *J Biol Chem* 1997; **272**: 18779–18789

14 **Okumura M**, Yamamoto M, Sakuma H, Kojima T, Maruyama T, Jamali M, Cooper D, Yasuda K. Leptin and high glucose stimulate cell proliferation in MCF-7 human breast cancer cells: reciprocal involvement of PKC-alpha and PPAR expression. *Biochim Biophys Acta* 2002; **1592**: 107

15 **Wang X**, Kilgore M. Signal cross-talk between estrogen receptor alpha and beta and the peroxisome proliferator-activated receptor gamma1 in MDA-MB-231 and MCF-7 breast cancer cells. *Mol Cell Endocrinol* 2002; **194**: 123

16 **Suchanek KM**, May FJ, Robinson JA, Lee WJ, Holman NA, Monteith GR, Roberts-Thomson SJ. Peroxisome proliferator-activated receptor alpha in the human breast cancer cell lines MCF-7 and MDA-MB-231. *Mol Carcinog* 2002; **34**: 165-171

17 **Stoll BA**. Linkage between retinoid and fatty acid receptors: implications for breast cancer prevention. *Eur J Cancer Prev* 2002; **11**: 319-325

18 **Stoll BA**. N-3 fatty acids and lipid peroxidation in breast cancer inhibition. *Br J Nutr* 2002; **87**: 193-198

19 **Inadera H,** Nagai S, Dong HY, Matsushima K. Molecular analysis of lipid-depleting factor in a colon-26-inoculated cancer cachexia model. *Int J Cancer* 2002; **101**: 37-45

20 **Dobbie Z**, Muller PY, Heinimann K, Albrecht C, D'Orazio D, Bendik I, Muller H, Bauerfeind P. Expression of COX-2 and Wnt pathway genes in adenomas of familial adenomatous polyposis patients treated with meloxicam. *Anticancer Res* 2002; **22**: 2215-2220

21 **Sunami E**, Tsuno NH, Kitayama J, Saito S, Osada T, Yamaguchi H, Tomozawa S, Tsuruo T, Shibata Y, Nagawa H. Decreased synthesis of matrix metalloproteinase-7 and adhesion to the extracellular matrix proteins of human colon cancer cells treated with troglitazone. *Surg Today* 2002; **32**: 343-350

22 **Theocharis S**, Kanelli H, Politi E, Margeli A, Karkandaris C, Philippides T, Koutselinis A. Expression of peroxisome proliferator activated receptor-gamma in non-small cell lung carcinoma: correlation with histological type and grade. *Lung Cancer* 2002; **36**: 249-255

23 **Bogazzi F**, Ultimieri F, Raggi F, Costa A, Gasperi M, Cecconi E, Mosca F, Bartalena L, Martino E. Peroxisome proliferator activated receptor gamma expression is reduced in the colonic mucosa of acromegalic patients. *J Clin Endocrinol Metab* 2002; **87**: 2403-2406

24 **Takashima T**, Fujiwara Y, Higuchi K, Arakawa T, Yano Y, Hasuma T, Otani S. PPAR-gamma ligands inhibit growth of human esophageal adenocarcinoma cells through induction of apoptosis, cell cycle arrest and reduction of ornithine decarboxylase activity. *Int J Oncol* 2001; **19:** 465-471

25 **Sato H**, Ishihara S, Kawashima K, Moriyama N, Suetsugu H, Kazumori H, Okuyama T, Rumi MA, Fukuda R, Nagasue N, Kinoshita Y. Expression of peroxisome proliferator-activated receptor (PPAR) gamma in gastric cancer and inhibitory effects of PPARgamma agonists. *Br J Cancer* 2000; **83**: 1394-1400

26 **Terashita Y**, Sasaki H, Haruki N, Nishiwaki T, Ishiguro H, Shibata Y, Kudo J, Konishi S, Kato J, Koyama H, Kimura M, Sato A, Shinoda N, Kuwabara Y, Fujii Y. Decreased peroxisome proliferator-activated receptor gamma gene expression is correlated with poor prognosis in patients with esophageal cancer. *Jpn J Clin Oncol* 2002; **32**: 238-243

27 **Chen GG**, Lee JF, Wang SH, Chan UP, Ip PC, Lau WY. Apoptosis induced by activation of peroxisome-proliferator activated receptor-gamma is associated with Bcl-2 and NF-kappaB in human colon cancer. *Life Sci* 2002; **70**: 2631-2646

28 **Evangelou A**, Letarte M, Marks A, Brown TJ. Androgen modulation of adhesion and antiadhesion molecules in PC-3 prostate cancer cells expressing androgen receptor. *Endocrinology* 2002; **143**: 3897-3904

29 **Eisen SF**, Brown HA. Selective estrogen receptor (ER) modula-

tors differentially regulate phospholipase D catalytic activity in ER-negative breast cancer cells. *Mol Pharmacol* 2002; **62**: 911-920

30 **Aoyama Y**. Experimental studies on the effects of the combined use of N-(4-hydroxyphenyl)retinamide (4-HPR) and tamoxifen (TAM) for estrogen receptor (ER)-negative breast cancer. *Kurume Med J* 2002; **49**: 27-33

31 **Galbiati E**, Caruso PL, Amari G, Armani E, Ghirardi S, Delcanale M, Civelli M. Pharmacological actions of a novel, potent, tissue-selective benzopyran estrogen. *J Pharmacol Exp Ther* 2002; **303:** 196-203

32 **Lovat PE**, Oliverio S, Ranalli M, Corazzari M, Rodolfo C, Bernassola F, Aughton K, Maccarrone M, Hewson QD, Pearson AD, Melino G, Piacentini M, Redfern CP. GADD153 and 12-lipoxygenase mediate fenretinide-induced apoptosis of neuroblastoma. *Cancer Res* 2002; **62:** 5158-5167

33 **Belev B**, Aleric I, Vrbanec D, Petrovecki M, Unusic J, Jakic-Razumovic J. Nm23 gene product expression in invasive breast cancer-immunohistochemical analysis and clinicopathological correlation. *Acta Oncol* 2002; **41:** 355-361

34 **Kintscher U**, Goetze S, Wakino S, Kim S, Nagpal S, Chandraratna RA, Graf K, Fleck E, Hsueh WA, Law RE. Peroxisome proliferator-activated receptor and retinoid X receptor ligands inhibit monocyte chemotactic protein-1-directed migration of monocytes. *Eur J Pharmacol* 2000; **401**: 259-270

35 **Hirase N**, Yanase T, Mu Y, Muta K, Umemura T, Takayanagi R, Nawata H. Thiazolidinedione suppresses the expression of erythroid phenotype in erythroleukemia cell line K562. *Leuk Res* 2000; **24**: 393-400

36 **Gurnell M**, Wentworth JM, Agostini M, Adams M, Collingwood TN, Provenzano C, Browne PO, Rajanayagam O, Burris TP, Schwabe JW, Lazar MA, Chatterjee VK. A dominant-negative peroxisome proliferator-activated receptor gamma (PPARgamma) mutant is a constitutive repressor and inhibits PPARgamma-mediated adipogenesis. *J Biol Chem* 2000; **275**: 5754-5759

37 **Asou H**, Verbeek W, Williamson E, Elstner E, Kubota T, Kamada N, Koeffler HP. Growth inhibition of myeloid leukemia cells by troglitazone, a ligand for peroxisome proliferator activated receptor gamma, and retinoids. *Int J Oncol* 1999; **15**: 1027-1032

38 **Esteller M**, Fraga MF, Paz MF, Campo E, Colomer D, Novo FJ, Calasanz MJ, Galm O, Guo M, Benitez J, Herman JG. Cancer epigenetics and methylation. *Science* 2002; **297**: 1807-1808

39 **Yamakawa-Karakida N**, Sugita K, Inukai T, Goi K, Nakamura M, Uno K, Sato H, Kagami K, Barker N, Nakazawa S. Ligand activation of peroxisome proliferator-activated receptor gamma induces apoptosis of leukemia cells by down-regulating the c-myc gene expression via blockade of the Tcf-4 activity. *Cell Death Differ* 2002; **9**: 513-526

40 **Oyama Y**, Akuzawa N, Nagai R, Kurabayashi M. PPARgamma ligand inhibits osteopontin gene expression through interference with binding of nuclear factors to A/T-rich sequence in THP-1 cells. *Circ Res* 2002; **90**: 348-355

41 **Abe A**, Kiriyama Y, Hirano M, Miura T, Kamiya H, Harashima H, Tokumitsu Y. Troglitazone suppresses cell growth of KU812 cells independently of PPARgamma. *Eur J Pharmacol* 2002; **436**: 7-13

42 **Harris SG**, Smith RS, Phipps RP. 15-deoxy-Delta 12,14-PGJ2 induces IL-8 production in human T cells by a mitogen-activated protein kinase pathway. *J Immunol* 2002; **168**: 1372-1379

43 **Anderson SP**, Yoon L, Richard EB, Dunn CS, Cattley RC, Corton JC. Delayed liver regeneration in peroxisome proliferator-activated receptor-alpha-null mice. *Hepatology* 2002; **36**: 544-554

44 **Rumi MA**, Sato H, Ishihara S, Ortega C, Kadowaki Y, Kinoshita Y. Growth inhibition of esophageal squamous carcinoma cells by peroxisome proliferator-activated receptor-gamma ligands. *J Lab Clin Med* 2002; **140**: 17-26

45 **Ohta T,** Elnemr A, Yamamoto M, Ninomiya I, Fushida S, Nishimura GI, Fujimura T, Kitagawa H, Kayahara M, Shimizu K, Yi S, Miwa K. Thiazolidinedione, a peroxisome proliferator-activated receptor-gamma ligand, modulates the E-cadherin/beta-catenin system in a human pancreatic cancer cell line, BxPC-3. *Int J Oncol* 2002; **21**: 37-42

46 **Kawakami S**, Arai G, Hayashi T, Fujii Y, Xia G, Kageyama Y, Kihara K. PPARgamma ligands suppress proliferation of human urothelial basal cells *in vitro*. *J Cell Physiol* 2002; **191**: 310-319

47 **Toyota M,** Miyazaki Y, Kitamura S, Nagasawa Y, Kiyohara T, Shinomura Y, Matsuzawa Y. Peroxisome proliferator-activated receptor gamma reduces the growth rate of pancreatic cancer cells through the reduction of cyclin D1. *Life Sci* 2002; **70**: 1565-1575

48 **Li HL**, Zhang HW, Chen DD, Zhong L, Ren XD, Si-Tu R. JTE-522, a selective COX-2 inhibitor, inhibits cell proliferation and induces apoptosis in RL95-2 cells. *Acta Pharmacol Sin* 2002; **23**:631-637

49 **Li HL**, Chen DD, Li XH, Zhang HW, Lu YQ, Ye CL, Ren XD. Changes of NF-kB, p53, Bcl-2 and caspase in apoptosis induced by JTE-522 in human gastric adenocarcinoma cell line AGS cells: role of reactive oxygen species. *World J Gastroenterol* 2002; **8**: 431-435

50 **Li HL**, Chen DD, Li XH, Zhang HW, Lu JH, Ren XD, Wang CC. JTE-522-induced apoptosis in human gastric adenocarcinoma cell line AGS cells by caspase activation accompanying cytochrome C release, membrane translocation of Bax and loss of mitochondrial membrane potential. *World J Gastroenterol* 2002; **8**: 217-223

51 **Li HL**, Ren XD, Zhang HW, Ye CL, Lv JH, Zheng PE. Synergism between heparin and adriamycin on cell proliferation and apoptosis in human nasopharyngeal carcinoma CNE2 cells. *Acta Pharmacol Sin* 2002; **23**: 167-172

52 **Li HL,** Ye KH, Zhang HW, Luo YR, Ren XD, Xiong AH, Situ R. Effect of heparin on apoptosis in human nasopharyngeal carcinoma CNE2 cells. *Cell Res* 2001; **11**: 311-315

53 **Tian G**, Yu JP, Luo HS, Yu BP, Yue H, Li JY, Mei Q. Effect of nimesulide on proliferation and apoptosis of human hepatoma SMMC-7721 cells. *World J Gastroenterol* 2002; **8**: 483-487

54 **Wu YL**, Sun B, Zhang XJ, Wang SN, He HY, Qiao MM, Zhong J, Xu JY. Growth inhibition and apoptosis induction of Sulindac on Human gastric cancer cells. *World J Gastroenterol* 2001; **7**: 796-800

55 **Wang X**, Lan M, Wu HP, Shi YQ, Lu J, Ding J, Wu KC, Jin JP, Fan DM. Direct effect of croton oil on intestinal epithelial cells and colonic smooth muscle cells. *World J Gastroenterol* 2002; **8**: 103-107

56 **Niu ZS**, Li BK, Wang M. Expression of p53 and C-myc genes and its clinical relevance in the hepatocellular carcinomatous and pericarcinomatous tissues. *World J Gastoenterol* 2002; **8**: 822-826

57 **Liu S**, Wu Q, Ye XF, Cai JH, Huang ZW, Su WJ. Induction of apoptosis by TPA and VP-16 is through translocation of TR3. *World J Gastroenterol* 2002; **8:** 446-450

58 **Xu CT**, Huang LT, Pan BR. Current gene therapy for stomach carcinoma. *World J Gastroenterol* 2001; **7**: 752-759

59 **Wu YL**, Sun B, Zhang XJ, Wang SN, He HY, Qiao MM, Zhong J, Xu JY. Growth inhibition and apoptosis induction of Sulindac on Human gastric cancer cells. *World J Gastroenterol* 2001; **7**: 796-800

60 **Hou L**, Li Y, Jia YH, Wang B, Xin Y, Ling MY, Lü S. Molecular mechanism about lymphogenous metastasis of hepatocarcinoma cells in mice. *World J Gastroenterol* 2001; **7**: 532-536

61 **Xu AG**, Li SG, Liu JH, Gan AH. Function of apoptosis and expression of the proteins Bcl-2, p53 and C-myc in the development of gastric cancer. *World J Gastroenterol* 2001; **7**: 403-406

62 **Liu XJ,** Yang L, Wu HB, Qiang O, Huang MH, Wang YP. Apoptosis of rat hepatic stellate cells induced by anti-focal adhesion kinase antibody. *World J Gastroenterol* 2002; **8**: 734-738

63 **Zhang XL**, Liu L, Jiang HQ. Salvia miltiorrhiza monomer IH764-3 induces hepatic stellate cell apoptosis via caspase-3 activation. *World J Gastroenterol* 2002; **8**: 515-519

64 **Sun BH**, Zhang J, Wang BJ, Zhao XP, Wang YK, Yu ZQ, Yang DL, Hao LJ. Analysis of in vivo patterns of caspase 3 gene expression in primary hepatocellular carcinoma and its relationship to p21(WAF1) expression and hepatic apoptosis. *World J Gastroenterol* 2000; **6**: 356-360

65 **Farilla L**, Hui H, Bertolotto C, Kang E, Bulotta A, Di Mario U, Perfetti R. Glucagon-Like Peptide-1 Promotes Islet Cell Growth and Inhibits Apoptosis in Zucker Diabetic Rats. *Endocrinology* 2002; **143:** 4397-4408

66 **Higashitsuji H**, Higashitsuji H, Nagao T, Nonoguchi K, Fujii S, Itoh K, Fujita J. A novel protein overexpressed in hepatoma accelerates export of NF-kappaB from the nucleus and inhibits p53-dependent apoptosis. *Cancer Cell* 2002; **2**: 335-346

Edited by Pang LH and Wang XL

P.O.Box 2345, Beijing 100023,China
Fax: +86-10-85381893
E-mail: wjg@wjgnet.com www.wjgnet.com

World J Gastroenterol 2003;9(8):1689-1696
World Journal of Gastroenterology
 ISSN 1007-9327

• LIVER CANCER •

S-phase delay in human hepatocellular carcinoma cells induced by overexpression of integrin b1

Yu-Long Liang, Ting-Wen Lei, Heng Wu, Jian-Min Su, Li-Ying Wang, Qun-Ying Lei, Xi-Liang Zha

Yu-Long Liang, Heng Wu, Li-Ying Wang, Qun-Ying Lei, Xi-Liang Zha, Department of Biochemistry and Molecular Biology, Shanghai Medical College, Fudan University, Shanghai 200032, China
Ting-Wen Lei, Department of Biochemistry, Guiyang Medical College, Guiyang 550004, Guizhou Province, China
Jian-Min Su, Department of Chemistry, Shanghai Medical College, Fudan University, Shanghai 200032, China
Supported by Grants from the National Natural Science Foundation of China, No.30000083 and Shanghai Municipal Government Science and Technology Committee, No.00JC14042
Correspondence to: Dr. Xi-Liang Zha, Department of Biochemistry and Molecular Biology, Shanghai Medical College, Fudan University, 138 Yi Xue Yuan Road, Shanghai 200032, China. xlzha@shmu.edu.cn
Telephone: +86-21-54237696 **Fax**: +86-21-64179832
Received: 2003-03-05 **Accepted:** 2003-04-01

Abstract

AIM: To clarify the mechanisms of integrin overexpression in negatively regulating the cell cycle control of hepatocellular carcinoma cells SMMC-7721.

METHODS: The cell cycle pattern was determined by flow cytometry. The mRNA and protein expression levels were assayed by RT-PCR and Western blot, respectively. Stable transfection was performed by Lipofectamine 2000 reagent, and cells were screened by G418.

RESULTS: Overexpression of α5β1 or β1 integrin induced S-phase delay in SMMC-7721 cells, and this delay was possibly due to the accumulation of cyclin-dependent kinase inhibitors (CKIs) $p21^{cip1}$ and $p27^{kip1}$. The decrease of protein kinase B (PKB) phosphorylation was present in this signaling pathway, but focal adhesion kinase (FAK) was not involved. When phosphorylation of PKB was solely blocked by wortmannin, $p27^{kip1}$ protein level was increased. Moreover, S-phase delay was recurred when attachment of the parental SMMC-7721 cells was inhibited by the preparation of poly-HEME, and this cell cycle pattern was similar to that of β1-7721 or α5β1-7721 cells.

CONCLUSION: S-phase delay induced by overexpression of integrin β1 subunit is attributed to the decrease of PKB phosphorylation and subsequent increases of $p21^{cip1}$ and $p27^{kip1}$ proteins, and may be involved in the unoccupied α5β1 because of lack of its ligands.

Liang YL, Lei TW, Wu H, Su JM, Wang LY, Lei QY, Zha XL. S-phase delay in human hepatocellular carcinoma cells induced by overexpression of integrin β1. *World J Gastroenterol* 2003; 9(8): 1689-1696
http://www.wjgnet.com/1007-9327/9/1689.asp

INTRODUCTION

Extracellular matrix (ECM) is consisted of many components, such as collagen, glycoproteins, elastin, and proteoglycans that in addition to providing a scaffold for tissue, regulate many fundamental cellular processes such as proliferation, survival, migration and differentiation[1,2]. Many cell types require anchorage to ECM to proliferate[3]. If lacking attachment to ECM, they will undergo anoikis[2, 4]. Integrins activate growth-promoting signaling pathways that are responsible for the anchorage, and two such pathways appear to be involved. One is that integrins facilitate growth factor-mediated activation of extracellular signal-regulated protein kinase (ERK); the other is that integrins activate the c-Jun NH_2-terminal kinase (JNK)[2, 5]. In addition, serine/threonine protein kinase, PKB, has emerged as a crucial regulator in the integrin pathway, which can be controlled through phosphatidylinositol-3' kinase (PI3K)[6]. Integrins, often together with growth factor receptors, up-regulate cyclins D and E and down-regulate CKIs $p21^{cip1}$, $p27^{kip1}$, and $p57^{kip2}$[2, 7]. This action allows cells to pass through the G1/S transition and complete the cell cycle.

Many studies, however, have demonstrated that integrins give rise to growth inhibition rather than growth stimulation[8-13]. Integrin α5β1 has been often observed to be lost in cancerous areas other than in its normal counterpart tissues[14]. It is apparent from these studies that integrin signaling may play a major role in negative control of cell growth, which may be lost in some cancer cells, and the mechanisms of this effect are not completely known yet.

In this study we have further investigated the inhibition role of integrin α5β1 in human hepatocellular carcinoma cell line, SMMC-7721. We analyzed the effect of these cells with or without adhesion to ECM. These studies identified overexpression of β1 subunit or α5β1 inhibited cell cycle progression at S-phase, and this inhibition maybe resulted from the up-regulation of cdk2 inhibitors $p21^{cip1}$ and $p27^{kip1}$ and involved in the unoccupied β1 because of relative lack of its ligands.

MATERIALS AND METHODS

Materials and antibodies

Poly-HEME, wortmannin, FN and LN were all obtained from Sigma, and geneticin (G418) was purchased from Calbiochem (San Diego, CA). Monoclonal antibodies used were directly against cyclin D1 (Santa Cruz), cdk2 (Santa Cruz), integrin β1 (BD Transduction Laboratories, Lexington, KY), phosphorylated FAK (anti-phosphotyrosine clone PT-66, Sigma) and β-actin (Santa Cruz). Goat anti-human integrin α5 polyclonal antibody was also purchased from Santa Cruz. Other antibodies used were those against FAK (Santa Cruz), $p21^{cip1}$ (Santa Cruz), $p27^{kip1}$ (Oncogene Research Products, Cambridge, MA), Ser473-phosphorylated form of PKB and PKB (Cell Signaling). Horseradish peroxidase conjugated anti-mouse, rabbit or goat IgG were purchased from Calbiochem (San Diego, CA).

Cell culture

Human hepatocellular carcinoma cell line SMMC-7721 was obtained from the Liver Cancer Institute, Zhongshan Hospital (Shanghai, China). SMMC-7721 cells were grown in RPMI 1640 medium (Gibco BRL) supplemented with 100 $mL \cdot L^{-1}$ calf bovine serum (CBS), 100×10^3 $U \cdot L^{-1}$ penicillin and 100×10^3 $U \cdot L^{-1}$ streptomycin sulfate. Integrin-overexpressing transfectant

cell lines were maintained in the same medium as above plus 500 μg/ml geneticin (Gibco BRL).

Plasmid construction and stable transfections

pECE vector containing human full-length cDNA of integrin β1 was presented generously by Dr. Mara Brancaccio (Department of Genetics, University of Torino, Torino, Italy). Complementary DNA of β1 integrin cleaved from the pECE plasmid by *EcoR* I was subcloned into pcDNA3 vector to generate pcDNA3-β1. pcDNA3-α5 expression vector was presented kindly by Dr. Sue E. Craig (School of Biological Sciences, University of Manchester, Manchester, UK). Stable transfections were performed using LIPOFECTAMINE™ 2000 (LF2000) reagent (Life Technologies, Grand Island, NY) according to the manufacturer's instructions. Briefly, logarithmically growing cells were transfected with 1 μg of plasmids and 2 μl of LF2000 reagent. At 48 h after transfection, the selective medium containing 1 mg/ml geneticin (G418) antibiotic (Calbiochem) was replaced, and then the cell clones were selected and identified.

Plating experiments

Mock and integrin transfected cells were seeded on the tissue culture plates coated with either FN (15 μg/ml) or LN (15 μg/ml), grown for 60 minutes, and followed by phase-contrast microscopy or protein extraction.

Flow cytometry

Cells were starved by exposure to SFM for 48 h, the harvested cells were then grown in normal growth medium containing 10 % CBS for 12-16 h, the time span covered the duration of normal S phase. At the end of incubation, the cells were digested with 2 mM EDTA in PBS and rinsed twice with ice-cold PBS solution, then fixed by adding them dropwise into 75 % ice-cold ethanol while vortexing, followed by incubation on ice for 60 min. The fixed cells were washed with ice-cold PBS and incubated at 37 ℃ for 30 min in 0.5 ml PBS solution containing 20 μg/ml RNase A, 0.2 % Triton X-100, 0.2 mM EDTA and 20 μg/ml of propidium iodide. DNA content was determined by FACS analysis (Becton Dickinson). The percentage of cells in G0/G1, S, and G2/M phases was determined using the Modfit program.

RNA isolation and RT-PCR

RT-PCR was performed to quantify the level of mRNA, which was isolated using Trizol system (Watson Biotechnologies, Shanghai, China) according to the manufacturer's guidelines. Complementary DNA synthesis was performed essentially as described previously[15], except that 2 μg of total RNA was used for cDNA synthesis, and the primer used was oligo $(dT)_{15}$. For amplification, 2-μl cDNA product was used in a final volume of 50 μl with 5 units of Taq polymerase (SABC, Luoyang, China). The primer pairs for $p27^{kip1}$ and $p21^{cip1}$ were described previously[16,17]. Primers for β-actin[16] were used as the internal control. The expected product sizes were p27, 471 bp; p21, 159 bp and β-actin, 412 bp.

Cell lysis and immunoblotting

Cells cultured under the same conditions as cell cycle analysis were collected, and then washed twice with ice-cold PBS and lysed in 1×SDS lysis buffer (50 mM Tris (pH 6.8), 2 % SDS, 10 % glycerol, 100 μg/ml PMSF, 10 μg/ml leupeptin and 5 mM Na_3VO_4) for 10 min on ice. Cell lysates were boiled and clarified by centrifugation at 12 000 g at 4 ℃ for 10 min. Protein concentration was determined with Hartree assay. Immunoblotting analyses using the enhanced chemiluminescence (ECL) detection system (Perfect, Shanghai, China) were carried out as described previously[18].

RESULTS

Overexpression of integrin α5β1 in SMMC-7721 cells

We transfected the full-length cDNA of genes ITGA5 (α5) or ITGB1 (β1) alone, or α5 and β1 together into a human hepatocellular carcinoma cell line, SMMC-7721, respectively. The pcDNA3 empty vector was the control plasmids, and cells transfected with pcDNA3 were regarded as the mocked cells. The overexpressed transfectant cell lines were mainly screened for increased expression of α5 or β1 in protein levels by Western analysis, and designated as α5-7721, β1-7721 and α5β1-7721, respectively. As shown in Figure 1A, integrin α5 expression was increased to 2-fold in α5-7721 or α5β1-7721 cells compared with the mocked cells. Meanwhile, β1-7721 and α5β1-7721 transfectants had more than 2.5-fold amount in integrin β1 protein level (Figure 1B). The β1 subunits appeared as two bands in Western blot because of variable post-translational modification (mainly N-glycosylation). The hypoglycosylated lower band (Figure 1B) was tentatively identified as biosynthetic precursor of β1 subunit. The band with lower migration rate (upper band in Figure 1B) of integrin β1 subunit was in hyperglycosylated forms, and mainly located in plasma membrane[19-21].

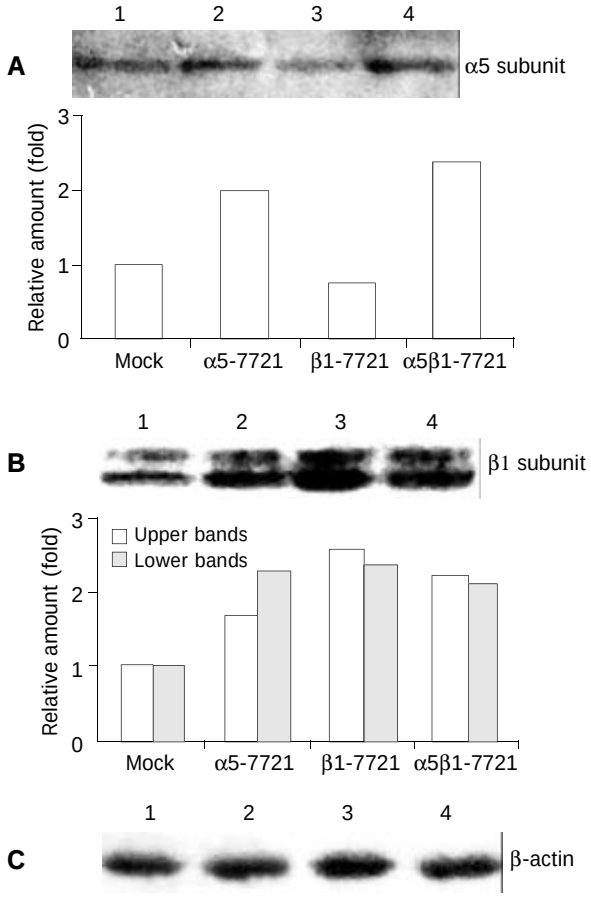

Figure 1 Integrin α5 and β1 protein levels in α5-, β1- and α5β1 transfected SMMC-7721 cells. (A) The expression level of α5 chain was increased in α5-7721 and α5β1-7721 cells. (B) Two forms of β1 integrin were due to different levels of β1-chain glycosylation. The hypoglycosylated lower band was tentatively identified as biosynthetic precursor of β1 subunit, the hyperglycosylated upper band was mature subunits, exposed in part on the cell surface (the 130-kDa product). Immunoblot assay showed that protein levels of the mature form were elevated in the transfectants, especially in β1-7721 and α5β1-7721 cells. (C) The protein level of β-actin showed an equal loading amount in each well. Lane 1, mock cells; lane 2, α5-7721; lane 3, β1-7721; lane 4, α5β1-7721. Each point in the graphs was the mean value from three separate experiments.

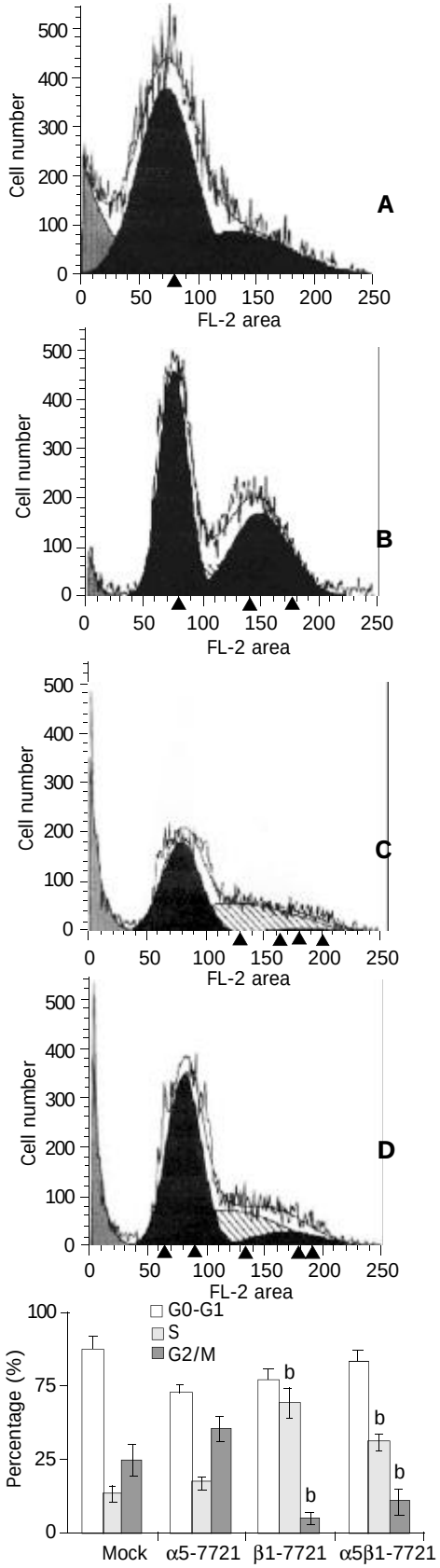

Figure 2 S-phase delay was induced in β1- and α5β1-transfectant cells. For cell cycle analysis, transfected and mocked cells were synchronized by exposure to SFM for 48 h, then grown in RPMI1640 medium containing 10 % CBS and penicillin / streptomycin solution. Twelve or 16 h later, the cells were collected and analysed for flow cytometry as described under "Materials and Methods". A, mocked cells; B, α5-7721 cells; C, β1-7721 cells; D, α5β1-7721 cells. Each bar in graph represented the mean ± SD obtained from three independent experiments. The S-phase delay was significantly different in β1-7721 and α5β1-7721 cells (n=3, ^bP<0.01 *vs* mocked cells).

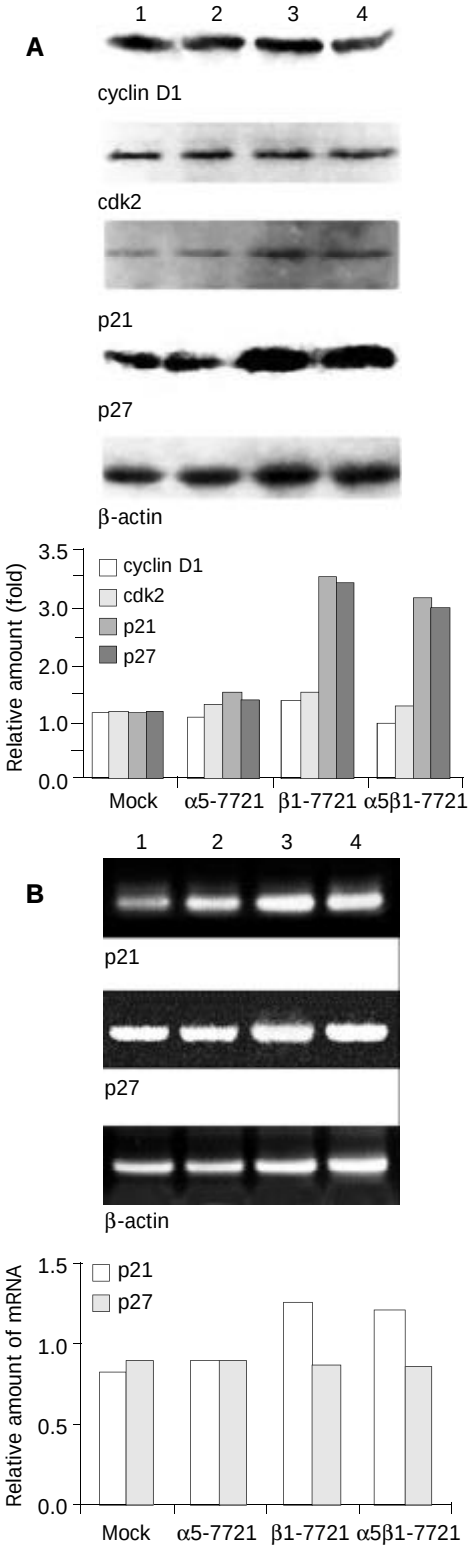

Figure 3 Message RNA and / or protein levels of cell cycle regulatory genes $p21^{cip1}$ and $p27^{kip1}$ in β1-7721 and α5β1-7721 transfectants, but not that of cyclin D1 and cdk2. (A) Immunoblot assay showed the protein level of cyclin D1 and cdk2 were not apparently affected, but $p21^{cip1}$ and $p27^{kip1}$ protein levels were increased in β1-7721 and α5β1-7721 cells. The protein level of β-actin was detected to assess the loading amount in each well in SDS-PAGE gel. (B) Message RNA levels of $p21^{cip1}$ and $p27^{kip1}$ were assessed by RT-PCR, and normalized by that of β-actin. It was apparent that mRNA level of $p21^{cip1}$ was increased in β1- and α5β1- transfected cells. However, the $p27^{kip1}$ mRNA amount was the same as control. Each result represented three separate experiments. Lane 1, mocked cell; lane 2, α5-7721; lane 3, β1-7721; lane 4, α5β1-7721.

Induction of S-phase delay by transfection of integrin β1 subunit

In the previous study, we showed that overexpression of integrin α5β1 or β1 subunit had negative effects on cell growth[11]. To elucidate the mechanisms of cell cycle perturbation induced by overexpressing integrins, flow cytometry analyses were applied. Cell cycle parameters were compared between transfected cells and mocked cells. Similar patterns of the cell cycle were found in α5-7721 and mocked cells (Figure 2). But in β1-7721 and α5β1-7721 transfectants, we observed a significant increase in fraction of cells in S phase of the cell cycle, as shown in Figure 2. This was accompanied by a decrease in proportion of cells in G2/M phases of the cell cycle. These changes were specific for the transfection events containing β1-plasmids, that is, at this point, the pattern of α5β1-7721 was similar to that of β1-7721 cells. These results were obtained from the cells synchronized partly in G0/G1 phase by exposure to serum-free medium. Therefore, these data showed that S-phase delay was probably due to enhanced production of exogenous β1 integrin.

$p21^{cip1}$ and $p27^{kip1}$ were up-regulated in β1 or α5β1 transfectant cell lines

To clarify the mechanism by which S-phase delay was induced in β1-7721 and α5β1-7721 cells, we investigated whether cyclins and cdks were involved in this situation. Expression level of cyclin D1 was examined because this protein was always referred to as a sensor molecule to the extracellular cues[22]. It was shown that cyclin D1 expression was not changed, neither was the cdk2 protein (Figure 3A). As evidenced recently, enhanced $p21^{cip1}$ and/or $p27^{kip1}$ expression was considered to be associated with G1 cell cycle arrest[23, 24], and under some circumstances, with S-phase delay in some cell types[25, 26]. So, we further examined whether β1-chain overexpression could induce $p21^{cip1}$ and $p27^{kip1}$ in β1-7721 and α5β1-7721 cells. As shown in Figure 3A, a significant increase (2-fold amount) of $p21^{cip1}$ protein levels was noted in β1-7721 and α5β1-7721 cells compared with the mocked cells or α5-7721 cells. Meanwhile, $p27^{kip1}$ protein level was also increased to 2.5-fold. We also found that the mRNA level of $p21^{cip1}$ increased, although that of $p27^{kip1}$ maintained the same as control (Figure 3B). Interestingly, we found that overexpression of β1 gene in SMMC-7721 cells induced S-phase delay in this study. The above findings showed that this S-phase delay might be attributed to the increased expression of $p21^{cip1}$ and $p27^{kip1}$.

Phosphorylated form of PKB was inhibited in β1 and α5β1 transfectants and this might result in accumulation of $p21^{cip1}$ and $p27^{kip1}$

To determine how overexpressing α5β1 integrins transferred signals from membrane to cytosol or nucleus to modulate the expression of CKIs $p21^{cip1}$ and $p27^{kip1}$, we examined the two important signaling molecules mediated by integrins, FAK and PKB. The results showed that neither FAK nor its tyrosine phosphorylated form was affected (Figure 4A). However, levels of Ser473-phosphorylated form of PKB were decreased in β1-7721 and α5β1-7721 cells in comparison with the control cells, but total amount of PKB protein was not apparently affected (Figure 4B).

In recent years, evidences have shown that activated PKB protein may phosphorylate $p21^{cip1}$, and induce its degradation through the ubiquitin-26S proteasome pathway[6,27]. But evidences indicating $p27^{kip1}$ phosphorylation by PKB are few. In this study, decrease of phosphorylated PKB (Figure 4B) and accumulation of $p27^{kip1}$ (Figure 3A) occurred concomitantly in β1-7721 or α5β1-7721 cells. To obtain support, we further performed an experiment to block the phosphorylated form of PKB. It is well known that Ser-473 phosphorylation of PKB, on behalf of its active forms, appears to be catalyzed by phosphoinositide-dependent kinase 1 (PDK1) and integrin-linked kinase (ILK)[28, 29], and that PI3K is located upstream of both ILK and PKB[6]. So the PI3K inhibitor wortmannin was explored in this study. Following serum starvation, cells were cultured in the medium with 100 nM wortmannin for 24 h or 48 h. We investigated the level of phosphorylation of PKB and $p27^{kip1}$ by immunostaining. The data showed that phosphorylation of PKB was blocked, and expression of $p27^{kip1}$ was increased at the same time compared with control cells (Figure 5). Therefore, the decrease of phosphorylated form of PKB was at least in part, responsible for $p27^{kip1}$ protein accumulation.

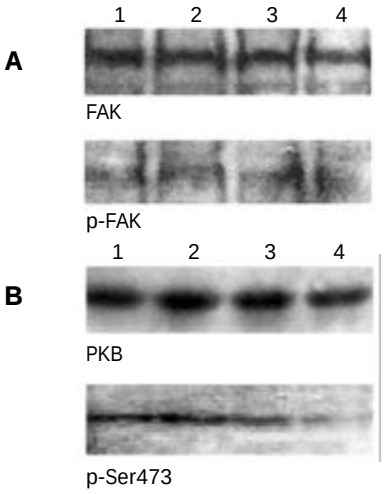

Figure 4 Activation of PKB, but not FAK, was downregulated in β1- and α5β1- transfected cells. (A) FAK activation was assessed by phosphotyrosine- specific antibody, followed by stripping and reprobing with anti-FAK antibody. (B) PKB and its Ser473-phosphorylated forms were determined by 10 % SDS-PAGE with the equal loading amount. The loading amount control is shown in Figures 1C and 3A. Lane 1, mock cells; lane 2, α5-7721; lane 3, β1-7721; lane 4, α5β1-7721. Results were representative of 4 repeated experiments.

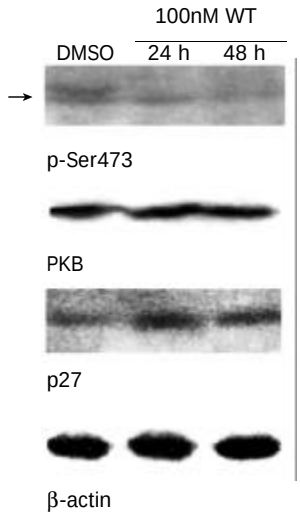

Figure 5 Ser473-phosphorylated form of PKB was decreased, but $p27^{kip1}$ protein level was increased concomitantly in SMMC-7721 parental cells treated with the PI3K inhibitor wortmannin. The parental SMMC-7721 cells were starved with serum-free medium for 48 h, then grown in normal medium / 10 % CBS containing DMSO (as control, 24 h) or 100 nM wortmannin for

the indicated times. The amount of DMSO did not exceed 0.1 %, which was determined not to damage the cells. Equal amount of wortmannin was added again after grown for 24 h. The level of Ser473-phosphorylated form of PKB (*arrow*) was declined, but $p27^{kip1}$ protein level was elevated with the treatment of wortmannin in SMMC-7721 cells. Results were representative of at least 3 repeated experiments. Abbreviation: DMSO, dimethylsulfoxide; WT, wortmannin.

Inhibition of cell cycle was possibly due to the relative lack of ECM

Integrins, in general, promote the focal adhesion protein activities such as FAK and cell cycle progression[2]. So we ponder why overexpression of integrin β1 subunit can repress the level of phosphorylated PKB and the cell cycle. Here, we performed plating experiments to elucidate its mechanism. First, we observed the morphological change of cells that were plated on LN- or FN- coated dishes and grown for 60 minutes (Figure 6). It was found that β1-7721 and α5β1-7721 cells were prone to attachment and spreading, perhaps to the cell cycle progression. Next, we determined the changes of phosphorylated FAK and phosphorylation of PKB in cells attaching on LN and FN. As mentioned above (Figure 4A), total amount of FAK and its phosphorylated forms were not affected in cells cultured in the flasks without coating of LN or FN. But the level of tyrosine phosphorylated FAK was increased in cells, which were plated on LN- or FN- coated dishes and grown for the indicated times (Figure 7A, and data not shown for FN-coated dishes). Moreover, the level of Ser473 phosphorylated form of PKB was similar to that of phosphorylated FAK under the same condition (Figure 7B, and data not shown for FN-coated dishes). Finally, protein level of $p27^{kip1}$ was declined in β1-7721 and α5β1-7721 cells (Figure 7C). These findings demonstrated that an important role of LN or FN in the molecular changes of β1-7721 or α5β1-7721 cells, especially, in PKB phosphorylation and $p27^{kip1}$ protein levels. On the contrary, when attachment of the parental cells to ECM was blocked by plating them onto poly-HEME-coated petri dishes, the percentage of cells in S-phase was increased from 13.08 % to 37.33 % (Figure 8). That is, when the parental SMMC-7721 cells were prevented from interaction with ECM through the preparation of poly-HEME, the same effects of S-phase accumulation took place as that in β1-7721 or α5β1-7721 cells. These results suggested that S-phase delay induced by overexpressing β1 in SMMC-7721 cells might be the result of the relative lack of ECM.

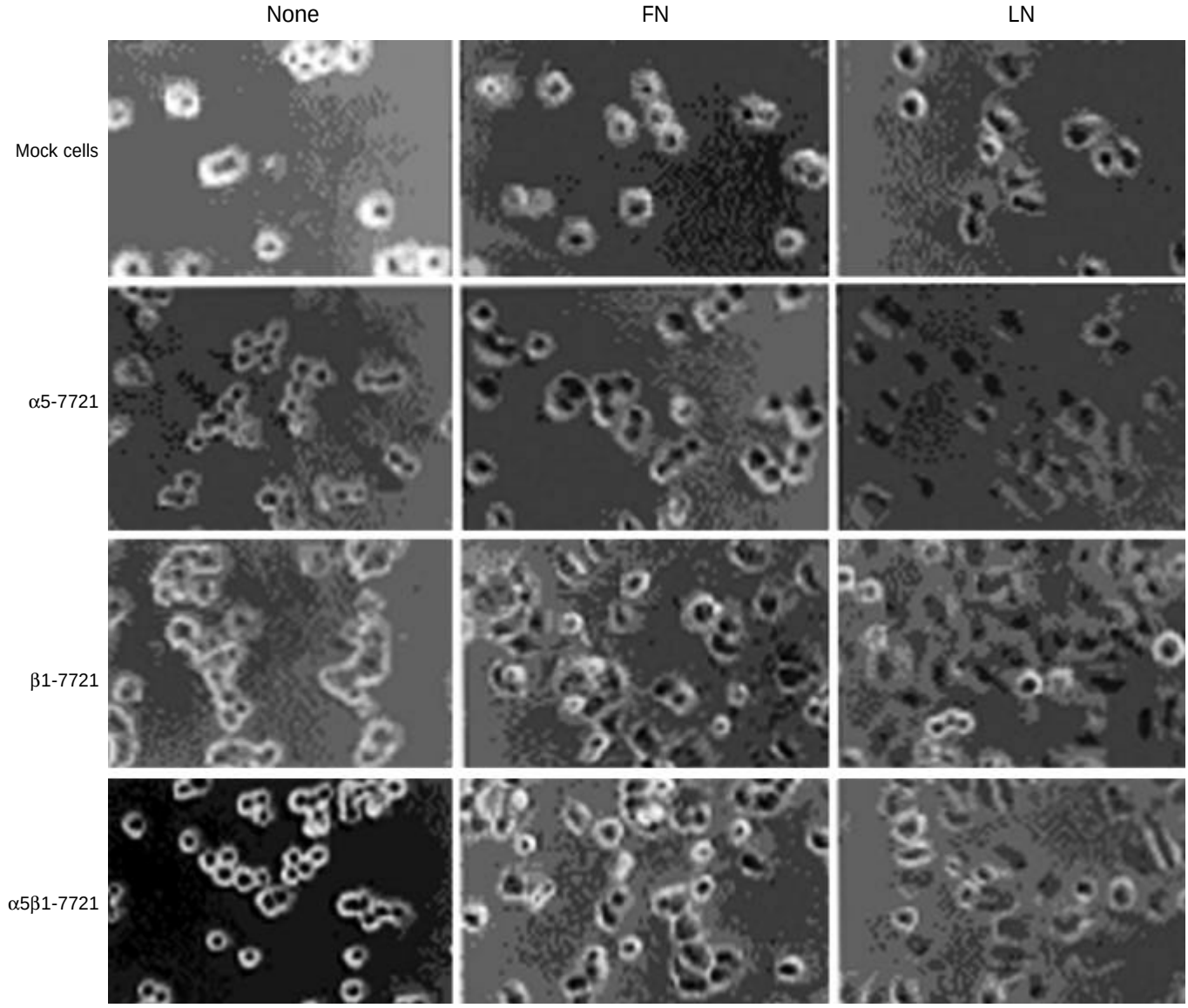

Figure 6 β1-7721 and α5β1-7721 cells subjected to spreading on fibronectin- or laminin- coated culture dishes. The mocked and transfected cells were plated on FN- or LN- coated tissue culture plates in normal medium for 60 min, then cells on the plates were photographed by phase-contrast microscopy with a digital camera. Abbreviations: FN, fibronectin; LN, laminin.

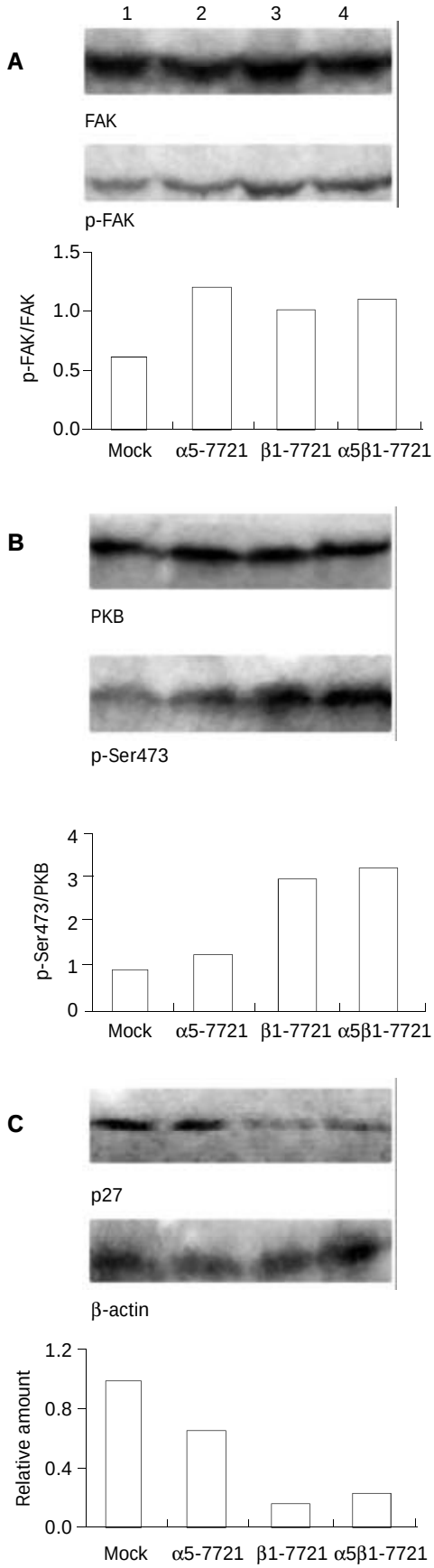

Figure 7 Effects of laminin on transfected cells. Protein levels of phosphorylated FAK (A) and Ser473-phosphorylated form of PKB (B) were increased in the transfected cells, especially in β1-7721 and α5β1-7721 cells grown in the LN-coated culture dishes for 60 minutes. (C) Under the same condition, $p27^{kip1}$ protein level was decreased in β1-7721 and α5β1-7721 cells. Lane 1, mock cells; lane 2, α5-7721; lane 3, β1-7721; lane 4, α5β1-7721. Each result represented at least 3 independent experiments.

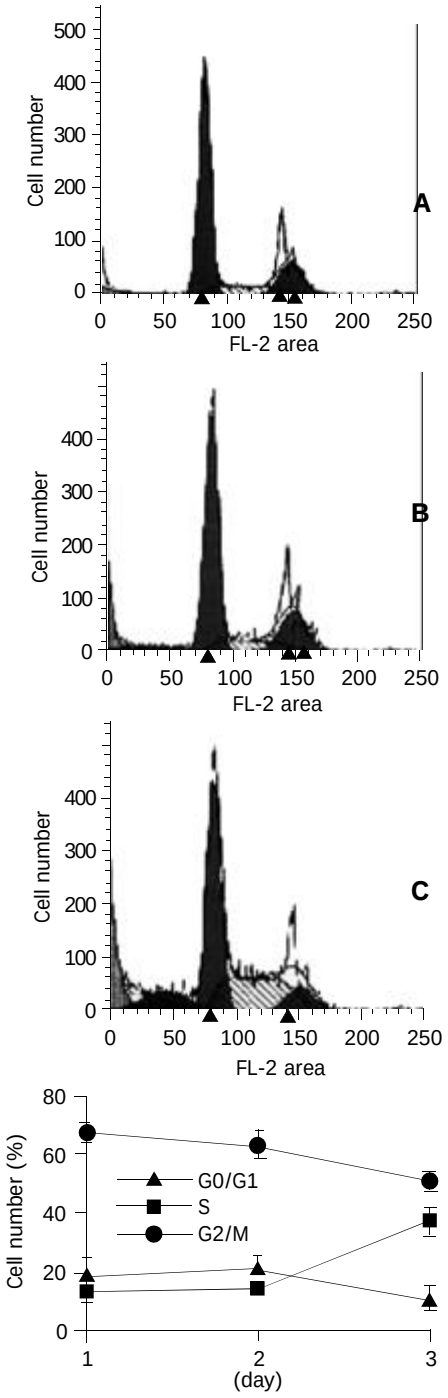

Figure 8 The percentage of cells in S phase was increased in SMMC-7721 cells plated on poly-HEME-coated petri dishes. The parental SMMC-7721 cells were plated on poly-HEME-coated petri dishes, and cultured in normal medium for 24 h (A), 48 h (B) or 72 h (C), respectively, then collected and analysed by flow cytometry. The cell cycle pattern (C) was similar to that of β1-7721 or α5β1-7721 cells.

DISCUSSION

We examined the effects of overexpressed α5β1 or β1 on tumor cell proliferation, which provide the evidence that overexpression of α5β1 or β1 inhibits the proliferation of human hepatocellular carcinoma cell line SMMC-7721 and this inhibition may be related to the insufficient ligands for overexpressed β1 integrins. This finding also demonstrated that the inhibition of cell cycle was due to a specific growth arrest at S-phase that involved an increase in the protein level of $p21^{cip1}$ and $p27^{kip1}$.

This study showed that cyclin D1 expression was not affected by transfection events. So the early G1 phase

progression may not be influenced under this condition. However, the protein levels of $p21^{cip1}$ and $p27^{kip1}$ were increased in β1 or α5β1 transfectant cells, which might be the major reason why S-phase delay occurred. It was previously reported that $p21^{cip1}$ and $p27^{kip1}$ were assembly factors rather than inhibitors of cdk4/6 kinases[30], but were inhibitors of cdk2 kinase, which is the key kinase contributing to G1/S transition and S phase progression. One CKI protein, $p21^{cip1}$, the first cyclin-dependent kinase inhibitor to be identified[31], has also a separate cdk2 binding site in its N-terminal region (amino acid 53-58) and optimal cyclin/cdk inhibition requires binding to this site as well as one of the cyclin binding domains. Furthermore, $p21^{cip1}$ interacts with proteins such as PCNA, c-Myc and E2Fs that control DNA replication and other S phase events[32]. Meanwhile, evidences have shown that $p27^{kip1}$ plays a key role in the regulation of the proliferation of tumor cells in response to signals from ECM[13]. Therefore, increased $p21^{cip1}$ and $p27^{kip1}$ proteins can induce S-phase delay in β1- and α5β1-transfected cells.

In many cell types, the intracellular concentration of $p27^{kip1}$ is mainly controlled at the posttranscriptional level, and its degradation is initiated by phosphorylation with a target enzyme, cdk2[33] or other enzymes, such as PKB[6], and completed by the ubiquitin-proteasome pathway. $p21^{cip1}$ protein can also be phosphorylated by PKB[6]. In this study, we found that PKB level of phosphorylated form was decreased in β1- or α5β1- transfected cells, accompanied by the increase of $p21^{cip1}$ and $p27^{kip1}$ to a certain extent. These findings indicate that the decrease of active form of PKB may interpret the accumulation of $p21^{cip1}$ and $p27^{kip1}$ *bona fide*, which in turn, interferes with the cell cycle at S phase.

This study suggested that overexpression of β1 or α5β1 integrin in SMMC-7721 cells could induce S-phase delay. The mechanism underlying this phenomenon may be due to two kinds of possibilities. One is "integrin-mediated death" (IMD) described by Stupack and his colleagues[34, 35], that is, an unligated integrin promotes apoptosis of cells. It is well known that α5β1 integrin, in general, acts as the effector protein of cell proliferation, such as endothelial cells in the vascular system[36]. In this study, however, we showed that overexpression of β1 or α5β1 induced S-phase delay. When cells were plated on FN/LN-coated culture dishes, they were subjected to attachment and spreading compared with the mocked and α5-7721 cells. Moreover, for the parental cells, they underwent S-phase delay and apoptosis when they were deprived of attachment by plating them on poly-HEME-coated petri dishes. Therefore, we postulated that the relative lack of ECM might be involved in S-phase delay triggered by overexpression of β1 or α5β1 integrin gene in SMMC-7721 cells. Another possibility is the trans-dominant integrin inhibition, which is defined as the occupancy of one integrin by its ligand, can inhibit the functions of other integrins[37-40]. For example, integrin α5β1 is essential for angiogenesis[36], but $\alpha_v\beta3$ may suppress the functions of integrin α5β1, if β3 integrins prevail in the endothelial cells[41]. It was reported that the basal integrin repertoire in hepatocellular carcinoma cells was characterized by the expression of several potential laminin receptors of the integrin family, such as α1β1, α2β1 and α6β1[42-47]. So the overexpression of β1 may preferentially dimerize with α1, α2 and α6, the subunits of the receptors of laminin or collagen (they were lost in this *in vitro* model). Therefore, if these α subunits are occupied, the functions of integrin α5β1 may be suppressed, including its capacity to block cell cycle arrest.

ACKNOWLEDGEMENTS

We are grateful to Dr. Mara Brancaccio from the University of Torino (Torino, Italy), and Dr. Sue E. Craig from the University of Manchester (Manchester, UK) for their gifts of the plasmids. We also acknowledge the Chinese Medicine Board (CMB) in New York, U.S.A. for its kind support to our research.

REFERENCES

1 **Lukashev ME**, Werb Z. ECM signalling: orchestrating cell behaviour and misbehaviour. *Trends Cell Biol* 1998; **8:** 437-441
2 **Giancotti FG**, Ruoslahti E. Integrin signaling. *Science* 1999; **285:** 1028-1032
3 **Assoian RK**. Anchorage-dependent cell cycle progression. *J Cell Biol* 1997; **136:** 1-4
4 **Frisch SM**, Francis H. Disruption of epithelial cell-matrix interactions induces apoptosis. *J Cell Biol* 1994; **124:** 619-626
5 **Schwartz MA**. Integrin signaling revisited. *Trends Cell Biol* 2001; **11:** 466-470
6 **Nicholson KM**, Anderson NG. The protein kinase B / Akt signalling pathway in human malignancy. *Cell Signal* 2002; **14**: 381-395
7 **Sherr CJ**, Roberts JM. CDK inhibitors: positive and negative regulators of G1-phase progression. *Genes Dev* 1999; **13:** 1501-1512
8 **Giancotti FG**, Mainiero F. Integrin-mediated adhesion and signaling in tumorigenesis. *Biochim Biophys Acta* 1994; **1198:** 47-64
9 **Giancotti FG**, Ruoslahti E. Elevated levels of the α5β1 fibronectin receptor suppress the transformed phenotype of Chinese hamster ovary cells. *Cell* 1990; **60:** 849-859
10 **Varner JA**, Emerson DA, Juliano RL. Integrin α5β1 expression negatively regulates cell growth: reversal by attachment to fibronectin. *Mol Biol Cell* 1995; **6:** 725-740
11 **Zhou GF**, Ye F, Cao LH, Zha XL. Overexpression of integrin α5β1 in human hepatocellular carcinoma cell line suppresses cell proliferation in vitro and tumorigenicity in nude mice. *Mol Cell Biochem* 2000; **207:** 49-55
12 **Wang D**, Sun L, Zborowska E, Willson JK, Gong J, Verraraghavan J, Brattain MG. Control of type II transforming growth factor-β receptor expression by integrin ligation. *J Biol Chem* 1999; **274:** 12840-12847
13 **Henriet P**, Zhong ZD, Brooks PC, Weinberg KI, DeClerck YA. Contact with fibrillar collagen inhibits melanoma cell proliferation by up-regulating $p27^{KIP1}$. *Proc Natl Acad Sci USA* 2000; **97**: 10026-10031
14 **Su JM**, Gui L, Zhou YP, Zha XL. Expression of focal adhesion kinase and α5 and β1 integrins in carcinomas and its clinical siginificance. *World J Gastroenterol* 2002; **8**: 613-618
15 **Munsterberg AE**, Lassar AB. Combinatorial signals from the neural tube, floor plate and notochord induce myogenic bHLH gene expression in the somite. *Development* 1995; **121:** 651-660
16 **Takano Y**, Kato Y, van Diest PJ, Masuda M, Mitomi H, Okayasu I. Cyclin D2 overexpression and lack of p27 correlate positively and cyclin E inversely with a poor prognosis in gastric cancer cases. *Am J Pathol* 2000; **156**: 585-594
17 **Chen B**, He L, Savell VH, Jenkins JJ, Parham DM. Inhibition of the interferon-gamma / signal transducers and activators of transcription (STAT) pathway by hypermethylation at a STAT-binding site in the $p21^{WAF1}$ promoter region. *Cancer Res* 2000; **60:** 3290-3298
18 **Kim J**, Han I, Kim Y, Kim S, Oh ES. C-terminal heparin-binding domain of fibronectin regulates integrin-mediated cell spreading but not the activation of mitogen-activated protein kinase. *Biochem J* 2001; **360:** 239-245
19 **Heino J**, Ignotz RA, Hemler ME, Crouse C, Massague J. Regulation of cell adhesion receptors by transforming growth factor-β. Concomitant regulation of integrins that share a common β1 subunit. *J Biol Chem* 1989; **264:** 380-388
20 **Bellis SL**, Newman E, Friedman EA. Steps in integrin β1-chain glycosylation mediated by TGFβ1 signaling through Ras. *J Cell Physiol* 1999; **181:** 33-44
21 **Yan Z**, Chen M, Perucho M, Friedman E. Oncogenic Ki-ras but not oncogenic Ha-ras blocks integrin β1-chain maturation in colon epithelial cells. *J Biol Chem* 1997; **272:** 30928-30936
22 **Howe A**, Aplin AE, Alahari SK, Juliano RL. Integrin signaling and cell growth control. *Curr Opin Cell Biol* 1998; **10:** 220-231
23 **Sherr CJ**, Roberts JM. Inhibitors of mammalian G1 cyclin-dependent kinases. *Genes Dev* 1995; **9:** 1149-1163
24 **Harper JW**, Adami GR, Wei N, Keyomarsi K, Elledge SJ. The p21

Cdk-interacting protein Cip1 is a potent inhibitor of G1 cyclin-dependent kinases. *Cell* 1993; **75:** 805-816

25 **Zhang Y**, Rishi AK, Dawson MI, Tschang R, Farhana L, Boyanapalli M, Reichert U, Shroot B, Van Buren EC, Fontana JA. S-phase arrest and apoptosis induced in normal mammary epithelial cells by a novel retinoid. *Cancer Res* 2000; **60:** 2025-2032

26 **Shenberger JS**, Dixon PS. Oxygen induces S-phase growth arrest and increases p53 and $p21^{WAF1/CIP1}$ expression in human bronchial smooth-muscle cells. *Am J Respir Cell Mol Biol* 1999; **21:** 395-402

27 **Brazil DP**, Hemmings BA. Ten years of protein kinase B signalling: a hard Akt to follow. *Trends Biochem Sci* 2001; **26:** 657-664

28 **Delcommenne M**, Tan C, Gray V, Rue L, Woodgett J, Dedhar S. Phosphoinositide-3-OH kinase-dependent regulation of glycogen synthase kinase 3 and protein kinase B/AKT by the integrin-linked kinase. *Proc Natl Acad Sci USA* 1998; **95:** 11211-11216

29 **Persad S**, Attwell S, Gray V, Mawji N, Deng JT, Leung D, Yan J, Sanghera J, Walsh MP, Dedhar S. Regulation of protein kinase B/Akt-serine 473 phosphorylation by integrin-linked kinase: critical roles for kinase activity and amino acids arginine 211 and serine 343. *J Biol Chem* 2001; **276:** 27462-27469

30 **Sherr CJ**. The Pezcoller lecture: cancer cell cycles revisited. *Cancer Res* 2000; **60:** 3689-3695

31 **el-Deiry WS**, Tokino T, Velculescu VE, Levy DB, Parsons R, Trent JM, Lin D, Mercer WE, Kinzler KW, Vogelstein B. WAF1, a potential mediator of p53 tumor suppression. *Cell* 1993; **75:** 817-825

32 **Dotto GP**. $p21^{WAF1/Cip1}$: more than a break to the cell cycle? *Biochim Biophys Acta* 2000; **1471:** M43-M56

33 **Elledge SJ**, Harper JW. The role of protein stability in the cell cycle and cancer. *Biochim Biophys Acta* 1998; **1377:** M61-M70

34 **Stupack DG**, Puente XS, Boutsaboualoy S, Storgard CM, Cheresh DA. Apoptosis of adherent cells by recruitment of caspase-8 to unligated integrins. *J Cell Biol* 2001; **155:** 459-470

35 **Cheresh DA**, Stupack DG. Integrin-mediated death: an explanation of the integrin-knockout phenotype? *Nat Med* 2002; **8:** 193-194

36 **Yang JT**, Rayburn H, Hynes RO. Embryonic mesodermal defects in α5 integrin-deficient mice. *Development* 1993; **119:** 1093-1105

37 **Schwartz MA**, Ginsberg MH. Networks and crosstalk: integrin signalling spreads. *Nat Cell Biol* 2002; **4:** E65-E68

38 **Blystone SD**, Graham IL, Lindberg FP, Brown EJ. Integrin αvβ3 differentially regulates adhesive and phagocytic functions of the fibronectin receptor α5β1. *J Cell Biol* 1994; **127:** 1129-1137

39 **Diaz-Gonzalez F**, Forsyth J, Steiner B, Ginsberg MH. Trans-dominant inhibition of integrin function. *Mol Biol Cell* 1996; **7:** 1939-1951

40 **Blystone SD**, Slater SE, Williams MP, Crow MT, Brown EJ. A molecular mechanism of integrin crosstalk: αvβ3 suppression of calcium/calmodulin- dependent protein kinase II regulates α5β1 function. *J Cell Biol* 1999; **145**: 889- 897

41 **Simon KO**, Nutt EM, Abraham DG, Rodan GA, Duong LT. The αvβ3 integrin regulates α5β1-mediated cell migration toward fibronectin. *J Biol Chem* 1997; **272:** 29380-29389

42 **Volpes R**, van den Oord JJ, Desmet VJ. Integrins as differential cell lineage markers of primary liver tumors. *Am J Pathol* 1993; **142:** 1483-1492

43 **Scoazec JY**, Fléjou JF, D'Errico A, Fiorentino M, Zamparelli A, Bringuier AF, Feldmann G, Grigioni WF. Fibrolamellar carcinoma of the liver: composition of the extracellular matrix and expression of cell-matrix a cell-cell adhesion molecules. *Hepatology* 1996; **24:** 1128-1136

44 **Torimura T**, Uneo T, Kin M, Inuzuka S, Sugawara H, Tamaki S, Tsuji R, Sujaku K, Sata M, Tanikawa K. Coordinated expression of integrin α6β1 and laminin in hepatocellular carcinoma. *Hum Pathol* 1997; **28:** 1131-1138

45 **Ozaki I**, Yamamoto K, Mizuta T, Kajihara S, Fukushima N, Setoguchi Y, Morito F, Sakai T. Differential expression of laminin receptors in human hepatocellular carcinoma. *Gut* 1998; **43**: 837-842

46 **Masumoto A**, Arao S, Otsuki M. Role of β1 integrins in adhesion and invasion of hepatocellular carcinoma cells. *Hepatology* 1999; **29:** 68-74

47 **Nejjari M**, Hafdi Z, Dumortier J, Bringuier AF, Feldmann G, Scoazec JY. α6β1 integrin expression in hepatocarcinoma cells: regulation and role in cell adhesion and migration. *Int J Cancer* 1999; **83:** 518-525

Edited by Zhang JZ and Wang XL

P.O.Box 2345, Beijing 100023,China
Fax: +86-10-85381893
E-mail: wjg@wjgnet.com www.wjgnet.com

World J Gastroenterol 2003;9(8):1697-1701
World Journal of Gastroenterology
 ISSN 1007-9327

• LIVER CANCER •

Comparison between chemoembolization combined with radiotherapy and chemoembolization alone for large hepatocellular carcinoma

Wei-Jian Guo, Er-Xin Yu, Lu-Ming Liu, Jie Li, Zhen Chen, Jun-Hua Lin, Zhi-Qiang Meng, Yi Feng

Wei-Jian Guo, Jie Li, Yi Feng, Department of Oncology, Xinhua Hospital of Shanghai Second Medical University, 1665 Kongjiang Road, Shanghai 200092, China
Er-Xin Yu, Lu-Ming Liu, Zhen Chen, Jun-Hua Lin, Zhi-Qiang Meng, Cancer Hospital of Fudan University, Shanghai 200032, China
Correspondence to: Wei-Jian Guo, MD, Department of Oncology, Xinhua Hospital of Shanghai Second Medical University, 1665 Kongjiang Road, Shanghai 200092, China. guoweijian1@sohu.com
Received: 2003-04-02 **Accepted:** 2003-05-19

Abstract

AIM: To investigate the efficacy of transcatheter arterial chemoembolization (TACE) combined with radiotherapy for unresectable large hepatocellular carcinoma (HCC).

METHODS: From June 1994 to June 1999, a total of 76 patients with large unresectable HCC were treated with TACE followed by external-beam irradiation. 89 patients with large HCC, who underwent TACE alone during the same period, served as the control group. Clinical features, therapeutic modalities, acute effects and survival rates were analyzed and compared between TACE plus irradiation group and TACE alone group. A multivariate analysis of nine clinical variables and one treatment variable (irradiation) was performed by the Cox proportional hazards model.

RESULTS: The clinical features and therapeutic modalities except irradiation between the two groups were comparable ($P>0.05$). The objective response rate (RR) in TACE plus irradiation group was higher than that in TACE alone group (47.4 % *vs* 28.1 %, $P<0.05$). The overall survival rates in TACE plus irradiation group (64.0 %, 28.6 %, and 19.3 % at 1, 3, 5 years, respectively) were significantly higher than those in TACE alone group (39.9 %, 9.5 %, and 7.2 %, respectively, $P=0.0001$). Cox proportional hazards model analysis showed that tumor extension and Child grade were significant and were independent negative predictors of survival, while irradiation was an independent positive predictor of survival.

CONCLUSION: TACE combined with radiotherapy is more effective than TACE alone, and is a promising treatment for unresectable large HCC.

Guo WJ, Yu EX, Liu LM, Li J, Chen Z, Lin JH, Meng ZQ, Feng Y. Comparison between chemoembolization combined with radiotherapy and chemoembolization alone for large hepatocellular carcinoma. *World J Gastroenterol* 2003; 9(8): 1697-1701
http://www.wjgnet.com/1007-9327/9/1697.asp

INTRODUCTION

Hepatocellular carcinoma (HCC) is a common cancer in Asia. In China, there has been an increasing trend in the incidence and mortality of HCC during the past two decades. The age-adjusted rate of death per 100 000/year was 20.37 in 1990's. Patients with HCC usually have a poor prognosis. Surgery is the only potential cure, and there has been a great progress in surgery over the past decades[1]. However, the overall 5-year survival rates are still not above 5 % as the number of resected cases is limited due to advanced lesions or associated liver disease[2-4]. Most of the patients with HCC are subjected to various forms of non-surgical therapy. Transcatheter arterial chemoembolization (TACE) has become one of the most popular forms of nonsurgical treatment in Asia. TACE application to HCC has demonstrated good results in reducing the size of tumor and improving survival[5-10]. However, within or around the capsule, which is supplied by both arterial and portal blood, tumor cells remain viable, which are often responsible for later recurrence[11]. Even in several prospective randomized trials, TAE failed to improve significantly the survival of patients with HCC[12,13]. Further treatment was needed to eradicate the residual tumor cells. We have found in a clinical trial that TACE combined with irradiation may be a good method for large unresectable HCC[14]. In the present study, we compared the effects of TACE plus irradiation with that of TACE alone for the treatment of large unrectable HCC.

MATERIALS AND METHODS

Patients

During the past decade, patients with unresectable HCC underwent TACE therapy as the first line treatment at the Cancer Hospital of Fudan University, but parts of patients underwent TACE combined with radiotherapy or were given percutaneous ethanol injection (PEI) in clinical trials by some doctors. Included in the present study were 76 patients with unresectable large HCC who underwent TACE combined with radiotherapy between June 1994 and June 1999. The criteria for entry into this study were as follows: (1) The tumor / liver volume ratio was not above 0.7:1. (2) The lesion was detectable by ultrasound (US) and computed tomography (CT). (3) The level of serum transaminase was under 80 IU/L. (4) There was no evidence of extrahepatic metastasis, or ascites, or severe cirrhosis (class C according to Child's classification). (5) Karnofsky performance score $\geqslant$70. During the same period, a total of 127 patients underwent TACE alone as a routine therapy. 89 patients who complied with the above criteria served as the control group. In 61 (80.0 %) patients in TACE plus irradiation group and 73 patients (82.0 %) in control group, the diagnosis of HCC was confirmed by cytological examination. Diagnosis in the remaining patients was made on the basis of characteristic findings by ultrasound, CT and angiography, and high serum α-fetoprotein (AFP) levels. None of the patients underwent surgical resection owing to advanced tumor stage and/or location of the lesion, or because of refusal of surgery. Informed consent was obtained from all patients and their relatives.

Treatments

TACE procedure was performed as follows. The tip of a catheter

was introduced into the appropriate hepatic artery, and 5-fluorouracil (1.0 g, 5-Fu, Xudong Haipu Pharmaceutical Inc., Shanghai, China) and cisplatin (40-60 mg, CDDP, Qilu Pharmaceutical Factory, Jinan, China) or doxorubicin hydrochloride (30-50 mg, Adriamycin, Main Luck Pharmaceutical Inc., Shenzhen, China) were injected, followed by a mixture of iodized oil (5-20 ml, Lipiodol, Huaihai Pharmaceutical Factory, Shanghai, China) and mitomycin C (10-20 mg, MMC, Kyowa Hakko Kogyo Co., LTD, Tokyo, Japan) was injected slowly under fluoroscopic control. In some patients embolization with a gelatin sponge (1×1×10 mm, Gelfoam. the 3rd Pharmaceutical Factory of Nanjing, Nanjing, China) was performed at the same time. TACE procedures were performed at 4 to 10 week intervals, and patients received 1 to 4 times of TACE.

In the TACE plus irradiation group, radiotherapy was started 4 to 8 weeks after TACE. Twenty-six patients with a solitary tumor within a 9 cm diameter received limited-field radiotherapy. Radiation was delivered through a pair of opposed anterior-posterior fields using a 6 MV or 18 MV linear accelerator. Field sizes ranged from 64 cm^2 to 144 cm^2. The fractions were 1.8 to 2.0 Gy daily, given five times a week. The total dose ranged from 30 Gy to 50 Gy, depending on the proportion of normal liver excluded from the high-dose volume and the Child' s grade. For 50 patients with a solitary tumor of more than 9 cm diameter or with multinodular or diffuse lesions, whole or partial liver irradiation with a moving strip technique[14] was performed. The total midline dose ranged from 19.5 to 30 Gy. Ten patients whose tumor reduced to 9 cm or smaller after whole or partial liver irradiation had a boost to residual disease to a total dose of 36 to 42Gy.

Effects evaluation

The effects on the tumor were assessed by US and CT, together with AFP levels in cases with increased baseline values. Changes in tumor size were assessed in terms of percent regressing on CT and US, using World Health Organization criteria. Cumulative survival was determined by the Kaplan-Meier method from the first day of treatment.

Statistical analysis

The difference of clinical features, therapeutic modalities, response rate (RR) and AFP decreasing rate between the 2 groups were analyzed by chi-square test. The difference of survival was assessed by log-rank test. *P* value <0.05 was considered significant.

To assess the relatively prognostic importance of factors in predicting survival, a multivariate analysis of nine clinical variables, including sex, age, AFP level, number of lesions, tumor size, tumor extension, portal thrombosis, Child grade, and Okuda stage, and one treatment variable (irradiation), was performed by Cox proportional hazards model.

RESULTS

Clinical features and therapeutic modalities

The nine clinical features before treatment in the two groups are shown in Table 1. Only the rate of two lobes invasion in TACE plus irradiation group was slightly, but not significantly higher than that in control group. The other features in two groups were similar (*P*>0.05). There was no significant difference of TACE times and spongostan use between two groups (Table 1). Thus, the clinical features and therapeutic modalities, except irradiation, were comparable between these two groups.

Effects on tumor

In the TACE plus irradiation group, 5 patients (6.6 %) showed a complete response (CR), and 31 patients (40.8 %) showed a partial response (PR). Tumor size was unchanged in 30 cases (39.5 %), and increased in 10 cases (13.2 %). The objective response rate (RR) was 47.4 %. 48 patients had increased AFP values (>20 ng/ml) before treatment. In 23 of these cases (47.9 %), AFP level reduced by more than 50 %. In the control group, CR was observed in 2 patients (2.3 %) and PR was observed in 23 patients (25.8 %). Tumor size was unchanged in 44 cases (49.4 %) and increased in 20 cases (22.5 %). The RR was 28.1 %. The rate of AFP level, reducing by more than 50 %, was 29.0 % (20/69). The RR and AFP reduction rate in the TACE plus irradiation group increased significantly compared with that in the control group (*P*<0.05).

Table 1 Clinical features and therapeutic modalities in two groups

		TACE group cases (%)	TACE plus irradiation group cases (%)	*P* value
Sex	Male	75 (84.3)	68 (89.5)	
	Female	14 (15.7)	8 (10.5)	0.327
Age	<60 years	66 (74.2)	57 (75.0)	
	⩾60 years	23 (25.8)	19 (25.0)	0.901
AFP	<400 ng/ml	45 (50.6)	42 (55.3)	
	⩾400 ng/ml	44 (49.4)	34 (44.7)	0.547
No. of lesions	Solitary	59 (66.3)	51 (67.1)	
	Multiple	30 (33.7)	25 (32.9)	0.912
Tumor	1 lobe	72 (81.9)	52 (68.4)	
extension[a]	2 lobe	17 (19.1)	24 (31.6)	0.064
Tumor size	5-10 cm	51 (57.3)	47 (61.8)	
	>10 cm	38 (42.7)	29 (38.2)	0.554
Portal	Absent	67 (75.3)	62 (81.6)	
thrombosis	Present	22 (24.7)	14 (18.4)	0.329
Child grade	A	74 (83.2)	63 (82.9)	
	B	15 (16.8)	13 (17.1)	0.996
Okuda stage	I	24 (27.0)	29 (38.2)	
	II	65 (73.0)	46 (60.5)	
	III		1 (1.3)	0.155
TACE times	1	27 (30.3)	27 (35.5)	
	2	42 (47.2)	28 (36.8)	
	3	15 (16.9)	11 (14.5)	
	4	5 (5.6)	10 (13.2)	0.253
Spongostan use	No	48 (53.9)	44 (57.9)	
	Yes	41 (46.1)	32 (42.1)	0.610

[a]Hepatic lobes were classified as two lobes: right lobe and left lobe.

Survival and Cox model analysis

In the TACE plus irradiation group, the median follow-up time was 26 months (ranged from 10 to 84 months). Fifty-two patients died, 21 patients were still alive, and the remaining 3 patients were lost to follow-up. In the control group, the median follow-up time was 24 months (ranged from 10 to 70 months). Seventy-five patients died, 9 patients were still alive, and 5 patients were lost to follow-up. The data were obtained and analyzed in January 2001.

The survival curve for patients from the two groups is shown in Figure 1. The overall survival rates at 1, 3, and 5 years from the TACE plus irradiation group were 64.0 %, 28.6 %, and 19.3 %, respectively (median survival, 19 months), and 39.9 %, 9.5 %, and 7.2 %, respectively from the control group (median survival, 10 months). The survival rates in TACE plus irradiation group were significantly higher than those in control group (*P*=0.0001).

Multivariate analysis using the Cox proportional hazards model showed that both tumor extension and Child grade were significant and independent negative predictors of survival, while irradiation was an independent positive predictor of survival (Table 2).

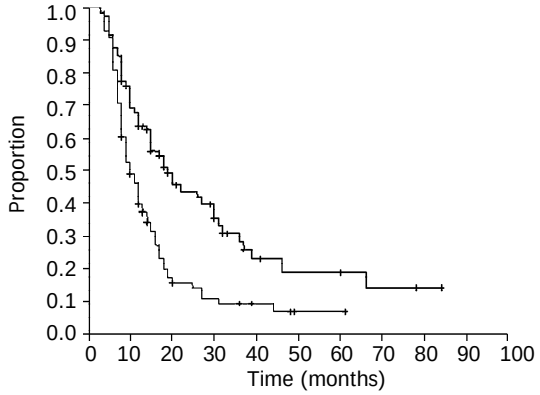

Figure 1 Cumulative survival curves for patients in two groups. The patients in TACE plus irradiation group survived significantly longer than did those in TACE alone group (P=0.0001).

Table 2 Multivariate analysis of major prognostic factors by the Cox proportional hazards model

Variabes	Regression coefficient	Hazard ratio	*P* value
Tumor extension	0.8708	2.3888	0.0016
Child grade	0.5685	1.7655	0.0200
Irradiation or not	-0.7256	0.4840	0.0002

DISCUSSION

TACE is a combination of target chemotherapy and arterial embolization that has both selective ischemic and chemotherapeutic effects on HCC. TACE is an excellent debulking procedure. Surgically resected specimens showed that TACE effectively destroyed malignant cells, not only in the main tumors, but also in daughter tumors, extracapsular invasion, and intraportal neoplastic thrombi. TACE was proved to be effective in treating HCC, and has been widely used for patients with unresectable HCC in Asia[5-10]. It was even found that the effects of TACE was comparable to that of resection in some subpopulations of patients with operable HCC[15]. However, TACE is not a curative method. Tumor cells remain viable, especially in and around the capsule, and tumors may recur by the blood supply from the collateral circulation or portal vein[11]. The long-term efficacy of TACE was disappointing. 1, 3, and 5 year survival rates were around 50 %, 20 %, and 6 %, respectively[5-10]. In the present study, the RR and 5 year survival rate in the TACE control group were 28.1 % and 7.2 %, respectively, which were approximate to the results in the literature. Nevertheless, in some prospective randomized trials, TACE therapy failed to improve the survival of patients significantly[12,13]. Segmental TACE has been shown to yield 5 year survival rate (30 %) for patients with lesions less than 5 cm, but it is suitable only for small tumors. Thus, multimodality treatments are necessary, especially for large HCC.

Radiotherapy has not played a significant role in treating HCC because of the poor tolerance of the liver. The benefit of radiotherapy is still uncertain. Whole liver irradiation at or above 35Gy in a 3-4 week period is known to cause a high incidence of radiation hepatitis, yet this dose level is not enough to control the tumor. In contrast to whole liver irradiation, small portions of the liver can be irradiated up to 50-60 Gy in 5-6 weeks without significant long-term morbidity. Limited-field high dose irradiation (40-60Gy) and three-dimension conformal radiotherapy have been found to be effective for relatively small unresectable HCC, even with portal vein thrombosis[16-20].

The combination of TACE with radiotherapy may remedy the limitation of each alone and have synergistic effects. Tumor shrinkage after TACE allows the use of smaller irradiation fields, which permits higher tumor doses and improves the normal liver tolerance. Combination therapy also serves the purpose of eliminating residual cancer cells after TACE. Furthermore, the anticancer drug retained in the tumor may have a radiosensitizing effect[21]. The anticancer drug, when it is mixed with lipiodol, has been reported to maintain relatively high concentrations in tumors as long as 27 days and decrease to a trace level after 47 days[22]. In 1990, Yoshikawa *et al*.[23] reported that the combination therapy was more effective than TACE or radiotherapy alone in a preliminary study encompassing a small number of cases. From then on, this combination regimen was carried out to treat HCC by more investigators, and was found to be an effective method for HCC[24-29]. Seong *et al*.[26] reported that 30 patients with HCC who were treated by TACE combined with radiotherapy had 3 year survival rate of 22.2 %, and a median survival of 17 months. The results of our study also suggested that TACE followed by irradiation was a promising approach for large HCC. The RR and 5 year survival rate were 47.4 % and 19.3 %, respectively, in 76 patients with very large tumors ($\geqslant$5 cm in all cases, >10 cm in 38.2 % of the cases, while two hepatic lobes were involved in 31.6 % of the cases). In addition, the results of the Cox proportional hazards model analysis showed that irradiation was an independent positive predictor of survival, and further confirmed that TACE combined with radiotherapy was more effective than TACE alone.

The results of combination therapy in the present study appeared to be comparable to those in other reports of multimodality therapy. Second-look resection after TACE yielded the highest 5 year survival rate (56 %)[30, 31], but only a few patients had the opportunity of resection following TACE. PEI after TACE yielded higher survival rates at 1, 2, and 3 years than TACE alone did[32-37], but the survival rates after 4 years dropped, and it was suitable only for tumors <8 cm. Tanaka *et al*.[37] reported that 83 patients with HCC who were treated by TACE-PEI had 5 and 7 year survival rates of 35 % and 14 %, respectively, but most of the patients (71.1 %) in their study had tumors of less than 5 cm in diameter. The results of our study showed that TACE combined with radiotherapy was effective even for very large tumors.

The optimal radiation dose in the combined therapy is unclear. It is well known that the inhibiting effect of radiotherapy on most tumors depends on the irradiation dose. It has been found that the radiation dose is a significant factor for predicting the objective response and the survival in treating HCC[14, 19], but liver tolerance should be considered at the same time. Recently, conformal radiotherapy has been introduced for the treatment of intrahepatic malignancies and dose-volume histogram analysis was used to quantify the tolerance of the liver by some investigators[20,38-40]. They suggested the irradiation dose level by normal liver volume to be radiated depended on the percentage of normal liver receiving more than 50 % of the prescribed isocenter dose, 66Gy for less than 33 %, 48Gy for 33-66 %, and 24Gy (whole liver) for more than 66 % in 1.5Gy twice a day fractionation with concurrent bromodeoxyuridine[38,39]. Introduction of conformal radiotherapy and dose-volume histogram analysis into the study of the combined therapy will help to give an optimal and tangible dose.

The Cox proportional hazards model showed that tumor extension was a significant and independent negative predictor

of survival. The prognosis of patients with invasion in two hepatic lobes was worse than that of patients with one hepatic lobe invasion. This may be because the tumor was barely controlled by combined therapy or TACE alone treatment plus the chance of metastases rose when there was invasion in two lobes. The degree of cirrhosis (classified by Child grade) is also an independent negative predictor of survival. This is in agreement with previous studies[35, 36].

In summary, our results demonstrate that TACE combined with radiotherapy is a promising treatment for large HCC. Prospectively randomized, controlled multi -center clinical trials are needed to confirm the advantageous effects of combined therapy over TACE or radiotherapy alone. In addition, further clarification about an optimal radiation dose and the optimal interval between TACE and radiotherapy are also needed.

ACKNOWLEDGEMENTS

We would like to thank Mrs. Margaret-Hiatt Rosen, Director of Admission, the Mead School, Stanford, US, for her correction of the English translation of the paper.

REFERENCES

1 **Zhou XD**, Tang ZY, Yang BH, Lin ZY, Ma ZC, Ye SL, Wu ZQ, Fan J, Qin LX, Zheng BH. Experience of 1000 patients who underwent hepatectomy for small hepatocellular carcinoma. *Cancer* 2001; **91**: 1479-1486

2 **Faivre J**, Forman D, Esteve J, Obradovic M, Sant M. Survival of patients with primary liver cancer, pancreatic cancer and biliary tract cancer in Europe. *Eur J Cancer* 1998; **34**: 2184-2190

3 **El-Serag HB**, Mason AC, Key C. Trends in survival of patients with hepatocellular carcinoma between 1977 and 1996 in the United States. *Hepatology* 2001; **33**: 62-65

4 **El-Serag HB**. Hepatocellular carcinoma: an epidemiologic view. *J Clin Gastroenterol* 2002; **35**(5 Suppl 2): S72-78

5 **Poon RT**, Ngan H, Lo CM, Liu CL, Fan ST, Wong J. Transarterial chemoembolization for inoperable hepatocellular carcinoma and postresection intrahepatic recurrence. *J Surg Oncol* 2000; **73**: 109-114

6 **Lo CM**, Ngan H, Tso WK, Liu CL, Lam CM, Poon RT, Fan ST, Wong J. Randomized controlled trial of transarterial lipiodol chemoembolization for unresectable hepatocellular carcinoma. *Hepatology* 2002; **35**: 1164-1171

7 **Savastano S**, Miotto D, Casarrubea G, Teso S, Chiesura-Corona M, Feltrin GP. Transcatheter arterial chemoembolization for hepatocellular carcinoma in patients with Child's grade A or B cirrhosis: a multivariate analysis of prognostic factors. *J Clin Gastroenterol* 1999; **28**: 334-340

8 **Sithinamsuwan P**, Piratvisuth T, Tanomkiat W, Apakupakul N, Tongyoo S. Review of 336 patients with hepatocellular carcinoma at Songklanagarind Hospital. *World J Gastroenterol* 2000; **6**: 339-343

9 **Levy I**, Verstandig A, Sasson T, Wolf D, Krichon I, Libson E, Levensart P, Papo O, Yurim O, Id A, Shouval D. Transarterial oil chemoembolization for hepatocellular carcinoma, in 100 cases. *Harefuah* 2000; **138**: 89-93

10 **Ueno K** , Miyazono N, Inoue H , Nishida H , Kanetsuki I , Nakajo M. Transcatheter arterial chemoembolization therapy using iodized oil for patients with unresectable hepatocellular carcinoma: evaluation of three kinds of regimens and analysis of prognostic factors. *Cancer* 2000; **88**: 1574-1581

11 **Tang ZY**, Yu YQ, Zhou XD, Yang BH, Lin ZY, Lu JZ, Ma ZC, Ye SL, Liu KD. Three decades' experience in surgery of hepatocellular carcinoma. *Gan To Kagaku Ryoho* 1997; **24**(Suppl): 126-133

12 **Pelletier G**, Ducreux M, Gay F, Luboinski M, Hagege H, Dao T, Van Steenbergen W, Buffet C, Rougier P, Adler M, Pignon JP, Roche A. Treatment of unresectable hepatocellular carcinoma with lipiodol chemoembolization: a multicenter randomized trial. Groupe CHC. *J Hepatol* 1998; **29**: 129-134

13 **Bruix J**, Llovet JM, Castells A, Montana X, Bru C, Ayuso MC, Vilana R, Rodes J. Transarterial embolization versus symptomatic treatment in patients with advanced hepatocellular carcinoma: results of a randomized, controlled trial in a single institution. *Hepatology* 1998; **27**: 1578-1583

14 **Guo WJ**, Yu EX. Evaluation of combined therapy with chemoembolization and irradiation for large hepatocellular carcinoma. *Br J Radiol* 2000; **73**: 1901-1907

15 **Lee HS**, Kim KM, Yoon JH, Lee TR, Suh KS, Lee KU, Chung JW, Park JH, Kim CY. Therapeutic efficacy of transcatheter arterial chemoembolization as compared with hepatic resection in hepatocellular carcinoma patients with compensated liver function in a hepatitis B virus-endemic area: a prospective cohort study. *J Clin Oncol* 2002; **20**: 4459-4465

16 **Seong J**, Park HC, Han KH, Chon CY. Clinical results and prognostic factors in radiotherapy for unresectable hepatocellular carcinoma: a retrospective study of 158 patients. *Int J Radiat Oncol Biol Phys* 2003; **55**: 329-336

17 **Tokuuye K**, Sumi M, Kagami Y, Murayama S, Kawashima M, Ikeda H, Ueno H, Okusaka T, Okada S. Radiotherapy for hepatocellular carcinoma. *Strahlenther Onkol* 2000; **176**: 406-410

18 **Seong J**, Park HC, Han KH, Lee DY, Lee JT, Chon CY, Moon YM, Suh CO. Local radiotherapy for unresectable hepatocellular carcinoma patients who failed with transcatheter arterial chemoembolization. *Int J Radiat Oncol Biol Phys* 2000; **47**: 1331-1335

19 **Park HC**, Seong J, Han KH, Chon CY, Moon YM, Suh CO. Dose-response relationship in local radiotherapy for hepatocellular carcinoma. *Int J Radiat Oncol Biol Phys* 2002; **54**: 150-155

20 **Cheng SH**, Lin YM, Chuang VP, Yang PS, Cheng JC, Huang AT, Sung JL. A pilot study of three-dimensional conformal radiotherapy in unresectable hepatocellular carcinoma. *J Gastroenterol Hepatol* 1999; **14**: 1025-1033

21 **Seong J**, Kim SH, Suh CO. Enhancement of tumor radioresponse by combined chemotherapy in murine hepatocarcinoma. *J Gastroenterol Hepatol* 2001; **16**: 883-889

22 **Raoul JL**, Heresbach D, Bretagne JF, Ferrer DB, Duvauferrier R, Bourguet P, Messner M, Gosselin M. Chemoembolization of hepatocellular carcinoma. A study of the biodistribution and pharmacokinetics of doxorubicin. *Cancer* 1992; **70**: 585-590

23 **Yoshikawa M**, Ebara M, Ohto M, Miyoshi T. A combination treatment of transcatheter arterial embolization (TAE) and irradiation for hepatocellular carcinoma (HCC): evaluation for therapeutic efficacy in comparison with TAE or irradiation alone. *Nippon Shokakibyo Gakkai Zasshi* 1990; **87**: 225-234

24 **Yamada K**, Soejima T, Sugimoto K, Mayahara H, Izaki K, Sasaki R, Maruta T, Matsumoto S, Hirota S, Sugimura K. Pilot study of local radiotherapy for portal vein tumor thrombus in patients with unresectable hepatocellular carcinoma. *Jpn J Clin Oncol* 2001; **31**: 147-152

25 **Guo WJ**, Song MZ, Yu EX. Transcatheter arterial chemoembolization combined with external radiation for primary liver cancer. *Zhonghua Zhongliu Zazhi* 1999; **21**: 25-28

26 **Seong J**, Keum KC, Han KH, Lee DY, Lee JT, Chon CY, Moon YM, Suh CO, Kim GE. Combined transcatheter arterial chemoembolization and local radiotherapy of unresectable hepatocellular carcinoma. *Int J Radiat Oncol Biol Phys* 1999; **43**: 393-397

27 **Chia-Hsien Cheng J**, Chuang VP, Cheng SH, Lin YM, Cheng TI, Yang PS, Jian JJ, You DL, Horng CF, Huang AT. Unresectable hepatocellular carcinoma treated with radiotherapy and/or chemoembolization. *Int J Cancer* 2001; **96**: 243-252

28 **Guo WJ**, Yu EX, Yi C, Wu WY, Lin JH. Prognostic factors influencing survival in patients with large hepatocellular carcinoma receiving combined transcatheter arterial chemoembolization and radiotherapy. *Zhonghua Ganzangbing Zazhi* 2002; **10**: 167-169

29 **Zeng ZC**, Tang ZY, Wu ZQ, Ma ZC, Fan J, Qin LX, Zhou J, Wang JH, Wang BL, Zhong CS. Phase I clinical trial of oral furtulon and combined hepatic arterial chemoembolization and radiotherapy in unresectable primary liver cancers, including clinicopathologic study. *Am J Clin Oncol* 2000; **23**: 449-454

30 **Fan J**, Tang ZY, Yu YQ, Wu ZQ, Ma ZC, Zhou XD, Zhou J, Qiu SJ, Lu JZ. Improved survival with resection after transcatheter arterial chemoembolization (TACE) for unresectable hepatocellular carcinoma. *Dig Surg* 1998; **15**: 674-678

31 **Tang ZY**. Hepatocellular carcinoma. *J Gastroenterol Hepatol*

2000; **15**(Suppl): G1-7

32 **Kamada K**, Kitamoto M, Aikata H, Kawakami Y, Kono H, Imamura M, Nakanishi T, Chayama K. Combination of transcatheter arterial chemoembolization using cisplatin-lipiodol suspension and percutaneous ethanol injection for treatment of advanced small hepatocellular carcinoma. *Am J Surg* 2002; **184**: 284-290

33 **Li C**, Shi Z, Hao Y. Combined percutaneous ethanol injection through liver puncture and transcatheter hepatic arterial chemoembolization for hepatocellular carcinoma. *Zhonghua Zhongliu Zazhi* 2001; **23**: 490-492

34 **Koda M**, Murawaki Y, Mitsuda A, Oyama K, Okamoto K, Idobe Y, Suou T, Kawasaki H. Combination therapy with transcatheter arterial chemoembolization and percutaneous ethanol injection compared with percutaneous ethanol injection alone for patients with small hepatocellular carcinoma: a randomized control study. *Cancer* 2001; **92**: 1516-1124

35 **Allgaier HP**, Deibert P, Olschewski M, Spamer C, Blum U, Gerok W, Blum HE. Survival benefit of patients with inoperable hepatocellular carcinoma treated by a combination of transarterial chemoembolization and percutaneous ethanol injection-a single-center analysis including 132 patients. *Int J Cancer* 1998; **79**: 601-605

36 **Lencioni R**, Paolicchi A, Moretti M, Pinto F, Armillotta N, Di Giulio M, Cicorelli A, Donati F, Cioni D, Bartolozzi C. Combined transcatheter arterial chemoembolization and percutaneous ethanol injection for the treatment of large hepatocellular carcinoma: local therapeutic effect and long-term survival rate. *Eur Radiol* 1998; **8**: 439-444

37 **Tanaka K**, Nakamura S, Numata K, Kondo M, Morita K, Kitamura T, Saito S, Kiba T, Okazaki H, Sekihara H. The long term efficacy of combined transcatheter arterial embolization and percutaneous ethanol injection in the treatment of patients with large hepatocellular carcinoma and cirrhosis. *Cancer* 1998; **82**: 78-85

38 **Dawson LA**, Normolle D, Balter JM, McGinn CJ, Lawrence TS, Ten Haken RK. Analysis of radiation-induced liver disease using the Lyman NTCP model. *Int J Radiat Oncol Biol Phys* 2002; **53**: 810-821

39 **Robertson JM**, McGinn CJ, Walker S, Marx MV, Kessler ML, Ensminger WD, Lawrence TS. A phase I trial of hepatic arterial bromodeoxyuridine and conformal radiation therapy for patients with primary hepatobiliary cancers or colorectal liver metastases. *Int J Radiat Oncol Biol Phys* 1997; **39**: 1087-1092

40 **Cheng JC**, Wu JK, Huang CM, Liu HS, Huang DY, Cheng SH, Tsai SY, Jian JJ, Lin YM, Cheng TI, Horng CF, Huang AT. Radiation-induced liver disease after three-dimensional conformal radiotherapy for patients with hepatocellular carcinoma: dosimetric analysis and implication. *Int J Radiat Oncol Biol Phys* 2002; **54**: 156-162

Edited by Zhang JZ

P.O.Box 2345, Beijing 100023,China
Fax: +86-10-85381893
E-mail: wjg@wjgnet.com www.wjgnet.com

World J Gastroenterol 2003;9(8):1702-1706
World Journal of Gastroenterology
 ISSN 1007-9327

• LIVER CANCER •

Role of preoperative selective portal vein embolization in two-step curative hepatectomy for hepatocellular carcinoma

Wu Ji, Jie-Shou Li, Ling-Tang Li, Wu-Hong Liu, Kuan-Sheng Ma, Xiang-Tian Wang, Zhen-Ping He, Jia-Hong Dong

Wu Ji, Jie-Shou Li, Ling-Tang Li, Research Institute of General Surgery, Nanjing General Hospital of Nanjing PLA Command Area, Nanjing 210002, Jiangsu Province, China
Wu Ji, Wu-Hong Liu, Xiang-Tian Wang, Department of General Surgery, Kunming General Hospital of Chengdu PLA Command Area, Kunming 650032, Yunnan Province, China
Kuan-Sheng Ma, Zhen-Ping He, Jia-Hong Dong, Hepatobiliary Surgery Center, Southwest Hospital, Third Military Medical University, Chongqing 400038, China
Correspondence to: Wu Ji, MD, Institute of General Surgery, Nanjing General Hospital of Nanjing PLA Command Area, 305 Eastern Zhongshan Road, Nanjing, 210002, Jiangsu Province, China. jiwusky@sohu.com
Telephone: +86-25-4826808 Ext 58007 **Fax:** +86-25-4820160
Received: 2002-11-06 **Accepted:** 2002-12-07

Abstract

AIM: To determine the feasibility and role of ultrasound-guided preoperative selective portal vein embolization (POSPVE) in the two-step hepatectomy of patients with advanced primary hepatocellular carcinoma (HCC).

METHODS: Fifty patients with advanced HCC who were not suitable for curative hepatectomy were treated by ultrasound-guided percutaneous transhepatic POSPVE with fine needles. The successful rate, side effects and complications of POSPVE, changes of hepatic lobe volume and two-step curative hepatectomy rate after POSPVE were observed.

RESULTS: POSPVE was successfully performed in 47 (94.0 %) patients. In patients whose right portal vein branches were embolized, their right hepatic volume decreased and left hepatic volume increased gradually. The ratio of right hepatic volume to total hepatic volume decreased from 62.4 % before POSPVE to 60.5 %, 57.2 % and 52.8 % after 1, 2 and 3 weeks respectively. The side effects included different degree of pain in liver area (38 cases), slight fever (27 cases), nausea and vomiting (9 cases). The level of aspartate alanine transaminase (AST), alanine transaminase (ALT) and total bilirubin (TBIL) increased after POSPVE, but returned to preoperative level in 1 week. After 2-4 weeks, two-step curative hepatectomy for HCC was successfully performed on 23 (52.3 %) patients. There were no such severe complications as ectopic embolization, local hemorrhage and bile leakage.

CONCLUSION: Ultrasound-guided percutaneous transhepatic POSPVE with fine needles is feasible and safe. It can extend the indications of curative hepatectomy of HCC, and increase the safety of hepatectomy.

Ji W, Li JS, Li LT, Liu WH, Ma KS, Wang XT, He ZP, Dong JH. Role of preoperative selective portal vein embolization in two-step curative hepatectomy for hepatocellular carcinoma. *World J Gastroenterol* 2003; 9(8): 1702-1706
http://www.wjgnet.com/1007-9327/9/1702.asp

INTRODUCTION

Hepatocellular carcinoma (HCC) is one of the most common malignant tumors of mankind. It threatens our life severely[1-5]. In China, HCC is responsible for about 130 000 deaths every year. It has ranked second of cancer mortality since 1990[6,7]. Surgical resection of the tumors is considered the only potentially curative therapy, and it is regarded as the first choice for the treatment of HCC. Many factors can affect hepatectomy, such as tumor size, location, multifocality and patients' status, hepatic function. Besides, 80 % of them are complicated with cirrhosis in China. So the extension of hepatectomy of HCC is greatly limited. Hepatectomy with less hepatic volume resected may be helpful to the safety of the operation, but this may not be a radical cure, and even lead to tumor residual. Hepatectomy with more hepatic volume resected will lead to postoperative hepatic failure, infection, hemorrhage and even death. So only 15 % to 30 % patients have a chance of receiving curative hepatectomy[8-10]. Most HCC patients are in late stages at the time of diagnosis. They are considered not suitable for operation. Researchers have proposed the concept of "two-step hepatectomy", and some progresses have been made in the past decades[11-15]. In 1986, Kinoshita *et al*[16] reported the experience of two-step hepatectomy after POSPVE. This is a completely new method. The purpose is to induce atrophy of the embolized (tumor) lobe and compensatory hypertrophy of the remnant lobe. The result is an increase of the remnant liver volume and a decreased ratio of resected volume to total liver volume. In recent years, reports of two-step hepatectomy after preoperative selective portal vein embolization (POSPVE) gradually increased[17-22]. But there are no such clinical reports in China.

In this study, based on an analysis of the feasibility and safety of ultrasound-guided percutaneous transhepatic POSPVE with fine needles in 50 HCC patients, we discussed the role of POSPVE in the two-step curative hepatectomy for moderate and advanced HCC.

MATERIALS AND METHODS

Eligibility of patients

This study involved 50 HCC patients. There were 36 males and 14 females. Forty three (86.0 %) patients were hepatitis surface antigen (HBsAg) positive, and 34 (68 %) were complicated with cirrhosis. Child-Pugh' s classification showed that 14 (28 %) patients were grade A, 33 (66 %) grade B, 3 (6 %) grade C. The diameter of space occupying lesions ranged from 8.1 to 16.3 cm, averaging 13.6 cm. The criteria of these patients included: HCC located in one side of the liver, with no confirmed portal vein thrombosis and distant metastasis. The ratio of hepatic volume to be resected to total hepatic volume was more than 50 % for those patients with cirrhosis and 60 % for those without cirrhosis. Those patients with coexisted morbidity-related diseases, poor life expectancy, multinodular or diffuse intrahepatic tumor, prothrombin activity less than 50 %, or platelet count lower than 50×10^9/L were excluded from the study.

Methods

One hundred microgram dolantin and 25 mg phenergan were

injected into the muscle before POSPVE. The liver, tumor and the portal vein branch to be embolized were carefully examined, located and confirmed by ultrasound. Local anesthesia was adopted with 2 % lidocaine transcutaneously down to liver surface. Under ultrasound guidance, we punctured percutaneously and transhepatically with a 21-gague PTC needle from the side of ultrasound head. When the needle was inserted into the portal vein branch to be embolized, the internal part of the needle was taken away, and dark red portal vein blood could be seen (Figure 1). Then embolic material was slowly injected into the portal vein. It consisted of a mixture of ethanol and iodized oil with a rate of 1:2. And 0.4 ml/kg was regarded as the standard dosage. Real-time ultrasonic scan showed that tiny spot echoes in the embolized portal vein branch appeared and diffused into the carcinoma. Intensified echoes appeared in some areas. After that, the fine needle was slowly pulled out. Flexible fabric bandage was used to cover the puncture spot. The patients inhaled oxygen after returning back to the ward. Changes of vital signs were monitored for 12 to 24 hours. They were given fluid infusion and anti-inflammation, hemorrhage prevention, liver function protection and analgesics treatments.

The successful rate of POSPVE, side effects and complications after POSPVE, changes of blood routine, liver function, and renal function were observed to evaluate the feasibility and safety of ultrasound-guided percutaneous transhepatic POSPVE with fine needles. Serial changes of hepatic lobe volume calculated with volume CT, ratio of right hepatic lobe volume to total hepatic volume, two-step curative hepatectomy rate after POSPVE were observed to evaluate the role of POSPVE in the two-step hepatectomy of HCC.

Statistical method

Quantitative variables were expressed as mean ± standard error of the mean. The statistical software SPSS10.0 was used. *P* value <0.05 was considered significant.

RESULTS

Feasibility and safety of POSPVE

Ultrasound-guided percutaneous transhepatic POSPVE with fine needles was successfully performed in 47 of 50 patients. The successful rate was 94.0 % (Figure 1). Three patients failed to finish the operation. The right portal vein branches were difficult to locate under ultrasound guidance because of the tumor compression in 2 of them, and one patient could not tolerate the irritation of embolic material. There were 44 right portal vein embolizations and 3 left portal vein embolizations. The side effects included different degree of pain in liver area (38 cases), slight fever (27 cases), nausea and vomiting (9 cases). The level of aspartate alanine transaminase (AST), alanine transaminase (ALT) and total bilirubin (TBIL) increased in 31 cases after POSPVE, but returned to preoperative level in 1 week. There were no such severe complications as ectopic embolization, local hemorrhage and bile leakage.

Role of POSPVE in two-step curative hepatectomy of HCC

In 44 patients whose right portal vein branches were embolized, the right hepatic volume decreased, the left hepatic volume increased and the ratio of right liver volume to total liver volume decreased gradually (Figures 2-3) (Table 1). Two to four weeks later, curative hepatectomies were successfully performed in 23 (52.3 %) patients (Figures 4-5). There were 6 irregular right hepatectomies, 15 regular right hepatectomies, and 2 right trisegmentectomies. All these 23 patients recovered smoothly, without any severe complications like hepatic failure, hemorrhage and infection. They were discharged 11 to 20 days after operations. The other 27 patients who could not receive curative hepatectomy after POSPVE were treated by transcatheter artery embolization (TAE) or chemotherapy, immune therapy and so on.

Table 1 Serial changes of liver volume and ratio of right hepatic lobe volume to total hepatic volume after right portal vein embolization

	Right liver volume (cm^3)	Left liver volume (cm^3)	Right liver volume / total liver volume (%)
Before POSPVE	592.4±98.5	352.2±65.2	62.4±7.6
1 week after POSPVE	571.7±104.0	378.6±127.9	60.5±9.3
2 weeks after POSPVE	547.7±118.3[a,c]	405.9±130.2[a,c]	57.2±11.2[a,c]
3 weeks after POSPVE	509.1±123.8[b,c,e]	446.1±143.5[b,d,e]	52.8±12.3[b,c,e]

[a]$P<0.05$, [b]$P<0.01$, *vs* before POSPVE; [c]$P<0.05$, [d]$P<0.01$, *vs* 1 week after POSPVE, [e]$P<0.05$, [f]$P<0.01$, *vs* 2 weeks after POSPVE.

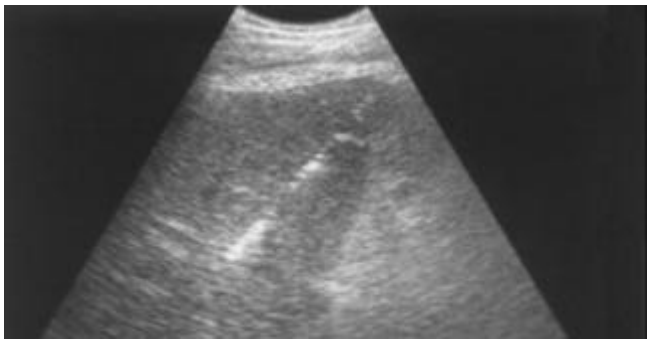

Figure 1 The fine needle was inserted into the right portal vein branch under ultrasound guidance. After embolization material was injected, tiny spot echoes appeared in the portal vein branch and diffused to the carcinoma area.

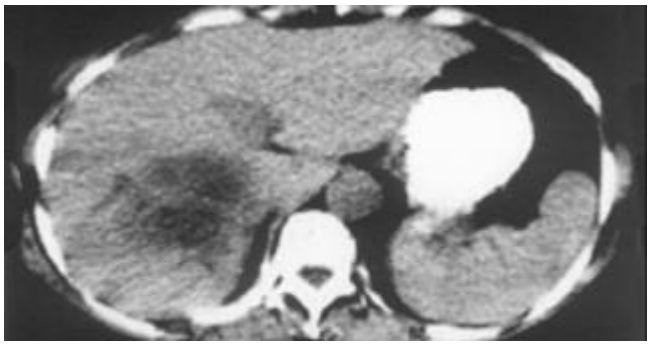

Figure 2 Before POSPVE, CT scan showed a 13.2 cm×10.8 cm HCC in the right lobe of liver. A right semihepatectomy was scheduled to perform.

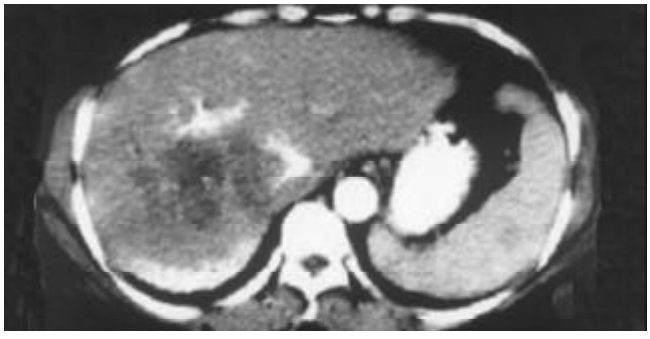

Figure 3 Three weeks after right POSPVE, CT scan showed increased volume of left lobe and decreased volume of right lobe. Iodized oil deposit still could be seen in the right portal vein branch.

Figure 4 Three weeks after right POSPVE, a right semihepatectomy was performed. In the operation, significant hypertrophy of left lobe was confirmed.

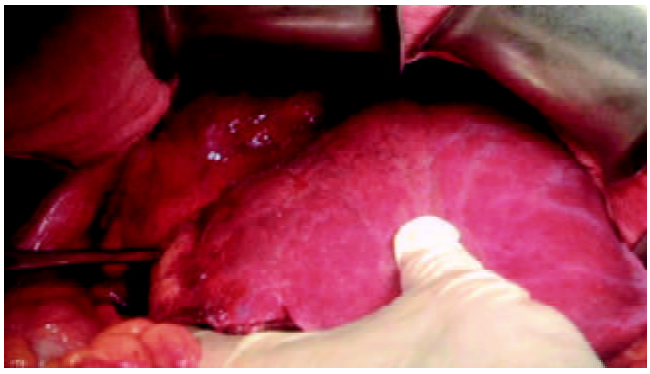

Figure 5 In the same operation, significant atrophy of right lobe and HCC could be seen. There was iodized oil deposit in the carcinoma area.

DISCUSSION

Rous and Larimore observed in 1920 that portal vein ligation in rabbit led to atrophy of the ipsilateral hepatic lobe and hypertrophy of the contralateral lobe. In 1956, Schalm confirmed it by occluding the portal vein branch. These observations provided the foundation for the study of liver regeneration after portal vein branch embolization. In 1975, Honjo found that portal vein ligation could significantly prolong the survival span of advanced HCC patients whose tumors could not be resected during operations. In 1986, Kinoshita published the first report demonstrating the efficacy of POSPVE before curative resection on primary and metastatic HCC. After that, POSPVE was gradually accepted in preparing large hepatectomy for HCC. It has been confirmed that POSPVE can extend the indication of curative hepatectomy for HCC, increase the safety of hepatectomy, and improve the long-term survival rate after the operation[23-32].

Portal vein blood supply is very important for both liver and HCC. Portal vein branch ligation or embolization results in redistribution of portal vein blood that is essential to liver regeneration. Most portal blood rich in hepatatrophic substances, such as insulin, glucagon and hepatocyte growth factor, flows toward the future remaining lobe. This leads to atrophy of the ipsilateral hepatic lobe and hypertrophy of the contralateral lobe. Harada *et al*[33] observed that POSPVE induced hepatocyte apoptosis and atrophy of the embolized lobe. Increased sinusoidal volume in this lobe may be attributable to hepatocyte deletion. Cells in the nonembolized lobe entered a highly active phase of proliferation within 2 weeks after POSPVE. Further evidences of cellular proliferation were provided by the increased nonembolized lobar volume and numerical density of hepatocyte nuclei (Nv). They concluded that the favorable role of POSPVE was attributed to a net gain of functional hepatocyte mass and early induction of hepatocyte proliferation. Shimizu *et al*[34] demonstrated that expression of proliferating cell nuclear antigen (PCNA) and mitotic index (MI) of hepatocytes in nonembolized lobe increased greatly. The amount of mitochondrial DNA-binding proteins increased 200-300 % of the preoperative level at 12 hours after ligation of left branch of the portal vein, before an increase of 390 % in mitochondrial DNA content at 24 hours, and was parallel to an increase of 240 % in mitochondrial mRNA at 12 hours. These results suggest that the energy supply for liver regeneration is achieved through enhancement of mitochondrial DNA replication as well as transcription, in which mitochondrial DNA-binding proteins probably play regulatory roles. Chijiiwa *et al*[35-37] found that the volume of nonembolized left lobe significantly increased after right POSPVE, with a significant increase in percentage of the left lobe to total liver volume. Concentrations of AMP, ADP, and ATP, and hepatic energy charge levels in the nonembolized left lobe were similar to those of the control liver. These results suggest that right POSPVE increased the volume of nonembolized left lobe, while keeping the hepatic engery charge and ATP levels similar to the control liver, thereby increasing the total amount of ATP and hepatic energy reserve of the nonembolized lobe in proportion to its volume increase at the time of surgery.

Two major techniques have been reported to access the portal vein: direct catheterization of the ileocolic vein and the percutaneous approach[38,39]. The former involves an open technique in which the ileocolic vein is cannulated at laparotomy. It is usually used when the carcinoma can not be resected during operation. This method can also be used when interventional facilities are not available for the percutaneous approach. The later can be finished under ultrasound guidance with local anesthesia. There are two major kinds of methods. One is to insert a catheter percutaneously into the portal vein branch, the other is to puncture the portal vein branch by a fine needle under ultrasound guidance. Most reports used the catheterization method. But it is technically complicated and expensive. Percutaneous approach with a fine needle is easy to perform, and patients suffer less and resume faster. But it has not been widely accepted. Its feasibility, safety and efficiency have not been discussed based on a large sample[40,41]. In this study, POSPVE with a fine needle was feasible in 47 of 50 HCC patients. The successful rate was 94.0 %. The complication rate was low, and there was no severe complication. The side effects were moderate. In 44 patients whose right portal veins were embolized, their right hepatic volume decreased and left hepatic volume increased, the ratio of hepatectomy decreased gradually. By inducing hypertrophy of the remaining liver, hepatectomies were successfully performed in 23 patients. The two-step curative hepatectomy after POSPVE was 52.3 %. All the patients recovered smoothly. It is concluded from this study that ultrasound-guided percutaneous transhepatic POSPVE with a fine needle is feasible, safe and effective. It extends the indication of curative hepatectomy for moderate and advanced HCC. This is the first report on the role of POSPVE in the treatment of HCC in China. Estimating the volume of the lobe that will remain after hepatectomy is thought to be mandatory for all patients undergoing extensive hepatic resection. If this volume is not large enough in terms of the risk of postoperative liver failure, then POSPVE is indicated. According to a criterion based on liver volumetry, POSPVE is usually indicated for patients who will undergo right trisegmentectomy, left trisegmentectomy, or right hepatectomy for cirrhosis patients. Many methods have been used to estimate the lobar volume. In this series, we used volume CT to calculate the exact volume of every lobe, and regard the ratio of hepatic volume to be resected to total hepatic

volume is more than 50 % for those patients with cirrhosis and 60 % for those without cirrhosis. The degree of hypertrophy induced in nonembolized lobe showed a large interindividual difference. It has been reported that male, diabetes mellitus and cirrhosis are negative factors, and cholestasis is a positive factor. Other factors that may influence the role of POSPVE include embolization materials and their dosage and extent[42-46]. Cyanoacrylate, lipiodol, gelatin sponge, thrombin, fibrin glue, gelfoam, and alcohol have been used as embolization materials. Their effects are controversial. We used lipidol and alcohol routinely as embolization materials throughout the study period. The functional burden placed on the liver by POSPVE using these materials was minimal and transient, as reflected in the slight elevation of AST, ALT and total bilirubin level. It was reported that the average future remaining hepatic volume increased by 28 % within 2 weeks after POSPVE. The rate of average hepatectomy decreased from 70.0 % before POSPVE to 62.2 %, and the two-step hepatectomy rate was 63.3 % to 77.4 %. But in this series, the two-step curative hepatectomy rate after POSPVE was 52.3 %. We think the main reason is that most patients in our study were male and coexisted with cirrhosis. They have been reported to be the negative regulatory factors of POSPVE. Besides, we used the method of ultrasound-guided percutaneous transhepatic POSPVE with a fine needle. It is safe, feasible and effective. The disadvantage of this method lies in that the embolization materials usually used are ethanol and iodized oil. So, it is mainly the distant branches of portal vein that are embolized. Besides, the role of ethanol is dosage dependent, while a large dosage is unbearable for most patients.

Although the concept of POSPVE appears to be well accepted and the procedure is performed ever more widely, there are a number of issues on which a general consensus has not yet been reached, such as the optimum duration between POSPVE and hepatectomy, the most suitable embolizing material and method of portal vein cannulation, the rate of technical failure and complications, and factors that accelerate or suppress the effect of POSPVE[32]. The fact that POSPVE is well tolerated might enlarge its indications in the future. POSPVE will be used not only for patients with possibly insufficient remaining liver volume after hepatectomy, but also for those whose curative operation may not be very safe.

REFERENCES

1 **Tang ZY**. Hepatocellular carcinoma-cause, treatment and metastasis. *World J Gastroenterol* 2001; **7**: 445-454
2 **Makuuchi M**, Imamura H, Sugawara Y, Takayama T. Progress in surgical treatment of hepatocellular carcinoma. *Oncology* 2002; **62**(Suppl): 74-81
3 **Fan J**, Wu ZQ, Tang ZY, Zhou J, Qiu SJ, Ma ZC, Zhou XD, Ye SL. Multimodality treatment in hepatocellular carcinoma patients with tumor thrombi in portal vein. *World J Gastroenterol* 2001; **7**: 28-32
4 **Makuuchi M**. Remodeling the surgical approach to hepatocellular carcinoma. *Hepatogastroenterology* 2002; **49**: 36-40
5 **Curley SA**, Cusack JC Jr, Tanabe KK, Stoelzing O, Ellis LM. Advances in the treatment of liver tumors. *Curr Probl Surg* 2002; **39**: 449-571
6 **Zhao WH**, Ma ZM, Zhou XR, Feng YZ, Fang BS. Prediction of recurrence and prognosis in patients with hepatocellular carcinoma after resection by use of CLIP score. *World J Gastroenterol* 2002; **8**: 237-242
7 **Qin LX**, Tang ZY. The prognostic significance of clinical and pathological features in hepatocellular carcinoma. *World J Gastroenterol* 2002; **8**: 193-199
8 **Rabe C**, Pilz T, Klostermann C, Berna M, Schild HH, Sauerbruch T, Caselmann WH. Clinical characteristics and outcome of a cohort of 101 patients with hepatocellular carcinoma. *World J Gastroenterol* 2001; **7**: 208-215
9 **Yip D**, Findlay M, Boyer M, Tattersall MH. Hepatocellular carcinoma in central sydney: a 10-year review of patients seen in a medical oncology department. *World J Gastroenterol* 1999; **5**: 483-487
10 **Fan J**, Ten GJ, He SC, Guo JH, Yang DP, Wang GY. Arterial chemoembolization for hepatocellular carcinoma. *World J Gastroenterol* 1998; **4**: 33-37
11 **Li L**, Wu PH, Li JQ, Zhang WZ, Lin HG, Zhang YQ. Segmental transcatheter arterial embolization for primary hepatocellular carcinoma. *World J Gastroenterol* 1998; **4**: 511-512
12 **Chen MS**, Li JQ, Zhang YQ, Lu LX, Zhang WZ, Yuan YF, Guo YP, Lin XJ, Li GH. High-dose iodized oil transcatheter arterial chemoembolization for patients with large hepatocellular carcinoma. *World J Gastroenterol* 2002; **8**: 74-78
13 **Wang JH**, Lin G, Yan ZP, Wang XL, Cheng JM, Li MQ. Stage II surgical resection of hepatocellular carcinoma after TAE: A report of 38 cases. *World J Gastroenterol* 1998; **4**: 133-136
14 **Sithinamsuwan P**, Piratvisuth T, Tanomkiat W, Apakupakul N, Tongyoo S. Review of 336 patients with hepatocellular carcinoma at songklanagarind hospital. *World J Gastroenterol* 2000; **6**: 339-343
15 **Schmid R**. Prospect of gastroenterology and hepatology in the next century. *World J Gastroenterol* 1999; **5**: 185-190
16 **Kinoshita H**, Sakai K, Hirohashi K, Igawa S, Yamasaki O, Kubo S. Preoperative portal vein embolization for hepatocellular carcinoma. *World J Surg* 1986; **10**: 803-808
17 **Elias D**, Ouellet JF, De Baere T, Lasser P, Roche A. Preoperative selective portal vein embolization before hepatectomy for liver metastases: long-term results and impact on survival. *Surgery* 2002; **131**: 294-299
18 **Azoulay D**, Castaing D, Smail A, Adam R, Cailliez V, Laurent A, Lemoine A, Bismuth H. Resection of nonresectable liver metastases from colorectal cancer after percutaneous portal vein embolization. *Ann Surg* 2000; **231**: 480-486
19 **Wakabayashi H**, Okada S, Maeba T, Maeta H. Effect of preoperative portal vein embolization on major hepatectomy for advanced-stage hepatocellular carcinomas in injured livers: a preliminary report. *Surg Today* 1997; **27**: 403-410
20 **Wakabayashi H**, Yachida S, Maeba T, Maeta H. Evaluation of liver function for the application of preoperative portal vein embolization on major hepatic resection. *Hepatogastroenterology* 2002; **49**: 1048-1052
21 **Tominaga M**, Ku Y, Iwasaki T, Fukumoto T, Muramatsu S, Kusunoki N, Suzuki Y, Fujino Y, Kuroda Y. Effect of portal vein embolization on function of the nonembolized lobes of the liver: Evaluation by first-pass hepatic lidocaine extraction in dogs. *Surgery* 2002; **132**: 424-430
22 **Nagino M**, Kamiya J, Kanai M, Uesaka K, Sano T, Yamamoto H, hayakawa N, Nimura Y. Right trisegment portal vein embolization for biliary tract carcinoma: Technique and clinical utility. *Surgery* 2000; **127**: 155-160
23 **Imamura H**, Shimada R, Kubota M, Matsuyama Y, Nakayama A, Miyagawa S, Makuuchi M, Kawasaki S. Preoperative portal vein embolization: an audit of 84 patients. *Hepatology* 1999; **29**: 1099-1105
24 **Gerunda GE**, Bolognesi M, Neri D, Merenda R, Miotto D, Barbazza F, Zangrandi F, Bisello M, Valmasoni M, Gangemi A, Gagliesi A, Faccioli AM. Preoperative selective portal vein embolization (PSPVE) before major hepatic resection. Effectiveness of doppler estimation of hepatic blood flow to predict the hypertrophy rate of non-embolized liver segments. *Hepatogastroenterology* 2002; **49**: 1405-1411
25 **Kubo S**, Shiomi S, Tanaka H, ShutoT, Takemura S, Mikami S, Uenishi T, Nishino Y, Hirohashi K, Kawamura E, Kinoshita H. Evaluation of the effect of portal vein embolization on liver function by (99m)tc-galactosyl human serum albumin scintigraphy. *J Surg Res* 2002; **107**: 113-118
26 **De Baere T**, Roche A, Elias D, Lasser P, Lagrange C, Bousson V. Preoperative portal vein embolization for extension of hepatectomy indications. *Hepatology* 1996; **24**: 1386-1391
27 **Abdalla EK**, Barnett CC, Doherty D, Curley SA, Vauthey JN. Extended hepatectomy in patients with hepatobiliary malignancies with and without preoperative portal vein embolization. *Arch Surg* 2002; **137**: 675-680
28 **Gerunda GE**, Neri D, Merenda R, Barbazza F, Zangrandi F,

Meduri F, Bisello M, Valmasoni M, Gangemi A, Faccioli AM. Effectiveness of preoperative selective portal vein embolization before extensive hepatic resection. *Liver Transpl* 2002; **8**: 405-407

29 **Sugawara Y**, Yamamoto J, Higashi H, Yamasaki S, Shimada K, Kosuge T, Takayama T, Makuuchi M. Preoperative portal embolization in patients with hepatocellular carcinoma. *World J Surg* 2002; **26**: 105-110

30 **Lee KC**, Kinoshita H, Hirohashi K, Kubo S, Iwasa R. Extension of surgical indications for hepatocellular carcinoma by portal vein embolization. *World J Surg* 1993; **17**: 109-115

31 **Wakabayashi H**, Ishimura K, Okano K, Karasawa Y, Goda F, Maeba T, Maeta H. Application of preoperative portal vein embolization before major hepatic resection in patients with normal or abnormal liver parenchyma. *Surgery* 2002; **131**: 26-33

32 **Tanaka H**, Hirohashi K, Kubo S, Shuto T, Higaki I, Kinoshita K. Preoperative portal vein embolization improves prognosis after right hepatectomy for hepatocellular carcinoma in patients with impaired hepatic function. *Br J Surg* 2000; **87**: 879-882

33 **Harada H**, Imamura H, Miyagawa S, Kawasaki S. Fate of the human liver after hemihepatic portal vein embolization: Cell kinetic and morphometric study. *Hepatology* 1997; **26**: 1162-1170

34 **Shimizu Y**, Suzuki H, Nimura Y, Onoue S, Nagino M, Tanaka M, Ozawa T. Elevated mitochondrial gene expression during rat liver regeneration after portal vein ligation. *Hepatology* 1995; **22**: 1222-1229

35 **Chijiiwa K**, Saiki S, Noshiro N, Kameoka N, Nakano K, Tanaka M. Effect of preoperative portal vein embolization on liver volume and hepatic energy status of the nonembolized liver lobe in humans. *Eur Surg Res* 2000; **32**: 94-99

36 **Kawai M**, Naruse K, Komatsu S, Kobayashi S, Nagino M, Nimura Y, Sokabe M. Mechanical stress-dependent secretion of interleukin 6 by endothelial cells after portal vein embolization: Clinical and experimental studies. *J Hepatol* 2002; **37**: 240-246

37 **Uemura T**, Miyazaki M, Hirai R, Matsumoto H, Ota T, Ohashi R, Shimizu N, Tsuji T, Inoue Y, Namba M. Different expression of positive and negative regulators of hepatocyte growth in growing and shrinking hepatic lobes after portal vein branch ligation in rats. *In J Mol Med* 2000; **5**: 173-179

38 **Tsuge H**, Mimura H, Kawata N, Orita K. Right portal vein embolization before extended right hepatectomy using laparoscopic catheterization of the ileocolic vein: a prospective study. *Surg Laparosc Endosc* 1994; **4**: 258-263

39 **Lu MD**, Chen JW, Xie XY, Liang LJ, Huang JF. Portal vein embolization by fine needle ethanol injection: experimental and clinical studies. *World J Gastroenterol* 1999; **5**: 506-510

40 **Seymour K**, Manas D, Charnley RM. During liver regeneration following right portal vein embolization the growth rate of liver metastases is more rapid than that of the liver parenchyma. *Br J Surg* 1999; **86**: 1482-1483

41 **Madoff DC**, Hicks ME, Vauthey JN, Charnsangavej C, Morello FA Jr, Ahrar K, Wallace MJ, Gupta S. Transhepatic portal vein embolization: anatomy, indications, and technical considerations. *Radiographics* 2002; **22**: 1063-1076

42 **Tanaka H**, Hirohashi K, Kubo S, Ikebe T, Tsukamoto T, Hamba H, Shuto T, Wakasa K, Kinoshita H. Influence of histological inflammatory activity on regenerative capacity of liver after percutaneous transhepatic portal vein embolization. *J Gastroenterol* 1999; **34**: 100-104

43 **Kaneko T**, Nakao A, Takagi H. Clinical studies of new material for portal vein embolization: Comparison of embolic effect with different agents. *Hepatogastroenterology* 2002; **49**: 472-477

44 **Yamakado K**, Takeda K, Nishide Y, Jin J, Matsumura K, Nakatsuka A, Hirano T, Kato N, Nakagawa T. Portal vein embolization with steel coil and absolute ethanol: a comparative experimental study with canine liver. *Hepatology* 1995; **22**: 1812-1818

45 **Lu MD**, YY Y, Ren W. A study of portal vein embolization with absolute ethanol injection in cirrhotic rats. *World J Gastroenterol* 1998; **4**: 415-417

46 **Lu MD**, Liang LJ, Huang JF, Ye WJ, Yang QS, Peng BG, Xie XY. Portal vein embolization with ethanol injection via a fine needle in dogs. *Surg Today* 1995; **25**: 416-420

Edited by Zhang JZ and Wang XL

P.O.Box 2345, Beijing 100023,China
Fax: +86-10-85381893
E-mail: wjg@wjgnet.com www.wjgnet.com

World J Gastroenterol 2003;9(8):1707-1712
World Journal of Gastroenterology
 ISSN 1007-9327

• COLORECTAL CANCER •

Contribution of eIF-4E inhibition to the expression and activity of heparanase in human colon adenocarcinoma cell line: LS-174T

Yu-Jie Yang, Ya-Li Zhang, Xu Li, Han-Lei Dan, Zhuo-Sheng Lai, Ji-De Wang, Qun-Ying Wang, Hai-Hong Cui, Yong Sun, Ya-Dong Wang

Yu-Jie Yang, Ya-Li Zhang, Xu Li, Han-Lei Dan, Zhuo-Sheng Lai, Ji-De Wang, Qun-Ying Wang, Hai-Hong Cui, Yong Sun, Ya-Dong Wang, Chinese PLA Institute of Digestive Disease, Nanfang Hospital, First Military Medical University, Guangzhou 510515, Guangdong Province, China
Supported by the National Natural Science Foundation of China, No. 30171053
Correspondence to: Dr. Yu-Jie Yang, Chinese PLA Institute of Digestive Disease, Nanfang Hospital, First Military Medical University, Guangzhou 510515, Guangdong Province, China. yujiey@fimmu.edu.cn
Telephone: +86-20-61641530
Received: 2003-03-04 **Accepted:** 2003-04-03

Abstract

AIM: Heparanase degrades heparan sulfate proteoglycans (HSPGs) and is a critical mediator of tumor metastasis and angiogenesis. Recently, it has been cloned as a single gene family and found to be a potential target for antimetastasis drugs. However, the molecular basis for the regulation of heparanase expression is still not quite clear. The aim of this study was to determine whether the expression of eukaryotic initiation factor 4E (eIF-4E) correlated with the heparanase level in tumor cells and to explore the correlation between heparanase expression and metastatic potential of LS-174T cells.

METHODS: A 20-mer antisense s-oligodeoxynucleotide (asODN) targeted against the translation start site of eIF-4E mRNA was introduced into LS-174T cells by lipid-mediated DNA-transfection. eIF-4E protein and mRNA levels were detected by Western blot analysis and RT-PCR, respectively. Heparanase activity was defined as the ability to degrade high molecular weight (40-100 kDa) radiolabeled HS (heparan sulfate) substrate into low molecular weight (5-15 kDa) HS fragments that could be differentiated by gel filtration chromatography. The invasive potential of tumor cell *in vitro* was observed by using a Matrigel invasion assay system.

RESULTS: The 20-mer asODN against eIF-4E specifically and significantly inhibited eIF-4E expression at both transcriptional and translational levels. As a result, the expression and activity of heparanase were effectively retarded and the decreased activity of heparanase resulted in the decreased invasive potential of LS-174T.

CONCLUSION: eIF-4E is involved in the regulation of heparanase production in colon adenocarcinoma cell line LS-174T, and its critical function makes it a particularly interesting target for heparanase regulation. This targeting strategy in antisense chemistry may have practical applications in experimental or clinical anti-metastatic gene therapy of human colorectal carcinoma.

Yang YJ, Zhang YL, Li X, Dan HL, Lai ZS, Wang JD, Wang QY, Cui HH, Sun Y, Wang YD. Contribution of eIF-4E inhibition to the expression and activity of heparanase in human colon adenocarcinoma cell line: LS-174T. *World J Gastroenterol* 2003; 9(8): 1707-1712
http://www.wjgnet.com/1007-9327/9/1707.asp

INTRODUCTION

For a malignant tumor cell to metastasize, it must break away from its neighbors, force its way through the surrounding stroma, and penetrate basement membranes to enter the stroma and the circulation. When it arrives at its destination, these steps must be repeated in reverse order[1]. A critical event in the process of cancer invasion and metastasis is therefore degradation of various constituents of the extracellular matrix (ECM) including collagen, laminin, fibronectin, and heparan sulfate proteoglycans (HSPGs). The malignant cell is able to accomplish this task through the concerted sequential action of enzymes such as metalloproteinases, serine proteases, and endoglycosidases[2,3]. Among these enzymes, an endo-β-glucuronidase (heparanase) selectively degrades the heparan sulfate chains of HSPGs which are essential and ubiquitous macromolecules associated with the cell surface and ECM of a wide range of cells and tissues[4,5]. Heparanase cleaves heparan sulfate (HS) and has been implicated in many important pathological processes, including tumor metastasis and angiogenesis[6, 7]. Therefore, heparanase plays an essential role in these pathological processes which makes it a potentially important target for cancer therapy and be helpful to investigate the mechanism, by which the expression of heparanase is regulated.

Eukaryotic initiation factor 4E (eIF-4E) is a 25 kDa mRNA cap-binding phosphoprotein that is rate-limiting for the initiation of cap-dependent mRNA translation by the eIF-4F translation initiation complex[8,9]. Overexpression of eIF-4E has been found in human carcinoma tissues and tumor cell lines. The factor (eIF-4E)[10] dramatically impacts upon the quantitative expression of key malignancy-related genes and can be considered as a critical determinant of malignancy. It seems that involvement of eIF-4E in tumor progression is more closely associated with the impact of enhanced eIF-4E activity on specific, malignancy-related molecules such as ODC, c-myc, cyclin D1, VEGF or MMP-9. Cooperative overexpression of these potent molecules leads to occurrence of tumorigenic phenotype that conspires to drive metastatic progression. The aim of this study was to determine whether eIF-4E was involved in the regulation of heparanase expression and to postulate the probable mechanism.

MATERIALS AND METHODS

Materials

Cell lines Human colon adenocarcinoma cell line LS-174T was an ATCC cell line and was maintained in RPMI 1640 supplemented with 2 mM L-glutamine and 10 % FCS at 37 ℃ in a humidified atmosphere containing 5 % CO_2.

Antisense oligonucleotides Oligonucleotides containing

phosphorothioate were customarily-made and purified with high-performance liquid chromatography. The eIF-4E antisense oligonucleotide comprised the following sequence[11]: 5' -AGTCGCCATCTTAGATCGAT-3' (20 mer), complementary to nucleotides (nt) -11 to +9 of human eIF-4E mRNA. The complementary sense sequence used was 5' -ATCGATCTA AGATGGCGACT-3' . Sense oligonucleotide was used as controls in each of the antisense oligonucleotide experiments.

Methods

Antisense oligonucleotide treatments The day before transfection, the cells were trysinized, counted and plated in a 5×10^6 cells/60-mm dish so that 90-95 % confluency was reached on the day of transfection. As it was a unique cationic lipid formulation, LIPOFECTAMlNE 2000 was more convenient in that it could be used in the presence of serum containing media, by adding it directly to the culture without washing the cells. For transfecting oligonucleotides to cells, the LIPOFECTAMlNE 2000 reagent (Invitrogen) was used according to the manufacturer' s instructions. Briefly, LIPOFECTAMlNE 2000 reagent and oligonucleotides (ODNs) were diluted separately into RPMI 1640 medium and ODNs were mixed with liposome in a charge ratio of 1:2. The mixtures were incubated at room temperature for 20 min to form complexes and then ODN-LIPOFECTAMlNE 2000 reagent complexes was added directly to each well and mixed gently by rocking the plate back and forth. The ODNs were delivered to tumor cells at the final concentration of 2 μmol/L. Tumor cells were incubated in the presence of oligonucleotides/ LIPOFECTAMlNE 2000 reagent mixture for 24 h and 48 h for RT-PCR assays or Western blot.

Semi-quantitative RT-PCR analysis of eIF-4E mRNA Total RNA was extracted by the guanidine salts and phenol-chloroform method. cDNA was prepared from 2 μg of total RNA, using poly-T as primer and MuLV reverse transcriptases (Promega). For PCR amplification, one-fourth of the reverse transcription product and 0.3 μmol/L of each oligonucleotide as primers were used. After one denaturation step at 96 ℃ for 3 minutes, 30 cycles of amplification were performed: denaturation at 94 ℃ for 45 s, annealing at 55 ℃ for 45 s, synthesis at 72 ℃ for 1 minute, and extension at 72 ℃ for 5 minutes. Oligonucleotides for eIF-4E expression analysis were sense primer 5' AGATGGCGACTGTCGAACC3' , antisense primer 5' CAGCGCCACATACATCAT3' [12]. To check cDNA quality, GAPDH was amplified using sense primer 5' CTGGCGCTGAGTACGTCGTG3' and antisense primer 5' CAGTCTTCTGGGTGGCAGTG3' . One-tenth of the amplified products was run on 2 % agarose gels in 1×Tris borate buffer and visualized with ethidium bromide.

Western blot analysis Total proteins were extracted at 48 h after transfection. Cells were lysed in RIPA buffer [10 mM Tris-HCl (pH 7.4), 1 % deoxycholate, 1 % NP40, 150 mM NaCl, 0.1 % SDS, 0.2 mM phenylmethylsulfonyl fluoride, 1 μg/ml aprotinin and 1 μg/ml leupeptin. The lysates were then centrifuged at 10 000×g for 15 min to remove debris. Protein content of the lysate was determined by using Bradford assay (Bio-Rad). For each sample, equal amounts (50 μg) of protein lysates were analyzed on a sodium dodecyl sulfate-10 % or 12 % polyacrylamide gel. Proteins were electroblotted onto Immobilon PVDF membranes (Millipore, Bedford, MA), blocked for 1 h in 5 % dry skim milk, and then incubated with the indicated antibodies. The antibodies used and their dilutions were as follows: 1:500 mouse monoclonal anti-eIF-4E (BD Biosciences), 1:700 rabbit polyclonal anti-heparanase (a kind gift from Mark D. Hulett). The secondary antibodies used were those in an enhanced chemiluminescence detection kit (Amersham) and were chosen according to the species used for the primary antibodies. Exposure times varied with the antibodies used and ranged from 5 to 60 s.

Assays for heparanase activity Heparanase activity was defined as the ability to degrade high molecular weight (40-100 kDa) radio-labeled HS substrate into low molecular weight (5-15 kDa) HS fragments[13-15], which could be differentiated by gel filtration chromatography[16,17]. Radiolabeled HS substrate was prepared by metabolically labeling the extracellular matrix with [^{35}S] as described[16,17]. Soluble substrate was made by releasing ^{35}S-labeled HS proteoglycans from the culture plate with trypsin, and incubated with cell homogenates which were prepared by suspending 10^6 cells in 0.2 ml of aq. 0.1 % (v/v) Triton X-100 and disrupted by freezing and thawing three times in a solid CO_2/ethanol mixture. Samples were taken from the above supernate fractions. Protein concentrations were estimated by a Bio-Rad Coomassie protein assay kit (Bio-Rad Laboratories) using BSA as a standard. Cell lysates containing 50 μg of protein were incubated at 37 ℃ for 24 h in 10 mM sodium phosphate-citrate buffer, pH 6.0, with 20-25 000 cpm of ^{35}S-labeled HS substrate. The incubation medium was centrifuged and the supernatant was analyzed by gel filtration on a Sepharose CL-6B column (0.7×25 cm). Fractions (0.2 ml) were eluted with PBS and their radioactivity was measured. Degradation fragments of HS side chains were eluted from Sepharose CL-6B at 0.5<Kav<0.8 (peak II). A nearly intact HSPG was eluted just after the Vo (Kav<0.2, peak I). Each experiment was repeated at least three times and the variation of elution positions (Kav values) did not exceed ±15 %. Blue dextran and phenol red were added to the sample to mark the excluded (V_0) and included (Vt) volumes, respectively.

***In vitro* invasion assays** *In vitro* invasion assays were performed using modified Boyden chambers, 24-well plates. Polycarbonate filters (8 μm porosity), used to separate the upper compartment, were coated with 50 μg Matrigel. After the lower wells were filled with 600 μl of culture media, supplemented with 0.1 % BSA and 50 μg solubilized Matrigel as a chemo-attractant. The cells in media containing 2 μM oligonucleotides, 1 % FBS at a density of 10^6 cells/ml were resuspended. Gelled Matrigel was gently washed with warmed serum free-culture media. 100 μl of the cell suspension was put onto the Matrigel. Chambers were placed in a 37 ℃ incubator with 5 % CO_2/95 % air for 48 h. Then, the cells remaining on the upper surface of the membrane were removed with a cotton swab and the filters were fixed and stained with a solution of methanol/Coomassie blue 0.1 % in acetic acid (1:3). Cells that had invaded the lower surface of the filter were counted under an inverted microscope. 10 fields per well were counted. The invasion score of untreated control cells was taken as 100 % and that of treated cells was expressed as a percentage of control. All experiments were performed in duplicate and the results from 3 separate sets of experiments were averaged.

RESULTS

Down-regulation effects of antisense oligonucleotides on eIF-4E expression

LS-174T cells were treated with either antisense oligonucleotides, sense control oligonucleotides or saline for 24 h or 48 h in the presence of liposome. By using quantitative RT-PCR analysis, a high level of eIF-4E mRNA was shown in LS-174T cell lines, and treatment with antisense oligonucleotides at concentrations up to 2 μM, induced a significant decrease in the eIF-4E mRNA expression levels compared to control groups. There was no down-regulation of eIF-4E expression in the sense oligonucleotide-treated cells (Figure 1). In order to verify that the decrease in mRNA expression levels corresponded also to

decreases in protein levels, Western blot analysis was performed (Figure 2). We used eIF-4E standard antigen (BD Transduction Laboratories) as a positive control. A significant reduction of eIF-4E protein level was observed in LS-174T cell line, treated with antisense oligonucleotides. In contrast, there was no apparent down-regulation of eIF-4E protein levels in the cells exposed to sense oligonucleotides in comparison with untreated ones.

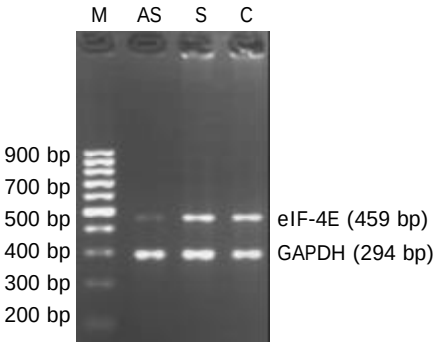

Figure 1 eIF-4E and GAPDH mRNA expression in oligonucleotide-treated human colon adenocarcinoma cells. AS. anti-sense oligonucleotide-transfected cells; S. sense oligonucleotide-transfected cells; C. cells treated with liposome only as control. LS-174T cells were treated with 2 μM oligonucleotides, according to the optimal condition of this cell line in the preliminary experimental results. The numbers under each band showed the relative amount of eIF-4E fragments normalized to that of GAPDH by densitometry. The results suggest that antisense oligonucleotides against eIF-4E inhibit eIF-4E mRNA expression in LS-174T cells, and sense oligonucleotides have no inhibitory effect on eIF-4E mRNA expression.

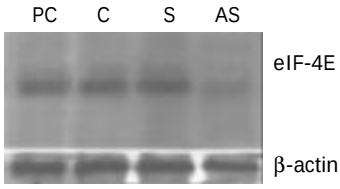

Figure 2 eIF-4E protein expression in oligonucleotide-treated colon adenocarcinoma cells. Protein extracts were prepared from oligonucleotide-treated cells at 48 h after transfection. Cell lysates were size-fractionated by 12 % SDS-PAGE, and immunodetection on the blotted membrane was performed using the eIF-4E MAb. AS, antisense oligonucleotide-treated cells; S. sense oligonucleotide-treated cells; C, cells treated with liposome only; PC, eIF-4E standard antigen (derived from a human neuroblastoma cell line) as a positive control marker.

eIF-4E down-regulation is correlated with alterations in expression of heparanase protein

It has shown that eIF-4E may be involved in regulating a variety of tumor invasion-associated molecules[10]. We investigated the relationship between eIF-4E overexpression and the effects of this expression on heparanase levels in metastatic colon adenocarcinoma cell line. Substantial alterations in the levels of both 50 kDa and 65 kDa heparanase protein expression were observed in the transfectants. In LS-174 cell lines treated with asODN, eIF-4E down-regulation appeared to be associated with the decrease in heparanase protein expression. A 50 kDa protein, corresponding to the expected active mature heparanase according to published data[18], was detected at lower levels in LS-174T cells transfected with antisense oligonucleotides. And so did a 65 kDa protein, which corresponded to the expected size for unprocessed heparanase. In the meantime, heparanase protein levels did not change apparently in the cells treated with sense oligonucleotides or liposome only. Our data demonstrated that eIF-4E did affect the expression of heparanase protein of LS-174T cells under these experimental conditions (Figure 3).

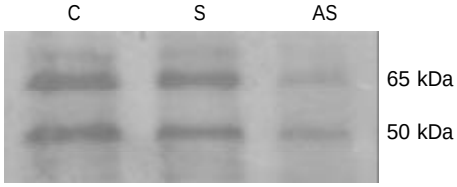

Figure 3 Western blot analysis of heparanase expression in LS-174T cells. The colon adenocarcinoma cells were lysed, and Western blot analysis was performed with an anti-human heparanase polyclonal antibody. AS, antisense oligonucleotide-treated cells; S. sense oligonucleotide-treated cells; C, cells treated with liposome only. Cells treated with antisense oligonucleotides showed markedly reduced levels of heparanase protein compared to cells treated with sense oligonucleotides or saline in the presence of liposome. The approximately 65-kDa protein represents a heparanase precursor, whereas the 50-kDa protein is a processed form, and data showed that both of them were less expressed while eIF-4E was inhibited.

Alteration in heparanase activity

Heparanase activity was determined by degradation of purified ECM [^{35}S] HS using gel filtration chromatography analysis. Degradation fragments eluted in peak II were shown to be degradation products of HS. In this experiment, incubation of an equal amount of protein with sulfate-labeled ECM resulted in release of high level HS degradation fragments (Peak II) in the samples derived from the cells treated with sense oligonucleotides or liposome alone, whereas degradation was less pronounced during incubation of ECM with extracts derived from the cells treated with antisense oligonucleotides (Figure 4). Heparanase activity was also expressed as the total amount of radioactivity eluted in peak II multiplied by the Kav of peak II, thereby representing both the total amount and the size of HS-degradation fragments. The result was consistent with heparanase expression at the protein level. Thus, the alteration of heparanase protein seen by immunostaining was also reflected by a decreased heparanase activity found in the extracts derived from the tumor cells treated with antisense oligonucleotides. These results suggested that the high levels of heparanase were parallel to over-expressed eIF-4E in LS-174T cells and the expression of heparanase might be regulated by eIF-4E in these tumor cells.

Inhibition of heparanase suppresses in vitro invasiveness of LS-174T cells

We first examined whether the variation of eIF-4E expression was associated with heparanase activity in LS-174T cells and its consequent influence on the invasive potential of these tumor cells (Figure 5). The effect of this antisense sequence on invasive capacity was studied *in vitro* by measuring the ability of tumor cells to cross a barrier composed of Matrigel. In these conditions, the invasiveness of LS-174T cells was reduced to 23 % by this antisense sequence. In a control experiment, cells treated at the same concentration of sense oligonucleotides did not show any significantly inhibitory effect on tumor cells invasion as compared to the untreated ones. These results argued that eIF-4E was involved in the regulation of heparanase expression and might further influence the invasive potential of tumor cells.

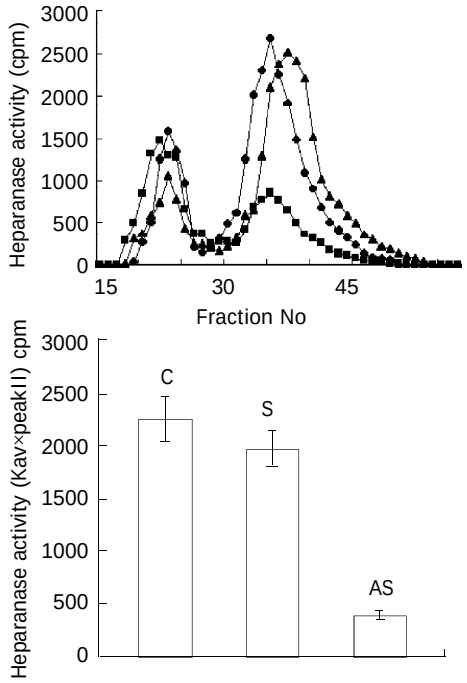

Figure 4 Effects of eIF-4E down-regulation upon enzyme activity of heparanase. Cells were treated for 48 h with antisense oligonucleotide (■), sense oligonucleotide (▲) or liposome only(◆). The soluble fraction from transfected, freezed and thawed LS-174T cells was incubated with ^{35}S-labeled HS. The incubation medium was then subjected to gel filtration over Sepharose CL-6B. Low-molecular-weight HS degradation fragments (peak II) were mainly produced during incubation with medium conditioned by sense oligonucleotide infected cells. The cells treated with antisense oligonucleotide exhibited low levels of heparanase activity as compared to untreated ones. Heparanase activity was also expressed as Kav×total cpm eluted in peak II.

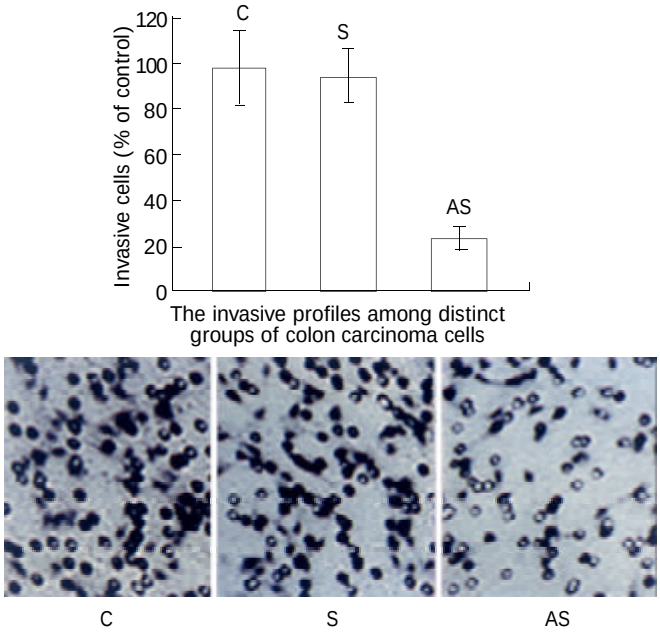

Figure 5 Invasive profiles of LS-174T cells measured *in vitro* using Matrigel as ECM barrier in modified Boyden chambers. The invasiveness of the cells on Matrigel was normalized to 100 % (control, untreated cells). Compared with the control, antisense oligonucleotide reduced invasion to 23 %. Sense sequence didn't have a significant influence on invasive potential of LS-174T cells. These results suggest that alteration of heparanase activity via inhibition of the expression of eIF-4E results in decreased invasiveness in LS-174T cells. The small rings are membrane pores.

DISCUSSION

Inhibition of tumor invasion is an attractive approach for the treatment of highly malignant tumors. Tumor cell invasion is characterized by secretion of enzymes that facilitate tumor cell spread by degrading ECM surrounding the tumors and solubilizing the vascular basement[19]. Thus, heparanase, which degrades HSPG in ECM, is an attractive target for the development of new antimetastatic drugs because of evidences implicating the enzyme in tumor cell invasion. Heparanase facilitates tumor cell invasion and metastasis by at least two different mechanisms. First, it breaks down physical barriers to invasion through degradation of HS chains of HSPGs which are the chief components in BM and ECM, not cleaved by MMPs. Second, it may regulate angiogenesis, tissue repair, inflammation and lipid metabolism by releasing HS-bound growth factor (bFGF) and lipoprotein lipase, which may be a pertinent molecular mechanism for tumor metastasis. Prior reports have mentioned that heparanase is involved in the metastatic potential of various tumor cells, however heparanase as a key regulator of tumor metastasis has not been established with regard to the lack of purified enzymes and cDNA of the gene[20-24]. Two studies concerned with cloning and sequencing of mammalian heparanase and new findings not only confirmed previous studies but revealed that heparanase played an important role in invasion and metastasis of tumor cells[25,26].

As judged by semi-quantitative RT-PCR, heparanase mRNA was increased in human malignancies and xenografts of human breast, colon, lung, prostate, ovary, and pancreas tumors, compared with the corresponding normal tissues[27]. Further support for the role of heparanase in tumour metastasis came from transfection studies where the metastatic ability of lymphoma and melanoma cell lines was substantially enhanced when they were stably transfected with the heparanase gene[25,28]. Additional evidences for heparanase involvement in tumour metastasis came from the *in vivo* administration of heparanase inhibitors, with a dramatic reduction (90 %) in the incidence of tumour metastases reported in a number of tumour models when animals were treated with heparanase inhibitors[29,30]. As to human colon carcinoma[31], heparanase mRNA and protein accumulated even at early stages in the progression of neoplastic disorders, and their levels increased gradually as cells progressed from severe dysplasia through well-differentiated to poorly differentiated colon carcinoma. Adjacent, morphologically normal colonic tissue showed no expression of the enzyme. Deeply invading colon carcinoma cells and the adjacent desmoplastic stromal fibroblasts showed high levels of heparanase mRNA and protein. These results suggest that increased expression of heparanase as in tumor cells indicates less differentiation and more invasive ness. Considering the key role of heparanase in the metastasis of tumor cells, it seems very important to investigate the mechanism by which the expression of heparanase in tumor cells is regulated. Virtually nothing is known about the factors that upregulate heparanase expression and activity in malignant cells, and the molecular basis of this upregulation at the gene level has not been delineated yet. Our research dealed with the translational regulation of heparanase via modulation of the mRNA cap-binding phosphoprotein, eIF-4E and probed the subsequent alterations of invasive potential in LS-174T cells.

To date, Overexpression of eIF-4E has been found in human carcinoma tissues and tumor cell lines. A recent publication[32] also suggested that increased expression of eIF-4E might be an early event in the development human colon cancer. Investigators have found that eIF-4E is increased in both colon adenomas and carcinomas. A compelling body of evidences now indicates that eIF-4E is centrally involved not only in

cellular transformation, but also in tumor formation, invasion and metastasis. The major intracellular signaling pathways involved in tumor growth and malignancy induce eIF-4E activity. MAP kinase activation stimulates MNK-mediated phosphorylation and activation of eIF-4E directly, while activation of the pI3 kinase/PTEN/AKT pathway ultimately yields phosphorylation and inactivation of 4E-BP1, and subsequent release of eIF-4E. Zimmer *et al*[10] indicated that increased eIF-4E activity might provide a central regulatory step facilitating tumor invasion and metastasis via upregulation of selected, potent gene products (such as bFGF, VEGF, MMP-9 and CD44v6). In this report, the colon adenocarcinoma cell line also showed expression of eIF-4E. By transfecting LS-174T cells with a 20-mer antisense s-oligodeoxynucleotide targeted against eIF-4E at well tolerated doses, eIF-4E expression was specifically and significantly inhibited at transcriptional and translational levels. Furthermore, as eIF-4E protein expression decreased, the expression and activity of heparanase were effectively retarded as well and the tumor cells also displayed a reduced invasive potential. It seems that heparanase down-regulation is closely correlated with alterations in the expression of eIF-4E. This study firstly demonstrated that eIF-4E might be involved in the regulatory processes of heparanase in colon adenocarcinoma cell line LS-174T. However, the mechanisms underlying these regulatory events remain unclear, since eIF-4E has the potential to alter gene expression at levels including translational initiation, mRNA splicing, mRNA 3' -end processing, mRNA nucleocytoplasmic transport, and protection against 5' -exonucleolytic degradation[33]. Possible roles of eIF-4E in regulatory processes of heparanase expression remain unidentified and the mechanism deserves further investigation.

Our results, together with the previous reports, indicate that constitutively high-level expression of eIF-4E in tumor cells is involved in the regulation of heparanase expression, although the exact mechanism is not quite certain. Since matrix metalloprotease 9 (MMP-9) and CD44 expression are directly related to metastatic capacity, they are certainly to be governed by enhanced eIF-4E activity. Therefore, eIF-4E antisense strategy should be an effective treatment against tumour invasion and metastasis. This targeting strategy in antisense chemistry may have practical applications in experimental or clinical anti-metastatic gene therapy of human colorectal carcinoma.

ACKNOWLEDGMENTS

This work was supported by a grant from National Natural Science Foundation of China. We thank Mr. Liu Rong, Wang Yadong for their technical assistance.

REFERENCES

1 **Poste G**, Fidler IJ. The pathogenesis of cancer metastasis. *Nature* 1980; **283**: 139-146
2 **Stetler Stevenson WG**, Aznavoorian S, Liotta LA. Tumor cell interactions with the extracellular matrix during invasion and metastasis. *Annu Rev Cell Biol* 1993; **9**: 541-573
3 **Duffy MJ**. The role of proteolytic enzymes in cancer invasion and metastasis. *Clin Exp Metastasis* 1992; **10**: 145-155
4 **Toyoshima M**, Nakajima M. Human heparanase. Purification, characterization, cloning, and expression. *J Biol Chem* 1999; **274**: 24153-24160
5 **Iozzo RV**, Murdoch AD. Proteoglycans of the extracellular environment: clues from the gene and protein side offer novel perspectives in molecular diversity and function. *FASEB J* 1996; **10**: 598-614
6 **Parish CR**, Freeman C, Hulett MD. Heparanase: a key enzyme involved in cell invasion. *Biochim Biophys Acta* 2001; **1471**: M99-108
7 **Vlodavsky I**, Friedmann Y. Molecular properties and involvement of heparanase in cancer metastasis and angiogenesis. *J Clin Invest* 2001; **108**: 341-347
8 **Rhoads RE**, Joshi-Barve S, Rinker-Schaeffer C. Mechanism of action and regulation of protein synthesis initiation factor 4E: effects on mRNA discrimination, cellular growth rate, and oncogenesis. *Prog Nucleic Acid Res Mol Biol* 1993; **46**: 183-219
9 **Sonenberg N**, Gingras AC. The mRNA 5' cap-binding protein eIF4E and control of cell growth. *Curr Opin Cell Biol* 1998; **10**: 268-275
10 **Zimmer SG**, DeBenedetti A, Graff JR. Translational control of malignancy: the mRNA cap-binding protein, eIF-4E, as a central regulator of tumor formation, growth, invasion and metastasis. *Anticancer Res* 2000; **20**: 1343-1351
11 **De Benedetti A**, Joshi-Barve S, Rinker-Schaeffer C, Rhoads RE. Expression of antisense RNA against initiation factor eIF-4E mRNA in HeLa cells results in lengthened cell division times, diminished translation rates, and reduced levels of both eIF-4E and the p220 component of eIF-4F. *Mol Cell Biol* 1991; **11**: 5435-5445
12 **Anthony B**, Carter P, De Benedetti A. Overexpression of the proto-oncogene / translation factor 4E in breast-carcinoma cell lines. *Int J Cancer* 1996; **65**: 858-863
13 **Bame KJ**, Hassall A, Sanderson C, Venkatesan I, Sun C. Partial purification of heparanase activities in Chinese hamster ovary cells: evidence for multiple intracellular heparanases. *Biochem J* 1998; **336**(Pt 1): 191-200
14 **Pikas DS**, Li JP, Vlodavsky I, Lindahl U. Substrate specificity of heparanases from human hepatoma and platelets. *J Biol Chem* 1998; **273**: 18770-18777
15 **Freeman C**, Parish CR. A rapid quantitative assay for the detection of mammalian heparanase activity. *Biochem J* 1997; **325**(Pt 1): 229-237
16 **Gilat D**, Hershkoviz R, Goldkorn I, Cahalon L, Korner G, Vlodavsky I, Lider O. Molecular behavior adapts to context: heparanase functions as an extracellular matrix-degrading enzyme or as a T cell adhesion molecule, depending on the local pH. *J Exp Med* 1995; **181**: 1929-1934
17 **Matzner Y**, Bar-Ner M, Yahalom J, Ishai-Michaeli R, Fuks Z, Vlodavsky I. Degradation of heparan sulfate in the subendothelial extracellular matrix by a readily released heparanase from human neutrophils. Possible role in invasion through basement membranes. *J Clin Invest* 1985; **76**: 1306-1313
18 **Hulett MD**, Hornby JR, Ohms SJ, Zuegg J, Freeman C, Gready JE, Parish CR. Identification of active-site residues of the pro-metastatic endoglycosidase heparanase. *Biochemistry* 2000; **39**: 15659-15667
19 **Nakajima M**, Irimura T, Di Ferrante D, Di Ferrante N, Nicolson GL. Heparan sulfate degradation: relation to tumor invasive and metastatic properties of mouse B16 melanoma sublines. *Science* 1983; **220**: 611-613
20 **Ishai-Michaeli R**, Eldor A, Vlodavsky I. Heparanase activity expressed by platelets, neutrophils, and lymphoma cells releases active fibroblast growth factor from extracellular matrix. *Cell Regul* 1990; **1**: 833-842
21 **Vlodavsky I**, Bar-Shavit R, Ishai-Michaeli R, Bashkin P, Fuks Z. Extracellular sequestration and release of fibroblast growth factor: a regulatory mechanism? *Trends Biochem Sci* 1991; **16**: 268-271
22 **Eisenberg S**, Sehayek E, Olivecrona T, Vlodavsky I. Lipoprotein lipase enhances binding of lipoproteins to heparan sulfate on cell surfaces and extracellular matrix. *J Clin Invest* 1992; **90**: 2013-2021
23 **Vlodavsky I**, Eldor A, Haimovitz-Friedman A, Matzner Y, Ishai-Michaeli R, Lider O, Naparstek Y, Cohen IR, Fuks Z. Expression of heparanase by platelets and circulating cells of the immune system: possible involvement in diapedesis and extravasation. *Invasion Metastasis* 1992; **12**: 112-127
24 **Eccles SA**. Heparanase: breaking down barriers in tumors. *Nat Med* 1999; **5**: 735-736
25 **Vlodavsky I**, Friedmann Y, Elkin M, Aingorn H, Atzmon R, Ishai-Michaeli R, Bitan M, Pappo O, Peretz T, Michal I, Spector L, Pecker I. Mammalian heparanase: gene cloning, expression and function in tumor progression and metastasis. *Nat Med* 1999;

5: 793-802

26 **Hulett MD**, Freeman C, Hamdorf BJ, Baker RT, Harris MJ, Parish CR. Cloning of mammalian heparanase, an important enzyme in tumor invasion and metastasis. *Nat Med* 1999; **5**: 803-809

27 **McKenzie E**, Tyson K, Stamps A, Smith P, Turner P, Barry R, Hircock M, Patel S, Barry E, Stubberfield C, Terrett J, Page M. Cloning and expression profiling of Hpa2, a novel mammalian heparanase family member. *Biochem Biophys Res Commun* 2000; **276**: 1170-1177

28 **Vlodavsky I**, Elkin M, Pappo O, Aingorn H, Atzmon R, Ishai-Michaeli R, Aviv A, Pecker I, Friedmann Y. Mammalian heparanase as mediator of tumor metastasis and angiogenesis. *Isr Med Assoc J* 2000; **2**(Suppl): 37-45

29 **Miao HQ**, Elkin M, Aingorn E, Ishai-Michaeli R, Stein CA, Vlodavsky I. Inhibition of heparanase activity and tumor metastasis by laminarin sulfate and synthetic phosphorothioate oligodeoxynucleotides. *Int J Cancer* 1999; **83**: 424-431

30 **Parish CR**, Freeman C, Brown KJ, Francis DJ, Cowden WB. Identification of sulfated oligosaccharide-based inhibitors of tumor growth and metastasis using novel *in vitro* assays for angiogenesis and heparanase activity. *Cancer Res* 1999; **59**: 3433-3441

31 **Friedmann Y**, Vlodavsky I, Aingorn H, Aviv A, Peretz T, Pecker I, Pappo O. Expression of heparanase in normal, dysplastic, and neoplastic human colonic mucosa and stroma. Evidence for its role in colonic tumorigenesis. *Am J Pathol* 2000; **157**: 1167-1175

32 **Rosenwald IB**, Chen JJ, Wang S, Savas L, London IM, Pullman J. Upregulation of protein synthesis initiation factor eIF-4E is an early event during colon carcinogenesis. *Oncogene* 1999; **18**: 2507-2517

33 **Rhoads RE**. Cap recognition and the entry of mRNA into the protein synthesis initiation cycle. *Trends Biochem Sci* 1988; 13: 52-56

Edited by Zhang JZ and Wang XL

P.O.Box 2345, Beijing 100023,China
Fax: +86-10-85381893
E-mail: wjg@wjgnet.com www.wjgnet.com

World J Gastroenterol 2003;9(8):1713-1718
World Journal of Gastroenterology
 ISSN 1007-9327

• COLORECTAL CANCER •

Refinement of heterozygosity loss on chromosome 5p15 in sporadic colorectal cancer

Shi-Feng Xu, Zhi-Hai Peng, Da-Peng Li, Guo-Qiang Qiu, Fang Zhang

Shi-Feng Xu, Zhi-Hai Peng, Da-Peng Li, Guo-Qiang Qiu, Fang Zhang, Department of General Surgery, Shanghai First People' s Hospital, Shanghai 200080, China
Supported by the National Natural Science Foundation of China, No. 30080016
Correspondence to: Dr. Zhi-Hai Peng, Department of General Surgery, Shanghai First People' s Hospital, 85 Wujin Road, Shanghai 200080, China. pengpzhb@online.sh.cn
Telephone: +86-21-63240090 Ext 3102
Received: 2003-03-20 **Accepted:** 2003-04-17

Abstract

AIM: To refine the loss of heterozygosity on chromosome 5p15 and to identify the new tumor suppressor gene (s) in colorectal tumorigenesis.

METHODS: Sixteen polymorphic microsatellite markers were analyzed on chromosome 5 and another 6 markers were applied on chromosome 5p15 in 83 cases of colorectal and normal DNA by PCR. PCR products were electrophoresed on an ABI 377 DNA sequencer. Genescan 3.1 and Genotype 2.1 software were used for LOH scanning and analysis.

RESULTS: We observed 2 distinct regions of frequent allelic deletions on Chromosome 5, at D5S416 on 5p15 and D5S428-D5S410 on 5q. Another 6 polymorphric microsatellite markers were applied to 5p15 and the minimal region of frequent loss of heterozygosity was established on 5p15 spanning the D5S416 locus.

CONCLUSION: Through our detailed deletion mapping studies, we have found a critical and precise location of 5p deletions, 5p15.2-5p15.3, which must contain one or more unknown tumor suppressor gene (s) of colorectal cancer.

Xu SF, Peng ZH, Li DP, Qiu GQ, Zhang F. Refinement of heterozygosity loss on chromosome 5p15 in sporadic colorectal cancer. *World J Gastroenterol* 2003; 9(8): 1713-1718
http://www.wjgnet.com/1007-9327/9/1713.asp

INTRODUCTION

Colorectal cancer is one of the most common malignant tumors threatening people' s health[1,2]. Its occurrence has been rising over the past 3 decades[3]. Now, colorectal cancer is the second cause of death in Western countries, and the fourth in China[4]. It is clear that improvement in its prognosis will not be achieved without a better understanding of its etiology and tumor biology. In recent years, the genetic basis of human tumors has been increasingly elucidated. A growing number of studies have shown that the molecular events controlling tumorigenesis involve abnormal cell growth promoted by activation of proto-oncogenes and/or inactivation of tumor suppressor genes[5,6]. Identification of novel tumor suppressor genes has been facilitated by loss of heterozygosity (LOH) studies that have guided the localization of minimally deleted regions on chromosomes[6,7]. In colorectal cancers, frequent allelic loss has been identified on chromosomes 5q (30 %), 8p (40 %), 17p (75-80 %), 18q (80 %), and 22q (20-30 %)[8,9].

Previous allelotype analyses of chromosome 5 in colorectal cancer mainly focused on the long arm (5q), where a high frequency of allelic deletions of 5q21-22 was reported, implicating the *APC/MCC* genes[10-13]. However, alterations of the short arm of chromosome 5 have not been studied extensively in colorectal cancers. In this study, 16 polymorphic microsatellite markers were applied to chromosome 5. As a result of the high frequence of LOH on the loci of D5S416, another 6 microsatellite markers from chromosomal region 5p15, spanning the D5S416 were precisely localized.

MATERIALS AND METHODS

Materials

This study was based on 83 patients with colorectal cancer including 40 men and 43 women, who were treated at the Surgical Department in Shanghai First People' s Hospital, China, between 1998 and 1999. The patients' age ranged from 31 to 84 years with a median of 66. All the patients were confirmed by pathology, and staged by Duke' s criteria. Eight, 21, 40, 14 cases were of Duke' s stages A, B, C and D, respectively. 23 cases were well differentiated, 39 moderately differentiated, 6 poorly differentiated adenocarcinoma, and 15 cases were mucinous adenocarcinoma. HNPCC patients were ruled out by Amsterdam criteria[14,15]. Each patient gave his were or her informed consent for the use of his or her tissues in this study.

Methods

DNA extraction The cancerous and adjacent normal tissues were freshly frozen within 30 min after being removed. These tissues were then cut into cubes of approximately 2 mm^3 and immediately frozen in liquid nitrogen. DNA was extracted using standard methods with proteinase K digested and phenol/chloroform purified.

Microsatellite markers and PCR Initially, 83 cases of colorectal cancer were analyzed by PCR using 16 microsatellite markers which were mapped to chromosome 5. DNA samples were analyzed as normal/tumor pairs using primers for the following microsatellite loci(location/heterozygosity): D5S1981-(5P15.3/0.73), D5S406-(5P15.3/0.78), D5S630-(5P15.3/0.89), D5S416(5P15.2/0.77), D5S419-(5P13.3/0.80), D5S418-(5P13.1/0.80), D5S407-(5q11.2/0.86), D5S647-(5q12.2/0.82), D5S424-(5q13.2/0.76), D5S428-(5q14.1/0.76), D5S2027-(5q21.1/0.78), D5S471-(5q23.1/0.75), D5S2115-(5q31.1/0.76), D5S410-(5q33.2/0.79), D5S400-(5q35.1/0.81), D5S408-(5q35.3/0.73). As a result of the high frequency of LOH in D5S416, 6 additional microsatellite markers from chromosomal region 5p15 were employed to span the D5S416 locus. DNA samples were also analyzed as normal/tumor pairs for the following microsatellite loci (location/heteozygosity): D5S1987-(5p15.3/0.87), D5S1991-(5p15.3/0.68), D5S1954-

(5p15.3/0.69), D5S1963-(5p15.2/0.69), D5S2114-(5P15.2/0.87), D5S486-(5p15.1/0.74). Polymorphic microsatellite markers were analyzed by PCR (GeneAmp PCR System 9700, PE Applied Biosystems Fostercity CA, USA). PCR conditions were as follows: 5 μl total volume with approximately 1.4 ng of DNA as a template with 10× standard buffer, 0.3 μl Mg^{2+}, 0.8 μl deoxynucleotide triphosphates, 0.3 unit of Hot-start taq polymerase and 0.06 ml of each oligonucleotide primer, with the forward primer fluorescence labeled with HEX, FAM or NED. The "touch-down" was applied. Cycling conditions consisted of 3 stages: an initial denaturation at 96 ℃ for 12 min in stage I; 14 cycles each at 94 ℃ for 20 s, at 63-56 ℃ for 1 min (decrease 0.5 ℃ per cycle) and at 72 ℃ for 1 min in stage II, 35 cycles each at 94 ℃ for 20 s, at 56 ℃ for 1 min and at 72 ℃ for 1 min in stage III.

LOH analysis A portion of each PCR product (0.5 μl) was combined with 0.1 μl of Genescan 500 size standard (PE Applied Biosystems Fostercity CA, USA) and 0.9 ul of formamide loading buffer. After denaturation at 96 ℃ for 5 min, the products were electrophoresed on a 5 % polyacrylamide gel on an ABI 377 DNA sequencer (PE Applied Biosystems Fostercity CA, USA) for 3 hours. Genotype 2.1 software displayed individual gel lanes as electrophoretograms with a given size, height, and area for each detected fluorescent peak. Stringent criteria were used to score the samples. Alleles were defined as the two highest peaks within the expected size range. A ratio of T1:T2/N1:N2 of less than 0.67 or greater than 1.50 was scored as a loss of heterozygosity (Figure 1). Most amplifications of normal DNA produced two PCR products indicating heterozygosity. A single fragment amplified from normal DNA (homozygote) and those PCR reactions in which fragments were not clearly amplified, were scored as not informative. The LOH frequency of a locus was equal to the ratio between allelic loss and informative cases.

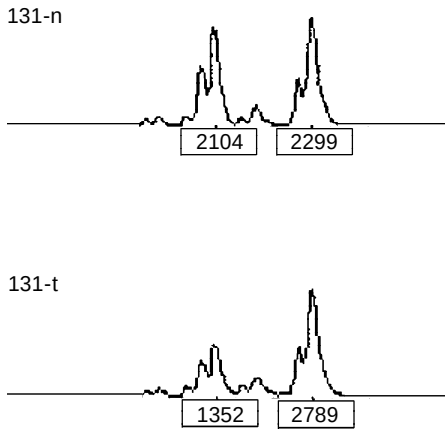

Figure 1 Representative LOH in tumor. "*n*" is normal DNA, "*t*" is tumor DNA. The peak heights are indicated below the corresponding alleles. Allele ratio=(t1:t2)/(n1:n2)=(1 352:2 789)/(2 104:2 299)=0.53. Allele ratio of less than 0.67 or greater than 1.50 was scored as LOH.

RESULTS

LOH analysis of colorectal cancers

Eighty-three colorectal cancers were analyzed for LOH at the 16 marker loci spanning chromosome 5 with the following most likely order: pter-D5S1981-D5S406-D5S630-D5S416-D5S419-D5S418-D5S407-D5S647-D5S424-D5S641-D5S428-D5S2027-D5S471-D5S2115-D5S410-D5S400-D5S408-qter[16] (Table 1 and Figure 2). We observed 2 distinct regions of frequent allelic deletions on chromosomes at D5S416 on 5p15 and D5S428-D5S410 on 5q.

LOH mapping of 5p15 region

The chromosomal region spanning D5S416 locus on chromosome 5p was further investigated using a saturation mapping strategy with another 6 microstellite markers that are localized and closely spaced within this region (Figure 3). Eighty-three paired normal and tumor DNA samples were analyzed for LOH at these loci which further refined the resolution of the deletion map to a genomic segment of approximately 1 centimorgan (cM) and established the minimal region of frequent chromosomal loss at D5S416 locus. Based on the databases described previously, the most likely order of these markers was pter-D5S630-D5S1987-D5S1991-D5S1954-D5S1963-D5S416-D5S2114-D5S486[16] (Table 2). Overall, preferential deletions of D5S416 were observed in 26/54 colorectal cancers and deletions of the 2 markers, D5S1954 and D5S1963 (approximately 1 cM centromeric to D5S416), were seen in 33.3 % (16/48) and 21.1 % (12/57), respectively. Thus, the majority of observed interstitial deletions were localized within a 1 cM genomic segment encompassing the D5S416 locus.

Table 1 The ratios of LOH of all loci on chromosome 5

Loci	Map location	Number of informative cases (%)	LOH No (%)
D5S1981	p15.3	24 (28.92)	3 (12.50)
D5S406	p15.3	26 (31.33)	5 (19.23)
D5S630	p15.3	65 (78.31)	8 (12.31)
D5S416	**p15.2**	**54 (65.06)**	**26 (48.15)**
D5S419	p13.3	63 (75.90)	7 (11.11)
D5S418	p13.1	66 (79.52)	15 (22.73)
D5S407	q11.2	51 (61.45)	10 (19.61)
D5S647	q12.2	74 (89.16)	16 (21.62)
D5S424	q13.2	36 (43.37)	8 (22.22)
D5S428	**q14.1**	**61 (73.49)**	**23 (37.70)**
D5S2027	**q21.1**	**46 (55.42)**	**15 (32.61)**
D5S471	**q23.1**	**62 (74.70)**	**24 (38.71)**
D5S2115	**q31.1**	**59 (71.08)**	**19 (32.20)**
D5S410	**q33.2**	**18 (21.69)**	**8 (44.44)**
D5S400	q35.1	28 (33.73)	4 (14.39)
D5S408	q35.3	61 (73.49)	6 (9.84)

Table 2 The ratios of LOH of the loci on 5p15 region

Loci	Map location	Space of two loci (cM)	Number of informative cases (%)	LOH No (%)
D5S630	p15.3	2.2	65 (78.31)	8 (12.31)
D5S1987	p15.3	4.7	67 (80.31)	11 (16.42)
D5S1991	p15.3	0.6	50 (60.24)	6 (12.00)
D5S1954	**p15.3**	**0.1**	**48 (57.83)**	**16 (33.33)**
D5S1963	**p15.2**	**0.8**	**57 (68.67)**	**12 (21.05)**
D5S416	**p15.2**	1.0	**54 (65.06)**	**26 (48.15)**
D5S2114	p15.2	2.2	53 (63.86)	7 (13.21)
D5S486	p15.1		60 (72.29)	10 (16.67)

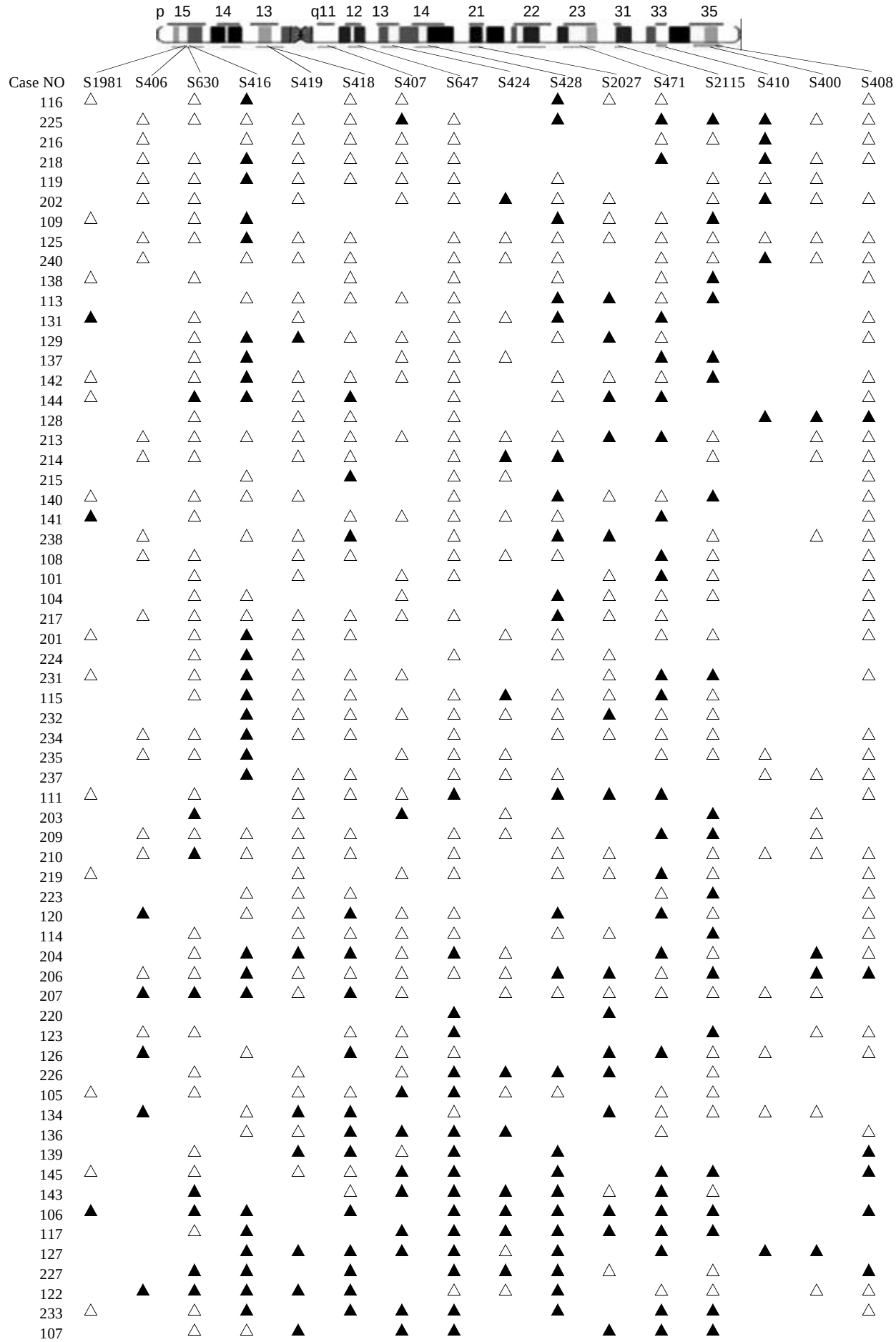

Figure 2 LOH map of chromosome 5 in colorectal cancer. ▲ LOH; △ retaining heterozygosity; neither ▲ or △ is non-informative. We can clearly figure out the two regions of the high rates of LOH on chromosome 5, one is D5S416 on 5p15, the other is D5S428-D5S410 on 5 q.

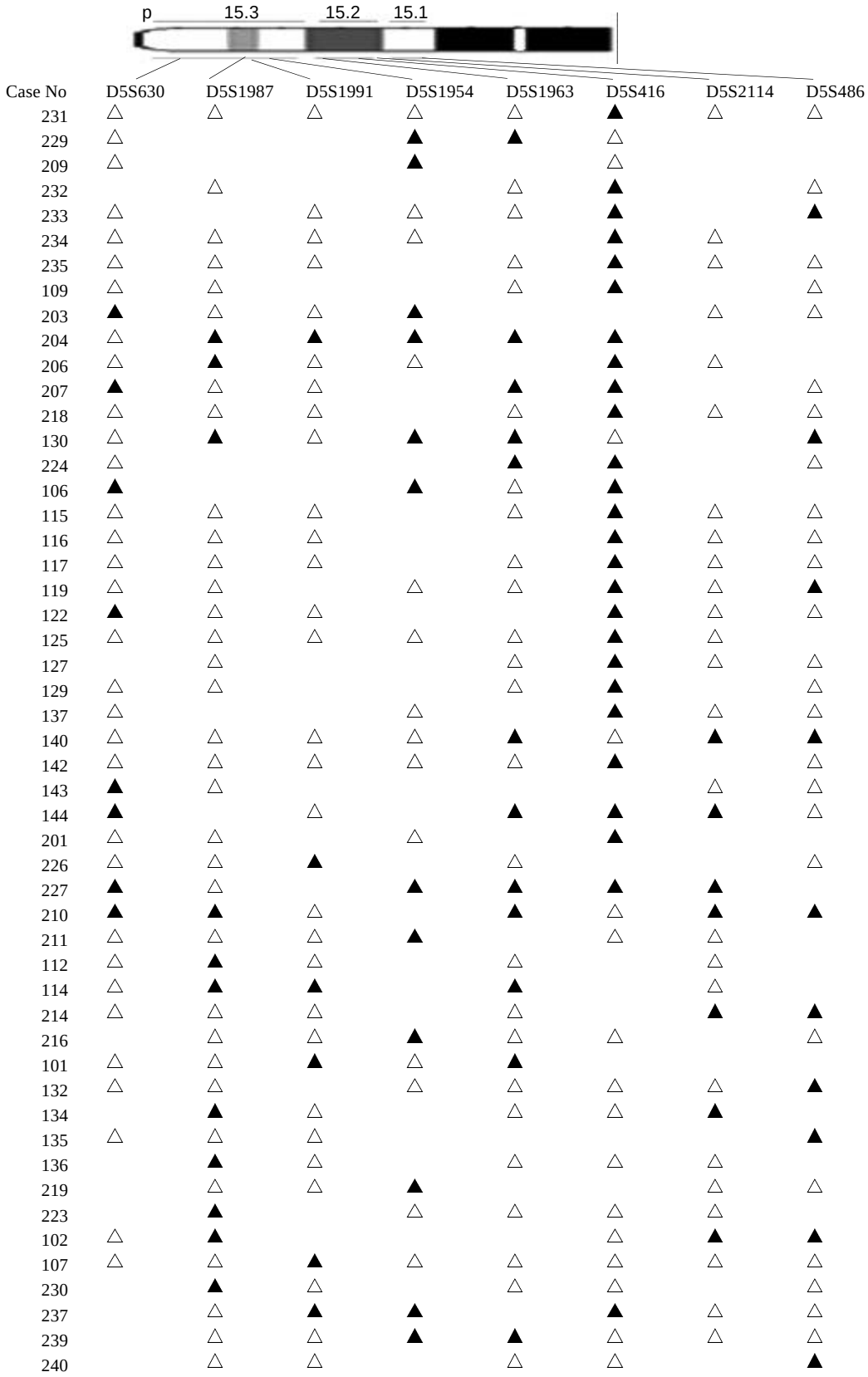

Figure 3 LOH map of 5p15 in colorectal cancer. ▲ LOH; △ retaining heterozygosity; neither ▲ or △ is non-informative.

DISCUSSION

Inactivation of tumor suppressor genes appears to be one of the genetic mechanisms involved in the development of colorectal cancer[17-19]. This process includes mutation of one allele, followed by a deletion of the remaining one (LOH) or homozygous deletion of both alleles[20]. Allelic deletions detected as LOH have been proved useful for mapping regions of DNA that contain tumor suppressor genes. LOH at specific chromosomal regions strongly suggests the existence of tumor suppressor genes at the relevant segment[21,22]. We performed deletion mapping analyses of chromosome 5 markers in 83 sporadic colorectal cancers, using 16 microsatellite markers. Analysis of the deletion map (Figure 2), together with the frequency of LOH obtained for each locus (Table 1) allowed us to identify two regions on chromosome 5 displaying high rates of LOH.

The 5q14-q22 region (D5S428-D5S410) has been frequently deleted in colorectal cancer. Ashton-Rickardt is the first author to describe the *APC/MCC* region as being frequently deleted in sporadic colorectal cancer[10]. Since then, several reports have indicated a high frequency of LOH at this region[11-13]. Our study also identified it, which proved our ways right.

The other region is 5p15 (D5S416). Further mapping of 5p15 region defined a minimal region of frequent deletion spanning the D5S416 locus (Figure 3). Based on this map, the majority of allelic deletions were localized within 1 cM chromosomal segment encompassing the 3 loci (D5S1954, D5S1963 and D5S416). Of these, D5S416 was the most frequently deleted locus (48.15 %), while the other 2 markers, D5S1954 and D5S1963, demonstrated allelic losses of 33.33 % and 21.05 %, respectively. Thus, the high LOH frequency and the patterns of allelic losses of chromosome 5p15.2-5p15.3 suggest that this region may be preferentially deleted in colorectal cancer and could potentially harbor important tumor suppressor genes in colorectal development and progression. A database search has identified four candidate genes, *PDCD6*[23-27], *TERT*[28-29], *T RIP13*[30,31] and *POLS*[32-34] with suggestive tumor suppressor gene functions. The programmed cell death gene, *PDCD6*, is a member of the family of intracellular Ca^{2+}-binding proteins and a part of the apoptotic machinery controlled by T-cell receptor (TCR) Fas, and glucocorticoid signals[23-27]. *TERT* encodes a reverse transcriptase required for the replication of chromosome termini and plays a role in telomere elongation. Although telomerase expression is a hallmark of cancer[35], the mice lacking the RNA component of telomerase (mTERC) exhibit progressive telomere shortening and chromosomal instability associated with epithelial tumors[28]. *TRIP13*, thyroid receptor interacting protein 13, is a transcription factor that regulates expression of a variety of specific target genes such as the human papilloma virus type16 E1(HPV16E1) which is important in cervical carcinoma[30,31]. *POLS* gene, a topoisomerase-related functional protein-4-1, encodes polymerase (DNA directed) signal within the deleted region. The yeast homolog TRF4 plays a critical role in chromosome segregation by coordinating between DNA replication and sister chromatid cohesion[32, 33]. The data strongly support the importance of the *POLS* gene, which is critical for TRF4' s essential and repair functions. Cell cycle analysis has revealed that *TRF4/POLS* is associated with chromosomes in G1, S and G2 phases[34]. The presence of these genes at the 5p15.2-5p15.3 interval suggests that they may target tumor suppressor genes of these deletions in colorectal cancer. It will be helpful for us to find the tumor suppressor genes through studying their functions.

In summary, through our detailed deletion mapping studies, we have found a critical and precise location of 5p deletions, 5p15.2-5p15.3, which must contain one or more unknown tumor suppressor gene(s) of colorectal cancer.

REFERENCES

1 **Zhang ZS**, Zhang YL. Progress in research of colorectal cancer in China. *Shijie Huaren Xiaohua Zazhi* 2001; **9**: 489-494

2 **Zhang YL**, Zhang ZS, Wu BP, Zhou DY. Early diagnosis for colorectal cancer in China. *World J Gastroenterol* 2002; **8**: 21-25

3 **Becker N.** Epidemiology of colorectal cancer. *Radiologe* 2003; **43**: 98-104

4 **Yu JP**, Dong WG. Current situation about early diagnosis of cancer of large intestine. *Shijie Huaren Xiaohua Zazhi* 1999; **7**: 553-554

5 **Lasko D**, Cavenee W, Nordenskjold M. Loss of constitutional heterozygosity in human cancer. *Annu Rev Genet* 1991; **25:** 281-314

6 **Cliby W**, Ritland S, Hartmann L, Dodson M, Halling KC, Keeney G, Podratz KC, Jenkins RB. Human epithelial ovarian cancer allelotype. *Cancer Res* 1993; **53**: 2393-2398

7 **Peng Z,** Ling Y, Bai S. Loss of heterozygosity on chromosome 3 in sporadic colorectal carcinoma. *Zhonghua Yixue Zazhi* 2001; **81**: 336-339

8 **Vogelstein B**, Fearon ER, Kern SE, Hamilton SR, Preisinger AC, Nakamura Y, White R. Allelotype of colorectal carcinomas. *Science* 1989; **244**: 207-211

9 **Weber TK**, Conroy J, Keitz B, Rodriguez-Bigas M, Petrelli NJ, Stoler DL, Anderson GR, Shows TB, Nowak NJ. Genome-wide allelotyping indicates increased loss of heterozygosity on 9p and 14q in early age of onset colorectal cancer. *Cytogenet Cell Genet* 1999; **86**: 142-147

10 **Ashton-Rickardt PG,** Dunlop MG, Nakamura Y, Morris RG, Purdie CA, Steel CM, Evans HJ, Bird CC, Wyllie AH. High frequency of APC loss in sporadic colorectal carcinoma due to breaks clustered in 5q21-22. *Oncogene* 1989; **4**: 1169-1174

11 **Okamoto M**, Sato C, Kohno Y, Mori T, Iwama T, Tonomura A, Miki Y, Utsunomiya J, Nakamura Y, White R. Molecular nature of chromosome 5q loss in colorectal tumors and desmoids from patients with familial adenomatous polyposis. *Hum Genet* **85**: 595-599

12 **Iacopetta B**, DiGrandi S, Dix B, Haig C, Soong R, House A. Loss of heterozygosity of tumour suppressor gene loci in human colorectal carcinoma. *Eur J Cancer* 1994; **30A**: 664-670

13 **Zhang F**, Zhou C, Ling Y, Qiu G, Bai S, Liu W, He L, Peng Z. Allelic analysis on chromosome 5 in sporadic colorectal cancer patients. *Zhonghua Zhongliu Zazhi* 2002; **24**: 458-460

14 **Vasen HF**, Mecklin JP, Khan PM, Lynch HT. The international collaborative group on hereditary non-polyposis colorectal cancer (ICG-HNPCC). *Dis Colon Rectum* 1991; **34**: 424-425

15 **Vasen HFA**, Watson P, Mecklin JP, Lynch HT. New clinical criteria for hereditary nonpolyposis colorectal cancer(HNPCC, Lynch syndrome) proposed by the International Collaborative group on HNPCC. *Gastroenterology* 1999; **116**: 1453-1456

16 http://www.ncbi.nlm.nih.gov/mapview/maps.cgi?org=hum&chr=5

17 **Kataoka M**, Okabayashi T, Johira H, Nakatani S, Nakashima A, Takeda A, Nishizaki M, Orita K, Tanaka N. Aberration of p53 and DCC in gastric and colorectal cancer. *Onco/Rep* 2000; **7**: 99-103

18 **Zhou CZ**, Peng ZH, Zhang F, Qiu GQ, He L. Loss of heterozygosity on long arm of chromosome 22 in sporadic colorectal carcinoma. *World J Gastroenterol* 2002; 8: 668-673

19 **Komarova NL,** Lengauer C, Vogelstein B, Nowak MA. Dynamics of genetic instability in sporadic and familial colorectal cancer. *Cancer Biol Ther* 2002; **1**: 685-692

20 **Dong JT.** Chromosomal deletions and tumor suppressor genes in prostate cancer. *Cancer Metastasis Rev* 2001; **20**: 173-193

21 **Baker SJ**, Fearon ER, Nigro JM, Hamilton SR, Preisinger AC, Jessup JM, Van Tuinen P, Ledbetter DH, Barker DF, Nakamura Y, White R, Vogelstein B. Chromosome 17 deletions and p53 gene mutations in colorectal carcinomas. *Science* 1989; **244**: 217-221

22 **Kinzler KW**, Nibert MC, Vogelstein B, Bryan TM, Levy DB, Smith KJ, Preisinger AC, Hamiton SR, Hedge P, Markham A, Carlson M, Joslyn G, Groden J. Identification of gene located at chromosome 5q21 that is mutated in colorectal cancers. *Science* 1991; **251**: 1366-1370

23 **Vito P**, Lacana E, D'Adamio L. Interfering with apoptosis: Ca (2+)-binding protein ALG-2 and Alzheimer's disease gene ALG-3. *Science* 1996; **271:** 521-524

24 **Krebs J,** Klemenz R. The ALG-2/AIP-complex, a modulator at the interface between cell proliferation and cell death? A hypothesis. *Biochim Biophys Acta* 2000; **1498**: 153-161

25 **Jung YS**, Kim KS, Kim KD, Lim JS, Kim JW, Kim E. Apoptosis-linked gene 2 binds to the death domain of Fas and dissociates from Fas during Fas-mediated apoptosis in Jurkat cells. *Biochem Biophys Res Commun* 2001; **288:** 420-426

26 **Krebs J,** Saremaslani P, Caduff R. ALG-2: a Ca2+ -binding modulator protein involved in cell proliferation and in cell death. *Biochim Biophys Acta* 2002; **1600**: 68-73

27 **Kitaura Y,** Satoh H, Takahashi H, Shibata H, Maki M. Both ALG-2 and peflin, penta-EF-hand (PEF) proteins, are stabilized by dimerization through their fifth EF-hand regions. *Arch Biochem Biophys* 2002; **399**: 12-18

28 **Artandi SE,** Chang S, Lee SL, Alson S, Gottlieb GJ, Chin L,

DePinho RA. Telomere dysfunction promotes non-reciprocal translocations and epithelial cancers in mice. *Nature* 2000; **406:** 641-645

29 **Poole JC,** Andrews LG, Tollefsbol TO. Activity, function, and gene regulation of the catalytic subunit of telomerase (hTERT). *Gene* 2001; **269**: 1-12

30 **Lee JW,** Choi HS, Gyuris J, Brent R, Moore DD. Two classes of proteins dependent on either the presence or absence of thyroid hormone for interaction with the thyroid hormone receptor. *Mol Endocrinol* 1995; **9**: 243-254

31 **Yasugi T,** Vidal M, Sakai H, Howley PM, Benson JD. Two classes of human papillomavirus type 16 E1 mutants suggest pleiotropic conformational constraints affecting E1 multimerization, E2 interaction, and interaction with cellular proteins. *J Virol* 1997; **71:** 5942-5951

32 **Wang Z**, Castano IB, De Las Penas A, Adams C, Christman MF. Pol kappa: A DNA polymerase required for sister chromatid cohesion. *Science* 2000; **289:** 774-779

33 **Carson DR,** Christman MF. Evidence that replication fork components catalyze establishment of cohesion between sister chromatids. *Proc Natl Acad Sci U S A* 2001; **98**: 8270-8275

34 **Wang Z,** Casatano IB, Adams C, Vu C, Fitzhugh D, Christman MF. Structure / function analysis of the *Saccharomyces* cerevisiae Trf4 / Pol Sigma DNA polymerase. *Genetics* 2002; **160**: 381-391

35 **Granger MP,** Wright WE, Shay JW. Telomerase in cancer and aging. *Crit Rev Oncol Hematol* 2002; **41**: 29-40

Edited by Ma JY and Wang XL

P.O.Box 2345, Beijing 100023,China
Fax: +86-10-85381893
E-mail: wjg@wjgnet.com www.wjgnet.com

World J Gastroenterol 2003;9(8):1719-1724
World Journal of Gastroenterology
 ISSN 1007-9327

• COLORECTAL CANCER •

Isolation of a novel member of small G protein superfamily and its expression in colon cancer

Wei Yan, Wen-Liang Wang, Feng Zhu, Sheng-Quan Chen, Qing-Long Li, Li Wang

Wei Yan, Wen-Liang Wang, Feng Zhu, Sheng-Quan Chen, Qing-Long Li, Li Wang, Department of Pathology, Xijing Hospital, Fourth Military Medical University, Xi' an 710032, Shaanxi Province, China
Supported by National Natural Science Foundation of China, No. 30270667
Correspondence to: Professor Wen-Liang Wang, Department of Pathology, Xijing Hospital, Fourth Military Medical University, Xi' an 710032, Shaanxi Province, China. wlwang@fmmu.edu.cn
Telephone: +86-29-3224893 **Fax:** +86-29-3284284
Received: 2003-03-02 **Accepted:** 2003-03-26

Abstract

AIM: APMCF1 is a novel human gene whose transcripts are up-regulated in apoptotic MCF-7 cells. In order to learn more about this gene's function in other tumors, we cloned its full length cDNA and prepared its polyclonal antibody to investigate its expression in colon cancers with immunohistochemistry.

METHODS: With the method of 5' rapid amplification of cDNA end (RACE) and EST assembled in GenBank, we extended the length of APMCF1 at 5' end. Then the sequence encoding the APMCF1 protein was amplified by RT-PCR from the total RNA of apoptotic MCF-7 cells and cloned into the prokaryotic expression vector pGEX-KG to construct recombinant expression vector pGEX-APMCF1. The GST-APMCF1 fusion protein was expressed in *E. coli* and used to immunize rabbits to get the rabbit anti-APMCF1 serum. The specificity of polyclonal anti-APMCF1 antibody was determined by Western blot. Then we investigated the expression of Apmcf1 in colon cancers and normal colonic mucosa with immunohistochemistry.

RESULTS: A cDNA fragment with a length of 1 745 bp was obtained. APMCF1 was mapped to chromosome 3q22.2 and spanned at least 14.8 kb of genomic DNA with seven exons and six introns contained. Bioinformatic analysis showed the protein encoded by APMCF1 contained a small GTP-binding protein (G proteins) domain and was homologous to mouse signal recognition particle receptor β(SRβ). A coding region covering 816 bp was cloned and polyclonal anti-APMCF1 antibody was prepared successfully. The immunohistochemistry study showed that APMCF1 had a strong expression in colon cancer.

CONCLUSION: APMCF1 may be the gene coding human signal recognition particle receptor β and belongs to the small-G protein superfamily. Its strong expression pattern in colon cancer suggests it may play a role in colon cancer development.

Yan W, Wang WL, Zhu F, Chen SQ, Li QL, Wang L. Isolation of a novel member of small G protein superfamily and its expression in colon cancer. *World J Gastroenterol* 2003; 9(8): 1719-1724
http://www.wjgnet.com/1007-9327/9/1719.asp

INTRODUCTION

Apoptosis or programmed cell death (PCD) is a form of cell death in human and other multicellular organisms[1-15]. It is a genetically controlled program of cellular selfdestruction, which is of central importance to the development and homeostasis of almost all animals, and also a highly regulated process involving a large number of genes that are conserved in all metazoans. A variety of genes have been found to take part in the process of apoptosis, such as the TNF/FasL family, the Bcl-2 family, the ICE/CED-3 family, oncogenes, tumor suppressor genes and the genes encoding heat shock proteins[16-24]. APMCF1 is a novel human gene fragment we cloned in 1999. Its transcript was found to be up-regulated in apoptotic MCF-7 cells, which might play a role in apoptosis of tumor cells[25]. As its 5' end is not complete, the functional study of this gene has not been performed. In order to learn more about this gene' s biological functions, we extended its 5' cDNA end and found it was a gene homologous to mouse SRβ. Then polyclonal antibody against this gene' s product was prepared and protein expression of APMCF1 in human colon cancer and normal colonic mucosa was examined with immunohistochemistry method.

MATERIALS AND METHODS

Main reagents

Reverse transcription kit was from TaKaRa. Pfu and Tf1 Taq DNA polymerase were from Promega. TRIzol Reagent was from Gibco. Retinoid acid (RA) was from Sigma.

Cell lines and specimens

MCF-7 cell line was kept by our lab oratory and maintained in DMEM medium supplemented with 100 mL/L fetal bovine serum. The cells were induced to apoptosis by RA with the method described before[25]. Fifty five tissue specimens of colon cancer and 5 tissue specimens of normal colonic mucosa were obtained from surgically resected tissues of patients with hepatocellular carcinoma in Xijing Hospital of Fourth Military Medical University. The tumor tissues consisted of 25 well-differentiated, 23 moderately differentiated, and 7 poorly differentiated colon cancer specimens, All the tissues were fixed in 100mL/L buffered formalin phosphate and embedded in paraffin wax.

5' RACE

A human EST named AGENCOURT_8343738 was initially identified with APMCF1 cDNA sequence(AF141882) by running a BLASTN search against the public database of ESTs (dbEST). It shared 98 % identification with APMCF1 but had more than 325 nucleotide acids at the 5' end. Then we designed a reverse transcription primer against this sequence. The total RNA extracted from the apoptotic MCF-7 cells with TRIzol reagent according to the manufacturer' s instructions was used as reverse transcription template. While transcription, 5' cap sequence was added according to the protocol of SMART™ PCR cDNA synthesis kit (Clontech). RT-PCR was

performed using the cap sequence as a sense primer, reverse transcription primer as a antisense primer. The sequences of the primers were as follows: sense primer (cap sequence), 5' TACGGCTGCGAGAAGACGACAGAA 3', and antisense primer, 5' CAGGCAATTTTAGCCAGCCATTT 3' (reverse transcription primer). A total of 30 cycles of PCR reactions were performed: at 95 ℃ for 15 s, at 68 ℃ for 5 min. Then 5 μL PCR products was extracted as a template for the next 30 cycles with the same PCR parameters. The resulting PCR fragment (810 bp) was subcloned into the pEGM-T easy vector (Promega) for sequencing.

Bioinformatics

The fragment of 810 bp was used as a bait to search the Genbank database and a homologous sequence FLJ14619 was found. Then all these ESTs were retrieved and a coontig was assembled from overlapping ESTs. A full length cDNA sequence of APMCF1 was obtained and identified in human genomic database. The putative cleavage site of the signal peptide was predicted by using Signal P server (http://www.cbs.dtu.dk/services/Signal P). The gene localization of APMCF1 on the chromosome was analyzed with the HTGS database (http://www.ncbi.nlm.nih.gov).

Construction of recombinant pGEX-APMCF1

The entire APMCF1 coding region was amplified by PCR by using upstream and downstream primers, which introduce a *Bam*HI and *Sal* I site respectively according to the conjunct sequence. The sequences of the primers were as follows: sense primer, 5' AGGATCCTCATCCATGGCTTCCG 3', and antisense primer, 5' ACGCGTCGACCTGCCTCTCAGGCAAT 3'. The PCR product was cloned into the pGEM-T easy vector for sequencing. Then the fragment containing the ORF of APMCF1 was released from the recombinant plasmid by cutting with *Bam*HI and *Sal* I, and subcloned into the prokaryotic expression vector pGEX-KG. The recombinant plasmid was termed pGEX-APMCF1.

Preparation of polyclonal antibody to APMCF1

The GST-APMCF1 fusion protein was expressed in *E. coli* DH5α and purified on glutathione-Sepharose 4B according to the manufacturer's instructions. After the purified protein was separated by 100 g/L sodium dodecylsulfate-poluacrylamide gel electrophoresis (SDS-PAGE), it was then transferred from the gel to nitrocellulose. The specific strip corresponding to the antigenic protein was excised and cut into very small pieces for immunizing rabbits. The specificity of the anti-APMCF1 antibodies was identified by Western blot.

Immunohistochemical staining

All the colon cancer specimens were fixed in 100 mL/L buffered formalin and embedded in paraffin. ABC technique was adopted for immunohistochemical staining. Briefly, deparaffinized sections were treated with 30 mL/L H_2O_2 in methanol for 30 minutes to abolish the endogenous peroxidase activity. Sections were further blocked with 10 mL/L normal goat serum for 0.5 hour, followed by incubation with polyclonal rabbit anti-APMCF1 serum (1:100) at 4 ℃ overnight. The sections were then washed in phosphate buffer solution (PBS) (0.01 mol/L, pH 7.2) and sequentially incubated with biotinylated goat anti-rabbit IgG followed by avidin-biotin horseradish peroxidase complex following the manufacturer's instructions (ABC kit, Sigma. USA). Staining was developed by immersing slides in 0.5 g/L diaminobenzidine tetrahydrochloride (DAB) with 3.3 g/L hydrogen peroxide. All slides were counterstained with haematoxylin, dehydrated and mounted. PBS substituting for the primary antibody was used as the negative control.

The intensity of staining for APMCF1 in colon cancer tissues and normal colonic mucosa tissues was scored for each specimen on a scale of 0 to 3, in which 0=negative staining, 1=weakly positive staining, 2=moderately positive staining, and 3=strongly positive staining. The percentage of positive cells in each specimen was estimated and scored on a scale of 0 to 4, in which 0=negative, 1=positive staining in 1 % to 25 % of cells counted, 2 in 26 % to 50 %, 3 in 51 % to 75 %, and 4 in 76 % to 100 %. Each section was evaluated for the sum of these two parameters. Group means of expression scores of APMCF1 antigens were compared by using ANOVA followed by Fisher's protected *t* test. $P<0.05$ was considered statistically significant.

RESULTS

Identification of human APMCF1

With 5' RACE and assembled homologous ESTs, the 5' end of original APMCF1 cDNA sequence was extended successfully. The length of new sequence was 1 745 bp. It was mapped to chromosome 3q22.2 and spanned at least 14.8 kb of genomic DNA with seven exons and six introns contained. Sequence analysis revealed that APMCF1 encoded a protein of 271 aa, with an ATG initiation codon at nt 17-19. The deduced APMCF1 protein contained no putative N-glycosylation site, and no typical signal cleavage site was revealed by searching on the signal P server. There was a transmembrane helice from 37 aa to 54 aa predicted by the method of TMpred. It contained a small GTP-binding protein (G proteins) domain and it was homologous to mouse signal recognition particle receptor β(SRβ) both in nucleic acid and amino acid sequence by 86 % and 89 % respectively. Further analysis showed that APMCF1 protein was homologous to gene products of SRβ from species ranging from mice to yeast. This indicated that APMCF1 protein was a human SRβ gene and also was a well conserved protein (Figure 1).

Identification of polyclonal antibody to APMCF1

To detect APMCF1 protein, we generated anti-human APMCF1 antibody by immunizing rabbit with the purified GST-APMCF1 fusion protein. On immunoblots, this anti-APMCF1 antibody specifically recognized GST-APMCF1 fusion protein, the dominant band was the expected 56-ku molecular size. No band was evident in the blot of the same samples using a preimmune rabbit serum. When the antibody was preabsorbed with GST-APMCF1 fusion protein, the corresponding band was no longer observed, confirming the antibody specificity (Figure 2).

Expression of APMCF1 in colon cancer

Fifty five cases of colon cancer tissues and 5 cases of normal colonic mucosa were examined for expression of APMCF1 by using immunohistochemistry. Specific cytoplasmic staining for APMCF1 was observed in 44 out of 55 cases of carcinomas (80 %) and 4 out of 5 normal mucosa. All of the positive samples had cytoplasmic staining, suggesting that APMCF1 might be a cytoplasmic protein. The positive ratios of APMCF1 in well-differentiated, moderately differentiated, and poorly differentiated carcinomas were 80 %, 74 % and 86 % respectively. A significantly high expression level of APMCF1 was found in poorly and moderately differentiated colon cancer, compared with that of normal tissue (Figures 3). There were also differences between different histological grades of colon cancer, but these differences did not reach statistical significance (Table 1).

A

```
                                                    a cca cgc gtc tca tcc
17   atg gct tcc gcg gac tcg cgc cgg gtg gca gat ggc ggc ggt gcc
      M   A   S   A   D   S   R   R   V   A   D   G   G   G   A
62   ggg ggc acc ttc cag ccc tac cta gac acc ttg cgg cag gag ctg
      G   G   T   F   Q   P   Y   L   D   T   L   R   Q   E   L
107  cag cag acg gac cca acg ctg ttg tca gta gtg gtg gcg gtt ctt
      Q   Q   T   D   P   T   L   L   S   V   V   V   A   V   L
152  gcg gtg ctg ctg acg cta gtc ttc tgg aag tta atc cgg agc aga
      A   V   L   L   T   L   V   F   W   K   L   I   R   S   R
197  agg agc agt cag aga gct gtt ctt ctt gtt ggc ctt tgt gat tcc
      R   S   S   Q   R   A   V   L   L   V   G   L   C   D   S
242  ggg aaa acg ttg ctc ttt gtc agg ttg tta aca ggc ctt tat aga
      G   K   T   L   L   F   V   R   L   L   T   G   L   Y   R
287  gac act cag acg tcc att act gac agc tgt gct gta tac aga gtc
      D   T   Q   T   S   I   T   D   S   C   A   V   Y   R   V
332  aac aat aac agg ggc aat agt ctg acc ttg att gac ctt ccc ggc
      N   N   N   R   G   N   S   L   T   L   I   D   L   P   G
377  cat gag agt ttg agg ctt cag ttc tta gag cgg ttt aag tct tca
      H   E   S   L   R   L   Q   F   L   E   R   F   K   S   S
422  gcc agg gct att gtg ttt gtt gtg gat agt gca gca ttc cag cga
      A   R   A   I   V   F   V   V   D   S   A   A   F   Q   R
467  gag gtg aaa gat gtg gct gag ttt ctg tat caa gtc ctc att gac
      E   V   K   D   V   A   E   F   L   Y   Q   V   L   I   D
512  agt atg ggt ctg aag aat aca cca tca ttc tta ata gcc tgc aat
      S   M   G   L   K   N   T   P   S   F   L   I   A   C   N
557  aag caa gat att gca atg gca aaa tca gca aag tta att caa cag
      K   Q   D   I   A   M   A   K   S   A   K   L   I   Q   Q
602  cag ctg gag aaa gaa ctc aac acc tta cga gtt acc cgt tct gct
      Q   L   E   K   E   L   N   T   L   R   V   T   R   S   A
647  gcc ccc agc aca ctg gac agt tcc agc act gcc cct gct cag ctg
      A   P   S   T   L   D   S   S   S   T   A   P   A   Q   L
692  ggg aag aaa ggc aaa gag ttt gaa ttc tca cag ttg ccc ctc aaa
      G   K   K   G   K   E   F   E   F   S   Q   L   P   L   K
737  gtg gag ttc ctg gag tgc agt gcc aag ggt gga aga ggg gac gtg
      V   E   F   L   E   C   S   A   K   G   G   R   G   D   V
782  ggc tct gct gac atc cag gac ttg gag aaa tgg ctg gct aaa att
      G   S   A   D   I   Q   D   L   E   K   W   L   A   K   I
827  gcc tga gag gca gct cta aag cac aag acc tgg atg tgt gac aca
      A   *
872  cag ttt tgg aaa aag gtc tgt ggt agt ctg gag ttg atg agg aag
917  ggg tac aag atg tgg tta gaa aca ttt ctt tgt tct gga aac aaa
962  gta ctg ttg aaa cca gct tgg aat ttt ttt ttt ttt ttt ttt taa
1007 gtt cag ttc tcc ctt atg gct gcc ttt caa aca agt acc ttt tat
1052 ctg atg cct gta tct tcc ctt tgt taa ggt gta act tga tgt agg
1097 gtc aag gtt ttt gtg aca aca ggc aga ctc cac aca gag agg ata
1142 tga tga gaa tat ggc cat cac ctg aaa agt ttt ctt atc ttc tgt
1187 gct ttt ggt ccc tgg aaa caa atc cgc cta tgt atg aag cta gtt
1232 gat ttc cag ttg cac tat ttc cag ttg cct ctg aag ttc aca ggc
1277 aat aca ttg tct agt cct ttg cga att tct ctg att tgt ggg cac
1322 agt tat gaa gtt tcc cca cat gtg aag aca ggt aca aaa tag cag
1367 agc caa gca gac agt ggg tct att ctt cat tag ctc agt gac ttg
1412 tcc aca ctc gtc tta gca ctt acg ttt caa aag ctt gtc aca aac
1457 cct tgg agt cat tcc cag ata ata gaa ctg gaa atg ata aat ccc
1502 cta atg cca agg gtc tag tgt gtt ctt agt ggt tat act ggg aag
1547 tgt gtg gag att tag gtg ctg ctc tgc tgc tct gga tgg ctg aag
1592 gct cct ggg cca tct tca tgt gct gct tga aga gct cct att ttg
1637 tac tcc tgg cta gaa tgc tgt gga aca aat aca aag tga aaa aag
1682 ttc tct gta gat ttc tga agt gca tat tca ttg atg cca aga aaa
1727 aaa aaa agt tgc ctt ttt g
```

B

```
APMCF1       (1) MASADSRRVADGGGAGGTFQPYLDTLRQELQQTDPTLLSVVVAVLAVLLT
Mouse        (1) MASANTRRVGDG--AGGAFQPYLDSLRQELQQRDPTLLSVAVALLAVLLT
C. elegan    (1) -------------------------MDKIDFNDPTTLAVLATAVIGLLT
Drosophila   (1) -----MDKLNEN-----ARQ------RKQIKLGEIDTGPIIVALLLGFIA
Saccharomyces(1) -------------------------MLSNTLIIACLLVIGTTIALIAVQ

APMCF1      (51) LVFWKLIRSRRSSQRAVLLVGLCDSGKTLLFVRLLT--GLYRDTQTSITD
Mouse       (49) LVFWKFIWSRKSSQRAVLFVGLCDSGKTLLFVRLLT--GQYRDTQTSITD
C. elegan   (25) VLLLVLKSFASSNKNRVLFVGLMDCGKTTIFTQLSQKEAEYPTTTKTYTS
Drosophila  (35) VAIFVILRRRSAGRKDFLLTGLSESGKSAIFMQLIH--GKFPATFTSIKE
Saccharomyces(25) KASSKTGIKQKSYQPSIIIAGPQNSGKTSLLTLLTT--DSVRPTVVSQEP

APMCF1      (99) SCAVYRVNNNRGNSLTLIDLPGHESLRLQFLERFKSS---AGAIVFVVDS
Mouse       (97) SSAIYKVNNNRGNSLTLIDLPGHESLRFQLLDRFKSS---ARAVVFVVDS
C. elegan   (75) MVENKITLRIKDKEKEIIDYPGNDRLRQKLIENHLHSR-SLLRIVFVVDS
Drosophila  (83) NVGDYRTG-S--ASARLVDIPGHYRVRDKCLELYKHR---AKGIVFVVDS
Saccharomyces(73) LSAADYDG----SGVTLVDFPGHVKLRYKLSDYLKTRAKFVKGLIFMVDS

APMCF1     (146) AAFQREVKDVAEFLYQVLIDSMG-LKNTPSFLIACNKQDIAMAKSAKLIQ
Mouse      (144) AAFQREVKDVAEFLYQVLIDSMA-LKNSPSLLIACNKQDIAMAKSAKLIQ
C. elegan  (124) AAFSKNARDVAELFYTVALEN----VDKVPILIACHKQDLSLAKTEKVIR
Drosophila (127) VTAHKDIRDVADFLYTILSDS---ATQPCSVLVLCNKQDQTTAKSAQVIK
Saccharomyces(119) TVDPKKLTTTAEFLVDILSITESSCENGIDILIACNKSELFTARPPSKIK

APMCF1     (195) QQLEKELNTLRVTRS-----AAPSTLYSSSTAPAQLGKKGKE-FEFSQLP
Mouse      (193) QQLEKELNTLRVTRS-----AAPSTLDSSSTAPAQLGKKGKE-FEFSQLP
C. elegan  (170) NSLEKEIGLINKSRA-----AALIGTDGSEEKRSTLTDTGID-FKWEDLK
Drosophila (174) SLLESELHTVRDTRSR----KLQSVGDEDGSKSITLGKPGRD-FEFSHIA
Saccharomyces(169) DALESEIQKVIERRKKSLNEVERKINEEDYAENTLDVLQSTDGFKFANLE

APMCF1     (239) -LKVEFLECSAKGGRGDVGSADIQDLEKWLAKIA
Mouse      (237) -LKVEFLECSAKGGRGDTGSADIQDLEKWLAKIA
C. elegan  (214) KQEVSFVSTSSNSE--DFG---VHEIASFVRA--
Drosophila (219) -QNIQFAEASAK----DT---ELDPLTDWLARLL
Saccharomyces(219) ASVVAFEGSINK----RK----ISQWREWIDEKL
```

Figure 1 Nucleotide and Predicted Amino Acid Sequence of the APMCF1 cDNA and sequence alignment of APMCF1 wth the protein from other species. A: The full-length gene sequence and amino acids sequence of APMCF1; B: Alignment was done by using the Align software in Vector NTI. Dark gray background shows identity with at lease five aligned residues in different species. The gray region represents the sequence conserved among different species.

Table 1 Expression of APMCF1 in colon cancer and normal colon

Histological type	*n*	Expression of APMCF1	Positive rate (%)
A) Well differentiated	25	4.20±1.02	80
B) Moderately differentiated	23	4.78±1.10	74
C) Poorly differentiated	7	5.18±1.89	86
D) Normal	5	3.84±1.73	80

Expression score (mean ± SE) in different histological grades of colon cancer and normal colon tissue. Statistically significant differences: B *versus* D, $P<0.05$; C *versus* D, $P<0.01$.

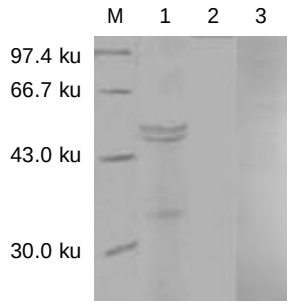

Figure 2 Immunoblotting of APMCF1 in GST-APMCF1 (56 ku) using antiserum, normal rabbit serum before immunization and antiserum preabsorbed with GST-APMCF1. M: Protein marker; 1: antiserum; 2: rabbit serum before immune from GST-APMCF1; 3: antiserum absorbed in the peptides used for immunization (control antibody).

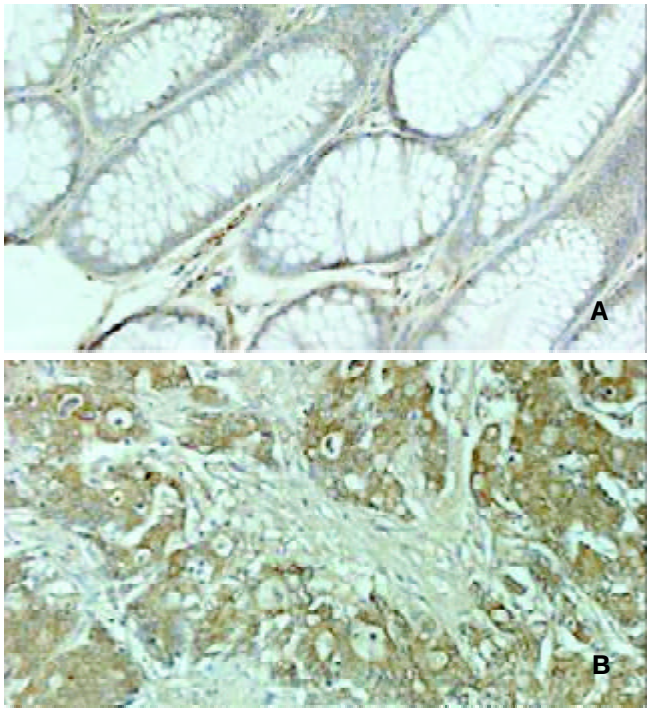

Figure 3 Expression of AMPCF1 in normal colon tissue and colon cancer (×200). A. Normal colon tissue; B. Colon cancer.

DISCUSSION

We have successfully extended the 5' end of APMCF1. The new sequence contains an open-reading frame of 816 bp that encodes a protein with a predicted molecular mass of 30ku. By searching the GenBank, it was found that the amino acid sequence of APMCF1 was homologous to mouse signal recognition particle receptor β(SRβ) and conserved in several other species, including *Caenorhabditis elegans*, *Saccharomyces cerevisia* and *Drosophila melanogaster*. This indicates that APMCF1 is likely a human SRβ gene and also a well conserved protein. The conservation of APMCF1 implies that it may have a very important function, since it remains stable during the evolution of species[26,27].

The mammalian SRP receptor, also known as docking protein, is composed of two subunits, SRα and SRβ. Based on the study results in mouse and canine, both of them are required to target nascent secretory and membrane proteins to the membrane of endoplasmic reticulum (ER). SRβ anchors alpha subunit to the ER membrane during this course[26,28-30]. The result of conserved domain searching showed that APMCF1 containd a GTPase domain closely related to ADP-ribosylation factor family (ARF) and Sar1p-like members of the Ras-family of small GTPases, suggesting it belongs to the small GTP-binding protein (G proteins) superfamily[31-36].

Over 100 members of the Ras superfamily of GTPases have been found so far. Based on both their sequence homology and function, they have been subdivided into at least six families: Ras, Rho, Rab, Arf, Ran, and Rad/Gem[37-42]. Each family, in turn, is comprised of several members with distinct expression, cellular localization and biological activities. Among these members, both Ras and Rho GTPases can mediate key cellular processes in response to diverse stimuli, such as cell growth, apoptosis, lipid metabolism, cytoarchitecture, membrane trafficking, and transcriptional regulation. The Rab and Sar1/Arf families regulate vesicle trafficking, and the Ran family regulates nucleocytoplasmic transport and microtubule organization. However, the negative aspect of these multifunctional proteins arises in the context of scenarios that cause their constitutive activation (i.e. point mutations or overexpression) and render them insensitive to regulatory signals. In this case, these GTPases trigger specific signals that lead to uncontrolled cell growth, enhanced angiogenesis, inhibition of apoptosis, and genetic instability, all of which result in tumor development[43-48].

From the analysis of bioinfomatics we can see that APMCF1 might be a new member of small-G protein superfamily. It may have the potential function to regulate the survival, proliferation, differentiation and apoptosis of cells as well as other small-G protein members such as Ras and Rho. Preliminary studies also showed that transcripts of APMCF1 were up-regulated in apoptotic MCF-7 cells, indicating it might play a role in apoptosis of tumor cells. So it is necessary to know expression pattern of APMCF1 in various tissues, especially in tumors. In the present study, APMCF1 was expressed highly in poorly and moderately differentiated colon cancers compared with that in normal colon mucosa, perhaps indicating its possible biological function in tumor development. It is early to say there are some relationship between the expression of APMCF1 and tumorigenesis before further study has been done. But it will be very interesting and worthy to further study these aspects in the future.

REFERENCES

1 **Lan J**, Xiong YY, Lin YX, Wang BC, Gong LL, Xu HS, Guo GS. *Helicobacter pylori* infection generated gastric cancer through p53-Rb tumor-suppressor system mutation and telomerase reactivation. *World J Gastroenterol* 2003; **9**: 54-58

2 **Guo XZ**, Shao XD, Liu MP, Xu JH, Ren LN, Zhao JJ, Li HY, Wang D. Effect of bax, bcl-2 and bcl-xL on regulating apoptosis in tissues of normal liver and hepatocellular carcinoma. *World J Gastroenterol* 2002; **8**: 1059-1062

3 **Hengartner MO**. The biochemistry of apoptosis. *Nature* 2000; **407**: 770-776

4 **Li HL**, Chen DD, Li XH, Zhang HW, Lu YQ, Ye CL, Ren XD.

Changes of NF-kB, p53, Bcl-2 and caspase in apoptosis induced by JTE-522 in human gastric adenocarcinoma cell line AGS cells: role of reactive oxygen species. *World J Gastroenterol* 2002; **8**: 431-435

5 **Qin LX**, Tang ZY. The prognostic molecular markers in hepatocellular carcinoma. *World J Gastroenterol* 2002; **8**: 385-392

6 **Javelaud D**, Besancon F. Inactivation of p21WAF1 sensitizes cells to apoptosis via an increase of both p14ARF and p53 levels and an alteration of the Bax/Bcl-2 ratio. *J Biol Chem* 2002; **277**: 37949-37954

7 **Huang ZH**, Fan YF, Xia H, Feng HM, Tang FX. Effects of TNP-470 on proliferation and apoptosis in human colon cancer xenografts in nude mice. *World J Gastroenterol* 2003; **9**: 281-283

8 **Chen G**, Goeddel DV. TNF-R1 signaling: a beautiful pathway. *Science* 2002; **296**: 1634-1635

9 **Shi M**, Wang FS, Wu ZZ. Synergetic anticancer effect of combined quercetin and recombinant adenoviral vector expressing human wild-type p53, GM-CSF and B7-1 genes on hepatocellular carcinoma cells *in vitro*. *World J Gastroenterol* 2003; **9**: 73-78

10 **Hatoum A**, El-Sabban ME, Khoury J, Yuspa SH, Darwiche N. Overexpression of retinoic acid receptors alpha and gamma into neoplastic epidermal cells causes retinoic acid-induced growth arrest and apoptosis. *Carcinogenesis* 2001; **22**: 1955-1963

11 **Daigle JL**, Hong JH, Chiang CS, McBride WH. The role of tumor necrosis factor signaling pathways in the response of murine brain to irradiation. *Cancer Res* 2001; **61**: 8859-8865

12 **Yu JL**, Rak JW, Coomber BL, Hicklin DJ, Kerbel RS. Effect of p53 status on tumor response to antiangiogenic therapy. *Science* 2002; **295**: 1526-1528

13 **Holtzman MJ**, Green JM, Jayaraman S, Arch RH. Regulation of T cell apoptosis. *Apoptosis* 2000; **5**: 459-471

14 **Afford S**, Randhawa S. Apoptosis. *Mol Pathol* 2000; **53**: 55-63

15 **Liu JW**, Tang Y, Shen Y, Zhong XY. Synergistic effect of cell differential agent-II and arsenic trioxide on induction of cell cycle arrest and apoptosis in hepatoma cells. *World J Gastroenterol* 2003; **9:** 65-68

16 **Urquhart JL**, Meech SJ, Marr DG, Shellman YG, Duke RC, Norris DA. Regulation of Fas-mediated apoptosis by N-ras in melanoma. *J Invest Dermatol* 2002; **119**: 556-561

17 **Nikitin AY**, Liu CY, Flesken-Nikitin A, Chen CF, Chen PL, Lee WH. Cell lineage-specific effects associated with multiple deficiencies of tumor susceptibility genes in Msh2(-/-)Rb(+/-) mice. *Cancer Res* 2002; **62**: 5134-5138

18 **Suzuki Y**, Honma T, Hayashi S, Ajioka Y, Asakura H. Bcl-2 expression and frequency of apoptosis correlate with morphogenesis of colorectal neoplasia. *J Clin Pathol* 2002; **55**: 212-216

19 **Schmitz I**, Kirchhoff S, Krammer PH. Regulation of death receptor-mediated apoptosis pathways. *Int J Biochem Cell Biol* 2000; **32**: 1123-1136

20 **Chen Y**, Wu Q, Song SY, Su WJ. Activation of JNK by TPA promotes apoptosis via PKC pathway in gastric cancer cells. *World J Gastroenterol* 2002; **8**: 1014-1018

21 **Cohen O**, Kimchi A. DAP-kinase: from functional gene cloning to establishment of its role in apoptosis and cancer. *Cell Death Differ* 2001; **8**: 6-15

22 **Baliga BC**, Kumar S. Role of Bcl-2 family of proteins in malignancy. *Hematol Oncol* 2002; **20**: 63-74

23 **Broceno C**, Wilkie S, Mittnacht S. RB activation defect in tumor cell lines. *Proc Natl Acad Sci U S A* 2002; **99**: 14200-14205

24 **Neurath MF**, Finotto S, Fuss I, Boirivant M, Galle PR, Strober W. Regulation of T-cell apoptosis in inflammatory bowel disease: to die or not to die, that is the mucosal question. *Trends Immunol* 2001; **22**: 21-26

25 **Yan W**, Li Q, Zhu F. Apoptosis-related genes cloned by improved subtractive hybridization. *Zhonghua Zhongliu Zazhi* 2001; **23**: 193-195

26 **Miller JD**, Tajima S, Lauffer L, Walter P. The beta subunit of the signal recognition particle receptor is a transmembrane GTPase that anchors the alpha subunit, a peripheral membrane GTPase, to the endoplasmic reticulum membrane. *J Cell Biol* 1995; **128**: 273-282

27 **Boettner B**, Van Aelst L. The role of Rho GTPases in disease development. *Gene* 2002; **286**: 155-174

28 **Hortsch M**, Labeit S, Meyer DI. Complete cDNA sequence coding for human docking protein. *Nucleic Acids Res* 1988; **16**: 361-362

29 **Exton JH**. Regulation of phospholipase D. *FEBS Lett* 2002; **531**: 58-61

30 **Ehrhardt A**, Ehrhardt GR, Guo X, Schrader JW. Ras and relatives-job sharing and networking keep an old family together. *Exp Hematol* 2002; **30**: 1089-1106

31 **Vaidehi N**, Floriano WB, Trabanino R, Hall SE, Freddolino P, Choi EJ, Zamanakos G, Goddard WA 3rd. Prediction of structure and function of G protein-coupled receptors. *Proc Natl Acad Sci U S A* 2002; **99**: 12622-12627

32 **Bacher G**, Pool M, Dobberstein B. The ribosome regulates the GTPase of the beta-subunit of the signal recognition particle receptor. *J Cell Biol* 1999; **146**: 723-730

33 **Larsen N,** Samuelsson T, Zwieb C. The Signal Recognition Particle Database (SRPDB). *Nucleic Acids Res* 1998; **26**: 177-178

34 **Bacher G**, Lutcke H, Jungnickel B, Rapoport TA, Dobberstein B. Regulation by the ribosome of the GTPase of the signal-recognition particle during protein targeting. *Nature* 1996; **381**: 248–251

35 **Alto NM**, Soderling J, Scott JD. Rab32 is an A-kinase anchoring protein and participates in mitochondrial dynamics. *J Cell Biol* 2002; **158**: 659-668

36 **Raugei G**, Ramponi G, Chiarugi P. Low molecular weight protein tyrosine phosphatases: small, but smart. *Cell Mol Life Sci* 2002; **59**: 941-949

37 **Shimada J**, Shakhnovich EI. The ensemble folding kinetics of protein G from an all-atom Monte Carlo simulation. *Proc Natl Acad Sci U S A* 2002; **99**: 11175-11180

38 **Lambert JM**, Lambert QT, Reuther GW, Malliri A, Siderovski DP, Sondek J, Collard JG, Der CJ. Tiam1 mediates Ras activation of Rac by a PI (3) K-independent mechanism. *Nat Cell Biol* 2002; **4**: 621-625

39 **Malumbres M**, Pellicer A. RAS pathways to cell cycle control and cell transformation. *Front Biosci* 1998; **3**: d887-912

40 **Bar-Sagi D**, Hall A. Ras and Rho GTPases: a family reunion. *Cell* 2000; **103**: 227-238

41 **Henriksson ML**, Sundin C, Jansson AL, Forsberg A, Palmer RH, Hallberg B. Exoenzyme S shows selective ADP-ribosylation and GTPase-activating protein (GAP) activities towards small GTPases *in vivo*. *Biochem J* 2002; **367**(Pt 3): 617-628

42 **Thompson PW**, Randi AM, Ridley AJ. Intercellular adhesion molecule (ICAM)-1, but not ICAM-2, activates RhoA and stimulates c-fos and rhoA transcription in endothelial cells. *J Immunol* 2002; **169**: 1007-1013

43 **Aresta S**, De Tand-Heim MF, Beranger F, De Gunzburg J. A novel Rho GTPase-activating-protein interacts with Gem, a member of the Ras superfamily of GTPases. *Biochem J* 2002; **367**(Pt 1): 57-65

44 **Neves SR**, Ram PT, Iyengar R. G protein pathways. *Science* 2002; **296**: 1636-1639

45 **Aznar S**, Lacal JC. Rho signals to cell growth and apoptosis. *Cancer Lett* 2001; **165**: 1-10

46 **Price LS**, Collard JG. Regulation of the cytoskeleton by Rho-family GTPases:implications for tumour cell invasion. *Semin Cancer Biol* 2001; **11**: 167-173

47 **Hall A**. Rho GTPases and the actin cytoskeleton. *Science* 1998; **279**: 509-514

48 **Takai Y**, Sasaki T, Matozaki T. Small GTP-binding proteins. *Physiol Rev* 2001; **81**: 153-208

Edited by Zhu LH

P.O.Box 2345, Beijing 100023,China
Fax: +86-10-85381893
E-mail: wjg@wjgnet.com www.wjgnet.com

World J Gastroenterol 2003;9(8):1725-1728
World Journal of Gastroenterology
 ISSN 1007-9327

• COLORECTAL CANCER •

Effect of retinoic acid on cell proliferation kinetics and retinoic acid receptor expression of colorectal mucosa

Hong-Bo Wei, Xiao-Yan Han, Wei Fan, Gui-Hua Chen, Ji-Fu Wang

Hong-Bo Wei, Xiao-Yan Han, Department of Gastrointestinal Surgery, The Third Affiliated Hospital, Sun Yat-Sen University, Guangzhou 510630, China
Wei Fan, Department of Nuclear Medicine, Cancer Center, Sun Yat-Sen University, Guangzhou 510060, China
Gui-Hua Chen, Ji-Fu Wang, Department of Gastrointestinal Surgery, The First Affiliated Hospital, Sun Yat-Sen University, Guangzhou 510080, China
Supported by Natural Science Foundation of Guangdong Province, No.010742
Correspondence to: Dr. Hong-Bo Wei, Department of Gastrointestinal Surgery, The Third Affiliated Hospital, Sun Yat-Sen University, Guangzhou 510630, China. drwhb@21cn.com
Telephone: +86-20-85516867 Ext 2228
Received: 2002-08-24 **Accepted:** 2003-02-11

Abstract

AIM: To investigate the effect of retinoic acid (RA) on cell proliferation kinetics and retinoic acid receptor (RAR) expression of colorectal mucosa.

METHODS: One hundred sixty healthy male Wistar rats were randomly divided into 4 groups. Rats in groups I and II were subcutaneously injected with dimethylhydrazine (DMH) (20 mg/kg, once a week,) for 7 to 13 weeks, while groups III and IV were injected with normal saline. Rats in groups II and III were also treated with RA (50 mg/kg, every day, orally) from 7th to 15th week, thus group IV was used as a control. The rats were killed in different batches. The expressions of proliferating cell nuclear antigen (PCNA), nucleolar organizer region-associated protein (AgNOR) and RAR were detected.

RESULTS: The incidence of colorectal carcinoma was different between groups I (100 %) and II (15 %) (P<0.01). The PCNA indices and mean AgNOR count in group II were significantly lower than those in group I (F=5.418 and 4.243, P<0.01). The PCNA indices and mean AgNOR count in groups I and II were significantly higher than those in the groups III and IV (in which carcinogen was not used) (F=5.927 and 4.348, P<0.01). There was a tendency in group I that the longer the induction with DMH the higher PCNA index and AgNOR count expressed (F=7.634 and 6.826, P<0.05). However, there was no such tendency in groups II, III and IV (F=1.662 and 1.984, P>0.05). The levels of RAR in normal and cancerous tissues in groups treated with RA were significantly higher than those in groups not treated with RA (F=6.343 and 6.024, P<0.05).

CONCLUSION: RA decreases the incidence of colorectal carcinoma induced by DMH. Colorectal cancer tissue is associated with abnormal expression of PCNA, AgNOR and RAR. RA inhibits the expression of PCNA and AgNOR, and increases RAR concentration in colorectal tissues.

Wei HB, Han XY, Fan W, Chen GH, Wang JF. Effect of retinoic acid on cell proliferation kinetics and retinoic acid receptor expression of colorectal mucosa. *World J Gastroenterol* 2003; 9(8): 1725-1728
http://www.wjgnet.com/1007-9327/9/1725.asp

INTRODUCTION

The occurrence and development of colorectal carcinoma usually need a long and multistep process. Intervention treatment to block the canceration course from precancerous lesion of colorectal carcinoma is an important step to decrease the incidence of colorectal carcinoma. Some results obtained from *in vitro* experiments have shown that retinoic acid (RA) plays a role in blocking canceration induced by carcinogen and promotes normal differentiation of leucocythemia cells[1-3]. However, the effect of RA on colorectal carcinoma, especially on cell proliferation kinetics and the expression of retinoic acid receptor (RAR) of colorectal mucosa, has not be reported. To provide theoretic data on prevention and treatment of colorectal carcinoma, we investigated the effect of RA on cell proliferation kinetics and expression of RAR of colorectal mucosa.

MATERIALS AND METHODS

Animals and groups

One hundred sixty healthy male Wistar rats (body weight 134±12 g) were randomly divided into 4 groups. There were 40 rats in each group. Rats in group I and II were subcutaneously injected with dimethylhydrazine (DMH) (20 mg/kg, once a week,) for 7 to 13 weeks, while groups III and IV were injected with normal saline. Rats in groups II and III were treated with RA (50 mg/kg, every day, orally) from 7th to 15th week, group IV was used as a control. Eight rats in each group were killed randomly at 7th, 14th and 21st week in each group. The other rats were killed at 28th week. The number of colorectal carcinoma lesions was examined, and the normal colorectal tissues were also collected. The colorectal samples were fixed with 10 % formalin and embedded in paraffin. The expression of proliferating cell nuclear antigen (PCNA) and nucleolar organizer region-associated protein (AgNOR) was studied.

Detection of PCNA and AgNOR

Normal colorectal tissues (n=8) and the colorectal tissues (n=8) free of cancer induced by DMH after 7, 14, 21 and 28 weeks, were included. The samples including well-differentiated adenocarcinoma (n=8) and poorly differentiated adenocarcinoma (n=8) were also collected.

The immunohistochemical staining method was used to detect PCNA indices[4-7]. Representative regions with a double blind method were selected, and at least 1 000 cells were counted. The rates of positive cells over total cells counted were defined as the PCNA indices. Ploton one-step method was used for the detection of AgNOR count[8-11].

Detection of retinoic acid receptor (RAR)

Specimen disposal The mesentery tissues were removed and

part of the colorectal tissues was cut to pieces and placed in DMEM buffer. A tissue was homogenated by a high speed disperser, 4 000 r.min^{-1} for 10 min and a homogenizer 4 000 r.min^{-1} for 30 min and then by centrifugation 1 000 r. min^{-1} for 30 min. The buffer was added to the deposit, and the suspension was centrifugated, 750 r. min^{-1}for 15 min. Finally, the deposit was made to nucleus fluid. DNA concentration was determined by the dimethylamine method. The rest part of tissues was treated with liguid nitrogen and preserved in an ultra cold storage freezer.

Receptor radio-ligand binding test[16-20] All the procedures of the test were carried out at 4 ℃. 0.1 ml of nucleus fluid and 0.05 ml of 3H-atRA (2×10^{-6} mol/L) and 0.05 ml of buffer were mixed at different concentrations (the end concentration was 0.1-10 nM, with 6 concentration points). At the same time, the control test tube of non-specific binding was 200-time of unlabelled 9-cis-atRA. After 20 h, the reaction mixture was filtered with a multi-head collecting device and the free RA was removed, and examined by the filter membrane method. Saturation binding curve, Scatchard diagram and receptor maximum dissociation constant KD were analyzed by a receptor radio-ligand binding analyzing software.

Statistical analysis

Experimental results were analyzed by variance analysis and chi-square test with SPSS software. Statistical significance was determined at $P<0.05$.

RESULTS

Incidence of colorectal carcinoma

At the 14th week after induction, 12.5 % of rats in group I developed colorectal carcinoma, but colorectal carcinoma was not found in group II. At the 21st and 28th weeks, the incidence of colorectal carcinoma reached 60 % and 100 % respectively in group I, compared with 12 % and 20 % respectively in group II. There were significant differences between the two groups ($P<0.05$ and $P<0.01$). All the carcinomas were adenocarcinomas. In group I, 12 cases of adenocarcinoma were well-differentiated and 9 cases were poorly-differentiated. All the 4 cases in group II were well-differentiated (Table 1).

Table 1 Incidence (%) of colorectal carcinoma in the groups

Weeks	*n*	Number of cancer			
		I	II	III	IV
7	8	0	0	0	0
14	8	1(12.5)	0	0	0
21	8	5(60.5)	1(12.5)	0	0
28	15	15(100.0)	3(20.0)	0	0

Expression of PCNA indices

At the 7th week, PCNA indices reached 96.75±6.88 and 95.50±14.01, respectively, in group I and group II, which were significantly higher than those in group III and group IV (34.38±6.30 and 33.63±4.75, respectively, $P<0.01$). In metaphase and late-phase, PCNA indices in group I and group II were continuously increased, especially in group I. PCNA indices in group I reached 168.13±14.34 at the 28th week and approached the level of well-differentiated adenocarcinoma (169.13±11.68), but were still significantly lower than that of poorly-differentiated adenocarcinoma (181.63±23.38, $P<0.05$). Analysis of variance showed that there was a tendency in group I that the longer the induction with DMH the higher the PCNA index ($F=7.634$, $P<0.05$). However, there was no such tendency in groups II, III and IV ($F=1.662$, $P>0.05$).

In comparison between the groups, the results showed that PCNA indices in group I and group II were significantly higher than those in groups III and IV at all stages of carcinoma induction ($F=5.927$, $P<0.01$). Moreover, PCNA index in group I was significantly higher than that in groups II at all stages ($F=5.418$, $P<0.01$), except at the 7th week (Table 2).

Table 2 Expression of PCNA indices in groups

Weeks	*n*	I	II	III	IV
7	8	96.75±6.88	95.50±14.01	34.38±6.30	33.63±4.75
14	8	110.88±15.51	97.88±8.90	35.13±3.91	35.88±2.17
21	8	149.50±15.15	98.25±25.09	36.00±3.46	34.13±4.39
28	8	168.13±14.34	98.88±25.30	35.88±4.29	33.13±4.32
Well-differentiated adenocarcinoma	8	169.13±11.68	-	-	-
Poorly differentiated adenocarcinoma	8	181.63±23.38	-	-	-

Expression of AgNOR count

At the 7th week, AgNOR count reached 3.78±0.88 and 3.71±9.95, respectively, in group I and group II, which was significantly higher than that in group III and group IV ($P<0.05$). As the time of induction with DMH prolonged, the AgNOR count in group I was continuously increased. Analysis of variance showed that there was a tendency in group I that the longer the induction with DMH the higher the AgNOR count ($F=6.826$, $P<0.05$). However, there was no such tendency in groups II, III and IV ($F=1.984$, $P>0.05$). At the 28th week, the AgNOR count already approached the level of well-differentiated adenocarcinoma, but was still significantly lower than that of poorly-differentiated adenocarcinoma ($P<0.05$).

In comparison between the groups, the results showed that the AgNOR counts in group I and group II were significantly higher than those in groups III and IV at all stages of carcinoma induction ($F=4.348$, $P<0.05$). The AgNOR count was significantly higher in group I than that in group II at all stages ($F=4.243$, $P<0.05$), except at the 7th week (Table 3).

Table 3 Expression of AgNOR count in groups

w	*n*	AgNOR count ($\bar{x}\pm s$)			
		I	II	III	IV
7	8	3.78±0.88	3.71±0.95	2.17±0.53	2.45±1.06
14	8	5.15±1.87	4.30±0.84	2.20±0.86	2.16±0.80
21	8	7.54±0.73	4.39±0.62	2.20±0.77	2.49±0.90
28	8	9.37±0.71	4.75±0.98	2.35±1.01	2.38±1.04
Well-differentiated adenocarcinoma	8	9.93±1.47	-	-	-
Poorly-differentiated adenocarcinoma	8	11.14±1.86	-	-	-

Table 4 RAR count (fmol/μg DNA) and KD (nmol) in cells. ($\bar{x}\pm s$)

Group	*n*	Bmax	KD
I	6	1.16±0.34	1.99±0.25
II	6	1.78±0.36	2.16±0.18
III	6	2.61±0.55	2.39±0.43
IV	6	2.64±0.22	2.45±0.23
Cancer tissue	6	1.02±0.21	1.74±0.16

Expression of RAR

Six samples of colorectal and cancer tissues were collected randomly from groups I, II, III and IV respectively. Expressions

of RAR were detected, Bmax and KD were calculated. The Bmax and KD in group I approached the level of cancer tissues (1.02±0.21 and 1.74±0.16, $P>0.05$). The Bmax and KD in group II were significantly higher than those in group I, but significantly lower than those in groups III and IV, ($F=6.343$ and 6.024, $P<0.05$).

DISCUSSION

Recently, the mechanism of preventing carcinoma by RA has been studied by scholars all over the world. Some researchers reported that leukaemia cells could respond to the effect of differentiation induced by RA to put up the potential of diphasic differentiation[21-23]. Some reported that RA could result in reversion of liver cancer cells[24,25]. In our research, we found that the incidence of carcinoma developed in RA treatment group (group II) was significantly lower than that in group I during inducetion. The results showed that retinoic acid (RA) had an effect on blocking canceration induced by carcinogen and decreased the incidence of colorectal cancer.

PCNA is the 36 KD polypeptide which is synthesized and expressed just in proliferating cells. It has been proved that PCNA expression is related to cell generation cycle[11,12]. Expression of PCNA increases in G_1 phase gradually, reaches pinnacle in S phase, and decreases in G_2/M phase. It plays an important role in understanding cell generation state to detect PCNA indices. The higher the PCNA expression, the higher the cell malignancy trend[12-15]. Our experimental results showed that there was a tendency in group I that the longer the interval induced by DMH, the higher the PCNA index would be ($P<0.05$). At the 28th week, the PCNA indices already approached the level of well-differentiated adenocarcinoma, but were still significantly lower than that of poorly-differentiated adenocarcinoma ($P<0.05$). The PCNA indices in group II were higher than those in groups III and IV, but still lower than those in group I. RA may have an effect on blocking canceration induced by carcinogen and decreasing the incidence of colorectal carcinoma. The mechanism is not clear, maybe it is related to blocking the transition of cancer cells from G_0/G_1 phase to S_1,G_2+M phase. Our results also showed that RA could not block canceration entirely.

AgNOR is the biochemical symbol of rDNA and transcription. AgNOR count can reflect the cell active state and cell malignant trend of carcinoma[8-10]. We found that AgNOR count of colorectal mucosa cells in group II was significantly lower than that in group I, but significantly higher than that in groups III and IV during the period of inducement. The reasonable explanation was that RA could inhibit the process of canceration induced by carcinogen but could not block canceration entirely.

Our results showed that there were plenty of RARs in colorectal tissues. The normal RAR contents in colorectal cells were 2.64 f mol/μg DNA, and KD was 2.45 nmol. However, RAR contents in colorectal cancer cells decreased significantly (1.02 f mol/μg DNA, and 1.74 nmol). It is possible that the development of colorectal carcinoma is related to abnormal expression of RAR, and especially decrease of RAR content. After interference treatment with RA, the expression of RAR increased. The carcinogenic course induced by DMH was slowed down distinctly. The results revealed that RA had an effect on inhibiting cellular proliferation and RA could regulate the expression of RAR[24-30].

There are plenty of similarities between human colorectal cancer and experimental colorectal cancer. However, it is possible that colorectal cancer occurs in total colorectal mucosa under the action of carcinogenic factor. It is possible that clinical application of RA can inhibit the precancerous lesion of colorectal carcinoma, block the canceration course, and decrease the incidence of colorectal cancer[31-35]. It is expected that clinical application of RA after colorectal operation would prevent and decrease the recurrence of carcinoma.

REFERENCES

1 **Adachi Y**, Itoh F, Yamamoto H, Iku S, Matsuno K, Arimura Y, Imai K. Retinoic acids reduce matrilysin (matrix metalloproteinase 7) and inhibit tumor cell invasion in human colon cancer. *Tumour Biol* 2001; **22**: 247-253

2 **Szeto W**, Jiang W, Tice DA, Rubinfeld B, Hollingshead PG, Fong SE, Dugger DL, Pham T, Yansura DG, Wong TA, Grimaldi JC, Corpuz RT, Singh JS, Frantz GD, Devaux B, Crowley CW, Schwall RH, Eberhard DA, Rastelli L, Polakis P, Pennica D. Overexpression of the retinoic acid-responsive gene Stra6 in human cancers and its synergistic induction by Wnt-1 and retinoic acid. *Cancer Res* 2001; **61**: 4197-4205

3 **Paulsen JE**, Lutzow-Holm C. *In vivo* growth inhibition of human colon carcinoma cells (HT-29) by all-trans-retinoic acid, difluoromethylornithine, and colon mitosis inhibitor, individually and in combination. *Anticancer Res* 2000; **20**: 3485-3489

4 **Wu W**, Zhang X, Yan X, Wang J, Zhang J, Li Y. Expressions of beta-catenin, p53 and proliferating cell nuclear antigen in the carcinogenesis of colorectal adenoma. *Zhonghua Zhongliu Zazhi* 2002; **24**: 264-267

5 **Boonsong A**, Curran S, McKay JA, Cassidy J, Murray GI, McLeod HL.Topoisomerase I protein expression in primary colorectal cancer and lymph node metastases. *Hum Pathol* 2002; 33: 1114-1119

6 **Izawa H**, Yamamoto H, Ikeda M, Ikeda K, Fukunaga H, Yasui M, Ikenaga M, Sekimoto M, Monden T, Matsuura N, Monden M. Analysis of cyclin D1 and CDK expression in colonic polyps containing neoplastic foci: a study of proteins extracted from paraffin sections. *Oncol Rep* 2002; **9**: 1313-1318

7 **Kohno H**, Tanaka T, Kawabata K, Hirose Y, Sugie S, Tsuda H, Mori H. Silymarin, a naturally occurring polyphenolic antioxidant flavonoid, inhibits azoxymethane-induced colon carcinogenesis in male F344 rats. *Int J Cancer* 2002; **101**: 461-468

8 **Barnett KT**, Fokum FD, Malafa MP. Vitamin E succinate inhibits colon cancer liver metastases. *J Surg Res* 2002; **106**: 292-298

9 **Lavezzi AM**, Ottaviani G, De Ruberto F, Fichera G, Matturri L. Prognostic significance of different biomarkers (DNA content, PCNA, karyotype) in colorectal adenomas. *Anticancer Res* 2002; **22**: 2077-2081

10 **McKay JA**, Douglas JJ, Ross VG, Curran S, Loane JF, Ahmed FY, Cassidy J, McLeod HL, Murray GI. Analysis of key cell-cycle checkpoint proteins in colorectal tumours. *J Pathol* 2002; **196**: 386-393

11 **Ohishi T**, Kishimoto Y, Miura N, Shiota G, Kohri T, Hara Y, Hasegawa J, Isemura M. Synergistic effects of (-)-epigallocatechin gallate with sulindac against colon carcinogenesis of rats treated with azoxymethane. *Cancer Lett* 2002; **177**: 49-56

12 **Yamada Y**, Yoshimi N, Hirose Y, Matsunaga K, Katayama M, Sakata K, Shimizu M, Kuno T, Mori H. Sequential analysis of morphological and biological properties of beta-catenin-accumulated crypts, provable premalignant lesions independent of aberrant crypt foci in rat colon carcinogenesis. *Cancer Res* 2001; **61**: 1874-1876

13 **Hung LC**, Pong VF, Cheng CR, Wong FI, Chu RM. An improved system for quantifying AgNOR and PCNA in canine tumors. *Anticancer Res* 2000; **20**: 3273-3280

14 **Derenzini M**, Trere D, Pession A, Govoni M, Sirri V, Chieco P. Nucleolar size indicates the rapidity of cell proliferation in cancer tissues. *J Pathol* 2000; **191**: 181-186

15 **Eminovic-Behrem S**, Trobonjaca Z, Petrovecki M, Dobi-Babic R, Dujmovic M, Jonjic N. Prognostic significance of DNA ploidy pattern and nucleolar organizer regions (AgNOR) in colorectal carcinoma. *Croat Med J* 2000; **41**: 154-158

16 **Ofner D**. *In situ* standardised AgNOR analysis: a simplified method for routine use to determine prognosis and chemotherapy efficiency in colorectal adenocarcinoma. *Micron* 2000; **31**: 161-164

17 **Sugai T**, Nakamura SI, Habano W, Uesugi N, Sato H, Yoshida T, Orii S. Usefulness of proliferative activity, DNA ploidy pattern and p53 products as diagnostic adjuncts in colorectal adenomas and intramucosal carcinomas. *Pathol Int* 1999; **49**: 617-625

18 **Nanashima A**, Yamaguchi H, Shibasaki S, Sawai T, Yasutake T, Tsuji T, Nakagoe T, Ayabe H. Proliferation of hepatic metastases of colorectal carcinoma: relationship to primary tumours and prognosis after hepatic resection. *J Gastroenterol Hepatol* 1999; **14**: 61-66
19 **Guan RJ**, Ford HL, Fu Y, Li Y, Shaw LM, Pardee AB. Drg-1 as a differentiation-related, putative metastatic suppressor gene in human colon cancer. *Cancer Res* 2000; **60**: 749-755
20 **Lee MO**, Han SY, Jiang S, Park JH, Kim SJ. Differential effects of retinoic acid on growth and apoptosis in human colon cancer cell lines associated with the induction of retinoic acid receptor beta. *Biochem Pharmacol* 2000; **59**: 485-496
21 **Sarraf P**, Mueller E, Smith WM, Wright HM, Kum JB, Aaltonen LA, de la Chapelle A, Spiegelman BM, Eng C.Loss-of-function mutations in PPAR gamma associated with human colon cancer. *Mol Cell* 1999; **3**: 799-804
22 **Nicke B**, Riecken EO, Rosewicz S. Induction of retinoic acid receptor beta mediates growth inhibition in retinoid resistant human colon carcinoma cells. *Gut* 1999; **45**: 51-57
23 **Zheng Y**, Kramer PM, Lubet RA, Steele VE, Kelloff GJ, Pereira MA. Effect of retinoids on AOM-induced colon cancer in rats: modulation of cell proliferation, apoptosis and aberrant crypt foci. *Carcinogenesis* 1999; **20**: 255-260
24 **Teraishi F**, Kadowaki Y, Tango Y, Kawashima T, Umeoka T, Kagawa S, Tanaka N, Fujiwara T. Ectopic p21sdi1 gene transfer induces retinoic acid receptor beta expression and sensitizes human cancer cells to retinoid treatment. *Int J Cancer* 2003; **103**: 833-839
25 **Narayanan BA**, Narayanan NK, Simi B, Reddy BS. Modulation of inducible nitric oxide synthase and related proinflammatory genes by the omega-3 fatty acid docosahexaenoic acid in human colon cancer cells. *Cancer Res* 2003; **63**: 972-979
26 **Wei HB**, Wang JF, Chen GH. Effect of retinoic acid (RA) on the T-lymphocyte subsets and T-cell colony of patients with colorectal cancer. *Ai Zheng* 2003; **22**: 202-205
27 **Lee MO**, Kang HJ. Role of coactivators and corepressors in the induction of the RARbeta gene in human colon cancer cells. *Biol Pharm Bull* 2002; **25**: 1298-1302
28 **Tao L**, Kramer PM, Wang W, Yang S, Lubet RA, Steele VE, Pereira MA.Altered expression of c-myc, p16 and p27 in rat colon tumors and its reversal by short-term treatment with chemopreventive agents. *Carcinogenesis* 2002; **23**: 1447-1454
29 **Ahmed KM**, Shitara Y, Takenoshita S, Kuwano H, Saruhashi S, Shinozawa T. Association of an intronic polymorphism in the midkine (MK) gene with human sporadic colorectal cancer. *Cancer Lett* 2002; **180**: 159-163
30 **Li Y**, Zhang H, Xie M, Hu M, Ge S, Yang D, Wan Y, Yan B. Abundant expression of Dec1/stra13/sharp2 in colon carcinoma: its antagonizing role in serum deprivation-induced apoptosis and selective inhibition of procaspase activation. *Biochem J* 2002; **367** (Pt2): 413-422
31 **Ye J**, Lu H, Zhou J, Wu H, Wang C. Inhibitory effect of all-trans-retinoid and polyphenon-100 on microsatellite instability in a colon cancer line. *Zhonghua Yixue Yichuanxue Zazhi* 2002; **19**: 190-193
32 **Wong NA**, Pignatelli M. Beta-catenin-a linchpin in colorectal carcinogenesis? *Am J Pathol* 2002; **160**: 389-401
33 **Lamprecht SA**, Lipkin M. Cellular mechanisms of calcium and vitamin D in the inhibition of colorectal carcinogenesis. *Ann N Y Acad Sci* 2001; **952**: 73-87
34 **Paulsen JE**, Elgjo K. Effect of tumour size on the *in vivo* growth inhibition of human colon carcinoma cells (HT-29) by colon mitosis inhibitor. *In Vivo* 2001; **15**: 397-401
35 **Parlesak A**, Menzl I, Feuchter A, Bode JC, Bode C. Inhibition of retinol oxidation by ethanol in the rat liver and colon. *Gut* 2000; **47**: 825-831

Edited by Xia HHX and Wang XL

P.O.Box 2345, Beijing 100023,China
Fax: +86-10-85381893
E-mail: wjg@wjgnet.com www.wjgnet.com

World J Gastroenterol 2003;9(8):1729-1733
World Journal of Gastroenterology
 ISSN 1007-9327

• COLORECTAL CANCER •

Expression of tumor related genes NGX6, NAG-7, BRD7 in gastric and colorectal cancer

Xiao-Mei Zhang, Shou-Rong Sheng, Xiao-Yan Wang, Jie-Ru Wang, Jiang Li

Xiao-Mei Zhang, Xiao-Yan Wang, Department of Digestion Medicine, Xiangya Hospital, Central South University, Changsha 410008, Hunan Province, China
Shou-Rong Sheng, Department of Digestion Medicine, The Third Xiangya Hospital, Central South University, Changsha 410013, Hunan Province, China
Jie-Ru Wang, Jiang Li, Carcinoma Research Institute, Xiangya Medical School, Central South University, Changsha 410078, Hunan Province, China
Supported by the Natural Science Foundation of Hunan Province No.01JJY2102 and the National "863 Program" of China, No.102-10-01-05
Correspondence to: Dr. Shou-Rong Sheng, Department of Digestion Medicine, The Third Xiangya Hospital, Central South University, Changsha 410013, Hunan Province, China. tangyy@public.cs.hn.cn
Telephone: +86-731-4316667 **Fax:** +86-731-4316667
Received: 2003-04-02 **Accepted:** 2003-05-19

Abstract

AIM: NGX6, NAG-7 and BRD7 genes are tumor related genes, which have been newly cloned by positional candidate cloning strategy. This study was designed to investigate the expression levels of NGX6, NAG-7 and BRD7 genes in human gastric and colorectal cancer tissues, and their corresponding normal tissues, and to investigate whether these genes play a role in the pathogenesis of gastric and colorectal cancers.

METHODS: Reverse transcription-polymerase chain reaction (RT-PCR), dot hybridization and Northern blot analysis were used to compare the expression levels of NGX6, NAG-7 and BRD7 genes in 34 gastric cancer tissues and 34 colorectal cancer tissues with their corresponding normal tissues of the same patients, respectively.

RESULTS: Among the 34 colorectal cancer specimens and the 34 gastric cancer specimens, the expression of NGX6 in 25 colorectal cancer tissues was absent or very weak (73.5 %) by RT-PCR analysis. The down-regulation rate of NGX6 in colorectal cancer tissues was significantly higher than that in corresponding normal tissues (26.5 %,9/34) ($P<0.005$). Moreover, the down-regulation of NGX6 was significantly correlated with lymph node and/or distance metastases. Patients with lymph node and/or distance metastasis had much higher down-regulation rate of NGX6 than patients without metastases (93.8 % *vs* 55.6 %, $P<0.05$). However no correlation was found between the expression of NGX6 and pathologic type of colorectal cancer in this study, and also the expression of NGX6 did not display any difference between gastric cancer and corresponding normal tissues (58.8 % *vs* 70.6 %, $P>0.25$). Dot hybridization and Northern blot analysis confirmed the results of RT-PCR. Furthermore, NAG-7 and BRD7 mRNA was not up- or down-regulated in gastric and colorectal cancers compared with their corresponding normal tissues in our study.

CONCLUSION: The down-regulation of NGX6 may be closely associated with tumorigenesis and metastasis of colorectal carcinoma. However, it may not contribute to the development and progression of gastric carcinoma. In addition, the expression levels of NAG-7, and BRD7 did not alter in gastric and colorectal cancers. This seems to suggest that NAG-7 and BRD7 genes may not play a role in gastric and colorectal carcinogenesis.

Zhang XM, Sheng SR, Wang XY, Wang JR, Li J. Expression of tumor related genes NGX6, NAG-7, BRD7 in gastric and colorectal cancer. *World J Gastroenterol* 2003; 9(8): 1729-1733
http://www.wjgnet.com/1007-9327/9/1729.asp

INTRODUCTION

Gastric cancer (GC) is a leading cause of carcinoma morbidity and mortality in China[1]. Meanwhile, the occurrence of colorectal cancer (CRC) has been rising in the past 3 decades. At present, CRC is the fourth cause of death in China[2,3]. It is well known that a multistep process associated with multiple gene abnormalities including inactivation of tumor suppressor genes and activation of oncogenes may be related to the occurrence of these diseases, but the molecular basis of these diseases is still not well understood[4-11]. Recently modern molecular genetic analyses have clarified that multiple chromosome alterations are frequently found in GC and CRC[12-16]. Nonrandom and significant losses of heterozygosity (LOH) at 9p, 3p and 6q have been detected to be more significant by cytogenetic studies, indicating that there may be more than one tumor suppressor gene (TSG) associated with GC and CRC located in these regions[17-24]. Unfortunately, homozygous deletions and point mutations of the known tumor suppressor genes such as p16/MTS1 gene (9p21),VHL gene (3p25-26), PPARγ gene (3p24.2-25) and FHIT gene (3p14.2) have seldom been observed in GC and CRC. These results suggest that these genes might not play important roles in gastric and colorectal tumorigenesis, and several other tumor suppressor genes in these region may contribute to the occurrence and development of GC and CRC[25-33]. NGX6, NAG-7 and BRD7 genes located at 9p21-22, 3p25 and 6q22.1-6q22.33, respectively, are novel tumor related genes cloned by positional candidate cloning strategy. In previous studies, all of them were found to be potential tumor suppressor genes associated with nasopharyngeal carcinoma (NPC)[34-39]. To investigate whether NGX6, NAG-7 and BRD7 genes also play a role in the pathogenesis of gastric and colorectal carcinoma, we analyzed the expression levels of NGX6, NAG-7 and BRD7 genes in 34 human gastric carcinoma tissues, 34 human colorectal carcinoma tissues and their corresponding normal tissues by RT-PCR, dot hybridization and Northern blot analysis.

MATERIALS AND METHODS

Tumor specimens

Fresh surgical specimens of thirty-four gastric carcinomas (GC), thirty-four colorectal carcinomas (CRC) and their corresponding normal tissues were obtained from the Xiang

ya Hospital Affiliated to Central South University from January 2000 to July 2000. All tumor specimens were confirmed by pathological diagnosis. Each freshly resected specimen was immediately stored in liquid nitrogen until analysis. Histologically, in the 34 cases of gastric carcinoma, 4 were well-differentiated adenocarcinomas, 22 poorly-differentiated adenocarcinomas, 6 signet ring cell carcinomas and 2 mucoid carcinomas. There were 18 males and 16 females, their age ranged from 30 to 68 years (mean age, 51.7 years). Six cases had lymph node and/or distance metastases. In the 34 cases of colorectal carcinoma, 6 were poorly-differentiated adenocarcinomas, 27 well-differentiated adenocarcinomas and 1 signet ring cell carcinoma. There were 20 males and 14 females, their age ranged from 17 to 72 years (mean age, 47.4 years). Sixteen cases had lymph node and/or distance metastases. No patient had received chemotherapy or radiation therapy before surgery.

RT-PCR

Total RNA was isolated using Trizol reagent (Gibco-BRL, Gaithersburg, MD, USA) according to the protocol provided by the manufacturer. After being treated with DNase-I (Promega), 1-2 μg of total RNA was reversely transcribed into complementary DNA (cDNA) with oligo (dT) using cDNA synthesis kit (Promega). Then 1 μl cDNA product was used as the template to amplify specific fragments in a 25 μl reaction mixture. The PCRs were performed using Taq polymerase and the buffer (Promega) supplied with 0.2 mM dNTPs and 0.2 μM primers. RT-PCR reaction was carried out with an initial denaturation at 95 ℃ for 5 min, followed by 35 cycles at 94 ℃ for 50 s, annealing temperature (56 ℃) for 50 s, at 72 ℃ for 60 s, and final extension at 72 ℃ for 10 min. At the same time, a housekeeping gene, $GAPDH_1$ or $GAPDH_2$ was amplified as an internal control to normalize the relative levels of cDNA, in which primers generated a PCR product of 475 bp or 760 bp. An aliquot (10 μl) of each reaction products was analyzed by 1.0 % agarose gel electrophoresis.

Primers corresponding to NGX6, NAG-7 and BRD7 sequences were designed with WWW Primer Picking (Primer 3) and synthesized by TaKaRa. Gene-specific forward and reverse primers for NGX6, NAG-7 and BRD7 genes were designed to produce PCR products of 780 bp, 466 bp and 270 bp, respectively. Primer sequences were as follows: NGX6F1, 5'-GAA CGT GGT GGA AAT ACA GA-3'; NGX6R1, 5'-TTC TAC ATC TTC TTT GGC CC-3'; NAG-7F1, 5'-ACATCAGCTTGGAGTTATTGA-3'; NAG-7R1,5'-GAAATGTACCACCCTACA-3'; BRD7F1, 5'-TGGAAGCCTCTCACAAGCT-3'; BRD7R1, 5'-TGTGTACTAATGCCATGAT-3'; $GAPDH_1$F1, 5'-GTCATCCATGACAACTTTGGTATC-3'; $GAPDH_1$R1, 5'-CTGTAGCCAAATTCGTTGTCATAC-3'; $GAPDH_2$F1, 5'-CGAGATCCCTCCAAAATCAA-3'; $GAPDH_2$R1, 5'-TGCTGTAGCCAAATTCGTTG-3'.

Northern blot analysis

Total RNA was isolated from human gastric and colorectal carcinomas and their corresponding normal tissues by Trizol reagent (Gibco-BRL), and transferred to nylon membrane according to the standard procedure. Hybridization was performed as previously described. 30 μg RNA was separated by electrophoresis through denaturing agarose gels, and blotted onto the nylon membranes (Clontech). RNA was permanently attached to the membrane by UV illumination for 150 s (GS Gene Linker, Bio-Rad, USA), and the membranes were dried in a vacuum at 80 ℃ for 2 h and sealed in a plastic bag for use. The hybridization probes were obtained by RT-PCR amplification. NGX6, NAG-7 and BRD7 cDNA probes were random-prime labeled with [α-^{32}P]dCTP using primer-a-gene random labeling kit (Promega, USA) following the protocol. Hybridization with RNA blots was carried out at 68 ℃ overnight in Express Hyb TM hybridization solution (Clontech) in rolling bottles. The membranes were washed twice at room temperature in 2×saline sodium citrate (SSC), 0.05 % SDS for 10 min, once at 42 ℃ in 1×SSC, 0.1 % SDS for 15 min and once at 50 ℃ in 0.1×SSC, 0.1 % (w/v) SDS for 30 min, exposure to film (Eastman Kodak, Rochester, NY, USA) for 4 d at -70 ℃. After exposure, the blot was again hybridized with a GAPDH probe.

Dot blot analysis

GAPDH and NGX6, NAG-7 and BRD7 cDNA fragments containing open reading frame from cDNA of gastric or colorectal carcinoma samples were obtained by RT-PCR. These cDNAs were reclaimed and purified by using a Kit according to the instruction of its manufacturer (Shanghai Huashun Co.). After alkali dissolution, GAPDH and NGX6, NAG-7 and BRD7 cDNA were blotted onto nylon membranes. cDNA permanently was attached to the membrane by UV illumination for 150 s, and the membranes were dried in a vacuum at 80 ℃ for 2 h to fix the cDNA. 10 μg total RNA was isolated from 10 cases of human gastric carcinomas, 10 cases of colorectal carcinomas and 10 cases of each corresponding normal tissues respectively, and was reversely-transcribed into cDNA probes with oligo (dT) and [α-^{32}P] dCTP using cDNA synthesis kit after treated with DNase I and RNasin at 37 ℃ for 1 h to remove contaminated DNA (1 μg total RNA of each case was used). Then the four cDNA probes were hybridized with GAPDH and NGX6, NAG-7 and BRD7 cDNA blots respectively as Northern hybridization described above.

Statistical analysis

Chi-square test was used for the comparison between two groups. A P value less than 0.05 was considered statistically significant.

RESULTS

Expression of NGX6, NAG-7 and BRD7 genes in gastric and colorectal cancer tissues by RT-PCR

In 34 pairs of CRC and corresponding normal tissues, 25 (73.5 %) showed decreased or absent expression of NGX6 in cancer samples compared with their corresponding normal tissues. The expression of NGX6 in colorectal carcinoma was significantly lower than that in normal tissues (χ^2=15.06, P<0.005). Representative cases of NGX6 expression detected by RT-PCR are shown in Figure 1. The down-regulation rate of NGX6 in the patients with lymph-node and/or distance metastases was 93.8 % (15/16), significantly higher than that in those without lymph-node or distance metastases (55.6 %, 10/18) (P<0.05). The down-regulation rates of NGX6 in well differentiated and poorly differentiated adenocarcinomas were 46.2 % and 85.7 %, respectively. There was no apparent relevance between NGX6 down-expression and pathologic type of colorectal carcinomas (P>0.05).

In 34 pairs of GC and their corresponding normal tissue specimens, NGX6 expression was detected in 20 GC tissues (58.8 %) and 24 corresponding normal tissues (70.6 %) as an expected PCR product of 780 bp in length. The expression level of NGX6 did not display any difference between gastric carcinoma and its corresponding normal tissues (χ^2=1.03, P>0.05).

NAG-7 expression was detected in 88.2 % (30/34) GC tissues and 82.3 % (28/34) corresponding normal tissues as well as in 76.2 % (26/34) CRC tissues and 76.2 % (26/34) corresponding normal tissues as an expected PCR product of 466 bp in length. BRD7 expression was detected in all samples

as an expected PCR product of 270 bp in length. The expression level of NAG-7 and BRD7 did not display any significant difference between cancer samples and normal tissues (P>0.05).

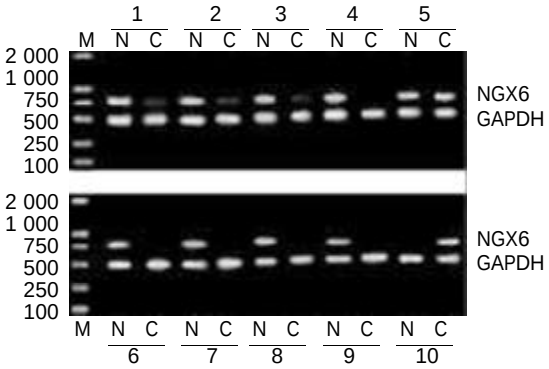

Figure 1 Expression of NGX6 in colorectal carcinoma and its corresponding normal tissues was examined by RT-PCR. The RT-PCR products with NGX6 primers produced 780 bp fragments and GAPDH primers produced 466 bp fragments. Lane M, DL-2000 marker; Lane N, normal tissues; Lane C, colorectal carcinoma tissues. This figure showed the representative results from several individual patients.

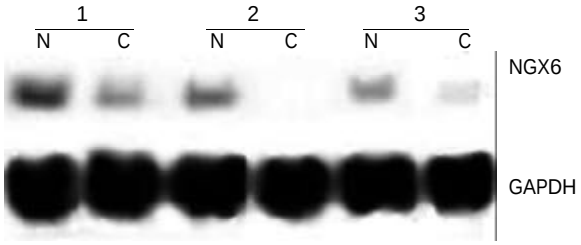

Figure 2 Northern blot was used to detect the expression abundance of NGX6 gene in human colorectal carcinoma and its adjacent normal tissues. The expression level of NGX6 was down-regulated in colorectal carcinoma tissues. C, human colorectal carcinoma tissue; N, adjacent normal colorectal tissue.

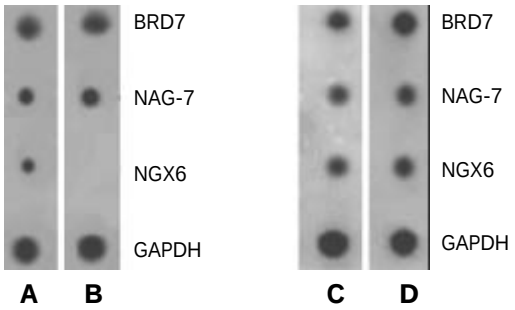

Figure 3 Dot hybridization analysis of NGX6, NAG-7 and BRD7 gene expression profiles in human colorectal and gastric carcinomas and their corresponding normal tissues. NGX6, NAG-7 and BRD7 cDNAs obtained by RT-PCR were blotted onto nylon membranes (Clontech) respectively. The membranes were respectively hybridized with each type of cDNA probes. (A: corresponding normal colorectal epithelial tissues, B: colorectal carcinoma, C: corresponding normal gastric epithelial tissues, D: gastric carcinoma.) NGX6 was down-regulated in colorectal carcinoma tissues, however it was expressed at the same level in the gastric cancer samples and normal tissues.

Expression of NGX6, NAG-7 and BRD7 genes in gastric and colorectal carcinoma tissues by Northern blot analysis and dot hybridization

Northern blot analysis and dot hybridization were performed to further investigate the expression of NGX6, NAG-7 and BRD7. Northern blot analysis showed that NGX6 was expressed as one single transcript of 2.4 kb, corresponding well with the size of the cloned cDNA. NGX6 was strongly expressed in its corresponding normal colorectal epithelial tissues, whereas faint signals or no signals were found in colorectal carcinoma tissues. Representative cases of NGX6 expression detected by Northern hybridization are shown in Figure 2. However, no signals were discerned in gastric carcinoma and its corresponding normal epithelial tissues. NAG-7 and BRD7 mRNA was expressed at the same level in the cancer samples and normal tissues. The results of dot hybridization were consistent with those of Northern analysis. Both dot hybridization and Northern analysis confirmed the results of RT-PCR. The expression of NGX6 was significantly down-regulated in colorectal carcinoma tissues.

DISCUSSION

NGX6, NAG-7 and BRD7 genes located at 9p21-22, 3p25 and 6q22.1-6q22.33 respectively are novel tumor related genes that were cloned by positional candidate cloning strategy. The cDNA sequence of NGX6, NAG-7 and BRD7 genes compared with Genbank and EMBO database using the BLAST program has verified that all of them are unique genes with no homology to any previously reported human genes, and their GenBank accession numbers are AF188239, AF086709 and AF179285, respectively. The NGX6 gene encodes a transmembrane protein of 338 amino acids containing four transmembrane regions, an EGF-like domain signature and a number of potential phosphorylation sites for protein kinase C (PKC), casein kinase II, tyrosine kinase and several N-myristylation sites. The NAG-7 gene encodes a transmembrane protein of 94 amino acids including one PKC phosphorylation site and one myristylation site. The BRD7 gene encodes a protein of 508 amino acids including a bromodomain and several important phosphorylation sites. In our previous study, their mRNA expression levels in nasopharyngeal carcinoma (NPC) cells were all significantly lower than those in normal nasopharyngeal epithelium. The proliferation rate of NPC cells was slower after transfection with these genes. The growth of xenografts was also inhibited after the transfected cells were injected into nude mice *in vivo*. These results suggest that the downregulation of these genes might play important roles in the occurrence and development of NPC[34-39].

Allelic imbalance or loss of heterozygosity (LOH) studies have been used to identify regions on chromosomes that may contain putative tumor suppressor genes. Deletions of chromosome 9p, 3p, and 6q regions have been observed at a high frequency in many types of sporadic tumors, including gastric and colorectal cancers[17-24]. NGX6, NAG-7 and BRD7 genes located at 9p21-22, 3p25 and 6q22.1-6q22.33 respectively, are the frequent sites of LOH in GC and CRC. We were interested in investigating if expression of NGX6, NAG-7 and BRD7 genes was altered in GC and CRC. In this study, RT-PCR, Northern blot and dot hybridization were used to detect the expression abundance of the three genes in gastric and colorectal carcinoma tissues, as well as their corresponding normal tissues. The results of RT-PCR showed that the down-regulation rate of NGX6 in colorectal carcinoma tissues with lymph-node or distant metastases was significantly higher than that both in its corresponding normal tissues (P<0.005) and in carcinomas without lymph-node or distant metastases (P<0.05). Dot hybridization and Northern analysis confirmed the results of RT-PCR. However, no significant correlation was found between the expression of NGX6 and pathologic type of colorectal carcinomas. The results suggest that down-regulation of NGX6 might be closely associated with the

development, progression and metastasis of CRC. It is reasonable to predict that the NGX6 gene plays an important role in suppressing CRC tumorigenesis; losses of its function may contribute to the development of CRC. Deletion of this gene may occur as a later event associated with tumor progress, and may contribute to the metastatic potential of CRC. So, it is speculated that NGX6 gene located on chromosomes 9p21-22 may be a candidate tumor suppressor gene and a putative metastasis suppressor gene associated with CRC. The possible mechanism of this gene suppressing CRC tumorigenesis remains unclear. We speculated that the possible mechanism might be as follows. Firstly, NGX6 gene may be involved in cell cycle regulation and play an important role in tumor growth suppression. Our previous studies showed that significant accumulation of cells in the G0-G1 fraction was observed in HNE_1 cell transfected with NGX6 gene by using flow cytometric analysis, and several genes related to cell cycle and transcription regulation were differentially expressed in NGX6 overexpressed nasopharyngeal carcinoma cells by cDNA array assay[34,35,40]. Combined with our data presented here, it is reasonable to speculate that deletion or down-regulation of NGX6 gene in colorectal cancer may contribute to tumor cell proliferation and tumor metastasis. Secondly, NGX6 gene encodes a putative transmembrance protein including an important structural feature-EGF-like domain signature. In our study, NGX6 gene was significantly down-regulated in CRC, indicating that NGX6 protein might function as an inhibited membrane receptor or a negative growth factor in the initiation and progression of CRC. However, many previous studies showed that the proteins with EGF-like domains such as EGF, TGF-a were overexpressed in tumor tissues and might play a role in promoting tumor growth and metastasis[41-43]. Recently, Williams *et al*[44] identified two novel mucin genes, which encoded two putative transmembrane mucins with EGF-like domains and were commonly downregulated in colorectal carcinoma. This detection further confirmed that the transmembrance protein with EGF-like domain could act as a suppressive membrane receptor or a negative growth factor. Finally, NGX6 gene may exert functions by up-regulating and down-regulating some proteins. Recently, Li *et al*[45] found that seven proteins were up-regulated and seven proteins were down-regulated in NGX6 transfected cells using high-resolution two-dimensional electrophoresis. These proteins included Fas, zinc-finger protein (ZNF), RAB, and Ah receptor-interacting protein (AIP), which may affect the signaling pathway, alter the cell metabolism, and inhibit cell proliferation, induce cell apoptosis and prevent tumor invasion. Therefore, all these protein roles on cells indicate that NGX6 gene has the capacity to suppress both NPC and CRC tumorigenesis.

In this study, we did not find the existence of up- or down-regulated NGX6 in 34 gastric carcinoma specimens and their corresponding normal tissues by RT-PCR. The expression of NAG-7 and BRD7 genes did not display any significant difference between gastric and colorectal carcinomas and their corresponding normal tissues. The results of RT-PCR were also confirmed by Northern blot analysis and dot hybridization. This seems to suggest that NAG-7 and BRD7 genes play no roles in the pathogenesis of gastric and colorectal carcinomas, and NGX6 gene may not contribute to the occurrence and development of gastric carcinoma.

In summary, the results of this study have shown that NGX6 is down-regulated in colorectal carcinoma, and the down-regulation of this gene has a close correlation with lymph node or distant metastasis of CRC, suggesting that NGX6 plays an important role in tumor suppression. However the mechanism of this gene is still unclear. Further studies are needed to better understand the function of this novel gene and its role in CRC tumorigenesis *in vivo*.

REFERENCES

1 **Deng DJ**. Progress of gastric cancer etiology: N-nitrosamides 1999s. *World J Gastroenterol* 2000; **6**: 613-618
2 **Zhang YL**, Zhang ZS, Wu BP, Zhou DY. Early diagnosis for colorectal cancer in China. *World J Gastroenterol* 2002; **8**: 21-25
3 **Yu J P,** Dong WG. Current situation about early diagnosis of cancer of large intestine. *Shijie Huaren Xiaohua Zazhi* 1999; **7**: 553-554
4 **Fiocca R,** Luinetti O, Villani L, Mastracci L, Quilici P, Grillo F, Ranzani GN. Molecular mechanisms involved in the pathogenesis of gastric carcinoma: interactions between genetic alterations, cellular phenotype and cancer histotype. *Hepatogastroenterology* 2001; **48**: 1523-1530
5 **Yustein AS**, Harper JC, Petroni GR, Cummings OW, Moskaluk CA, Powell SM. Allelotype of gastric adenocarcinoma. *Cancer Res* 1999; **59**: 1437-1441
6 **Song ZJ**, Gong P, Wu YE. Relationship between the expression of iNOS,VEGF,tumor angiogenesis and gastric cancer. *World J Gastroenterol* 2002; **8**: 591-595
7 **Liu LX**, Liu ZH, Jiang HC, Qu X, Zhang WH, Wu LF, Zhu AL, Wang XQ, Wu M. Profiling of differentially expressed genes in human gastric carcinoma by cDNA expression array. *World J gastroenterol* 2002; **8**: 580-585
8 **He XS**, Su Q, Chen ZC, He XT, Long ZF, Ling H, Zhang LR. Expression, deletion [was deleton] and mutation of p16 gene in human gastric cancer. *World J Gastroenterol* 2001; **7**: 515-521
9 **Li XG**, Song JD, Wang YQ. Differential expression of a novel colorectal cancer differentiation-related gene in colorectal cancer. *World J Gastroenterol* 2001; **7**: 551-554
10 **Lou MJ**, Lai MD. Identification of differentially expressed genes in normal mucosa, adenoma and adenocarcinomas of cilon by SSH. *World J Gastroenterol* 2001; **7**: 726-731
11 **Hu JY**, Li GC, Wang WM, Zhu JG, Li YF, Zhou GH, Sun QB. Transfection of colorectal cancer cells with chemokine MCP-3 (monocyte chemotactic protein-3) gene retards tumor growth and inhibits tumor metastasis. *World J Gastroenterol* 2002; **8**: 1067-1072
12 **Wang Y**, Zheng E, Ke Y. Studies of loss of heterozygosity (LOH) in Chinese human gastric cancer tissues. *Zhonghua Zhongliu Zazhi* 1998; **20**: 116-118
13 **Gayet J**, Zhou XP, Duval A, Rolland S, Hoang JM, Cottu P, Hamelin R. Extensive characterization of genetic alterations in a series of human colorectal cancer cell lines. *Oncogene* 2001; **20**: 5025-5032
14 **Lai MD**. Gene changes of Chinese colorectal cancer. *Shijie Huaren Xiaohua Zazhi* 2001; **9**: 1227-1232
15 **Qin LX**. Chromosomal aberrations related to metastasis of human solid tumors. *World J Gastroenterol* 2002; **8**: 769-776
16 **Zhou CZ**, Peng ZH, Zhang F, Qiu GQ, He L. Loss of heterozygosity on long arm of chromosome 22 in sporadic colorectal carcinoma. *World J Gastroenrerol* 2002; **8**: 668-673
17 **Chetty R**, Naidoo R, Tarin M, Sitti C. Chromosome 2p, 3p, 5q and 18q status in sporadic gastric cancer. *Pathology* 2002; **34**: 275-281
18 **Weber TK**, Conroy J, Keitz B, Rodriguez-Bigas M, Petrelli NJ, Stoler DL, Anderson GR, Shows TB, Nowak NJ. Genome-wide allelotyping indicates increased loss of heterozygosity on 9p and 14q in early age of onset colorectal cancer. *Cytogenet Cell Genet* 1999; **86**: 142-147
19 **Martignetti JA**, Gelb BD, Pierce H, Picci P, Desnick RJ. Malignant fibrous histiocytoma: inherited and sporadic forms have loss of heterozygosity at chromosome bands 9p21-22-evidence for a common genetic defect. *Genes Chromosomes Cancer* 2000; **27**: 191-195
20 **Zhang Y**, Lai M. Microsatellite alterations on chromosome 9p21-22 in sporadic colorectal cancer. *Zhonghua Binglixue Zazhi* 1999; **28**: 418-421
21 **Kim NG**, Kim JJ, Ahn JY, Seong CM, Noh SH, Kim CB, Min JS, Kim H. Putative chromosomal deletions on 9P, 9Q and 22Q occur preferentially in malignant gastrointestinal stromal tumors. *Int J Cancer* 2000; **85**: 633-638
22 **Carvalho B**, Seruca R, Buys CH, Kok K. Novel expressed sequences obtained by means of a suppression subtractive hybridisation analysis from the 6q21 region that is frequently deleted in gastric cancer. *Eur J Cancer* 2002; **38**: 1126-1132
23 **Carvalho B**, van der Veen A, Gartner F, Carneiro F, Seruca R, Buys CH, Kok K. Allelic gains and losses in distinct regions of chromosome 6 in gastric carcinoma. *Cancer Genet Cytogenet* 2001; **131**: 54-59

24 **Carvalho B**, Seruca R, Carneiro F, Buys CH, Kok K. Substantial reduction of the gastric carcinoma critical region at 6q16.3-q23.1. *Genes Chromosomes Cancer* 1999; **26**: 29-34

25 **Gunther T**, Schneider-Stock R, Pross M, Manger T, Malfertheiner P, Lippert H, Roessner A. Alterations of the p16/MTS1-tumor suppressor gene in gastric cancer. *Pathol Res Pract* 1998; **194**: 809-813

26 **Shim YH**, Kang GH, Ro JY. Correlation of p16 hypermethylation with p16 protein loss in sporadic gastric carcinomas. *Lab Invest* 2000; **80**: 689-695

27 **Tsujie M**, Yamamoto H, Tomita N, Sugita Y, Ohue M, Sakita I, Tamaki Y, Sekimoto M, Doki Y, Inoue M, Matsuura N, Monden T, Shiozaki H, Monden M. Expression of tumor suppressor gene p16(INK4) products in primary gastric cancer. *Oncology* 2000; **58**: 126-136

28 **Dai CY**, Furth EE, Mick R, Koh J, Takayama T, Niitsu Y, Enders GH. p16 (INK4a) expression begins early in human colon neoplasia and correlates inversely with markers of cell proliferation. *Gastroenterology* 2000; **119**: 929-942

29 **Trzeciak L**, Hennig E, Kolodziejski J, Nowacki M, Ostrowski J. Mutations, methylation and expression of CDKN2a/p16 gene in colorectal cancer and normal colonic mucosa. *Cancer Lett* 2001; **163**: 17-23

30 **Noguchi T**, Muller W, Wirtz HC, Willers R, Gabbert HE. FHIT gene in gastric cancer: association with tumour progression and prognosis. *J Pathol* 1999; **188**: 378-381

31 **Thiagalingam S**, Lisitsyn NA, Hamaguchi M, Wigler MH, Willson JK, Markowitz SD, Leach FS, Kinzler KW, Vogelstein B. Evaluation of the FHIT gene in colorectal cancers. *Cancer Res* 1996; **56**: 2936-2939

32 **Wijnhoven BP**, Lindstedt EW, Abbou M, Ijzendoorn Y, de Krijger RR, Tilanus HW, Dinjens WN. Molecular genetic analysis of the von Hippel-Lindau and human peroxisome proliferator-activated receptor gamma tumor-suppressor genes in adenocarcinomas of the gastroesophageal junction. *Int J Cancer* 2001; **94**: 891-895

33 **Miyakis S**, Sourvinos G, Liloglou TL, Stathopoulos GP, Field JK, Spandidos DA. The Von Hippel-Lindau (VHL) tumor-suppressor gene is not mutated in sporadic human colon adenocarcinomas. *Int J Cancer* 2000; **88**: 503-505

34 **Yang JB**, Bin LH, Li ZH, Zhang XF, Qian J, Zhang BC, Zhou M, Xie Y, Deng LW, Li GY. Refined localization and cloning of a novel putative tumor suppressor gene associated with nasopharyngeal carcinoma on chromosome 9p21-22. *Aizheng* 2000; **19**: 6-9

35 **Yang J,** Tang X, Deng L. Detailed deletion mapping of chromosome 9p21-22 in nasopharyngeal carcinoma. *Zhonghua Zhongliu Zazhi* 1999; **21**: 419-421

36 **Xie Y**, Deng L, Jiang N, Zhan F, Cao L, Qiu Y, Tang X, Li G. Molecular cloning of a novel gene located on chromosome 3p25.3 and an analysis of its expression in nasopharyngeal carcinoma. *Zhonghua Yixue Yichuan Xue Zazhi* 2000; **17**: 225-228

37 **Xie Y**, Bin L, Yang J, Li Z, Yu Y, Zhang X, Cao L, Li G. Molecular cloning and characterization of NAG-7: a novel gene downregulated in human nasopharyngeal carcinoma. *Chin Med J (Engl)* 2001; **114**: 530-534

38 **Yu Y**, Zhang BC, Xie Y, Cao L, Zhou M, Zhan FH, Li GY. Analysis and molecular cloning of differentially expressing genes in nasopharyngeal carcinoma. *Shengwu Huaxue Yu Shengwu Wuli Xuebao* 2000; **32**: 327-332

39 **Yu Y**, Xie Y, Cao L, Zhang BC, Zhou M, Zhan FH, Li GY. Molecular Cloning and functional primary study of a novel candidate tumor suppressor gene related with nasopharyngeal carcinoma. *Shengwu Huaxue Yu Shengwu Wuli Jinzhan* 2000; **27:** 319-324

40 **Ma J**, Li J, Zhou J, Li XL, Tang K, Zhou M, Yang JB, Yan Q, Shen SR, Hu GX, Li GY. Profiling genes differentially expressed in NGX6 overexpressed nasopharyngeal carcinoma cells by cDNA array. *J Cancer Res Clin Oncol* 2002; **128**: 683-690

41 **Choi JH**, Kim HC, Lim HY, Nam DK, Kim HS, Yi SY, Shim KS, Han WS. Detection of transforming growth factor-alpha in the serum of gastric carcinoma patients. *Oncology* 1999; **57**: 236-241

42 **Xia L**, Yuan YZ, Xu CD, Zhang YP, Qiao MM, Xu JX. Effects of epidermal growth factor on the growth of human gastric cancer cell and the implanted tumor of nude mice. *World J Gastroenterol* 2002; **8**: 455-458

43 **Ghanem MA**, Van Der Kwast TH, Den Hollander JC, Sudaryo MK, Mathoera RB, Van den Heuvel MM, Noordzij MA, Nijman RJ, van Steenbrugge GJ. Expression and prognostic value of epidermal growth factor receptor, transforming growth factor-alpha, and c-erb B-2 in nephroblastoma. *Cancer* 2001; **92**: 3120-3129

44 **Williams SJ**, McGuckin MA, Gotley DC, Eyre HJ, Sutherland GR, Antalis TM. Two novel mucin genes down-regulated in colorectal cancer identified by differential display. *Cancer Res* 1999; **59**: 4083-4089

45 **Li J**, Tan C, Xiang Q, Zhang X, Ma J, Wang JR, Yang J, Li W, Shen SR, Liang S, Li G. Proteomic detection of changes in protein synthesis induced by NGX6 transfected in human nasopharyngeal carcinoma cells. *J Protein Chem* 2001; **20**: 265-271

Edited by Zhang JZ and Wang XL

P.O.Box 2345, Beijing 100023,China
Fax: +86-10-85381893
E-mail: wjg@wjgnet.com www.wjgnet.com

World J Gastroenterol 2003;9(8):1734-1738
World Journal of Gastroenterology
 ISSN 1007-9327

• COLORECTAL CANCER •

Transcriptional gene expression profiles of HGF/SF-met signaling pathway in colorectal carcinoma

Xue-Nong Li, Yan-Qing Ding, Guo-Bing Liu

Xue-Nong Li, Yan-Qing Ding, Department of Pathology, First Military Medical University, Guangzhou 510515, Guangdong Province, China
Guo-Bing Liu, Department of Obstetrics & Gynecology, Nanfang Hospital, Guangzhou 510515, Guangdong Province, China
Supported by National Natural Science Foundation of China, No. 30170486 and No.30170423
Correspondence to: Dr. Xue-Nong Li, Department of Pathology, First Military Medical University, Guangzhou 510515, Guangdong Province, China. leexue0@163.com
Telephone: +86-20-61648223
Received: 2002-12-28 **Accepted:** 2003-04-01

Abstract

AIM: To explore the transcriptional gene expression profiles of HGF/SF-met signaling pathway in colorectal carcinoma to understand mechanisms of the signaling pathway at so gene level.

METHODS: Total RNA was isolated from human colorectal carcinoma cell line LoVo treated with HGF/SF (80 ng/L) for 48 h. Fluorescent probes were prepared from RNA labeled with cy3-dUTP for the control groups and with cy5-dUTP for the HGF/SF-treated groups through reverse-transcription. The probes were mixed and hybridized on the microarray at 60 ℃ for 15-20 h, then the microarray was scanned by laser scanner (GenePix 4000B). The intensity of each spot and ratios of Cy5/Cy3 were analyzed and finally the differentially expressed genes were selected by GenePix Pro 3.0 software. 6 differential expression genes (3 up-regulated genes and 3 down-regulated genes) were selected randomly and analyzed by β-actin semi-quantitative RT-PCR.

RESULTS: The fluorescent intensities of built-in negative control spots were less than 200, and the fluorescent intensities of positive control spots were more than 5000. Of the 4004 human genes analyzed by microarray, 129 genes (holding 3.22 % of the investigated genes) revealed differential expression in HGF/SF-treated groups compared with the control groups, of which 61 genes were up-regulated (holding 1.52 % of the investigated genes) and 68 genes were down-regulated (holding 1.70 % of the investigated genes), which supplied abundant information about target genes of HGF/SF-met signaling.

CONCLUSION: HGF/SF-met signaling may up-regulate oncogenes, signal transduction genes, apoptosis-related genes, metastasis related genes, and down-regulate a number of genes. The complexity of HGF/SF-met signaling to control the gene expression is revealed as a whole by the gene chip technology.

Li XN, Ding YQ, Liu GB. Transcriptional gene expression profiles of HGF/SF-met signaling pathway in colorectal carcinoma. *World J Gastroenterol* 2003; 9(8): 1734-1738
http://www.wjgnet.com/1007-9327/9/1734.asp

INTRODUCTION

HGF/SF-met signaling is a pathway by stimulation of c-met via its ligand hepatocyte growth factor /scatter factor (HGF/SF), leading to a considerable variety of biological and biochemical effects on the cells[1-3]. HGF/SF, a multifunctional cell growth factor, is yielded by interstitial cells such as fibroblast, neuroglial cell, glial cell, fat-storing cell and macrophage[3,4]. It binds to the c-met receptor specifically, inducing a series of conformational changes of signaling proteins by activating JAK[5], phosphatidylinositol 3-kinase (PI-3 K)[6], phospholipase C-γ[7], Raf-1 kinase[8] etc, by which it transmits the signal to the nuclear transcription machines to control certain gene transcription and expressions. Finally it affects the cell proliferation, differentiation, locomotion and other cell functions[9-12]. HGF/SF has been proved to have mitogen, motogen, morphogen activity for almost all epithelial cells, and to promote adhesiveness, invasiveness, motion and metastasis and stimulation for blood vessel growth of cancer cells[8-13]. It was revealed to have anti-cytotoxin and anti-apoptosis for cancer cells in the recent investigation[11,12]. It is evidenced that abnormal activation of HGF/SF-met signaling plays an important or critical causal role in tumor progression and invasion and metastasis. However, little is known about the target genes and gene expression profiles by which HGF/SF exerts biological functions through start-up of transcriptional gene expression.

In the present study, we aimed to explore the transcriptional gene expression profiles by activating HGF/SF-met signaling in colorectal carcinoma cells using the microarray technology by which thousands of genes could be detected at the same time.

MATERIALS AND METHODS

Reagents

Hepatocyte growth factor/scatter factor (HGF/SF), ethidium bromide(EB), and SDS were purchased from Sigma. AMV reverse transcriptase, oligo(dT), dNTP, Taq, and agarose were Promega products. Trypsin, Cy3-dUTP, and Cy5-dUTP were purchased from Amersham Phamacia, and Oligotex mRNA midi kit from Qiagen, and other reagents from Shanghai Biostar Co.

Cells and cell culture

Human colorectal carcinoma cell line LoVo was routinely cultured in RPMI-1640 medium with 10 % FCS, incubated at 37 ℃ with 5 % CO_2. The well-grown cells at the logarithmic growth phase were treated with HGF/SF (80 ng/L) for 24-48 h in the same medium containing 2.5 % FCS. The blank control groups were treated with D-Hanks solution in the same culture condition as HGF/SF-treated groups. Triduplication of the experiments was for the microarray assay.

Construction of microarrays

The genes for HGEC-40S microarray containing 4096 cDNA spots (including 92 negative and positive control spots) were provided by Shanghai Biostar Co. These genes were amplified by PCR with universal primers and then purified by the routine method[13-15]. The purity of PCR products was supervised by agarose electrophoresis and then the PCR products were

dissolved in 3 X SSC solution. The target genes were spotted on siliconlated slides (TeleChem Inc) by using Cartesian 7500 spotting robotics (Cartesian Inc), then hydrated for 2 h, dried for 0.5 h, UV cross-linked by UVP CL-1000 at 65 mJ/cm, and then treated with 0.2 % SDS(10min), H_2O (10 min) and 0.2 % $NaBH_4$ (10 min). Finally the slides were dried again and ready for use.

Probe preparation

Total RNA was isolated from human colorectal carcinoma cell line LoVo by the routine method[13-15]. And then they were tested by hot-stabilization experiments and RNA electrophoresis. cDNA probes were prepared through reverse transcription in 50 μl reaction system in reference to Schena *et al*[15]. The fluorescent probes derived from cDNA reverse-transcripted from RNA were labeled with cy3-dUTP for the control groups and with cy5-dUTP for the HGF/SF-treated groups. The two kinds of probes were mixed equally after ethanol precipitation, then inspissated by vacuum to 50 μl, purified by using S-200 columns, and finally dissolved in hybridizing solution (20 μl 5×SSC+0.2 % SDS).

Microarray hybridization[16-19]

After denatured at 95 ℃ water bath, the microarray was prehybridized with 6 μl hybridization solutions 1 and 2 (Biostar) at 42 ℃ for 6 h. The probe mixtures were added on the prehybridized microarray, denatured at 95 ℃ for 5 min, then inoculated in hybridization cabin at 60 ℃ for 15-20 h. After the glass cover was removed, the microarray was washed in solutions 1 (2×SSC+0.2 % SDS), and 2 (0.1×SSC+0.2 % SDS) and 3 (0.1×SSC) for 10 min each, then dried at room temperature.

Detection and analysis

GenePix 4000B laser scanner (Axon) was used to scan microarray, with laser power 3.72 and photomultiplier tube volts 750. GenePix Pro 3.0 software was used for analysis of intensity of each spot and ratio of Cy5/Cy3 from the acquired images. The intensities of Cy3 and Cy5 were normalized by a coefficient according to the ratio of the located 40 housekeeping genes. The standards for differentially expressed genes were as follows: the ratio of Cy5/Cy3 was more than 4 or less than 0.25, and the intensity value of Cy3 and Cy5 was more than 200.

Verification by RT-PCR[20,21]

RT-PCR primers were designed by Omiga 2.0 software with basic reaction parameters as follows: primer length 18-22 bp, primer % GC 40-60 %, primer Tm 55 ℃; PCR products length 100-600 bp, PCR products % GC 40-60 %, and PCR products Tm 82.5 ℃. The primer sequences were as follows:

CAMK4 (321 bp): 5' GAGACCCTTCTCCAATCC3'
5' GAACTTCAAAACCCACAGC 3'
SHPG (555 bp): 5' ACATCTCCCCTTTGCTAACG 3'
5' GCCACAGTACCCTCATAACTCC 3'
Heregulin (424 bp): 5' TGCTCAACAGCAACATCC 3'
5' TCATACATCTGCCCCTCC 3'
p130 (523 bp): 5' GCACTTCAGTGTTCTAATCG 3'
5' GGCTATTCTCCTTAATGTACC 3'
DAP-1 (322 bp): 5' ACATGAGACACCACATTCC 3'
5' ACGACACAGTTGCTGACC 3'
TRAMP (381 bp): 5' ATTCGCAAGAAAAGCACC 3'
5' GTAGAACGCACTAAGCTGACC 3'
β-actin (206 bp): 5' GGCGGCACCACCATGTACCCT 3'
5' AGGGGCCGGACTCGTCATCATACT 3'

Components of the reverse transcription reaction system were as follows: oligo (dT) 0.5 μl, AMV5x buffer 4 μl, dNTP (10 mM) 1 μl RNasin (20u/ μl) 1 μl, AMV (10u/ μl) 0.5 μl, and DEPC-treated water 12 μl. Components of PCR reaction system were as follows: 10X PCR buffer 2 μl, cDNA 5 μl, dNTP (10 mM) 1 μl, forward primer 1 μl (1 μM), reverse primer 1 μl (1 μM), β-actin forward primer 0.5 μl (0.2 μM), β-actin reverse primer 0.5 μl (0.2 μM), Taq DNA polymerase (2U/ μl) 1 μl, and DEPC-treated water 8 μl, PCR amplification consisted of 35 cycles of denaturation for 60-90 s at 94 ℃, annealing for 60-90 s at 56 ℃, and extension for 90-120 s at 72 ℃. After 35 turns of the cycle, it ended after extension at 72 ℃ for 7 min. DEPC-treated water was replaced with DNA template for the negative control. 1.5 % agarose gel electrophoresis with ethidium bromide was used for the analysis of PCR products. Bandleader 3.0 software was applied to detect the density of bands of PCR products. The value of gene expression was calculated from percent of the ratio of band density of PCR product and the band density of β-actin.

Statistical methods

Data for gene expression were analyzed by two sided Student' s *t* test using SPSS 10.0 software and the significant value was $P<0.05$.

RESULTS

Total RNA electrophoresis and hot-stabilization test

The values of D_{260}/D_{280} for control and HGF/SF-treated groups were 2.022, 2.103 respectively. After hot stabilization test the 18S and 28S bands of total RNA extracts were as clear as before the test (Figure 1).

Microarray quality control

The fluorescent intensities of built-in negative control including rice U2 RNA gene, HCV coat protein gene, spotting solution (without DNA) as blank spots were lower than 200, while the intensities of built-in 40 house-keeping genes as positive control spots were larger than 5000. Normalization coefficient was 1.028. The odds of spot average intensities with background for HGF/SF-treated groups and the control groups were 10.254, 12.856 respectively. The ratio of Cy5/Cy3 by self-check test was 0-1.7, with the average 1.0112.

Scanning results of microarray

The scanning images for HGF/SF-treated groups labeled with Cy5 and images for control groups labeled with Cy3 showed lower noise background and appropriate spot intensity of signal with clear circle appearance. The overlaying image for bicolor fluorescence label is shown in Figure 2.

Filter of the differential expression genes

Of the 4 004 human genes analyzed by microarray, 129 differential expression genes were identified by the filter standard mentioned above. Among the 129 differential expression genes, 61 genes were up-regulated and 68 genes were down-regulated. The up-regulated genes by HGF/SF-met signaling consisted of cell growth factor genes, cell surface receptor genes, angiogenesis genes, cell cycle positive-regulation genes, calcium-, MAPK signaling-related genes and nuclei-receptor genes, etc. The down-regulated genes by HGF/SF-c-met signaling were cell death correlation receptor genes, transmembrane-4 superfamily, cell cycle negative- regulation genes, calcium-, MAPK signaling-related negative genes, cytoskeleton rearrangement inhibitor, anti-oncogene and protease inhibitor, etc.

Results of RT-PCR

To validate the reliability of microarray results, 6 differential expression genes (3 up-regulated genes and 3 down-regulated genes) were selected randomly and analyzed by β-actin semi-quantitative RT-PCR. Expressions of the 6 differential genes by RT-PCR were confirmed to be consistent with the results of microarray (shown in Figure 3 and Figure 4). The average

relative densities of bands detected by Bandlead 3.0 computer program showed significant differences (P<0.05) between HGF/SF-treated groups and control groups except SHPG, heregulin, and DAP-1 groups.

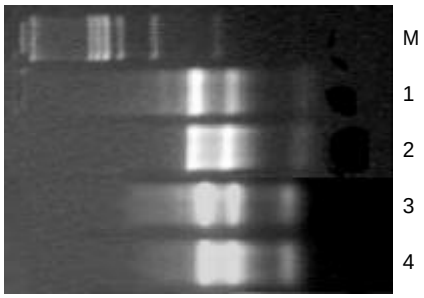

Figure 1 Result of total RNA electrophoresis and hot-stabilization test. M: PCR marker; 1: RNA of HGF/SF-treated group; 2: RNA of control group; 3: RNA of HGF/SF-treated group after hot-treatment; 4: RNA of control group after hot-treatment.

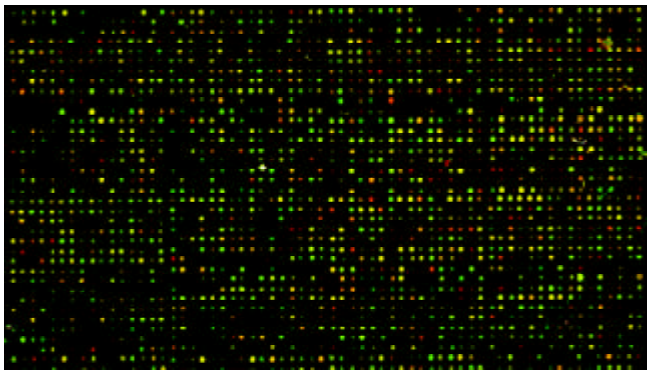

Figure 2 The overlaying image for bicolor fluorescence label on gene chip. red: high expression; green: low expression; yellow: no change in expression.

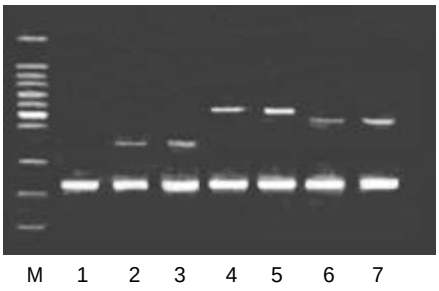

Figure 3 Result of RT-PCR for up-regulated genes. M: 100 bp DNA ladder marker; 1: negative control; 2: CAMK4 blank control; 3: CAMK4 HGF 80 ng/ml; 4: SHPG blank control; 5: SHPG HGF 80 ng/ml; 6: Heregulin blank control; 7: Heregulin HGF 80 ng/ml.

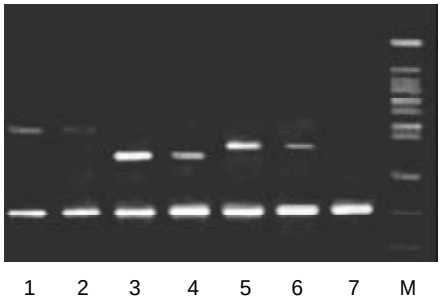

Figure 4 Result of RT-PCR for down-regulated genes. 1: p130 blank control; 2: p130 HGF 80 ng/ml; 3: DAP-1 blank control; 4: DAP-1 HGF 80 ng/ml; 5: TRAMP blank control; 6: TRAMP HGF 80 ng/ml; 7: negative control; M: 100 bp DNA ladder marker.

DISCUSSION

Reliability of the microarray assay

Gene chip, or DNA chip, including oligonucleotide chip synthesized *in situ* and cDNA microarray by direct-spot or cDNA array[22-24], is a key technique platform[25-27] in post-genome times for its striking superiority of high-throughput, high-parallelity, high-sensitivity, micromation and automatization. cDNA microarray is a mature and widespread technique. Its stability, reliability and reproducibility have been confirmed by many investigators[28-31]. The microarray experiment in this research was successful and under strict quality control, with mRNA in good quality and no degradation tested by the test of hot-stabilization. In our experiment the built-in positive and negative control showed the qualified results, the scanning images showed lower noise background, and the positive spots indicated high intensity of signal with clear circle appearance. All the parameters such as odds of spot average intensity with background for the HGF/SF-treated group and for the control, normalization coefficient, and ratio of Cy5/Cy3 by self-check test were in accord with theoretic values of successful experiment. The expressions of the 6 differential expression genes randomly selected by RT-PCR were confirmed to be consistent with the results of microarray. These results indicate satisfactory reliability of the microarray experiment.

Superiority of microarray for study of target genes related to the HGF/SF-met signaling

It has been evidenced that HGF/SF-met signaling plays an important, even a critical role in tumor progression, invasion and metastasis. Hamasuna *et al*[32] showed that HGF/SF activated membrane type metalloproteinases (MT1-MMP) in dosage-related manner and decreased wild-type metalloproteinases inhibitor TIMP-2 mRNA. They indicated that glioblastoma cells U251 excreted more MMP-2 protein and MMP-2 mRNA expression increased by 2.5 fold by HGF/SF stimulation. Abouader *et al*[33] argued that HGF/SF-met signaling was a key molecule path for control of glioblastoma cells growth, progression, invasion and metastasis. Recently Webb *et al*[34] have confirmed that HGF/SF-met-uPA -plasmin pathway exists in some tumor cell lines and is related to invasion, metastasis and other malignant behaviors. Only a few genes can be investigated by the traditional technology of molecular biology and the whole transcriptional gene expression profiles of HGF/SF-met signaling pathway can hardly be explored. In this paper the transcriptional gene expression profiles of HGF/SF-met signaling pathway in colorectal carcinoma cells were discussed for the first time so as to explore the target genes related to the signaling pathway. The results indicated that HGF/SF-met signaling might activate oncogenes, signal transduction genes, apoptosis-related genes, metastasis related genes and many other genes with up-regulation effects, and meanwhile it might down-regulate a number of genes. It is suggested that a complex signaling-adjusting-gene-expression network may be in existence, and contribute to extensive gene transcription effects and comprehensive biological roles. The complexity of HGF/SF-met signaling to control the gene expression was revealed as a whole by the gene chip technology, by which it manifested incomparable superiority.

Transcriptional gene expression profiles of HGF/SF-met signaling

Of the 4 004 human genes analyzed by microarray (totally 4 096 spots, subtracted 92 built-in positive and negative control

spots), 129 genes (holding 3.22 % of the investigated genes) revealed differential expression in the HGF/SF-treated groups compared with the control groups, which supplied abundant information about target genes of HGF/SF-met signaling. Among the 129 differential expression genes, 61 genes were up-regulated (holding 1.52 % of the investigated genes), and 68 genes were down-regulated (holding 1.70 % of the investigated genes). The expressions of some differential genes analyzed by microarray, for instance, collagenase IV[35], catenin[36], were consistent with the results reported in literatures that they were uncovered by traditional technology. Still a number of genes with differential expression not reported previously were found in our investigation. Some of them are genes with unknown function. Some genes with elevated expression by HGF/SF stimulation not reported previously are listed as following: Syndeans-2, calmodulin-dependent protein kinase IV(CaMK4), cadherein 8, protocadherin, calcium-dependent serine protein kinase (CASK), human keractnocyte growth factor(KGF), Heregulin, angiogenin, *etc*. In a word, the up-regulated genes by HGF/SF stimulation usually belong to cell growth factor genes, cell surface receptor genes, angiogenesis genes, cell cycle positive-regulation genes, calcium-, MAPK signaling-related genes, transcription factor, cytoskeleton regulation genes, and nuclei-receptor genes. These up-regulation genes stimulating cell growth, promoting cell transformation, resisting apoptosis, facilitating cell locomotion, accelerating signal conduction, and promoting vascularization and extracellular matrix lysis[37-44], may provide a foundation for mitogen, motogen, and morphogen activity in HGF/SF-met signaling pathway further.

Versatile effects on down-regulated gene expression by HGF/SF-met signaling have been found in this microarray assay. The genes of reduced expression by HGF/SF stimulation not reported previously include dual-specificity phosphatase 6 (DUSP6), SPINT2 (serine protease inhibitor, Kunitz-type 2, hepatocyte growth factor activator inhibitor type 2), TIMP1(tissue inhibitor of metalloproteinases 1), elastase inhibitive factor, TAPA1(Target of antiproliferative antibody 1, CD81), MRP-1 (motility-related protein 1, CD9), PRB2/p130, pRB2/p107, TRAMP (TNF receptor-related apoptosis mediating protein, DR3), WD40, DAP-1, etc. On the whole, the adjustability of multi-aspects and multi-targets in down-regulation of gene expression in colorectal carcinoma cells by HGF/SF-met signaling was revealed by microarray assay. The down-regulated genes by HGF/SF stimulation usually belong to cell death correlated receptor genes, transmembrane-4 superfamily, cell cycle negative-regulation genes, calcium and MAPK signaling-related negative genes, cytoskeleton rearrangement inhibitors, anti-oncogene and protease inhibitors. These genes are responsible for the negative control of cell function, which makes reinforcement and maintenance in stimulation of cell growth, promotion of cell transformation, resistance to apoptosis, facilitation for cell locomotion, acceleration of signal transduction, promotion of vascularization and lysis of extracellular matrix[45-56]. These are another annotation for mitogen, motogen, and morphogen activity of HGF/SF-met signaling pathway in tumor progression, also the first confirmation of pluripotency and versatility in regulation of gene expression by HGF/SF-met signaling.

The transcriptional gene expression profiles induced by HGF/SF-met signaling pathway in the colorectal carcinoma cells were described by cDNA microarray technology, and meanwhile the complexity and pluripotency of regulation in gene expression were also revealed for the first time. A majority of the genes with differential expression can be explained by the existing scientific theories, although some of them have unknown-function and a few of them cannot be explained reasonably for the time being, which deserve further investigation.

REFERENCES

1 **Stuart KA,** Riordan SM, Lidder S, Crostella L, Williams R, Skouteris GG. Hepatocyte growth factor / scatter factor-induced intracellular signalling. *Int J Exp Pathol* 2000; **81:** 17-30

2 **Ueoka Y**, Kato K, Kuriaki Y, Horiuchi S, Terao Y, Nishida J, Ueno H, Wake N. Hepatocyte growth factor modulates motility and invasiveness of ovarian carcinomas via Ras-mediated pathway. *Br J Cancer* 2000; **82:** 891-899

3 **Delehedde M,** Sergeant N, Lyon M, Rudland PS, Fernig DG. Hepatocyte growth factor / scatter factor stimulates migration of rat mammary fibroblasts through both mitogen-activated protein kinase and phosphatidylinositol 3-kinase / Akt pathways. *Eur J Biochem* 2001; **268:** 4423-4429

4 **Liu ZX**, Nickel CH, Cantley LG. HGF promotes adhesion of ATP-depleted renal tubular epithelial cells in MAPK-dependent manner. *Am J Physiol Renal Physiol* 2001; **281**: 62-70

5 **Rodrigues GA**, Park M, Schlessinger J. Activation of the JNK pathway is essential for transformation by the Met oncogene. *EMBO J* 1997; **16**: 2634-2645

6 **Awasthi V,** King RJ. PKC, p42 / p44 MAPK, and p38 MAPK are required for HGF-induced proliferation of H441 cells. *Am J Physiol Lung Cell Mol Physiol* 2000; **279**: 942-949

7 **Day RM**, Cioce V, Breckenridge D, Castagnino P, Bottaro DP. Differential signaling by alternative HGF isoforms through c-Met: activation of both MAP kinase and PI 3-kinase pathways is insufficient for mitogenesis. *Oncogene* 1999; **18:** 3399-3406

8 **Abounader R**, Ranganathan S, Kim BY, Nichols C, Laterra J. Signaling pathways in the induction of c-met receptor expression by its ligand scatter factor / hepatocyte growth factor in human glioblastoma. *J Neurochem* 2001; **76:** 1497-1508

9 **Sipeki S**, Bander E, Buday L, Farkas G, Bacsy E, Ways DK, Farago A. Phosphatidylinositol 3-kinase contributes to Erk1 / Erk2 MAP kinase activation associated with hepatocyte growth factor-induced cell scattering. *Cell Signal* 1999; **11**: 885-890

10 **Wong AS**, Leung PC, Auersperg N. Hepatocyte growth factor promotes in vitro scattering and morphogenesis human cervical carcinoma cells. *Gynecol Oncol* 2000; **78**: 158-165

11 **Hiscox S,** Jiang WG. Association of the HGF / SF receptor, c-met, with the cell-surface adhesion molecule, E-cadherin, and catenins in human tumor cells. *Biochem Biophys Res Commun* 1999; **261:** 406-411

12 **Kitamura S,** Kondo S, Shinomura Y, Kanayama S, Miyazaki Y, Kiyohara T, Hiraoka S, Matsuzawa Y. Met / HGF receptor modulates bcl-w expression and inhibits apoptosis in human colorectal cancers. *Br J Cancer* 2000; **83:** 668-673

13 **Luo YQ,** Wu MC, Cong WM. Gene expression of hepatocyte growth factor and its receptor in HCC and nontumorous liver tissues. *World J Gastroenterol* 1999; **5:** 119-121

14 **Liu LX**, Jiang HC, Liu ZH, Zhou J, Zhang WH, Zhu AL, Wang XQ, Wu M. Integrin gene expression profiles of human hepatocellular carcinoma. *World J Gastroenterol* 2002; **8:** 631-637

15 **Schena M,** Shalon D, Heller R, Chai A, Brown PO, Davis RW. Parallel human genome analysis: microarray-based expression monitoring of 1000 genes. *Proc Natl Acad Sci U S A* 1996; **93:** 10614-10619

16 **Heller RA**, Schena M, Chai A, Shalon D, Bedilion T, Gilmore J, Woolley DE, Davis RW. Discovery and analysis of inflammatory disease-related genes using cDNA microarrays. *Proc Natl Acad Sci U S A* 1997; **94**: 2150-2155

17 **Schena M,** Shalon D, Davis RW, Brown PO. Quantitative monitoring of gene expression patterns with a complementary DNA microarray. *Science* 1995; **270:** 467-470

18 **Shirota Y,** Kaneko S, Honda M, Kawai HF, Kobayashi K. Identification of differentially expressed genes in hepatocellular carcinoma with cDNA microarrays. *Hepatology* 2001; **33:** 832-840

19 **Raouf A**, Seth A. Discovery of osteoblast-associated genes using cDNA microarrays. *Bone* 2002; **30:** 463-471

20 **Verhofstede C,** Fransen K, Marissens D, Verhelst R, van der Groen G, Lauwers S, Zissis G, Plum J. Isolation of HIV-1 RNA from plasma: evaluation of eight different extraction methods. *J Virol Methods* 1996; **60**: 155-159

21 **Mannhalter C,** Koizar D, Mitterbauer G. Evaluation of RNA isolation methods and reference genes for RT-PCR analyses of rare target RNA. *Clin Chem Lab Med* 2000; **38:** 171-177

22 **Orr MS,** Scherf U. Large-scale gene expression analysis in molecular target discovery. *Leukemia* 2002; **16:** 473-477
23 **Bashyam MD**. Understanding cancer metastasis: an urgent need for using differential gene expression analysis. *Cancer* 2002; **94**: 1821-1829
24 **Ramaswamy S**, Golub TR. DNA microarrays in clinical oncology. *J Clin Oncol* 2002; **20:** 1932-1941
25 **Lakhani SR**, Ashworth A. Microarray and histopathological analysis of tumours: the future and the past? *Nat Rev Cancer* 2001; **1:** 151-157
26 **Bertucci F,** Houlgatte R, Nguyen C, Viens P, Jordan B R, Birnbaum D. Gene expression profiling of cancer by use of DNA arrays: how far from the clinic? *Lancet Oncol* 2001; **2:** 674-682
27 **Balmain A.** Cancer genetics: from Boveri and Mendel to microarrays. *Nat Rev Cancer* 2001; **1:** 77-82
28 **Xu S,** Mou H, Lu G, Zhu C, Yang Z, Gao Y, Lou H, Liu X, Cheng Y, Yang W. Gene expression profile differences in high and low metastatic human ovarian cancer cell lines by gene chip. *Chin Med J* 2002; **115:** 36-41
29 **Lu T,** Liu J, Le Cluyse EL, Zhou YS, Cheng ML, Waalkes MP. Application of cDNA microarray to the study of arsenic-induced liver diseases in the population of Guizhou, China. *Toxicol Sci* 2001; **59:** 185-192
30 **Shen XZ,** Chow JF, Koo MW, Cho CH. Gene expression profiles in gastric mucosa of sleep deprivation rats. *World J Gastroenterol* 2000; **6:** 754-758
31 **Cheung ST,** Chen X, Guan XY, Wong SY, Tai LS, Ng IO, So S, Fan ST. Identify metastasis-associated genes in hepatocellular carcinoma through clonality delineation for multinodular tumor. *Cancer Res* 2002; **62**: 4711-4721
32 **Hamasuna R,** Kataoka H, Moriyama T, Itoh H, Seiki M, Koono M. Regulation of matrix metalloproteinase-2 (MMP-2) by hepatocyte growth factor / scatter factor (HGF / SF) in human glioma cells: HGF / SF enhances MMP-2 expression and activation accompanying up-regulation of membrane type-1 MMP. *Int J Cancer*, 1999; **82:** 274-281
33 **Abounader R,** Ranganathan S, Lal B, Fielding K, Book A, Dietz H, Burger P, Laterra J. Reversion of human glioblastoma malignancy by U1 small nuclear RNA / ribozyme targeting of scatter factor / hepatocyte growth factor and c-met expression. *J Natl Cancer Inst* 1999; **91:** 1548-1556
34 **Webb CP,** Hose CD, Koochekpour S, Jeffers M, Oskarsson M, Sausville E, Monks A, Vande Woude GF. The geldanamycines are potent inhibitor of the hepatocyte growth factor / scatter factor-Met-urokinase plasminogen activator-plasmin proteolytic netwok. *Cancer Res*, 2000; **60:** 342-349
35 **Nabeshima K,** Inoue T, Shimao Y, Okada Y, Itoh Y, Seiki M, Koono M. Front-cell-specific expression of membrane-type 1 matrix metalloproteinase and gelatinase A during cohort migration of colon carcinoma cells induced by hepatocyte growth factor / scatter factor. *Cancer Res* 2000; **60:** 3364-3369
36 **Hiscox S,** Jiang WG. Hepatocyte growth factor / scatter factor disrupts epithelial tumour cell-cell adhesion: involvement of beta-catenin. *Anticancer Res* 1999; **19:** 509-517
37 **Contreras HR,** Fabre M, Granes F, Casaroli-Marano R, Rocamora N, Herreros AG, Reina M, Vilaro S. Syndecan-2 expression in colorectal cancer-derived HT-29 M6 epithelial cells induces a migratory phenotype. *Biochem Biophys Res Commun* 2001; **286:** 742-751
38 **Munesue S,** Kusano Y, Oguri K, Itano N, Yoshitomi Y, Nakanishi H, Yamashina I, Okayama M. The role of syndecan-2 in regulation of actin-cytoskeletal organization of Lewis lung carcinoma-derived metastatic clones. *Biochem J* 2002; **363:** 201-209
39 **Tamura N,** Tai Y, Sugimoto K, Kobayashi R, Konishi R, Nishioka M, Masaki T, Nagahata S, Tokuda M. Enhanced expression and activation of Ca(2+) / calmodulin-dependent protein kinase IV in hepatocellular carcinoma. *Cancer* 2000; **89:** 1910-1916
40 **Williams CL,** Phelps SH, Porter RA. Expression of Ca2+ / calmodulin-dependent protein kinase types II and IV, and reduced DNA synthesis due to the Ca2+ / calmodulin-dependent protein kinase inhibitor KN-62 (1-[N,O-bis(5-isoquinolinesulfonyl)-N-methyl-L- tyrosyl]-4-phenyl piperazine) in small cell lung carcinoma. *Biochem Pharmacol* 1996; **51:** 707-715
41 **Wilson SE,** Weng J, Chwang EL, Gollahon L, Leitch AM, Shay JW. Hepatocyte growth factor (HGF), keratinocyte growth factor (KGF), and their receptors in human breast cells and tissues: alternative receptors. *Cell Mol Biol Res* 1994; **40:** 337-350
42 **Hijazi MM,** Thompson EW, Tang C, Coopman P, Torri JA, Yang D, Mueller SC, Lupu R. Heregulin regulates the actin cytoskeleton and promotes invasive properties in breast cancer cell lines. *Int J Oncol* 2000; **17:** 629-641
43 **Etoh T,** Shibuta K, Barnard GF, Kitano S, Mori M. Angiogenin expression in human colorectal cancer: the role of focal macrophage infiltration. *Clin Cancer Res* 2000; **6:** 3545-3551
44 **Lixin R,** Efthymiadis A, Henderson B, Jans DA. Novel properties of the nucleolar targeting signal of human angiogenin. *Biochem Biophys Res Commun* 2001; **284**: 185-193
45 **Rao CN,** Lakka SS, Kin Y, Konduri SD, Fuller GN, Mohanam S, Rao JS. Expression of tissue factor pathway inhibitor 2 inversely correlates during the progression of human gliomas. *Clin Cancer Res* 2001; **7:** 570-576
46 **Kataoka H,** Uchino H, Denda K, Kitamura N, Itoh H, Tsubouchi H, Nabeshima K, Koono M. Evaluation of hepatocyte growth factor activator inhibitor expression in normal and malignant colonic mucosa. *Cancer Lett* 1998; **128:** 219-227
47 **Longo N,** Yanez-Mo M, Mittelbrunn M, de la Rosa G, Munoz ML, Sanchez-Madrid F, Sanchez-Mateos P. Regulatory role of tetraspanin CD9 in tumor-endothelial cell interaction during transendothelial invasion of melanoma cells. *Blood* 2001; **98:** 3717-3726
48 **Hashida H,** Takabayashi A, Tokuhara T, Taki T, Kondo K, Kohno N, Yamaoka Y, Miyake M. Integrin alpha3 expression as a prognostic factor in colon cancer: Association with MRP-1 / CD9 and KAI1 / CD82. *Int J Cancer* 2002; **97:** 518-525
49 **Luo D,** Liu QF, Gove C, Naomov NV, Su JJ, Williams R. Analysis of N-ras gene mutation and p53 gene expression in human hepatocellular carcinomas. *World J Gastroenterol* 1998; **4:** 97-99
50 **Wang L,** Lu W, Chen YG, Zhou XM, Gu JR. Comparison of gene expression between normal colon mucosa and colon carcinoma by means of messenger RNA differential display. *World J Gastroenterol* 1999; **5:** 533-534
51 **Sun BH,** Zhang J, Wang BJ, Zhao XP, Wang YK, Yu ZQ, Yang DL, Hao LJ. Analysis of in vivo patterns of caspase 3 gene expression in primary hepatocellular carcinoma and its relationship to p21(WAF1) expression and hepatic apoptosis. *World J Gastroenterol* 2000; **6:** 356-360
52 **Wu BP,** Zhang YL, Zhou DY, Gao CF, Lai ZS. Microsatellite instability, MMR gene expression and proliferation kinetics in colorectal cancer with famillial predisposition. *World J Gastroenterol* 2000; **6:** 902-905
53 **Berditchevski F,** Odintsova E. Characterization of integrin-tetraspanin adhesion complexes: role of tetraspanins in integrin signaling. *J Cell Biol* 1999; **146:** 477-492
54 **Tanaka N,** Ogi K, Odajima T, Dehari H, Yamada S, Sonoda T, Kohama G. pRb2 / p130 protein expression is correlated with clinicopathologic findings in patients with oral squamous cell carcinoma. *Cancer* 2001; **92:** 2117-2125
55 **Paggi MG,** Giordano A. Who is the boss in the retinoblastoma family? The point of view of Rb2 / p130, the little brother. *Cancer Res* 2001; **61:** 4651-4654
56 **Classon M,** Dyson N. p107 and p130: versatile proteins with interesting pockets. *Exp Cell Res* 2001; **264:** 135-147

Edited by Zhao P and Wang XL

P.O.Box 2345, Beijing 100023,China
Fax: +86-10-85381893
E-mail: wjg@wjgnet.com www.wjgnet.com

World J Gastroenterol 2003;9(8):1739-1742
World Journal of Gastroenterology
 ISSN 1007-9327

• VIRAL HEPATITIS •

Pathogenicity of GB virus C on virus hepatitis and hemodialysis patients

Wan-Fu Zhu, Li-Min Yin, Peng Li, Jian Huang, Hui Zhuang

Wan-Fu Zhu, Li-Min Yin, Peng Li, Jian Huang, Hui Zhuang, Department of Microbiology, School of Basic Medical Sciences, Peking University, Beijing 100083, China
Supported by the National Natural Science Foundation of China, No.39870695
Correspondence to: Professor Wan-Fu Zhu, Department of Microbiology, School of Basic Medical Sciences, Peking University, Beijing 100083, China. zhuwanfu@sun.bjmu.edu.cn
Telephone: +86-10-82801599 **Fax:** +86-10-82801599
Received: 2003-01-04 **Accepted:** 2003-02-13

Abstract

AIM: To determine the pathogenicity of GB virus C (GBV-C) on liver and the effects of its co-infection on the clinical features and prognosis of patients with hepatitis B and C.

METHODS: Cross-sectional study was carried out in 413 patients with acute, chronic hepatitis B or liver cirrhosis, and in 67 hemodialysis patients. A 20-month prospective cohort study was carried out in 95 hepatitis B and 80 hepatitis C patients. A reverse transcriptase nested polymerase chain reaction (RT-nPCR) of the 5'-noncoding region was used to detect circulating GBV-C RNA. Liver function was determined by an automated analyzer for all patients.

RESULTS: The prevalence of GBV-C in the high-risk populations with the virus transmitted via blood was high, ranging from 16.2 to 28.8 %. Co-infection with GBV-C in hepatitis B patients did not affect the clinical features of the disease or liver function. The dialysis patients infected with GBV-C alone did not develop functional changes to the liver. Prospective cohort study showed that GBV-C co-infection did not affect the clinical features, prognosis or negative serum conversion rate of chronic hepatitis B and C.

CONCLUSION: The results suggest that GBV-C has no marked pathogenicity on liver, so it may not be a hepatitis virus.

Zhu WF, Yin LM, Li P, Huang J, Zhuang H. Pathogenicity of GB virus C on virus hepatitis and hemodialysis patients. *World J Gastroenterol* 2003; 9(8): 1739-1742
http://www.wjgnet.com/1007-9327/9/1739.asp

INTRODUCTION

Hepatitis B and C viruses (HBV, HCV) jointly contribute to 90 % of cases of post-transfusion non-A, non-B hepatitis (HNANB). The remaining 10 % of cases could not be attributed to any of the other known hepatitis viruses or other factors such as alcohol, drug, or any disease related causes[1,2]. These cases are named non-A-E hepatitis (HNA-E) and may be caused by an unknown viral agent. In 1995 and 1996, GB virus-C (GBV-C) and hepatitis G virus (HGV) were cloned by Simons *et al.* and Linnen *et al.*, respectively, in the United States[3,4]. Sequence analysis revealed that these two viruses had 85 % and 95 % identical nucleotide and amino acid sequences, respectively. And now these two viruses are named as GBV-C. Initially, GBV-C was isolated from the serum of patients with HNA-E[3,4]. However, there are still a lot of arguments up to now on the pathogenicity of GBV-C on liver and on whether GBV-C is an aetiological agent of HNA-E[5,6]. The prevalence of GBV-C in patients with chronic hepatitis B or chronic hepatitis C is very common, because of the similar transmission routes[7-12]. In the present study, we investigated the prevalence of GBV-C and evaluated its pathogenicity on liver with a cross-sectional study in 413 patients with acute, chronic hepatitis B, or liver cirrhosis, and in 67 hemodialysis patients. We also carried out a 20-month prospective cohort study in 95 patients with chronic hepatitis B and 80 patients with chronic hepatitis C. The results suggest that GBV-C has no marked pathogenicity on liver, so it may not be a new hepatitis virus.

MATERIALS AND METHODS

Patients

A total of 413 inpatients with confirmed diagnoses of acute, chronic hepatitis B or liver cirrhosis in two hospitals for infectious diseases in Beijing from January to December 2000 were enrolled in this study. Anti-HAV IgM, anti-HCV, anti-HDV and anti-HEV antibodies were all negative in these patients. Serum samples of the inpatients were collected and tested to assess liver biochemical characteristics on the day of admission. The rest serum was tested and stored at -80 ℃ for pathogen analysis.

Serum samples of hemodialysis patients with renal failure were collected from 67 patients in 3 general hospitals from December 2001 to March 2002 in Beijing. All samples were stored at -30 ℃ before analysis.

A cohort of 95 patients with chronic hepatitis B and 80 patients with chronic hepatitis C was enrolled from villages of a county in Zhoukou area, Henan Province. All patients were infected with HBV or HCV from 1991 to 1992 as a consequence of blood donation. All the patients had persistently elevated serum alanine aminotransferase (ALT) (at least 1.5 times the upper limit of the normal level) and were positive for serum HBV DNA or HCV RNA as detected by PCR or RT-PCR, respectively. All the patients were negative for serum anti-HAV IgM and anti-HEV. The average disease course of these patients was 3 years when investigation and confirming diagnosis were carried out in April 1994. All the patients of the cohort showed no evidence of liver cirrhosis or hepatocellular carcinoma in regular ultrasonic graphic examinations. All the patients were followed up twice, i.e., 6 and 20 months after the first investigation.

Laboratory examination

For GBV-C RNA detection, RNA was first extracted from 50 μl of serum using a commercial RNA extraction kit (Promega, Z5110). Reverse transcriptase and nested polymerase chain reactions (RT-nPCR), 35 cycles for two round, were performed using a PCR machine (SABC Thinker Series II, Sino-American Biotechnology Company, China). The primers used were from

the 5' -noncoding region of the GBV-C genome, outer primers (sense, 5' -TCTTGGTAGCCACTATAGGTG-3' , and antisense, 5' -GGCAAAGCCTATTGGTCAAG-3'), and inner primers (sense, 5' -AGAAAGAGCACGGTCCACAG-3' , and antisense, 5' -CCACTGGTCCTTGTCAACTC-3'). The amplified product (158 base pairs) was visualized under ultraviolet light after gel electrophoresis and stained with ethidium bromide. GBV-C RNA was assessed in duplicate sera and scored as positive only when consistent results were obtained. Liver biochemistry tests including alanine aminotransferase (ALT), aspartate aminotransferase (AST), total bilirubin (TBil), direct bilirubin (DBil), total protein (Tp), and serum albumin/globulin ratio (A/G) were measured with an automated analyzer.

Statistical analysis

Data in the text and tables were expressed as $\bar{x}\pm s$. Student' s *t*-test and one-way analysis of variance were used for statistical analysis according to the data obtained. For all tests, *P* values less than 0.05 were considered to be statistically significant, and *P* values less than 0.01 were considered to be greatly statistically significant.

RESULTS

Of the serum samples from 413 patients infected with HBV, 67 were co-infected with GBV-C (16.22 %). 169 cases had integrated clinical data. The patients suffering from acute, chronic hepatitis B or liver cirrhosis were grouped on the basis of the presence or absence of GBV-C co-infection, and the levels of ALT, AST, TBil, DBil, Tp of the different groups were compared (Table 1).

Results shown in Table 1 indicated that there was no significant difference in the serum biochemistry characteristics of 3 types of patients (acute, chronic hepatitis B and liver cirrhosis) between GBV-C RNA infected group and non-infected group ($P>0.05$).

11 of the 67 dialysis patients were GBV-C RNA positive (16.42 %) and the positive rate of GBV-C RNA increased with the number of times of dialysis. The comparison of serum ALT and AST levels in 67 patients infected with different viruses is shown in Table 2.

Table 2 Comparison of serum ALT and AST in dialysis patients with different virus infection

Group	*n*	Average dialysis times	ALT/IU·L^{-1}	AST/IU·L^{-1}
(1) HBV DNA(+) HCV RNA(-) GBV-C RNA(-)	11	243.75±224.53	31.63±22.32	35.12±18.06
(2) HBV DNA(-) HCV RNA(+) GBV-C RNA(-)	6	306.67±296.41	30.67±9.45	25.00±12.28
(3) HBV DNA(-) HCV RNA(-) GBV-C RNA(+)	8	353.40±309.45	20.67±11.72	17.00±1.00
(4) HBV DNA(-) HCV RNA(-) GBV-C RNA(-)	37	116.45±103.02	15.37±6.83	20.00±7.04

Table 1 Comparison of biochemistry characteristics in all types of patients with or without GBV-C infection

Group	*n*	ALT/IU·L^{-1}	AST/IU·L^{-1}	TBil/μmol·L^{-1}	DBil/μmol·L^{-1}	Tp/g·L^{-1}
Acute hepatitis B						
GBV-C RNA(+)	13	1173.92±961.98	565.69±405.32	5.18±3.47	3.54±2.66	68.44±12.14
GBV-C RNA(-)	33	1380.27±906.14	620.06±405.32	6.52±6.61	4.57±4.51	67.84±12.42
Chronic hepatitis B						
GBV-C RNA(+)	24	366.33±237.36	289.42±201.32	6.48±7.34	3.98±4.50	71.30±8.57
GBV-C RNA(-)	35	312.91±432.82	227.29±292.17	3.29±5.58	2.21±4.24	71.06±7.66
Liver cirrhosis						
GBV-C RNA(+)	30	71.67±74.13	96.73±87.21	5.54±7.44	3.62±5.33	66.46±8.75
GBV-C RNA(-)	34	92.68±80.33	106.15±94.81	7.67±10.30	5.20±5.80	62.58±10.99
Total						
GBV-C RNA(+)	67	400.51±585.36	255.22±301.71	5.73±6.81	3.69±4.46	68.80±9.61
GBV-C RNA(-)	102	578.63±807.04	314.98±345.05	5.85±7.85	3.87±4.80	67.21±10.92

No significant difference ($P>0.05$) was found in all the biochemistry characteristics between hepatitis B patients with or without GBV-C infection.

Table 3 Comparison of biochemistry characteristics between chronic hepatitis B patients with or without GBV-C infection

GBV-C RNA	*n*	A/G	ALT/IU·L^{-1}	AST/IU·L^{-1}	TBil/μmol·L^{-1}
(1) Positive group	24	1.65±0.26	90.84±48.43	43.21±31.56	5.91±1.86
(2) Negative group	71	1.63±0.21	95.36±51.96	44.45±38.07	7.66±1.95

No significant difference ($P>0.05$) was found in all the biochemistry characteristics between the two groups.

Table 4 Comparison of biochemistry characteristics between chronic hepatitis C patients with or without GBV-C infection

GBV-C RNA	*n*	A/G	ALT/IU·L^{-1}	AST/IU·L^{-1}	TBil/μmol·L^{-1}
(1) Positive group	23	1.82±0.30	110.23±59.61	45.96±40.11	4.53±1.55
(2) Negative group	57	1.65±0.25	97.65±56.74	52.94±48.00	5.77±1.73

No significant difference ($P>0.05$) was found in all the biochemistry characteristics between the two groups.

On statistic analysis, ALT levels were significantly different between groups 1 and 4 ($P<0.01$) and groups 2 and 4 ($P<0.05$). AST levels were also significantly different between groups 1 and 4 ($P<0.01$). The results showed a significant elevation in the levels of ALT and AST in hemodialysis patients infected with HBV or HCV compared with that in those not infected with the two viruses. Significant difference ($P<0.05$) was found in dialysis times between groups 2 and 4, and groups 3 and 4. Three patients had abnormal liver function (ALT>40 IU/L, AST>40 IU/L), among them one was infected with HCV, the other two were infected with HBV. Serum ALT and AST levels were normal in patients with GBV-C infection alone.

A cohort study was carried out in 95 patients with chronic hepatitis B and 80 patients with chronic hepatitis C enrolled from villages in Henan Province. Serum GBV-C was positive in 24 (25.26 %) chronic hepatitis B patients and 23 (28.75 %) chronic hepatitis C patients (Tables 3 and 4).

When following up the patients 6 months later, we found that 23 of the 95 chronic hepatitis B patients (24.21 %) became HBV DNA negative and 21 of the 80 (26.25 %) chronic hepatitis C patients became HCV RNA negative. GBV-C RNA could not be detected in 12.50 % (3/95) chronic hepatitis B patients and in 17.39 % (4/80) chronic hepatitis C patients. Table 5 and Table 6 show the biochemistry characteristics of chronic hepatitis B and C patients.

Table 5 Comparison of biochemistry characteristics between chronic hepatitis B patients with or without GBV-C infection at the 6-month follow-up

Group	*n*	A/G	ALT/IU·L^{-1}	AST/IU·L^{-1}	TBil/μmol·L^{-1}
(1) HBV DNA(+) GBV-C RNA(+)	14	1.74±0.19	93.29±60.67	29.14±13.87	7.64±5.47
(2) HBV DNA (+) GBV-C RNA (-)	58	1.73±0.18	62.33±41.67	27.68±11.99	6.10±2.09
(3) HBV DNA (-) GBV-C RNA (+)	7	1.61±0.11	30.00±7.80	21.57±8.18	7.57±3.41
(4) HBV DNA (-) GBV-C RNA (-)	16	1.64±0.14	32.65±17.01	26.65±11.96	7.71±2.76

Significant difference ($P<0.05$) was found only in ALT between group 1 and group 3, group 2 and group 4. No significant difference ($P>0.05$) was found in other biochemistry characteristics among the 4 groups.

Table 6 Comparison of biochemistry characteristics between chronic hepatitis C patients with or without GBV-C infection at the 6-month follow-up

Group	*n*	A/G	ALT/IU·L^{-1}	AST/IU·L^{-1}	TBil/μmol·L^{-1}
(1) HCV RNA(+) GBV-C RNA(+)	11	1.76±0.17	127.11±82.12	41.13±19.07	7.49±5.82
(2) HCV RNA(+) GBV-C RNA (-)	48	1.82±0.20	71.62±47.74	26.05±12.49	7.97±3.91
(3) HCV RNA (-) GBV-C RNA(+)	8	1.60±0.13	33.11±8.08	22.97±9.78	7.26±4.25
(4) HCV RNA (-) GBV-C RNA (-)	13	1.60±0.14	30.74±20.01	24.65±11.84	7.65±3.23

Significant difference ($P<0.05$) was found both in ALT between group 1 and group 3, group 2 and group 4, and in AST between group 1 and group 4. No significant difference ($P>0.05$) was found in other biochemistry characteristics among the 4 groups.

At the 20-month follow up, the biochemistry characteristics of chronic hepatitis B and C patients were compared between two groups: one with and the other without GBV-C co-infection (Tables 7 and 8). At this time point, 26.0 % (25/95) chronic hepatitis B patients and 20.0 % (16/80) chronic hepatitis C patients were lost in the follow up.

Table 7 Comparison of biochemistry characteristics between chronic hepatitis B patients with or without GBV-C infection after 20 months

Group	*n*	ALT/IU·L^{-1}	AST/IU·L^{-1}
(1) HBV DNA(+) GBV-C RNA(+)	8	52.13±44.90	44.25±28.42
(2) HBV DNA (+) GBV-C RNA (-)	30	44.40±37.26	34.67±24.23
(3) HBV DNA (-) GBV-C RNA (+)	8	28.14±15.36	25.29±17.21
(4) HBV DNA (-) GBV-C RNA (-)	24	25.15±11.59	25.73±13.16

Significant difference ($P<0.05$) was found only in ALT and AST between group 1 and group 3, and group 2 and group 4.

Table 8 Comparison of biochemistry characteristics between chronic hepatitis C patients with or without GBV-C infection after 20 months

Group	*n*	ALT/IU·L^{-1}	AST/IU·L^{-1}
(1) HCV RNA(+) GBV-C RNA(+)	6	72.24±73.87	49.29±48.49
(2) HCV RNA(+) GBV-C RNA (-)	22	42.43±39.10	32.91±30.57
(3) HCV RNA (-) GBV-C RNA(+)	7	26.98±24.47	25.11±19.07
(4) HCV RNA (-) GBV-C RNA (-)	29	25.39±13.16	26.74±16.99

Significant difference ($P<0.05$) was found only in ALT and AST between group 1 and group 3, and group 2 and group 4.

After 20-month follow up, correlation was seen between the abnormal levels of the liver biochemistry characteristics and HBV DNA in chronic hepatitis B patients. However, no correlation was found between the abnormal levels of the liver function and co-infection with GBV-C. The same result was found in chronic hepatitis C patients. During the period of follow up for 20 months, 50.00 % (8/16) hepatitis B patients with GBV-C infection and 44.44 % (24/54) hepatitis B patients without GBV-C infection became HBV DNA undetectable. 53.85 % (7/13) hepatitis C patients with GBV-C infection and 56.86 % (29/51) hepatitis C patients without GBV-C infection became HCV RNA undetectable. The rates of negative serum conversion of HBV DNA and HCV RNA were not significantly different between the two groups.

DISCUSSION

Since GBV-C was cloned, there have been a lot of arguments on the pathogenicity of GBV-C. Although a number of reports have indicated that GBV-C can induce acute, chronic, and even fulminant hepatitis[13-16], most of the clinical observations have demonstrated that GBV-C infection alone has little significance in causing liver damage in human[17-20]. There were 363 research publications on GBV-C/HGV in MEDLINE database from 1999 to February 2001, among which only 8 supported GBV-C pathogenicity on the liver. Most researches implicated that no correlation existed between GBV-C and liver diseases. Patients with HBV or HCV co-infected with GBV-C did not have different clinical manifestations and outcomes when compared with patients with HBV or HCV infection alone[21-23].

GBV-C, HBV and HCV have a similar route of transmission. Many of the reports limited their research on the prevalence of GBV-C in hepatitis B and hepatitis C patients and had relatively small numbers of cases. Therefore, it was difficult for them to draw a definite conclusion on GBV-C pathogenicity on the liver. The subjects of this study were a large sample in the high-risk population with GBV-C infection (hepatitis B, hepatitis C and hemodialysis patients). This work combined the cross-sectional and prospective cohort studies and applied the methods of cross-experimental design and analysis. Therefore, it could analyze more reasonably the pure effects of GBV- C infection on liver.

All data in this study were pooled from experiments carried out by many graduate students and repeated many times. Hepatitis B, hepatitis C and hemodialysis patients belonged to the high-risk population transmitted via blood. Previous investigations have shown that there was no significant difference between the prevalence rates of GBV-C in patients with HNA-E and of the aforementioned high-risk population (P>0.05)[23-25]. So these findings do not support the argument that GBV-C was the etiological factor of HNA-E. No significant difference was seen in the abnormal level of liver biochemistry characteristics between positive and negative serum GBV-C RNA in acute, chronic hepatitis B or liver cirrhosis patients (P>0.05). But the abnormal level of liver biochemistry characteristics correlated well with HBV DNA. Therefore, these results demonstrated that co-infection with GBV-C did not affect the liver biochemistry characteristics and illness. Infection with HBV or HCV could elevate the level of liver enzymes (ALT and AST) in hemodialysis patients, but infection with GBV-C did not demonstrate such effects. So these results showed that the hemodialysis patients had no abnormal liver biochemistry characteristics when infected with GBV-C alone without the known hepatitis virus co-infection. The dynamic observation in 3 follow-ups of the cohort of chronic hepatitis B and C patients during a period of 20 months indicated that co-infection with GBV-C did not significantly affect the illness, outcome or rate of negative serum conversion. In summary, this work demonstrates that, though GBV-C is highly prevalent in high-risk populations with virus infection via blood, it seems to have no pathogenicity on the liver and therefore may not be a hepatitis virus.

ACKNOWLEDGMENTS

We are very grateful to Prof. Liu Shu-Lin for his revision of the manuscript.

REFERENCES

1 **Alter HJ,** Seeff LB. Transfusion associated hepatitis. In: Zuckerman AJ, Thomas HC, eds. Viral Hepatitis. *London: Churchill Livingstone* 1998: 489-513
2 **Karayiannis P,** Pickering J, Zampino R, Thomas HC. Natural history and molecular biology of hepatitis G virus / GB virus C. *Clin Diagn Virol* 1998; **10**: 103-111
3 **Simons JN,** Leary TP, Dawson GJ, Pilot-Matias TJ, Muerhoff AS, Schlauder GG, Desai SM, Mushahwar IK. Isolation of novel virus-like sequences associated with human hepatitis. *Nat Med* 1995; **1**: 564-569
4 **Linnen J,** Wages J Jr, Zhang-Keck ZY, Fry KE, Krawczynski KZ, Alter H, Koonin E, Gallagher M, Alter M, Hadziyannis S, Karayiannis P, Fung K, Nakatsuji Y, Shih JW, Young L, Piatak M Jr, Hoover C, Fernandez J, Chen S, Zou JC, Morris T, Hyams KC, Ismay S, Lifson JD, Kim JP. Molecular cloning and disease association of hepatitis G virus: a transfusion-transmissible agent. *Science* 1996; **271**: 505-508
5 **Grassi M,** Mammarella A, Sagliaschi G, Granati L, Musca A, Traditi F, Pezzella M. Persistent hepatitis G virus (HGV) infection in chronic hemodialysis patients and non-B, non-C chronic hepatitis. *Clin Chem Lab Med* 2001; **39**: 956-960
6 **De Filippi F,** Lampertico P, Soffredini R, Rumi MG, Lunghi G, Aroldi A, Tarantino A, Ponticelli C, Colombo M. High prevalence, low pathogenicity of hepatitis G virus in kidney transplant recipients. *Dig Liver Dis* 2001; **33**: 477-479
7 **Halasz R,** Weiland O, Sallberg M. GB virus C / hepatitis G virus. *Scand J Infect Dis* 2001; **33**: 572-580
8 **Kleinman S.** Hepatitis G virus biology, epidemiology, and clinical manifestations: Implications for blood safety. *Transfus Med Rev* 2001; **15**: 201-212
9 **Li G,** Ma HH, Lau GK, Leung YK, Yao CL, Chong YT, Tang WH, Yao JL. Prevalence of hepatitis G virus infection and homology of different viral strains in southern China. *World J Gastroenterol* 2002; **8**: 1081-1087
10 **Yan J,** Chen LL, Luo YH, Mao YF, He M. High frequencies of HGV and TTV infections in blood donors in hangzhou. *World J Gastroenterol* 2001; **7**: 637-641
11 **Yan J,** Dennin RH. A high frequency of GBV-C / HGV coinfection in hepatitis C patients in Germany. *World J Gastroenterol* 2000; **6**: 833-841
12 **Yan J**, Chen LL, Lou YL, Zhong XZ. Investigation of HGV and TTV infection in sera and saliva from non-hepatitis patients with oral diseases. *World J Gastroenterol* 2002; **8**: 857-862
13 **Kocabas E,** Antmen B, Yarkin F, Serin M, Aksungur P, Tanyeli A, Kilinc Y, Aksaray N. Prevalence of GB virus C / hepatitis G virus infection in pediatric patients receiving multiple transfusions in southern Turkey. *Turk J Pediatr* 1999; **41**: 81-90
14 **Tanaka T,** Hess G, Tanaka S, Kohara M. The significance of hepatitis G virus infection in patients with non-A to C hepatic diseases. *Hepatogastroenterology* 1999; **46**: 1870-1873
15 **Yoshiba M,** Okamoto H, Mishiro S. Detection of the GBV-C hepatitis virus genome in serum from patients with fulminant hepatitis of unknown aetiology. *Lancet* 1995; **346**: 1131-1132
16 **Xu JZ,** Yang ZG, Le MZ, Wang MR, He CL, Sui YH. A study on pathogenicity of hepatitis G virus. *World J Gastroenterol* 2001; **7**: 547-550
17 **Sathar M,** Soni P, York D. GB virus C / hepatitis G virus (GBV-C / HGV): still looking for a disease. *Int J Exp Pathol* 2000; **81**: 305-322
18 **Pessoa MG,** Terrault NA, Detmer J, Kolberg J, Collins M, Hassoba HM, Wright TL. Quantitation of hepatitis G and C viruses in the liver: evidence that hepatitis G virus is not hepatotropic. *Hepatology* 1998; **27**: 877-880
19 **Sarrazin C,** Ruster B, Lee JH, Kronenberger B, Roth WK, Zeuzem S. Prospective follow-up of patients with GBV-C / HGV infection: specific mutational patterns, clinical outcome, and genetic diversity. *J Med Virol* 2000; **62**: 191-198
20 **Shindo M,** Arai K, Okuno T. Long-term follow-up of hepatitis G virus / GB virus C replication in liver during and after interferon therapy in patients coinfected with hepatitis C and G viruses. *J Gastroenterol* 1999; **34**: 680-687
21 **Fattovich G,** Ribero ML, Favarato S, Azzario F, Donato F, Giustina G, Fasola M, Pantalena M, Portera G, Tagger A. Influence of GB virus-C / hepatitis G virus infection on the long-term course of chronic hepatitis B. *Liver* 1998; **18**: 360-365
22 **Kao JH,** Chen PJ, Lai MY, Chen W, Chen DS. Effects of GB virus-C / hepatitis G virus on hepatitis B and C viremia in multiple hepatitis virus infections. *Arch Virol* 1998; **143**: 797-802
23 **Yu ML,** Chuang WL, Dai CY, Lu SN, Wang JH, Huang JF, Chen SC, Lin ZY, Hsieh MY, Tsai JF, Wang LY, Chang WY. The serological and molecular epidemiology of GB virus C / hepatitis G virus infection in a hepatitis C and B endemic area. *J Infect* 2001; **42**: 61-66
24 **Li P,** Zhu WF, An WF, Li ZJ, Wang SP, Zhuang H. Cohort study on pathogenicity of hepatitis G virus mixed infection with hepatitis B and C virus. *Zhongguo Gonggong Weisheng* 2002; **18**: 911-913
25 **Huang J,** Zhu WF, Li Z, Sun JY, Hao W, Wang XM, Li P, Zhuang H. Pathogenicity study of hepatitis G virus mixed infection in chronic hepatitis B and C patients. *Ziran Kexue Jinzhan* 2002; **12**: 307-310

Edited by Pang LH

P.O.Box 2345, Beijing 100023,China
Fax: +86-10-85381893
E-mail: wjg@wjgnet.com www.wjgnet.com

World J Gastroenterol 2003;9(8):1743-1746
World Journal of Gastroenterology
 ISSN 1007-9327

• VIRAL HEPATITIS •

Novel assay of competitively differentiated polymerase chain reaction for screening point mutation of hepatitis B virus

Xiao-Mou Peng, Xue-Juan Chen, Jian-Guo Li, Lin Gu, Yang-Su Huang, Zhi-Liang Gao

Xiao-Mou Peng, Xue-Juan Chen, Jian-Guo Li, Lin Gu, Yang-Su Huang, Zhi-Liang Gao, Department of Infectious Diseases, the Third Affiliated Hospital, Zhongshan University, Guangzhou 510630, Guangdong Province, China
Supported by the Science Foundation of Guangdong Province, No. 99M04801G
Correspondence to: Xiao-Mou Peng, Department of Infectious Diseases, the Third Affiliated Hospital, Zhongshan University, Guangzhou 510630, China. xiaomoupeng@hotmail.com
Telephone: +86-20-85516867 Ext 2019 **Fax:** +86-20-85515940
Received: 2003-04-12 **Accepted:** 2003-05-17

Abstract

AIM: Point mutation, one of the commonest gene mutations, is the most important molecular pathogenesis of cancer and chronic infection. The commonest methods for detection of point mutation are based on polymerase chain reaction (PCR). These techniques, however, cannot be used in large scale screening since they are neither accurate nor simple. For this reason, this study established a novel method of competitively differentiated PCR (CD-PCR) for screening point mutation in clinical practice.

METHODS: Two competitively differentiated primers for mutant-type and wild-type templates respectively with an identically complemented region in 3' end except for last 2 base pairs and a different non-complemented region in 5' end were designed. Thus, competitive amplification might be carried out at a lower annealing temperature at first, and then differentiated amplification at a higher annealing temperature when primers could not combine with initial templates. The amplification was performed in one-tube. The products of CD-PCR were detected using microplate hybridization assay. CD-PCR was evaluated by detecting G1896A variant of hepatitis B virus (HBV) in form of recombinant plasmids and in sera from patients with hepatitis B, and compared with allele-specific PCR (AS-PCR) and competitive AS-PCR.

RESULTS: CD-PCR was successfully established. It could clearly distinguish wild-type and mutant-type plasmid DNA of G1896A variant when the amount of plasmid DNA was between 10^2-10^8copies/reaction, while for AS-PCR and competitive AS-PCR, the DNA amount was between 10^2-10^4copies/reaction. CD-PCR could detect one copy of G1896A variant among 10-100 copies of wild-type plasmid DNA. The specificity of CD-PCR was higher than those of AS-PCR and competitive AS-PCR in the detection of HBV G1896A variant in sera from patients with hepatitis B. CD-PCR was independent of the amount of HBV DNA in serum. HBV G1896A variant was more often found in HBeAg (-) patients with a lower level of detectable viremia than that with a higher level of detectable viremia (P=0.0192).

CONCLUSION: CD-PCR is more specific since it is less influenced by the amount of initial templates and the cross amplification between mutant- and wild-type amplified products. It is also simple and time-saving. Thus, CD-PCR might be useful in routine gene typing and point mutation screening. HBV G1896A or other more important mutations have to be routinely detected in patients with a detectable level of viremia after HBeAg/antibody conversion in clinical practice.

Peng XM, Chen XJ, Li JG, Gu L, Huang YS, Gao ZL. Novel assay of competitively differentiated polymerase chain reaction for screening point mutation of hepatitis B virus. *World J Gastroenterol* 2003; 9(8): 1743-1746
http://www.wjgnet.com/1007-9327/9/1743.asp

INTRODUCTION

Point mutation is one of the commonest gene mutations not only in human genome but also in genome of pathogens. It is the most important molecular pathogenesis of cancer and chronic infection[1-3]. The commonest method for detecting point mutation is based on polymerase chain reaction (PCR), which can be divided into two types. One type is to analyze the PCR products using direct sequencing, restriction fragment length polymorphism and single strand conformation polymorphism[4-7]. This type of technique is usually accurate, but cannot be used in routine clinical examination since it needs additional manipulation. The other type is allele specific-PCR (AS-PCR), sequence specific-PCR or amplification refractory mutation system[8-13]. This type of techniques is usually simple, but its specificity is influenced by the amount of initial templates of PCR. This deficiency was not so obvious when this type of methods was used to detect point mutation or gene typing of human gene in the past since the initial templates in these samples could be controlled[8,12,13]. Some investigators, however, have made efforts to improve AS-PCR by introducing competitive mechanism, and established the so-called bidirectional AS-PCR and competitive PCR in order to decrease the influence of the amount of initial templates on its specificity[14-19]. AS-PCR has been used to detect point mutation of pathogens recently[10, 20-22]. However, the specificity of AS-PCR in detection of pathogen mutations was challenged by uncontrollable amount of initial templates and the requisition of high sensitivity. For these reasons, a novel method of competitively differentiated polymerase chain reaction (CD-PCR) was established in this study and compared with AS-PCR and competitive AS-PCR in the detection of G1896A variant of HBV.

MATERIALS AND METHODS

Materials

One hundred serum samples with (hepatitis B surface antigen) HBsAg(+), anti-(hepatitis B e antigen) HBe(+) and anti-(hepatitis B core antigen) HBc(+), 60 serum samples with HBsAg(+), HBeAg(+) and anti-HBc(+) and 40 serum samples without HBV serum markers were collected. The serum markers were demonstrated by enzyme-linked immunoabsorbent assay. Recombinant plasmid pG1896A was constructed as described

before[23]. TZ19U-HBV that contained double copies of HBV DNA (adw) was a gift from Professor Huang Zhimin (Zhongshan University, Guangzhou, China) and was used as wild-type DNA control. T4 DNA ligase and pfu DNA polymerase were purchased from Promega (USA). DNA gel extraction kits and plasmid isolation kits were purchased from Qiagen (Germang). Anti-digoxigenin and anti-fluorescein labeled with horseradish peroxidase were purchased from Roche (USA). Primers shown in Table 1 were designed with the Omega 2 software and synthesized in Bioasia Biological Engineering Company (Shanghai, China).

Table 1 Primers and probes for detecting of HBV G1896A variant

Denomination	Sequence(5'→3')
BIO-PCP	BIO-GAGAC TCTAA GGCTT CTCGA TACAG AGCTG AGG
PCA	GCAGT ATGGT GAGGT GAGCA ATGCT CAG
DIG-PCMd	DIG-CTCAC GCTAC ATTGT GTGCC TTGGG TGGCT TCA
DIG-PCMc	DIG-TGTGC CTTGG GTGGC TTCA
FLU-PCWd	FLU-GTCCG TAGTC TCGTT GTGCC TTGGG TGGCT TGG
FLU-PCWc	FLU-TGTGC CTTGG GTGGC TTGG
PCS	CCACC GTGAA CGCCC ATCAG
PCSc	CCCGA ATTCC ACCGT GAACG CCCAT CAG
PCAc	CCCAA GCTTG CAGTA TGGTG AGGTG AGCAA TG

BIO: the abbreviation of biotin; DIG: the abbreviation of digoxigenin; FLU: the abbreviation of fluorescein.

Methods

Principles of CD-PCR Two competitively differentiated primers (CDP) with different labels in 5' end were designed. CDP had a complemented region of 17-20 bp long with penultimate mismatch and a 3' terminus matching the mutant or the normal bases of the templates. The annealing temperature of this part was about 52-54 ℃. There was also a non-complemented region of 14 bp long, which was different from each other in 5' end. The total annealing temperature of CDP was about 75-80 ℃. PCR was performed in one tube. Competitive amplification was performed first when CDP competed for templates under lower annealing temperature. After certain amounts of products of each primer were obtained, differentiated amplification was then performed under higher annealing temperature when CDP could only use its own products as templates. This amplification model would keep the products ratio of mutant and wild templates and allow the templates to be fully amplified.

G1896A variant detected by CD-PCR Wild-type and G1896A mutant-type plasmids were used for the optimization of CD-PCR. A total volume of 30 μl was used in the final conditions of PCR reaction. The reaction mixture consisted of 10 mmol/L Tris-HCl, pH 8.5,50 mmol/L KCl, 1.5 mmol/L $MgCl_2$, 0.2 mmol/L dNTPs, 2U pfu DNA polymerase, 20 pmol FLU-PCWd, 20 pmol DIG-PCMd, 20 pmol PCA and 5 μl plasmid or extracted DNA. The cycling conditions were as follows: 3 cycles (first set) at 94 ℃ for 40 s, at 52 ℃ for 40 s and at 72 ℃ for 90 s followed by 35 cycles (second set) at 94 ℃ for 40 s, and at 72 ℃ for 90 s. The PCR products were then hybridized with solidified biotin-labeled probe PCP in two wells of microplate. The color reaction was obtained after captured PCR products reacted with anti-DIG or anti-FLU respectively, which were conjugated with horseradish peroxidase.

G1896A variant detected by competitive AS-PCR Except for the replacement of primer FLU-PCWd and DIG-PCMd with primer FLU-PCWc and DIG-PCMc, the components of competitive AS-PCR were similar to CD-PCR. The cycling conditions were as follows: 25 cycles (first set) at 94 ℃ for 40 s, at 60 ℃ for 40 s, and at 72 ℃ for 90 s followed by 10 cycles (second set) at 94 ℃ for 40 s, at 52 ℃ for 40 s, and at 72 ℃ for 90 s. The PCR products were then detected similar to CD-PCR.

G1896A variant detected by AS-PCR Except for the absence of FLU-PCWc, the components and the cycling conditions were similar to competitive CD-PCR. The PCR products were visualized under an ultraviolet transilluminator.

Quantification of serum HBV DNA by fluorescent quantitive PCR The HBV DNA level of 200 sera was detected using fluorescent quantitive PCR following the instruction (Taqmen, Roche).

DNA sequencing A fragment of HBV precore in positive or negative sera by all three methods and in sera that were positive for AS-PCR and competitive AS-PCR, and negative for CD-PCR was analyzed using DNA sequencing after it was amplified using primers PCSc and PCAc and cloned into plasmid pUC19.

RESULTS

Detection of HBV G1896A variant in recombinant plasmid DNA

The typical results of HBV G1896A variant detected by means of AS-PCR, competitive AS-PCR and CD-PCR are shown in Figure 1. To detect G1896A variant, the sensitivity of AS-PCR was 10^3 copies/reaction, and there was non-specific amplification when the amount of wild-type initial templates was higher than 10^4 copies/reaction. For competitive AS-PCR, the wild-type and mutant-type plasmid DNA could be clearly distinguished when the initial templates were 10^2-10^4 copies/reaction. CD-PCR could clearly distinguish them in the range of 10^2-10^8 copies/reaction. There was some degree of non-specific reaction when the amount of initial templates was higher than 10^4 copies/reaction, but the difference of color intensities between wild-type and mutant-type product wells was obvious. CD-PCR could detect one variant G1896A copy among 100 wild-type copies of DNA when the initial templates were 10^2-10^5 copies/reaction, but one out of 10 copies when the initial templates were 10^5-10^8 copies/reaction.

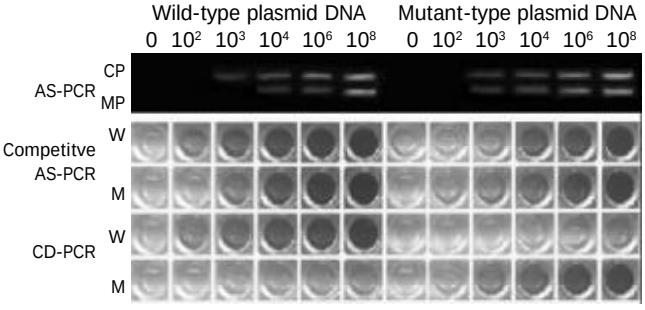

Figure 1 HBV G1896A variant detected by AS-PCR, competitive AS-PCR and CD-PCR using its wild-type or mutant-type recombinant plasmid DNA as objects. CP: common product band; MP: mutant product band; W: wild-type products; M: mutant-type products.

Detection of HBV G1896A variant in sera

Among 200 sera, HBV DNA was positive in 104 cases using AS-PCR, in 119 cases using competitive AS-PCR and in 122 cases using CD-PCR. The sensitivity for HBV DNA detection by CD-PCR was similar to that of competitive AS-PCR, but higher than that of AS-PCR (χ^2=5.47, P=0.0193). The results of G1896A variant in sera are shown in Table 2. Among the 104 cases with positive HBV DNA detected by all the three methods, there were 33 positive cases, and 31 negative cases

of G1896A variant detected by both CD-PCR and AS-PCR, and 40 cases that were positive by AS-PCR but not by CD-PCR.

Table 2 HBV G1896A variant and its relationship with HBV serum markers

	Cases	CD-PCR(%)		CAS-PCR(%)		AS-PCR(%)	
		HBV DNA(+)	G1896A variant	HBV DNA(+)	G1896A variant	HBV DNA(+)	G1896A variant
HBsAg(+)/ HBeAg(+)	60	100.0	6.7	100.0	63.3[b]	93.3	55.0[b]
HBsAg(+)/ HBeAg(-)	100	62.0[c]	38.0	59.0	46.0	48.0	40.0
HBsAg(-)/ HBeAg(-)	40	0	0	0	0	0	0

[b]$P<0.01$, compared with group of CD-PCR, χ^2 test, [c]$P<0.05$, compared with group of AS-PCR, χ^2 test.

The results of DNA sequencing

HBV G1896A mutation was confirmed by DNA sequencing in 3 positive sera by all the three methods, and excluded in 3 negative sera by all the three methods and in 4 sera that were positive by AS-PCR and competitive AS-PCR, but negative by CD-PCR.

The relationship between G1896A variant and HBV DNA level

The relationship between G1896A variant detected by AS-PCR, competitive AS-PCR and CD-PCR and HBV DNA level in the sera is shown in Table 3. More G1896A variants were found in patients with positive HBeAg by AS-PCR and competitive AS-CR. These could be false positives. These false-positive findings occurred more often in patients with a higher level of HBV DNA in serum. CD-PCR seemed more specific since only 4 patients were found to be infected with both wild-type HBV and G1896A variants in HBeAg positive cases. By CD-PCR, HBV G1896A variant was more often found in HBeAg (-) patients with a lower level of viremia (P=0.0192).

Table 3 Relationship between G1896A variant and HBV DNA level in serum

	HBeAg(+)(n=56)		HBeAg(-) (n=48)	
	$\leqslant 10^6$copies / ml (n=14)	$>10^6$ copies / ml(n=42)	$\leqslant 10^6$ copies / ml(n=28)	$>10^6$ copies / ml(n=20)
AS-PCR	2	31	21	19
Competitive AS-PCR	2	35	23	20
CD-PCR	2	2	21[a]	8

[a]Compared with HBeAg(-) group with a level higher than 10^6 copies / ml of HBV DNA in serum, Fisher's exact possibility test, P=0.0192.

DISCUSSION

AS-PCR has been considered as a simplest and quickest method for the detection of known point mutations[5,10-19]. False positive results, however, seem inevitable since the amplification of wild-type templates by allele-specific or sequence-specific primers for mutant-type templates can not be completely prevented. Once non-specific products occur, they will be amplified subsequently. Thus the ratio of specific and non-specific products will decrease, and become even smaller as the plateau of PCR reaches at the late stage. It is understandable that false band will occur when a large amount of initial templates or too many cycles are used in AS-PCR. To improve the specificity of AS-PCR, the specificity of primers was designed by introducing penultimate mismatch[24], and the cycles of specific amplification were reduced by introducing basic amplification[6,25]. The application of competitive mechanism is another important step to improve AS-PCR.

Competitive AS-PCR and bidirectional or tetra-primer AS-PCR are common assays that have a competitive mechanism[6,14-19,25]. Bidirectional or tetra-primer AS-PCR is in fact a competition for PCR system, while competitive AS-PCR is the competition for both templates and PCR system. However, these PCRs can not exclude the non-specific amplification from initial templates in each cycle. For competitive AS-PCR, it is possible to reduce the influence of initial templates, but a new problem will occur, which is that the initial products will become the templates for non-specific amplification in subsequent cycles. This might be the underlying mechanism that the competitive AS-PCR seemed worse than AS-PCR in this study. Therefore, to reduce the influence of the initial templates and products would be a very important measure to improve AS-PCR assay on specificity of amplification

For CD-PCR, competitive amplification was performed first, and followed by differentiated amplification, which was different from competitive AS-PCR. This protocol would allow allele- or sequence-specific amplification to begin at a low level of templates. Thus, the influence of initial templates could be controlled to a minimal level. After a few cycles, differentiated amplification was carried out under higher annealing temperature at which primers could not combine with initiated templates and the initial products could not be used as templates for non-specific amplification in subsequent cycles under higher annealing temperature either. These might be the mechanisms that CD-PCR had much better performance than that of AS-PCR and competitive AS-PCR in this study. The molecular weights of wild-type and mutant-type products were the same, therefore, products of CD-PCR could not be distinguished by electrophoresis. It was convenient and time-saving when microplate hybridization assay was used to demonstrate the products in this study. Automatic detection was possible too when CD-PCR was adapted to real-time fluorescent PCR assay as used in AS-PCR or competitive AS-CR[26,27]. CD-PCR could also be used by combining with other high resolution techniques[28,29]. It could be used in gene typing for organ transplantation or gene polymorphism in addition to the detection of gene point mutations as AS-PCR[30,31].

Detectable viremia was found in sera of some patients with hepatitis B after HBeAg/antibody conversion[32-34]. This type of viremia resulted in G1896A mutation in 60.4 % out of such patients, especially in patients with a much lower level of HBV DNA. This result is conformable to the fact that the replication ability of G1896A variant has decreased[35], and suggests that G1896A or other more important mutations have to be detected in patients with a detectable level of viremia after HBeAg/ antibody conversion in clinical practice.

REFERENCES

1 **Bressac B**, Kew M, Wands J, Ozturk M. Selective G to T mutations of p53 gene in hepatocellular carcinoma from southern Africa. *Nature* 1991; **350**: 429-431

2 **Steinberg JL**, Yeo W, Zhong S, Chan JY, Tam JS, Chan PK, Leung NW, Johnson PJ. Hepatitis B virus reactivation in patients undergoing cytotoxic chemotherapy for solid tumours: precore / core mutations may play an important role. *J Med Virol* 2000; **60**: 249-255

3 **Yoo BC**, Park JW, Kim HJ, Lee DH, Cha YJ, Park SM. Precore and core promoter mutations of hepatitis B virus and hepatitis B e antigen-negative chronic hepatitis B in Korea. *J Hepatol* 2003; **38**: 98-103

4 **Chen RY**, Edwards R, Shaw T, Colledge D, Delaney WE 4th, Isom

H, Bowden S, Desmond P, Locarnini SA. Effect of the G1896A precore mutation on drug sensitivity and replication yield of lamivudine-resistant HBV *in vitro*. *Hepatology* 2003; **37**: 27-35

5 **Peng XM**, Peng WW, Yao JL. Codon 249 mutations of p53 gene in development of hepatocellular carcinoma. *World J Gastroenterol* 1998; **4**: 125-127

6 **Peng XM**, Yao CL, Chen XJ, Peng WW, Gao ZL. Codon 249 mutations of p53 gene in non-neoplastic liver tissues. *World J Gastroenterol* 1999; **5**: 324-326

7 **Ding Y**, Le XP, Zhang QX, Du P. Methylation and mutation analysis of p16 gene in gastric cancer. *World J Gastroenterol* 2003; **9**: 423-426

8 **Suzuki F**, Suzuki Y, Tsubota A, Akuta N, Someya T, Kobayashi M, Saitoh S, Arase Y, Ikeda K, Kumada H. Mutations of polymerase, precore and core promoter gene in hepatitis B virus during 5-year lamivudine therapy. *J Hepatol* 2002; **37**: 824-830

9 **Moses JH**, Greville WD, Downes J, McClenahan W, Kennedy A, Dunckley H. A new HLA-A*02 allele, A*0234, detected by polymerase chain reaction using sequence-specific primers (PCR-SSP). *Tissue Antigens* 2000; **55**: 175-177

10 **Ma CL**, Fang DX, Chen HB, Li FQ, Jin HY, Li SQ, Tan WG. A mutation specific polymerase chain reaction for detecting hepatitis B virus genome mutations at nt551. *World J Gastroenterol* 2003; **9**: 509-512

11 **Hodgson DR**, Foy CA, Partridge M, Pateromichelakis S, Gibson NJ. Development of a facile fluorescent assay for the detection of 80 mutations within the p53 gene. *Mol Med* 2002; **8**: 227-237

12 **Stoehr R**, Knuechel R, Boecker J, Blaszyk H, Schmitt R, Filbeck T, Hofstaedter F, Hartmann A. Histologic-genetic mapping by allele-specific PCR reveals intraurothelial spread of p53 mutant tumor clones. *Lab Invest* 2002; **82**: 1553-1561

13 **Kirby GM**, Batist G, Fotouhi-Ardakani N, Nakazawa H, Yamasaki H, Kew M, Cameron RG, Alaoui-Jamali MA. Allele-specific PCR analysis of p53 codon 249 AGT transversion in liver tissues from patients with viral hepatitis. *Int J Cancer* 1996; **68**: 21-25

14 **Waterfall CM**, Eisenthal R, Cobb BD. Kinetic characterisation of primer mismatches in allele-specific PCR: a quantitative assessment. *Biochem Biophys Res Commun* 2002; **299**: 715-722

15 **Horvath AD**, Kirov SA, Karaulanov EE, Ganev VS. Detection of apoB-100 R3500Q mutation by competitive allele-specific polymerase chain reaction. *J Clin Lab Anal* 2001; **15**: 256-259

16 **Sasvari-Szekely M**, Gerstner A, Ronai Z, Staub M, Guttman A. Rapid genotyping of factor V Leiden mutation using single-tube bidirectional allele-specific amplification and automated ultrathin-layer agarose gel electrophoresis. *Electrophoresis* 2000; **21**: 816-821

17 **Hamajima N**, Saito T, Matsuo K, Kozaki K, Takahashi T, Tajima K. Polymerase chain reaction with confronting two-pair primers for polymorphism genotyping. *Jpn J Cancer Res* 2000; **91**: 865-868

18 **Hamajima N**, Saito T, Matsuo K, Tajima K. Competitive amplification and unspecific amplification in polymerase chain reaction with confronting two-pair primers. *J Mol Diagn* 2002; **4**: 103-107

19 **McKinzie PB**, Parsons BL. Detection of rare K-ras codon 12 mutations using allele-specific competitive blocker PCR. *Mutat Res* 2002; **517**: 209-220

20 **Gramegna M**, Lampertico P, Lobbiani A, Colucci G. Detection of the hepatitis B virus major pre-core mutation by the amplification refractory mutation system technique. *Res Virol* 1993; **144**: 307-309

21 **Nainan OV**, Khristova ML, Byun K, Xia G, Taylor PE, Stevens CE, Margolis HS. Genetic variation of hepatitis B surface antigen coding region among infants with chronic hepatitis B virus infection. *J Med Virol* 2002; **68**: 319-327

22 **Kinoshita M**, Seno T, Fukui T, Shin S, Tsubota A, Kumada H. A detection method for point mutation in the precore region of human hepatitis B virus (HBV)-DNA using mutation-site-specific assay. *Clin Chim Acta* 1994; **228**: 83-90

23 **Peng XM**, Gu L, Chen XJ, Huang YS, Gao ZL. The Defect and Improvement of Allele-specific PCR during Detection of G1896A Variant of Hepatitis B Virus. *J Practical Med* 2003; **19**: 467-469

24 **Fishbein WN**, Davis JI, Foellmer JW, Nieves S, Merezhinskaya N. A Competitive Allele-specific Oligomers Polymerase Chain Reaction Assay for the cis Double Mutation in AMPD1 that is the Major Cause of Myo-adenylate Deaminase Deficiency. *Mol Diagn* 1997; **2**: 121-128

25 **Hersberger M**, Marti-Jaun J, Hanseler E, Speck RF. Rapid detection of the CCR2-V64I, CCR5-A59029G and SDF1-G801A polymorphisms by tetra-primer PCR. *Clin Biochem* 2002; **35**: 399-403

26 **Glaab WE**, Skopek TR. A novel assay for allelic discrimination that combines the fluorogenic 5' nuclease polymerase chain reaction (TaqMan) and mismatch amplification mutation assay. *Mutat Res* 1999; **430**: 1-12

27 **Suemizu H**, Ohnishi Y, Maruyama C, Tamaoki N. Two-color allele-specific polymerase chain reaction (PCR-SSP) assay of the leptin receptor gene (Leprdb) for genotyping mouse diabetes mutation. *Exp Anim* 2001; **50**: 435-439

28 **Tian H**, Brody LC, Fan S, Huang Z, Landers JP. Capillary and microchip electrophoresis for rapid detection of known mutations by combining allele-specific DNA amplification with heteroduplex analysis. *Clin Chem* 2001; **47**: 173-185

29 **McClay JL**, Sugden K, Koch HG, Higuchi S, Craig IW. High-throughput single-nucleotide polymorphism genotyping by fluorescent competitive allele-specific polymerase chain reaction (SNiPTag). *Anal Biochem* 2002; **301**: 200-206

30 **Donohoe GG**, Laaksonen M, Pulkki K, Ronnemaa T, Kairisto V. Rapid single-tube screening of the C282Y hemochromatosis mutation by real-time multiplex allele-specific PCR without fluorescent probes. *Clin Chem* 2000; **46**: 1540-1547

31 **See D**, Kanazin V, Talbert H, Blake T. Electrophoretic detection of single-nucleotide polymorphisms. *Biotechniques* 2000; **28**: 710-714

32 **Seo Y**, Yoon S, Nakaji M, Yano Y, Nagano H, Ninomiya T, Hayashi Y, Kasuga M. Hepatitis B virus DNA in anti-HBe-positive asymptomatic Carriers. *Intervirology* 2003; **46**: 43-49

33 **Yotsuyanagi H**, Hino K, Tomita E, Toyoda J, Yasuda K, Iino S. Precore and core promoter mutations, hepatitis B virus DNA levels and progressive liver injury in chronic hepatitis B. *J Hepatol* 2002; **37**: 355-363

34 **Yuen MF**, Sablon E, Yuan HJ, Hui CK, Wong DK, Doutreloigne J, Wong BC, Chan AO, Lai CL. Relationship between the development of precore and core promoter mutations and hepatitis B e antigen seroconversion in patients with chronic hepatitis B virus. *J Infect Dis* 2002; **186**: 1335-1338

35 **Karino Y**, Toyota J, Sato T, Ohmura T, Yamazaki K, Suga T, Nakamura K, Sugawara M, Matsushima T, Hino K. Early mutation of precore (A1896) region prior to core promoter region mutation leads to decrease of HBV replication and remission of hepatic inflammation. *Dig Dis Sci* 2000; **45**: 2207-2213

Edited by Yuan HT and Wang XL

P.O.Box 2345, Beijing 100023,China
Fax: +86-10-85381893
E-mail: wjg@wjgnet.com www.wjgnet.com

World J Gastroenterol 2003;9(8):1747-1751
World Journal of Gastroenterology
 ISSN 1007-9327

Identification of *H. pylori* strain specific DNA sequences between two clinical isolates from NUD and gastric ulcer by SSH

Feng-Chan Han, Min Gong, Han-Chong Ng, Bow Ho

Feng-Chan Han, Min Gong, Han-Chong Ng, Bow Ho, Department of Microbiology, Faculty of Medicine, National University of Singapore, 5 Science Drive 2, Singapore 117595, Republic of Singapore
Supported by the NMRC-Sponsored Project, Grant number: R-182-000-037-213
Correspondence to: Feng-Chan Han, Institute of Genetic Diagnosis, Fourth Military Medical University, 169 Changle West Road, Xi' an 710033, Shaanxi Province, China. biohanfc@hotmail.com
Telephone: +86-29-3374772 **Fax:** +86-29-3285729
Received: 2003-04-08 **Accepted:** 2003-05-17

Abstract

AIM: The genomes of *Helicobacter pylori* (*H. pylori*) from different individuals are different. This project was to identify the strain specific DNA sequences between two clinical *H. pyl*ori isolates by suppression subtractive hybridization (SSH).

METHODS: Two clinical *H. pylori* isolates, one from gastric ulcer (GU, tester) and the other from non-ulcer dyspepsia (NUD, driver), were cultured and the genomic DNA was prepared and submitted to *Alu* I digestion. Then two different adaptors were ligated respectively to the 5'-end of two aliquots of the tester DNA fragments and SSH was made between the tester and driver DNA. The un-hybridized tester DNA sequences were amplified by two sequential PCR and cloned into pGEM-T-Easy Vector. The tester strain specific inserts were screened and disease related DNA sequences were identified by dot blotting.

RESULTS: Among the 240 colonies randomly chosen, 50 contained the tester strain specific DNA sequences. Twenty three inserts were sequenced and the sizes ranged from 261 bp to 1 036 bp. Fifteen inserts belonged to the *H.pylori* plasmid pHPO100 that is about 3.5 kb and codes a replication protein A. Other inserts had patches of homologous to the genes of *H.pylori* in GenBank. Various patterns of dot blots were given and no GU strain unique DNA sequences were found when 4 inserts were used as probes to screen the genomic DNA from 27 clinical isolates, 8 from GU, 12 from duodenum ulcer (DU), 4 from GU-DU, 2 from NUD and 1 from gastric cancer (GC). But a 670 bp DNA fragment (GU198) that was a bit homologous to the 3'-end of the gene of thymidylate kinase was positive in 7 GU strains (7/8), 3 GU-DU strains (3/4) and 3 DU strains (3/12). A 384 bp fragment (GU79) of the replication gene A (repA) was positive only in 4 *H.pylori* isolates, 2 from GU and 2 from GU-DU.

CONCLUSION: Differences exist in the genes of different *H.pylori* isolates. SSH is very effective to screen *H.pylori* strain specific DNA sequences between two clinical isolates, and some of these sequences may have clinical significance.

Han FC, Gong M, Ng HC, Ho B. Identification of *H. pylori* strain specific DNA sequences between two clinical isolates from NUD and gastric ulcer by SSH. *World J Gastroenterol* 2003; 9(8): 1747-1751
http://www.wjgnet.com/1007-9327/9/1747.asp

INTRODUCTION

Helicobacter pylori (*H. pylori*) is a microaerophilic Gram-negative bacterium that colonizes the stomach in more than half of the world population. It is the causative agent of chronic gastritis and contributes to peptic ulcer[1, 2] and also plays an important role in the pathogenesis of gastric cancer[3-16]. When one is infected by this bacterium, the clinical outcome depends on the interaction of virulent effects of the bacterium, the host response, and the environment[18]. The genomes of *H.pylori* from different individuals are quite different and each one contains about 1 600 genes, among which almost 320 genes are dispensable and 100 genes are strain unique[17-19]. Genes that are present in one strain and absent or substantially different in the others can be of great biological interest[20].

H. pylori strains with the cag pathogenicity island (PAI) can induce more severe inflammation, proliferation and apoptosis in the gerbil mucosa than do the strains partial or complete lack of the cag PAI[21]. In contrast to the $CagA^-$ *H. pylori* infection, $CagA^+$ *H. pylori* infection is associated with a higher prevalence of p53 mutation in gastric adenocarcinoma[22]. In addition to the *cag* island, other polymorphic loci that appear clinically relevant have to be identified.

We screened the strain specific DNA sequences between two clinical isolates and tried further to identify the disease related sequences. Different methods, such as microarray[19,21], and subtractive hybridization[18, 23,24] could be used for bacterial strain specific DNA screening. Suppression subtractive hybridization (SSH), in which the genomic DNA sample containing the sequences of interest is called "tester", and the reference sample is called "driver", is a powerful approach for assessing the DNA sequence differences among the closely related bacterial strains.

MATERIALS AND METHODS

H.pylori growth and genomic DNA extraction

H. pylori clinical isolates preserved in the brain heart infusion broth (BHI, Gibco) supplemented with 100 mL/L horse serum (Gibco) and 200 mL/L glycerol (BDH) were inoculated on the *H.pylori* selective chocolate blood agar containing 40 g/L blood agar base No.2 (Oxoid) and 50 mL/L horse blood (Gibco). Antibiotics were also used at the following concentrations: vancomycin (Sigma) 3 mg/L, trimethoprim (Sigma) 5 mg/L, nalidixic acid (Sigma) 10 mg/L and amphotericin B (Sigma) 2 mg/L. The plates were incubated in microaerobic atmosphere (50 mL/L CO_2) in a CO_2 incubator (Forma Scientific) at 37 ℃ for up to 5 days. *H.pylori* genomic DNA was extracted following Bow's method[25].

Driver and tester DNA preparations

The subtractive DNA library was made by using the PCR-select bacterial genome subtraction kit (Clontech) with Akopyants NS's method (*Proc Natl Acad Sci U S A.* 1998;95: 13108) as reference, but with some change at certain procedures. Genomic DNA of an *H.pylori* strain from gastric ulcer (GU) was used as the tester, and DNA of a strain from non-ulcer dyspepsia (NUD) was used as the driver. The

sequences of the adaptors and primers were listed as followings: adaptor 1, 5'-CTAATACGACTCACTATAGGGCTCGAGCGGCCGCCCGGGCAGGT-3',5'-ACCTGCCCGG-3',adaptor 2R, 5'-CTAATACGACTCACTATAGGGCAGCGTGGTCGCGGCCGAGGT-3',5'-ACCTCGGCCG-3',P1,5'-CTAATACGACTCACTATAGGGC-3', NP1, 5'-TCGAGCGGCCGCCCGGGCAGGT-3', NP2, 5'-AGCGTGGTCGCGGCCGAGGT-3'. In brief, 4 μg of the tester or driver genomic DNA was digested with 40 units of *Alu*I (New England Biolabs) in 400 μL reaction volume at 37 ℃ for 16 hours. The DNA fragments were then extracted with phenol and precipitated with ethanol, and resuspended in sterile distilled water at a final concentration of 300 mg/L. Two aliquots of tester DNA (120 ng each) were ligated separately to the two adaptors (2 μmol/L final concentration) at 16 ℃ for 16 hours, each in a total volume of 10 μL, with 1 μL (New Engl and Biolabs, 400 units) of T4 DNA ligase in the buffer supplied by the manufacturer. After ligation, 1 μL of 0.2 mol/L EDTA was added, and the sample was heated at 70 ℃ for 5 minutes to inactivate the ligase and then stored at -20 ℃.

Suppression subtractive hybridization

Two microliters of the driver DNA fragments (600 ng) were added to 1 μL (12 ng) of each adaptor-ligated tester DNA (50:1 ratio). One microliter of 4×hybridization buffer (2 mol/L NaCl, 200 mmol/L Hepes, pH 8.0, 0.8 mmol/L EDTA) was added to each tube, and the solution was overlaid with a drop of mineral oil. The DNA fragments were then denatured at 98 ℃ for 2 minutes, and allowed to anneal at 65 ℃ for 1.5 hours. After the first hybridization, the two samples (one with adaptor 1, the other with adaptor 2R) were combined and 300 ng more heat-denatured driver DNA dissolved in 2 μL of 1× hybridization buffer was added. The 10 μL mixture was allowed to hybridize at 65 ℃ for an additional 14 hours. After being diluted to 200 μL with dilution buffer (50 mmol/L, NaCl, 20 mmol/L Hepes, pH8.3, 0.2 mmol/L EDTA), the sample was heated at 65 ℃ for 10 minutes, and stored at -20 ℃.

The first and second PCRs

The first PCR mixture (25 μL) containing 1 μL of the above diluted DNA, 1 μL of 10 μmol/L PCR primer P1, 2 μL of 2.5 mmol/L dNTPs, 2.5 μL of 10×PCR reaction buffer, and 5 μL of the Advantage 2 Polymerase Mix (Clontech) was incubated in a thermal cycler (Perkin-Elmer 2400) at 72 ℃ for 2 minutes and subjected to 25 cycles at 94 ℃ for 30 s, at 66 ℃ for 30 s, and at 72 ℃ for 1.5 minutes. Seven microliters of the PCR products were analyzed by 15 g/L agarose gel electrophoresis. The products were then diluted 40-fold in 10 mmol/L Tris· HCl (pH 7.5). The second PCR mixture (25 μL) contained 1 μL of the diluted first PCR products, 1 μL of the nest PCR primers (NP1 and NP2, 10 μmol/L each), 2 μL of 2.5 mmol/L dNTPs, 2.5 μL of 10×PCR reaction buffer, and 5 μL of the Advantage 2 Polymerase Mix. The cycling program was 12 cycles at 94 ℃ for 30 s, at 68 ℃ for 30 s, and at 72 ℃ for 1.5 minutes, followed by further extension at 72 ℃ for 5 minutes. The PCR products were analyzed by 15 g/L agarose gel electrophoresis, purified by using the Quaquick Spin PCR Purification Kit (Qiagen) and cloned into the pGEM- T Easy Vector (Promega) following the protocols. The recombinant plasmids were transformed into *E. coli Top*[10], which was then cultured overnight on the selective agar plates containing 20 μL of 50 g/L ampicillin, 35 μL of 100 mmol/L IPTG and 40 μL of 20 g/L X-gal. White colonies were randomly picked and suspended in 100 μL of Luria-Bertani medium containing ampicillin in an eppendorf tube and cultured at 37 ℃ for 2 hours. One microliter of the cell suspension, after being frozen and thawed three times, was used as templates and the inserts were amplified under condition as in the second PCR except for 25 cycles. The sizes of the inserts were identified by agarose gel electrophoresis.

Strain specific insert screening and disease related DNA sequence identification

One microliter of each PCR product (10 ng) was dotted on the Hybond N+ membrane (Amersham) in duplicating forms and DNA fixation was carried out by irradiation under a UV transilluminator (Vilber Lourmat) for 5 minutes. The *Alu*I-digested DNA fragments of the tester and driver *H.pylori* were used as probes and dot blotting was preformed using the ECL direct nucleic acid labeling and detection system (Amersham Phamacia Biotech). The pre-hybridization and hybridization were carried out in the hybridization oven (Amersham) at 42 ℃ for 1 hour and 12 hours respectively. After stringently washing the Hybond N+ membrane (twice for 20 minutes in 6 mol/L Urea, 4 g/L SDS and 0.1×SSC, and twice for 5 minutes in 2× SSC), the chemiluminenscence signals were detected by exposure of the Hyperfilm to the membrane for 5 to 30 minutes. The inserts that gave positive results to the tester probes and negative to the driver probes were sequenced using a Big Dye Terminator DNA sequencing kit (Perkin-Elmer) and ABI automated sequencer. The sequences were then submitted to gene and protein homologous analysis. In the same way, by dotting 100 ng of each genomic DNA from different *H.pylori* isolates on the membrane and using the inserts interested as probes, the disease related DNA sequences were identified. In the above cases, 1 ng of each probe DNA was dotted on the membrane to be used as positive control.

RESULTS

Tester strain specific DNA sequencing and homologous analysis

After SSH between the tester and driver DNA fragments, about 900 colonies grew on the ampicillin plates and two thirds of them were white in color. Two hundred and forty white colonies

Table 1 Homologous analysis of some strain specific DNA sequences

Inserts	GenBank accesion No.	Homolog/genes or proteins	DNA matches
GU79	AF056496	*H.pylori* plasmid pHPO100/ RepA, $2e^{-53}$	1882-2265
GU150	AE000629	Carbamoyl-phosphate synthetase, $3e^{-29}$	1029-1229
GU185	AE000595	Putative outer membrane p1, $7e^{-24}$	2993-3177
GU198	AE001560	Thymidylate kinase, $2e^{-10}$	640-717
GU210	AE000590	Hypothetical protein , $3e^{-33}$	789-396
GU212	AE000531	Type II restriction enzyme R protein, $4e^{-26}$	1-597
GU223	AE000647	Hypothetical protein, $4e^{-16}$	7724-8193
GU234	AE000650	Site specific DNA-methyltransferase, $3e^{-54}$	9070-8752
GU235	AE000547	Toxin-like outer membrane protein, $2e^{-64}$	13943-14494

were randomly chosen and the inserts were amplified using the primers as in the nest PCR. By dotting and fixing the equal amount of each PCR product in replica form on the membrane, dot blotting was carried out using the *Alu*I digested DNA fragments as probes (Figure 1). Fifty tester strain specific DNA sequences were screened and 23 of them were sequenced. The sizes of the inserts ranged from 261 to 1 036 bp. Blast analysis showed that, of the 23 inserts sequenced, 15 belonged to parts of the *H.pylori* plasmid pHPO100 (Table1 only shows GU79) and 2 of them contained the same fragment. The size of this plasmid is 3 520 bp, which codes a replication protein A (RepA, 1 842-2 765) and an unknown protein (2 762-3 520). The other 8 inserts were homologous to genes of *H.pylori* in GenBank to different extent (Table1).

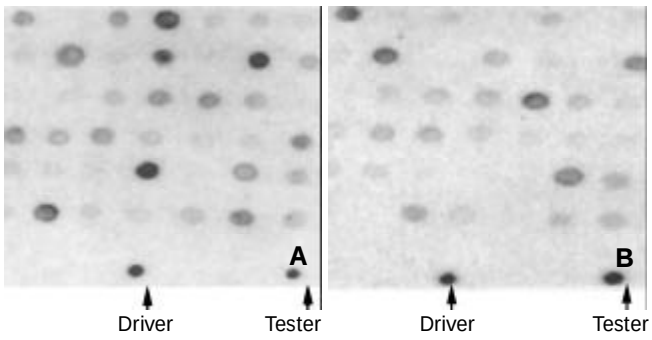

Figure 1 Dot blotting to screen the tester strain specific inserts by using the *Alu* I digested tester DNA (A) and driver DNA (B) as probes. The arrowheads indicate the spots of positive controls.

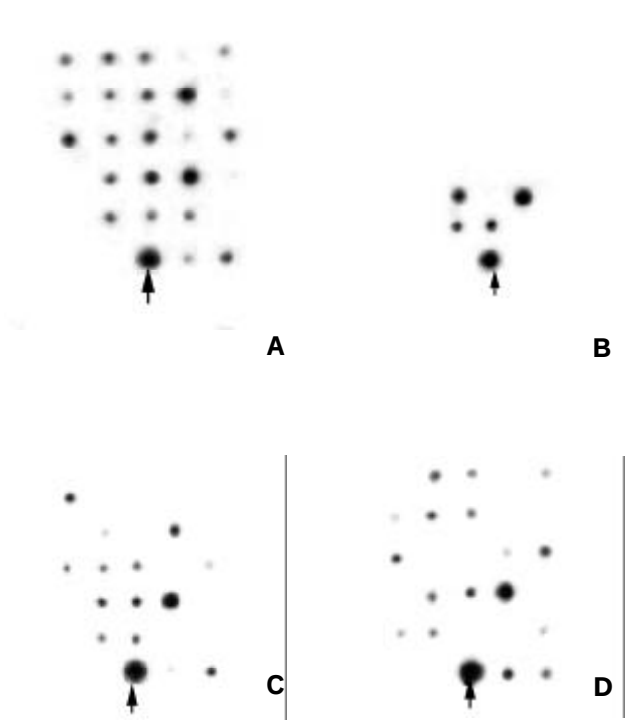

Figure 2 Dot blotting for identification the disease related DNA sequences in 27 different clinical isolates by using GU210 (A), GU79 (B), GU198 (C) and GU235 (D) as probes. The arrowheads indicate the spots of positive controls.

Disease related DNA sequence screening

We next chose 4 tester strain specific DNA sequences as probes to screen the genomic DNA of *H.pylori* with different clinical background, 8 from GU, 12 from duodenum ulcer (DU), 4 from GU-DU, 2 from NUD and 1 from gastric cancer (GC), to know if some of them were specific for the GU isolates. We found that the 4 different inserts gave 4 different dot blotting profiles (Figure 2) and there were no GU strain unique sequences. But a DNA fragment GU198 (670 bp) that was a bit (78 bp) homologous to the 3' -end of the gene of hymidylate kinase was positive in 7 of the 8 GU strains, 3 of the 4 GU-DU strains, and 3 of the 12 DU strains. It was also positive in one of the 2 NUD strains and the GC strain. The replication gene A fragment GU79 (384 bp) was positive in 4 *H.pylori* isolates, 2 from GU and 2 from GU-DU.

DISCUSSION

A remarkable feature of *H.pylori* is the high diversity of its genomic DNA[26-29]. Clinical isolates of *H.pylor*i from different individuals show enormous variations in their genomes or genes[30-33]. The genetic diversity is represented in many forms, including point mutations and inserted sequences[34]. Such variation has given rise to the notion that *H. pylori* has a very plastic genome, and that such plasticity confers a selective advantage on a bacterium that must co-evolve with its host over the course of decades[17]. Based on this, it is conceivable that there are different DNA sequences between two genomes of *H.pylori* with different clinical background.

SSH is a powerful technique that has been applied to research in many different fields. In studies of eukaryotic systems, application of subtraction techniques typically focuses on differential gene expression between two cDNA populations rather than differences between genomes (Diatchenko L. *Proc Natl Acad Sci U S A* 1996; 93: 6025). This is because eukaryotic genomes are too complex for existing subtraction technologies. In contrast, bacterial genomes are considerably smaller, and are even less complex than many eukaryotic cDNA populations. Thus, subtraction methods can be used to identify sequences that are present in one bacterial genome, but absent in another. It requires only about several micrograms of genomic DNA, takes only several days, and does not involve the physical separation of single strain and double strain molecules. Furthermore, the suppression PCR prevents undesirable amplification while enrichment of target molecules proceeds. Even so, the conditions of the SSH were carefully optimized in this experiment. By comparing the genomic DNA digestion efficiency of *Hae* III, *Rsa* I and *Alu* I, *Alu* I was finally selected. The time of the adaptor ligation should be within 16 hours to avoid ligation between the DNA fragments. The ratio of tester and driver DNA was 1:50 in the first hybridization. In this way, we established a GU strain specific DNA sequence library.

When we used the tester and driver DNA fragments as probes to hybridize separately with different PCR products of the subtracted inserts, the tester specific DNA sequences were screened. Of the 23 sequenced DNA fragments, 15 were homologous to the *H.pylori* plasmid pHPO100. The size of this plasmid is about 3.5 kb and codes a replication protein A, which appears to be the predominant plasmid replication protein of *H. pylori* and has the highly conserved (76-96 %) amino acid sequence and may play an important role in the DNA sequence exchange between plasmid and the chromosome[35]. Thus the protein may increase the gene diversity and have the pathogenic significance. Other inserts had patches of homologous to the genes of different *H.pylori* proteins in GenBank. The results indicate that SSH can be used to screen the strain specific DNA sequences between clinical isolates even though the dominant subtracted fragments come from the plasmid of the tester strain.

When we tried to find out if some of the tester strain specific DNA sequences were unique to GU strains, no such DNA sequences were identified. Whereas a DNA fragment GU198

that is partly homologous to the gene of thymidylate kinase was positive in 7 of the 8 GU strains, 3 of the 4 GU-DU strains, and only 3 of the 12 DU strains. This is also of clinical significance. Study on identification of this DNA fragment is still going on.

Several aspects regarding the identification of disease related DNA sequences need to be discussed. First, the tester strain specific DNA sequences mean that, comparing with the driver strain, these sequences are unique to the tester strain, other strains from GU patients may share or may not share these sequences. Second, since the strain specific genes account for about 6 % of the whole genes of a given *H.pylori* strain[19], more colonies should be screened and more DNA fragments be used to identify the disease specific DNA sequences. Third, dot blotting can be used as a primary screening method, and, if possible, Southern blotting be employed for further identification. Fourth, it is better to choose the plasmid free *H. pylori* for the strain specific DNA sequence screening. Since the copies of a plasmid in the bacterium are often more than that of a gene in its genome, amplification of the subtracted gene sequences coming from the genome would be suppressed in the PCR and, as a result, the dominant strain specific DNA sequences would belong to the plasmid. Although about 50 % of *H. pylori* strains carry cryptic plasmids ranging in size from 2 to about 100 kb[35,36], the role of these plasmids is not well understood. In this investigation, the repA gene was positive in 4 *H.pylori* strains, 2 from GU (2/8), and 2 from GU-DU (2/4). This may be due to the homologous of the genomic DNA to the repA or the insertion of the repA fragment into the genome (De Ungria MC. *Plasmid* 1999; 41: 97) or the plasmid DNA being not eliminated during genomic DNA preparation. Study on the relationship between repA gene and the disease state of the patients is also necessary.

Anyway, we have successfully screened some tester strain specific DNA sequences by SSH, and this study is one of the few attempts trying to identify the disease specific genes using *H.pylori* clinical isolates[23]. Though we failed to get the disease specific DNA sequences, we believe that, at least, some tester strain specific sequences may have significantly high positive rates in strains with similar background to the tester strain. This may aid in the effective diagnosis and treatment of *H. pylori* infection and have the potential value for pathogenic investigation of this bacterium.

ACKNOWLEDGEMENT

Mr. Mun-Fai Loke, from Department of Microbiology, National University of Singapore, prepared some of the *H. pylori* clinical isolates.

REFERENCES

1 **Israel DA**, Peek RM. Pathogenesis of *Helicobacter pylori*-induced gastric inflammation. *Aliment Pharmacol Ther* 2001; **15**: 1271-1290
2 **Sanders MK,** Peura DA. *Helicobacter pylori*-Associated Diseases. *Curr Gastroenterol Rep* 2002; **4**: 448-454
3 **Dawsey SM**, Mark SD, Taylor PR, Limburg PJ. Gastric cancer and *H pylori*. *Gut* 2002; **51**: 457-458
4 **Blaser MJ**. Linking *Helicobacter pylori* to gastric cancer. *Nat Med* 2000; **6**: 376-377
5 **Unger Z**, Molnar B, Pronai L, Szaleczky E, Zagoni T, Tulassay Z. Mutant p53 expression and apoptotic activity of *Helicobacter pylori* positive and negative gastritis in correlation with the presence of intestinal metaplasia. *Eur J Gastroenterol Hepatol* 2003; **15**: 389-393
6 **Yang Y,** Deng CS, Peng JZ, Wong BC, Lam SK, Xia HH. Effect of *Helicobacter pylori* on apoptosis and apoptosis related genes in gastric cancer cells. *Mol Pathol* 2003; **56**: 19-24
7 **Wang RT**, Wang T, Chen K, Wang JY, Zhang JP, Lin SR, Zhu YM, Zhang WM, Cao YX, Zhu CW, Yu H, Cong YJ, Zheng S, Wu BQ. *Helicobacter pylori* infection and gastric cancer: evidence from a retrospective cohort study and nested case-control study in China. *World J Gastroenterol* 2002; **8**: 1103-1107
8 **Meining A**, Riedl B, Stolte M. Features of gastritis predisposing to gastric adenoma and early gastric cancer. *J Clin Pathol* 2002; **55**: 770-773
9 **Lan J,** Xiong YY, Lin YX, Wang BC, Gong LL, Xu HS, Guo GS. *Helicobacter pylori* infection generated gastric cancer through p53-Rb tumor-suppressor system mutation and telomerase reactivation. *World J Gastroenterol* 2003; **9**: 54-58
10 **Cai L**, Yu SZ, Zhang ZF. *Helicobacter pylori* infection and risk of gastric cancer in Changle County, Fujian Province, China. *World J Gastroenterol* 2000; **6**: 374-376
11 **Liu HF**, Liu WW, Fang DC, Wang GA, Teng XC. Relationship between *Helicobacter pylori* infection and gastric precancerous lesions: a follow-up study. *Shijie Huaren XiaohuaZazhi* 2002; **10**: 912-915
12 **Miehlke S**, Kirsch C, Dragosics B, Gschwantler M, Oberhuber G, Antos D, Dite P, Lauter J, Labenz J, Leodolter A, Malfertheiner P, Neubauer A, Ehninger G, Stolte M, Bayerdorffer E. *Helicobacter pylori* and gastric cancer: current status of the Austrian in Czech German gastric cancer prevention trial (PRISMA Study). *World J Gastroenterol* 2001; **7**: 243-247
13 **Yao YL**, Xu B, Song YG, Zhang WD. Overexpression of cyclin E in Mongolian gerbil with *Helicobacter pylori*-induced gastric precancerosis. *World J Gastroenterol* 2002; **8**: 60-63
14 **Zhang Z,** Yuan Y, Gao H, Dong M, Wang L, Gong YH. Apoptosis, proliferation and p53 gene expression of *H. pylori* associated gastric epithelial lesions. *World J Gastroenterol* 2001; **7**: 779-782
15 **Xue FB,** Xu YY, Wan Y, Pan BR, Ren J, Fan DM. Association of *H.pylori* infection with gastric carcinoma: a Meta analysis. *World J Gastroenterol* 2001; **7**: 801-804
16 **Liu HF**, Liu WW, Fang DC, Wang GA, Teng XC. Effect of *Helicobacter pylori* infection on bax protein expression in patients with gastric precancerous lesions. *Shijie Huaren Xiaohua Zazhi* 2003; **11**: 22-24
17 **Bjorkholm BM**, Oh JD, Falk PG, Engstrand LG, Gordon JI. Genomics and proteomics converge on *Helicobacter pylori*. *Curr Opin in Microbiol* 2001; **4**: 237-245
18 **Agron PG**, Macht M, Radnedge L, Skowronski EW, Miller W, Andersen GL. Use of subtractive hybridization for comprehensive surveys of prokaryotic genome differences. *FEMS Microbiology Letters* 2002; **10468**: 1-8
19 S**alama N,** Guillemin K, McDaniel TK, Sherlock G, Tompkins L, Falkow S. A whole genome microarray reveals genetic diversity among *Helicobacter pylori* strains. *Proc Natl Acad Sci U S A* 2000;**97**: 14668-14673
20 **Blaser MJ,** Berg DE. *Helicobacter pylori* genetic diversity and risk of human disease. *J Clin Invest* 2001; **107**: 767-773
21 I**srael DA**, Salama N, Arnold CN, Moss SF, Ando T, Wirth HP, Tham KT, Camorlinga M, Blaser MJ, Falkow S, Peek RM Jr. *Helicobacter pylori* strain-specific differences in genetic content, identified by microarray, influence host inflammatory responses. *J Clin Invest* 2001; **107**: 611-620
22 **Shibata A**, Parsonnet J, Longacre TA, Garcia MI, Puligandla B, Davis RE, Vogelman JH, Orentreich N, Habel LA. CagA status of *Helicobacter pylori* infection and p53 gene mutations in gastric adenocarcinoma.*Carcinogenesis* 2002; **23**: 419-424
23 **Kersulyte D,** Velapatino B, Dailide G, Mukhopadhyay AK, Ito Y, Cahuayme L, Parkinson AJ, Gilman RH, Berg DE. Transposable element ISHp608 of *Helicobacter pylori*: nonrandom geographic distribution, functional organization, and insertion specificity. *J Bacteriol* 2002; **184**: 992-1002
24 **Kersulyte D**, Mukhopadhyay AK, Shirai M, Nakazawa T, Berg DE. Functional organization and insertion specificity of IS607, a chimeric element of *Helicobacter pylori*. *J Bacteriol* 2000; **182**: 5300-5308
25 **Hua JS**, Zheng PY, Fong TK, Mar KM, Bow H. *Helicobacter pylori* acquistion of metronidazole resistance by natural transformation *in vitro*. *World J Gastroenterol* 1998; **4**: 385-387

26 **Suerbaum S**. Genetic variability within *Helicobacter pylori*. *Int J Med Microbiol* 2000; **290**: 175-181

27 **Yakoob J,** Hu GL, Fan XG, Yang HX, Liu SH, Tan DM, Li TG, Zhang Z. Diversity of *Helicobacter pylori* among Chinese persons with *H. pylori* infection. *APMIS* 2000; **108**: 482-486

28 **Israel DA**, Salama N, Krishna U, Rieger UM, Atherton JC, Falkow S, Peek RM Jr. *Helicobacter pylori* genetic diversity within the gastric niche of a single human host. *Proc Natl Acad Sci U S A* 2001; **98**: 14625-14630

29 **Nobusato A**, Uchiyama I, Kobayashi I. Diversity of restriction-modification gene homologues in *Helicobacter pylori*. *Gene* 2000; **259**: 89-98

30 **Tomasini ML**, Zanussi S, Sozzi M, Tedeschi R, Basaglia G, De Paoli P. Heterogeneity of cag Genotypes in *Helicobacter pylori* Isolates from Human Biopsy Specimens. *J Clin Microbiol* 2003; **41**: 976-980

31 **Ji WS**, Hu JL, Qiu JW, Peng DR, Shi BL, Zhou SJ, Wu KC, Fan DM. Polymorphism of flagellin A gene in *Helicobacter pylori*. *World J Gastroenterol* 2001; **7**: 783-787

32 **Pride DT**, Meinersmann RJ, Blaser MJ. Allelic Variation within *Helicobacter pylori* babA and babB. *Infect Immun* 2001; **69**: 1160-1171

33 **Azuma T,** Yamakawa A, Yamazaki S, Fukuta K, Ohtani M, Ito Y, Dojo M, Yamazaki Y, Kuriyama M. Correlation between variation of the 3' region of the cagA gene in *Helicobacter pylori* and disease outcome in Japan. *J Infect Dis* 2002; **186**: 1621-1630

34 **Nobusato A**, Uchiyama I, Ohashi S, Kobayashi I. Insertion with long target duplication: a mechanism for gene mobility suggested from comparison of two related bacterial genomes. *Gene* 2000; **259**: 99-108

35 **Hofreuter D**, Haas R. Characterization of two cryptic *Helicobacter pylori* plasmids: a putative source for horizontal gene transfer and gene shuffling. *J Bacteriol* 2002; **184**: 2755-2766

36 **Hosaka Y**, Okamoto R, Irinoda K, Kaieda S, Koizumi W, Saigenji K, Inoue M. Characterization of pKU701, a 2.5-kb plasmid, in a Japanese *Helicobacter pylori* isolate. *Plasmid* 2002; **47**: 193-200

Edited by Zhang JZ

P.O.Box 2345, Beijing 100023,China
Fax: +86-10-85381893
E-mail: wjg@wjgnet.com www.wjgnet.com

World J Gastroenterol 2003;9(8):1752-1755
World Journal of Gastroenterology
 ISSN 1007-9327

Seroprevalence of *Helicobacter pylori* in school-aged Chinese in Taipei City and relationship between ABO blood groups

Tzee-Chung Wu, Liang-Kung Chen, Shinn-Jang Hwang

Tzee-Chung Wu, Division of Gastroenterology and Nutrition, Children' s Medical Center, Taipei Veterans General Hospital; School of Medicine, National Yang-Ming University, Taipei, Taiwan
Liang-Kung Chen, Shinn-Jang Hwang, Department of Family Medicine, Taipei Veterans General Hospital; School of Medicine, National Yang-Ming University, Taipei, Taiwan
Correspondence to: Dr. Tzee-Chung Wu, Division of Gastroenterology and Nutrition, Children' s Medical Center, Taipei Veterans General Hospital, No. 201, Shih-Pai Road Sec 2, Taipei, 11217 Taiwan. tcwu@vghtpe.gov.tw
Telephone: +886-2-2875-7190 **Fax**: +886-2-2876-7109
Received: 2003-04-02 **Accepted:** 2003-04-24

Abstract

AIM: To explore the seropositive rate of antibodies against *H. pylori* (anti-HP) in Taipei City and to compare the relationship of ABO blood groups and *H. pylori* infection.

METHODS: In 1993, high school students in Shih-Lin District were randomly selected for blood samplings by their registration number at school. In addition, similar procedures were performed on the well-children clinics of Taipei Veterans General Hospital. Besides, randomly selected sera from the adults who took the physical examination were recruited for evaluation. Informed consents were obtained from all the subjects before blood samplings and parents were simultaneously informed for those who were younger than 18-year-old. Blood tests for anti-HP and ABO blood groupings were performed by enzyme-linked immunosorbent assay. Chi square tests were used for the comparisons between seroprevalence of *H. pylori* and ABO blood groups.

RESULTS: Totally, 685 subjects were recruited (260 children aged 1-14 years, 425 high school students aged 15-18 years) were evaluated, and another 88 adult healthy volunteers were studied as well for comparison. The age-specific seropositive rate of anti-HP was 1.3 % at age 1-5 years, 7.7 % at age 6-10 years, and 11.5 % at age 11-14 years. The seroprevalence of *H. pylori* infection was abruptly increased in young adolescence: 18.6 % at age 15 years, 28.1 % at age 16 years, 32.4 % at age 17 years and 41.0 % at age 18 years, respectively. In the 425 high school students, ABO blood groupings were performed, which disclosed 48.5 % (206/425) of blood group O, 24 % (102/425) of blood group A, 21.8 % (93/425) of blood group B and 5.6 % (24/425) of blood group AB. In comparison of the subjects with blood group O and the other blood groups, no statistical significance could be identified in the seroprevalence of *H. pylori* (P=0.99).

CONCLUSION: The seroprevalence of *H. pylori* infection in Taipei City in adults is similar to the developed countries, and the abrupt increase of *H. pylori* during high school may be resulted from marked increase of interpersonal social activities. Although blood group O was reported to be related to *H. pylori* infection in previous literature, we found no association between *H. pylori* infection and ABO blood groups.

Wu TC, Chen LK, Hwang SJ. Seroprevalence of *Helicobacter pylori* in school-aged Chinese in Taipei City and relationship between ABO blood groups. *World J Gastroenterol* 2003; 9 (8): 1752-1755
http://www.wjgnet.com/1007-9327/9/1752.asp

INTRODUCTION

Helicobacter pylori (*H. pylori*) infection is the most common chronic bacterial infection in the world. Previous seroepidemiologic studies indicated that about 50 % of adults in the developed countries and nearly 90 % of adults in the developing countries were positive of serum antibodies against *H. pylori*[1]. Chronic *H. pylori* infection may be related to several conditions, including chronic gastritis[2,3], peptic ulcer disease[4,5], primary gastric lymphoma (mostly mucosa-associated lymphoid tissue, MALToma)[6,7], and gastric adenocarcinoma[8,9].

The seroprevalence of *H. pylori* infection of adults in Taiwan varied from 54.4 % to 59 % in previous reports, which was similar to developed countries[10-12]. However, the seroprevalence of *H. pylori* infection was low in the preschool children in Taiwan. The seropositive rate of antibodies against *H. pylori* was 8.1 % in 2 551 healthy preschool children aged 3-6 years[13], and it was significantly increased to 21.1 % in young adolescence[14]. Therefore, marked increase of interpersonal social activities during the school age was proposed to be the most likely source of *H. pylori* infection.

People with blood group O have been noted to be more susceptible to peptic ulcer disease for decades without appropriate explanations[15,16]. In 1993, Boren *et al*[17] reported that people with blood group O had more *H. pylori* receptors, and Lewis^b antigens mediated the attachment of *H. pylori* to the gastric mucosa. Furthermore, higher density of colonization of *H. pylori* was noted in the gastric mucosa of people with blood group O[18]. However, absence of correlation between *H. pylori* infection and ABO blood groups was reported in some following studies[19,20].

In Taiwan, blood group O was reported to correlate with the prevalence of *H. pylori* infection in patients with gastroduodenal diseases[21], but it remained unknown for those asymptomatic individuals who were infected by *H. pylori*. Therefore, we conducted a study to evaluate the relationship between *H. pylori* and ABO blood groups in those healthy volunteers in Taipei City to clarify the possible association.

MATERIALS AND METHODS

We conducted a cross-sectional survey among senior high schools in the Shih-Lin District, Taipei City in 1993. All the recruited subjects were randomly selected in each age group (from 15 to 18) according to the registration number in schools. Blood samplings were performed after the informed consents were signed by themselves or their parents (if the subjects were younger than 18-year-old). In addition, children at age 1 to 14 years from the well-children clinics of Taipei Veterans General Hospital were recruited if their parents agreed with the study

and signed the informed consents. Moreover, we randomly collected the sera of adults who underwent physical examinations from the Department of Physical Examination to evaluate the seroprevalence of *H. pylori*. This study was evaluated and approved by the Ethical Committee of Taipei Veterans General Hospital.

The blood samples were centrifuged and the sera were stored in aliquot at -80 ℃ until analysis. The serum antibodies against *H. pylori* were tested by the commercial enzyme-linked immunosorbent assay (ELISA) kit (HEL-P test, AMRAD, Sydney, Australia). In addition, ABO blood groupings were also done by the ELISA test (Gamma Biologicals, Houston, TX, USA). ABO blood groupings were not performed in children from the well-children clinics because we reserved the sera from the blood samplings in the beginning, which were not possible for ABO blood groupings by the commercial kit.

Data of the recruited individuals were expressed in categories. The comparisons of seroprevalence of *H. pylori* between each ABO blood group were evaluated by chi-square test or Fisher' s exact test if appropriate. A *P* value of less than 0.05 would be considered statistically significant. All the available data were analyzed by a computer program (SPSS, Chicago, IL, USA).

RESULTS

Totally, 685 subjects were recruited, including 260 children aged 1-14 years from the Well-children Clinic, and 425 young adolescents aged 15-18 years from high school students in Shih-Lin District, Taipei City. In addition, sera of 88 randomly selected subjects from the Department of Physical Examination were evaluated for the referential seroprevalence of *H. pylori* in adults (Table 1).

Table 1 Age and sex distribution of seroprevalence of antibodies against *Helicobacter pylori* (anti-HP), and comparisons between sex and age groups

Age	Male		Female		*P*
	Anti-HP (+)/*n*	(%)	Anti-HP (+)/*n*	(%)	
1-5	0/26	0	1/42	2.4	0.32
6-10	4/39	10.3	2/39	5.1	0.40
11-14	9/53	17.0	3/51	5.9	0.08
Subtotal	13/118	11.0	6/132	4.5	0.06
15	7/34	20.6	11/63	17.5	0.72
16	9/38	23.7	27/90	30	0.46
17	21/65	32.3	24/74	32.4	0.99
18	14/41	34.1	11/20	55.0	0.14
Subtotal	51/179	28.5	73/246	29.7	0.79
Adults	27/49	55.1	19/39	48.7	0.56
Total	91/346	26.3	98/417	23.5	0.37

The age-specific seropositive rate of antibodies against *H. pylori* was 1.3 % at age 1-5 years, 7.7 % at age 6-10 years, and 11.5 % at age 11-14 years. The seroprevalence of *H. pylori* infection abruptly increased in young adolescence: 18.6 % at age 15 years, 28.1 % at age 16 years, 32.4 % at age 17 years and 41.0 % at age 18 years, respectively. In randomly selected adults, the seropositive rate of anti-HP reached 52.3% (Figure 1).

In the 425 randomly selected high school students, ABO blood groupings were performed, which disclosed 48.5 % (206/425) blood group O, 24 % (102/425) blood group A, 21.8 % (93/425) blood group B and 5.6 % (24/425) blood group AB. Further analysis on the ABO blood groupings and seroprevalence of *H. pylori* demonstrated that seropositive rate of anti-HP was 27.7 % (57/206) in blood group O, 31.4 % (32/102) in blood group A, 30.1 % (28/93) in blood group B, and 29.2 % (7/24) in blood group AB (Table 2). In comparison of the subjects with blood group O with the other blood groups, no statistical difference could be identified in the seroprevalence of *H. pylori* (*P*=0.98). Neither was the difference significant among the groups as for being vulnerable to *H. pylori* infection.

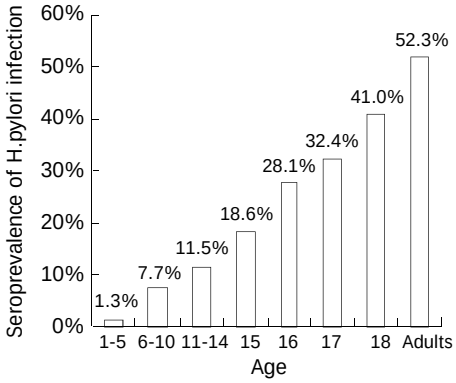

Figure 1 Age-specific seroprevalence of *H. pylori* infection in 773 healthy subjects in Taipei.

Table 2 Relationship of ABO blood groups and seropositivity of antibodies against *Helicobacter pylori* (anti-HP) infection

Blood group	Serum anti-HP (+)	Serum anti-HP (-)	*P*
O	57 (27.7%)	149 (72.3%)	-
A	32 (31.4%)	70 (68.6%)	0.99
B	28 (30.1%)	65 (69.9%)	0.99
AB	7 (29.2%)	17 (60.8%)	0.99
Total	124 (100%)	301 (100%)	

DISCUSSION

H. pylori infection is the most prevalent chronic bacterial infection in the world. Despite of the worldwide infection, the transmission pattern remains uncertain. *H. pylori* infection is rare before first two decades of life in developed countries, ranging from 6 % to 16 %[22-24]. However, children in Gambia and Nigeria are almost all infected by *H. pylori* at age of 5 years[25,26]. According to the previous reports, the seroprevalence of *H. pylori* infection in Taiwanese preschool children (3-6 years old) was 8.1 %, with the age-dependent progression (4.5 % in 3-year-old children, 4.4 % in 4-year-old children, 9.4 % in 5-year-old children, and 11.7 % in 6-year-old children)[13]. Furthermore, the seropositivity of antibodies against *H. pylori* was reported to be 21.1 % in adolescents[14], and 54.4 % in adults over 30-year-old in Taiwan[10]. Moreover, age-specific prevalence of *H. pylori* infection in patients with gastroduodenal diseases was 11.1 % in those aged 1 to 20, 73.1 % at age 21-30, and 79.8 % at age 51-60 in Central Taiwan[27]. In this seroepidemiological study, we also found a similar pattern of age-dependent progression. However, the seroprevalence of *H. pylori* in this study (1.3 % at age 1-5 years, 7.7 % at age 6-10 years, and 11.5 % at age 11-14 years) was significantly lower than that in the Taiwan islandwide survey. The better socioeconomic status in Taipei City may account for the differences of seroprevalence of *H. pylori* infection. However, the seroprevalence of *H. pylori* infection among adults in Taipei City was about the average of the Taiwan islandwide survey.

The transmission pattern of *H. pylori* currently remains uncertain, but the role of fecal-oral route seems to be minor[28,29]. The genotypic study did not support oral-oral transmission

pattern of *H. pylori* infection, either[30]. Intrafamilial and person-to-person transmission has been shown being more important in *H. pylori* infection[31,32]. Risk factors analysis of *H. pylori* infection has been extensively performed including gender, race, family income, type of housing, location of housing, water supply, health status, and keeping pets, but only the socioeconomic status was better confirmed[33-36]. Broutet *et al* [37] proposed that male gender deserve more attention in epidemiological studies of *H. pylori* infection. In this study, the male predominance of *H. pylori* infection was observed. However, similar findings were not supported in previous epidemiological reports despite of different areas, ethnicity, and age[38-41]. The sex difference of *H. pylori* infection at age 11-14 years was unclear, which deserves further investigations.

The seropositive rate of anti-HP increased abruptly in subjects at age 15 years to 18 years (18.6 % to 41.0 %) in this study. The estimated annual incidence was 7.5 % in this cross-sectional survey, which might be resulted from the extensive social activities at this stage. On the other hand, smoking is an important factor in *H. pylori* infection, particularly in young adults[42,43]. Most smokers start smoking at their young adolescence. Therefore, smoking may be another explanation of such an abrupt increase of *H. pylori* infection among people aged 15 to 18.

People with blood group O were found more susceptible to peptic ulcer disease for decades without known cause until the relationship between Lewis^b antigens and the attachment of *H. pylori* to gastric mucosa was observed[15-18]. However, the correlation between *H. pylori* infection and ABO blood types was not supported in some reports[19,20]. Nevertheless, Lin *et al*[21] demonstrated the close relationship between *H. pylori* infection and blood group O patients with gastroduodenal diseases in Central Taiwan. In our study, healthy individuals rather than symptomatic patients with blood group O were not particularly vulnerable to *H. pylori* infection.

In conclusion, the abrupt increase of *H. pylori* infection in high school students was noted with the estimated yearly incidence to be 7.5 %. Subjects with blood group O do not increase clinical susceptibility to *H. pylori* infection than those with other blood groups.

REFERENCES

1 **Megraud F.** Epidemiology of *Helicobacter pylori* infection. *Gastroenterol Clin North Am* 1993; **22:** 73-88
2 **Czinn SJ,** Dahms BB, Jacobs GH, Kaplan B, Rothstein FC. Campylobacter-like organisms in association with symptomatic gastritis in children. *J Pediatr* 1986; **109**: 80-83
3 **Ashorn M.** What are the specific features of *Helicobacter pylori* gastritis in children? *Ann Med* 1995; **27:** 617-620
4 **Rauws EA,** Tytgat GN. Cure of duodenal ulcer associated with eradication of *Helicobacter pylori*. *Lancet* 1990; **1:** 1233-1235
5 **Macarthur C,** Saunders N, Feldman W. *Helicobacter pylori*, gastroduodenal disease, and recurrent abdominal pain in children. *JAMA* 1995; **273:** 729-734
6 **Wotherspoon AC.** Gastric lymphoma of mucosa-associated lymphoid tissue and *Helicobacter pylori*. *Annu Rev Med* 1998; **49:** 289-299
7 **Wu TC,** Chen LK, Lai CR. Primary gastric lymphoma associated with *Helicobacter pylori* in a child. *J Ped Gastroenterol Nutr* 2001; **32:** 608-610
8 **Parsonnet J,** Friedman GD, Vandersteen DP, Chang Y, Vogelman JH, Orentreich N, Sibley RK. *Helicobacter pylori* infection and the risk of gastric carcinoma. *N Engl J Med* 1991; **325:** 1127-1131
9 **Nomura A,** Stemmermann GN. *Helicobacter pylori* and gastric cancer. *J Gastroenterol Hepatol* 1993; **8:** 294-303
10 **Lin JT,** Wang JT, Wang TH, Wu MS, Lee TK, Chen CJ. *Helicobacter pylori* infection in a randomly selected population, healthy volunteers, and patients with gastric ulcer and gastric adenocarcinoma. A seroprevalence study in Taiwan. *Scand J Gastroenterol* 1993; **28:** 1067-1072
11 **Lin JT,** Wang JT, Wu MS, Wang TH, Lee TK, Chen CJ. Seroprecalence study of *Helicobacter pylori* infection in patients with gastroduodenal diseases. *J Formos Med Assoc* 1994; **93:** 122-127
12 **Lin JT,** Wang LY, Wang JT, Wang TH, Tang CS, Chen CJ. A nested case-control study on the association between *Helicobacter pylori* infection and gastric cancer risk in a cohort of 9775 men in Taiwan. *Anticancer Res* 1995; **15:** 603-606
13 **Lin DB,** Nieh WT, Wang HM, Hsiao MW, Ling UP, Changlai SP. Seroepidemiology of *Helicobacter pylori* infection among preschool children in Taiwan. *Am J Trop Med Hyg* 1999; **61:** 554-558
14 **Wang LY,** Lin JT, Cheng YW, Chou SSJ, Chen SJ. Seroepidemiology of *Helicobacter pylori* among adolescents in Taiwan. *Chin J Microbiol Immunol* 1996; **29:** 10-17
15 **Clark CA,** Wyn EJ, Haddock DRW, Howel-Evans AW, McConnell RB, Sheppard PM. ABO blood groups and secretor character in duodenal ulcer. *Br Med J* 1956; **2:** 725-731
16 **Mentis A,** Blackwell CC, Weir DM, Spiliadis C, Dailianas A, Skandalis N. ABO blood group, secretor status, and detection of *Helicobacter pylori* among patients with gastric or duodenal ulcers. *Epidemiol Infect* 1991; **106:** 221-229
17 **Boren T,** Falk P, Roth KA, Larson G, Normark S. Attachment of *H. pylori* to human gastric epithelium mediated by blood type group antigens. *Science* 1993; **262:** 1892-1895
18 **Atherton JC,** Tham KT, Peek RM Jr, Cover TL, Blaser MJ. Density of *Helicobacter pylori* infection *in vivo* as assessed by quantitative culture and histology. *J Infect Dis* 1996; **174:** 552-556
19 **Loffeld RJ,** Stobberingh E. *Helicobacter pylori* and ABO blood groups. *J Clin Pathol* 1991; **44:** 516-517
20 **Niv Y,** Fraser G, Delpre G, Neeman A, Leiser A, Samra Z. *Helicobacter pylori* infection and blood groups. *Am J Gastroenterol* 1996; **91:** 101-104
21 **Lin CW,** Chang YS, Wu SC, Cheng KS. *Helicobacter pylori* in gastric biopsies of Taiwanese patients with gastroduodenal diseases. *Jpn J Med Sci Biol* 1998; **51:** 13-23
22 **De Giacomo C,** Lisato L, Negrini R, Licardi G, Maggiore G. Serum immune response to Helicobacter pylori in children: epidemiologic and clinical applications. *J Pediatr* 1991; **199:** 205-210
23 **Thomas JE,** Whatmore AM, Barer MR, Eastham EJ, Kehoe MA. Serodiagnosis of *Helicobacter pylori* infection in children. *J Clin Microbiol* 1990; **28:** 2641-2646
24 **Oderda G,** Vaira D, Holton J. Age-related increase of *Helicobacter pylori* prevalence in symptom-free and in dyspeptic children. *Lancet* 1992; **340:** 671-672
25 **Holcombe C,** Tsimiri S, Elridge J, Jones DM. Prevalence of antibody to *Helicobacter pylori* in children in northern Nigeria. *Trans R Soc Trop Med Hyg* 1993; **87:** 19-21
26 **Sullivan PB,** Thomas JE, Wight DG, Neale G, Eastham EJ, Corrah T. *Helicobacter pylori* in Gambian children with chronic diarrhea and malnutrition. *Arch Dis Child* 1990; **65:** 189-191
27 **Lin CW,** Chang YS, Lai PY, Cheng KS. Prevalence and heterogeneity of *Helicobacter pylori* in gastric biopsies of patients with gastroduodenal diseases. *J Microbiol Immunol Infect* 1997; **30:** 61-71
28 **Webb PM,** Knight T, Newell DG, Elder JB, Forman D. *Helicobacter pylori* transmission: evidence from a comparison with hepatitis A virus. *Eur J Gastroenterol Hepatol* 1996; **8:** 439-441
29 **Lin DB,** Tsai TP, Yang CC. Association between seropositivity of antibodies against hepatitis A virus and *Helicobacter pylori*. *Am J Trop Med Hyg* 2000; **63:** 189-191
30 **Luman W,** Zhao Y, Ng HS, Ling KL. *Helicobacter pylori* infection is unlikely to be transmitted between partners: evidence from genotypic study in partners of infected patients. *Eur J Gastroenterol Hepatol* 2002; **14:** 521-528
31 **Tindberg Y,** Bengtsson C, Granath F, Blennow M, Nyren O, Granstrom M. *Helicobacter pylori* infection in Swedish school children: lack of evidence of child-to-child transmission outside the family. *Gastroenterology* 2001; **121:** 310-316
32 **Wizla-Derambure N,** Michaud L, Ategbo S, Vincent P, Ganga-Zandzou S, Turck D, Gottrand F. Familial and community environmental risk factors for *Helicobacter pylori* infection in children and adolescents. *J Ped Gastroenterol Nutr* 2001; **33:** 58-63
33 **Graham DY,** Malaty HM, Evans DG, Evans DJ Jr, Klein PD, Adam E. Epidemiology of *Helicobacter pylori* in an asymptomatic popu-

lation in the United States. Effect of age, race, and socioeconomic status. *Gastroenterology* 1991; **100:** 1495-1501

34 **Fiedorek SC,** Malaty HM, Evans DL, Pumphrey CL, Casteel HB, Evans DJ Jr, Granham DY. Factors influencing the epidemiology of *Helicobacter pylori* infection in children. *Pediatrics* 1991; **88:** 578-582

35 **Stone MA,** Taub N, Barnett DB, Mayberry JF. Increased risk of infection with *Helicobacter pylori* in spouses of infected subjects: observations in a general population sample from the UK. *Hepato-Gastroenterology* 2000; **47:** 433-436

36 **Brown LM.** *Helicobacter pylori*: epidemiology and routes of transmission. *Epidemiologic Reviews* 2000; **22:** 283-297

37 **Broutet N,** Sarasqueta AM, Sakarovitch C, Cantet F, Lethuaire D, Megraud F. *Helicobacter pylori* infection in patients consulting gastroenterologists in France: prevalence is linked to gender and region of residence. *Eur J Gastroenterol Hepatol* 2001; **13:** 677-684

38 **Elitsur Y,** Short JP, Neace C. Prevalence of *Helicobacter pylori* infection in children from urban and rural West Virginia. *Dig Dis Sci* 1998; **43:** 773-778

39 **Sinha SK,** Martin B, Sargent M, McConnell JP, Bernstein CN. Age at acquisition of *Helicobacter pylori* in a pediatric Canadian First Nations population. *Helicobacter* 2002; **7:** 76-85

40 **Leal-Herrera Y,** Torres J, Perez-Perez G, Gomez A, Monath T, Tapia-Conyer R, Munoz O. Serologic IgG response to urease in *Helicobacter pylori*-infected persons from Mexico. *Am J Trop Med Hyg* 1999; **60:** 587-592

41 **Lin JT,** Wang LY, Wang JT, Wang TH, Chen CJ. Ecological study of association between *Helicobacter pylori* infection and gastric cancer in Taiwan. *Dig Dis Sci* 1995; **40:** 385-388

42 **Brenner H,** Rothenbacher D, Bode G, Adler G. Relation of smoking and alcohol and coffee consumption to active *Helicobacter pylori* infection: cross sectional study. *Br Med J* 1997; **315:** 1489-1492

43 **Kopanski Z,** Schlegel-Zawadzka M, Golec E, Witkowska B, Micherdzinski J, Cienciala A, Kustra Z. The significance of selected epidemiologico-clinical factors in the prevalence of the *Helicobacter pylori* infection in young males. *Eur J Med Res* 1997; **2:** 358-360

Edited by Xu XQ

P.O.Box 2345, Beijing 100023,China
Fax: +86-10-85381893
E-mail: wjg@wjgnet.com www.wjgnet.com

World J Gastroenterol 2003;9(8):1756-1761
World Journal of Gastroenterology
 ISSN 1007-9327

Construction and characterization of bivalent vaccine candidate expressing HspA and M_r18 000 OMP from *Helicobacter pylori*

Zheng Jiang, Ai-Long Huang, Xiao-Hong Tao, Pi-Long Wang

Zheng Jiang, Xiao-Hong Tao, Pi-Long Wang, Department of Gastroenterology, the First Affiliated Hospital, Chongqing University of Medical Sciences, Chongqing 400016, China
Ai-Long Huang, Institute of Viral Hepatitis, Chongqing University of Medical Sciences, Chongqing 400010, China
Correspondence to: Dr. Zheng Jiang, Department of Gastroenterology, the First Affiliated Hospital, Chongqing University of Medical Sciences, Chongqing 400016, China. jianggooddoctor@mail.china.com
Telephone: +86-23-68891218
Received: 2003-01-11 **Accepted:** 2003-03-10

Abstract

AIM: To construct a recombinant vector which can express outer membrane protein (OMP) with M_r18 000 and heat shock protein A (HspA) from *Helicobacter pylori* (*H. pylori*) in *E. coli* BL21, and to exploit the possibility for obtaining the vaccine conferring protection from *H. pylori* infection.

METHODS: The target gene of HspA was amplified from *H. pylori* chromosome by PCR, and then inserted into the prokaryotic expression vector pET32a (+) by restrictive endonuclease enzyme *kpn* I, *Bam*H I simultaneously. The recombinant vector was used to sequence, and then together with pET32a (+)/Omp_{18}, digested by restrictive endonuclease enzyme *Hind* III and *Bam*H I simultaneously. pET32a(+)/HspA and Omp_{18} were recovered from 1 % agarose gel by gel kit, and ligated with T_4 ligase by *Bam*H I digested viscidity end. The recombinant plasmid of pET32a(+)/HspA/Omp_{18} was transformed and expressed in *E. coli* BL21 (DE3) under induction of IPTG. After purification, its antigenicity of the fusion protein was detected by Western blot.

RESULTS: Enzyme digestion analysis and sequencing showed that the target genes were inserted into the recombinant vector, composed of 891 base pairs, encoded objective polypeptides of 297 amino acid residues. Compared with GenBank reported by Tomb *et al,* there were 1.3 % and 1.4 % differences in obtained *H. pylori* nucleotide sequence and amino acid residues, respectively. SDS-PAGE analysis showed that relative molecule mass (M_r) of the expressed product was M_r 51 000, M_r of protein expressed by pET32a (+) was about M_r 20 000, and soluble expression product accounted for 18.96 % of total bacterial protein. After purification with Ni^{+2}-NTA agarose resins, the purification of recombinant fusion protein was about 95 %. Western blot showed that recombinant fusion protein could be recognized by the patients' serum infected with *H. pylori* and anti-Omp_{18} monoclone, suggesting that this protein had good antigenicity.

CONCLUSION: The gene coding for *H. pylori* M_r18 000 OMP and HspA was cloned and expressed successfully. The results obtained lay the foundation for development of *H. pylori* protein vaccine and a quick diagnostic kit.

Jiang Z, Huang AL, Tao XH, Wang PL. Construction and characterization of bivalent vaccine candidate expressing HspA and M_r18 000 OMP from *Helicobacter pylori*. *World J Gastroenterol* 2003; 9(8): 1756-1761
http://www.wjgnet.com/1007-9327/9/1756.asp

INTRODUCTION

Helicobacter pylori (*H.pylori*) is a microaerophilic, spiral and gram-negative bacillus first isolated from human gastric antral epithelium in 1982. It has been recognized as a human-specific gastric pathogen that colonizes the stomaches of at least half the world's population[1], and there are approximately thousands of newly infected people annually. Most infected individuals are asymptomatic. However, in some individuals, their infections are associated with the development of peptic ulcer, gastric adenocarcinoma, mucosa-associated lymphoid tissue (MALT) lymphoma and primary gastric non-Hodgkin's lymphoma[2-20], moreover with extradigestive diseases[21-37]. This organism was recently categorized as a class I carcinogenetic factor by the World Health Organization, and direct evidence of carcinogenesis was recently demonstrated in an animal model[38,39]. Although there are many methods for eradication of *H. pylori* infection, such as bi-, tri- drug therapy, the definitive curative effects were acquired by using a serial of antibiotics, which has led to resistant *H. pylori*. Meantime medical side effects, patients' endurance and compliance were challenged. This has drawn increasing interests of scientists in developing *H. pylori* vaccine so as to reduce and prevent *H. pylori* infection, extinct diseases associated with *H. pylori* infection. Immunization against this bacterium represents a cost-effective strategy to reduce global *H. pylori*-gastric cancer and peptic ulcer rates[40]. To date, *H. pylori* vaccine candidate antigens identified include urease enzyme, VacA, and so on[41-50]. M_r18 000 and HspA are outer membrane proteins of *H. pylori*, and the vaccines prepared with M_r18 000 OMP and HspA respectively were used to inoculate Balb/c mice, 70-80 % of experimental mice were protected. In order to acquire a better immunocompetent effect, some investigators suggested that bi-valent antigen vaccine was possibly superior to single antigen. So in this study, the recombinant plasmid encoding *H. pylori* M_r18 000 OMP and HspA genes was constructed and expressed in BL21 to explore the possibility for obtaining a vaccine conferring protection from *H. pylori* infection.

MATERIALS AND METHODS

Material

A well-characterized strain of *H. pylori* was afforded by the Department of Microbiology, Chongqing University of Medical Sciences. Top10, BL21 *E.coli* strains and pET32a (+), pET32a(+)/Omp_{18} plasmid, anti-Omp_{18} antibody were provided by the Institute of Viral Hepatitis of Chongqing University of Medical Sciences. Restriction endonuclease enzymes (*Kpn* I, *Hind* III, *Bam*HI) and T_4DNA ligase were purchased from Promega, *Tag*DNA polymerase was produced by the Immunology Department of Beijing University of Medical Sciences. Isopropyl-β-D-thiogalactopyranoside (IPTG), dNTP and oligonucleotide primers were obtained from Sigma.

Cloning of H.pylori HspA gene

Oligonucleotide primers were designed to amplify *H. pylori* open reading frame (ORFs) of HspA based on GenBank. The primers had a *KpnI* site incorporated into the 5' end and a *Bam*HI site at the 3' end and their sequences were as follows (5'-3'): CCGGTACCATGAAGTTTCAACCATTAGG (forward) and CCGGATCCGTGTTTTTTGTGATCATGAC (reverse). The reverse 5' end stop codon TAA was banned. Genomic DNA prepared from Chinese *H. pylori* strains was used as the template in PCR. The PCR consisted of 30 cycles of denaturation at 94 ℃ for 60 s, annealing at 52 ℃ for 50 s, and an extension step at 72 ℃ for 50 s. The products were visualized on 10 g· L^{-1} agarose gel and purified using a PCR purification kit. After digestion with the restriction endonuclease enzymes *Bam*HI and *KpnI* simultaneously, the purified products were cloned into the compatible sites of the expression vector pET32a (+) by using T_4 DNA ligase at a molar ratio of 4:1 at 4 ℃ overnight.

Construction of recombinant plamids

After the above connected products were transfected into Top10, pET32a(+)/HspA was selected and identified by the methods reported by Jiang *et al*[51]. After pET32a(+)/HspA and pET32a(+)/Omp_{18} were digested by restrictive endonuclease enzymes *Bam*HI and *Hind* III simultaneously, the segments of Omp_{18} and pET32a(+)/HspA were recycled by gel extract kit, and ligated by using T_4 DNA ligase at a molar ratio of 4:1 at 4 ℃ overnight. pET32a(+)/HspA /Omp_{18} was selected, appraised by PCR or enzyme digestion (Figure 1).

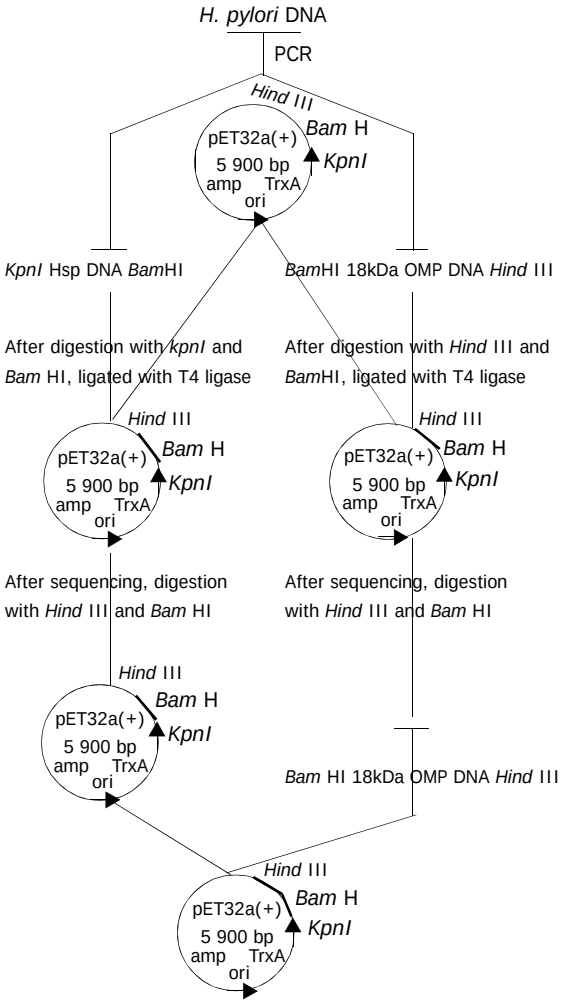

Figure 1 Schematic construction of plasmid pET32a(+)/HspA-Omp_{18}.

Extraction and expression of recombinant plasmid

The single bacterial colony (Top10/pET32a (+)/HspA/Omp_{18}) was picked, and cultivated in 2 ml LB broth containing 100 mg· L^{-1} of ampicillin, at 300 r· min^{-1} at 37 ℃ overnight, then recombinant plasmids were extracted according to the manufacturer's instructions, in the meantime, identified by PCR and restriction endonuclease enzyme digestion. The recombinant plasmid was transfected into competent BL21 (DE3) *E.coli* strains by using standard procedures reported by Jiang *et al*. BL21 *E.coli* strains containing recombinant plasmid were grown until mid-log phase (optical density at 600 nm=0.5 to 1.0), and then induced to express recombinant fusion protein by adding 1 mmol· L^{-1} IPTG for 4 h. Following induction, bacteria were harvested by centrifugation at 12 000 r· min^{-1} for 2 min, resuspended in protein-buffer and seethed for 5 min. Total proteins were electrophoresed on 150 g· L^{-1} SDS-PAGE gel and stained with Coomassie. The rate of recombinant fusion protein to total protein was deduced by Image Master Totallab v1.11 software.

Immunoblotting analysis of the recombinant fusion protein

Due to C end of recombinant fusion antigen with six histidines, the recombinant fusion antigen was purified by using Ni^{2+}-NTA agarose resin. Briefly, 500 ml of bacteria cultivated suspension was prepared, centrifugated, resuspended with the buffer liquid (50 mmol· L^{-1} phosphate, 300 mmol· L^{-1} NaCl, pH 7.0), and sonicated by ultrasonic wave with the energy of 600W×35 % for 40 min, and ultracentrifugated for 15 min at 10 000 r· min^{-1} at 4 ℃. The sonicated recombinant fusion antigen was purified by using Ni^{2+}-NTA agarose resin with abluent (50 mmol· L^{-1} phosphate, 300 mmol· L^{-1} NaCl, 20 mmol· L^{-1} imidazole, pH 7.80) and lavation (50 mmol· L^{-1} phosphate, 300 mmol· L^{-1} NaCl, 250 mmol· L^{-1} imidazole, pH 7.80) respectively, and quantified. The antigenicity of expressed recombinant fusion protein was determined by immunoblotting. Following electrophoretic transfer of SDS-PAGE-separated (150 g· L^{-1} acrylamide) recombinant fusion protein to 0.45 μm pore size PVDF membrane, and after a 30-min wash in tris-saline blotting buffer, antigen-impregated PVDF strips were incubated with the sera of patients infected with *H. pylori* and anti-Omp_{18} antibody for 2 h at RT. After a washing, the protein was detected by incubating the strips in alkaline phosphatase-conjugated goat anti-man IgG antibody for 1 h at RT.

RESULTS

PCR amplification of H.pylori HspA gene

According to literature[55], *H. pylori* HspA ORF was amplified by PCR with Chinese *H. pylori* strain's chromosomal DNA as the templates. The cloning products were electrophoresed and visualized by10 g· L^{-1} agarose gel (Figure 2). It revealed that the size of HspA DNA fragment amplified by PCR was between 250-500 base pairs, and contained a gene of approximately 357 nucleotides, and was compatible with the previous reports[55].

Identification of recombinant vector by PCR or restriction enzyme digestion

pET32a(+)/HspA identification by PCR After the single colony of Top10 *E. coli* /recombinant pET32a(+)/HspA was picked and incubated in 2 ml LB broth containing 100 mg· L^{-1} of ampicillin at 300 r· min^{-1} at 37 ℃ overnight, then 50 μl was incubated and seethed for 10 min, with the genomes of supernate and recombinant vector as templates respectively, products were amplified by PCR under the condition as mentioned above. The PCR products were visualized by 10

g· L^{-1} agarose gel electrophoresis (Figure 3). It indicated that recombinant plasmid contained the objective gene. At the same time, it was successful in transfecting recombinant plasmid into Top10 *E. coli*.

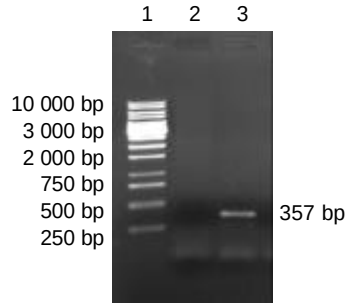

Figure 2 10 g·L^{-1} agarose gel electrophoresis of HspA DNA fragment amplified by PCR from Helicobacter pylori. Lane 1. PCR marker, Lane 2. Negative control, Lane 3. PCR products.

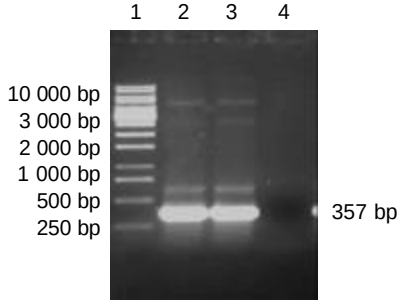

Figure 3 The identification of recombinant vector by PCR. Lane 1. DNA Marker, Lane 2, 3. PCR products with the template of Top10/recombinant vector, and recombinant vector respectively, Lane 4. Negative control.

pET32a(+)/HspA-Omp$_{18}$ identification by restriction enzyme digestion Recombinant plasmids pET32a(+)/HspA-Omp$_{18}$ were digested by single, bi-, tri-enzyme digestion with *Hind*III, *KpnI* and *Bam*HI, respectively, then digestive products were visualized on 10 g· L^{-1} agarose gel (Figure 4). It demonstrated that recombinant plasmids were digested to 357 bp, 528 bp DNA fragment, and contained the objective gene.

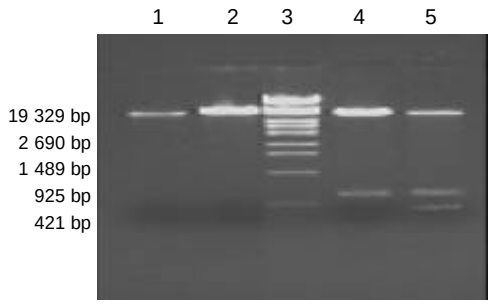

Figure 4 Identification of recombinant plasmid by restriction enzyme digestion. Lane 1. pET32a(+)/HspA digested by *Bam*HI, Lane 2. pET32a(+)/HspA-Omp$_{18}$ digested by *Bam*HI, Lane 3. DNA marker, Lane 4. pET32a(+)/HspA-Omp$_{18}$ digested by *Bam*HI and *Hind* III simultaneously, Lane 5. pET32a(+)/HspA-Omp$_{18}$ digested by kpnI, *Bam*HI and *Hind* III simultaneously.

Sequence analysis of cloned HspA, M_r18 000 OMP nucleotide

The nucleotide sequence of the cloned genes M_r18 000 OMP and HspA inserted into pET32a (+) was analyzed by automated sequencing across the cloning junction, using the universal primer T_7. The results showed that the cloned genes M_r18 000 OMP and HspA were connected by *Bam*H I enzyme digestion adhesion end. The cloned HspA genes contained 357 nucleotides with a promoter codon coding a putative protein of 119 amino acid residues with a calculated molecular mass of M_r13 000, and provided a putative signal peptide. Compared with previous reports, 5 base pairs of the cloned gene and 2 amino acid residues (G→D, A→S) encoded were changed. The cloned gene M_r18 000 OMP and its encoding protein sequences were published in GenBank (AF374387).

Analysis of the recombinant fusion protein

After pET32a(+)/HspA-Omp$_{18}$ was transfected into BL21 *E. coli* strains, the strains with high expressions of fusion proteins were selected. BL21 (DE3) *E.coli* strains containing recombinant plasmid were grown until mid-log phase (optical density at 600 nm=0.4 to 0.6), and then induced to express recombinant fusion protein by adding of 1 mmol· L^{-1} IPTG for 4 h. Following induction, bacteria were harvested by centrifugation at 12 000 r· min^{-1} for 5 min, resuspended in protein-buffer and seethed for 5 min. Total protein was electrophoresed on 150 g· L^{-1} SDS-PAGE gel and stained with Coomassie. Its molecular mass was M_r 51 000 by 150 g· L^{-1} SDS-PAGE gel analysis. After the recombinant bacteria were sonicated by ultrasonic wave and ultracentrifuged (10 000 r· min^{-1}, 15 min, 4 ℃), the level of soluble fusion protein in the supernate was about 18.96 % of total cellular protein. After purification by Ni^{2+}-NTA agarose resin columniation, the purity of recombinant fusion protein was about 95 % (Figure 5).

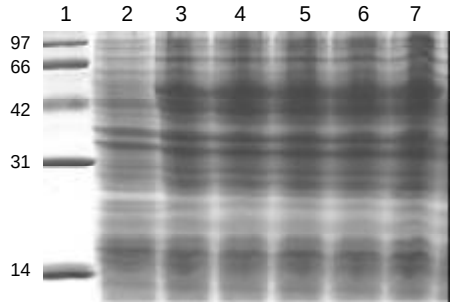

Figure 5 150 g·L^{-1} SDS-PAGE of total protein in recombinant vector expressed in BL21 *E.coli*. Lane 1. Standard protein marker (M_r 14; 31; 42; 66; 97×10^3), Lane 2. Bacterial protein expressed in BL21 after induction for 4 hours with IPTG, Lane 3-7. Expression of recombinant vector in BL21 after induction for 4 h with IPTG.

Antigenicity of recombinant fusion protein

After bacteria BL21/pET32a(+)/HspA-Omp$_{18}$, BL21/pET32a (+), BL21/pET32a(+)/HspA were induced to cultivate by adding of 1 mmol· L^{-1} IPTG for 4 h respectively, 1 ml of cultivated medium was respectively ultracentrifuged, resuspended in protein-buffer and seethed for 5 min. Total protein was electrophoresed on 150 g· L^{-1} SDS-PAGE gel, and then the proteins of SDS-PAGE-separated (150 g· L^{-1} acrylamide) were transferred to 0.45 μm pore size PVDF membrane at 14V, at 4 ℃ overnight. Following a 30-min wash in tris-saline blotting buffer, antigen-impregated PVDF strips were incubated with the sera of patients infected with *H. pylori* and anti-Omp$_{18}$ antibody for 2 h at RT. After a washing, the proteins were detected by incubating the strips in alkaline phosphatase-conjugated goat anti-man IgG antibody for 1 h at RT. In this study, antigen-impregated PVDF strips of BL21/pET32a(+)/HspA-Omp$_{18}$ were recognized by anti-Omp$_{18}$ antibody, showing brown strip corresponding to the site of the

recombinant fusion protein. Antigen-impregated PVDF strips of BL21/pET32a(+)/HspA were recognized by patient' s sera infected with *H. pylori*, also showing brown strip corresponding to the site of the fusion protein, while antigen-impregated PVDF strips of BL21/pET32a(+) were not recognized by patient' s sera infected with *H. pylori* (Figure 6).

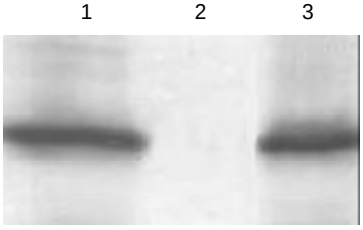

Figure 6 Antigenic analysis of the expression of recombinant vector by Western blot. Lane 1. BL21 / pET32a(+) / HspA-Omp$_{18}$, Lane 2. BL21 / pET32a(+), Lane 3. BL21 / pET32a(+) / HspA.

DISCUSSION

Heat shock phenomena were found by a geneticist Ritossa in studying on change of drosophila cell chromosome stimulated by heat in 1962. Heat shock protein, found by Tissiers *et al* in 1974, indwells in man, microbe, foliage, and animal. It belongs to secretory protein, and accounts for 5 % of total cellular proteins. When cells are stimulated by environment, Hsps are induced to synthesize. A series of heat shock proteins, such as HspA, HspB, Hsp60, and Hsp70, synthesized by *H. pylori*, play a significant role in *H. pylori* pathogenesis, for example, taking part in regulation of cell immunization, initiating auto-immunoreaction of gastric epithelial cell, serving as a promotor in development of chronic gastric pathological changes, and mediating recognition and adhesion of pathogens with host. HspA and HspB genes encode 118, 545 amino acid residues respectively, corresponding to calculated molecular mass of M_r 13 000, 58 200. HspA is consisted of two domains: N domain is conservative sequence, associated with immune appearance; C domain is composed of 27 amino acid residues, including 8 histidines, and 4 cysteines. So the frame is a nickel combinative region, and plays a role in nickel ion translation and presentation. The experiments suggested that HspA, B were important factors in *H. pylori* conglutination and *H. pylori* active proteins stabilization under the extremely unfavorable conditions, meantime they increase urease activity. Others suggested that Hsp60 and HopZ (*H. pylori* outer membrane protein Z) of *H. pylori* were associated with *H. pylori* adhesion. HspA and HspB were homologous with *E. coli* GroEs and GroEI, associated with auto-immunoreaction, which might lead to the production of damaging auto-antibody. Animal experiments demonstrated that mice fed with HspA, B resulted in coronary artery sclerosis[52].

The outer membrane is a continuous structure on the surface of gram-negative bacteria and an asymmetric bilayer with phospholipids in the inner monolayer and the bulky glycolipid lipopolysaccharide (LPS). In the outer monolayer, *H. pylori* as bacterial pathogens, has particular significance as a potential target for inducing host protective immunity and escaping from the host' s immune system. Outer membrane vaccines have been used with considerable success to induce protection against a number of organisms, including the heat shock protein in *H. pylori*, urease A, and B. M_r18 000 OMP is a lipoprotein (Lpp20) belonging to other outer membrane protein[53]. In an earlier study, immunoreactive species-specific M_r19 500 *H. pylori* OMP actually was Lpp20-M_r18 000 OMP. The Lpp20 antigen appears to be commonly expressed in all *H. pylori* strains examined so far. Furthermore, no cross-reaction was shown when antibodies (polyclonal and monoclonal) to *H. pylori* Lpp20 were used to immunoscreen closely related species of helicobacter, campylobacter, or a diverse range of other bacteria. It shows that the Lpp20 gene to be unique to *H. pylori*[54]. Keenan *et al* demonstrated the protein was expressed on the surface of the bacteria by immunolabeling of *H. pylori* with gold-labeled anti-Lpp20 antibodies. Bacterial lipoproteins have been well described, not only as vaccine target candidates, but also as immunostimulatory molecules.

In order to overcome the weak antigenicity of a single antigen, *H. pylori* M_r18 000 OMP and HspA gene were amplified by PCR, and inserted into pET32a(+) vector simultaneously in our study. The pET32a(+) vector was designed for cloning and high-level expression of peptide sequences with the 109aa Trx.· Tag™ thioredoxin protein. Cloning sites were available to produce objective proteins also containing cleavable His· Tag and s· Tag™ sequences for detection and purification. The expressed protein of pET32a(+) vector had a putative molecular mass of M_r 20 000, so the expression of recombinant vector was a fusion protein with a calculated molecular mass of M_r 51 000, consistent with our results. Compared with the reports, 1.8 % of the cloned genes was mutated, and 1.7 % of amino acid residues was changed. The reasons for the discrepancy might be as follows: (1) *H. pylori* chromosomal DNA as templates was different, (2) there were heterogeneity among *H. pylori* strains, and (3) *H. pylori* was provided with the ability of transformation, which could lead to *H. pylori* variation and genome reset[54]. But there was much homogeneity between them.

Todoroki *et al*[55] investigated the effect of DNA vaccines encoding *H. pylori*-heat shock proteins A and B (pcDNA3.1-hspA and -hspB) on inducing immune responses against *H. pylori* in mice. C57BL/six mice aged 5 weeks were immunized by a single injection of 10microg of pcDNA3.1-hspA and pcDNA3.1-hspB into intracutaneous tissue. Plasmid DNA lacking the inserted Hsp was injected as a control. The results demonstrated that DNA vaccines encoding *H. pylori*-Hsp induced significant immune response against *H. pylori*, decreased gastric mucosal inflammation, indicating that a pcDNA3.1-hspA or -hspB DNA vaccine can be a new approach against *H. pylori* in human. Jiang *et al*[51] reported that recombinant fusion OMP$_{18}$ protein also had good antigenicity. While being an immunogenic marker, the patient sera infected with *H. pylori* M_r 18 000 Omp antigen showed high sensitivity and specificity[56]. Moreover, a significant association was found between the serologic response to M_r 18 000 Omp antigen and malignant outcome of *H. pylori* infection[57]. So the serum test for detecting antibody with lower-molecular-weight proteins of *H. pylori* could be used to identify *H. pylori*-infected patients at risk of peptic ulcer or malignancy. A recently published study also identified M_r 18 000 Omp as a candidate following the successful immunization of mice with purified recombinant antigen. In our study, the purified M_r 51 000 recombinant fusion HspA-Omp$_{18}$ protein could be recognized by patients' sera infected with *H. pylori* and anti-Omp$_{18}$ monoclonal antibody, and the purified M_r 33 000 recombinant fusion HspA protein could also be recognized by patients' sera. The results demonstrated that recombinant fusion protein had good antigenicity. These showed that M_r 51 000 recombinant fusion HspA-Omp$_{18}$ protein would not only provide HspA characteristics, but possess M_r 18 000 Omp specialty. Meantime, M_r 51 000 recombinant fusion HspA-Omp$_{18}$ protein was suggested to be a true vaccine candidate and not merely an immunogenic marker for *H. pylori* infection.

In addition to construction of the recombinant vector, looking for living carriers would be a key step. Immunization via the mucosal or intracutaneous-inoculated route offers the advantage that has the potential to stimulate both mucosal and systemic immunity. It is simple, safe and can be used for the

immunization of a large population. Bacillus Calmette-Guerin (BCG), the attenuated strain of mycobacterium bovid and the current vaccine against tuberculosis, has been widely used as a living, innately immunogenic vehicle for multiple protective recombinant antigens for vaccines against pathogenic microorganisms. With the aim of developing a recombinant vaccine, vaccines against human immunodeficiency virus, diphtheria, pertussis, tetanus (DPT), and parasite[58-68] have been investigated. We are developing a living carrier-BCG to provide a mucosal or intracutaneous-inoculated vaccine vector to deliver M_r 51 000 recombinant fusion HspA-Omp_{18} protein to antigen-presenting cells on mucosal surface. We believe that before long, *H. pylori* vaccine could be constructed successfully for eradicating *H. pylori* infection and *H. pylori* associated diseases.

REFERENCES

1 **Michetti P**, Kreiss C, Kotloff KL, Porta N, Blanco JC, Bachmann D, Herranz M, Saldinger PF, Corthesy-Theulaz I, Losonsky G, Nichols R, Simon J, Stolte M, Ackerman S, Monath TP, Blum AL. Oral immunization with urease and Escherichia coli heat-labile Enterotoxin is safe and immunogenic in *Helicobacter pylori*-infected adults. *Gastroenterology* 1999; **116**: 804-812

2 **Hiyama T**, Haruma K, Kitadai Y, Masuda H, Miyamoto M, Ito M, Kamada T, Tanaka S, Uemura N, Yoshihara M, Sumii K, Shimamoto F, Chayama K. Clinicopathological features of gastric mucosa-associated lymphoid tissue lymphoma: a comparison with diffuse large B-cell lymphoma without a mucosa-associated lymphoid tissue lymphoma component. *J Gastroenterol Hepatol* 2001; **16**: 734-739

3 **Nakamura S**, Matsumoto T, Suekane H, Takeshita M, Hizawa K, Kawasaki M, Yao T, Tsuneyoshi M, Iida M, Fujishima M. Predictive value of endoscopic ultrasonography for regression of gastric low grade and high grade MALT lymphomas after eradication of *Helicobacter pylori*. *Gut* 2001; **48**: 454-460

4 **Uemura N**, Okamoto S, Yamamoto S, Matsumura N, Yamaguchi S, Yamakido M, Taniyama K, Sasaki N, Schlemper RJ. *Helicobacter pylori* infection and the development of gastric cancer. *N Engl J Med* 2001; **345**: 784-789

5 **Kate V**, Ananthakrishnan N, Badrinath S. Effect of *Helicobacter pylori* eradication on the ulcer recurrence rate after simple closure of perforated duodenal ulcer: retrospective and prospective randomized controlled studies. *Br J Surg* 2001; **88**: 1054-1058

6 **Xue FB**, Xu YY, Wan Y, Pan BR, Ren J, Fan DM. Association of H. pylori infection with gastric carcinoma: a Meta analysis. *World J Gastroenterol* 2001; **7**: 801-804

7 **Xia HHX**, Fan XG, Talley NJ. Clarithromycin resistance in *Helicobacter pylori* and its clinical relevance. *World J Gastroenterol* 1999; **5**: 263-265

8 **Peng ZS**, Liang ZC, Liu MC, Ouang NT. Studies on gastric epithelial cell proliferation and apoptosis in *Hp* associated gastric ulcer. *Shijie Huaren Xiaohua Zazhi* 1999; **7**: 218-219

9 **Xiao SD**, Liu WZ. Current statue in treatment of *Hp* infection. *Shijie Huaren Xiaohua Zazhi* 1999; **7**: 3-4

10 **Meyer JM**, Silliman NP, Dixon CA, Siepman NY, Sugg JE, Hopkins RJ. *Helicobacter pylori* and early duodenal ulcer status post-treatment: a review. *Helicobacter* 2001; **6**: 84-92

11 **Casella G**, Buda CA, Maisano R, Schiavo M, Perego D, Baldini V. Complete regression of primary gastric MALT-lymphoma after double eradication *Helicobacter pylori* therapy: role and importance of endoscopic ultrasonography. *Anticancer Res* 2001; **21**(2B): 1499-1502

12 **Hurenkamp GJ**, Grundmeijer HG, Van Der Ende A, Tytgat GN, Assendelft WJ, Van Der Hulst RW. Arrest of chronic acid suppressant drug use after successful *Helicobacter pylori* eradication in patients with peptic ulcer disease: a six-month follow-up study. *Aliment Pharmacol Ther* 2001; **15:** 1047-1054

13 **Guo CQ**, Wang YP, Liu GY, Ma SW, Ding GY, Li JC. Study on *Helicobacter pylori* infection and-p^{53}, c-erbB-2 gene expression in carcinogenesis of gastric mucosa. *Shijie Huaren Xiaohua Zazhi* 1999; **7**: 313-315

14 **Hiyama T**, Haruma K, Kitadai Y, Masuda H, Miyamoto M, Ito M, Kamada T, Tanaka S, Uemura N, Yoshihara M, Sumii K, Shimamoto F, Chayama K. Clinicopathological features of gastric mucosa-associated lymphoid tissue lymphoma: a comparison with diffuse large B-cell lymphoma without a mucosa-associated lymphoid tissue lymphoma component. *J Gastroenterol Hepatol* 2001; **16**: 734-739

15 **Hu PJ**. *Hp* and gastric cancer: challenge in the research. *Shijie Huaren Xiaohua Zazhi* 1999; **7**: 1-2

16 **Quan J**, Fan XG. Progress in experimental research of *Helicobacter pylori* infection and gastric cancinoma. *Shijie Huaren Xiaohua Zazhi* 1999; **7**: 1068-1069

17 **Delchier JC**, Lamarque D, Levy M, Tkoub EM, Copie-Bergman C, Deforges L, Chaumette MT, Haioun C. *Helicobacter pylori* and gastric lymphoma: high seroprevalence of CagA in diffuselarge B-cell lym phoma but not in low-grade lymphoma of mucosa-associatedlymphoid tissue type. *Am J Gastroenterol* 2001; **96**: 2324-2328

18 **Morgner A**, Miehlke S, Fischbach W, Schmitt W, Muller-Hermelink H, Greiner A, Thiede C, Schetelig J, Neubauer A, Stolte M, Ehninger G, Bayerdorffer E. Complete remission of primary high-grade B-cell gastric lymphoma after cure of *Helicobacter pylori* infection. *J Clin Oncol* 2001; **19**: 2041-2048

19 **Zhang XQ**, Lin SR. Progress in research on the relationship between *Hp* and stomach cancer. *Shijie Huaren Xiaohua Zazhi* 2000; **8**: 206-207

20 **Hua JS**. Effect of *Hp*: cell proliferation and apoptosis on stomach cancer. *Shijie Huaren Xiaohua Zazhi* 1999; **7**: 647-648

21 **Armitage GC**. Periodontal infections and cardiovascular disease-how strong is the association? *Oral Dis* 2000; **6**: 335-350

22 **Tsai CJ**, Huang TY. Relation of *Helicobacter pylori* infection and angiographically demonstrated coronary artery disease. *Dig Dis Sci* 2000; **45**: 1227-1232

23 **Gocyk W**, Niklinski T, Olechnowicz H, Duda A, Bielanski W, Konturek PC, Konturek SJ. *Helicobacter pylori*, gastrin and cyclooxygenase-2 in lung cancer. *Med Sci Monit* 2000; **6**:1085-1092

24 **Tsang KW**, Lam WK, Kwok E, Chan KN, Hu WH, Ooi GC, Zheng L, Wong BC, Lam SK. *Helicobacter pylori* and upper gastrointestinal symptoms in bronchiectasis. *Eur Respir J* 1999; **14**: 1345-1350

25 **Caselli M**, Zaffoni E, Ruina M, Sartori S, Trevisani L, Ciaccia A, Alvisi V, Fabbri L, Papi A. *Helicobacter pylori* and chronic bronchitis. *Scand J Gastroenterol* 1999; **34**: 828-830

26 **Dauden E**, Jimenez-Alonso I, Garcia-Diez A. *Helicobacter pylori* and idiopathic chronic urticaria. *Int J Dermatol* 2000; **39**: 446-452

27 **Ojetti V**, Armuzzi A, De-Luca A, Nucera E, Franceschi F, Candelli M, Zannoni GF, Danese S, Di-Caro S, Vastola M, Schiavino D, Gasbarrini G, Patriarca G, Pola P, Gasbarrini A. *Helicobacter pylori* infection affects eosinophilic cationic protein in the gastric juice of patients with idiopathic chronic urticaria. *Int Arch Allergy Immunol* 2001; **125**: 66-72

28 **Vainio E**, Huovinen S, Liutu M, Uksila J, Leino R. Peptic ulcer and *Helicobacter pylori* in patients with lichen planus. *Acta Derm Venereol* 2000; **80**: 427-429

29 **Szlachcic A**, Sliwowski Z, Karczewska E, Bielanski W, Pytko-Polonczyk J, Konturek SJ. *Helicobacter pylori* and its eradication in rosacea. *J Physiol Pharmacol* 1999; **50**: 777-786

30 **Avci O**, Ellidokuz E, Simsek I, Buyukgebiz B, Gunes AT. *Helicobacter pylori* and Behcet's disease. *Dermatology* 1999; **199**: 140-143

31 **Yazawa N**, Fujimoto M, Kikuchi K, Kubo M, Ihn H, Sato S, Tamaki T, Tamaki K. High seroprevalence of *Helicobacter pylori* infection in patients with systemic sclerosis: association with esophageal involvement. *J Rheumatol* 1998; **25**: 650-653

32 **Emilia G**, Longo G, Luppi M, Gandini G, Morselli M, Ferrara L, Amarri S, Cagossi K, Torelli G. *Helicobacter pylori* eradication can induce platelet recovery in idiopathic thrombocytopenic purpura. *Blood* 2001; **97**: 812-814

33 **Parkinson AJ**, Gold BD, Bulkow L, Wainwright RB, Swaminathan B, Khanna B, Petersen KM, Fitzgerald MA. High prevalence of *Helicobacter pylori* in the Alaska native population and association with low serum ferritin levels in young adults. *Clin Diagn Lab Immunol* 2000; **7**: 885-888

34 **Konno M**, Muraoka S, Takahashi M, Imai T. Iron-deficiency anemia associated with *Helicobacter pylori* gastritis. *J Pediatr Gastroenterol Nutr* 2000; **31**: 52-56

35 **Annibale B**, Lahner E, Bordi C, Martino G, Caruana P, Grossi C, Negrini R, Delle-Fave G. Role of *Helicobacter pylori* infection in

pernicious anaemia. *Dig Liver Dis* 2000; **32**: 756-762
36 **Choe YH**, Kwon YS, Jung MK, Kang SK, Hwang TS, Hong YC. *Helicobacter pylori*-associated iron-deficiency anemia in adolescent female athletes. *J Pediatr* 2001; **139**: 100-104
37 **Kaptan K**, Beyan C, Ural AU, Cetin T, Avcu F, Gulsen M, Finci R, Yalcin A. *Helicobacter pylori*-is it a novel causative agent in Vitamin B12 deficiency? *Arch Intern Med* 2000; **160**: 1349-1353
38 **Watanabe T**, Tada M, Nagai H, Sasaki S, Nakao M. *Helicobacter pylori* infection induces gastric cancer in Mongolian Gerbils. *Gastroenterol* 1998; **115**: 642-648
39 **Honda S**, Fujioka T, Tokieda M, Satoh R, Nishizono A, Nasu M. Development of *Helicobacter pylori*-induced gastric carcinoma in Mongolian Gerbils. *Cancer Res* 1998; **58**: 4255-4259
40 **Hatzifoti C**, Wren BW, Morrow JW. *Helicobacter pylori* vaccine strategies-triggering a gut reaction. *Immuno Today* 2000; **21**: 615-619
41 **Dieterich C**, Bouzourene H, Blum AL, Corthesy-Theulaz IE. Urease-based mucosal immunization against Helicobacter heilmannii infection induces corpus atrophy in mice. *Infect Immun* 1999; **67**: 6206-6209
42 **Liu X**, Hu J, Zhang X, Fan D. Oral immunization of mice with attenuated Salmonella typhimurium expressing *Helicobacter pylori* urease B subunit. *Chin Med J* 2002; **115**: 1513-1516
43 **Lee CK**, Soike K, Hill J, Georgakopoulos K, Tibbitts T, Ingrassia J, Gray H, Boden J, Kleanthous H, Giannasca P, Ermak T, Weltzin R, Blanchard J, Monath TP. Immunization with recombinant Helicobacter pylori urease decreases colonization levels following experimental infection of rhesus monkeys. *Vaccine* 1999; **17:** 1493-1505
44 **Solnick JV**, Canfield DR, Hansen LM, Torabian SZ. Immunization with recombinant *Helicobacter pylori* urease in specific-pathogen-free rhesus monkeys (Macaca mulatta). *Infect Immun* 2000; **68**: 2560-2565
45 **Satin B**, Del Giudice G, Della Bianca V, Dusi S, Laudanna C, Tonello F, Kelleher D, Rappuoli R, Montecucco C, Rossi F. The neutrophil-activating protein (HP-NAP) of *Helicobacter pylori* is a protective antigen and a major virulence factor. *J Exp Med* 2000; **191**: 1467-1476
46 **Chen Y**, Zhang ZS, Wang JD, Zhou DY. Cloning and expression of adhesion gene hpaA of *Helicobacter pylori*. *J First Mil Med Univ* 2000; **20**: 210-213
47 **Chen Y**, Wang J, Shi L. *In vitro* study of the biological activities and immunogenicity of recombinant adhesin of *Heliobacter pylori* rHpaA. *Zhonghua Yixue Zazhi* 2001; **81**: 276-279
48 **Kim BO**, Shin SS, Yoo YH, Pyo S. Peroral immunization with *Helicobacter pylori* adhesin protein genetically linked to cholera toxin A2B subunits. *Clin Sci* 2001; **100**: 291-298
49 **Kotloff KL**, Sztein MB, Wasserman SS, Losonsky GA, DiLorenzo SC, Walker RI. Safety and immunogenicity of oral inactivated whole-cell Helicobacter pylori vaccine with adjuvant among volunteers with or without subclinical infection. *Infect Immun* 2001; **69**: 3581-3590
50 **Goto T**, Nishizono A, Fujioka T, Ikewaki J, Mifune K, Nasu M. Local secretory immunoglobulin A and postimmunization gastritis correlate with protection against *Helicobacter pylori* infection after oral vaccination of mice. *Infect Immun* 1999; **67**: 2531-2539
51 **Jiang Z**, Tao XH, Huang AL, Wang PL. A study of recombinant protective *H. pylori* antigens. *World J Gastroenterol* 2002; **8**: 308-311
52 **Metzler B**, Mayr M, Oietrich H, Singh M, Wiebe E, Xu Q, Wick G. Inhibition of arteriosclerosis by T-cell depletion in normocholesterolemic rabbits immunized with heat shock protein 65. *Arterioscler thromb vasc boil* 1999; **19**: 1905-1911
53 **Keenan J**, Oliaro J, Domigan N, Potter H, Aitken G, Allardyce R, Roake J. Immune response to an 18-kilodalton outer membrane antigen identifies Lipoprotien 20 as a *Helicobacter pylori* vaccine candidate. *Infect Immun* 2000; **68**: 3337-3343
54 **Alm RA**, Bina J, Andrews BM, Dolg P, Hancock REW, Trust TJ. Comparative genomics of *Helicobacter pylori*: analysis of the outer membrane protein families. *Infect immun* 2000; **68**: 4155-4168
55 **Todoroki I**, Joh T, Watanabe K, Miyashita M, Seno K, Nomura T, Ohara H, Yokoyama Y, Tochikubo K, Itoh M. Suppressive effects of DNA vaccines encoding heat shock protein on *Helicobacter pylori*-induced gastritis in mice. *Biochem Biophys Res Commun* 2000; **277**: 159-163
56 **Shiesh SC**, Sheu BS, Yang HB, Tsao HJ, Lin XZ. Serologic response to lower-molecular-weight proteins of *Helicobacter pylori* is related to clinical outcome of *Helicobacter pylori* infection in Taiwmn. *Dig Dis Sci* 2000; **45**: 781-788
57 **Raymond J**, Sauvestre C, Kalach N, Bergeret M, Dupont C. Immunoblotting and serology for diagnosis of *Helicobacter pylori* infection in children. *Pediatr Infect Dis J* 2000; **19**: 118-121
58 **Kawahara M**, Hashimoto A, Toida I, Honda M. Oral recombinant mycobacterium bovis bacillus calmette-guerin expressing HIV-1 antigens as a freeze-dried vaccine induces long-term, HIV-specific mucosal and systemic immunity. *Clin Immunol* 2002; **105**: 326-331
59 **Kawahara M**, Matsuo K, Nakasone T, Hiroi T, Kiyono H, Matsumoto S, Yamada T,Yamamoto N, Honda M. Combined intrarectal / intradermal inoculation of recombinant mycobacterium bovis bacillus calmette-guerin (BCG) induces enhanced immune responses against the inserted HIV-1 V3 antigen. *Vaccine* 2002; **21**: 158-166
60 **Young SL**, O'Donnell MA, Buchan GS. IL-2-secreting recombinant bacillus Calmette Guerin can overcome a Type 2 immune response and corticosteroid-induced immunosuppression to elicit a Type 1 immune response. *Int Immunol* 2002; **14**: 793-800
61 **Young S**, O'Donnell M, Lockhart E, Buddle B, Slobbe L, Luo Y, De Lisle G, Buchan G. Manipulation of immune responses to Mycobacterium bovis by vaccination with IL-2- and IL-18-secreting recombinant bacillus Calmette Guerin. *Immunol Cell Biol* 2002; **80**: 209-215
62 **Zheng C**, Xie P, Chen Y. Recombinant Mycobacterium bovis BCG producing the circumsporozoite protein of Plasmodium falciparum FCC-1 / HN strain induces strong immune responses in BALB / c mice. *Parasitol Int* 2002; **51**: 1-7
63 **Mederle I**, Bourguin I, Ensergueix D, Badell E, Moniz-Peireira J, Gicquel B, Winter N. Plasmidic versus insertional cloning of heterologous genes in Mycobacterium bovis BCG: impact on *in vivo* antigen persistence and immune responses. *Infect Immun* 2002; **70**: 303-314
64 **Zheng C**, Xie P, Chen Y. Immune response induced by recombinant BCG expressing merozoite surface antigen 2 from Plasmodium falciparum. *Vaccine* 2001; **20**: 914-919
65 **Chujoh Y**, Matsuo K, Yoshizaki H, Nakasatomi T, Someya K, Okamoto Y, Naganawa S, Haga S, Yoshikura H, Yamazaki A, Yamazaki S, Honda M. Cross-clade neutralizing antibody production against human immunodeficiency virus type 1 clade E and B' strains by recombinant Mycobacterium bovis BCG-based candidate vaccine. *Vaccine* 2001; **20**: 797-804
66 **Hiroi T**, Goto H, Someya K, Yanagita M, Honda M, Yamanaka N, Kiyono H. HIV mucosal vaccine: nasal immunization with rBCG-V3J1 induces a long term V3J1 peptide-specific neutralizing immunity in Th1- and Th2-deficient conditions. *J Immunol* 2001; **167**: 5862-5867
67 **Ohara N**, Matsuoka M, Nomaguchi H, Naito M, Yamada T. Protective responses against experimental Mycobacterium leprae infection in mice induced by recombinant Bacillus Calmette-Guerin over-producing three putative protective antigen candidates. *Vaccine* 2001; **19**: 1906-1910
68 **Luo Y**, Chen X, Szilvasi A, O'Donnell MA. Co-expression of interleukin-2 and green fluorescent protein reporter in mycobacteria: *in vivo* application for monitoring antimycobacterial immunity. *Mol Immunol* 2000; **37**: 527-536

Edited by Zhang JZ, Zhu LH and Wang XL

P.O.Box 2345, Beijing 100023,China
Fax: +86-10-85381893
E-mail: wjg@wjgnet.com www.wjgnet.com

World J Gastroenterol 2003;9(8):1762-1766
World Journal of Gastroenterology
 ISSN 1007-9327

cagA and vacA genotype of *Helicobacter pylori* associated with gastric diseases in Xi'an area

Wen Qiao, Jia-Lu Hu, Bing Xiao, Kai-Chun Wu, Dao-Rong Peng, John C Atherton, Hui Xue

Wen Qiao, Hui Xue, Department of Gastroenterology, First Hospital, Xi' an Jiaotong University, Xi' an 710061, Shaanxi Province, China
Jia-Lu Hu, Kai-Chun Wu, Dao-Rong Peng, Department of Gastroenterology, Xijing Hospital, Fourth Military Medical University, Xi' an 710032, Shaanxi Province, China
Bing Xiao, Department of Gastroenterology, Nanfang Hospital, First Military Medical University, Guangzhou 510515, Guangdong Province, China
John C Atherton, Division of Gastroenterology and Institute of Infections and Immunity, University Hospital, Nottingham NG7 2UH, England
Correspondence to: Dr. Wen Qiao, Department of Gastroenterology, First Hospital, Xi' an Jiaotong University, Xi' an 710061, Shaanxi Province, China. xhy1202@ sohu.com
Telephone: +86-29-5324101 **Fax:** +86-29-5263190
Received: 2003-01-11 **Accepted:** 2003-03-05

Abstract

AIM: To establish stock of clinical *Helicobacter pylori* (*H. pylori*) isolates, to perform cagA and vacA typing of these isolates, to evaluate the relationship between genotypes of cagA and vacA and upper gastrointestinal diseases and to assess the association of vacA genotypes with presence of the pathogenicity marker-cagA.

METHODS: Clinical *H.pylori* strains were isolated from the antrum of 259 patients in Clumbia agar. The isolated *H. pylori* strains were identified by histology, and16SrRNA PCR. CagA genotypes were detected by colony hybridization, the probe was derived from the cloned plasmid PcagA, and digested by *Eco*RI-*Hin*dIII and the isolated PcagA DNA fragment was radioactively labelled by the random priming method. vacA genes types (s,m)and subtypes (s1a, s1b, s2) were typed by PCR. Vacuolating toxin was detected with neutral red absorb test. The results were treated statistically by χ^2 test, *t* test, and rank sum test.

RESULTS: A total of 192 clinical *H.pylori* strains were isolated and the stock of *Helicobacter pylori* was established. The total positive rate of cagA was 87 % in all gastric diseases, and 95 % in gastric cancer group. There was a difference between gastric cancer group and the other groups ($P<0.05$) except duodenal ulcer group. The expression of type s1 of vacA was more than type s2 ($P<0.05$), and, the expression of type m1 was equal to type m2. In gastric cancer group, there was a difference between s1a and s1b ($P<0.05$), and s1a was more than s1b. Vacuolating toxins were more in Xi'an area isolates.

CONCLUSION: The cagA$^+$ vacA type s1 clinical isolates are more in Xi'an area, but this can not serve as an index to predict gastric cancer.

Qiao W, Hu JL, Xiao B, Wu KC, Peng DR, Atherton JC, Xue H. cagA and vacA genotype of *Helicobacter pylori* associated with gastric diseases in Xi'an area. *World J Gastroenterol* 2003; 9 (8): 1762-1766
http://www.wjgnet.com/1007-9327/9/1762.asp

INTRODUCTION

Helicobacter pylori (*H. pylori*) is an important human pathogen that causes chronic gastritis and is associated with development of peptic ulcer diseases, and gastric malignancies[1]. Epidemiological studies have shown that *H. pylori* is a class 1 carcinogen for gastric adenocarcinoma, which is one of the most common cancers worldwide, and the odds ratio for developing gastric cancer is 3.8 to 8.7 in *H.pylori* infected subjects[2-6]. The pathophysiological mechanism by which *H.pylori* leads to gastric cancer has not yet been defined, although many hypotheses have been put forward.

The genetic variability among *H.pylori* strains is relatively high[7]. Approximately 50-60 % of *H. pylori* strains contain cytotoxin-associated (cagA) gene and consequently produce 128 ku CagA protein[8,9]. The presence of cagA is associated with gastric cancer, gastric mucosal atrophy, and duodenal ulcer. CagA is a part of a large genomic entity, designating the pathogenicity (cag) island[10,11], which contains multiple genes that are related to the virulence and pathogenicity of *H. pylori* strains. Therefore, the presence of cagA can be considered as a marker for this genomic pathogenicity island and is associated with more virulent *H.pylori* strains.

Another important virulence factor, produced by approximately 50 % of *H. pylori* strains, is a cytotoxin that induces formation of vacuolates in mammalian cells *in vitro* and leads to cell death[12]. The toxin is encoded by vacA gene, which is virtually present in all *H.pylori* strains[13]. The existence of different allelic variants in two parts of this gene has been described[14-17]. The N-terminal signal (s) region occurs as either a s1a, s1b or s2 allele. The middle (m) region is present as a m1 or m2 allele. The mosaic structure of vacA gene accounts for differences in cytotoxin production between strains[18-20].

The aim of this study was to detect and type the virulence-associated cagA and vacA genes of clinical *H.pylori* isolates in Xi'an area of China. Finally, the clinical relevance of vacA and cagA genotyping was investigated with gastric cancer and precancerous conditions.

MATERIALS AND METHODS

Bacterial isolation and culture

A total of 192 *H.pylori* isolates were obtained from patients undergoing upper gastrointestinal examination. The diagnosis obtained by endoscopy and histology was recorded for all the patients from whom the strains were isolated. Following primary isolation, *H.pylori* strains were grown on Columbia agar with 50 mL/L frozen-melting sheep blood, 100 mL/L fetal bovine serum, and Skirrow's antibiotic supplement in a microaerophilic atmosphere for 5 days at 37 ℃, then frozen at -70 ℃. Most of the strains were frozen four to six passages after primary isolation. Subsequent analyses were performed on strains derived from the frozen stocks. The isolated *H.pylori* strains were identified by histology, and16SrRNA PCR.

Plasmid DNA preparation

A signal bacteria clone was incubated at 37 ℃ overnight, harvested, and suspended in 0.5 mol/L EDTA-1M Tris-HCl

(pH 8.0), 10 mol/L NaOH and 100 g/L SDS was added, mixed, then 5 mol/L KAc and ice HAc were added. The mixture was centrifuged at 12 000 r/min for 10 min. The supernatant was extracted with phenol-chloroform followed by with chloroform. After extraction, the DNA solution was mixed with absolute ethanol and 3 mol/L NaAc at -20 ℃ for 20 min, washed with 700 mL/L ethanol, and dried. The DNA pellet was suspended in TE (10 mmol/L Tris-HCl, 1 mmol/L pH8.0 EDTA), and stored at -20 ℃.

DNA probes

The probe was derived from the cloned plasmid PcagA, and digested by *Eco*RI-*Hin*dIII. The enzyme digestion segment of PcagA was retrieved by DNA purification reagent kit (Baotaike Biotechnology Company). The isolated PcagA DNA fragment was radioactively labelled by the random priming method.

Colony hybridization

SDS of 100 g/L was added in fresh *H.pylori* liquid for 10 min, 2×SSC (1×SSC is 0.15 mol/L NaCl plus 0.015 mol/L sodium citrate) for 5 min, then *H.pylori* degeneration liquids were dotted on NC membranes which had been treated by 2×SSC, heated at 80 ℃ for 2 h. The membranes were put into pre-hybridization liquid (1×Denhardt, 1 g/L SDS, 5×SSC, 500 g/L deionised fomamide) at 42 ℃ for 3 h, then α-^{32}P labeled probes were added at 43.5 ℃ overnight. The membrane filters were subsequently washed once in 2×SSC-5 g/L SDS and three times in 0.1×SSC-1 g/L SDS, then exposed to X-ray film and their radioactivity was self-developing at -20 ℃ for 48 h. The film was developed and then fixed.

H.pylori chromosomal DNA extracts

Fresh *H. pylori* strains were harvested, suspended in 0.1 mol/L NaCl-10 mmol/L Tris-HCl-1 mmol/L EDTA (pH 8.0), and incubated at 37 ℃ for 15 min. NH_4Ac was added and the mixture was placed on ice for 5 min and extracted once with chloroform, mixed with isopropanol and placed on ice for 10 min. After extraction, the DNA solution was mixed with absolute ethanol at -20 ℃ for 1 h, washed with 700 mL/L ethanol, and dried. The DNA pellet was suspended in distilled water and stored at -20 ℃.

VacA genotyping

The vacA was typed by PCR. Table 1 shows the primer sequence of vacA. And Table 2 shows the system of PCR. The reaction condition was at 94 ℃ for 1 min, at 52 ℃ for 1 min, and at 72 ℃ for 1 min for 35 cycles and extension at 72 ℃ for 6 min. The PCR product was analyzed by 20 g/L agarose gel. The reference *H.pylori* strains were 60 190 (s1a/m1), 84 183 (s1b/m1) and 86 313 (s2/m2).

Cytotoxicity test on hela cells

Hela cells were cultured in plastic flasks in Dulbecco' s modified Eagle' s medium (DMEM) containing 25 mmol/L HEPES buffer (N-2-hydroxyethylpiperazine-N' -2-ethanesulfonic acid, pH7.2) and 100 g/L fetal bovine serum. Cells were maintained at 37 ℃ in a 50 mL/L CO_2 atmosphere. After cultured for 24 h, the cells were suspended with trypsin-EDTA and seeded in 96-well titration plates to make the density of cells of 10^4 per well. The supernatant prepared by water extracts from different strains was diluted two-fold from 1:2 to 1:32 and incubated with Hela cells for 12 h, then added 0.5 g/L neutral red- normal saline for 5 min, washed 3 times with 2 g/L BAS-normal saline and added HCl-ethanol. The absorbance was detected at 540 nm. When the detected value was more than 3 times of the negative control, it was defined as a positive result.

Table 2 The system of PCR

Constituents	Volume / per tube (μL)	Final concentration
Water	36	
10×PCR buffer	5	1×
4dNTP, 2.5mmol/L /each	4	0.2mmol/L each
primer 1.25 μmol/L	1	0.5 μmol/L
primer 2.25 μmol/L	1	0.5 μmol/L
$MgCl_2$, 50 mmol/L	1.5	1.5 mmol/L
Taq DNA polymerase, 5MU/L	0.5	0.1 MU/L
Template DNA	1	

Statistical analysis

χ^2 test, *t* test, and rank sum test were used for statistical analysis.

RESULTS

Presence of cagA gene

The presence of cagA gene was investigated in all clinical isolates by colony hybridization. *Eco*RI-*Hin*dIII-digested chromosomal DNA (Figure 1) was probed with an α ^{32}P-labelled DNA fragement internal to cagA. Typical examples of the results obtained with colony hybridization are reported in Figure 2. Of the 192 clinical isolates, 165 strains (86 %) had a positive hybridization dot, while 27 strains (14 %) did not show hybridization dot. In the 192 strains, the positive rate of gastric cancer group was 95 %, chronic superficial gastritis (CSG) 77 %, chronic atrophic gastritis (CAG) 86 %, gastric ulcer (GC) 69 %, and duodenal ulcer (DU) 95 %. There were differences between CAG and GU (P<0.05), and between GU and DU (P<0.05), but there were no statistical differences between CSG and CAG (P>0.05), and between CSG and GU (P>0.05).

Presence of signal sequence typing of vacuolating toxin gene

The signal sequence gene was typed by PCR in all *H. pylori* clinical isolates. The products of s1 and s2 were 259 bp and 286 bp, respectively. In the 192 strains, 174 strains (90.6 %) were s1 type, and 18 strains (9.4 %) were s2. The subtypes of s1 were typed by two pairs of primers (SS1-F/VA1-R and SS3-

Table 1 Oligonucleotide primers used for vacA typing

Gene and region amplified	Genotype identified	Primer designation	Primer sequence	Size of PCR product(bp)
Mid-region	m1/m2	VAG-F	5'CAATCTGTCCAATCAAGCGAG3'	567/642
		VAG-R	5'GCGTCAAAATAATTCCAAGG3'	
Signal sequence	s1/s2*	VA1-F	5'ATGGAAATACAACAAACACAC3'	259/286*
		VA1-R	5'CTGCTTGAATGCGCCAAAC3'	
	s1a	SS1-F#	5'GTCAGCATCACACCGCAAC3'	190
	s1b	SS3-F#	5'AGCGCCATACCGCAAGAC3'	187

vacA types s1 and s2 were differentiated on the size of the PCR product. # Used with reverse primer VA1-R.

F/VA1-R) (Table 3 and Figure 3). The product of s1a and s1b was 190 bp and 187 bp, respectively. In the 174 s1 type strains, 111 strains (63.8 %) were s1a, and 63 strains (36.2 %) were s1b (Figures 4, 5).

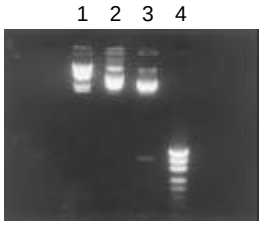

Figure 1 Restriction endonuclease *Eco*RI, *Hin*dIII digests of PcagA. 1. λDNA *Hin*dIIImarker, 2. PcagA, 3. Fragement digested by *Eco*RI-*Hin*dIII, 4. PUC18/MSPI marker.

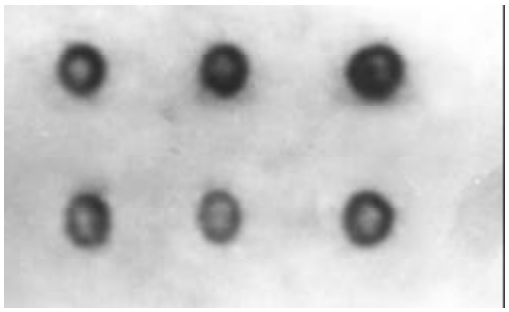

Figure 2 Colony hybridization detection of cagA. The positive hybridization dot.

Figure 3 PCR typing of vacA signal sequence. 1.PCR marker, 2. Type s2, 3. Type s1, 4. Standard strain 86313, 5. Standard strain 60 190.

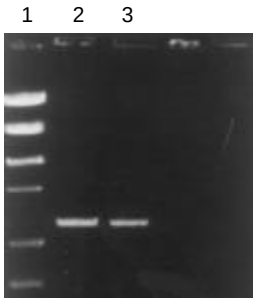

Figure 4 PCR typing of vacA s1a. 1. PCR marker, 2. Clinical isolates, 3. Standard strain 84 183.

Presence of middle region typing of vacuolating toxin gene

The middle region gene was also typed by PCR in all *H. pylori* clinical isolates. The products of m1 and m2 were 567 bp and 642 bp, respectively. In the 192 strains, 99 strains (51.6 %) were m1 type, and 93 strains(48.4%) were m2, (Table 4 and Figure 6).

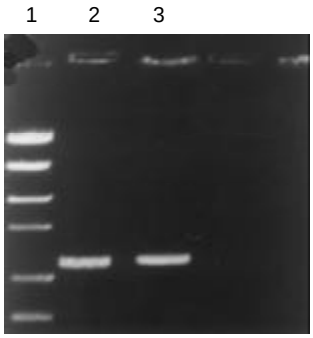

Figure 5 PCR typing of vacA mid-region. 1. PCR marker, 2. Clinical isolates, 3. Standard strain 84 183.

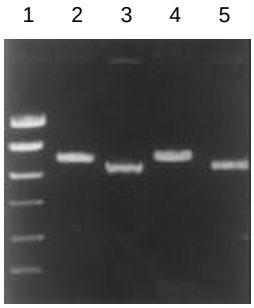

Figure 6 PCR typing of vacA s1a. 1. PCR marker, 2.Type m2, 3. Type m1, 4. Standard strain 86 313, 5. Standard strain 60 190.

Table 3 *H.pylori* signal sequence typing and gastric diseases

s type	GC	CSG	CAG	GU	DU	Total(%)
s1a	43a	14	37	5	12	111(57.8)
s1b	10	13	25	8	7	63(32.8)
s2	3	4	7	3	1	18(9.4)
Total	56	31	69	16	20	192(100.0)

[a]$P<0.05$ *vs* GU, CSG, CAG.

Table 4 *H.pylori* signal sequence typing and gastric diseases

m type	GC	CSG	CAG	GU	DU	Total(%)
m1	31	13	36	7	12	99(51.6)
m2	25	18	33	9	8	93(48.4)
Total	56	31	69	16	20	192(100.0)

No difference at all.

Presence of middle region typing and signal sequence of vacuolating toxin gene

In the 192 strains, 65 strains (33.9 %) were sla/m1, 34 strains (17.7 %) s1b/m1, 46 strains (24.0 %) s1a/m2, 29 strains (15.1 %) s1b/m2, and 18 strains (9.4 %) s2/m2.

Relationship between vacA typing and detecting of vacuolating cytotoxin activity in vitro

The maximum diluting times of positive result were the value of vacuolating toxin. Based on the maxium diluting unit, the strains were divided into three types: high toxin ($\geqslant$8), low toxin (1-8) and none toxin (less than 1). In the 192 strains, high toxin was 90 strains (46.9 %), low toxin 62 (32.3 %) and none toxin 40 (20.8 %, Table 5).

Relationship between cagA and vacA subtype

In the 165 cagA gene positive strains, 165 strains (100 %)

were vacA s1 type; 97 strains (58.8 %) vacA m1 type, and 78 strains (46.2 %, Table 6) vacA m2 type.

Table 5 Relationship between vacA typing and grade of vacuolating cytotoxin activity

vacA type	Grade of vacuolating cytotoxin activity		
	None	Low	High
s1a	5	38	68
s1b	17	24	22
s2	18	0	0
m1	10	30	59
m2	30	32	31

$P<0.05$, each group *vs* s1a, s1b, s2.

Table 6 Relationship between vacA typing, cagA gene and gastric diseases for 192 *H. pylori* isolates

vacA type	cagA+					Total(%)
	GC	CSG	CAG	GU	DU	
s1a	43	14	37	4	12	110(66.7)
s1b	10	10	22	6	7	55(33.3)
s2	0	0	0	0	0	0(0.0)
m1	31	12	36	6	12	97(58.8)
m2	22	12	23	4	7	78(46.2)

DISCUSSION

H. pylori is the major causative agent of chronic superficial gastritis and plays a central role in the etiology of peptic ulcer disease. Evidence suggests that *H. pylori* infection pre-exists in gastric carcinoma and precancerous lesions, and is a risk for development of gastric carcinoma. Cittelly showed that lower frequencies of cytotoxic genotypes such as cagA and vacA s1m1 were observed in patients with NAG (non atrophic gastritis), when compared to patients with GC (gastric cancer) or PU (peptic ulcer). He suggested that vacA and cagA could be used as markers for increased virulence. In 1994, *H. pylori* was designated as a class I carcinogen by the World Health Organization[21,22]. *H. pylori* infection is high among Chinese people (the infected rate is 40-70 %), and also high in gastric cancer. The mortality of gastric cancer ranks the first among malignancies. The results of epidemiologic surveys on the relationship between *H. pylori* and gastric cancer show that infection of *H.pylori* in Lanzhou, an area with a high occurrence of gastric cancer, is higher than that in Guangzhou, an area with a low occurrence of gastric cancer[23, 24].

Recent researches suggested that the positive cytotoxin-associated gene A of *H.pylori* was about 60 %. This toxin can induce severe inflammation of gastric mucosa and is related with peptic ulcer and gastric cancer[25]. We detected the cagA gene in 192 clinical strains by colony hybridization, with a total positive rate of 86 %. In gastric cancer and duodenal ulcer, *H.pylori* infection rate (91 %) was the highest in all gastric diseases. In gastric ulcer group it was the lowest, only 69 %. Our results suggest that positive cagA of *H.pylori* isolated strains is related with gastric diseases in Xi' an area, Because the expression of cagA positive strains in gastric cancer group was higher than that in chronic gastritis group and the difference was apparent ($P<0.05$). CagA can increase the serious consequences of carcinogenesis from chronic inflammation. The detectable rate of CagA antibody in human group in high occurrence region of gastric cancer was obviously higher than that in low occurrence area. Some researches have also proved that cagA positive strains are easy to cause inflammation of gastric mucosa and can stimulate hyperplasia of gastric mucosal cells. Many studies have shown that there is a relationship between cagA positive antibody and peptic ulcer and gastric cancer. One research suggested that development of more prominent gastritis and severe atrophy in cagA (+) patients was an indicator for the importance of cagA rather than *H. pylori* load. Our research was consistent with theirs[26, 27].

All strains have the gene encoding toxin vacA, but its structure varies, especially in the mid-region which may be type m1 or m2 and the region encoding the signal sequence (type s1a, s1b or s2). The final structure is a mosaic, and all combinations of signal sequence and mid-region types are found except s2/m1. A strain' s vacA structure determines its *in vitro* cytotoxin activity, with type m1 vacA being more active than type m2, type s1a being more active than type s1b, and type s2 vacA not producing detectable activity. Our results showed that the main genotype was s1a in gastric cancer group, and there was an apparent difference between s1a and s1b ($P<0.05$), and the s2 genotype was seldom found. In the meantime, there was no apparent difference between m1 and m2 ($P>0.05$). The expression of s1a type was different among gastric cancer, gastric ulcer, and chronic gastritis. In gastritis group, there was no difference between s1a type and s1b type. Andreson' s research showed that the presence of the cagA gene was correlated with that of vacA signal sequence type s1a. However, no clear differences were found in the distribution of cagA and vacA genotypes among patients with peptic ulcer or chronic gastritis in Estonia. The reason why the different regional distribution can cause different genotype of *H.pylori* is not clear[28].

Our results showed that the infected *H.pylori* in Xi' an area was mainly toxin strains. In the meantime, the expression of s1a and s1b in the toxin strains was obviously different ($P<0.05$), and there was no significant difference between m1 and m2 ($P>0.05$). This suggests that s2 type can not produce detectable vacuolating toxin, and s1 type can produce the toxin. The middle-region is not obviously related to toxin production. The toxin produced by s2 type may not effectively pass through cellular membrane[29].

In cagA positive strains, the main vacA subtype was s1a, about 67 %, and s1b was only 33 %, and there was an apparent difference between these two subtypes ($P<0.05$). But there was no difference between m1 and m2 ($P>0.05$). We found that s1 type was related with gastric cancer[30].

Inactivation of multiple antioncogenes and *H.pylori* infection may be involved in the development and progress of gastric carcinoma, and *H.pylori* infection may be associated with the inactivation of some oncogenes[31]. The genotype expression of *H.pylori* in gastric cancer was mainly $cagA^+$/s1a strains in Xi' an area, but this can not serve as an index to predict gastric cancer. The main genotype of vacA in chronic gastritis, gastric ulcer and duodenal ulcer is s1, but there is no difference between s1a, s1b, m1 and m2.

REFERENCES

1 **YaoYL**, Zhang WD. The relationship between *Helicobacter pylori* and gastric cancer. *Shijie Huaren Xiaohua Zazhi* 2001; **9**: 1045-1049

2 **Zhuang XQ**, Lin SR. Research of *Helicobacter pylori* infection in precancerous gastric lesions. *World J Gastroenterol* 2000; **6**: 428-429

3 **Vandenplas Y**. *Helicobacter pylori* infection. *World J Gastroenterol* 2000; **6**: 20-31

4 **Zhong Z**, Yuan Y, Gao H, Dong M, Wang L, Gong YH. Apoptosis, proliferation and p53 gene expression of *H. pylori* associated gastric epithelial lesions. *World J Gastroenterol* 2001; **7**: 779-782

5 **Gao H**, Wang JY, Shen XZ, Liu JJ. Effect of *Helicobacter pylori* infection on gastric epithelial cell proliferation. *World J Gastroenterol* 2000; **6**: 442-444

6 **Zhuang XQ**, Lin SR. Study on the relationship between *Helicobactr pylori* and gastric cancer. *Shijie Huaren XiaoHuaZazhi* 2000; **8**: 206-207

7 **Figueiredo C**, Van Doorn LJ, Nogueira C, Soares JM, Pinho C, Figueira P, Quint WG, Carneiro F. *Helicobacter pylori* genotypes are associated with clinical outcome in Portuguese patients and show a high prevalence of infections with multiple strains. *Scand J Gastroenterol* 2001; **36**: 128-135

8 **Li XJ**, Yan XJ, Liu ZG, Su CZ. Expression, purification and clinical research of *Helicobacter pylori* cytotoxin-associated gene A. *Shijie Huaren Xiaohua Zazhi* 2002; **10**: 271-274

9 **Abasiyanik MF**, Sander E, Salih BA. *Helicobacter pylori* anti-CagA antibodies: Prevalence in symptomatic and asymptomatic subjects in Turkey. *Can J Gastroenterol* 2002; **16**: 527-532

10 **Kidd M,** Lastovica AJ, Atherton JC, Louw JA. Conservation of the cag pathogenicity island is associated with vacA alleles and gastroduodenal disease in south african *Helicobacter pylori* isolates. *Gut* 2001; **49**: 11-17

11 **Hu WJ**, Li NS, Wang SL, Liu J, Tu ZX, Xu GM. Difference between cagA and cagM in cag I of *Helicobacter pylori* isolated from Chinese patients. *Shijie Huaren Xiaohua Zazhi* 2001; **9**: 405-409

12 **Ye GA**, Zhang WD, Liu LM, Shi L, Xu ZM, Chen Y, Zhou DY. vacA gene of *Helicobacter pylori*. *Shijie Huaren Xiaohua Zazhi* 2001; **9**: 593-595

13 **van Doorn LJ**. Detection of *Helicobacter pylori* virulence-associated genes. *Expert Rev Mol Diagn* 2001; **1**: 290-298

14 **Lin CW**, Wu SC, Lee SC, Cheng KS. Genetic analysis and clinical evaluation of vacuolating cytotoxin gene A and cytotoxin-associated gene A in taiwanese *Helicobacter pylori* isolates from peptic ulcer patients. *Scand J Infect Dis* 2000; **32**: 51-57

15 **Fallone CA**, Barkun AN, Gottke MU, Best LM, Loo VG, Veldhuyzen van Zanten S, Nguyen T, Lowe A, Fainsilber T, Kouri K, Beech R. Association of *Helicobacter pylori* genotype with gastroesophageal reflux disease and other upper gastrointestinal diseases. *Am J Gastroenterol* 2000; **95**: 659-669

16 **Shiesh SC**, Sheu BS, Yang HB, Tsao HJ, Lin XZ. Serologic response to lower-molecular-weight proteins of H. pylori is related to clinical outcome of *H. pylori* infection in Taiwan. *Dig Dis Sci* 2000; **45**: 781-788

17 **Yao YL**, Xu B, Song YG, Zhang WD. Overexpression of cyclin E in mongolian gerbil with *Helicobacter pylori*-induced gastric precancerosis. *World J Gastroenterol* 2002; **8**: 60-63

18 **Ji KY**, Hu FL. The development of *Helicobacter pylori* and cytokines. *Shijie Huaren Xiaohua Zazhi* 2002; **10**: 503-508

19 **Hou P**, Tu ZX, Xu GM, Gong YF, Ji XH, Li ZS. *Helicobacter pylori* vacA genotypes and cagA status and their relationship to associated diseases. *World J Gastroenterol* 2000; **6**: 605-607

20 **She FF**, Su DH, Lin JY, Zhou LY. Virulence and potential pathogenicity of coccoid *Helicobacter pylori* induced by antibiotics. *World J Gastroenterol* 2001; **7**: 254-258

21 **Xue FB,** Xu YY, Wan Y, Pan BR, Ren J, Fan DM. Association of *H. pylori* infection with gastric carcinoma: a meta analysis. *World J Gastroenterol* 2001; **7**: 801-804

22 **Cittelly DM**, Huertas MG, Martinez JD, Oliveros R, Posso H, Bravo MM, Orozco O. *Helicobacter pylori* genotypes in non atrophic gastritis are different of the found in peptic ulcer, premalignant lesions and gastric cancer in colombia. *Rev Med Chil* 2002; **130**: 143-151

23 **Wang GT**.The relationship between CagA/VacA strains and chronic gastric diseases. *Shijie Huaren XiaoHuaZazhi* 2001; **9**: 1335-1338

24 **Chen JP**, Shen DM, Yang ZB. CagA+ *Hp* broth culture filtrates induced malignant transformation on human gastric epithelial cells. *Shijie Huaren Xiaohua Zazhi* 2001; **9**: 617-621

25 **Wang CD**, Li JS, Chen LY. CagA and VacA do not predict *Helicobacter pylori*-associated gastroduodenal diseases. *Shijie Huaren Xiaohua Zazhi* 2002; **10**: 533-535

26 **Cai L**, Yu SZ, Zhang ZF. *Helicobacter pylori* infection and risk of gastric cancer in Changle County, Fujian Province, China. *World J Gastroenterol* 2000; **6**: 374-376

27 **Zhou JC**, Xu CP, Zhang JZ. The research development of cagA/CagA of *Helicobacter pylori* mocular biology. *Shijie Huaren XiaoHuaZazhi* 2001; **9**: 560-562

28 **Demirturk L**, Ozel AM, Yazgan Y, Solmazgul E, Yildirim S, Gultepe M, Gurbuz AK. CagA status in dyspeptic patients with and without peptic ulcer disease in turkey: Association with histopathologic findings. *Helicobacter* 2001; **6**: 163-168

29 **Andreson H**, Loivukene K, Sillakivi T, Maaroos HI, Ustav M, Peetsalu A, Mikelsaar M. Association of cagA and vacA genotypes of *Helicobacter pylori* with gastric diseases in estonia. *J Clin Microbiol* 2002; **40**: 298-300

30 **Park SM**, Park J, Kim JG, Yoo BC. Relevance of vacA genotypes of *Helicobacter pylori* to cagA status and its clinical outcome. *Korean J Intern Med* 2001; **16**: 8-13

31 **Wang XD**, Fang DC, Li W, Du QX, Liu WW. A study on relationship between infection of *Helicobacter pylori* and inactivation of antioncogenes in cancer and pre-cancerous lesion. *Shijie Huaren Xiaohua Zazhi* 2001; **9**: 984-987

Edited by Ma JY

P.O.Box 2345, Beijing 100023,China
Fax: +86-10-85381893
E-mail: wjg@wjgnet.com www.wjgnet.com

World J Gastroenterol 2003;9(8):1767-1771
World Journal of Gastroenterology
 ISSN 1007-9327

• BASIC RESEARCH •

Expression and activities of three inducible enzymes in the healing of gastric ulcers in rats

Jin-Sheng Guo, Chi-Hin Cho, Wei-Ping Wang, Xi-Zhong Shen, Chuen-Lung Cheng, Marcel Wing Leung Koo

Jin-Sheng Guo, Chi-Hin Cho, Wei-Ping Wang, Xi-Zhong Shen, Chuen-Lung Cheng, Marcel Wing Leung Koo, Department of Pharmacology, Faculty of Medicine, University of Hong Kong, Hong Kong
Jin-Sheng Guo, Xi-Zhong Shen, Division of Gastroenterology, Zhongshan Hospital, Fu Dan University, Shanghai 200032, China
Correspondence to: Marcel Wing Leung Koo, Department of Pharmacology, Faculty of Medicine, University of Hong Kong, Pokfulam, Hong Kong. wlkoo@hkusua.hku.hk
Telephone: +852-28199256 **Fax:** +852-28170859
Received: 2003-04-04 **Accepted:** 2003-05-20

Abstract

AIM: To explore the roles of nitric oxide synthase (NOS), heme oxygenase (HO) and cyclooxygenase (COX) in gastric ulceration and to investigate the relationships of the expression and activities of these enzymes at different stages of gastric ulceration.

METHODS: Gastric ulcers (kissing ulcers) were induced by luminal application of acetic acid. Gastric tissue samples were obtained from the ulcer base, ulcer margin, and non-ulcerated area around the ulcer margin at different time intervals after ulcer induction. The mRNA expression and protein levels of inducible and constitutive isoforms of NOS, HO and COX were analyzed with RT-PCR and Western blotting methods. The activities of the total NOS, inducible NOS (iNOS), HO, and COX were also determined.

RESULTS: Differential expression of inducible iNOS, HO-1 and COX-2 and enzyme activities of NOS, HO and COX were found in the gastric ulcer base. High iNOS expression and activity were observed on day 1 to day 3 in severely inflamed ulcer tissues. Maximum expressions of HO-1 and COX-2 and enzyme activities of HO and COX lagged behind that of iNOS, and remained at high levels during the healing phase.

CONCLUSION: The expression and activities of inducible NOS, HO-1 and COX-2 are found to be correlated to different stages of gastric ulceration. Inducible NOS may contribute to ulcer formation while HO-1 and COX-2 may promote ulcer healing.

Guo JS, Cho CH, Wang WP, Shen XZ, Cheng CL, Koo MWL. Expression and activities of three inducible enzymes in the healing of gastric ulcers in rats. *World J Gastroenterol* 2003; 9 (8): 1767-1771

http://www.wjgnet.com/1007-9327/9/1767.asp

INTRODUCTION

Nitric oxide synthase (NOS), heme oxygenase (HO) and cyclooxygenase (COX) are three important enzymes with constitutive and inducible isoforms. NOS catabolizes L-arginine to L-citrulline and nitric oxide (NO)[1,2], COX converts arachidonic acid to bioactive prostanoids[3,4], while HO metabolizes heme to biliverdin, carbon monoxide, and iron[5,6]. All these products play important roles in physiological and pathological conditions. The constitutive forms, namely eNOS, HO-2 and COX-1, are normally expressed in cells and tissues. Their expressions and activities are unaffected or only marginally modified during the process of inflammation. On the contrary, the inducible isoforms, namely iNOS, HO-1 and COX-2, are highly inducible in acute and chronic inflammation[7-9]. These induced enzymes may directly mediate the inflammatory reaction or contribute to the resolution of inflammation. Although the inducible property of these enzymes in inflammation has been proven and widely studied, their expression and activities at different stages of gastric ulceration have not been well defined. In this study, the temporal changes in the expressions and activities of these enzymes in rat stomaches during inflammation and ulcer healing were examined.

MATERIALS AND METHODS

Animals

The protocol of the study was approved by the Committee on the Use of Live Animals for Teaching and Research of University of Hong Kong. Male SD rats (weighing between 150-170 g) were fed on a standard laboratory diet (Ralston Purina Co., Chicago, IL) and kept inside a room with well-regulated temperature (22±1 ℃), humidity (65-70 %), and day/night cycle (12 h/12 h). The rats were starved for 24 h and water withdrawn 1 hour before the operation of the induction of gastric ulcer.

Preparation of gastric kissing ulcers

Gastric kissing ulcers were induced by luminal application of an acetic acid solution as previously described[10,11]. Briefly, the abdomen was opened under ether anesthesia, and the stomach was exposed. The anterior and posterior walls of the stomach were clamped together by a clip with metal rings of 11 mm internal diameter attached to both ends. Acetic acid solution (60 %, v/v) of 0.12 mL was injected with a syringe through the forestomach into the gastric lumen between the two rings. The acid solution was withdrawn 45 s later into the same syringe, and the operating site was disinfected with 70 % ethanol. Thereafter the animals were allowed to feed on standard diet and tap water *ad libitum* until collection of gastric tissue samples.

Sample collection

The rats were killed by ether anesthetization at 2 h, 6 h, 12 h, 1 d, 2 d, 3 d, 5 d, 8 d, and 15 d after ulcer induction and their stomachs were excised. The stomach was opened along the greater curvature and rinsed with cold normal saline, then blotted dry. The ulcer area (mm^2) was traced onto a transparency and then copied to a grid paper with 1 mm^2 square. The ulcer area was determined by counting the numbers of square it covered. Gastric tissues from the ulcer base, ulcer margin (1-2 mm adjacent to the ulcer base) and intact tissues around the ulcer margin were obtained and immediately frozen

in liquid nitrogen before storage at -70 ℃ until used for reverse transcription polymerase chain reaction (RT-PCR), Western blot and enzyme activities analysis. Gastric samples obtained from each time point were also fixed in 10 % buffered formalin for histological examinations. Gastric tissues from the rats without kissing ulcers were used as the control.

Histology

Paraffin embedded sections were prepared and hematoxylin and erosin staining (H&E) was used for morphological examinations of histological changes during tissue inflammation and ulcer healing.

RT-PCR analysis of mRNA expression

Total RNA was isolated from gastric tissues using Trizol reagent (Gibico BRL, Gathersburg, MD, USA). First strand complementary DNA (cDNA) was synthesized from 5 μg RNA by using oligo $(dT)_{20}$ primer with the thermoscript RT-PCR system (Gibico BRL). PCR cycles were performed for amplification of iNOS, eNOS, COX-1, COX-2, HO-1, HO-2 and β-actin cDNA using a PCR thermal cycler (Gene Amp PCR System 9700; Perkin-Elmer Corp., Norwalk, CT, USA) and oligonucleotides (Gibico BRL) of sequences are listed in Table 1. The number of PCR cycles was adjusted carefully to avoid saturation of the amplification system. PCR products were visualized by UV illumination (Bio-Rad, Hercules, CA, USA) after electrophoresis through 1 % agarose gel containing 0.5 μg/mL ethidium bromide. The gel photographs were scanned with a computerized densitometer (Multi-Analyst, Bio-Rad, Hercules, CA).

Table 1 Primer sequences of iNOS, eNOS, COX-1, COX-2, HO-1, HO-2 and β-actin

Primer	Primer sequences	Amplicon-length (bp)
HO-1	Sense: 5'-CAGTCGCCTCCAGAGTTTCC-3'	
	Antisense: 5'-TACAAGGAGGCCATCACCAGC-3'	284
HO-2	Sense: 5'-AGAAGTATGTGGATCGGA-3'	
	Antisense: 5'-TACTCAGGTCCAAGGCA-3'	242
COX-1	Sense: 5'-TGCTGCTGAGAAGGGAGTTCATTC-3'	
	Antisense: 5'-CAAGTCACACACACGGTTATGCTC-3'	403
COX-2	Sense: 5'-ACACTCTATCACTGGCATCC-3'	
	Antisense: 5'-GAAGGGACACCCTTTCACAT-3'	584
iNOS	Sense: 5' -TGGCTTGCCCTTGGAAGTTTCTC-3'	
	Antisense: 5'-TCCAGGCCATCTTGGTGGCAAGA-3'	574
eNOS	Sense: 5'-TACGGAGCAGCAAATCCAC-3'	
	Antisense: 5'-CAGGCTGCAGTCCTTTGATC-3'	812
β-actin	Sense:5'-GTGGGGCGCCCCAGGCACCA-3'	
	Antisense: 5'-CTCCTTAATGTCACGCACGATTTC-3'	540

Western blot analysis of NOS, HO and COX proteins

Gastric tissues for the analysis of protein expressions of iNOS, eNOS, HO-1, HO-2, COX-1 and COX-2 were homogenized in a proteinase inhibitor buffer (50 mmol/L Tris HCl, pH 7.5, 150 mmol/L NaCl, 0.5 % α-cholate sodium, 0.1 % SDS, 2 mmol/L EDTA, 1 % Triton X-100, 10 % glycerol, 1 mmol/L PMSF and aprotinin) and then centrifuged at 10 000 rpm for 15 min at 4 ℃. The supernatant was collected and the protein content was determined with dye-binding (Bio-Rad) method. 30 μg of total protein was loaded onto SDS-polyacrylamide gel and blotted onto hybrid C membranes (Amersham Life Science, Little Chalfont, Buckinghamshire, England) by electrophoresis. Pre-stained rainbrow recombinant protein molecular weight markers (Amersham International plc, Little Chalfont, Buckinghamshire, England) were used for molecular weight determinations. Membranes were blocked with blocking buffer containing 5 % fat free milk powder, 10 mmol/L Tris-HCl (pH 7.5), 100 mmol/L NaCl and 0.1 % Tween 20 for 1 h at room temperature. The blots were incubated overnight at 4 ℃ with 1:500 dilution of polycolonal antibodies against HO-1 and HO-2 (Stress-Gen, Victoria, Canada), monoclonal antibodies against iNOS and eNOS (Transduction Lab, Lexington, Kentucky, USA), polyclonal antibodies against COX-1 and COX-2 (Santa Cruz Biotechnology INC, Santa Cruz, California, USA). After washed in washing buffer for 30 min, the membranes were treated with HRP conjugated secondary antibody (1:5 000) (Bio-Rad) for 1 h at room temperature followed by another 30 min of washing. The ECL Western blotting system (Amersham Life Sciences) was used in accordance to the manufacturer's instructions for chemiluminescence of proteins, and the blots were then exposed to photographic films (Fuji Photo Film Co., Tokyo, Japan).

Determination of NOS activity

NOS activity in the gastric tissue was measured as the ability of tissue homogenates to convert L-[^{3}H]-arginine to L-[^{3}H]-citrulline[12]. Gastric samples were homogenized at 4 ℃ in a buffer containing 10 mmol/L HEPES (pH 7.2), 320 mmol/L surcose, 0.1 mmol/L EDTA, 1 mmol/L dithiothreitol, 10 μg/mL leupeptin, 2 μg/mL aprotinin (Sigma, St. Louis, MO, USA) and 1 mmol/L PMSF (Sigma), then centrifuged at 12 000 rpm for 30 min at 4 ℃. The supernatant was collected and the protein contents were measured. 100 μL of supernatant was then mixed with a buffered solution consisting of 0.7 mmol/L NADPH, 150 μmol/L $CaCl_2$, 7 mmol/L L-valine, 10 mmol/L HEPES (pH 7.2) and 1μ Ci [^{3}H]-L-arginine (Gibico BRL) and incubated at 37 ℃ for 30 min to determine the total NOS activity. For determination of the iNOS activity, 1 mmol/L EGTA was used to inhibit the activity of calcium-dependent constitutive eNOS. The reaction was stopped by adding 50 μL 20 % perchloric acid, 160 mL 1 mmol/L NaOH and 540 mL dilution solution containing 1 mmol/L each of L-arginine and DL-citrulline. The newly formed L-[^{3}H]-citrulline was separated from L-[^{3}H]-arginine by passing the reaction mixture over 1 mL AG50W-X8 resin columns (Bio-Rad), and the eluted labelled material was measured using a Beckman scintillation counter (LS-6500, Beckman Instrument, USA). The final result was expressed as pmol of L-[^{3}H]-citrulline formed per milligram of protein per 30 min.

Determination of HO activity

Heme oxygenase activity was measured as the ability of tissue homogenates to metabolize heme to bilirubin[13]. In brief, gastric tissues were homogenized in 0.1 mol/L potassium phosphate-buffered saline (pH 7.4) and centrifuged at 12 000 rpm for 30 min. Then 500 μL supernatant (about 4 mg total protein) was added to an equal volume of reaction mixture (2 mmol/L $MgCl_2$, 30 μmol/L hemin, 30 mg rat liver cytosol, 0.2 U glucose-6-phosphate dehydrogenase, 2 mmol/L glucose-6-phosphate, and 0.8 mmol/L NADPH), and incubated at 37 ℃ in the dark for 1 h. The formed bilirubin was extracted with benzene and the absorbance of bilirubin at 462 nm was measured against a baseline absorbance at 530 nm. Heme oxygenase activity was expressed as μg of bilirubin formed/mg protein per hour. The protein content in the supernatant was determined by dye-binding method with BSA as a standard.

Assessment of COX activity

Cyclooxygenase activity was measured as the ability of tissue homogenates to metabolize arachidonic acid to PGE_2 according to the method described by Tomlinson and Vane[7, 8]. Gastric tissues were homogenized at 4 ℃ in proteinase inhibitory

buffer containing 50 mmol/L Tris-Cl (pH 7.4), 3.15 % trisodium citrate, 1 mmol/L PMSF, 0.2 mmol/L leupeptin. The protein concentration in the homogenates was measured. Homogenates were incubated at 37 ℃ for 30 min in the presence of excess arachidonic acid (30 mmol/L). The samples were then boiled and centrifuged at 12 000 rpm for 30 min. The concentration of PGE_2 in the supernatant was measured by immunoassay, using R&D PGE_2 kits (R&D Systems, Inc. Minneapolis, MN, USA). Results were expressed as ng PGE_2 produced per mg protein in 30 min.

Statistical analysis

All the data were expressed as mean ± S.E.M. Statistical analysis was performed using Student' s *t*-test. Values of $P<0.05$ were considered statistically significant.

RESULTS

Morphology and histology

Two symmetrical ulcers were induced in the anterior and posterior walls of the stomach by acetic acid injection. The ulcer base was denuded of mucosal layers because of the necrotic changes and it reepithelized gradually during ulcer healing. Histological accumulation of neutrophils was found at 6 h and prominent inflammatory infiltration was observed at the ulcer base on day 1 to day 3 after ulcer induction. This period was defined as the inflammatory stage of gastric ulceration. After 3 days, the ulcer healed rapidly and was characterized by a reduction in ulcer area (Figure 1). There was intensive proliferation of epithelial cells at the ulcer margin, accompanied by the development of granulation tissues with angiogenesis. The period from day 3 onwards was considered to be the healing phase of gastric ulceration. Complete reepithelization of the ulcer craters was found in some stomaches on day 15 after ulcer induction.

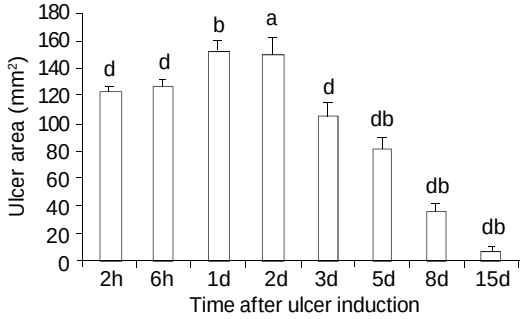

Figure 1 Sequential change of ulcer areas at different time points after ulcer induction. Significant decrease of ulcer area was found on day 3 after ulcer induction. The data were represented as mean ± S. E. M of 20 rats in each group, $^aP<0.05$ *vs* the 2 h group; $^bP<0.001$ *vs* the 2 h group; $^dP<0.001$ *vs* the day 1 group.

Expression of HO, NOS and COX mRNA

Basal levels of COX-2 and HO-1 mRNA expression were detected in normal and non-ulcerated gastric tissues around the ulcers, while expression of iNOS mRNA could only be detected in the ulcer tissue 6 h after ulcer induction. Dramatic increase in mRNA expression of HO-1, iNOS and COX-2 was found from 6 h onwards. High level of iNOS expression persisted for only 3 days then declined rapidly over the healing phase. The expression of HO-1 and COX-2 mRNA remained at high levels during the healing stage from day 3 to day 8. Unlike their inducible isoforms, mRNA expression of HO-2, eNOS and COX-1 was relatively stable. The HO-2 mRNA appeared to be slightly increased in the ulcer base at 12 h after ulcer induction (Figure 2).

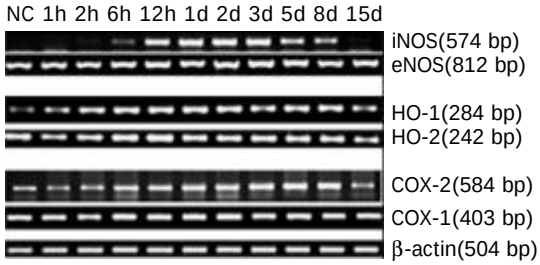

Figure 2 Time course of mRNA expression of inducible and constitutive isoforms of NOS, HO and COX in the ulcer bases. NC=normal control group.

Western blot analysis of HO, NOS and COX

A basal level of HO-1 protein was found in normal gastric tissues, while the iNOS and COX-2 proteins were undetectable. Acetic acid-induced ulceration resulted in a transient loss of HO-1 protein at 2 h, but re-appeared at 6 h and then increased persistently until its peak expression on day 3 to day 5. Its level decreased but still remained higher than normal during day 5 to day 15, at which the ulcer decreased in size and reepithelized.

Expression of COX-2 protein was found to be induced 6 h after ulcer induction and peaked on day 5. Afterwards it remained at a high level during the healing stage. Unlike HO-1 and COX-2, high level of iNOS protein was only detected at the inflammatory stage from day 1 to day 3. The protein expressions of HO-2, eNOS and COX-1 were relatively stable. Transient losses of eNOS and COX-1 proteins were observed at 2 h after acetic acid injection, and then gradually returned to normal levels during the healing process. The level of HO-2 protein was slightly increased after ulcer induction and peaked on day 1, then returned to normal level during ulcer healing (Figure 3).

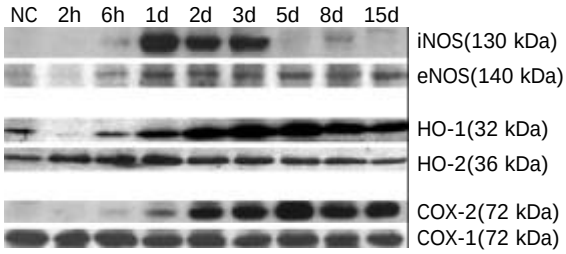

Figure 3 Western blot analysis of the protein levels of inducible and constitutive isoforms of NOS, HO and COX in the ulcer bases at different time after ulcer induction. NC= normal control group.

Expressions of iNOS and COX-2 in the ulcer margin were lower than those in ulcer base during the inflammatory phase. HO-1 expression in the ulcer margin was higher than that in non-ulcerated tissue but lower than that in the ulcer base both in the inflammatory and healing stages.

Enzyme activities of HO, NOS and COX

Marked increase of HO, NOS and COX activities at the ulcer base was found 6 h after ulcer induction. High level of iNOS activity was detected in ulcer base on day 1 to day 3, which was in consistent with the Western blot findings of iNOS protein expression. Similar trend was found in the margins but to a lesser extent (Figure 4). The activity of HO increased in 6 h and peaked on day 2, then remained at an elevated level on day 3 to day 8 (Figure 5). COX activity was persistently increased during the healing stage and was markedly elevated on day 15. Similar trend was found in the margin tissues but to a lesser extent (Figure 6). The trends for HO, NOS and COX activities in the ulcer margin were similar to those found in the ulcer base but with a lower value.

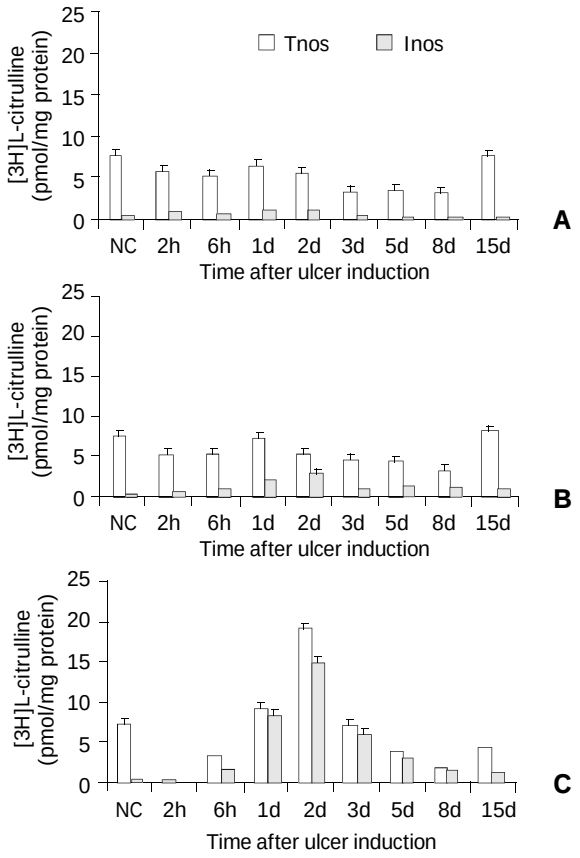

Figure 4 Total NOS (tnos) and iNOS (inos) activities at the non-ulcerated tissues (A), margins (B), and ulcer base (C) of acetic acid induced gastric ulcer. Each bar represents the mean ± S.E.M of 8 rats in each group. NC=normal control group.

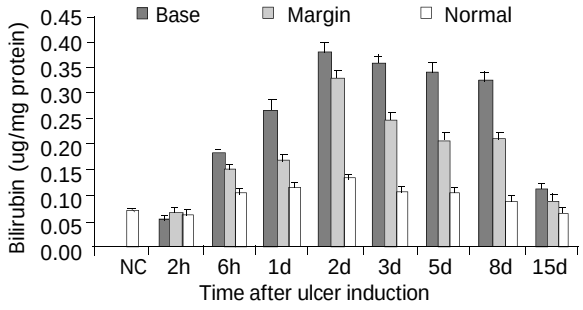

Figure 5 HO activities in the gastric tissues of normal control rats (NC) and the non-ulcerated tissues, ulcer margins and ulcer bases of acetic acid induced gastric ulcer. Each bar represents the mean ± S. E. M of 8 rats in each group.

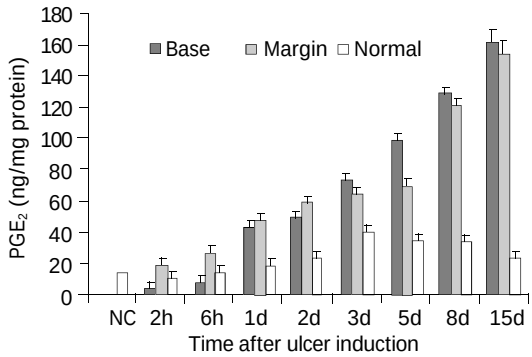

Figure 6 COX activities in the gastric tissues of normal control rats (NC) and the non-ulcerated tissues, ulcer margins and ulcer bases of acetic acid induced gastric ulcer. Each bar represents the mean ± S.E.M of 8 rats in each group.

DISCUSSION

In this study, the expression and activity patterns of NOS, HO and COX were investigated in rats with acetic acid-induced kissing ulcers. The results showed that the inducible isoforms of HO-1, iNOS and COX-2 were all up-regulated during the inflammatory phase. High expression and activity of iNOS were found to coincide with severe inflammation in the ulcer tissue, suggesting that it could be contributed by inflammatory cells that were involved in the inflammatory process. Maximum expressions and activities of HO-1 and COX-2 were found during the ulcer healing phase and thus they might play a role in ulcer healing.

It has been found that NO released from endothelial cells and neuronal cells by the constitutive isoform of NO synthase has regulatory roles in blood flow, motility and secretion. It also protects the gastrointestinal tract against injurious substances. NO produced from inflammatory cells by the inducible isoform of NOS has antimicrobial, antitumor and cytotoxic effects, but excessive amount may lead to peroxynitrite formation, protein tyrosine nitration, hydroxyl radical production and tissue damage[14, 15]. The present study also demonstrated that overexpression of iNOS on day 1 and day 2 after ulcer induction was accompanied by enlargement of ulcer crater. The expression of iNOS protein and activity were observed to be declined when the ulcer began to heal. NO generated from iNOS may also play a beneficial role during ulcer healing by inducing apoptosis in inflammatory cells[16].

The roles of HO-1 and COX-2 in gastric ulcer healing have not been clearly defined. HO-1 has been shown to possess cyto-protective and anti-inflammatory actions. Its expression is associated with the resolution of non-immune as well as immune-driven inflammation[9]. The role of HO-1 as an inflammatory defensive factor may be due to its conversion of oxidant heme to antioxidants biliverdin and bilirubin. It also elevates intracellular free iron levels to facilitate ferritin up-regulation, and regulation of vascular tension through CO generation. Moreover, a recent study has found that CO is able to inhibit the expression of lipopolysaccharide-induced pro-inflammatory cytokines and increase the anti-inflammatory cytokine through a pathway involving the mitogen-activated protein kinases (MAPK)[17]. Besides a role in resolution of inflammation, evidence has also been found that HO-1 may participate in the regulation of endothelial cells activation, proliferation and angiogenesis[18,19], which is essential for wound healing. In this study, the expression and activity of HO-1 were significantly elevated during early ulcer healing and this could be due to the contributory actions of HO-1 in inflammatory resolution and angiogenesis in tissue regeneration.

High expression of COX-2 protein and enzymatic activity of COX at the late ulcer healing stage were observed in this study. The expression of COX-1 protein was relatively stable, thus the change of COX activity might mainly be due to the change of protein level and activity of COX-2. Since tissue remodeling which includes reepithelization of gastric mucosa, maturation of granulation tissue, and reconstruction of extracellular matrix (ECM) mainly occurs at the late ulcer healing stage, the results of this study suggest that COX-2 may play an essential role in these remodeling processes. This is supported by the fact that non-selective as well as selective COX-2 inhibitors delay ulcer healing and prevent regeneration of the mucosa, maturation and angiogenesis in the ulcer base[20-26].

There may be interactions among NOS, HO and COX. HO may modulate NOS and COX systems since they are all heme-containing enzymes. NO and NO donors have been found to stimulate HO-1 expression in different cell lines[27-31] and NO was found to be able to stabilize HO-1 mRNA[32]. On the other hand, HO-1 may have a negative feedback regulation on NO production. Induction of HO-1 by cadmium, bismuth salts,

heme, and nitric oxide (NO) donors have been shown to inhibit the expression of iNOS[33, 34], while inhibition of HO-1 by its inhibitor enhanced iNOS expression. In the present study, a dramatic decrease of iNOS expression and activity was accompanied by an increase in expression and activity of HO-1 on day 5 after ulcer induction. This inverse relationship between iNOS and HO-1 expression and activities supports the existence of close interaction among these enzymes.

In summary, differential expression and activity patterns of inducible enzymes of iNOS, HO-1 and COX-2 during gastric ulceration and healing were found in the present study. The results indicate that iNOS may contribute to tissue inflammation during ulcer formation, while HO-1 and COX-2 may promote ulcer healing, since their expression and activities correlate with the resolving of inflammation and remodeling of ulcer tissues. Close interaction between iNOS and HO-1 may exist because the decrease of iNOS expression and activity coincide with the increase in expression and activity of HO-1. However, further experiments that enroll the use of selective blockers of these inducible enzymes should be conducted to substantiate these conclusions.

ACKNOWLEDGMENT

The authors wish to thank Hon Chueng Leung and Hau Leung So for their excellent technical assistance. This research was supported by RGC grant of the Hong Kong Research Council.

REFERENCES

1 **Griffith OW,** Stuehr DJ. Nitric oxide synthases: properties and catalytic mechanism. *Annu Rev Physiol* 1995; **57:** 707-736
2 **Marletta MA.** Nitric oxide synthase structure and mechanism. *J Biol Chem* 1993; **268:** 12231-12234
3 **DeWitt DL.** Prostaglandin endoperoxide synthase: regulation of enzyme expression. *Biochim Biophys Acta* 1991; **1083**: 121-134
4 **Marnett LJ,** Rowlinson SW, Goodwin DC, Kalgutkar AS, Lanzo CA. Arachidonic acid oxygenation by COX-1 and COX-2. Mechanisms of catalysis and inhibition. *J Biol Chem* 1999; **274:** 22903-22906
5 **Abraham NG,** Drummond GS, Lutton JD, Kappas A. The biological significance and physiological role of heme oxygenase. *Cell Physiol Biochem* 1996; **6:** 129-168
6 **Maines MD,** Trakshel GM, Kutty RK. Characterization of two constitutive forms of liver microsomal heme oxygenase. Only one molecular species of the enzyme is inducible. *J Biol Chem* 1986; **261:** 411-419
7 **Tomlinson A,** Appleton I, Moore AR, Gilroy DW, Willis D, Mitchell JA, Willoughby DA. Cyclo-oxygenase and nitric oxide synthase isoforms in rat carrageenin-induced pleurisy. *Br J Pharmacol* 1994; **113:** 693-698
8 **Vane JR,** Mitchell JA, Appleton I, Tomlinson A, Bishop-Bailey D, Croxtall J, Willoughby DA. Inducible isoforms of cyclooxygenase and nitric-oxide synthase in inflammation. *Proc Natl Acad Sci USA* 1994; **91:** 2046-2050
9 **Willis D,** Moore AR, Willoughby DA. Heme oxygenase isoform expression in cellular and antibody-mediated models of acute inflammation in the rat. *J Pathol* 2000; **190:** 627-634
10 **Chow JY,** Ma L, Zhu M, Cho CH. The potentiating actions of cigarette smoking on ethanol-induced gastric mucosal damage in rats. *Gastroenterology* 1997; **113:** 1188-1197
11 **Tsukimi Y,** Okabe S. Validity of kissing gastric ulcers induced in rats for screening of antiulcer drugs. *J Gastroenterol Hepatol* 1994; **9:** S60-S65
12 **Tepperman BL,** Brown JF, Whittle BJ. Nitric oxide synthase induction and intestinal epithelial cell viability in rats. *Am J Physiol* 1993; **265:** G214-G218
13 **Ishikawa K,** Sato M, Yoshida T. Expression of rat heme oxygenase in Escherichia coli as a catalytically active. Full-length form that binds to bacterial membrances. *Eur J Biochem* 1991; **202:** 161-165
14 **Beckman JS,** Koppenol WH. Nitric oxide, superoxide and peroxynitrite: the good, the bad, and ugly. *Am J Physiol* 1996; **271:** C1424-C1437
15 **Cho CH.** Current roles of nitric oxide in gastrointestinal disorders. *J Physiol Paris* 2001; **95:** 253-256
16 **Akiba Y,** Nakamura M, Mori M, Suzuki H, Oda M, Kimura H, Miura S, Tsuchiya M, Ishii H. Inhibition of inducible nitric oxide synthase delays gastric ulcer healing in the rat. *J Clin Gastroenterol* 1998; **27:** S64-S73
17 **Otterbein LE,** Bach FH, Alam J, Soares M, Tao Lu H, Wysk M, Davis RJ, Flavell R A, Choi AM. Carbon monoxide has anti-inflammatory effects involving the mitogen-activated protein kinase pathway. *Nat Med* 2000; **6:** 422-428
18 **Brouard S,** Otterbein LE, Anrather J, Tobiasch E, Bach FH, Choi AM, Soares MP. Carbon monoxide generated by heme oxygenase 1 suppresses endothelial cell apoptosis. *J Exp Med* 2000; **192:** 1015-1026
19 **Deramaudt BM,** Braunstein S, Remy P, Abraham NG. Gene transfer of human heme oxygenase into coronary endothelial cells potentially promotes angiogenesis. *J Cell Biochem* 1998; **68:** 121-127
20 **Mizuno H,** Sakamoto C, Matsuda K, Wada K, Uchida T, Noguchi H, Akamatsu T, Kasuda M. Induction of cyclooxygenase 2 in gastric mucosal lesions and its inhibition by the specific antagonist delays healing in mice. *Gastroenterology* 1997; **112:** 387-397
21 **Hudson N,** Balsitis M, Everitt S, Hawkey CJ. Angiogenesis in gastric ulcers: impaired in patients taking non-steroidal anti-inflammatory drugs. *Gut* 1995; **37:** 191-194
22 **Jones MK,** Wang H, Peskar BM, Levin E, Itani RM, Sarfeh, IJ, Tarnawski AS. Inhibition of angiogenesis by nonsteroidal anti-inflammatory drugs: insight into mechanisms and implications for cancer growth and ulcer healing. *Nat Med* 1999; **5:** 1418-1423
23 **Shigeta JJ,** Takahashi S, Okabe S. Role of cyclooxygenase-2 in the healing of gastric ulcers in rats. *J Pharmacol Exp Ther* 1998; **287:** 1383-1390
24 **Sun WH,** Tsuji S, Tsujii M, Gunawan ES, Sawaoka H, Kawai N, Iijima H, Kimura A, Kakiuchi Y, Yasumaru M, Sasaki Y, Kawano S, Hori M. Cyclo-oxygenase-2 inhibitors suppress epithelial cell kinetics and delay gastric wound healing in rats. *J Gastroenterol Hepatol* 2000; **15:** 752-761
25 **Brzozowski T,** Konturek PC, Konturek SJ, Sliwowski Z, Pajdo R, Drozdowicz D, Ptak A, Hahn EG. Classic NSAID and selective cyclooxygenase (COX)-1 and COX-2 inhibitors in healing of chronic gastric ulcers. *Microsc Res Tech* 2001; **53:** 343-353
26 **Brzozowski T,** Konturek PC, Konturek SJ, Schuppan D, Drozdowicz D, Kwiecien S, Majka J, Nakamura T, Hahn E. Effect of local application of growth factors on gastric ulcer healing and mucosal expression of cyclooxygenase-1 and –2. *Digestion* 2001; **64:** 15-29
27 **Alcaraz MJ,** Habib A, Lebret M, Creminon C, Levy-Toledano S, Maclouf J. Enhanced expression of heam oxygenase-1 by nitric oxide and antiinflammatory drugs in NIH 3T3 fibroblasts. *Br J Pharmacol* 2000; **130:** 57-64
28 **Hara E,** Takahashi K, Takeda K, Nakayama M, Yoshizawa M, Fujita H, Shirato K, Shibahara S. Induction of heme oxygenase-1 as a response in sensing the signals evoked by distinct nitric oxide donors. *Biochem Pharmacol* 1999; **58:** 227-236
29 **Durante W,** Kroll MH, Christodoulides N, Peyton KJ, Schafer AI. Nitric oxide induces heme oxygenase-1 gene expression and carbon monoxide production in vascular smooth muscle cells. *Circ Res* 1997; **80:** 557-564
30 **Hartsfield CL,** Alam J, Cook JL, Choi AMK. Regulation of heme oxygenase-1 gene expression in vascular smooth muscle cells by nitric oxide. *Am J Physiol* 1997; **273:** L980-L988
31 **Saudau K,** Pfeilschifter J, Brüne B. Nitrosative and oxidative stress induced heme oxygenase-1 accumulation in rat mesangial cells. *Eur J Pharmacol* 1998; **342:** 77-84
32 **Bouton C**, Demple B. Nitric oxide-inducible expression of heme oxygenase-1 in human cells. Translation-independent stabilization of the mRNA and evidence for direct action of nitric oxide. *J Boil Chem* 2000; **275**: 32688-32693
33 **Cavicchi M,** Gibbs L, Whittle BJ. Inhibition of inducible nitric oxide synthase in the human intestinal epithelial cell line, DLD-1, by the inducers of heme oxygenase-1, bismuth salts, and nitric oxide donors. *Gut* 2000; **47:** 771-778

Edited by Xu XQ and Wang XL

P.O.Box 2345, Beijing 100023,China
Fax: +86-10-85381893
E-mail: wjg@wjgnet.com www.wjgnet.com

World J Gastroenterol 2003;9(8):1772-1776
World Journal of Gastroenterology
 ISSN 1007-9327

• BASIC RESEARCH •

Role of TFF in healing of stress-induced gastric lesions

Shi-Nan Nie, Xiao-Ming Qian, Xue-Hao Wu, Shi-Yu Yang,Wen-Jie Tang, Bao-Hua Xu, Fang Huang, Xin Lin, Dong-Yan Sun, Hai-Chen Sun, Zhao-Shen Li

Shi-Nan Nie, Xiao-Ming Qian, Xue-Hao Wu, Shi-Yu Yang, Wen-Jie Tang, Bao-Hua Xu, Fang Huang, Xin Lin, Dong-Yan Sun, Hai-Chen Sun, Emergency Department, Nanjing General Hospital of Nanjing Command/Clinical School of Medical College of Nanjing University, Nanjing 210002, Jiangsu Province, China
Zhao-Shen Li, Department of Gastroenterology, Changhai Hospital, Second Military Medical University, Shanghai, 200433, China
Supported by the Key Project of the Tenth-Five-Year Plan Foundation of PLA, No.01Z059
Correspondence to: Shi-Nan Nie, Emergency Department, Nanjing General Hospital of Nanjing Command/Clinical School of Medical College of Nanjing University, Nanjing 210002, Jiangsu Province, China. shnnie630504@.sohu.com
Telephone: +86-25-4826808-58143
Received: 2003-03-05 **Accepted:** 2003-04-01

Abstract

AIM: To determine the changes of pS2 and ITF of TFF expression in gastric mucosa and the effect on ulcer healing of pS2, ITF to Water-immersion and restraint stress (WRS) in rats.

METHODS: Wistar rats were exposed to single or repeated WRS for 4 h every other day for up to 6 days.Gastric mucosal blood flow (GMBF) was measured by LDF-3 flowmeter and the extent of gastric mucosal lesions were evaluated grossly and histologically. Expression of pS2 and ITF mRNA was determined by RT-PCR. Immunohistochemistry was used to further detect the expression of pS2 and ITF.

RESULTS: WRS applied once produced numerous gastric mucosal erosions, but the number of these lesions gradually declined and GMBF restored at 2, 4, 8 h after stress. The area of gastric mucosal lesion was reduced by 64.9 % and GMBF was increased by 89.8 % at 8 h. The healing of stress-induced ulcerations was accompanied by increased expression of pS2 (0.51±0.14 *vs* 0.77±0.11, $P<0.01$) and ITF (0.022±0.001*vs* 0.177±0.010, $P<0.01$). The results were demonstrated further by immunohistochemistry of pS2 (0.95±0.11 *vs* 1.41±0.04, $P<0.01$) and ITF (0.134±0.001*vs* 0.253±0.01,$P<0.01$). With repeated WRS, adaptation to this WRS developed, the area of gastric mucosal lesions was reduced by 22.0 % after four consecutive WRS. This adaptation to WRS was accompanied by increased GMBF (being increased by 94.2 %), active cell proliferation in the neck region of gastric glands, and increased expression of pS2 (0.37±0.02 *vs* 0.77±0.01, $P<0.01$) and ITF (0.040± 0.001*vs* 0.372±0.010, $P<0.01$). The result was demonstrated further by immunohistochemistry of pS2 (0.55±0.04 *vs* 2.46±0.08, $P<0.01$) and ITF (0.134±0.001*vs* 0.354±0.070, $P<0.01$).

CONCLUSION: TFF may not only participate in the early phase of epithelial repair known as restitution(maked by increased cell migration),but also play an important role in the subsequent,protracted phase of glandular renewal(made by cell proliferation).

Nie SN, Qian XM, Wu XH, Yang SY, Tang WJ, Xu BH, Huang F, Lin X, Sun DY, Sun HC, Li ZS. Role of TFF in healing of stress-induced gastric lesions. *World J Gastroenterol* 2003; 9(8): 1772-1776
http://www.wjgnet.com/1007-9327/9/1772.asp

INTRODUCTION

Stress ulcer is a highly prevalent clinical complication. Fully understanding the mechanism of healing of stress-induced gastric lesions not only deepens our insights into stress ulcer, but also provides new ways for its prevention and treatment in clinical practice. The mechanism of the recovery of gastric mucosa after stress exposure has not been fully explained, the healing of stress ulcerations is a complex process which is affected by different factors. Current research has found that a variety of peptides are considered to play a crucial role in the control of mucosal integrity and repair. Among them, an important role was attributed to epidermal growth factor and transforming growth factor alpha[1-3].

Recently, a group of new peptides has been discovered, called TFF (trefoil factor family or trefoil peptides) because of their uniquely distinctive cysteine-rich "three-leaf" secondary structure, which probably protects these peptides from degradation by luminal acid and proteases within gastrointestinal tract. pS2 and intestinal trefoil factor (ITF) belong to the growing family of trefoil peptides[4,5].

The physiological role of TFF is poorly understood so far. The aim of the present study was to investigate the expression of pS2 and ITF in gastric mucosa of rats undergone WRS, and to probe the role of TFF in the early phase of epithelial repair of stress-induced gastric lesion.

MATERIALS AND METHODS

Induction of gastric adaptation to WRS: Thirty male Wistar rats, weighing 210-250 g (purchased from Xipuer-Bikai Experimental Animal Co. LTD, Shanghai) which had been fasted for 24 h with free access to water, were used. The animals were deprived of water 1 h before the experiment and divided into normal control group (n=6) and experimental control group (n=24). After being fasted for 24 h, the rats of normal control group were lightly anesthetized with ether and tied up on the rat board, the abdomen was opened, the stomach was exposed and GMBF was measured in the oxyntic gland area, gastric mucosa was sampled. The rats of experimental control group were divided into four subgroups (6 in each group) and exposed to WRS[6] for 4 h. They were killed either immediately (0 time: namely 0 h) or after 2 h, 4 h, 8 h. GMBF was measured and gastric mucosa was sampled as described below.

The rats of experimental control group were divided into four subgroups (6 each group) and exposed to repeated WRS[7]: The rats of group I were lightly anesthetized with ether, tied up on the rat board and exposed to WRS for 4 h by placing in water at 20-23 ℃ to the rat's xyphoid level at 10:00 AM on day 1. Then the rats were anesthetized with pentobarbital (30 mg· kg^{-1} i.p.), GMBF was measured and gastric mucosa was sampled. the rats of group II were treated similarly except that after WRS, they were removed from water and placed at

room temprature, and refed with food and water until 10:00 AM the next day, and starved again for 24 h, WRS was repeated. the rats of group III and IV were exposed to the 3rd or 4th WRS as described above.

Measurement of GMBF: GMBF was measured by using laser Doppler flowmetry (LDF-3 flowmeter, Nankai University, Tianjin, China). In brief, the rats were anesthetized with pentobarbital (30 mg· kg^{-1} i.p.), the abdomen was opened, the stomach was exposed and transected, the gastric contents were gently evacuated to the exterior through the cut made in the forestomach.Then, an optical probe was placed gently 0.5 mm above perpendicular to the mucosal surface in the oxyntic gland area to monitor GMBF displayed in mV (value of Doppler signal voltage) on the digital panel of the flowmeter. When GMBF became stable, four points were selected for measurement (one point for 1 minute) and the average value was calculated and expressed as *U/mV*.

Appreciation of UI: Mucosal lesions were evaluated by the score systems reported by Nie S[7]. Briefly, after the measurement of GMBF, the stomach was dissected out and opened along the greater curvature. The stomach was then examined with a 10×magnifier for the presence of erosions and scored as follows: 1 point for small round hemorrhagic erosion, 2 points when the length of hemorrhagic erosion was less than 1 mm, 3 points when the length was 1-2 mm, 4 points when the length was 2-3 mm, 5 points when the length was longer than 4 mm. The score value multiplied 2 when the width of erosion was larger than 1 mm.

Reverse-transcriptase-polymerase chain reaction (RT-PCR) for detection of messenger RNA (mRNA) for pS2 and ITF: The stomachs were removed from rats with intact gastric mucosa and from those exposed to single or repeated stress. Mucosal specimens (about 100 mg) were scraped off using a slide glass and immediately snap frozen in liquid nitrogen and stored at -80 ℃ until analysis. Total RNA was isolated from mucosal samples using a guanidium isothiocyanate/phenol chloroform single step extraction kit from Stratagene (Gibco BRL,USA). Following precipitation, the RNA was resuspended in RNAse-free TE buffer and the concentration was estimated by absorbance at 260 nm wavelength. Furthermore, the quality of each RNA sample was determined by running the agarosefomaldehyde electrophoresis. RNA samples were stored at -80 ℃ until analysis.

Single-strand cDNA was generated from 5 μg of total cellular RNA using StrataScript™ reverse transcriptase (Gibco BRL,USA) and oligo (dT) primers (Gibco BRL,USA). Briefly, 5 μg of total RNA was used as the template to synthesize complementary DNA with 2.5 U of Maloney murine leukemia virus reverse transcriptase in 5 μl of buffer containing 10 mM Tris-HCl, pH 8.3; 50 mM KCl, 5 mM $MgCl_2$; 1 mM of each deoxyribonucleoside triphosphate; 2.5 mM of oligo (dt) primers and 1.4 U μl^{-1} RNAse blocker. Reverse-transcription was performed at room temperature for 20 min, then at 37 ℃ for 15 min, at 90 ℃ for 5 min and at 5 ℃ for 10 min. The resulting complementary DNA was used as a template for subsequent polymerase chain reaction (PCR).

A 124-base pair (bp) fragment of pS_2 was amplified from single-stranded DNA by polymerase chain reaction (PCR) using two oligonucleotide primers for pS_2 sequence: Sense primer, 5' -CCATGGAGCACAAGGTGACCTG-3' and antisense primer, 5' -GGGAAGCCACAATTTATTCT-3' . A 221-base pair (bp) fragment of ITF was amplified from single-stranded DNA by polymerase chain reaction (PCR) using two oligonucleotide primers to ITF sequence: Sense primer, 5' -ATGGAGACCAGAGCCTTCTGGAC-3' and antisense primer, 5' -AGAGGTTTGAAGCACCAGGGC-3' . Concomitantly, amplification of the 521 bp fragment of rat β-actin was performed on the same RNA samples to assess RNA integrity, two oligonucleotide primers to β-actin sequence: Sense primer, 5' -TGGGACGATATGGAGAAGAT-3' and antisense primer, 5' -ATTGCCGATAGTGATGACCT-3' . The nucleotide sequences of the primers for pS_2 were based on the pulished cDNA sequences encoding pS2[8] and the nucleotide sequences of the primers for ITF were based on the published cDNA sequences encoding ITF[9]. The primers were synthesized by Bo-Ya Biotechnical Co. LTD, Shanghai, China.

Reaction mixture for PCR contained cDNA template (2 μl), 50 pmol of each primer, and 2.5 U of Termus aquaticus DNA (Promega) in 10 mM Tris-HCl (pH 8.8), 50 mM KCl, 1.5 mM $MgCl_2$, 0.5 mM dNTPs in a volume of 50 μl. RT blanks (no RNA included) were incubated in each analysis. The mixture was overlaid with 25 μl of mineral oil to prevent evaporation. Amplification was performed using a DNA thermal cycler for 35 cycles, each of which consisted of 2 min at 94 ℃ for denaturation, 45 s at 52 ℃ (pS_2) and at 50 ℃ (ITF) for annealing, and 1 min at 72 ℃ for extension. The final cycle included extension for 5 min at 72 ℃ to ensure full extension of the product. The number of amplification cycles was previously determined to keep amplification in linear to avoid the "plateau effect" associated with increased numbers of PCR cycles. 8 μl of each PCR -product was electrophoresed on 1.6 % agarose gel stained with ethidium bromide, and then visualized under UV light. Location of predicted PCR-product was confirmed by using DNA digest phix 174/Hae III as a stained size marker. The gel was then photographed under UV transillumination. In addition to size analysis by agarose gel electrophoresis,specificity of the primer pair for pS_2 and ITF was assessed by sequencing PCR products. For quantification,we determined the intensity of polymerase chain reaction products on the negative film of gel photographs according to Konturek PC *et al*[10]. Expression of the products was quantified using video image analysis system (TanonGIS-1000, Tanon Technical Co, LTD, Shanghai, China). An index of messenger RNA expression was determined in each sample using the following equation according to Konturek PC *et al*[11].

Immunocytochemistry: For histological assessment, the other half of the stomach was fixed in 10 % formalin, embedded in paraffin, and stained with hematoxylin and eosin. For immunohistochemistry, serial sections obtained from these paraffin blocks were dewaxed and rehydrated. Endogenous peroxidase was blocked with 3 % hydrogen peroxide for 15 min. Sections were then incubated for 35 min with a specific monoclonal antibody against pS_2 and ITF (Asgiraud, Italy), washed and incubated with biotinylated rabbit anti-mouse antibody. After 35 min incubation in avidin-biotin complex, the sections were incubated for 2 min in peroxidase substrate (diaminobenzidine, PBS, in addition to 0.3 percent of hydrogen peroxide) and counterstained with haematoxylin.

The intensity of pS_2 and ITF staining (Mean score) for each cell was graded according to the criteria described by Nie *et al*[6]. as follows: 0=no staining, I=weakly positive, II=moderately positive (cytoplasm positive but other cytoplasmic details also visible), or III=densely stained. The staining intensity was calculated in 300 consecutive cells in three regions of the gastric mucosa: Surface epithelium (top), neck region (neck) and basal portions of the gastric glands (base). The mean intensity per section and region was calculated. Negative control sections were processed immunohistochemically after replacing the primary antibody with an irrelevant monoclonal antibody or phosphate-buffered-saline (PBS).

Statistical analysis: Results were presented as *means±SD*. Statistical comparisons were made by Student' s *t* test.The linearly relevant analysis was applied to analyse the relationship between two variants, *P* values less than 0.05 were considered statistically significant.

RESULTS

Gastric lesion induced by single or repeated WRS: WRS applied once produced numerous gastric mucosal erosions in oxyntic mucosa with the mean lesion number of 45.32±1.41 per rat. No microscopic evidence of damage occurred in the forestomach. Microscopical examination of the mucosa after 4 h stress revealed widespread damage of the surface epithelium with many cells sloughed off into the gastric lumen and focal area of deep haemorrhagic necrosis (Figure 1). The number of stress lesions was gradually declined at 2, 4, 8 h after the end of stress. UI was reduced to about 20.8 % of the initial number at 8 h after the end of stress (Table 1). With repeated WRS, adaptative cytoprotection against stress was developed, UI in II, III, IV groups markedly reduced as compared with group I (P<0.01). UI after four consecutive WRS was 22 % of UI after one WRS. Cell proliferation in the neck regions of gastric glands was activated (Figure 2, Table 2).

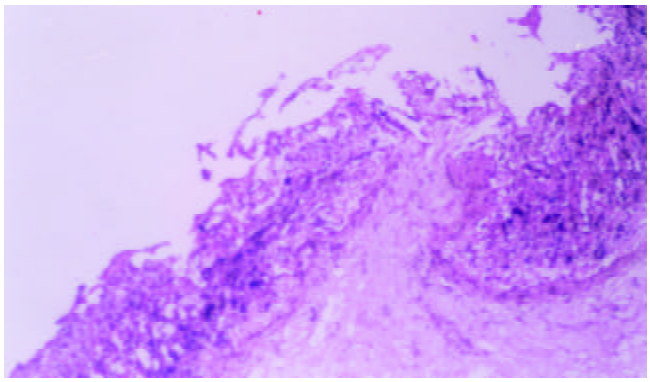

Figure 1 Necrosis appeared as craters in rats after exposed to single WRS for 4 h (HE×200).

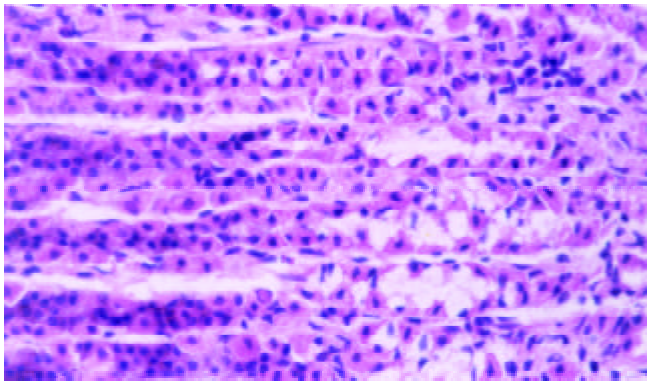

Figure 2 Foveolae and neck region elongated and the mucosa appeared thicker after rats exposed to 4th WRS for 4 h(HE×400).

Change of GMBF after single or repeated WRS: GMBF of normal rats was 424.70±7.72*U/mV*. GMBF significantly decreased after single exposure to WRS and restored at 2, 4, 8 h after the end of stress. It increased up to 94.5 % of normal value at 8 h after the end of stress (Table 1). GMBF of normal rats was 484.01±10.97*U/mV*. GMBF significantly decreased after single exposure to WRS.With repetitive challenge with WRS, there was an adaptive increase of it in experimental group, and GMBF of groups II, III, IV markedly increased as compared with that of group I (P<0.01). After the 4th time of WRS, the value of GMBF was almost restored to normal level (94.2 % of normal value). There was a significantly negative relevance between GMBF and UI (r=-0.953, P<0.01) (Table 2).

Expressions of pS_2 and ITF mRNA and immunohistochemical staining for expression of pS_2 and ITF proteins during recovery from stress damage: The expressions of pS_2 and ITF could be detected in normal gastric mucosa. They were expressed mainly in the regenerative zone of cytoplasm and weaker expressions were found at the basal portions of the gastric glands. The expressions of pS_2 and ITF in single WRS significantly decreased and was absent in the necrotic region, whereas repeated WRS significantly increased expression of pS_2 and ITF. In addition to the regenerative zone,other areas including the lumen of gastric glands also expressed pS_2 and ITF.

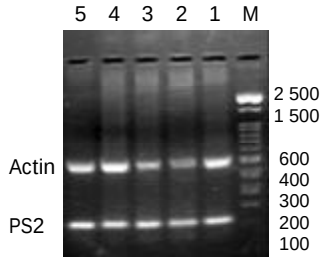

Figure 3 Messenger RNA expression of pS_2 mRNA and β-actin in gastric mucosa of rats after single exposure to WRS and in control intact rats (M=PCR size marker, 1=control group, 2=group 1, 3=group 2, 4=group 3, 5=group 4).

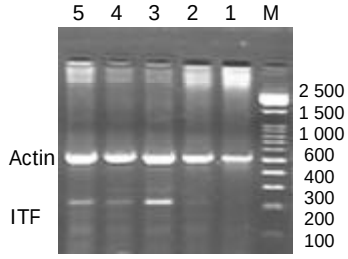

Figure 4 Messenger RNA expression of ITF mRNA and β-actin in gastric mucosa of rats after single exposure to WRS and in control intact rats (M=PCR size marker, 1=control group, 2=group 1, 3=group 2, 4=group 3, 5=group 4).

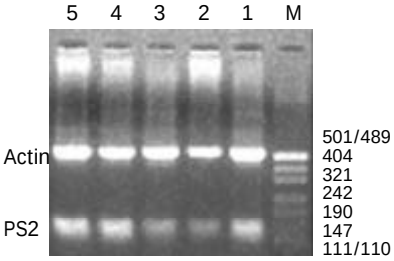

Figure 5 Messenger RNA expression of pS_2 mRNA and β-actin in gastric mucosa of rats after repeated exposure to WRS and in control intact rats (M=PCR size marker, 1=control group, 2=group I, 3=group II, 4=group III, 5=group IV).

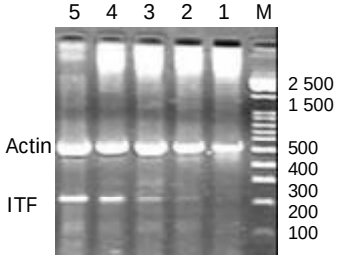

Figure 6 Messenger RNA expression of ITF mRNA and β-actin in gastric mucosa of rats after repeated exposure to WRS and in control intact rats (M=PCR size marker, 1=control group, 2=group I, 3=group II, 4=group III, 5=group IV).

Table 1 Changes of expression of pS_2, ITF, GMBF and UI in gastric mucosa after exposed to WRS

Group	GMBF (*U* / mV)	UI	Mean score (pS_2)	pS_2 / β-actin	Mean score (ITF)	ITF / β-actin
Control	424.70±7.72	0.00	1.65±0.03	0.78±0.11	0.003±0.001	0.004±0.0002
experimental						
1	274.56±13.0[b]	45.32±1.41	0.95±0.11[b]	0.51±0.14[b]	0.134±0.001[b]	0.022±0.01[b]
2	371.35±15.27[bd]	18.31±1.47[d]	1.63±0.14[d]	0.78±0.13[d]	0.259±0.01[bd]	0.287±0.008[bd]
3	417.451±12.31[d]	11.38±1.31[d]	1.53±0.13[bd]	0.71±0.12[d]	0.136±0.04[ad]	0.112±0.009[d]
4	401.32±8.95[d]	9.54±1.27[d]	1.41±0.04[bd]	0.77±0.11[ad]	0.235±0.01[bd]	0.177±0.01[ad]

[a]*P*<0.05 *vs* control group; [b]*P*<0.01 *vs* control group; [c]*P*<0.05 *vs* group 1; [d]*P*<0.01 *vs*r group 1.

Table 2 Changes of expression of pS_2, ITF, GMBF and UI in gastric mucosa after exposed to repeated WRS

Group	GMBF(*U* / mV)	UI	Mean score (pS_2)	pS_2 / β-actin	Mean score (ITF)	ITF / β-actin
Control	484.01±10.97	0.00	2.01±0.14	0.63±0.01	0.0003±0.001	0.004±0.0004
experimental						
I	321.87±8.85[b]	47.23±1.20	0.55±0.04[b]	0.37±0.02[b]	0.134±0.001[b]	0.040±0.001[b]
II	418.35±7.94[bd]	30.54±1.12[d]	1.51±0.03[bd]	0.42±0.01[bd]	0.194±0.05[bd]	0.108±0.009[bd]
III	446.09±10.98[bd]	20.75±1.54[d]	2.55±0.11[bd]	0.72±0.02[bd]	0.281±0.015[bd]	0.265±0.009[bd]
IV	455.95±11.81[bd]	10.39±1.18[d]	2.46±0.08[bd]	0.77±0.01[bd]	0.354±0.07[bd]	0.372±0.01[bd]

[a]*P*<0.05 *vs* control group; [b]*P*<0.01 *vs* control group; [c]*P*<0.05 *vs* group I; [d]*P*<0.01 *vs* group I.

The expressions of pS2 and ITF mRNA were increased during the healing after single WRS (pS2: 0.51±0.14 *vs* 0.77±0.11, *P*<0.01; ITF: 0.022±0.001*vs* 0.177±0.010, *P*<0.01) (Figure 3, 4). The same results were observed by immunohistochemistry (pS2: 0.95±0.11 *vs* 1.41±0.04, *P*<0.01; ITF: 0.134±0.001*vs* 0.253±0.01, *P*<0.01). With repeated WRS, adaptative cytoprotection against stress was developed.The expression of pS2 and ITF mRNA was increased by using RT-PCR (pS2: 0.37±0.02 *vs* 0.77±0.01, *P*<0.01; ITF: 0.040±0.001*vs*0.372±0.010, *P*<0.01) (Figure 5,6) and immunohistochemistry (pS2: 0.55±0.04 *vs* 2.46±0.08, *P*<0.01; ITF: 0.134±0.001*vs* 0.354±0.070, *P*<0.01). There was a significantly negative relevance between expressions of pS_2 or ITF and UI (*r*=-0.921, *P*<0.01; *r*=-0.965, *P*<0.01), and positive relevance was found between expressions of pS_2 or ITF and GMBF (*r*=0.826, *P* <0.05; *r*=0.854, *P*<0.05) (Table 2).

DISCUSSION

The cytoprotective functions in protecting gastrointestinal tract against ongoing damage may be accomplished in several ways, and evidences for participation in both the early phase of epithelial repair known as restitution (marked by increased cell migration but no proliferation), and in the subsequent, protracted phase of glandular renewal (marked by proliferation, differentiation and migration) have been published[12-14].

This study assessed for the first time immunohistochemical and RT-PCR analyses of pS2, ITF expression in rat gastric mucosa after exposure to water immersion and restrained stress. Our observation showed that expression of pS2 and ITF in gastric mucosa was enhanced shortly after the stress, leading us to hypothesize that this process might be mediated by pS2 and ITF.

The importance of trefoil peptides in the process of response to the damage action of strong irritants has not yet been evaluated.The members of the trefoil peptide family, including pS2 and ITF, share a common structural feature, which is a motif of six cysteine residues termed a trefoil or a P domain. There are increasing evidences that pS2 and ITF are important in maintaining the integrity of gastric mucosa and involved in the repair of ulcerated areas in gastrointestinal tract[15-19]. This is supported by an observation that increased expressions of pS2 and ITF were found in the ulcer-associated cell lineage (UACL), which is a glandular structure that develops in the area of gastrointestinal tract adjacent to ulcerated mucosa[20]. This is supported by the findings obtained from *in vitro* study which showed that pS2 and ITF exhibited a mitogenic effect on different cell lines[21,22]. Moreover, exogenously recombinant TFF has been shown to significantly attenuate the extent of acute mucosal injury induced by a variety of ulcerogens such as 96 % ethanol, indomethacin or stress[23], indicating that this peptide does exhibit gastroprotective activity.

The present study showed that, WRS applied once produced numerous gastric mucosal erosions. UI gradually declined at 2, 4, 8 h after the end of stress, the expression of pS2 and ITF was increased during the healing of stress-induced ulceration, there was not a correlation between the expression of pS2 or ITF and UI.

The facts that pS2 or ITF is over-expressed in gastric mucosa immediately after stress injury and that this peptide stimulates cell migration, strongly suggest that it might mediate the early phase healing of acute gastric lesion called restitution[24-28].

It has also been proposed that trefoil peptide family contribute to gastric mucosal defence and repair by affecting cell proliferation[29,30].

In the present study, we found this adaptation was accompanied by an increased mucosal cell proliferation and enhanced expressions of mRNA for pS2 and ITF, suggesting the involvement of pS2 and ITF in the adaptation process.

The major finding of this report was the demonstration for the first time that gastric adaptation to WRS involved overexpressions of mRNA for pS2 and ITF and an increased rate of cell proliferation in gastric mucosa, and enhanced cell proliferation was preceded by overexpressions of pS_2 and ITF mRNA, although the expressions of mRNA for pS_2 and ITF decreased in initial phase after exposure of gastric mucosa to WRS, suggesting that this trefoil peptide contributes to cell proliferation.

The present study also showed that with repeated WRS, adaptative cytoprotection against stress was developed, the mucosal lesions reduced markedly after 2nd, 3rd and 4th WRS. The expression of pS2 and ITF was increased. There was a significantly negative relevance between expressions of pS2 or ITF and UI.

After the 4th WRS, GMBF was almost restored to normal level. Therefore, during the process of tolerant cytoprotection, GMBF, UI and expression of pS2 and ITF showed regular

changes and there was a good relationship beween them.

Indeed, we have confirmed that WRS-adapted mucosa exhibits an augment GMBF, but it is not clear whether this factor could directly or indirectly account for the mucosal adaptation, or what could be the mechanism of this mucosal hyperemia in the stomach. TGFα has been shown to increase GMBF[2,31], while TFF can promote synthesis of TGFα. So hyperemia observed during the development of adaptation can be mediated, at least in part by the release of this peptide.

REFERENCES

1 **Brzozowski T,** Konturek SJ, Majka J, Dembinski A, Drozdowicz D. Epidermal growth factor, polyamines, and prostaglandins in healing of stress-induced gastric lesions in rats. *Dig Dis Sci* 1993; **38**: 276-283

2 **Konturek SJ,** Brzozowski T, Majka J, Dembinski A, Slomiany A, Slomiany BL. Transforming growth factor alpha and epidermal growth factor in protection and healing of gastric mucosal injury. *Scand J Gastroenterol* 1992; **27**: 649-655

3 **Konturek PC,** Ernst H, Brzozowski T, Ihlm A, Hahn EG, Konturek SJ. Expression of epidermal growth factor and transforming growth factor-alpha after exposure of rat gastric mucosa to stress. *Scand J Gastroenterol* 1996; **31**: 209-216

4 **Podolsky DK.** Mechanisms of regulatory peptide action in the gastrointestinal tract: trefoil peptides. *J Gastroenterol* 2000; **35** (Suppl 12): 69-74

5 **Tran CP,** Cook GA, Yeomans ND, Thim L, Giraud AS. Trefoil peptide TFF2 (spasmolytic polypeptide) potently accelerates healing and reduces inflammation in a rat model of colitis. *Gut* 1999; **44**: 636-642

6 **Nie SN,** Li ZS, Zhan XB, Gong YF, Tu ZX, Gong YF. Role of the pS2 in healing of stress-induced gastric lesions. *Wei Chang Bing Xue* 2002; **7**: 20-23

7 **Nie S,** Li Z, Zhan X, Tu Z, Xu G, Gong Y, Man X. Role of the pS (2) in gastric mucosa adaptative cytoprotection from stress. *Zhonghua Yixue Zazhi* 2002; **82**: 172-175

8 **Itoh H,** Tomita M, Uchino H, Kobayashi T, Kataoka H, Sekiya R, Nawa Y. cDNA cloning of rat pS2 peptide and expression of trefoil peptides in acetic acid-induced colitis. *Biochem J* 1996; **318**: 939-944

9 **Nie SN,** Li ZS, Zhan XB, Xu GM, Tu ZX, Gong YF. Role of the pS2,ITF in the early phase of epithelial repaire of stress-induced gastric lesion. *Jiefangjun Yixue Zazhi* 2002; **27**: 182-185

10 **Brzozowski T,** Konturek PC, Konturek SJ, Stachura J. Gastric adaptation to aspirin and stress enhances gastric mucosal resistance against the damage by strong irritants. *Scand J Gastroenterol* 1996; **31**: 118-125

11 **Konturek PC,** Brzozowski T, Pierzchalski P, Kwiecien S, Pajdo R, Hahn EG, Konturek SJ. Activation of genes for spasmolytic peptide, transforming growth factor alpha and for cyclooxygenase (COX)-1 and COX-2 during gastric adaptation to aspirin damage in rats. *Aliment Pharmacol Ther* 1998; **12**: 767-777

12 **Podolsky DK.** Mucosal immunity and inflammation. V. Innate mechanisms of mucosal defense and repair: The best offense is a good defense. *Am J Physiol* 1999; **277**: G495-499

13 **Wright NA.** Aspects of the biology of regeneration and repair in the human gastrointestinal tract. *Philos Trans R Soc Lond B Biol Sci* 1998; **353**: 925-933

14 **Podolsky DK.** Healing the epithelium: Solving the problem from two sides. *J Gastroenterol* 1997; **32**: 122-126

15 **Farrell JJ,** Taupin D, Koh TJ, Chen D, Zhao CM, Podolsky DK, Wang TC. TFF2/SP-deficient mice show decreased gastric proliferation, increased acid secretion, and increased susceptibility to NSAID injury. *J Clin Invest* 2002; **109**: 193-204

16 **Ulaganathan M,** Familari M, Yeomans ND, Giraud AS, Cook GA. Spatio-temporal expression of trefoil peptide following severe gastric ulceration in the rat implicates it in late-stage repair processes. *J Gastroenterol Hepatol* 2001; **16**: 506-512

17 **Longman RJ,** Douthwaite J, Sylvester PA, Poulsom R, Corfield AP, Thomas MG, Wright NA. Coordinated localisation of mucins and trefoil peptides in the ulcer associated cell lineage and the gastrointestinal mucosa. *Gut* 2000; **47**: 792-800

18 **McKenzie C,** Thim L, Parsons ME. Topical and intravenous administration of trefoil factors protect the gastric mucosa from ethanol-induced injury in the rat. *Aliment Pharmacol Ther* 2000; **14**: 1033-1040

19 **Cook GA,** Thim L, Yeomans ND, Giraud AS. Oral human spasmolytic polypeptide protects against aspirin-induced gastric injury in rats. *J Gastroenterol Hepatol* 1998; **13**: 363-370

20 **Alison MR,** Chinery R, Poulsom R, Ashwood P, Longcroft JM, Wright NA. Experimental ulceration leads to sequential expression of spasmolytic polypeptide, intestinal trefoil factor, epidermal growth factor and transforming growth factor alpha mRNAs in rat stomach. *J Pathol* 1995; **175**: 405-414

21 **Chinery R,** Coffey RJ. Trefoil peptides: Less clandestine in the intestine. *Science* 1996; **274**: 204

22 **Mashimo H,** Wu DC, Podolsky DK, Fishman MC. Impaired defense of intestinal mucosa in mice lacking intestinal trefoil factor. *Science* 1996; **274**: 262-265

23 **Babyatsky MW,** deBeaumont M, Thim L, Podolsky DK. Oral trefoil peptides protect against ethanol- and indomethacin-induced gastric injury in rats. *Gastroenterology* 1996; **110**: 489-497

24 **Saitoh T,** Mochizuki T, Suda T, Aoyagi Y, Tsukada Y, Narisawa R, Asakura H. Elevation of TFF1 gene expression during healing of gastric ulcer at non-ulcerated sites in the stomach: Semiquantification using the single tube method of polymerase chain reaction. *J Gastroenterol Hepatol* 2000; **15**: 604-609

25 **Poulsen SS,** Thulesen J, Christensen L, Nexo E, Thim L. Metabolism of oral trefoil factor 2 (TFF2) and the effect of oral and parenteral TFF2 on gastric and duodenal ulcer healing in the rat. *Gut* 1999; **45**: 516-522

26 **Dossinger V,** Kayademir T, Blin N, Gott P. Down-regulation of TFF expression in gastrointestinal cell lines by cytokines and nuclear factors. *Cell Physiol Biochem* 2002; **12**: 197-206

27 **Ito S,** Lacy ER, Rutten MJ, Critchlow J, Silen W. Rapid repair of injured gastric mucosa. *Scand J Gastroenterol Suppl* 1984; **101**: 87-95

28 **Konturek PC,** Brzozowski T, Konturek SJ, Elia G, Wright N, Sliwowski Z, Thim L, Hahn EG. Role of spasmolytic polypeptide in healing of stress-induced gastric lesions in rats. *Regul Pept* 1997; **68**: 71-79

29 **Konturek PC.** Physiological, immunohistochemical and molecular aspects of gastric adaptation to stress, aspirin and to *H. pylori*-derived gastrotoxins. *J Physiol Pharmacol* 1997; **48**: 3-42

30 **Modlin IM,** Poulsom R. Trefoil peptides: Mitogens, motogens, or mirages? *J Clin Gastroenterol* 1997; **25**(Suppl 1): S94-100

31 **Tepperman BL,** Soper BD. Effect of epidermal growth factor, transforming growth factor alpha and nerve growth factor on gastric mucosal integrity and microcirculation in the rat. *Regul Pept* 1994; **50**: 13-21

Edited by Zhao P and Wang XL

P.O.Box 2345, Beijing 100023,China
Fax: +86-10-85381893
E-mail: wjg@wjgnet.com www.wjgnet.com

World J Gastroenterol 2003;9(8):1777-1780
World Journal of Gastroenterology
 ISSN 1007-9327

• BASIC RESEARCH •

Cloning of human 15ku selenoprotein gene from H9 T cells

Ke-Jun Nan, Chun-Li Li, Yong-Chang Wei, Chen-Guang Sui, Zhao Jing, Hai-Xia Qin, Li-Jun Zhao, Bo-Rong Pan

Ke-Jun Nan, Chun-Li Li, Yong-Chang Wei, Chen-Guang Sui, Zhao Jing, Hai-Xia Qin, Department of Medical Oncology, First Hospital of Xi' an Jiaotong University, Xi' an 710061, Shaanxi Province, China
Li-Jun Zhao, The University of Georgia, Athens, Ga 30602, USA
Bo-Rong Pan, Department of Oncology, Xijing Hospital, Fourth Military Medical University, Xi' an 710032, Shaanxi Province, China
Supported by Science and Technology Research and Development Project of Shaanxi Province, No. 2002K10-G1
Correspondence to: Dr. Chun-Li Li, Department of Medical Oncology, First Hospital of Xi' an Jiaotong University, 1 Jiangkang Road, Xi' an 710061, Shaanxi Province, China. chun128@sohu.com
Telephone: +86-29-5324036 **Fax:** +86-29-5324086
Received: 2003-03-03 **Accepted:** 2003-03-29

Abstract

AIM: To clone human 15ku selenoprotein gene.

METHODS: H9 human T cells were cultured in RPMI1640 medium supplemented with 100 mL /L fetal calf serum. mRNA was isolated from the cells. cDNA library was constructed by RT-PCR. The human 15ku selenoprotein gene was obtained by PCR and cloned into T vector and sequenced.

RESULTS: A unique cDNA fragment about 1 244 bp was obtained. Sequence analysis identified an open reading frame within the cDNA. The gene had an in-frame TGA, which encoded selenocysteine (Sec), and a 3'-UTR SECIS element, which was required for synthesis of selenoprotein. The predicted protein molecular mass was about 15ku (162 residues). The result was identical with human liver 15ku selenoprotein gene published in Genbank.

CONCLUSION: Human 15ku selenoprotein gene can be successfully obtained from T cell line.

Nan KJ, Li CL, Wei YC, Sui CG, Jing Z, Qin HX, Zhao LJ, Pan BR. Cloning of human 15ku selenoprotein gene from H9 T cells. *World J Gastroenterol* 2003; 9(8): 1777-1780
http://www.wjgnet.com/1007-9327/9/1777.asp

INTRODUCTION

The trace element selenium (Se) is an essential human nutrient[1]. It has been shown to prevent cancers, especially liver and stomach cancers[2] in both epidemiological studies and clinical supplementation trials[3]. However, the mechanism by which Se suppresses tumor development remains unknown. Se is present in known human selenoproteins as amino acid selenocysteine (Sec)[4]. Sec is the active form of Se in selenoproteins and has important biological functions. Recently, a human 15ku selenoprotein (Sep15) containing Se in the form of Sec was identified. It was an acid protein with a PI value of 4.5. It was recently identified in human T cells[5, 6] and was present in various human tissues, such as liver, kidney, testis and brain, but it was highly expressed in epithelial cells of the prostate gland[6] and thyroid[5]. The level of this selenoprotein was reduced substantially in hepatocellular carcinoma[7] and in a malignant prostate cell line[8]. Furthermore, epidemiological data have indicated a statistically significant inverse correlation between Se in the diet and occurrence of liver cancer. These facts have provoked our interest to study Sep15. The recent finding that the gene of Sep15 was located on human chromosome 1p31, often affected in human cancer[9], also supports the hypothesis that this protein might play a role in the development of cancers[5]. To get a better understanding of the relationship between Sep15 and tumor, and the mechanism by which it suppresses the tumor, we firstly cloned the gene of this selenoprotein.

MATERIALS AND METHODS

Materials

H9 T cell line was purchased from ATCC. RPMI1640 was purchased from Gibco. Fetal bovine serum was from Hangzhou Sijiqing Company. Main biochemical reagents of T vector, T4 DNA ligase, *Taq* DNA polymerase and Trizol reagent were from Promega. Small amount plasmid extraction kit and PCR products purification kit were from Huashun Shengwu Engineering Company. Bacteria species JM109 was from the Department of Biochemistry of the Fourth Military Medical University. Agarose was from Huamei Shengwu Engineering Company. The restriction endonuclease *Not* I was from Takara. RNA extraction kit was from Promega. RT-PCR kit was from American Bior' s Company. The primers were synthesized by Georgia University of America. The forward primer was 5'-AGCGATGGCGGCTGGGCCGAG-3'. The backward primer was 5'-GATTTTTGAAACTTTTTATTTATA-3'.

Methods

mRNA extraction of H9 T cells H9 T cells were cultured in the RPMI1640 containing new born bovine serum under the condition of 50 mL/L CO_2 at 37 ℃ in a CO_2 incubator. About 10^7 H9 T cells were absolutely split with trizol reagent. Total RNA was extracted with chloroform, deposited with isopropanol, then dried at 37 ℃. mRNA was isolated with a mRNA purification kit from Promega[10]. The procedure in details was performed according to the instructions of the kit.
RT-PCR[11] By using the reverse transcription system from Promega[12], cDNA synthesis was performed according to the following instructions. mRNA previously extracted and random hexamers were used to synthesize first strand of cDNA[13], which was used to synthesize the double-strand DNA in the latter PCR[14]. PCR was performed as follows[15, 16]. The total volume of the PCR amplification system was 100 μL. First, 10 μL reverse transcription reaction liquid, 4 μL 20 pmol/L primers (each 2 μL), 8 μL 10 mmol/L dNTP, 10 μL 10×PCR reaction liquid, and 10U *Taq*DNA were added consecutively, then water was added to a total volume of 100 μL. The PCR was performed by incubating at 94 ℃ for 2 min, at 94 ℃ for 1 min, at 55 ℃ for 1 min, at 72 ℃ for 1 min, totally 35 cycles. The reaction mixture was incubated at 72 ℃ for 7 min. Finally all the PCR products were used for 10 g/L agarose gel electrophoresis to purify the products. Purification was performed according to the instructions of the gel extraction kit from Huashun Company.
Linkage and conversion 5 μL T vector, 1 μL T_4DNA ligase,

1 μL 10×buffer were added into previously purified PCR products, incubated at 16 ℃ overnight. 5 μL linkage products was picked up to infect competence bacteria of JM109. The conversion products were spread on a LB agarose plate containing ampicillin at 37 ℃ overnight.

Restriction endonuclease digestion and evaluation First, 3 monoclonal colonies were randomly chosen, and put into 10 g/L LB containing ampicillin, the culture was shaken at 37 ℃ overnight in air bath, then the plasmid of $P^{GEM\text{-}T\text{-}15ku\text{-}selenoprotein}$ was extracted. The procedure was performed according to the instructions of the low-dose plasmid extraction kit from Huashun Company. 5 μL previously extracted plasmid was digested with *Not* I. The reaction system containing 5 μL plasmid, 1 μL *Not* I, 2 μL 10×BSA buffer, 2 μL 10×H buffer, 2 μL 10×TritonX-100, and 8 μL sterilized water was performed at 37 ℃ for 3 hours. Finally 5 μL reaction mixture was used for 10 g/L agarose gel electrophoresis for 45 minutes. At the same time, the plasmid DNA was sent to the laboratory of Georgia University in America to sequence the DNA.

RESULTS

Sep15 gene amplification

After 35 cycles of RT-PCR, 5 μL PCR products were used for 10 g/L agarose gel electrophoresis. When compared with the DNA marker, cDNA fragment was between 1 000 bp and 2 000 bp. It was coincident with the length of purposed gene (Figure 1).

Figure 1 Agarose gel electrophoresis of RT-PCR amplified Sep15 gene fragment.

Sep15 gene cloning and its digestion and evaluation

After 3 monoclonal colonies were randomly chosen, the plasmid was extracted and digested with *Not* I. Then, 5 μL was used for 10 g/L agarose gel electrophoresis, the straps were found to be coincident with the length of purposed gene (Figure 2).

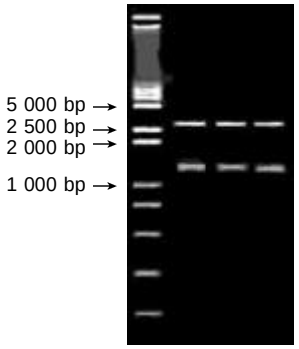

Figure 2 *Not* I cut plasmid of $P^{GEM\text{-}T\text{-}15ku\text{-}selenoprotein}$.

DNA sequencing

The sequencing of $P^{GEM\text{-}T\text{-}15ku\text{-}selenoprotein}$ showed that the Sep15 gene we cloned was completely coincident with the sequence in GenBank. It was 100 % homology with the human Sep15 gene. The sequences were as follows.

```
   1 agcgatggcg gctgggccga gtgggtgtct ggtgccggcg tttgggctac ggttgttgtt ggcgactgtg
  71 cttcaagcgg tgtctgcttt tggggcagag ttttcatcgg aggcatgcag agagttaggc ttttctagca
 141 acttgctttg cagctcttgt gatcttctcg gacagttcaa cctgcttcag ctggatcctg attgcagagg
 211 atgctgtcag gaggaagcac aatttgaaac caaaaagctg tatgcaggag ctattcttga agtttgtgga
 281 tgaaaattgg gaaggttccc tcaagtccaa gcttttgtta ggagtgataa acccaaactg ttcagaggac
 351 tgcaaatcaa gtatgtccgt ggttcagacc ctgtattaaa gcttttggac gacaatggga acattgctga
 421 agaactgagc attctcaaat ggaacacaga cagtgtagaa gaattcctga gtgaaaagtt ggaacgcata
 491 taaatcttgc ttaaattttg tcctatcctt ttgttacctt atcaaatgaa atattacagc acctagaaaa
 561 taatttagtt ttgcttgctt ccattgatca gtcttttact tgaggcatta aatatctaat taaatcgtga
 631 aatggcagta tagtccatga tatctaagga gttggcaagc ttaacaaaac ccatttttta taaatgtcca
 701 tcctcctgca tttgttgata ccactaacaa aatgctttgt aacagacttg cggttaatta tgcaaatgat
 771 agtttgtgat aattggtcca gttttacgaa caacagattt ctaaattaga gaggttaaca agacagatga
 841 ttactatgcc tcatgtgctg tgtgctcttt gaaaggaatg acagcagact acaaagcaaa taagatatac
 911 tgagcctcaa cagattgcct gctcctcaga gtctctccta tttttgtatt acccagcttt ctttttaata
 981 caaatgttat ttatagttta caatgaatgc actgcataaa aactttgtag cttcattatt gtaaaacata
1050 ttcaagatcc tacagtaaga gtgaaacatt cacaaagatt tgcgttaatg aagactacac agaaaacctt
1121 tctagggatt tgtgtggatc agatacatac ttggcaaatt tttgagtttt acattcttac agaaaagtcc
1191 atttaaaagt gatcatttgt aagaccaaaa tataaataaa aagtttcaaa aatc
```

DISCUSSION

Se was recognized as an essential trace element in human and animal' s life by WHO in 1978. The relationship between Se and many kinds of disease including cancer is a hot point of medical research[17, 18]. Usually, Se is incorporated into proteins in the forms of selenocysteine (Sec) and selenomethionine (SeMet). The term "selenoprotein" is restricted to the proteins which contain Se in the form of selenocysteine[19]. Selenoproteins are distinguished from proteins which nonspecifically incorporate selenomethionine not contributing to the biological function of the Se. About 21 specific selenoproteins have been identified in mammals and bacteria, and 18 of them could have biological functions attributed to them. Mammalian Se-containing proteins can be divided into three groups: proteins containing nonspecifically incorporated Se, specific Se-binding proteins, and specific selenocysteine-containing selenoproteins[5]. Selenoproteins with a known function identified so far include five glutathione peroxidases, two deiodinases, several thioredoxin reductases, and selenophosphate synthetase 2. Sep15, selenoprotein P, selenoprotein W, an 18-ku selenoprotein and several selenoproteins identified in silico from nucleotide sequence databases have been found to contain selenocysteine, but their functions are not known. Gel electrophoretic separation of tissue samples from rats labeled with ^{75}Se showed the existence of further Se-containing proteins[5].

It has been shown that Se could prevent cancer in a variety of animal model systems[20, 21]. Both epidemiological studies and supplementation trial supported its efficacy in humans[22]. However, the mechanism by which Se suppresses tumor development remains unknown[23]. Se is present in known human selenoproteins as selenocysteine. Selenocysteine represents the 21st amino acid and is encoded by UGA triplet in selenoprotein mRNA[24, 25]. Although UGA most often functions as a stop codon, UGA-encoded incorporation of selenocysteine into the growing polypeptide is determined by the presence of a specific stem-loop secondary structure within the 3' -untranslated region of the selenoprotein mRNA[26]. Sep15 was firstly found in human T cells, and it contains a selenocysteine residue encoded by TGA. Its coding sequence has no homology to known protein-encoding genes. Computer analysis of transcript map databases indicated that this gene included five exons and four introns[27]. Recent findings indicate that the chromosome, in which the gene of Sep15 is located, is a genetic locus commonly mutated or deleted in human

cancers. One in-frame TGA codon and two stem loop structures resembling selenocysteine insertion sequence (SECIS) elements were identified in the 3' -untranslated region of the gene, and only one of them was functional[9]. Examination of the available cDNA sequence of this protein revealed that two polymorphisms were located at position 811(C/T) and 1 125 (G/A)[28] within the 3' -untranslated region. They were organized into two alleles, C^{811}/G^{1125} and T^{811}/A^{1125} in the 68 %/32 % frequency distribution. These 3' -untranslated region polymorphisms resulted in changes in selenocysteine incorporation into protein and different response. To Se supplementation[9]. Human epidemiological studies have revealed that Se has a negative correlation with the occurrence of prostate cancer[29, 30] and lung cancer[31]. Moreover, recent investigations have shown that Se supplementation may be effective on the reduction of common human cancers, including prostate cancer[9], colon[32] cancer and lung cancer. Northern blot analysis of the human Sep15 mRNA demonstrated that the expression of Sep15 was significantly decreased in malignant prostate cancer cell line and in hepatocellular carcinoma cell line. The Sep15 protein levels in liver tumors, adjacent tissues, and normal hepatic tissue were significantly different. The Sep15 level was significantly decreased in tumors compared with that in the normal control. It was consistent with the observation that Sep15 protein was not detectable in mouse prostate adenocarcinoma cells, while normal mouse prostate showed a strong signal with Sep15 protein-specific antibodies.

Different expression patterns of the Sep15 protein in normal and malignant tissues, the occurrence of polymorphism associated with protein expression, the role of Se in differential regulation of polymorphisms, and loss of heterozygosity at the Sep15 locus in certain human tumor types make us suggest that Sep15 may be involved in cancer development[28]. We have cloned the gene of Sep15 in our country for the first time in order to study the expression of Sep15 protein in different tissue, its structure, function and the relationship with cancer due to the worldwide cancer[33-37] , and digestive in china[38-40].

REFERENCES

1 **Yu MW,** Horng IS, Hsu KH, Chiang YC, Liaw YF, Chen CJ. Plasma selenium levels and risk of hepatocellular carcinoma among men with chronic hepatitis virus infection. *Am J Epidemiol* 1999; **150**: 367-374

2 **Trobs M,** Renner T, Scherer G, Heller WD, Geiss HC, Wolfram G, Haas GM, Schwandt P. Nutrition, antioxidants, and risk factor profile of nonsmokers, passive smokers and smokers of the Prevention Education Program (PEP) in Nuremberg, Germany. *Prev Med* 2002; **34**: 600-607

3 **Popova NV**. Perinatal selenium exposure decreases spontaneous liver tumorogenesis in CBA mice. *Cancer Lett* 2002; **179**: 39-42

4 **Leblondel G,** Mauras Y, Cailleux A, Allain P. Transport measurements across Caco-2 monolayers of different organic and inorganic selenium: influence of sulfur compounds. *Biol Trace Elem Res* 2001; **83**: 191-206

5 **Behne D,** Kyriakopoulos A. Mammalian selenium-containing proteins. *Annu Rev Nutr* 2001; **21**: 453-473

6 **Korotkov KV,** Kumaraswamy E, Zhou Y, Hatfield DL, Gladyshev VN. Association between the 15-kDa selenoprotein and UDP-glucose:glycoprotein glucosyltransferase in the endoplasmic reticulum of mammalian cells. *J Biol Chem* 2001; **276**: 15330-15336

7 **Chin-Thin W,** Wei-Tun C, Tzu-Ming P, Ren-Tse W. Blood concentrations of selenium, zinc, iron, copper and calcium in patients with hepatocellular carcinoma. *Clin Chem Lab Med* 2002; **40**: 1118-1122

8 **Klein EA,** Thompson IM, Lippman SM, Goodman PJ, Albanes D, Taylor PR, Coltman C. SELECT: the selenium and vitamin E cancer prevention trial: rationale and design. *Prostate Cancer Prostatic Dis* 2000; **3**: 145-151

9 **Kumaraswamy E,** Malykh A, Korotkov KV, Kozyavkin S, Hu Y, Kwon SY, Moustafa ME, Carlson BA, Berry MJ, Lee BJ, Hatfield DL, Diamond AM, Gladyshev VN. Structure-expression relationships of the 15-kDa selenoprotein gene. Possible role of the protein in cancer etiology. *J Biol Chem* 2000; **275**: 35540-35547

10 **Li SW,** Gong JP, Wu CX, Shi YJ, Liu CA. Lipopolysaccharide induced synthesis of CD14 proteins and its gene expression in hepatocytes during endotoxemia. *World J Gastroenterol* 2002; **8**: 124-127

11 **Liu LX,** Jiang HC, Liu ZH, Zhou J, Zhang WH, Zhu AL, Wang XQ, Wu M. Integrin gene expression profiles of human hepatocellular carcinoma. *World J Gastroenterol* 2002; **8**: 631-637

12 **Jiang RL,** Lu QS, Luo KX. Cloning and expression of core gene cDNA of Chinese hepatitis C virus in cosmid pTM3. *World J Gastroenterol* 2000; **6**: 220-222

13 **Li Y,** Yang L, Cui JT, Li WM, Guo RF, Lu YY. Construction of cDNA representational difference analysis based on two cDNA libraries and identification of garlic inducible expression genes in human gastric cancer cells. *World J Gastroenterol* 2002; **8**: 208-212

14 **Li Y,** Lu YY. Applying a highly specific and reproducible cDNA RDA method to clone garlic up-regulated genes in human gastric cancer cells. *World J Gastroenterol* 2002; **8**: 213-216

15 **Zhao Y,** Wu K, Xia W, Shan YJ, Wu LJ, Yu WP. The effects of vitamin E succinate on the expression of c-jun gene and protein in human gastric cancer SGC-7901 cells. *World J Gastroenterol* 2002; **8**: 782-786

16 **Xue YW,** Zhang QF, Zhu ZB, Wang Q, Fu SB. Expression of cyclooxygenase-2 and clinicopathologic features in human gastric adenocarcinoma. *World J Gastroenterol* 2003; **9**: 250-253

17 **Ujiie S,** Kikuchi H. The relation between serum selenium value and cancer in Miyagi, Japan: 5-year follow up study. *Tohoku J Exp Med* 2002; **196**: 99-109

18 **Hara S,** Shoji Y, Sakurai A, Yuasa K, Himeno S, Imura N. Effects of selenium deficiency on expression of selenoproteins in bovine arterial endothelial cells. *Biol Pharm Bull* 2001; **24**: 754-759

19 **Mostert V.** Selenoprotein P: properties, functions, and regulation. *Arch Biochem Biophys* 2000; **376**: 433-438

20 **Riondel J,** Wong HK, Glise D, Ducros V, Favier A. The effect of a water-dispersible beta-carotene formulation on the prevention of age-related lymphoid neoplasms in mice. *Anticancer Res* 2002; **22**: 883-888

21 **Popova NV.** Perinatal selenium exposure decreases spontaneous liver tumorogenesis in CBA mice. *Cancer Lett* 2002; **179**: 39-42

22 **Nakaji S,** Fukuda S, Sakamoto J, Sugawara K, Shimoyama T, Umeda T, Baxter D. Relationship between mineral and trace element concentrations in drinking water and gastric cancer mortality in Japan. *Nutr Cancer* 2001; **40**: 99-102

23 **Calvo A,** Xiao N, Kang J, Best CJ, Leiva I, Emmert-Buck MR, Jorcyk C, Green JE. Alterations in gene expression profiles during prostate cancer progression: functional correlations to tumorigenicity and down-regulation of selenoprotein-P in mouse and human tumors. *Cancer Res* 2002; **62**: 5325-5335

24 **Korotkov KV,** Novoselov SV, Hatfield DL, Gladyshev VN. Mammalian selenoprotein in which selenocysteine (Sec) incorporation is supported by a new form of Sec insertion sequence element. *Mol Cell Biol* 2002; **22**: 1402-1411

25 **Zhang W,** Cox AG, Taylor EW. Hepatitis C virus encodes a selenium-dependent glutathione peroxidase gene. Implications for oxidative stress as a risk factor in progression to hepatocellular carcinoma. *Med Klin* 1999; **94** (Suppl 3): 2-6

26 **Mansur DB,** Hao H, Gladyshev VN, Korotkov KV, Hu Y, Moustafa ME, El-Saadani MA, Carlson BA, Hatfield DL, Diamond AM. Multiple levels of regulation of selenoprotein biosynthesis revealed from the analysis of human glioma cell lines. *Biochem Pharmacol* 2000; **60**: 489-497

27 **Hatfield DL,** Gladyshev VN. How selenium has altered our understanding of the genetic code. *Mol Cell Biol* 2002; **22**: 3565-3576

28 **Hu YJ,** Korotkov KV, Mehta R, Hatfield DL, Rotimi CN, Luke A, Prewitt TE, Cooper RS, Stock W, Vokes EE, Dolan ME, Gladyshev VN, Diamond AM. Distribution and functional consequences of nucleotide polymorphisms in the 3'-untranslated region of the human Sep15 gene. *Cancer Res* 2001; **61**: 2307-2310

29 **Brooks JD,** Metter EJ, Chan DW, Sokoll LJ, Landis P, Nelson WG, Muller D, Andres R, Carter HB. Plasma selenium level before diagnosis and the risk of prostate cancer development. *J Urol* 2001;

166: 2034-2038

30 **Gasparian AV,** Yao YJ, Lu J, Yemelyanov AY, Lyakh LA, Slaga TJ, Budunova IV. Selenium compounds inhibit I kappa B kinase (IKK) and nuclear factor-kappa B (NF-kappa B) in prostate cancer cells. *Mol Cancer Ther* 2002; **1**: 1079-1087

31 **Trobs M,** Renner T, Scherer G, Heller WD, Geiss HC, Wolfram G, Haas GM, Schwandt P. Nutrition, antioxidants, and risk factor profile of nonsmokers, passive smokers and smokers of the Prevention Education Program (PEP) in Nuremberg, Germany. *Prev Med* 2002; **34**: 600-607

32 **Casimiro C.** Etiopathogenic factors in colorectal cancer. Nutritional and life-style aspects. 2. *Nutr Hosp* 2002; **17**: 128-138

33 **Sun XW,** Shen BZ, Shi MS, Dai XD. Relationship between CD44v6 expression and risk factors in gastric carcinoma patients. *Shijie Huaren Xiaohua Zazhi* 2002; **10**: 1129-1132

34 **Zhou HB,** Zhang JM, Yan Y. Inactivation of DPC4 gene in colorectal carcinoma. *Shijie Huaren Xiaohua Zazhi* 2002; **10**: 1140-1142

35 **Zhou XD,** Yu JP, Ran ZX, Luo HS, Yu BP. Expression of cFLIP and p53 mutation in adenocarcinoma of colon. *Shijie Huaren Xiaohua Zazhi* 2002; **10**: 536-539

36 **Dong K,** Li B, Qin Y, Li CZ, Lui JY, Sun ZL, Sun ZF. Methylation pattern analysis in CpG islands of p15 and p16 tumor suppressor genes in pancreatic carcinoma tissue. *Shijie Huaren Xiaohua Zazhi* 2002; **10**: 1264-1267

37 **Cui M,** Zhang HJ, An LG. Tumor growth Inhibition by polysaccharide from Coprinus comatus. *Shijie Huaren Xiaohua Zazhi* 2002; **10**: 287-290

38 **Gong JQ,** Fang CH. Relationship between the oval cells and development of hepatocellular carcinoma in rats. *Shijie Huaren Xiaohua Zazhi* 2002; **10**: 1133-1139

39 **Yang L**, Wang YP, Wu DY, Zhang SM, Li JY, Zhang YC, Xin Y. Pathological behaviors and molecular mechanisms of signet-ring cell carcinoma and mucinous adenocarcinoma of stomach: a comparative study. *Shijie Huaren Xiaohua Zazhi* 2002; **10**: 516-524

40 **Zhu JS,** Zhu L, Wang L, Zhuang QX, Hu B, Da W, Chen WX, Chen GQ, Ma JQ. Autologous peripheral blood stem cell combined with high-dose arterial chemotherapy for advanced gastric cancer. *Shijie Huaren Xiaohua Zazhi* 2002; **10**: 1408-1411

Edited by Xu XQ and Wang XL

P.O.Box 2345, Beijing 100023,China
Fax: +86-10-85381893
E-mail: wjg@wjgnet.com www.wjgnet.com

World J Gastroenterol 2003;9(8):1781-1785
World Journal of Gastroenterology
 ISSN 1007-9327

• BASIC RESEARCH •

X-ray induced L02 cells damage rescued by new anti-oxidant NADH

Fa-Quan Liu, Ji-Ren Zhang

Fa-Quan Liu, Ji-Ren Zhang, Department of Oncology, Zhujiang Hospital, First Military Medical University, Guangzhou 510282, Guangdong Province, China
Supported by Healthcare Research Fundation of the Tenth Five-Year Plan of PLA, No, 01MA138
Correspondence to: Fa-Quan Liu, Department of Oncology, Zhujiang Hospital,First Military Medical University, Guangzhou, 510282, China. liufaquan@163.net
Telephone: +86-20-85143202 **Fax:** +86-20-85143200
Received: 2002-08-06 **Accepted:** 2002-10-18

Abstract

AIM: To explore molecular mechanism of nicotinamide adenine dinucleotide (NADH) antagonization against X-ray induced L02 cells damage.

METHODS: L02 liver cells were cultured in RPMI 1640, exposed to X-ray irradiation and continued to culture in the presence or absence of NADH. Cellular viability was analyzed by routine MTT methods. The percent age of apoptotic cells and positive expressions of p53, bax and bcl-2, fas, fasL proteins were determined by FCM. Level of intracellular ROS was determined by confocal microscope scanning. Morphological change was detected by scanning electron micrograph.

RESULTS: The viability of L02 cells was decreased with increasing dose of X-ray irradiation. NADH could not only eliminate the apoptosis induced by X-ray irradiation, but also up-regulate expression of bcl-2 protein and down-regulate expression of p53, bax, fas and fasL proteins ($P<0.05$). At the same time, NADH could reduce level of intracellular ROS in radiated L02 cells.

CONCLUSION: NADH has marked anti-radiation effect, its mechanism may be associated with up-regulation of bcl-2 expression and down-regulation of p53, bax fas and fasL expression, as well as decline of intracellular ROS. However, further investigation of its mechanism is worthwhile.

Liu FQ, Zhang JR. X-ray induced L02 cells damage rescued by new anti-oxidant NADH. *World J Gastroenterol* 2003; 9(8): 1781-1785
http://www.wjgnet.com/1007-9327/9/1781.asp

INTRODUCTION

Recent radiobiological studies have demonstrated that ionizing radiation can induce cell death. Exposure of cell to ionizing radiation over a wide dose range results in activation of cellular response pathways, including p53-dependent and p53-independent ways[1,2]. At the same time, apoptosis resulted from a coordinate sequence of biochemical events eventually leads to cell death. Among these,the generation of ROS with perturbation of prooxidant/antioxidant ratio, alterations in mitochondria structure and $\triangle \Psi m$, and diminutions of plasma membrane potential have been investigated[3,4]. The stabilized electrochemical gradient relies on a functional ion exchange via the electrogenic transporter Na+/K+-ATPase. Na+/K+-ATPase is an energy hungry process which consumes a major of cellular ATP production. Therefore, there may be a decrease of ATP level when apoptosis starts within a few minutes after ionizing irradiation. NADH, an important coenzyme, participates in three carboxyl cycles and ultimately produces ATP molecules. We added NADH to L02 cells undergoing X-ray irradiation *in vitro*, and observed change of survivals and apoptosis as well as radiation associated proteins which take part in signal transduction of apoptosis.

MATERIALS AND METHODS

Reagents

NADH (purity: 97 %) was gifted by Professor Birkmay from Chemical Department of Graz University. Monoclonal mouse anti-p53, bcl-2, bax antibodies and rat anti-Fas, FasL antibodies were from Beijing Zhongshan Biotechnology Company. PI/Annexin V kits were purchased from Immunotech (France). High FITC-labeled goat anti-mouse antibodies were from Zhongshan Company. H_2DCF probe was purchased from America Molecular Probe Company.

Cell lines and culture

Normal human liver cell line L02 was purchased from Shanghai Institute of Cell Biology, Chinese Academy of Sciences. The cells were cultured in RPMI 1640 supplemented with streptomycin (50 U/ml), glutamate (2 mM) and 10 % fetal bovine serum.

Induction of apoptosis

The L02 cells were seeded in 6-well tissue cultured plates, the supernatant was discarded and 0.01 M PBS (pH 7.4) was added. The L02 cells were X-ray-irradiated with 2.5, 5.0 and 7.5 Gy. The cells were then cultured in a complete medium in the presence or absence of NADH at a concentration of 400 ug/ml, respectively. Non-irradiated culture served as control.

MTT cell viability assay

The cells were seeded into 96-well dishes (5×10^3 cells/well), incubated for 24 h to allow attachment, treated with X-ray at 5.0 Gy, and continued to culture for 12, 24, 36, 48 h in the presence or absence of NADH. Absorbance was read at 570 nm by using DG3022 ELISA according to the routine MTT methods. The cellular viability was calculated as the amount of MTT uptake[5].

Assessment of apoptotic cells

The L02 cells were seeded at 5×10^4-5×10^5/ml in 6 well tissue cultured plates and cultured for 48 hours in RPMI-1640 medium containing 10 % FBS. Apoptosis was induced by X-ray irradiation, the LO2 cells were continued to culture for 24 h. A total of 5×10^5-5×10^6/ml cells were collected by centrifugation at 200 g (×5 min) and washed twice with ice-cold PBS (pH 7.4). Percent age of apoptosis was detected by flow cytometry according to PI/Annexin V kits.

Scanning electron microscope

24 hours following exposure to 2.5 Gy X-ray radiation, the L02 cells were fixed for 1 hour at room temperature using 4 % glutaraldehyde in PBS and proceeded for scanning electron microscopy as routine methods.

Protein expression of bcl-2, bax, fas, FasL and p53

The L02 cells were collected and then washed twice with ice-cold PBS, followed by fixation in 0.5 % paraformaldehyde at 4 ℃ for 30 min. The fixated cells were treated with PBS containing 0.1 % Triton-100 and washed twice. The treated cells of every tube were divided into five tubes and washed. The supernatant was aspirated. The antibodies against bcl-2, bax, p53, fas, FasL were added into each tube, mixed and incubated for 1 h at 37 ℃. The cells were washed twice and the FITC-labeled second antibodies were added for 30 min at 37 ℃. Then, the cells were washed twice with ice-cold PBS and resuspended with 500 μl PBS. 10 000 events were analyzed and the positive rate of protein expression was detected by FCM.

Determination of intracellular ROS concentration

The cell suspension was dispensed into special culture plates at a density of 2×10^4 cells per ml and incubated at 37 ℃, 5 % CO_2 for 48 h. The supernatant was removed and replaced with Hank' s solution , then exposed to 2.5 Gy X-ray radiation. The supernatant was discarded at once, and replaced with RPMI-1640 medium with or without NADH at a concentration of 400 ug/ml for 4 h, respectively. Non-irradiated culture served as control, followed by washing three times with Hank' s solution. Measurement of intracellular ROS concentration was described in literature. Briefly, the cells were loaded with 0.5 ml H_2DCF in DMSO solution at 5 μg/ml and incubated at 37 ℃ for 30 min. After washed three times with PBS, 0.5 ml PBS was loaded and the change of intracellular ROS was detected by scanning fluorescence intensity under confocal microscope.

RESULTS

X-ray treatment inhibited growth of L02 cells

The L02 cells were treated with different doses of X-ray irradiation. Cell survival was determined after 12, 24, 36, 46 h. Inhibition of growth in X-ray treated cells occurred in a dose-dependent manner (Figure 1). Survival of L02 cells decreased as the dose of X-ray increased. It was most obvious at 24 h post-irradiation.

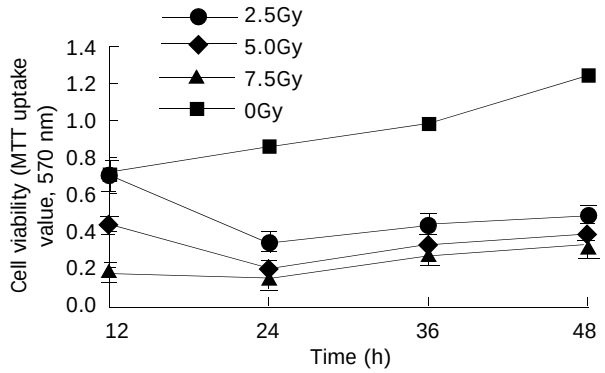

Figure 1 X-ray induced inhibition of growth of L02 cells.

NADH antagonized apoptosis of X-ray treated L02 cells

The L02 cells were treated with 2.5, 5.0, 7.5 Gy X-ray irradiation, then post-incubated in fresh complete RPMI 1640 medium containing NADH or NADH free drug for 24 h. Percent age of apoptosis was determined by FCM using PI/ Annexin V stain method. The results showed that NADH diminished apoptosis of L02 cells exposed to X rays. The percent age of apoptosis was (7.08±2.34) %, (28.16±2.46) %, (47.30±3.43) % in the absence of NADH. However, it was (6.04±0.86) %, (8. 25±1.64) %, (15.30±1.98) % in the presence of NADH. The difference was significant between L02 cells treated with 5.0 Gy,7.5 Gy X rays and cultured for 24 h in the presence of NADH and L02 cells cultured in the absence of NADH ($P<0.05$). These findings suggested that NADH was involved in cytoprotection by blocking the induction of apoptosis.

NADH rescued L02 cells damage from X-ray radiation

X-ray radiation could induce L02 cells damage. As shown in Figure 2, Part(b) and part(c) represented different morphologic changes of 2.5 Gy X-ray radiated L02 cells in the absence or presence of NADH. Part(a) represented the shamly irradiated L02 cells, which had normal liver cell surface structure with normal protuberance and volume. But, Part(b) had decreased protuberance and atrophy. However, degree of damage in L02 cells of part(c) group was becoming less than that of part(b). These suggested that NADH could rescue L02 cells damage from X-ray irradiation.

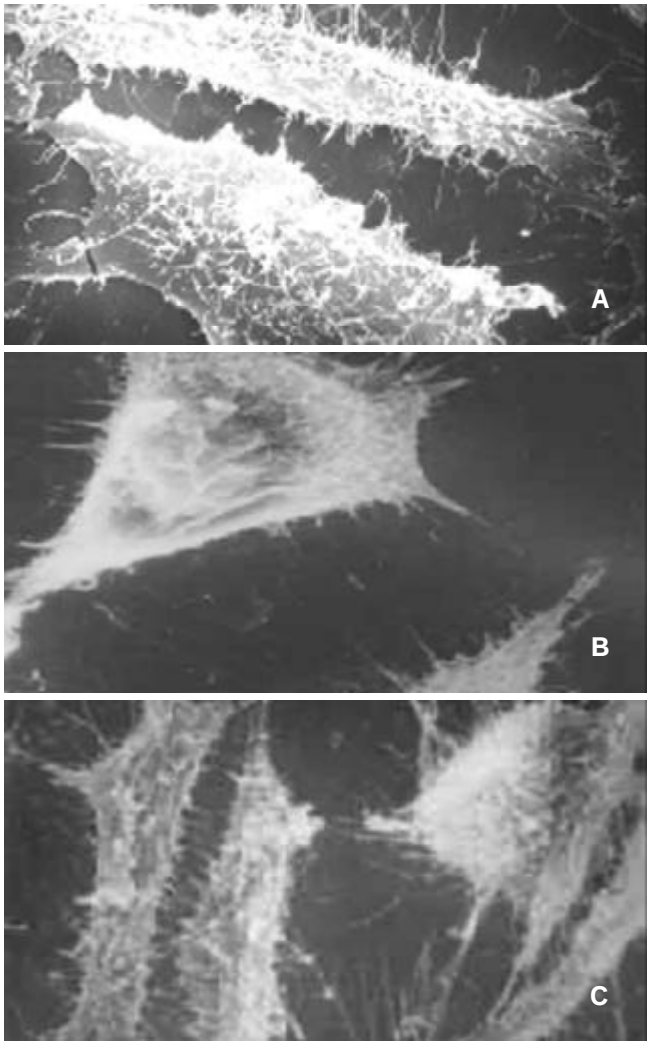

Figure 2 The result of scan electron microscopy. (a) Normal liver cell surface structure. (b) Irradiated hepatocytes with atrophy and decreased protuberance. (c) Morphological changes of hepatocytes irradiated and incubated in the presence of NADH.

Expression of p53, bax, bcl-2, Fas and Fas-L in L02 cells

The results of FCM analysis for p53, bax, bcl-2, Fas and FasL protein expression in X-ray irradiated and mockly irradiated

L02 cells are summarized in Table 1. Significantly high levels of p53, bax, Fas and Fas-L protein expression were detected in cells irradiated and cultured in the absence of NADH than in those cells cultured in the presence of NADH and mockly irradiated, but expression of bcl-2 protein tended to be low in L02 cells. Our results showed that NADH up-regulated expression of bcl-2 protein and down-regulated expression of p53, bax, bcl-2, Fas and FasL protein in L02 cells undergoing X ray irradiation. It might be one of the mechanisms that NADH rescues L02 cells injury from ionizing irradiation.

Table 1 Effect of NADH on regulation of apoptosis associated proteins in L02 cells treated with X-ray (n=3, $\bar{x}\pm s$)

Group	p53	Fas	FasL	bcl-2	bax
Mock IR	22.40±0.91	7.01±0.21	66.66±1.60	5.27±0.12	74.71±1.81
IR	37.4±1.11[a]	13.40±0.78[a]	74.40±1.09[a]	2.22±0.18[a]	86.76±2.14[a]
IR+NADH	26.93±6.73	11.29±1.40	68.93±1.88	3.62±1.34	71.60±2.92

Based on *t* test, "Mock IR" represented L02 cells of non-irradiated group. "IR+NADH" represented L02 cells irradiated and continued to culture in the presence of NADH. [a]P<0.05 *vs* Mock IR group and IR+NADH group.

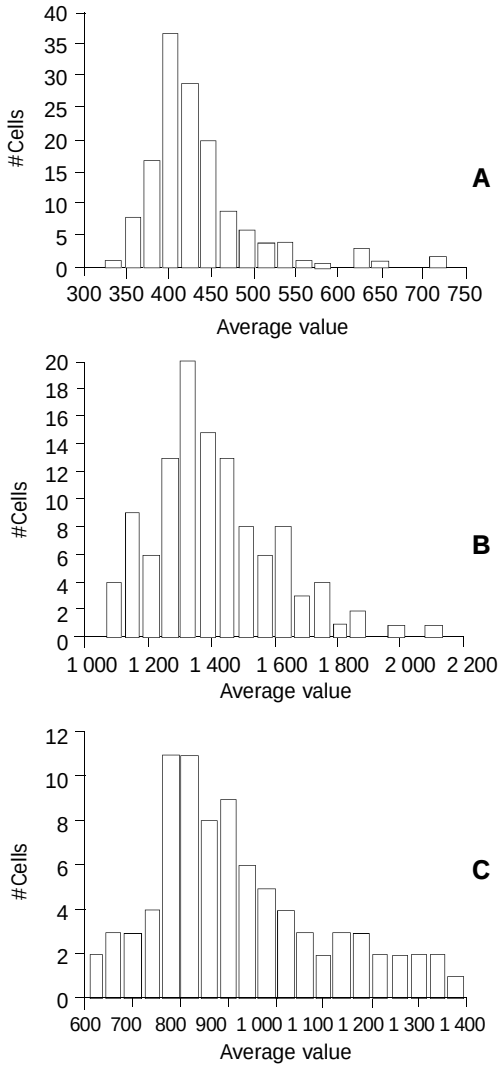

Figure 3A The change of intracellular H_2O_2 production in L02 cells cultured with or without NADH for 4 h after X-ray irradiation. (a) Sham irradiation group. (b and c) X-ray treated (2.5 Gy) L02 cells were respectively cultured in the absence or presence of NADH. Mean value of fluorescence was calculated according to the number of L02 cells. [a]P<0.05 compared with sham irradiation (a) and test group (c).

Determination of intracellular ROS

Figure 3A and Figure 3B show that 2.5 Gy X-ray irradiation increased the level of intracellular ROS after 4 h irradiation in L02 cells compared with that in L02 cells of sham irradiation group. However, NADH could reverse the effect of X-ray irradiation.

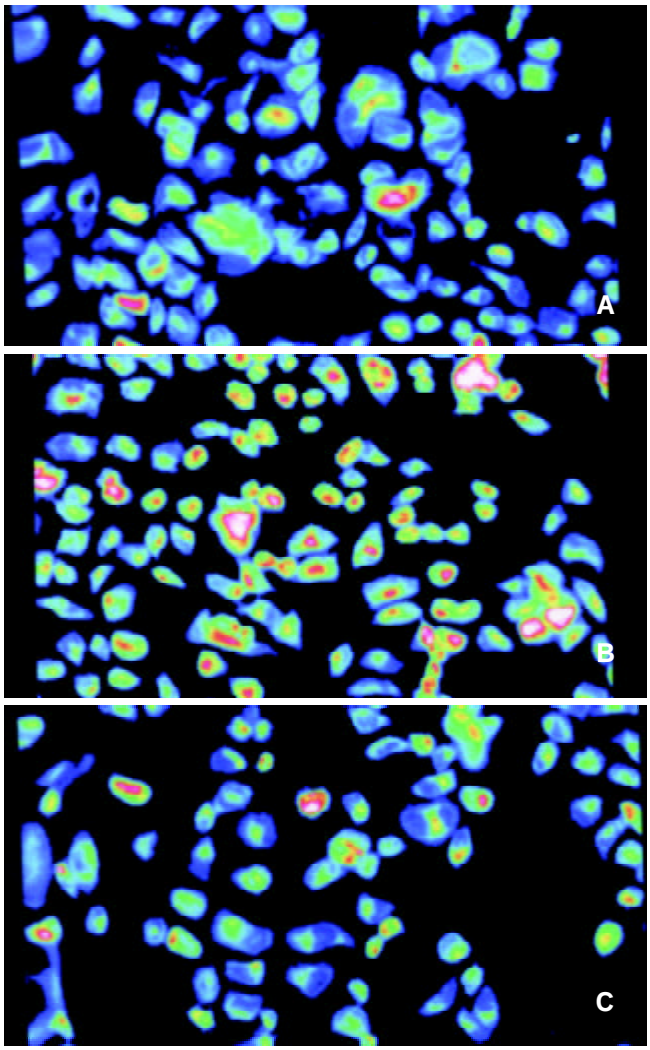

Figure 3B The graph showed the cell fluorescence change of intracellular ROS by confocal microscope scanning in L02 cells of different treatment.

DISCUSSION

When a cell exposed to ionizing irradiation, at least two signal-generating targets are activated, one at the membrane and the other at the DNA. Signal may also originate in cytoplasm[6,7]. These signal targets ultimately result in cell death or non-death stress response. Apoptosis, also called programmed cell death (PCD),is a peculiar form of cell death characterized by several morphological and biochemical aspects which are different from necrosis, an other form of death. X-ray irradiation is one of the ionizing radiations, which can cause both membrane and DNA damage to cells and result in cell apoptosis. How ionizing radiation triggers apoptosis is not known. It was reported that apoptosis mediated by DNA damage occurred via p53-dependent and p53-independent pathways[1,2]. However, several pathways of apoptosis have been reported. One of these is the Fas/FasL pathway, which involves binding of a death receptor to a death domain, initiating a cascade of proteases that leads to cell apoptosis[8]. In the present study, we tested whether apoptosis induced by X-ray irradiation

occurred via DNA damage or Fas/FasL pathway. Our results demonstrated that X-ray irradiation led to cell apoptosis by increasing positive rate of L02 cells expressing p53 and bax proteins, and decreasing positive rate of bcl-2 protein. At the same time, Fas and FasL expression in L02 cells exposed to irradiation was up-regulated as compared with that in mockly irradiated-cells.

Cellular sensitivity to radiation reflects a culmination of distinct molecular pathway including DNA repair, cell cycle checkpoint fidelity, and particularly apoptosis. Several oncogenes and tumor suppressor genes play a pivotal role in modulating the response of cells to radiation. An important molecule, p53, initiates responses to DNA damage, and affects the sensitivity of cells to apoptosis. Functional inactivation of p53 is associated with resistance to radiotherapy. Overexpression of wtp53 gene was found to be associated with increased cellular sensitivity to apoptosis induced by ionizing irradiation[9,10]. Bcl-2, an important regulator of apoptosis, was found to be associated with anti-apoptosis response. Over expression of bcl-2 by transferring bcl-2 gene into deficient cells has been associated with increased cellular resistance to induction of apoptosis by a variety of DNA-damaging agents including ionizing irradiation, drugs. However, bax, another member of bcl-2 family, as an inhibitor of apoptosis, can bind bcl-2 to form homo- and heterodimers. Rate of bcl-2 to bax may determine the extent to which apoptosis is induced or suppressed[11,12]. At the same time, high expression of wild - type p53 protein induced by ionizing irradiation appears to regulate expression of bcl-2, bax, p21 and p16 genes[13]. Our results showed that X-ray radiation induced DNA damage resulted in an increase of positivity of p53 and bax protein expression, and decrease of bcl-2 protein expression in L02 cells. But it is necessary to further confirm whether p53 may regulate expression of bcl-2 and bax genes.

Recently, it has been suggested that Fas/FasL system plays a key role in the regulation of apoptosis. Fas is located on the plasma membrane of hepatocytes abundantly, and FasL, a glycoprotein of 40 kd is located on the plasma membrane of the lymphocytes. The interaction of the Fas ligand and Fas receptor initiates a chemical process in the cells that leads to apoptosis. Fas, named CD95, expresses in alcoholic liver disease, viral hepatitis, hepatocarcinomas, and hepatocirrhosis[14-16]. Fas-FasL interaction may contribute to hepatocyte apoptosis in these patients. It was rarely reported that apoptosis induced by ionizing irradiation occurred via Fas-FasL interaction pathway, particularly apoptosis induced by Fas-FasL interaction itself in hepatocytes. It was recently reported that the Fas/Fas ligand system was involved in modulating keratocyte apoptosis induced by UV irradiation[17]. Newton reported that apoptosis induced by ionizing radiation required p53 and was regulated by the Bcl-2 protein family but did not require signals transduced by Fas and FADD/MORT1[18]. Our experiment indicated that X-ray irradiation enhanced the positive rate of L02 cells expressing Fas and FasL protein as compared with shamly irradiated cells. It is suggested that FasL-Fas interaction play an important role in liver cell apoptosis induced by X-ray irradiation. It is different from the model in which ionizing irradiation triggers apoptosis via p53-dependent activation of caspase-9.

Several biochemical alterations, including excessive generation of reactive oxygen species (ROS), calcium flux, Caspase activation, have been shown to be essential in cell apoptosis[19-21]. ROS plays a pivotal role in ionizing irradiation -induced cell apoptosis[22-24]. ROS, as a signal molecule, could regulate gene expression and mitochondria membrane potential[25,26]. Free radicals are an integral part of metabolism and formed continuously in the body. Many sources of stress heat, irradiation, hyperoxia, inflammation and any increases in metabolism including exercise, injury, and even repair processes lead to increased production of free radicals and associated reactive oxygen or nitrogen species (ROS/RNS)[27-29]. Evidences have shown that free radicals have important functions in the signal network of cells, including induction of growth and apoptosis and as killing tools of immunocompetent cells[30,31]. Massive intervention into the redox state by pharmaceutical doses of exogenous antioxidants should be considered with caution due to the ambiguous role of free radicals in regulation of growth, apoptosis, and cytotoxicity of immunocompetent cells. Our results showed that X-ray irradiation could give rise to increases of ROS generation after 4 h irradiation, but NADH could reverse the effect of X-ray irradiation, lower the level of intracellular ROS. These results indicated that NADH rescued L02 cells damage from X-ray irradiation by regulation of ROS generation.

NADH, a kind of important coenzyme, takes part in triggering biological anti-oxidation and regulating the expression of membrane glycoprotein receptors[32]. But it was seldom reported that NADH played a role in antagonizing ionizing irradiation induced apoptosis and regulating expression of membrane receptors. Recently, it was reported that the content of intracellular NADH changed after UV or ionizing irradiation[33,34]. Most of the results indicated that the content of intracellular NADH declined after ionizing irradiation or PDT treatment by confocal microscope scanning analysis. Pogue reported that the endogenous fluorescence signal attributable to reduced nicotinamide adenine dinucleotide (NADH) was measured in response to photodynamic therapy (PDT)-induced damage. Measurements on cells *in vitro* have showed that NADH fluorescence decreased relatively to that of controls after treatment with a toxic dose of PDT, as measured within 30 min after treatment. Similarly, assays of cell viability indicated that mitochondria function was reduced immediately after treatment in proportion to the dose delivered[35]. It was seldom reported that signal transduction molecules changed after ionizing irradiation by extraneously added NADH. Recent studies of repairing ionizing irradiation injury focused on antioxidant drugs. Bush reported that NAC could protect immune function and regulate expression of oncogenes in bone marrow cells exposed to ionizing irradiation[36]. Zhou found that bilobalide might block PC12 cells from reactive oxygen species-induced apoptosis in the early stage and then attenuate the elevation of c-Myc, p53, and Bax and activation of Caspase-3[37]. Our results indicated that expression of p53, bax, Fas and FasL proteins was up-regulated and expression of bcl-2 protein was down-regulated in L02 cells undergoing X-ray irradiation. However, when L02 cells undergoing X-ray irradiation continued to culture in the presence of NADH, expression of p53, bax, Fas and FasL proteins were down-regulated and expression of bcl-2 protein was up-regulated. At the same time, level of intracellular ROS declined, survival of cell increased. Our observations provide evidence that NADH is a new kind of radiation protector.

REFERENCES

1 **Caelles C**, Helmberg A, Karin M. p53-dependent apoptosis in the absence of transcriptional activation of p53-target genes. *Nature* 1994; **370**: 220-223

2 **Strasser A**, Harris AW, Jacks T, Cory S. DNA damage can induce apoptosis in proliferating lymphoid cells via p53-independent mechanisms inhibitable by Bcl-2. *Cell* 1994; **79**: 329-339

3 **Zamzami N**, Marchetti P, Castedo M, Zanin C, Vayssiere JL, Petit PX, Kroemer G. Reduction in mitochondrial potential constitutes an early irreversible step of programmed lymphocyte death *in vivo*. *J Exp Med* 1995; **181**: 1661-1672

4 **Zamzami N**, Marchetti P, Castedo M, Decaudin D, Macho A, Hirsch T, Susin SA, Petit PX, Mignotte B, Kroemer G. Sequence

reduction of mitochondrial transmembrane potential and generation of reactive oxygen species in early programmed cell death. *J Exp Med* 1995; **182**: 367-377

5 **Weller M**, Schmidt C, Roth W, Dichgans J. Chemotherapy of human malignant glioma: prevention of efficacy by dexamethasone? *Neurology* 1997; **48**: 1704-1709

6 **Godar DE,** Thomas DP, Miller SA, Lee W. Long-wavelength UVA radiation induces oxidative stress, cytoskeletal damage and hemolysis. *Photochem Photobiol* 1993; **57**: 1018-1026

7 **Liu ZG**, Baskaran R, Lea-Chou ET, Wood LD, Chen Y, Karin M, Wang JY. Three distinct signalling responses by murine fibroblasts to genotoxic stress. *Nature* 1996; **384**: 273-276

8 **Friesen C**, Herr I, Krammer PH, Debatin KM. Involvement of the CD95(APO-1/FAS) receptor/ligand system in drug-induced apoptosis in leukemia cells. *Nat Med* 1996; **2**: 574-577

9 **Burger H,** Nooter K, Boersma AW, Kortland CJ, Van den Berg AP, Stoter G. Expression of p53, p21/WAF/CIP, Bcl-2, Bax, Bcl-x, and Bak in radiation-induced apoptosis in testicular germ cell tumor lines. *Int J Radiat Oncol Biol Phys* 1998; **41**: 415-424

10 **Bandoh N**, Hayashi T, Kishibe K, Takahara M, Imada M, Nonaka S, Harabuchi Y. Prognostic value of p53 mutations, bax, and spontaneous apoptosis in maxillary sinus squamous cell carcinoma. *Cancer* 2002; **94**: 1968-1980

11 **Findley HW**, Gu L, Yeager AM, Zhou M. Expression and regulation of Bcl-2, Bcl-xl, and Bax correlate with p53 status and sensitivity to apoptosis in childhood acute lymphoblastic leukemia. *Blood* 1997; **89**: 2986-2993

12 **Latonen L**, Taya Y, Laiho M. UV-radiation induces dose-dependent regulation of p53 response and modulates p53-HDM2 interaction in human fibroblasts. *Oncogene* 2001; **20**: 6784-6793

13 **Miyashita T**, Krajewski S, Krajewska M, Wang HG, Lin HK, Liebermann DA, Hoffman B, Reed JC. Tumor suppressor p53 is a regulator of bcl-2 and bax gene expression *in vitro* and *in vivo*. *Oncogene* 1994; **9**: 1799-1805

14 **Hayashi N**, Mita E. Involvement of Fas system-mediated apoptosis in pathogenesis of viral hepatitis. *J Viral Hepat* 1999; **6**: 357-365

15 **Abdulkarim B**, Sabri S, Deutsch E, Vaganay S, Marangoni E, Vainchenker W, Bongrand P, Busson P, Bourhis J. Radiation-induced expression of functional Fas ligand in EBV-positive human nasopharyngeal carcinoma cells. *Int J Cancer* 2000; **86**: 229-237

16 **Li ZY**, Zou SQ. Fas counterattack in cholangiocarcinoma: a mechanism for immune evasion in human hilar cholangiocarcinomas. *World J Gastroenterol* 2001; **7**: 860-863

17 **Podskochy A**, Fagerholm P. The expression of Fas ligand protein in ultraviolet-exposed rabbit corneas. *Cornea* 2002; **21**: 91-94

18 **Newton K**, Strasser A. Ionizing radiation and chemotherapeutic drugs induce apoptosis in lymphocytes in the absence of Fas or FADD/MORT1 signaling. Implications for cancer therapy. *J Exp Med* 2000; **191**: 195-200

19 **Chan WH**, Yu JS. Inhibition of UV irradiation-induced oxidative stress and apoptotic biochemical changes in human epidermal carcinoma A431 cells by genistein. *J Cell Biochem* 2000; **78**: 73-84

20 **Pu Y**, Chang DC. Cytosolic Ca^{2+} signal is involved in regulating UV-induced apoptosis in hela cells. *Biochem Biophys Res Commun* 2001; **282**: 84-89

21 **Zhao QL**, Kondo T, Noda A, Fujiwara Y. Mitochondrial and intracellular free-calcium regulation of radiation-induced apoptosis in human leukemic cells. *Int J Radiat Biol* 1999; **75**: 493-504

22 **Li HL**, Chen DD, Li XH, Zhang HW, Lu YQ, Ye CL, Ren XD. Changes of NF-kB, p53, Bcl-2 and caspase in apoptosis induced by JTE-522 in human gastric adenocarcinoma cell line AGS cells: role of reactive oxygen species. *World J Gastroenterol* 2002; **8**: 431-435

23 **Lam M**, Oleinick NL, Nieminen AL. Photodynamic therapy-induced apoptosis in epidermoid carcinoma cells. Reactive oxygen species and mitochondrial inner membrane permeabilization. *J Biol Chem* 2001; **276**: 47379-47386

24 **Lin CP**, Lynch MC, Kochevar IE. Reactive oxidizing species produced near the plasma membrane induce apoptosis in bovine aorta endothelial cells. *Exp Cell Res* 2000; **259**: 351-359

25 **Ferlini C**, De Angelis C, Biselli R, Distefano M, Scambia G, Fattorossi A. Sequence of metabolic changes during X-ray-induced apoptosis. *Exp Cell Res* 1999; **247**: 160-167

26 **Kang CD**, Jang JH, Kim KW, Lee HJ, Jeong CS, Kim CM, Kim SH, Chung BS. Activation of c-jun N-terminal kinase/stress-activated protein kinase and the decreased ratio of Bcl-2 to Bax are associated with the auto-oxidized dopamine-induced apoptosis in PC12 cells. *Neurosci Lett* 1998; **256**: 37-40

27 **Chen YC**, Tsai SH, Lin-Shiau SY, Lin JK. Elevation of apoptotic potential by anoxia hyperoxia shift in NIH3T3 cells. *Mol Cell Biochem* 1999; **197**: 147-159

28 **Fehrenbach E**, Northoff H. Free radicals, exercise, apoptosis, and heat shock proteins. *Exerc Immunol Rev* 2001; **7**: 66-89

29 **Gorman AM**, Heavey B, Creagh E, Cotter TG, Samali A. Anti-oxidant-mediated inhibition of the heat shock response leads to apoptosis. *FEBS Lett* 1999; **445**: 98-102

30 **Elbim C**, Pillet S, Prevost MH, Preira A, Girard PM, Rogine N, Matusani H, Hakim J, Israel N, Gougerot-Pocidalo MA. Redox and activation status of monocytes from human immunodeficiency virus-infected patients: relationship with viral load. *J Virol* 1999; **73**: 4561-4566

31 **Goldshmit Y**, Erlich S, Pinkas-Kramarski R. Neuregulin rescues PC12-ErbB4 cells from cell death induced by H(2)O(2). Regulation of reactive oxygen species levels by phosphatidylinositol 3-kinase. *J Biol Chem* 2001; **276**: 46379-46385

32 **Birkmayer GJ**, Birkmayer W. Stimulation of endogenous L-dopa biosynthesis-a new principle for the therapy of Parkinson's disease: the clinical effect of nicotinamide adenine dinucleotide (NADH) and nicotinamide adenine dinucleotidephosphate (NADPH). *Acata Neurol Scand Suppl* 1989; **126**: 183-187

33 **Obi-Tabot ET**, Hanrahan LM, Cachecho R, Beer ER, Hopkins SR, Chan JC, Shapiro JM, LaMorte WW. Change in hepatocyte NADH fluorescence during prolonged hypoxia. *J Surg Res* 1993; **55**: 575-580

34 **Cristovao L**, Lechner MC, Fidalgo P, Leitao CN, Mira FC, Rueff J. Absence of stimulation of poly(ADP-ribose) polymerase activity in patients predisposed to colon cancer. *Br J Cancer* 1998; **77**: 1628-1632

35 **Pogue BW**, Pitts JD, Mycek MA, Sloboda RD, Wilmot CM, Brandsema JF, O'Hara JA. *In vivo* NADH fluorescence monitoring as an assay for cellular damage in photodynamic therapy. *Photochem Photobiol* 2001; **74**: 817-824

36 **Bush JA**, Ho VC, Mitchell DL, Tron VA, Li G. Effect of N-acetylcysteine on UVB-induced apoptosis and DNA repair in human and mouse keratinocytes. *Photochem Photobiol* 1999; **70**: 329-333

37 **Zhou LJ**, Zhu XZ. Reactive oxygen species-induced apoptosis in PC12 cells and protective effect of bilobalide. *J Pharmacol Exp Ther* 2000; **293**: 982-988

Edited by Wen CY and Wang XL

P.O.Box 2345, Beijing 100023,China
Fax: +86-10-85381893
E-mail: wjg@wjgnet.com www.wjgnet.com

World J Gastroenterol 2003;9(8):1786-1790
World Journal of Gastroenterology
 ISSN 1007-9327

• BASIC RESEARCH •

Effect of gastrin on differentiation of rat intestinal epithelial cells *in vitro*

Zhou Wang, Wei-Wen Chen, Ru-Liu Li, Bin Wen, Jing-Bo Sun

Zhou Wang, Wei-Wen Chen, Ru-Liu Li, Bin Wen, Piwei Institute, Guangzhou University of TCM, Guangzhou, 510405, Guangdong Province, China
Jing-Bo Sun, The Second Affiliated Hospital of Guangzhou University of TCM, Guangzhou, 510120, Guangdong Province, China
Supported by the Major State Basic Research Development Program of China (973 Program) No.G19990544 and the National Natural Science Foundation of China, No.39970906
Correspondence to: Dr. Wei-Wen Chen, Piwei Institute, Guangzhou University of TCM, Guangzhou, 510405, Guangdong Province, China. chenww@gzhtcm.edu.cn
Telephone: +86-20-36585080 **Fax:** +86-20-36586563
Received: 2003-03-04 **Accepted:** 2003-04-03

Abstract

AIM: To investigate the effect of gastrin on differentiation of IEC-6 cell line *in vitro*.

METHODS: IEC-6 cells were incubated with gastrin. On day 7 after treatment, cell morphology was examined by light microscope, and on day 20, the cellular ultrastructures were examined by electron microscope. After exposure to gastrin for 6 hours, villin mRNA was analyzed by reverse transcription-polymerase chain reaction, and on day 7, the expression of villin was examined by immunocytochemical analysis with laser confocal microscope.

RESULTS: After exposure to gastrin, IEC-6 cells showed differentiated phenotypes as villas enterocytes and contained an abundance of plasma, small nuclei with nucleoli, and were arranged regularly. There were numerous microvilli around edge of the cells, and several cells showed columnar structures. Villin mRNA expression in cytoplasm was increased in comparison with control.

CONCLUSION: Differentiated characteristics of villus enterocytes and phenotypic changes of rat intestinal epithelial cells (IEC-6) are induced by gastrin, and the effects of gastrin are correlated to increased villin expression.

Wang Z, Chen WW, Li RL, Wen B, Sun JB. Effect of gastrin on differentiation of rat intestinal epithelial cells *in vitro*. *World J Gastroenterol* 2003; 9(8): 1786-1790
http://www.wjgnet.com/1007-9327/9/1786.asp

INTRODUCTION

Gastrin stimulates cell proliferation in gastric mucosa under physiological conditions[1]. Studies have demonstrated that gastrin many increase ornithine decarboxylase activity of IEC-6 cells, cause intracellular polyamine synthesis, and therefore promote cell proliferation[2,3] and migration[4]. Polyamine has been demonstrated to be closely correlated to cytoskeleton reconstitution, an important process of cellular differentiation[5-9], but it is not clear yet whether gastrin plays roles in differentiation of IEC-6 cells. This study was to investigate gastrin-induced morphological changes of intestinal epithelial cell (IEC-6) and the intracellular expression of villin.

MATERIALS AND METHODS

Cell culture

IEC-6 cells (ATCC, Rockville, MD) were grown at 37 ℃ in a 900 mL· L^{-1} air-100 mL· L^{-1} CO_2 atmosphere in Dulbecco' s modified Eagle' s medium (pH7.2) containing 50 g· L^{-1} dFBS, 10 mg· L^{-1} insulin, 50 mg· L^{-1} gentamycin sulfate, and subcultured once a week. When cultured cells became confluence, they were dissociated with 0.5 g· L^{-1} trypsin and 0.2 g· L^{-1} EDTA, and seeded into 6-well cell culture plates. Pentagastrin (Sigma. Louis, MO) was dissolved in two or three drops of 300 g· L^{-1} ammonium hydroxide (sterile), the solution was adjusted to pH 7.5, and then diluted with medium to 62.5 mg· L^{-1} before use.

Morphology

Light microscopy Monolayer of IEC-6 cells was prepared on glass coverslips, which were placed in 6-well cell culture plates (Corning Glass Works). The cells were seeded at a concentration of 1.0×10^5 per well, and incubated at 37 ℃ in a 900 mL· L^{-1} air-100 mL· L^{-1} CO_2 atmosphere for 24 h. The media containing cDMEM 2 000 μL, PBS 490 μL and 10 μL pentagastrin solution were replaced to make a final concentration of pentagastrin 250 μg· L^{-1} in culture. The medium in control group was the same as that in the treatment group except gastrin. Cells were harvested on day 7 from the initial treatment. The coverslips were removed and fixed for 15 min at room temperature in 3.5 % paraformaldehyde in PBS, washed with distilled water, followed by HE staining and examined under light microscope.

Electron microscopy The cells were seeded in 6-well cell culture plates with a concentration of 1.0×10^5 per well under the same culture condition as above. Cultured cells were harvested on day 20 from the initial treatment of gastrin, washed with PBS, fixed in 2 % glutaraldehyde, postfixed in 1 % osmium tetroxide, dehydrated, and embedded in Epon, and examined under electron microscope.

Villin expression

mRNA level analysis After incubated with gastrin for 6 hours, cultured cells were harvested for extraction of total RNA with RNA TRIzol reagent (Gibco, Gaithersburg, MD). Isolation was performed according to the manufacturer' s protocols. The concentration of extracted RNA was determined. RT-PCR kit (Gibco, Gaithersburg, MD) was used for RT-PCR reaction following the attached protocol of the product. The primers (Seagon, Shanghai, China) were synthesized according to sequences of rat villin gene (GenBank™ accession number M98454) as follows: coding strand primer: 5' -ATG CCC AAG TCA AAG GCT CTC TCA ACA TCA C-3' , noncoding strand primer: 5' -TGC AAC AGT CGC TGG ACA TCA CAG G-3' [10]. The reference primers (Seagon, Shanghai, China) were according to sequences of rat β-actin gene (GenBank™ accession number AB028846) as follows: coding strand primer: 5' -TTC CAG CCT TCC TTC CTG G-3' , noncoding strand primer: 5' -TTG CGC TCA GGA GGA GCA AT-3' . 2 μL of

RT products was added to the PCR master mix. After incubation at 94 ℃ for 2 min, reaction was done for 35 cycles at 94 ℃ for 60 s, at 55 ℃ for 60 s, and at 72 ℃ for 30 s. The expected cDNA amplification products were 408 bp for villin and 238 bp for β-actin. After electrophoresis on agarose gel and staining with ethidium bromide, DNA bands were visualized with an ultraviolet transilluminator.

Protein level analysis On day 7 from the initial treatment, cultured cells were fixed for 15 min at room temperature in 3.5 % paraformaldehyde in PBS, and washed three times. For study of villin expression, the cells were permeabilized by incubation with 0.2 % Triton X-100 in PBS for 4 min, washed three times with PBS, and then treated with goat serum for 10 min. The permeabilized cells were incubated with goat anti-rat antibody with dilution of 1:100 in PBS (Santa Cruz) for 2 hours at room temperature, washed, and then incubated with FITC-conjugated rabbit anti-goat IgG with dilution of 1:50 in PBS (Sigma. Louis, MO). The treated cells were visualized under TCS SP confocal laser scanning microscope (Leica, Heidelberg, Germany).

RESULTS

Effect of gastrin on morphology of IEC-6 cells

Light microscopy Seven-days after treatment with gastrin, cells were arranged regularly with an abundance of plasma, and small nuclei with nucleoli. Typically differentiated cells showed a tendency to form microvilli on the edge, and remarkable cytoskeleton-like structure, which was similar to cytoskeleton distribution in well-differentiated enterocytes. Cells in control group contained sparse plasma, large nuclei without nucleoli, and were arranged irregularly (Figure1).

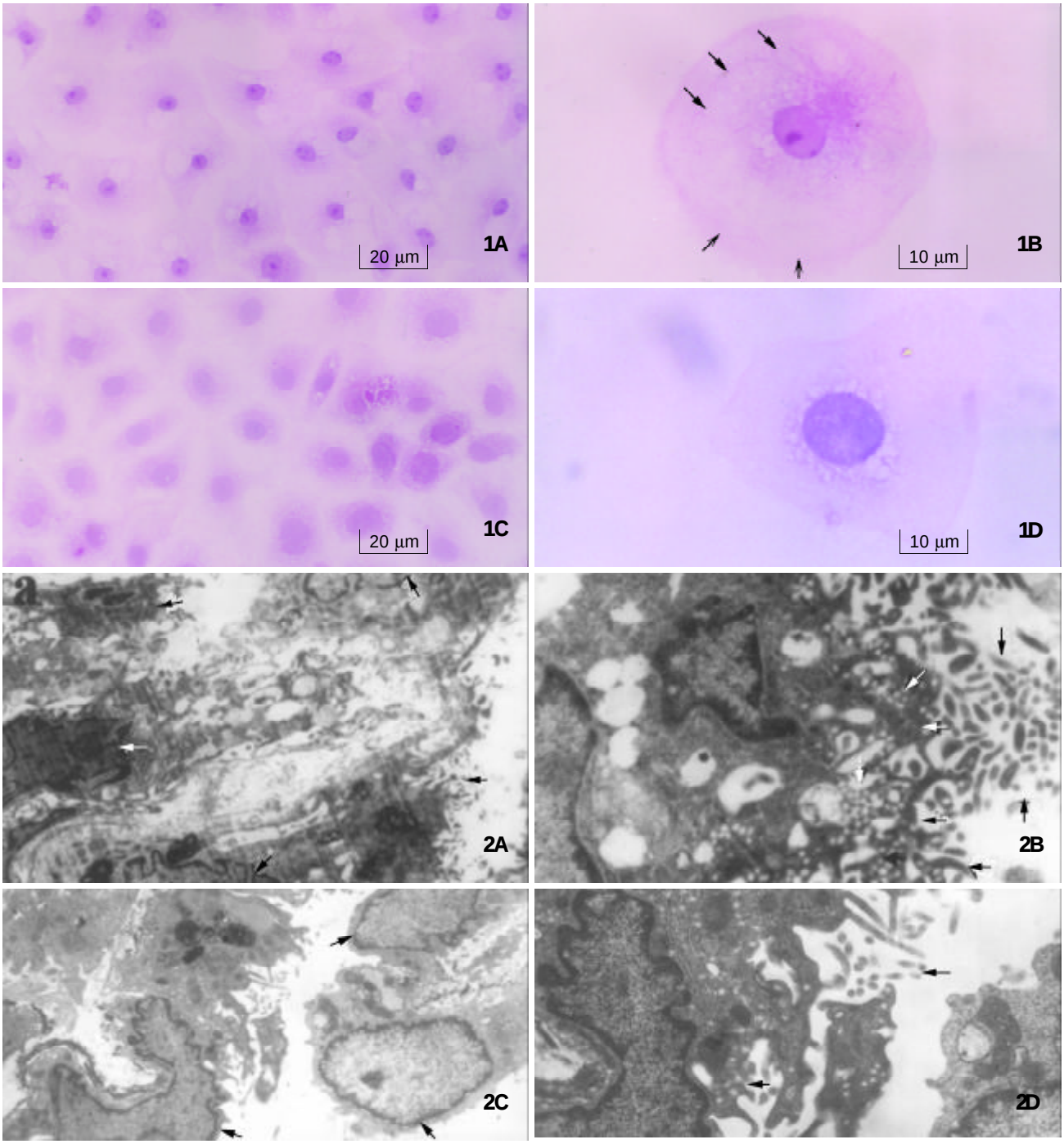

Figure 1 Morphology of IEC-6 cells. a: Gastrin-treated cells(250×) contained an abundance of plasma, small nuclei with nucleoli, and were arranged regularly. b: One of gastrin-treated cells (400×) showed the tendency to form microvilli on the edge(open

arrows), and cytoskeleton-like staining in plasma (solid arrows). c: Control cells (250×) contained sparse plasma, large nuclei without nucleoli, and were in irregular arrangement and immature shape. d: One of control cells (400×) showed no tendency to form microvilli on the edge, and nucleus was relatively larger and had no nucleolus.

Figure 2 Ultrastructural changes of IEC-6 cells. a: Gastrin-treated cells (5 000×, bar=1 μm) showed columnar structures(the nuclei were shown by open arrows) with numerous microvilli on the edge (solid arrows). b: Gastrin-treated cells (12 000×, bar=500 nm)developed numerous microvilli (open arrows) and lots of endocytic vesicles appeared under the apical membrane (solid arrows). c: Control cells (5 000×, bar=1 μm) were thin and flat. Relatively large nuclei (open arrows) and scanty plasma were observed. d: Only sparse microvilli (open arrow) and endocytic vesicles (solid arrow) were seen in control cells (12 000×, bar=500 nm).

Electron microscopy Twenty days after 20-day treatment with gastrin, numerous microvilli appeared on the edge of IEC-6 cells, many endocytic vesicles occurred under the apical membrane, and columnar structures were seen in some cells. Control cells were thin and flat, the nuclei were relatively large with scanty of cytoplasm. Only sparse microvilli were observed on the edge of control cells, and few endocytic vesicles were noticed (Figure 2).

Effect of gastrin on villin expression in IEC-6 cells

mRNA level After exposure to gastrin for 6 hours, villin mRNA expression in gastrin-treated cells was stronger than that in control cells (Figure 3).

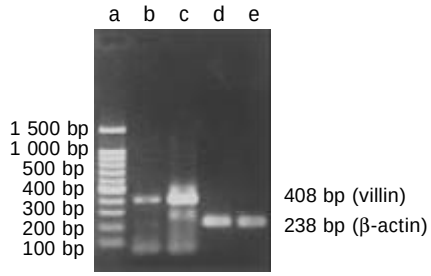

Figure 3 RT-PCR products from IEC-6 cells on agarose electrophoresis. a: Marker (brighter band: 500 bp), b: Control, c: Gastrin treated cells, d: β-actin(Control), e: β-actin (Gastrin).

Protein level On day 7 after treatment, plenty of cytoplasmic villins were observed obviously in gastrin-treated cells and few in control cells (Figure 4).

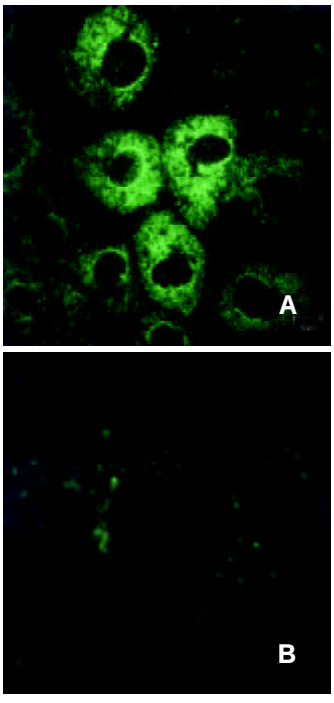

Figure 4 Villin expression in IEC-6 cells. a: Gastrin-treated cells (800×), b: Control cells (800×).

DISCUSSION

The barrier function of intestine is based on the physiological renewal or pathological repair of intestinal epithelia. The process includes proliferation, migration and terminal differentiation of the crypt cells. Development and differentiation of intestinal epithelia proceed in at least two distinct steps: the conversion of a nonepithelial cell to a protoepithelium, followed by a process of terminal differentiation. Terminal differentiation continues to occur in adult animals in the intestine[11], and is the last process. It not only indicates the completion of renewal or repair and the degree of differentiation, but also determines whether the new epithelia have physiological functions. There are two morphological characteristics in differentiated intestinal epithelia. One is the columnar shape cells with microvilli at the apical membrane, the other is organization of intestinal epithelial cells on a basement membrane into multicellular structures.

Intestinal epithelial cells (IEC-6) have features of undifferentiated small intestinal crypt cells[12], and are often used as a model of intestinal mucosal repair and cell differentiation[13,14]. The differentiation of intestinal crypt cell is a complex process, which is controlled by multiple factors. It has been known that several genes, such as p38 mitogen-activated protein kinases (p38MAPK)[15], Cdx gene family[16-20], pancreatic-duodenal homeobox (Pdxs) gene[21-23], sucrase-isomaltase (SI) gene[18,24,25], villin[26], activin[27], provoke cells towards the phenotype of differentiated villus enterocytes. Some cytokines such as epidermal growth factor (EGF)[6,7], insulin, insulin-like growth factor (IGF)-I and II[28,29], transforming growth factor (TGF)-β1[29], glucagon-like peptide-2 (GLP-2)[30] also have effects on the process. Astragalus injection could promote IEC-6 cell differentiation by inducing ODC activity and polyamine biosynthesis[31].

Moreover, the interaction between cells or between cells and extracellular matrix (ECM) also plays an important role in differentiation of IEC-6 cells[32]. Both humoral and matrix factors from intestinal mesenchyme are involved in intestinal epithelial differentiation and these factors appear to be organ specific[33,34]. And in conjunction with cell-cell contact and/or ECM, many regulatory cytokines such as enteroglucagon, interleukin-2 (IL-2), fibroblast growth factor (FGF), and EGF family members lead to specific differentiation signals[35]. Cdx2 gene provokes pleiotropic effects triggering cells towards the phenotype of differentiated villus enterocytes, but its expression is also modulated by basement membrane components[18].

Previous studies on differentiation of IEC-6 cells have found that laminin can lead the organization of IEC-6 cells on a basement membrane into multicellular structures[36], and the down-regulation of c-jun expression mediated by laminin might result in the event[37]. IEC-6 cell culture on Englebreth-Holm-Swarm (EHS) extracellular matrix proteins also displays morphological changes, correlated with loss of nuclear localization of c-myc protein and development of cell surface alkaline phosphatase (ALP) enzymatic activity[14]. And it has been documented that striking morphological and functional alterations can be induced by glucocorticoid in IEC-6 cells. These effects are consistent with the activation or modulation of multiple genes important in physiological functions of

absorptive villous cells[38]. Other data showed differentiation of IEC-6 cells was associated with upregulation of 11β-hydroxysteroid dehydrogenase (11β-HSD2) activity[39]. Members of the Cdx gene family play a fundamental role in both the establishment of the intestinal phenotype during development and maintenance of this phenotype via transcriptional activation of differentiated intestinal genes[40-43].

Our results showed that significantly morphological changes were observed in IEC-6 cells treated with gastrin in comparison with control group. The cells were in regular arrangement. Typically differentiated cell had an abundance of cytoplasm and a small nucleus containing nucleolus. There was a tendency to form microvilli and cytoskeleton-like structures were observed in the cytoplasm. Twenty-days after treatment of gastrin, a great number of microvilli appeared on the edges of the cells, and several cells displayed a simple columnar structure, and were fundamentally different from adenocarcinoma-like differentiation induced by Cdx1 transfection, which exhibited stratified columnar structure[16]. The absence of a multilayer structure indicated that these cells did not lose their contact inhibition characteristics, and they were not tumor cells. The existence of lots of endocytic vesicles as found under the apical membrane was also a typical feature of terminally differentiated enterocytes[11,44]. These results indicated that the cells might have the function of endocytosis as well as enterocytes. In control cells, only few microvilli were observed on the edge of cells with few endocytic vesicles.

Villin is one of the actin-binding proteins which have been reported to play a major role in the formation of the microvillus core bundle[45]. These proteins are known to modulate the dynamics of the actin cytoskeleton by mediating the state of actin polymerization and the spatial arrangement of actin protofilaments[46-49]. Villin may also respond to the apical calcium gradient, fragmenting actin microfilaments (MFs), and thus locally facilitate actin remodeling[50], and has a very important role in the alteration of cell morphology. The villin mRNA was expressed at high levels in the small intestine, to a lesser degree in the colon, and was not detected in the brain or liver[51]. The results indicate that villin is a kind of intestine-specific structure protein. In HT-29 cells, increase of villin mRNA levels was consistent with the process of enterocyte differentiation. Similarly, villin gene expression was induced in Caco-2 cells during postconfluence differentiation[51]. Immunolocalization studies on the distribution of the brush border-specific microvillar protein, villin, in human colonic mucosa indicated that localization of this protein was disrupted in certain dysplastic and neoplastic states. Thus, the expression and/or distribution of brush border-specific proteins such as villin may be useful markers for defects in the differentiation state of enterocytes[52].

Changes of cellular morphology and expression of mRNA and protein of villin in IEC-6 were investigated in order to observe the effects of gastrin on the differentiation of IEC-6 cells. The results showed that gastrin could obviously up-regulate villin expression at both mRNA and protein levels. These results were in consistent with the morphological alterations of these cells, and indicated that there was causality between the two events, i.e., gastrin induced characteristic features of differentiated enterocytes may account for its up-regulation to villin expression in IEC-6 cells. All these results indicate that gastrin can promote differentiation of IEC-6 cells, which is correlated to the up-regulation of villin expression.

ACKNOWLEDGEMENTS

We are grateful to Professor Peixun Wang, Associate Professors Weiwei Lei and Qin Xu, and Dr. Haibin Wang for their technical advice and excellent assistance.

REFERENCES

1 **Jonson L**, Bundgaard JR, Johnsen AH, Rourke IJ. Identification and expression of gastrin and cholecystokinin mRNAs from the turtle, Pseudemys scripta: evidence of tissue-specific tyrosyl sulfation(1). *Biochim Biophys Acta* 1999; **1435**: 84-93

2 **Wang JY**, McCormack SA, Viar MJ, Johnson LR. Secretin inhibits induction of ornithine decarboxylase activity by gastrin in duodenal mucosa and IEC-6 cells. *Am J Physiol* 1994; **267**(2Pt 1): G276-G284

3 **Zhang ZL**, Chen WW. Proliferation of intestinal crypt cells by gastrin-induced ornithine decarboxylase. *World J Gastroenterol* 2002; **8**: 183-187

4 **McCormack SA**, Wang JY, Viar MJ, Tague L, Davies PJ, Johnson LR. Polyamines influence transglutaminase activity and cell migration in two cell lines. *Am J Physiol* 1994; **267**(3Pt 1): C706-C714

5 **McCormack SA**, Wang JY, Johnson LR. Polyamine deficiency causes reorganization of F-actin and tropomyosin in IEC-6 cells. *Am J Physiol* 1994; **267**(3Pt 1): C715-C722

6 **McCormack SA**, Blanner PM, Zimmerman BJ, Ray R, Poppleton HM, Patel TB, Johnson LR. Polyamine deficiency alters EGF receptor distribution and signaling effectiveness in IEC-6 cells. *Am J Physiol* 1998; **274**(1Pt 1): C192-C205

7 **McCormack SA**, Ray RM, Blanner PM, Johnson LR. Polyamine depletion alters the relationship of F-actin, G-actin, and thymosin beta4 in migrating IEC-6 cells. *Am J Physiol* 1999; **276**(2Pt 1): C459-C468

8 **Teti D,** Visalli M, McNair H. Analysis of polyamines as markers of (patho)physiological conditions. *J Chromatogr B Analyt Technol Biomed Life Sci* 2002; **781**: 107-149

9 **Weiss TS,** Bernhardt G, Buschauer A, Thasler WE, Dolgner D, Zirngibl H, Jauch KW. Polyamine levels of human colorectal adenocarcinomas are correlated with tumor stage and grade. *Int J Colorectal Dis* 2002; **17**: 381-387

10 **Pinto D,** Robine S, Jaisser F, El Marjou FE, Louvard D. Regulatory sequences of the mouse villin gene that efficiently drive transgenic expression in immature and differentiated epithelial cells of small and large intestines. *J Biol Chem* 1999; **274**: 6476-6482

11 **Hikita C,** Vijayakumar S, Takito J, Erdjument-Bromage H, Tempst P, Al-Awqati Q. Induction of terminal differentiation in epithelial cells requires polymerization of hensin by galectin 3. *J Cell Biol* 2000; **151**: 1235-1246

12 **Quaroni A**, Wands J, Trelstad RL, Isselbacher KJ. Epithelioid cell cultures from rat small intestine. Characterization by morphologic and immunologic criteria. *J Cell Biol* 1979; **80**: 248-265

13 **Wroblewski R,** Jalnas M, Van Decker G, Bjork J, Wroblewski J, Roomans GM. Effects of irradiation on intestinal cells *in vivo* and *in vitro*. *Histol Histopathol* 2002; **17**: 165-177

14 **Wood SR,** Zhao Q, Smith LH, Daniels CK. Altered morphology in cultured rat intestinal epithelial IEC-6 cells is associated with alkaline phosphatase expression. *Tissue Cell* 2003; **35**: 47-58

15 **Houde M**, Laprise P, Jean D, Blais M, Asselin C, Rivard N. Intestinal epithelial cell differentiation involves activation of p38 mitogen-activated protein kinase that regulates the homeobox transcription factor Cdx2. *J Biol Chem* 2001; **276**: 21885-21894

16 **Soubeyran P**, Andre F, Lissitzky JC, Mallo GV, Moucadel V, Roccabianca M, Rechreche H, Marvaldi J, Dikic I, Dagorn JC, Iovanna JL. Cdx1 promotes differentiation in a rat intestinal epithelial cell line. *Gastroenterology* 1999; **117**: 1326-1338

17 **Freund JN**, Domon-Dell C, Kedinger M, Duluc I. The Cdx-1 and Cdx-2 homeobox genes in the intestine. *Biochem Cell Biol* 1998; **76**: 957-969

18 **Lorentz O**, Duluc I, Arcangelis AD, Simon-Assmann P, Kedinger M, Freund JN. Key role of the Cdx2 homeobox gene in extracellular matrix-mediated intestinal cell differentiation. *J Cell Biol* 1997; **139**: 1553-1565

19 **Taylor JK**, Levy T, Suh ER, Traber PG. Activation of enhancer elements by the homeobox gene Cdx2 is cell line specific. *Nucleic Acids Res* 1997; **25**: 2293-2300

20 **Moucadel V,** Soubeyran P, Vasseur S, Dusetti NJ, Dagorn JC, Iovanna JL. Cdx1 promotes cellular growth of epithelial intestinal cells through induction of the secretory protein PAP I. *Eur J Cell Biol* 2001; **80**: 156-163

21 **Yamada S**, Kojima H, Fujimiya M, Nakamura T, Kashiwagi A, Kikkawa R. Differentiation of immature enterocytes into

enteroendocrine cells by Pdx1 overexpression. *Am J Physiol Gastrointest Liver Physiol* 2001; **281**: G229-G236

22 **Yoshida S,** Kajimoto Y, Yasuda T, Watada H, Fujitani Y, Kosaka H, Gotow T, Miyatsuka T, Umayahara Y, Yamasaki Y, Hori M. PDX-1 induces differentiation of intestinal epithelioid IEC-6 into insulin-producing cells. *Diabetes* 2002; **51**: 2505-2513

23 **Kojima H,** Nakamura T, Fujita Y, Kishi A, Fujimiya M, Yamada S, Kudo M, Nishio Y, Maegawa H, Haneda M, Yasuda H, Kojima I, Seno M, Wong NC, Kikkawa R, Kashiwagi A. Combined expression of pancreatic duodenal homeobox 1 and islet factor 1 induces immature enterocytes to produce insulin. *Diabetes* 2002; **51**: 1398-1408

24 **Suh E**, Traber PG. An intestine-specific homeobox gene regulates proliferation and differentiation. *Mol Cell Biol* 1996; **16**: 619-625

25 **Taylor JK**, Boll W, Levy T, Suh E, Siang S, Mantei N, Traber PG. Comparison of intestinal phospholipase A / lysophospholipase and sucrase-isomaltase genes suggest a common structure for enterocyte-specific promoters. *DNA Cell Biol* 1997; **16**: 1419-1428

26 **Braunstein EM**, Qiao XT, Madison B, Pinson K, Dunbar L, Gumucio DL. Villin: A marker for development of the epithelial pyloric border. *Dev Dyn* 2002; **224**: 90-102

27 **Sonoyama K**, Rutatip S, Kasai T. Gene expression of activin, activin receptors, and follistatin in intestinal epithelial cells. *Am J Physiol Gastrointest Liver Physiol* 2000; **278**: G89-G97

28 **Jehle PM**, Fussgaenger RD, Blum WF, Angelus NK, Hoeflich A, Wolf E, Jungwirth RJ. Differential autocrine regulation of intestine epithelial cell proliferation and differentiation by insulin-like growth factor (IGF) system components. *Horm Metab Res* 1999; **31**: 97-102

29 **Kojima H**, Hidaka H, Matsumura K, Fujita Y, Nishio Y, Maegawa H, Haneda M, Yasuda H, Fujimiya M, Kikkawa R, Kashiwagi A. Concerted regulation of early enterocyte differentiation by insulin-like growth factor I, insulin, and transforming growth factor-beta1. *Proc Assoc Am Physicians* 1998; **110**: 197-206

30 **Kitchen PA**, Fitzgerald AJ, Goodlad RA, Barley NF, Ghatei MA, Legon S, Bloom SR, Price A, Walters JR, Forbes A. Glucagon-like peptide-2 increases sucrase-isomaltase but not caudal-related homeobox protein-2 gene expression. *Am J Physiol Gastrointest Liver Physiol* 2000; **278**: G425-G428

31 **Zhang ZL,** Chen WW. Effect of astragalus injection in promoting IEC-6 cell differentiation through activating ornithine decarboxylase. *Zhongguo Zhongxiyi Jiehe Zazhi* 2002; **22**: 439-443

32 **Wolpert S**, Wong ML, Bass BL. Matrix alters the proliferative response of enterocytes to growth factors. *Am J Surg* 1996; **171**: 109-112

33 **Ferretti E**, Li S, Wang J, Post M, Moore A. Mesenchymal regulation of differentiation of intestinal epithelial cells. *J Pediatr Gastroenterol Nutr* 1996; **23**: 65-73

34 **Karlsson L**, Lindahl P, Heath JK, Betsholtz C. Abnormal gastrointestinal development in PDGF-A and PDGFR-α deficient mice implicates a novel mesenchymal structure with putative instructive properties in villus morphogenesis. *Development* 2000; **127**: 3457-3466

35 **Burgess AW**. Growth control mechanisms in normal and transformed intestinal cells. *Philos Trans R Soc Lond B Biol Sci* 1998; **353**: 903-909

36 **Olson AD**, Pysher T, Bienkowski RS. Organization of intestinal epithelial cells into multicellular structures requires laminin and functional actin microfilaments. *Exp Cell Res* 1991; **192**: 543-549

37 **Wolpert SI**, Lally KM, Li J, Wang JY, Bass BL. Extracellular matrix modulates enterocyte growth via downregulation of c-jun but is independent of p21 and p27 expression. *J Gastrointest Surg* 1999; **3**: 319-324

38 **Quaroni A**, Tian JQ, Goke M, Podolsky DK. Glucocorticoids have pleiotropic effects on small intestinal crypt cells. *Am J Physiol* 1999; **277**(5Pt 1): G1027-G1040

39 **Pacha J,** Lisa V, Miksik I. Effect of cellular differentiation on 11beta-hydroxysteroid dehydrogenase activity in the intestine. *Steroids* 2002; **67**: 119-126

40 **Suh E**, Chen L, Taylor J, Traber PG. A homeodomain protein related to caudal regulates intestine-specific gene transcription. *Mol Cell Biol* 1994; **14**: 7340-7351

41 **Moucadel V,** Totaro MS, Dell CD, Soubeyran P, Dagorn JC, Freund JN, Iovanna JL. The homeobox gene Cdx1 belongs to the p53-p21(WAF)-Bcl-2 network in intestinal epithelial cells. *Biochem Biophys Res Commun* 2002; **297**: 607-615

42 **Soubeyran P**, Haglund K, Garcia S, Barth BU, Iovanna J, Dikic I. Homeobox gene Cdx1 regulates Ras, Rho and PI3 kinase pathways leading to transformation and tumorigenesis of intestinal epithelial cells. *Oncogene* 2001; **20**: 4180-4187

43 **Patterson AP,** Chen Z, Rubin DC, Moucadel V, Iovanna JL, Brewer HB Jr, Eggerman TL. Developmental regulation of apolipoprotein B mRNA editing is an autonomous function of small intestine involving homeobox gene Cdx1. *J Biol Chem* 2003; **278**: 7600-7606

44 **Vijayakumar S,** Takito J, Hikita C, Al-Awqati Q. Hensin remodels the apical cytoskeleton and induces columnarization of intercalated epithelial cells: processes that resemble terminal differentiation. *J Cell Biol* 1999; **144**: 1057-1067

45 **Athman R,** Louvard D, Robine S. The epithelial cell cytoskeleton and intracellular trafficking. III. How is villin involved in the actin cytoskeleton dynamics in intestinal cells? *Am J Physiol Gastrointest Liver Physiol* 2002; **283**: G496-G502

46 **Glenney JR Jr**, Bretscher A, Weber K. Calcium control of the intestinal microvillus cytoskeleton: its implications for the regulation of microfilaments organizations. *Proc Natl Acad Sci U S A* 1980; **77**: 6458-6462

47 **Mooseker MS**, Graves TA, Wharton KA, Falco N, Howe CL. Regulation of microvillus structure: calcium-dependent solation and cross-linking of actin filaments in the microvilli of intestinal epithelial cells. *J Cell Biol* 1980; **87**(3Pt 1): 809-822

48 **Ferrary E,** Cohen-Tannoudji M, Pehau-Arnaudet G, Lapillonne A, Athman R, Ruiz T, Boulouha L, El Marjou F, Doye A, Fontaine JJ, Antony C, Babinet C, Louvard D, Jaisser F, Robine S. *In vivo*, villin is required for Ca(2+)-dependent F-actin disruption in intestinal brush borders. *J Cell Biol* 1999; **146**: 819-830

49 **Coluccio LM**, Bretscher A. Reassociation of microvillar core proteins: making a microvillar core *in vitro*. *J Cell Biol* 1989; **108**: 495-502

50 **Vidali L,** Hepler PK. Actin and pollen tube growth. *Protoplasma* 2001; **215**: 64-76

51 **Hodin RA**, Shei A, Meng S. Transcriptional activation of the human villin gene during enterocyte differentiation. *J Gastrointest Surg* 1997; **1**: 433-438

52 **Carboni JM,** Howe CL, West AB, Barwick KW, Mooseker MS, Morrow JS. Characterization of intestinal brush border cytoskeletal proteins of normal and neoplastic human epithelial cells. A comparison with the avian brush border. *Am J Pathol* 1987; **129**: 589-600

Edited by Ren SY and Wang XL

P.O.Box 2345, Beijing 100023,China
Fax: +86-10-85381893
E-mail: wjg@wjgnet.com www.wjgnet.com

World J Gastroenterol 2003;9(8):1791-1794
World Journal of Gastroenterology
 ISSN 1007-9327

• BASIC RESEARCH •

Role of nucleation of bile liquid crystal in gallstone formation

Hai-Ming Yang, Jie Wu, Jin-Yi Li, Lin Gu, Min-Fei Zhou

Hai-Ming Yang, Jie Wu, Lin Gu, Department of Physics and Mathematics, Kunming Medical College, Kunming 650031, Yunnan Province, China
Jin-Yi Li, Department of Physics, Yunnan Normal University, Kunming 650092, Yunnan Province, China
Min-Fei Zhou, Department of Hepato-biliary Surgery, The Second Affiliated Hospital of Kunming Medical College, Kunming 650101, Yunnan Province, China
Supported by the National Natural Sciencce Foundation of China, No. 39960024, and Applied Basic Research Fund of Yunnan Provincial Science and Technology Committee, No. 1999C 0064M and Science Foundation of Yunnan Education Committee, No. 9912073
Correspondence to: Hai-Ming Yang, Physics and Mathematics Department of Kunming Medical College, 191 West Renming Road, Kunming 650031, Yunnan Province, China. yanghaiming88@hotmail.com
Telephone: +86-871-5338812
Received: 2003-01-04 **Accepted:** 2003-02-16

Abstract

AIM: To explore the role of bile liquid crystal in the process of gallbladder stone formation and to provide bases for preventing and treating cholelithiasis.

METHODS: 46 guinea pigs, half males and half females, were randomly divided into control group and stone-causing group. Normal feed and stoneleading feed were used respectively to raise guinea pigs in the control group and stone-causing group. The guinea pigs were killed in three batches during the raising period. Under polarizing microscope, the pattern changes of bile liquid crystal in the gallbladder biles of the guinea pigs in the control group and stone-causing group were dynamicly observed respectively in single-blind trial.

RESULTS: It was found that there were few crystals in the guinea pigs' biles of the control group, and their Malta cross was small and scattered, and existed in single form. With the increase of the feeding days, bile liquid crystals grew and Malta cross became bigger with their distribution densified, denser somewhere, but always existed in single form. While those of the stone-causing group had more bile liquid crystals, Malta cross was big and merged in strings. With the increase of the feeding days, bile liquid crystals grew in amount and strings of Malta cross increased and became bigger. The crosses in strings were arranged more and more regularly and they gradually changed into stone crystals.

CONCLUSION: Formation of gallbladder stone is a process of nucleation from different substances, and the causing-stone gallbladder bile is a constantly supersaturated solution, and bile liquid crystal is a nucleation factor in the formation of gallbladder stones. The process of nucleation includes gathering, merging and phase-changing of bile liquid crystals. The process of gathering, merging of bile liquid crystal is the key to nucleation.

Yang HM, Wu J, Li JY, Gu L, Zhou MF. Role of nucleation of bile liquid crystal in gallstone formation. *World J Gastroenterol* 2003; 9(8): 1791-1794
http://www.wjgnet.com/1007-9327/9/1791.asp

INTRODUCTION

Bile liquid crystal is a type of liquid crystal in the living beings' bile. Since American scholar Olszewski *et al*[1] found the substance of liquid crystal in the bile liquid of human body in 1973, some scholars at home and abroad have explored the matter of liquid crystal in the living beings' bile[2-4], but the relation between bile liquid crystal and formation of gallbladder stone has not been clarified so far. In order to explore the role of bile crystal in the process of gallbladder-stone formation and to provide certain bases for the prevention and treatment of gallbladder stone, we made dynamic observations and studied on the nucleation of bile liquid crystal in gallbladder stone through animal tests in guinea pigs.

MATERIALS AND METHODS

Materials

46 guinea pigs (provided by the animal branch of the Scientific Research Department in Kunming Medical College, with qualified animal testing certificate issued by Yunnan Province), each weighing about 300 grams, half males and half females, were randomly divided into control group (n=23) and stone-causing group (n=23).

Methods

Animal raising The control group was given normal feed which was provided by the animal branch of the Scientific Research Department in Kunming Medical College, while the stone-causing group was given stoneleading feed. The two groups were separately raised in flocks, with free access to water containing 1 % vitamin C.

Stone-causing feed The components of the stone-causing feed were as follows: starch 25 %, bran 25 %, glucose 12 %, lard 1.5 %, cholesterol 1.5 %, normal feed 35 %[5]. They were mixed evenly and made granule with feed machine.

Sample preparation Guinea pigs were killed in three batches. The first batch was killed after raised for 10 days, with 5 pigs in each group, totally 10 pigs in the 2 groups. The 2nd batch was killed after raised for 25 days, with 5 pigs in each group, totally 10 pigs in the 2 groups. The 3rd batch was killed after raised for 60 days, with 13 pigs in each group, totally 26 pigs in the 2 groups. The pigs were whacked at head to stupor with a blood vessel forceps, immediately cut open belly and their cystic duct was blocked with a blood vessel forceps to take out gallbladder and all bile. The bile was centrifugalized for 30 minutes with a China-made TGL-16B bench centrifuge, 4 000 r/min, and observed under polarizing microscope.

Polarizing microscope observation A China-made W-104 micro-sample advancer (precision of 0.2 μL) was used to stratify the centrifuged bile and drip 6.0 μL of it on a carrier flake, then it was covered with the cover-glass and the bile naturally spread out to form slices. Under an advanced polarizing microscope (BHSP model of Olympus, Japan), the pattern changes of the bile liquid crystal in the process of gallbladder stone formation were observed.

RESULTS

Patterns change of bile liquid crystals in control group

Under the perpendicular polarized microscope, the

morphological changes of bile liquid crystal in the gallbladder bile of guinea pigs in the control group were observed, and it was found that there were few matters of liquid crystal in gallbladder bile, and that the interference pattern, named Malta cross, was small and scattered, in single form. With the increase of the feeding days, bile liquid crystals grew larger and Malta cross became bigger with their distribution densified unevenly, but always existed in single form, as shown in Figure 1 (a), (b), (c) and (d). No regularly shaped stone crystal was found in the biles.

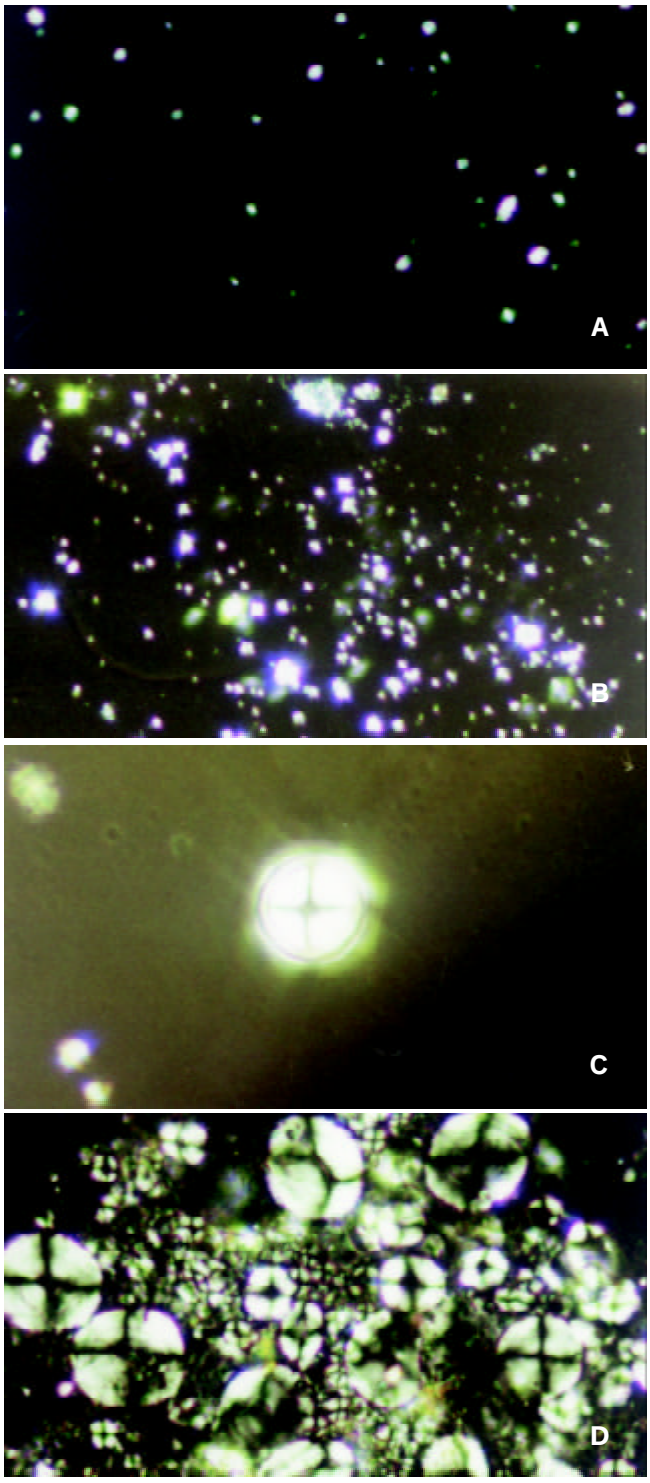

Figure 1 Malta cross showed in bile liquid crystals in gallbladders of guinea pigs in the control group: (a) Small and scattered crosses (10 days, ×400). (b) The crosses gradually grew in size and number (25 days, ×400). (c) Single big crosses (25 days, ×400). (d) Densely distributed crosses (60 days, ×400).

The pattern changes of bile liquid crystals in the stone-causing group

Under the polarizing microscope, the morphological changes of bile liquid crystal in guinea pigs' gallbladders in stone-causing group were observed, and it was found that there were more matters of liquid crystal in gallbladder biles, and that the interference pattern, Malta cross was big and merged into strings. With the increase of the feeding days, bile liquid crystals grew in number and strings of Malta crosses increased and became bigger. The crosses in strings were arranged more regularly so that they gradually phase-changed into stone crystals, as shown in Figure 2 (a), (b), (c) and (d). It exhibited variously shaped stone crystals in the biles, as shown in Figure 3 (a), (b), (c) and (d).

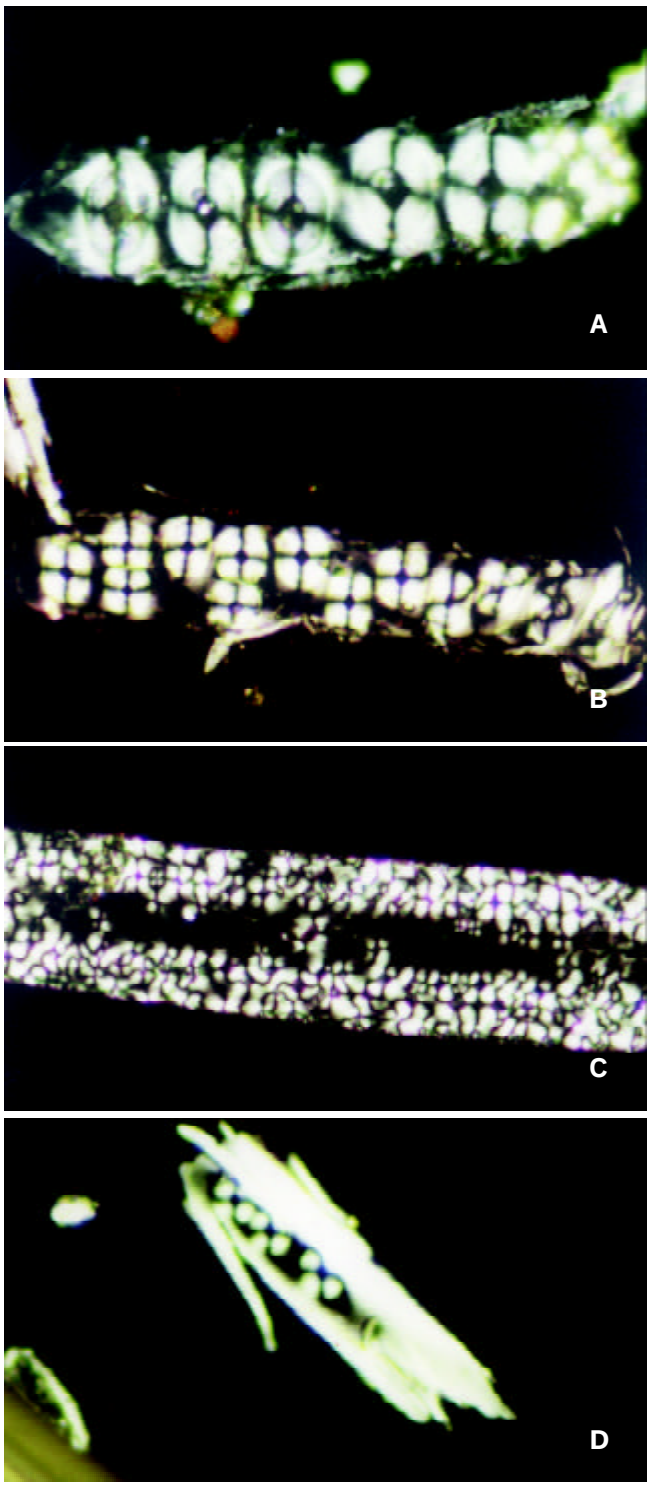

Figure 2 Malta cross shown in bile liquid crystals in gallblad-

ders of guinea pigs in the stone-causing group: (a) The cross merged into strings (10 days, ×400). (b) Gradually growing strings of the cross (25 days, ×200). (c) Strings of the cross in phase-changing (60 days, ×400). (d) Stone crystals nucleated by strings of the cross (60 days, ×200).

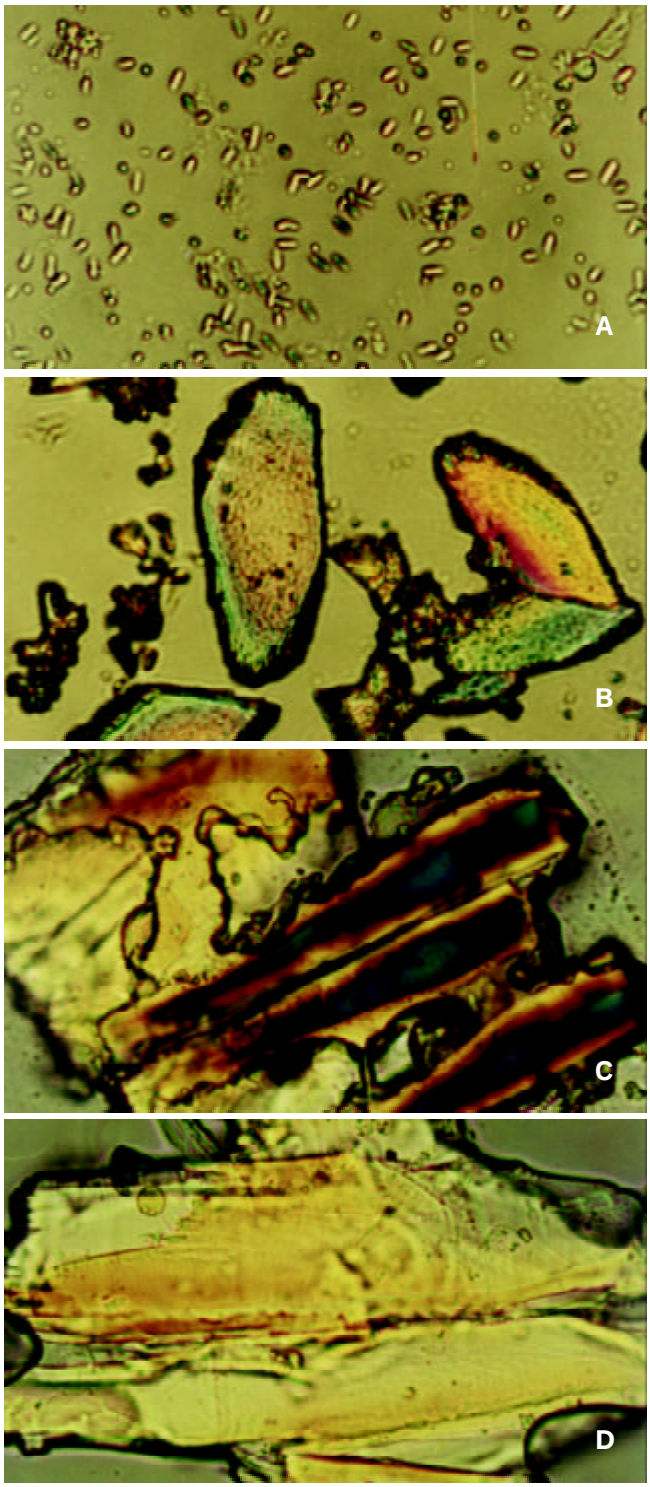

Figure 3 Gallbladder stone crystals in bile of the stone-causing group.

DISCUSSION

The cause of gallbladder stone is very complicated, various factors are involved[5-9]. The basic factor is now considered to be the change of compositions and physical-chemistry characteristics of biles, which results in cholesterol in the state of super-saturation in the bile. And it is very likely to form crystals, which is then deposited to form gallbladder stones. It also causes imbalance between nucleation-leading factors and antinucleation factors and abnormal function of the gallbladder and so on[10-19]. From the viewpoint of crystallogeny, in a system of solution, the precondition for solute to be separated out and to form crystal is that the solute in the system must be in the state of super-saturation, which is an unstable state in thermodynamics. Only in this state, can the solute be crystallized and separated out. The formation of crystals has two steps of nucleation and crystallization, it firstly forms a crystalline nucleus containing hundreds of molecules, then crystals grow. In a system of solution, spontaneous nucleation of solute often requires a very high degree of saturation, the supersaturated solution in this state is called unstably supersaturated solution. When a certain type of special nucleating factors is added, supersaturated solution of a relatively low degree also can produce nucleation, which is called heterogeneous nucleation, and the supersaturated solution in this state is called substably supersaturated solution[20,21]. Homogeneous nucleation of bile cholesterol requires a very high degree of saturation (estimated at about 300 %), which is not possible to occur in human body, and even less possible in guinea pigs' body. So the formation of gallbladder-stone should be a process of heterogeneous nucleation, stone-causing gallbladder bile should be a substably supersaturated solution, and bile liquid crystal should be a type of nucleating factors for gallbladder stones.

As we observed under the polarizing microscope, there were many substances of liquid crystal in the gallbladder bile of the guinea pigs in the stone-causing group, which were big and string of Malta crosses. With the increase of the feeding days, bile liquid crystals grew in number, more and more strings of Malta cross appeared and steadily became bigger and bigger, and their arrangement became more and more regular, and gradually phase-changed into stone crystals. These have proved that the formation of gallbladder stone is indeed a process of heterogeneous nucleation, and stone-causing gallbladder bile is a type of substably supersaturated solution, and that bile liquid crystal is a type of nucleating factors in gallbladder-stone. Its process of nucleation is such that bile liquid crystals get together, merge and phase change. In another word, single Malta crosses assemble into strings, then merge as slices, and finally phase-change into crystals. The assemblage and merger of bile liquid crystals are the key for nucleation. Although there were also substances of liquid crystal existing in gallbladder biles in the control group and bile crystals also increased with feeding time, they neither assembled nor merged, and Malta crosses always existed in single forms which were unable to nucleate to form stone. If some way can be found to prevent or retard the assemblage and merger of bile liquid crystals, i. e., formation of the nucleus, it will be of a great significance in theory and practice for prevention and treatment of cholelithiasis.

Cholesterol can not dissolve in water, but it can dissolve in bile. The concentration of cholesterol in bile is about 10-20 mmol/L, this concentration is about 10^6 times[22] denser than that of the solubility of cholesterol in water. Studies concerned pointed out that cholesterol in bile maintained its state of dissolution in forms of micelle and vesicle. Micelle is the polymer of cholesterol, phosphatide and cholate, while vesicle is the compound of cholesterol and phosphatide[23-31]. These two form a system of thermodynamic balance in bile so that they are interlinked and interconverted, and play the role of modulation for dissolution and separation of cholesterol. Under the effect of nucleation-leading factors and antinucleation factors in bile, vesicles in bile assemble, merge and separate out crystalline nuclei of cholesterol which then gradually grow up to form stones[32]. As we observed under the polarizing microscope, single Malta cross in bile liquid crystal of guinea pigs in stone-causing group, gradually assembled into strings,

then merged into slices, and finally phase-changed into stone crystals. The present study supports the above viewpoints from the studies of morphology. Whether bile crystal is such a kind of vesicles or vesicles aggregate and what factors cause or stop bile liquid crystal assembling and merging, still need to be further studied.

REFERENCES

1 **Olszewski MF**, Holzbach RT, Saupe A, Brown GH. Liquid crystals in human bile. *Nature* 1973; **242**: 336-337
2 **Yang HM,** Wu J, Li JY, Zhou JL, He LJ, Xu XF. Optic properties of bile liquid crystals in human body. *World J Gastroenterol* 2000; **6**: 248-251
3 **Yang H**, Wu J, Cu L, Zhou J, He L, Cao S. The optical properties of bile liguid crystals in organisms. *Chin J Biomedi Engin* 1999; **8**: 67-68
4 **Savina LV**, Kokueva OV, Golovanva ES, Kadygrob GV. Crystallooptic structures of bile in chronic acalculous cholecystitis. *Eksp Klin Gastroenterol* 2002; **128**: 59-62
5 **Han TQ,** Jiang ZY, Zhang SD. Research progress in formation of gallstone. *Zhongguo Shiyong Waike Zazhi* 2001; **21**: 123-125
6 **Zhang SD,** Han TQ. Prospects for studies of gallstone. *Waike Lilun Yu Shijian* 1999; **4**: 5-6
7 **Nishioka T,** Tazuma S, Yamashita G, Kajiyama G. Partial replacement of bile salts causes marked changes of cholesterol crystallization in supersaturated model bile systems. *Biochem J* 1999; **340**: 445-451
8 **Wang DQ,** Cohen DE, Lammert F, Carey MC. No pathophysiologic relationship of soluble biliary proteins to cholesterol crystallization in human bile. *J Lipid Res* 1999; **40**: 415-425
9 **Rubin M**, Pakula R, Konikoff FM. Microstructural analysis of bile: relevance to cholesterol gallstone pathogenesis. *Histol Histopathol* 2000; **15**: 761-770
10 **Wu ZD**. Surgery. 5th ed. Beijing: *People's Health Publishing House* 2002: 617-619
11 **Yu JP,** Sheng ZX, Luo HS. Practical Digestive Diseases. 1st ed. Beijing: *Science Press* 1999: 1228-1232
12 **Yang GH**. Pathology. 5th ed. Beijing: *People's Health Publishing House* 2001: 217-218
13 **Zhao JC,** Shu Y, Cheng NS, Xiao LJ, Zhu H. Changes of cholesterol metabolism in cholesterol gallstone formation in the rabbit. *Zhongguo Putong Waike Zazhi* 2000; **9**: 124-128
14 **Li QR,** Gong YH, Zhou JP, Gao Q, Pang BZ. Formation of gallstones by feeding on high cholesterol diet. *Zhonghua Linchuang Ganzangbingxue Zazhi* 2002; **18**: 320-321
15 **Zhang JH,** Yang KZ, Han BL. The kinetic mechanism of gallstone formation. *Zhongguo Putong Waike Zazhi* 2001; **16:** 424-426
16 **Ye SA,** Tang WH. Research progress in gallbladder's effect in the process of gallstone formation. *Guowai Yixue Waike Fence* 2001; **28**: 221-223
17 **Liu CL,** Higuchi WI. Cholesterol crystallite nucleation in supersaturated model biles from a thermodynamic standpoint. *Biochim Biophys* 2002; **1588**: 15-25
18 **Jirsa M,** Groen AK. Role of biliary proteins and non-protein factors in kinetics of cholesterol crystallisation and gallstone growth. *Front Biosci* 2001; **6**: E154-167
19 **Qin YL,** Tang WH. Research progress in glycoprotein in gallstone. *Guowai Yixue Waike Fence* 1999; **26**: 344-347
20 **Zhang KC,** Zhang LH. Crystal Growth Science and Technology. 2nd Edition. Beijing: *Science Press* 1997: 178-182
21 **Cheng JZ**. Modern Crystal Chemistry-Theories and Technique. 1st Edition. Beijing: *Higher Education Press* 2001: 126-131
22 **Zhang QY**. Diseases of the Biliary System. 1st Edition. Nanjing: *Jiangsu Science and Technology Press* 1997: 167
23 **Luk A**S, Kaler EW, Lee SP. Structural mechanisms of bile salt-induced growth of small unilamellar cholesterol-lecithin vescicles. *Biochemistry* 1997; **36**: 5633-5644
24 **Prigun NP,** Korolevich AN. Changes in human biliary vesicle sizes in pathological states. *Biofizika* 2002; **47**: 1095-1100
25 **Portincasa P,** Venneman NG, Moschetta A, van den Berg A, Palasciano G, vanBerge-Henegouwen GP, van Erpecum KJ. Quantitation of cholesterol crystallization from supersaturated model bile. *J Lipid Res* 2002; **43**: 604-610
26 **Venneman NG,** Huisman SJ, Moschetta A, vanBerge-Henegouwen GP, van Erpecum KJ. Efects of hydrophobic and hydrophilic bile salt mixtures on cholesterol crystallization in model biles. *Biochim Biophys Acta* 2002; **1583**: 221-228
27 **Moschetta A,** vanBerge-Henegouwen GP, Portincasa P, Palasciano G, van Erpecum KJ. Cholesterol crystallization in model biles: effects of bile salt and phospholipid species composition. *J Lipid Res* 2001; **42**: 1273-1281
28 **Moschetta A**, Frederik PM, Portincasa P, vanBerge-Henegouwen GP, van Erpecum KJ. Incorporation of cholesterol in sphingomyelin-phosphatidylcholine vesicles has profound effects on detergent-induced phase transitions. *J Lipid Res* 2002; **43**: 1046-1053
29 **Moschetta A**, vanBerge-Henegouwen GP, Portincasa P, Renooij WL, Groen AK, van Erpecum KJ. Hydrophilic bile salts enhance differential distribution of sphingomyelin and phosphatidylcholine between micellar and vesicular phases: potential implications for their effects *in vivo*. *J Hepatol* 2001; **34**: 492-499
30 **Eckhardt ER**, Moschetta A, Renooi j W, Goerdayal SS, van Berge-Henegouwen GP, van Erpecum KJ. Asymmetric distribution of phosphatidylcholine and sphingomyelin between micellar and vesicular phases. Potential implications for canalicular bile formation. *J Lipid Res* 1999; **40**: 2022-2033
31 **Sakomoto M**, Tazuma S, Chayama K. Less hydrophobic phosphatidylcholine species simplify biliary vesicle morphology, but induce bile metastability with a broad spectrum of crystal forms. *Biochem J* 2002; **362**: 105-112
32 **Gantz DL,** Wang DQ, Garey MC, Small DM. Cryoelectron microscopy of a nucleating model bile in vitreous ice: formation of primordial vesicles. *Biophys J* 1999; **76**: 1436-1451

Edited by Xu XQ and Zhu LH

P.O.Box 2345, Beijing 100023,China
Fax: +86-10-85381893
E-mail: wjg@wjgnet.com www.wjgnet.com

World J Gastroenterol 2003;9(8):1795-1798
World Journal of Gastroenterology
 ISSN 1007-9327

• BASIC RESEARCH •

Toxicities and therapeutic effect of 5-fluorouracil controlled release implant on tumor-bearing rats

Yin-Cheng He, Ji-Wei Chen, Jun Cao, Ding-Yu Pan, Jian-Guo Qiao

Yin-Cheng He, Ji-Wei Chen, Jun Cao, Ding-Yu Pan, Jian-Guo Qiao, Department of General Surgery, Zhongnan Hospital, Wuhan University, Wuhan 430071, Hubei Province, China
Correspondence to: Dr. Yin-Cheng He, Department of General Surgery, Zhongnan Hospital, Wuhan University, Wuhan 430071, Hubei Province, China. w030508h@public.wh.hb.cn
Telephone: +86-27-67812963
Received: 2002-12-10 **Accepted:** 2003-01-16

Abstract

AIM: To investigate the toxicities, biodistribution and anticancer effect of 5-fluorouracil controlled release implant (5-FUCI) on Walker 256 carcinosarcoma cells in Wistar rats.

METHODS: Experiment 1: Wistar rats were randomly divided into three groups (27 rats per group). Blank implant was implanted in left lobe of the liver, and rats were treated with saline solution (in group A) or 5-fluorouracil (subcutaneous injection, group B). 5-FUCI was inserted in left lobe of the liver (group C). The gastrointestinal and hematological toxicities were observed and contents of element F in group C were assayed. Experiment 2: on day 6 after Walker-256 carcinosarcoma transplantation in left lobe of the liver, 5-FUCI was implanted in right lobe of the liver (group E) or left lobe (group F), and rats in control group (group D) were inserted blank implant. Tumor inhibition rate and survival time were investigated.

RESULTS: 5-FUCI showed no obvious toxic effect, extraction of Evan's blue from gastrointestinal tissue was normal, the peripheral white blood cells and bone marrow nucleated cells were not reduced, compared with control group ($P>0.05$). Histological examination revealed that there were no visible changes in small intestinal mucosa, The concentration of 5-fluorouracil in left lobe of the liver was 9.84, 28, 34 times as much as those of right lobe of the liver, heart and kidney respectively after the implantation in group C. They kept a high level of fluorouracil in left lobe of the liver, ranging from (4.414±0.482) % to (7.800±0.804) %, for eight weeks. Survival days were 28.0±2.2, 30.0±3.2 and 38.7±6.7 d in group D, E and F, respectively.

CONCLUSION: 5-FUCI shows no obvious toxicities to gastrointestinal tract and myelotoxicity. After implantation, it kept a high level of 5- fluorouracil in surrounding tissues of the implant for eight weeks. Its antitumor effect on Walker-256 carcinosarcoma is demonstrated.

He YC, Chen JW, Cao J, Pan DY, Qiao JG. Toxicities and therapeutic effect of 5-fluorouracil controlled release implant on tumor-bearing rats. *World J Gastroenterol* 2003; 9(8): 1795-1798
http://www.wjgnet.com/1007-9327/9/1795.asp

INTRODUCTION

5-Fluorouracil (5-FU) is one of the most widely used chemotherapeutic drugs in the treatment of malignant gastrointestinal cancers[1-7], but its use has been limited by is systemic toxicities, i.e. severe gastrointestinal toxicities, hematological side effects, and severe disturbance in bone marrow[8,9]. Moreover, 5-FU has a serum half-life of only 10 minutes[10-13], further limiting its usefulness. To maximize the therapeutic effect of 5-FU and minimize any adverse effect, we developed silicone as a polymer matrix, and 5-FU as a model drug to prepare a controlled-release implant of 5-fluorouracil (5-FUCI, Figure 1) for delivering agents directly to the site of the tumor. Tube-type pellets made of silastic elastomer were of 2 mm in outer diameter, 0.5 mm in wall thickness and 25 mm in length. Per pellet contained 13.2 mg of 5-FU. The daily delivery dose of 5-FU was approximately 30 $\mu g \cdot d^{-1}$, zero-order release profiles lasted for 24 weeks *in vitro* (unpublished data). This study investigated its toxicities as compared with standard systemic therapy, the biodistribution of 5-FU after 5-FUCI was implanted in the liver of rats, and therapeutic effect on the Walker-256 carcinosarcoma in the liver of Wistar rats. Two experiments were performed.

MATERIALS AND METHODS

Experiment 1: Toxicity evaluation and biodistribution of 5-FUCI

5-FUCI and blank implant 5-FUCI and blank implants were prepared and kindly provided by Prof. Huaiying Wu (from Shanghai Medical University, China). 5-Fu was purchased from Shanghai Haipu Pharmaceutical Company.

Animals Adult male Wistar rats, weighing 300-320 g, were obtained from the Experimental Animal Center of Wuhan University, China. They were housed in stock cages (3 rats per cage) and given free access to water and the commercial laboratory rodent diet. Twelve hours prior to experiment, the rats were fasted, but allowed free access to water.

Implantation and treatment The rats were anesthetized with i.p. of sodium pentobarbital (40 $mg \cdot kg^{-1}$). All procedures were carried out aseptically. Then, they were randomly divided into three groups (27 rats per group) and received implantations.

Group A: A blank implant was implanted in left lobe of the liver. Subcutaneous injection of 1 ml saline solution was administered (daily×7, weekly×7).

Group B: A blank implant was implanted in left lobe of the liver. 5-FU (10 $mg \cdot kg^{-1}$) was subcutaneously injected (daily×7, weekly ×7).

Group C: 5-FUCI was implanted in left lobe of the liver. 1 ml saline solution was subcutaneously injected (daily×7, weekly ×7).

Counts of WBC and bone marrow nucleated cells Three rats per group were respectively anesthetized weekly, counts of the peripheral white blood cells and bone marrow nucleated cells were assessed. The jugular vein was isolated and received injection of 1 % Evan' s blue solution (1.0 $mg \cdot kg^{-1}$). The rats were killed by cervical dislocation at 45 min postinjection.

Toxicity evaluation of small intestine Two cm sections of the proximal jejunum were cut and weighed, and treated with 40 % trichloroacetic acid solution (1:8, w/v), then left at 25 ℃ overnight and centrifuged at 1 500 g for 10 min. The upper aqueous phase was collected and extraction of Evan' s blue

was measured by spectrophotometer.

Morphological changes of small intestinal mucosa The small intestine segments were collected, and haematoxylin and eosin stained slides were used. The area of small intestinal mucosal cells and integrated optical density (IOD) of inner mucosal surface of the small intestine were measured by using image analysis system (IBAS, Kontron Co. Ltd., Germany).

Assay of element F in group C To evaluate the biodistribution of 5-FU postimplantation, major organs (left/right lobe of the liver, heart, kidney) in group C were resected, adherent blood was removed and weighed. The contents of F were measured by an electron probe analyzer (JCXA-733, JEDL Co. Ltd., Japan).

Experiment 2: Antitumor activities of 5-FUCI

Preparation of TB rats Walker-256 carcinosarcoma cells were obtained from Chinese Center of Culture Preservation. On day 0 following laparotomy, 10^7 tumor cells of approximately 0.1 ml of cell suspension were transplanted in left lobe of the liver under slight ketamine anesthesia.

5-FUCI transplantation and treatment On day 6 after tumor transplantation, the tumor-bearing (TB) rats were randomly assigned to three groups (12 rats per group) for treatment and reoperated for insertion of 5-FUCI or blank implant.

Group D: The TB rats were treated by intratumoral implantation of a blank implant in left lobe of the liver.

Group E: 5-FUCI was implanted in right lobe of the liver.

Group F: The TB rats were treated by intratumoral implantation of 5-FUCI in left lobe of the liver.

Tumor volume and survival days On day 21, six rats per group were sacrificed, solid tumors were excised, weighed and the rate of tumor inhibition was calculated by the formula: (the tumor volume of control group- tumor volume of experimental group)/(the tumor volume of control group)×100 %. The life span of rest rats was investigated.

Pathological examination The tumor tissues taken from control group and experimental group were embedded in paraffin, and 5 μm sections were taken, stained with hematoxylin-eosin, and observed under light microscope to examine the therapeutic effect of 5-FUCI.

Statistical analysis

The differences between the mean values were analyzed for significance using the Student' s *t* test for independent samples. Survival time was examined with time sequence examination. $P \leqslant 0.05$ was considered to be statistically significant.

RESULTS

Changes of counts of WBC and bone marrow nucleated cells before and after treatment

Counts of the peripheral white blood cells in group B decreased from 11.5 g· L^{-1} before chemotherapy to 2.0 g· L^{-1} 3 weeks after treatment, but the data were not significantly different in group C compared with control group (group A, $P>0.05$). Counts of the bone marrow nucleated cells after subcutaneous injection of 5-FU decreased from 41.4×10^9· L^{-1} to 24.0×10^9· L^{-1}, and the data were normal in groups A and C ($P>0.05$).

Small intestinal mucosal image analysis

Morphological changes of small intestinal mucosa are listed in Tables 1 and 2.

Gastrointestinal toxicity

Gastrointestinal toxicity was positive by correlated with extraction of Evan' s blue from gastrointestinal tract. The results of extraction of Evan' s blue from small intestine are shown in Table 3.

Table 1 Changes of area of small intestinal mucosal cells (μm^2)

Time (weeks)	Group A	Group B	Group C
2	38.98±8.16	47.16±3.29	31.32±7.76[b]
4	35.07±5.70	42.25±4.42	28.81±1.98[b]
6	38.11±1.89	36.97±3.44	30.17±5.00
8	29.91±1.34	-	29.72±0.97
Mean	35.68±5.78	42.13±5.48[a]	30.00±4.15[ab]

[a]$P<0.05$ *vs* group A; [b]$P<0.05$ *vs* group B.

Table 2 Changes of IOD of inner mucosal surface of small intestine

Time (weeks)	Group A	Group B	Group C
2	0.406±0.020	0.248±0.069	0.453±0.051
4	0.417±0.110	0.290±0.017	0.409±0.024[b]
6	0.379±0.042	0.335±0.055	0.453±0.081
8	0.508±0.083	-	0.352±0.041[a]
Mean	0.427±0.080	0.295±0.051[a]	0.417±0.063[b]

[a]$P<0.05$ *vs* group A; [b]$P<0.05$ *vs* group B.

Table 3 Changes of extraction of Evan's blue from small intestine (μg· g^{-1})

Time (weeks)	Group A	Group B	Group C
0	0.860±0.051	0.840±0.045	0.870±0.035
1	0.903±0.045	0.980±0.145	0.847±0.083
2	0.797±0.086	1.123±0.172	1.243±0.169[a]
3	0.880±0.240	1.273±0.231	0.813±0.081[b]
4	0.917±0.349	1.275±0.230	0.823±0.067[b]
5	0.793±0.100	1.320±0.110[a]	0.863±0.115[b]
6	0.993±0.276	1.427±0.227	0.813±0.099[b]
7	0.890±0.226	1.010±0.014	0.923±0.250
8	0.873±0.116	-	0.853±0.131
Mean	0.881±0.183	1.253±0.323[a]	0.898±0.179[b]

[a]$P<0.05$ *vs* group A; [b]$P<0.05$ *vs* group B.

Biodistribution of 5-FU after implantation

After 5-FUCI implantation, the local high accumulation of 5-FU was demonstrated in the adjacent tissue surrounding 5-FUCI implant (in left lobe of the liver). On the other hand, the concentration of 5-FU was lower in right lobe of the liver, heart and kidney (Table 4).

Table 4 Contents of element F in group C in major organs (%)

Time (weeks)	Left lobe of liver	Right lobe of liver	Heart	Kidney
2	7.800±0.804	0.782±0.084[a]	0.143±0.050[ab]	0.174±0.144[ab]
4	6.560±0.694	0.645±0.233[a]	0.300±0.131[a]	0.272±0.136[a]
6	6.269±1.383	0.784±0.362[a]	0.288±0.232[a]	0.141±0.061[ab]
8	4.414±0.482	0.334±0.143[a]	0.162±0.067[a]	0.184±0.120[a]

[a]$P<0.05$ *vs* left lobe of the liver; [b]$P<0.05$ *vs* right lobe of the liver.

Observations of the anticancer effect

Changes of tumor volume and survival time in cancer-bearing rats are listed in Table 5. One animal in group F survived to the end of the experiment (50 days) and no viable tumor was found.

Table 5 Changes of tumor volume and survival days in tumor-bearing rats

Group	Tumor volume (cm^3)		Tumor inhibition rates (%)	Survival days (d)
	6 days of transplantation	21 days of transplantation		
Group D	0.021±0.010	2.762±1.384	-	28.0±2.2
Group E	0.030±0.014	1.844±0.904	33.2	30.0±3.2
Group F	0.027±0.012	0.102±0.117[ab]	96.3[b]	38.7±6.7[ab]

[a]$P<0.05$ *vs* group D, [b]$P<0.05$ *vs* group E.

Results of pathologic examination

5-FUCI implantation had no apparent pathological changes in the heart, liver, kidney and small intestine in group C. Some local effects of 5-FUCI were observed. The tumor cell proliferation in group D was very active (Figure 2). A number of focal necrosis were observed in group E (Figure 3) Most necrotic tissues were found at a distance of up to 1 cm from the implant in group F(Figure 4).

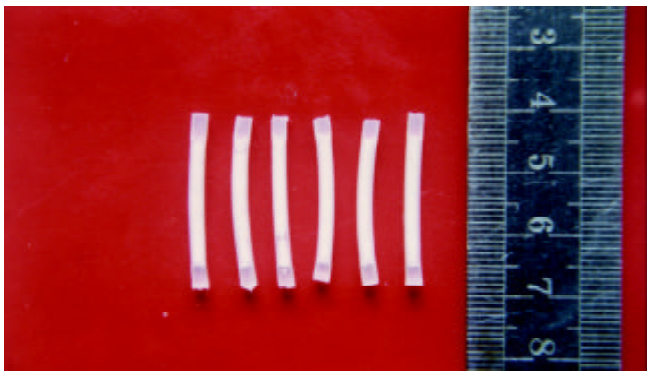

Figure 1 5-FUCI.

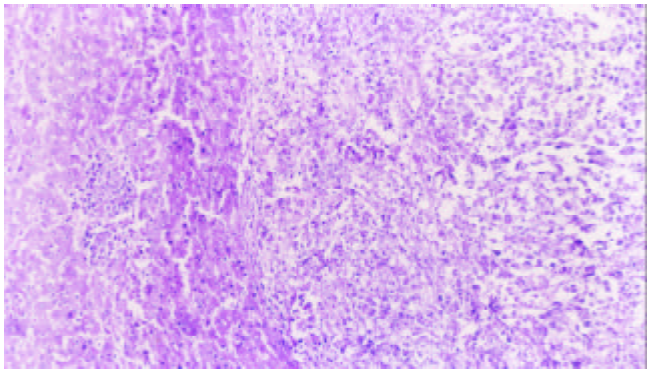

Figure 2 Tumor section (HE×100): tumor cell proliferation was active in group D.

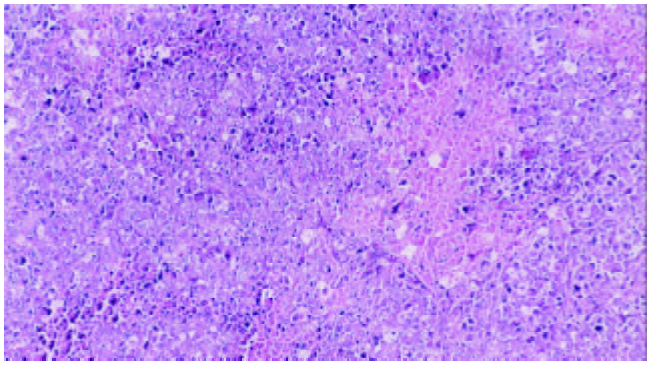

Figure 3 Tumor section (HE×100): a number of focal necrosis observed in group E.

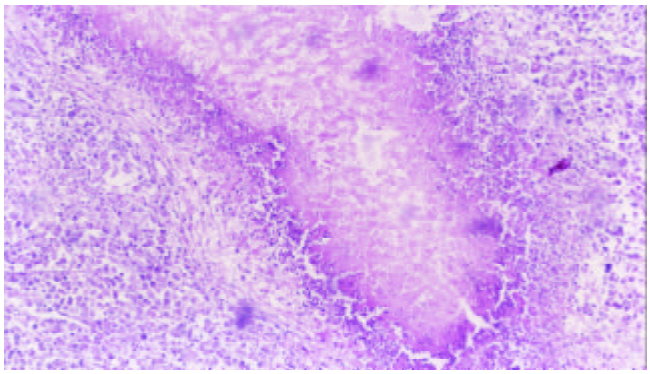

Figure 4 Tumor section (HE×100): the island of necrosis and lymphocytes infiltrated around the necrotic tissue found in group F.

DISCUSSION

Controlled release implant is a newly developed agent[14-17]. Different from other kinds of common or slow-released agents, it is capable of being administered through implantation to target organ, and can result in a therapeutically suitable plasma concentration of agents for an extended period of time[18-22], and exert a full antitumor action, despite the short half-life of drugs[23,24].

This study illustrated that the concentration of 5-FU in left lobe of the liver was 9.84, 28 and 34 times as much as that in right lobe of the liver, heart and kidney respectively after the implantation. It kept a high level of 5-FU in surrounding tissues of the implant, ranging from (4.414±0.482) % to (7.800±0.804) %, for eight weeks. 5-FUCI not only provided higher drug and /or drug metabolite concentrations in the tumor than the drug administered as an aqueous solution s.c. or systemically, but also resulted in a prolonged exposure of the tumor tissue to the drug and /or its metabolites. Consequently, 5-FUCI would be expected to improve effectiveness and to minimize the systemic toxicity associated with current systemic therapy of 5-FU[25-28].

New insights indicate that the toxicity of 5-FU is dose dependent, frequent low-dose infusions are less toxic to host than less frequent higher doses. No sign of systemic toxicities of 5-FUCI was detected because the daily delivery dose of 5-FUCI was only approximately 30 $\mu g \cdot d^{-1}$.

In previous studies, Smith *et al* demonstrated the sensitivity of tumor cells to 5-FU and dependence on drug concentration and exposure time[25,29]. If the exposure time was increased, the required drug concentration could be reduced. For example, the concentration of 5-FU that inhibited growth of 50-90 % (IC_{50}, IC_{90}) of BxPC-3 pancreatic cancer cells was eight to ten times less with a 72-h drug exposure than with a 24-h exposure[29]. We have shown that delivery of drugs administrated in 5-FUCI resulted in growth inhibition of Walker-256 carcinosarcoma cells that could hardly be accomplished with s.c. 5-FU solution.

Controlled release implant may enhance the pharmacological alternatives for the treatment of malignant tumors. Some researches have proved that tumor cell growth could be inhibited at a distance of 0.5-5 cm from the implant[30-32]. Therefore an implant needs to be inserted in many sites for multicenter or >5 cm neoplasms in outer diameter.

The data indicated that silicone pellets were transparent, and without fracture or apparent degradation after 8 weeks of implantation. In addition, a fibrous capsule was not detected around the pellets. Release of 5-FU from these pellets allows the drug to remain in the plasma for 1 to 8 weeks, in spite of its short plasma half-life (10 min)[10-13]. This was an

improvement compared with the injection of drugs. Administration of 5-FU by implantation of silastic elastomer seems to be a good candidate for 5-FU therapy. It suggests that 5-FUCI is a novel clinical approach and can offer an effective local chemotherapy.

REFERENCES

1 **Aboagye EO**, Saleem A, Cunningham VJ, Osman S, Price PM. Extraction of 5-fluorouracil by tumor and liver: a noninvasive positron emission tomography study of patients with gastrointestinal cancer. *Cancer Res* 2001; **61**: 4937-4941

2 **Xiao HB**, Cao WX, Yin HR, Lin YZ, Ye SH. Influence of L-methionine-deprived total parenteral nutrition with 5-fluorouracil on gastric cancer and host metabolism. *World J Gastroenterol* 2001; **7**: 698-701

3 **Liu LX**, Zhang WH, Jiang HC, Zhu AL, Wu LF, Qi SY, Piao DX. Arterial chemotherapy of 5-fluorouracil and mitomycin C in the treatment of liver metastases of colorectal cancer. *World J Gastroenterol* 2002; **8**: 663-667

4 **Chen XX**, Lai MD, Zhang YL, Huang Q. Less cytotoxicity to combination therapy of 5-fluorouracil and cisplatin than 5-fluorouracil alone in human colon cancer cell lines. *World J Gastroenterol* 2002; **8**: 841-846

5 **Cao S**, Rustum YM. Synergistic antitumor activity of irinotecan in combination with 5-fluorouracil in rats bearing advanced colorectal cancer: role of drug sequence and dose. *Cancer Res* 2000; **60**: 3717-3721

6 **Yoshikawa R**, Kusunoki M, Yanagi H, Noda M, Furuyama JI, Yamamura T, Hoshimoto-Tamaoki T. Dual antitumor effects of 5-fluorouracil on the cell cycle in colorectal carcinoma cells: a novel target mechanism concept for pharmacokinetic modulating chemotherapy. *Cancer Res* 2001; **61**: 1029-1037

7 **Van Kuilenburg AB**, Haasjes J, Richel D, Zoetekouw L, Van Lenthe H, De Abreu RA, Maring JG, Vreken P, Van Gennip AH. Clinical implications of dihydropyrimidine dehydrogenase (DPD) deficiency in patients with severe 5-fluorouracil-associated toxicity: identification of new mutations in the *DPD* gene. *Clin Cancer Res* 2000; **6**: 4705-4712

8 **Di Paolo A**, Danesi R, Falcone A, Cionini L, Vannozzi F, Masi G, Allegrini G, Mini E, Bocci G, Conte PF, Del Tacca M. Relationship between 5-fluorouracil disposition, toxicity and dihydropyrimidine dehydrogenase activity in cancer patients. *Ann Oncol* 2001; **12**: 1301-1306

9 **Van Kuilenburg AB**, Haasjes J, Richel DJ, Zoetekouw L, Van Lenthe H, De Abreu RA, Maring JG, Vreken P, Van Gennip AH. Clinical implications of dihydropyrimidine dehydrogenase (DPD) deficiency in patients with severe 5-fluorouracil-associated toxicity: identification of new mutations in the *DPD* gene. *Clin Cancer Res* 2000; **6**: 4705-4712

10 **Fraile RJ**, Baker LH, Buroker TR, Horwitz J, Vaitkevicius VK. Pharmacokinetics of 5-fluorouracil administered orally, by rapid intravenous and by slow infusion. *Cancer Res* 1980; **40**: 2223-2228

11 **Yi YM**, Yang TY, Pan WM. Preparation and distribution of 5-fluorouracil (125)I sodium alginate-bovine serum albumin nanoparticles. *World J Gastroenterol* 1999; **5**: 57-60

12 **Kuan HY**, Smith DE, Ensminger WD, Knol JA, De Remer SJ, Yang Z, Stetson PL. Regional pharmacokinetics of 5-fluorouracil in dogs: role of the liver, gastrointestinal tract, and lungs. *Cancer Res* 1998; **58**: 1688-1694

13 **Schlemmer HP**, Becker M, Bachert P, Dietz A, Rudat V, Vanselow B, Wollensack P, Zuna I, Knopp MV, Weidauer H, Wannenmacher M, Van Kaick G. Alterations of intratumoral pharmacokinetics of 5-fluorouracil in head and neck carcinoma during simultaneous radiochemotherapy. *Cancer Res* 1999; **59**: 2363-2369

14 **Saltzman WM**, Fung LK. Polymeric implants for cancer chemotherapy. *Adv Drug Deliv Rev* 1997; **26**: 209-230

15 **Dash AK**, Cudworth GC 2nd. Therapeutic applications of implantable drug delivery systems. *J Pharmacol Toxicol Methods* 1998; **40**: 1-12

16 **Takahashi T**. Development and clinical application of drug delivery systems for cancer treatment. *Int J Clin Oncol* 2002; **7**: 206–218

17 **Einmahl S**, Zignani M, Varesio E, Heller J, Veuthey JL, Tabatabay C, Gurny R. Concomitant and controlled release of dexamethasone and 5-fluorouracil from poly(ortho ester). *Int J Pharm* 1999; **185**: 189-198

18 **Itokazu M**, Kumazawa S, Wada E, Wenyi Y. Sustained release of adriamycin from implanted hydroxyapatite blocks for the treatment of experimental osteogenic sarcoma in mice. *Cancer Lett* 1996; **107**: 11-18

19 **Ramchandani M**, Robinson D. *In vitro* and *in vivo* release of ciprofloxacin from PLGA 50:50 implants. *J Control Release* 1998; **54**: 167-175

20 **Wang G**, Tucker IG, Roberts MS, Hirst LW. *In vitro* and *in vivo* evaluation in rabbits of a controlled release 5-fluorouracil subconjunctival implant based on poly (d, L-lactide-co-glycolide). *J Control Release* 1998; **54**: 167-175

21 **Kong Q**, Kleinschmidt-Demasters BK, Lillehei KO. Intralesionally implanted cisplatin cures primary brain tumor in rats. *J Surg Oncol* 1997; **64**: 268-273

22 **Kitchell BK**, Orenberg EK, Brown DM, Hutson C, Ray K, Woods L, Luck E. Intralesoinal sustained-release chemotherapy with therapeutic implants for treatment of canine sun-induced squamous cell carcinoma. *Eur J Cancer* 1995; **31**: 2093-2098

23 **Ning S**, Yu N, Brown DM, Kanekal S, Knox SJ. Radiosensitization by intratumoral administration of cisplatin in a sustained-release drug delivery system. *Radiother Oncol* 1999; **50**: 215-223

24 **Maeda M**, Moriuchi S, Sano A, Yoshimine T. New drug delivery system for water-soluble drugs using silicone and its usefulness for local treatment: application of GCV-silicone to GCV / HSV-tk gene therapy for brain tumor. *J Control Release* 2002; **84**: 15-25

25 **Smith JP**, Kanekal S, Patawaran MB, Chen JY, Jones RE, Orenberg EK, Yu NY. Drug retention and distribution after intratumoral chemotherapy with fluorouracil / epinephrine injectable gel in human pancreatic cancer xenografts. *Cancer Chemother Pharmacol* 1999; **44**: 267-274

26 **Tang WX**, Cheng PY, Luo YP, Wang RX. Interaction between cisplatin, 5-fluorouracil and vincristine on human hepatoma cell line (7721). *World J Gastroenterol* 1998; **4**: 418-420

27 **Deng LY**, Zhang YH, Xu P, Yang SM, Yuan XB. Expression of IL 1beta converting enzyme in 5-FU induced apoptosis in esophageal carcinoma cells. *World J Gastroenterol* 1999; **5**: 50-52

28 **Jin J**, Huang M, Wei HL, Liu GT. Mechanism of 5-fluorouracil required resistance in human hepatocellular carcinoma cell line Bel(7402). *World J Gastroenterol* 2002; **8**: 1029-1034

29 **Smith JP**, Stock E, Orenberg EK, Yu NY, Kanekal S, Brown DM. Intratumoral chemotherapy with a sustained-release drug delivery system inhibits growth of human pancreatic cancer xenografts. *Anticancer Drugs* 1995; **6**: 717-726

30 **Harper E**, Dang W, Lapidus RG, Garver RI Jr. Enhanced efficacy of a novel controlled release paclitaxel formulation (PACLIMER Delivery System) for local-regional therapy of lung cancer tumor nodules in mice. *Clin Cancer Res* 1999; **5**: 4242-4248

31 **Williams JA**, Dillehay LE, Tabassi K, Sipos E, Fahlman C, Brem H. Implantable biodegradable polymers for IUdR radiosensitization of experimental human malignant glioma. *J Neurooncol* 1997; **32**: 181-192

32 Yuan X, Fahlman C, Tabassi K, Williams JA. Synthetic, implantable, biodegradable polymers for controlled release of radiosensitizers. *Cancer Biother Radiopharm* 1999; **14**: 177-186

Edited by Zhang JZ and Wang XL

P.O.Box 2345, Beijing 100023,China
Fax: +86-10-85381893
E-mail: wjg@wjgnet.com www.wjgnet.com

World J Gastroenterol 2003;9(8):1799-1803
World Journal of Gastroenterology
 ISSN 1007-9327

• BASIC RESEARCH •

TLR4 mediates LPS-induced HO-1 expression in mouse liver: Role of TNF-α and IL-1β

Yong Song, Yi Shi, Li-Hua Ao, Alden H. Harken, Xian-Zhong Meng

Yong Song, Yi Shi, Department of Respiratory Diseases, Nanjing Jinling Hospital, School of Medicine, Nanjing University, Nanjing 210002, Jiangsu Province, China
Li-Hua Ao, Alden H. Harken, Xian-Zhong Meng, Department of Surgery, Box C-320, Health Sciences Center, University of Colorado, 4200 E. 9th Avenue, Denver, CO 80262, USA
Correspondence to: Yong Song, M.D., Ph D., Department of Respiratory Diseases, Nanjing Jinling Hospital, School of Medicine, Nanjing University, Nanjing 210002, Jiangsu Province, China. yong_song6310@yahoo.com
Telephone: +86-25-4810453 **Fax:** +86-25-4809843
Received: 2003-01-18 **Accepted:** 2003-03-03

Abstract

AIM: Heme oxygenase (HO)-1 catalyzes the conversion of heme to biliverdin, iron and carbon monoxide. HO-1 is induced by many stimuli including heme, Hb, heat stress, lipopolysaccharide (LPS) and cytokines. Previous studies demonstrated that LPS induced HO-1 gene activation and HO-1 expression in liver. However, the mechanisms of LPS-induced HO-1 expression in liver remain unknown. The effect of toll-like receptor-4 (TLR4) on LPS-induced liver HO-1 expression and the role of TNF-α and IL-1β in this condition were determined.

METHODS: HO-1 expression was determined by immunofluorescent staining and immunoblotting. Double immunofluorescent staining was performed to determine the cell type of HO-1 expression in liver.

RESULTS: A low dose of LPS significantly increased HO-1 expression in the liver which was localized in Kupffer cells only. Furthermore, HO-1 expression was enhanced by three doses of LPS. HO-1 expression was significantly inhibited in the liver of TLR4 mutant mice. While the liver HO-1 expression in TNF KO mice was much lower than that in C57 mice following the same LPS treatment, IL-1β KO had a slight influence on liver HO-1 expression following LPS treatment.

CONCLUSION: The present results confirm that macrophages are the major source of HO-1 in the liver induced by LPS. This study demonstrates that TLR4 plays a dominant role in mediating HO-1 expression following LPS. LPS-induced HO-1 expression is mainly mediated by endogenous TNF-α, but only partially by endogenous IL-1β.

Song Y, Shi Y, Ao LH, Harken AH, Meng XZ. TLR4 mediates LPS-induced HO-1 expression in mouse liver: Role of TNF-α and IL-1β. *World J Gastroenterol* 2003; 9(8): 1799-1803
http://www.wjgnet.com/1007-9327/9/1799.asp

INTRODUCTION

Heme oxygenase (HO) catalyzes the degradation of heme into biliverdin, iron and carbon monoxide[1-3]. Heme oxygenase has three known isoforms that consist of the inducible isoform heme oxygenase-1 (HO-1), the constitutive isoform heme oxygenase-2 and heme oxygenase-3. HO-1 is induced not only by its substrate, hemin, but also by oxidative stress, heat stress, UV irradiation, heavy metals, lipopolysaccharide (LPS) and cytokines[4-8]. This diversity of HO-1 inducers has provided further support for the speculation that HO-1 may play a vital function in maintaining cellular homeostasis, and some studies suggest that HO-1 can serve as a key biological molecule in the adaptation and/or defense against oxidative stress.

LPS is generally regarded as a key initiating factor in the pathogenesis of septic shock, and it stimulates inflammatory cells to produce cytokines, and other inflammatory mediators. HO-1 is induced by LPS in some cultured cell models *in vitro*[4,9], and also in lungs[10], kidneys and spleen[11,12] *in vivo*. It has been reported that HO-1 is induced in the liver after administration of LPS[11,13,14], but little is known about the mechanism of LPS-induced HO-1 expression in liver.

Studies have demonstrated that LPS induces cellular response by the signaling molecules belonging to the Toll-like receptor (TLR) family[15]. So far, six members (TLR1-6) have been reported and two of these, TLR2 and TLR4, have been shown to be essential for the recognition of distinct bacterial cell wall components[15,16]. TLR4 recognizes LPS, lipoteichoic acid and Taxol[17-19]. Recently, it was demonstrated that TLR4 mediated heat shock protein 60 signaling[20]. Although TLR4 is clearly critical to LPS signaling, the role of TLR4 in LPS-induced HO-1 expression has remained unclear. TLR4 mutation attenuates LPS-induced NF-κB activation and the production of cytokines[21,22]. Previous studies showed that cytokines, TNF-α, IL-α, or IL-1β induced HO-1 expression *in vitro*[8,23,24]. Do endogenous cytokines, TNF-α and IL-1β play a role in LPS-induced HO-1 expression?

The purposes of this study were to examine: the time course and localization of HO-1 expression in the liver by LPS stimulation, the role of TLR4 in LPS-induced liver HO-1 expression, whether LPS-induced HO-1 expression is dependent on TNF-α, and whether IL-1β plays a role in LPS-induced HO-1 expression.

MATERIALS AND METHODS

Animals

Male mice of the C57 BL/6, BALB/cJ and C.C3H-Tlr4Lps-d (TLR4 mutant) aged 8-10 weeks were obtained from Jackson Laboratory (Bar Harbor, ME). TNF-α knockout (TNF KO) mice of the same age range were generous gifts from Dr. David Riches of National Jewish Medical and Research Center (Denver, CO). IL-1β knockout (IL-1KO) mice were obtained from National Jewish Medical and Research Center (Denver, CO). The mice were kept on a 12-h light/dark cycle with free access to food and water. All animal experiments were approved by the University of Colorado Health Science Center Animal Care and Research Committee. During experiments, all the animals received humane care in compliance with the "Guide for the Care and Use of Laboratory Animals" [DHEW Publication No. (NIH) 85-23, revised in 1985, Office of Science and Health Reports, DRR/NIH, Bethesda, MD 20205].

Chemicals and reagents

Rabbit polyclonal antibody to HO-1 and the recombinant rat HO-1 were purchased from StressGen Biotechnologies Corp (Victoria, BC, Canada). Rat monoclonal antibody to mouse CD 68 was purchased from Serotec (Oxford, UK). Rat IgG and Cy3-conjugated goat anti-rabbit IgG were purchased from Jackson ImmunoResearch Laboratories (West Grove, PA). Fluorescein-conjugated wheat germ agglutinin was obtained from Molecular Probes (Eugene, OR). LPS (Escherichia coli, O55:B5) and all other chemicals were obtained from Sigma (St Louis, MO).

Experimental protocols

To determine HO-1 expression in the liver, the mice received either LPS (0.5 mg/kg) or normal saline by tail vein injection. To determine a time course of HO-1 expression, a single dose, two or three doses of LPS were used in each every 24 hours. After anesthesia and heparinization (40 mg/kg of pentobarbital sodium, ip), the liver tissue samples were prepared for the assessment of HO-1 expression. A portion of the liver tissue was embedded in a tissue-freezing medium and frozen in dry-ice-chilled isopentane. The remaining liver tissue was frozen in liquid nitrogen. All the samples were stored at -70 ℃ prior to use.

Immunofluorescent detection of HO-1 expression

Liver HO-1 expression was determined by immunofluorescent staining as previously described[25]. Tissue cryosections (5 μm thick) were prepared with a cryostat (IEC Minotome plus, Needham Heights, MA) and collected on poly-l-lysine-coated slides. All incubations were performed at room temperature. Sections were treated with a mixture of 70 % acetone and 30 % methanol for 5 min, and then fixed with 3 % paraformaldehyde for 20 min. Sections were washed with PBS, blocked with 10 % normal goat serum for 30 min, and incubated for 1 h with a polyclonal rabbit anti-HO-1 antibody (1:300 in PBS containing 1 % bovine serum albumin). Control sections were incubated with nonimmune rat IgG (5 mg/ml). After washed with PBS, sections were incubated with Cy3-conjugated goat anti-rabbit IgG (1:300 dilution with PBS containing 1 % bovine serum albumin). The cell surface was counterstained with fluorescein-conjugated wheat germ agglutinin, and the nucleus with *bis*-benzimide. The sections were mounted with aqueous media. Microscopic analysis was performed with a Leica DMRXA digital microscope (Germany) equipped with Slidebook software (I. I. I. Inc., Denver, CO).

Double immunofluorescent staining of HO-1 and macrophage

Double immunofluorescent staining was performed to determine the cell type stained positively of HO-1. CD68 (macrophages)-positive cells were studied. Tissue cryosections (5-μm thick) were prepared, fixed as described for staining of HO-1. Sections were blocked with 5 % normal goat serum + 5 % normal donkey serum for 30 min. Then slides were incubated for 1 h with a rat monoclonal antibody to mouse macrophages (CD68, 1:200) and rabbit polyclonal antibody to HO-1 (1:300). Control sections were incubated with non-immune rat IgG and rabbit IgG. After washed with PBS, the sections were incubated with Cy3-conjugated donkey anti-rat IgG (CD68) and FITC-conjugated goat anti-rabbit IgG (HO-1). The nucleus was counterstained with *bis*-benzimiade. The sections were washed with PBS, and then mounted on aqueous mounting media. Microscopic observation and photography were performed as described above.

Immunoblotting of HO-1

Liver tissue was homogenized with 4 volumes of homogenate buffer (PBS containing the protease inhibitor cocktail and 1 % Triton X100, pH 7.4), and centrifuged at 10 000×g for 20 min at 4 ℃. The resulting supernatant was collected and stored at -70 ℃ for immunoblotting of HO-1. Aliquots of protein (60 μg/lane) in the liver tissue homogenate were separated on a 4-20 % SDS-polyacrylamide gel (Bio-Rad, Hercules, CA). Separated proteins were blotted onto a nitrocellulose membrane (Bio-Rad, Hercules, CA), and equal loading was confirmed by densitometric assessment of protein band staining with Ponceau S solution. The membrane was rinsed in PBS and blocked for 1 h at room temperature with 5 % dry milk in PBS. The membrane was then incubated with a polyclonal rabbit anti-HO-1 antibody (1:1 000 dilution with 5 % dry milk in PBST) at room temperature for 1 h. Following an incubation with HRP-conjugated goat anti-rabbit IgG (1:10 000 dilution with 5 % dry milk in PBST), HO-1 bands were developed using ECL and visualized by exposure to Kodak X-Omat film (Eastman Kodak, Rochester, NY).

Statistical analysis

Data were expressed as mean ± standard error of the mean (SE). An analysis of variance (ANOVA) was performed with Statview 4.0 statistical analysis software (SAS Institute, Cary, NC), and a difference was accepted as significant if the P value was smaller than 0.05 as verified by the Bonferroni/ Dunn post hoc test.

RESULTS

Time course of liver HO-1 expression following LPS administration

Liver HO-1 expression in C57 mice after LPS administration was assessed by immunofluorescent staining and immunoblotting. HO-1 had low basal level expression in control liver by immunofluorescent staining (Figure 1A), but was barely detectable by immunoblotting (Figure 1B). A low dose (0.5 mg/kg) of LPS significantly increased HO-1 expression in the liver at 24 h after LPS administration. Furthermore, HO-1 expression was enhanced by three doses of LPS (Figure 1A and Figure 1B). The integrated intensity of HO-1 expression was significantly increased in liver of LPS-treated mice as compared with sham treatment mice (Figure 1C, $P<0.05$). However, cellular HO-1 level went down if animals were allowed to recover for 48 h following the last LPS injection, then gradually declined to control level at 72 h (data not shown).

Cell type involved in liver HO-1 expression

HO-1 protein was barely detectable in parenchymal liver cells following LPS stimulation, whereas high amounts of HO-1 were detectable in interstitial cells. To further characterize the cell types expressing HO-1, we attempted to localize the cell type(s) responsible for LPS-induced HO-1 expression in liver by double immunofluorescent staining. Rat anti-mouse CD68 monoclonal antibody and rabbit anti-HO-1 polyclonal antibody were used. We found that lower percentages of Kupffer cells exhibited positive staining for HO-1 in sham treatment. After three doses of LPS treatment, the majority of CD68 positive cells (>90 %) were HO-1 positive (Figure 2).

Effect of TLR4 on liver HO-1 expression

To examine the mechanism of regulation of liver HO-1 expression in response to LPS, we used C.C3H-Tlr4Lps-d mice, mice of TLR4 mutation. In BALB/cJ (wild type) mice, LPS-induced HO-1 expression in liver was comparable to C57 mice. In contrast, liver HO-1 expression in TLR4 mutant mice was significantly inhibited following the same treatment with LPS (Figure 3). These results suggested that mutation of

TLR4 exerted a dominant effect on liver HO-1 expression after LPS treatment.

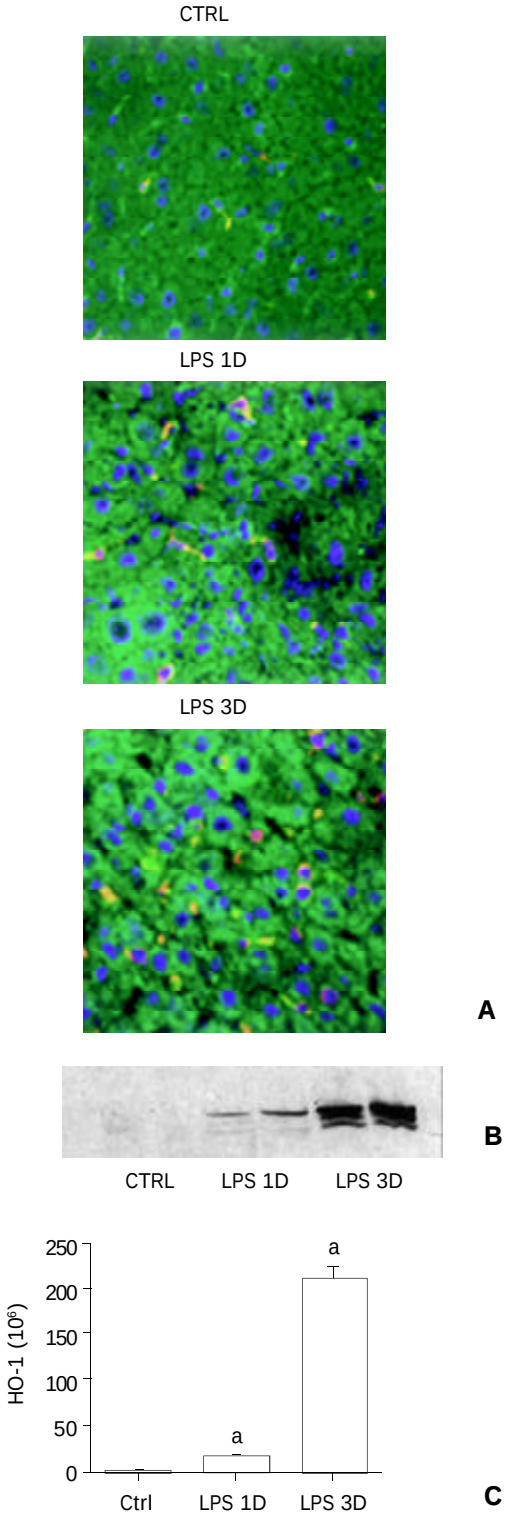

Figure 1 Liver HO-1 expression in wild type mice. A: Immunofluorescent detection of HO-1 in liver. After different doses of LPS or sham treatment, liver HO-1 expression of wild type (C57) mice were visualized by immunofluorescent staining with a specific rabbit polyclonal antibody against HO-1 followed by indocarbocyanine (Cy3)-conjugated anti-rabbit IgG (red). The cell surface was counterstained with fluorescein-conjugated wheat germ agglutinin (green), and the nucleus was counterstained with *bis*-benzimide (blue). HO-1 was present in liver of sham-treated animals (Ctrl). A single dose of LPS treatment increased liver HO-1 expression (LPS 1D). Furthermore, HO-1 expression was enhanced by three doses of LPS treatment (LPS 3D, magnification ×400). B: Immunoblotting detection of HO-1 in liver. C57 mice were treated with vehicle (Ctrl), single dose of LPS (LPS 1D) and three doses of LPS (LPS 3D). Liver tissue was homogenized, and immunoblotting analysis was performed. HO-1 protein was detected by immunoblotting with polyclonal rabbit antibody against HO-1. Data were representative of at least 2 experiments. C: Immunofluorescent staining to quantitate HO-1 expression. Liver HO-1 expression was determined by immunofluorescent staining. Integrated intensity of HO-1 positive signal was masked and quantified by using Slidebook software (I. I. I. Inc., Denver, CO). $^aP<0.05$ *vs.* sham.

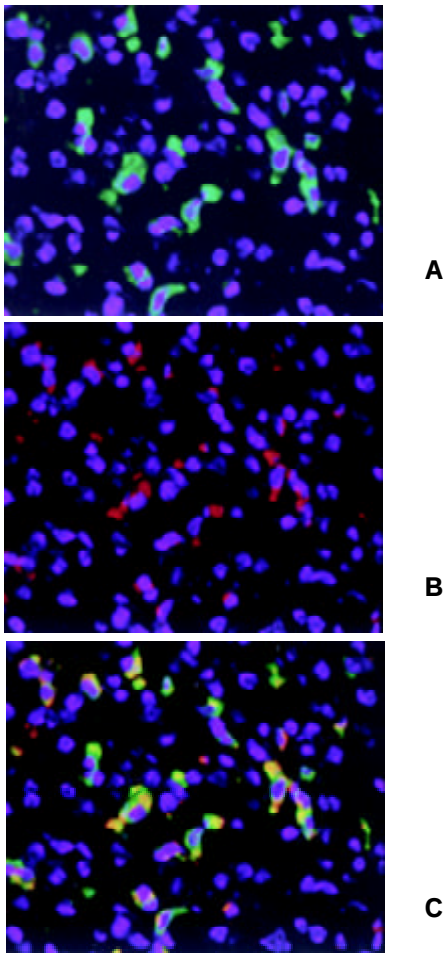

Figure 2 Double immunofluorescent staining of HO-1 localization in liver. After three doses of LPS treatment, HO-1 and CD68 in liver tissue were detected by double immunofluorescent staining with polyclonal rabbit antibody against HO-1 followed by FITC-conjugated anti-rabbit IgG (green) and monoclonal rat antibody against mouse CD68 followed by Cy3-conjugated anti-rat IgG (red). Cell nuclei were counterstained with *bis*-benzimide (blue). A: HO-1; B: Macrophages (Kupffer cells); C: HO-1 + Macrophages. magnification ×400.

Effect of TNF knockout on HO-1 expression

LPS is a potent inducer of TNF-α. Recent evidence suggests that LPS-induced TNF-α production is mediated through TLR4. Previous study demonstrated that TNF-α induced HO-1 expression in endothelial cells. Does TNF-α play an important role in LPS-induced HO-1 expression in liver? To examine the mechanism of regulation of liver HO-1 expression in response to LPS, we used C.C3H-Tlr4Lps-d mice, mice of TLR4 mutation. In BALB/cJ (wild type) mice, LPS-induced HO-1 expression in liver was comparable to C57 mice. In contrast, liver HO-1 expression in TLR4 mutant mice was significantly inhibited following same treatment as wild type mice (Figure 3). These results suggested that TLR4 exerted a dominant effect on liver HO-1 expression following LPS treatment.

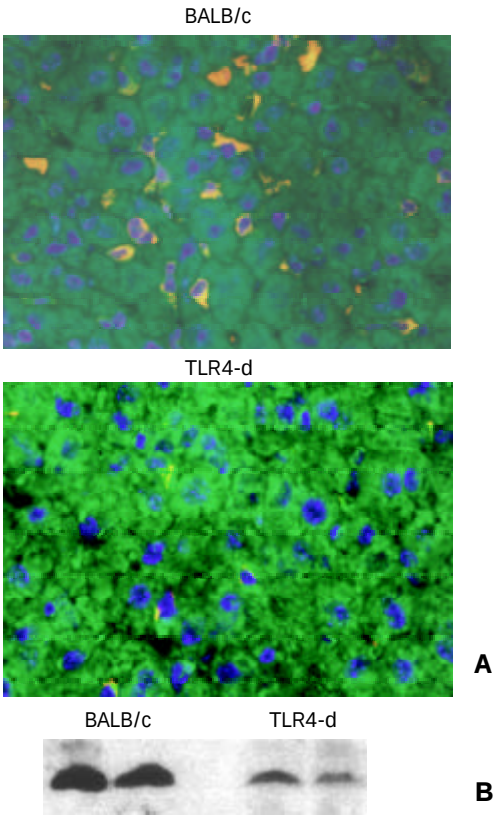

Figure 3 Effect of TLR4 mutation on liver HO-1 expression. A: Immunofluorescent detection of HO-1 in liver. After three doses of LPS treatment, liver HO-1 expression was visualized by immunofluorescent staining with a specific rabbit polyclonal antibody against HO-1, followed by indocarbocyanine (Cy3)-conjugated anti-rabbit IgG (red). The cell surface was counterstained with fluorescein-conjugated wheat germ agglutinin (green), and the nucleus was counterstained with *bis*-benzimide (blue). Liver HO-1 expression was abrogated in TLR4 mutated mice following LPS, but neither was influenced in BALB/c (control) mice (magnification ×400). B: Immunoblotting detection of HO-1 in liver. BALB/c and TLR4 mutated mice were treated with three doses of LPS. Liver tissue was homogenized, and immunoblotting analysis was performed. HO-1 protein was detected by immunoblotting with polyclonal rabbit antibody against HO-1. Data were representative of at least 2 experiments.

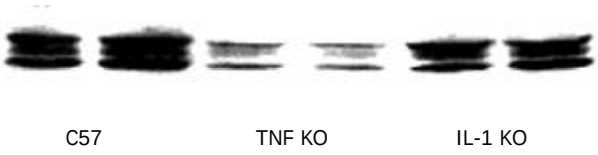

Figure 4 Effect of TNF KO and IL-1 KO on liver HO-1 expression. Immunoblotting detection of HO-1 in liver. C57, TNF KO and IL-1 KO mice were treated with three doses of LPS. Liver tissue was homogenized, and immunoblotting analysis was performed. HO-1 protein was detected by immunoblotting with polyclonal rabbit antibody against HO-1. Data were representative of at least 2 experiments.

Effect of IL-1b knockout on HO-1 expression

IL-1β is characteristically present in many inflammatory disorders. Although previous studies showed that IL-1β induced HO-1 expression *in vitro*, little is known about the role of endogenous IL-1β in LPS-induced HO-1 expression. We determined liver HO-1 expression in IL-1β KO mice. Mice were treated with LPS same as C57 mice. Compared with C57 mice, mice of IL-1β KO showed only a slight difference in liver HO-1 expression following LPS treatment (Figure 4), indicating that the expression of HO-1 following LPS was partially mediated by endogenous IL-1β.

DISCUSSION

In this study, we found that a low dose of LPS significantly increased HO-1 expression only in macrophages of wild type mice. This effect was further enhanced by the same dose of LPS for 3 consecutive days. However, HO-1 expression was significantly inhibited in TLR4 mutant mice. While liver HO-1 expression in TNF KO mice was much lower than that in C57 mice following the same LPS treatment, IL-1 KO had a slight influence on liver HO-1 expression following LPS treatment. The present results confirmed that macrophages were the major source of HO-1 in the lungs and liver as induced by LPS. This study demonstrated that TLR4 played a dominant role in mediating HO-1 expression following LPS. LPS-induced HO-1 expression was mainly mediated by endogenous TNF, but only partially by endogenous IL-1.

HO-1 is the rate-limiting enzyme in heme catabolism, and is also known as heat shock protein 32. Previous studies demonstrated that HO-1, besides its role in heme degradation, may also play a vital function in maintaining cellular homeostasis[26]. HO-1 is induced not only by its substrate, hemin, but also by oxidative stress, heat stress, UV irradiation, heavy metals, LPS and cytokines[4-8]. It has also been reported that HO-1 is induced in liver after LPS administration[11,13,14]. But most of studies just determined the changes of HO-1 mRNA in liver. Little is known about the time course and localization of HO-1 protein expression in liver. We examined liver HO-1 expression following LPS. We found that HO-1 had a low basal level expression in normal mouse liver by immunofluorescent staining. A low dose of LPS significantly increased HO-1 expression in the liver at 24 h after LPS administration. HO-1 expression was enhanced by three doses of LPS. Induction of HO-1, however, went down when animals were allowed to recover 48 h following the last LPS injection, then gradually declined to the control level by 72 h (data not shown). These results indicate that LPS-induced HO-1 expression in liver is in a dose-dependent fashion. Furthermore, we detected and localized HO-1 using immunofluorescent double staining. Hepatocytes were involved in the removal of plasma hemoglobin and some studies suggested that LPS mediated HO-1 mRNA accumulation in hepatocytes[7,13]. Interestingly, in the present study, most of HO-1 positive signals were co-localized in Kupffer cells. This finding formed a contrast to those from other animal models by hemin and LPS treatment. It is possible that the differences of experimental design, i.e, different stimuli, doses, and animals may lead to different results. In addition, the method of HO-1 staining by others was different from ours, it could be a reason for different expression of HO-1 in liver. Kupffer cells are the first line defense and effector cells in liver inflammatory response. The present results confirm that Kupffer cells are the major source of HO-1 in liver induced by LPS. HO-1 expression in Kupffer cells may play a protective role by inducing an adaptive hepatocellular stress response after LPS stimulation.

Studies demonstrated that LPS induced a cellular response by the signaling molecules belonging to the Toll-like receptor family[15]. TLR4 has been shown to be essential for the recognition of LPS, lipoteichoic acid (LTA) and Taxol[17-19]. Recently, it was demonstrated that TLR4 mediated heat shock protein 60 signaling[20]. Although TLR4 is clearly critical to LPS signaling, the role of TLR4 in LPS-induced HO-1 expression has remained unclear. To examine the mechanism of regulation of liver HO-1 expression in response to LPS, we determined liver HO-1 expression in TLR4 mutant mice. Liver

HO-1 expression in TLR4 mutant mice was significantly inhibited following the same treatment as wild type mice. This result suggests that TLR4 exerts a dominant effect on liver HO-1 expression after LPS treatment.

TNF-α is a pleiotropic early response cytokine and is rapidly produced by LPS stimulation. To determine the role of TNF-α in HO-1 expression following LPS *in vivo*, we subjected TNF KO mice to the same treatment as C57 mice. This treatment could also result in liver HO-1 expression comparable to that in the liver of C57 mice. We found that liver HO-1 expression in TNF KO mice was much lower than that in C57 mice following the same LPS treatment. This result suggests that LPS induces HO-1 expression mainly through endogenous TNF.

As an important inflammatory cytokine, IL-1 (IL-1α and IL-1β) induces HO-1 expression in endothelial cells and pancreatic islets[23-28]. Toll-like receptors belong to the IL-1 receptor family containing repeated leucine-rich motifs in their extracellular portion and are linked to a signaling pathway that involves the IL-1-receptor-associated kinase and NF-κB. It is likely that IL-1-induced HO-1 expression is mediated by TLR4. But it is unclear about the role of endogenous IL-1 in LPS-induced liver HO-1 expression. So, in the present study, IL-1 KO mice were used to determine liver HO-1 expression following LPS induction. Mice were treated with LPS the same as C57 mice. Compared with C57 mice, IL-1β KO has a slight influence on liver HO-1 expression following LPS treatment of IL-1β KO mice, indicating that the expression of HO-1 following LPS is partially mediated by endogenous IL-1β.

Taken together, the current study *in vivo* showed that TLR4 mutation attenuated LPS-induced HO-1 production in tissues. This provides a strong support to the hypothesis that TLR4 plays an important role in HO-1 signals. However, some aspects of its action remain unknown. What are the down stream signals of TLR4? In this context, future investigations are necessary to determine the signal transduction pathway of HO-1 expression induced by LPS.

REFERENCES

1 **Maines, MD.** The heme oxygenase system: a regulator of second messenger gases. *Annu Rev Pharmacol Toxicol* 1997; **37**: 517-554

2 **Maines, MD.** Heme oxygenase: function, multiplicity, regulatory mechanisms, and clinical applications. *FASEB J* 1988; **2**: 2557-2568

3 **Otterbein LE,** Choi AM. Heme oxygenase: colors of defense against cellular stress. *Am J Physiol Lung Cell Mol Physiol* 2000; **279**: L1029-L1037

4 **Camhi SL,** Alam J, Otterbein L, Sylvester SL, Choi AM. Induction of heme oxygenase-1 gene expression by lipopolysaccharide is mediated by AP-1 activaion. *Am J Respir Cell Mol Biol* 1995; **13**: 387-398

5 **Choi AM,** Alam J. Heme oxygenase-1: Function, regulation, and implication of a novel stress-inducible protein in oxidant-induced lung injury. *Am J Respir Cell Mol Biol* 1996; **5**: 9-19

6 **Keyse SM,** Tyrrell RM. Heme oxygenase is the major 32-kDa stress protein induced in human skin fibroblasts by UVA radiation, hydrogen peroxide, and sodium arsenite. *Proc Natl Acad Sci USA* 1989; **86**: 99-103

7 **Otterbein L,** Sylvester SL, Choi AM. Hemoglobin provides protection against lethal endotoxemia in rats: the role of heme oxygenase-1. *Am J Respir Cell Mol Biol* 1995; **13**: 595-601

8 **Terry CM,** Clikeman JA, Hoidal JR, Callahan KS. Effect of tumor necrosis factor-α and interleukin-1α on heme oxygenase-1 expression in human endothelial cells. *Am J Physiol* 1998; **274**(3Pt 2): H883-H891

9 **Camhi SL,** Alam J, Wiegand GW, Chin BY, Choi AM. Transcriptional activation of the HO-1 gene by lipopolysacchsride is mediated by 5' distal enhancers: role of reactive oxygen intermediates and AP-1. *Am J Respir Cell Mol Biol* 1998; **18**: 226-234

10 **Carraway MS,** Ghio AJ, Taylor JL, Piantadosi CA. Induction of ferritin and heme oxygenase-1 by endotoxin in the lung. *Am J Physiol* 1998; **275** (3Pt 1): L583-L592

11 **Oshiro S,** Takeuchi H, Matsumoto M, Kurata S. Transcriptional activation of heme oxygenase-1 gene in mouse spleen,liver and kidney cells after treatment with lipopolysacchride or hemoglobin. *Cell Biol Int* 1999; **23**: 465-474

12 **Suzuki T,** Takahashi T, Yamasaki A, Fujiwara T, Hirakawa M, Akagi R. Tissue-specific gene expression of heme oxygenase-1 (HO-1) and non-specific delta-aminolevulinate synthase (ALAS-N) in a rat model of septic multiple organ dysfunction syndrome. *Biochem Pharmacol* 2000; **60:** 275-283

13 **Bauer I,** Wanner GA, Rensing H, Alte C, Miescher EA, Wolf B, Pannen BH, Clemens MG, Bauer M. Expression pattern of heme oxygenase isoenzymes 1 and 2 in normal and stress-exposed rat liver. *Hepatology* 1998; **27**: 829-838

14 **Rizzardini M,** Zappone M, Villa P, Gnocchi P, Sironi M, Diomede L, Meazza C, Monshouwer M, Cantoni L. Kupffer cell depletion partially prevents hepatic heme oxygenase 1 messenger RNA accumulation in systemic inflammation in mice: role of interleukin 1beta. *Hepatology* 1998; **27**: 703-710

15 **Means TK,** Golenbock DT, Fenton MJ. The biology of toll-like receptors. *Cytokine Growth Factor Rev* 2000; **11**: 219-232

16 **Medvedev AE,** Kopydlowski KM, Vogel SN. Inhibition of lipopolysaccharide-induced signal transduction in endotoxin-tolerized mouse macrophages: dysregulation of cytokine, chemokine, and toll-like receptor 2 and 4 gene expression. *J Immnuol* 2000; **164**: 5564-5574

17 **Kawasaki K,** Akashi S, Shimazu R, Yoshida T, Miyake K, Nishijima M. Mouse toll-like receptor 4 MD-2 complex mediates lipopolysaccharide-mimetic signal transduction by Taxol. *J Biol Chem* 2000; **275**: 2251-2254

18 **Means TK,** Lien E, Yoshimura A, Wang S, Golenbock DT, Fenton MJ. The CD14 ligands lipoarabinomannan and lipopolysaccharide differ in their requirement for toll-like receptors. *J Immunol* 1999; **163**: 6748-6755

19 **Takeuchi O,** Hoshino K, Kawai T, Sanjo H, Takada H, Ogawa T, Takeda K, Akira S. Differential roles of TLR2 and TLR4 in recognition of gram-negative and gram-positive bacterial cell wall components. *Immunity* 1999; **11**: 443-451

20 **Ohashi K,** Burkart V, Flohe S, Kolb H. Cutting edge: heat shock protein 60 is a putative endogenous ligand of the toll-like receptor-4 complex. *J Immunol* 2000; **164**: 558-561

21 **Means TK,** Jones BW, Schromm AB, Shurtleff BA, Smith JA, Keane J, Golenbock DT, Vogel SN, Fenton MJ. Differnetial effects of a toll-like receptor antagonist on mycobacterium tuberculosis-induced macrophage response. *J Immunol* 2001; **166**: 4074-4082

22 **Nill MR,** Oberyszyn TM, Ross MS, Oberyszyn AS, Robertson FM. Temporal sequence of pulmonary cytokine gene expression in response to endotoxin in C3H / HeN endotoxin-sensitive and C3H / HeJ endotoxin-resistant mice. *J Leukoc Biol* 1995; **58**: 563-574

23 **Terry CM,** Clikeman JA, Hoidal JR, Callahan KS. TNF-α and IL-1α induce heme oxygenase-1 via protein kinase C, Ca^{2+}, and phospholipase A2 in endothelial cells. *Am J Physiol* 1999; **276**(5Pt 2): H1493-H1501

24 **Ye J,** Laychock SG. A protective role for heme oxygenase expression in pancreatic islets exposed to interleukin-1b. *Endocrinology* 1998; **139**: 4155-4163

25 **Song Y,** Ao L, Calkins CM, Raeburn CD, Harken AH, Meng X. Differential cardiopulmonary recruitment of neutrophils during hemorrhagic shock: a role for ICAM-1? *Shock* 2001; **16**: 444-448

26 **Horvath I,** MacNee W, Kelly FJ, Dekhuijzen PNR, Phillips M, Doring G, Choi AMK, Yamaya M, Bach FH, Willis D, Donnelly LE, Chung KF, Barnes PJ. "Haemoxygenase-1 induction and exhaled markers of oxidative stress in lung diseases", summary of the ERS research seminar in Budapest, Hungary, September,1999. *Eur Respir J* 2001; **18**: 420-430

27 **Kyokane T,** Norimizu S, Taniai H, Yamaguchi T, Takeoka S, Tsuchida E, Naito M, Nimura Y, Ishimura Y, Suematsu M. Carbon monoxide from heme catabolism protects against hepatobiliary dysfunction in endotoxin-treated rat liver. *Gastroenterology* 2001; **120**: 1227-1240

28 **West MA,** Bennet T, Seatter SC, Clair L, Bellingham J. LPS pretreatment reprograms macrophage LPS-stimulated TNF and IL-1 release without protein tyrosine kinase activation. *J Leukoc Biol* 1997; **61**: 88-95

Edited by Lu HM and Wang XL

P.O.Box 2345, Beijing 100023,China
Fax: +86-10-85381893
E-mail: wjg@wjgnet.com www.wjgnet.com

World J Gastroenterol 2003;9(8):1804-1807
World Journal of Gastroenterology
 ISSN 1007-9327

• BASIC RESEARCH •

Contractile effects and intracellular Ca^{2+} signalling induced by emodin in circular smooth muscle cells of rat colon

Tao Ma, Qing-Hui Qi, Wen-Xiu Yang, Jian Xu, Zuo-Liang Dong

Tao Ma, Qing-Hui Qi, Jian Xu, Zuo-Liang Dong, Department of Surgery, General Hospital of Tianjin Medical University, Tianjin 300052, China
Wen-Xiu Yang, Division of Biophysics, Department of Physics, Nankai University, Tianjin 300071, China
Supported by the National Natural Science Foundation of China, No.30171198
Correspondence to: Qing-Hui Qi, Department of Surgery, General Hospital of Tianjin Medical University, Tianjin 300052, China. mataoemail@yahoo.com.cn
Telephone: +86-22-84283767
Received: 2003-01-11 **Accepted:** 2003-03-10

Abstract

AIM: To investigate whether emodin has any effects on circular smooth muscle cells of rat colon and to examine the mechanism underlying its effect.

METHODS: Smooth muscle cells were isolated from the circular muscle layer of Wistar rat colon and the cell length was measured by computerized image micrometry. Intracellular Ca^{2+} ($[Ca^{2+}]i$) signalling was studied in smooth muscle cells using Ca^{2+} indicator Fluo-3 AM on a laser-scanning confocal microscope.

RESULTS: Emodin dose-dependently induced smooth muscle cells contraction. The contractile responses induced by emodin were inhibited by preincubation of the cells with ML-7 (an inhibitor of MLCK). Emodin caused a large, transient increase in $[Ca^{2+}]i$ followed by a sustained elevation in $[Ca^{2+}]i$. The emodin –induced increase in $[Ca^{2+}]i$ was unaffected by nifedipine, a voltage-gated Ca^{2+}-channel antagonist, and the sustained phase of the rising of $[Ca^{2+}]i$ was attenuated by extracellular Ca^{2+} removal with EGTA solution. Inhibiting Ca^{2+} release from ryanodine-sensitive intracellular stores by ryanodine reduced the peak increase in $[Ca^{2+}]i$. Using heparin, an antagonist of IP_3R, almost abolished the peak increase in $[Ca^{2+}]i$.

CONCLUSION: Emodin has a direct excitatory effect on circular smooth muscle cells in rat colon mediated via Ca^{2+}/CaM dependent pathways. Furthermore, emodin-induced peak $[Ca^{2+}]i$ increase may be attributable to the Ca^{2+} release from IP_3 sensitive stores, which further promote Ca^{2+} release from ryanodine-sensitive stores through CICR mechanism. Additionally, Ca^{2+} influx from extracellular medium contributes to the sustained increase in $[Ca^{2+}]i$.

Ma T, Qi QH, Yang WX, Xu J, Dong ZL. Contractile effects and intracellular Ca^{2+} signalling induced by emodin in circular smooth muscle cells of rat colon. *World J Gastroenterol* 2003; 9(8): 1804-1807

http://www.wjgnet.com/1007-9327/9/1804.asp

INTRODUCTION

Emodin (1, 3, 8-trihydroxy-6-methylanthraquinone) is an anthraquinone derivative isolated from *Rheum palmatum*[1]. Pharmaceutical preparations based on *Rheum palmatum* have been widely used in China for hundreds of years to treat gastrointestinal disorders[2-4]. The reported biological effects of emodin include antitumor, antibacterial and anti-inflammatory actions[5-7]. Emodin also possesses prokinetic effect on gastrointestinal smooth muscle. Stimulatory actions of emodin on gastrointestinal smooth muscle have been described in several studies, and emodin-induced contractions have been related to calcium ions[8-10]. However, the effects of emodin on the contractility of smooth muscle cells have not yet been explored. Thus, the present study was designed to determine whether emodin had any effects on circular smooth muscle cells of rat colon and to examine the mechanism underlying its effects.

MATERIALS AND METHODS

Materials

Fluo-3 AM (Molecular Probes,USA) was dissolved in DMSO (Sigma) and stored at -20 ℃. Pluronic F-127, collagenase type II, emodin, nifedipine, ryanodine, heparine, Egtazic acid (EGTA), trypsin inhibitor and HEPES were all purchased from Sigma Co. Ltd, USA. DMEM was purchased from GIBCO Co, USA, other chemicals were from LianXing BIO Co. Ltd (Beijing). Nifedipine, ryanodine and heparin were all dissolved in standard buffer and kept at 4 ℃.

Methods

Preparation of dispersed smooth muscle cells Smooth muscle cells were isolated from the circular muscle layer of Wistar rat colon as previously described with slight modifications[11]. Briefly, muscle strips were digested for 30 min at 31 ℃ in HEPES medium containing 0.1 % type II collagenase and 0.01 % trypsin inhibitor. The partly digested strips were washed with PBS, and muscle cells were allowed to disperse spontaneously for 30 min. The cells were harvested by filtration through 500 μm Nitex filter and centrifuged at 350 g for 10 min, and the filtrate (cell suspension) was equilibrated for 20 min before the experiment. For some experiments, cells were permeabilized with a brief exposure to saponin (75 μg/ml for 4 min) and equilibrated in a cytosolic buffer.

Measurement of muscle cell contraction Contraction was measured in smooth muscle cells by computerized image micrometry as described previously[12]. An aliquot consisting of 1×10^4 cells in 0.25 ml of medium was added to 0.1 ml of a solution containing the test agents. The reaction was interrupted at 1 min by adding 0.1 ml of acrolein at a final concentration of 0.1 %. Individual cell length was measured by computerized image micrometry. The average length of cells in the control state or after adding test agents was obtained from 50 cells randomly. The contractile response was defined as the decrease in the average length of the 50 cells and expressed in percentage as compared with control length.

Measurements of $[Ca^{2+}]i$ in smooth muscle cells Changes in $[Ca^{2+}]i$ were estimated by fluorescence measurement using

Ca^{2+} indicator Fluo-3 AM as described elsewhere[13], using a laser scanning confocal microscope(Radiance 2000; Bio-rad, Hertfordshire, UK).

Freshly dissociated smooth muscle cells were seeded onto glass coverslips and incubated with Fluo-3 working solution (Fluo-3 AM 5 μmol and Pluronic F-127 0.03 % dissolved in standard buffer) at 37 ℃ under an atmosphere of 5 % CO_2. After a loading period of 30 min, the cells were washed with PBS to remove extracellular Fluo-3 AM and incubated for an additional 20 min to allow complete desterilization of the cytosolic Fluo-3 AM.

Coverslips mounted on the chamber slide (Molecular Probe) were placed on the stage of the microscope. The fluorescence in the cell was excited at 488 nm by an argon-ion laser, emission at wavelength between 515-545 nm was detected by a photomultiplier. Changes in the Fluo-3 fluorescence intensity indicating fluctuations in cytosolic Ca^{2+} were recorded using T-series acquisition. After stable baseline fluorescence intensity was measured, 10 μl of an agent was added to extracellular medium to yield a 1/100 concentration, and the fluorescence intensity was recorded. The ratio representing the intracellular calcium variations related to the basal level was calculated. Baseline and sustained phases of agonist induced [Ca^{2+}]i were determined from the average of 5 data points. Peak [Ca^{2+}]i was determined from the average of 3 data points including the absolute maximum of the response.

Statistical analysis

Data represented means ± standard error of the mean. Values of *n* were the numbers of cells. Student' s *t*-test was performed and a *P*-value of less than 0.05 was considered statistically significant.

RESULTS

Effect of emodin on smooth muscle cell length

In resting state, the average length of isolated smooth muscle cells was 81.27±6.29 μm. The application of emodin to freshly isolated smooth muscle cells induced a reduction in cell length. This reduction in cell length reflected contraction of the smooth muscle cells. Emodin at concentrations of 5 to 100 μmol/L induced a concentration-dependent contraction (Figure 1). Maximal contraction of 17.26±3.51 % was observed with 50 μmol/L of emodin. In order to determine the signal mechanism underlying emodin-induced contraction, the effect of ML-7, an inhibitor of MLCK, on the cell contraction induced by emodin was examined. 36.61±4.69 % of the contractile response induced by 50 μmol/L emodin was inhibited by preincubation of the cells with ML-7(Figure 2).

Role of calcium in emodin-induced responses

The exposure of freshly isolated smooth muscle cells to emodin (50 μmol/L) induced an increase in [Ca^{2+}]i. The emodin-induced increase in [Ca^{2+}]i was a biphasic rise, consisting of a transient peak followed by a decline to steady-state level that remained significantly above baseline during scanning (Figures 3 and 4).

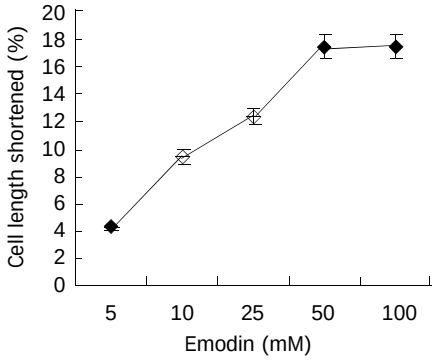

Figure 1 Contractile effect of emodin on isolated smooth muscle cell. Values were calculated as means ± SE from 3 experiments.

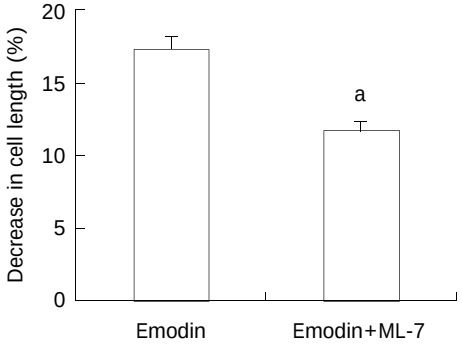

Figure 2 Effect of ML-7 on emodin-induced contraction of smooth muscle cells. Values were means ±SE of 3 experiments. [a]*P*<0.05 by Student's *t*-test.

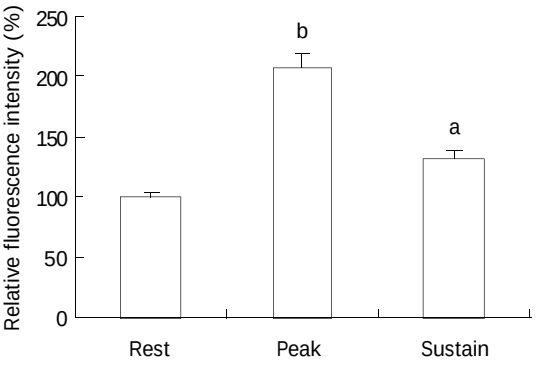

Figure 4 Average peak and sustained changes in [Ca^{2+}]i in response to emodin (50 μmol / L). [a]*P*<0.05, [b]*P*<0.001.

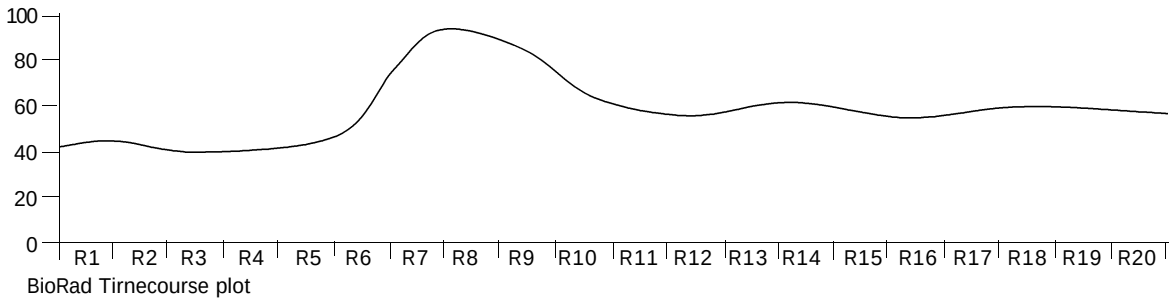

Figure 3 Timecourse changes of [Ca^{2+}]i induced by emodin in a circular colonic smooth muscle cells (analysed by BioRad Laserpix software).

To determine whether the emodin-induced increase in $[Ca^{2+}]i$ required calcium influx from extracellular medium, the effect of nifedipine, an antagonist of voltage-gated Ca^{2+} channel in response to emodin was investigated. Emodin was applied after 15 min-exposure to nifedipine. Exposing smooth muscle cells to nifedipine had no effect on the increase in $[Ca^{2+}]i$ induced by emodin ($P>0.05$). To further evaluate the role of extracellular Ca^{2+} influx to the emodin-induced rise in $[Ca^{2+}]i$, emodin was applied to cells incubation with Ca^{2+}-free extracellular solution. Removal of extracellular Ca^{2+} by EGTA solution significantly reduced the sustained changes in $[Ca^{2+}]i$ (Figure 4, $P<0.05$) compared with the sustained increase in $[Ca^{2+}]i$ induced by emodin, and had no effect on peak changes in $[Ca^{2+}]i$ (Figure 4, $P>0.05$).

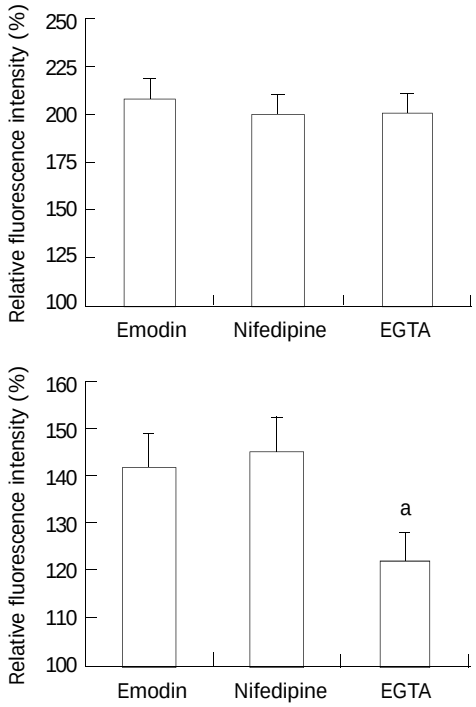

Figure 5 Average peak (top) and sustained (bottom) changes in $[Ca^{2+}]i$ in response to emodin under control conditions, in the presence of nifedipine, and EGTA solution. $n=15$. $^aP<0.05$ *vs* emodin group.

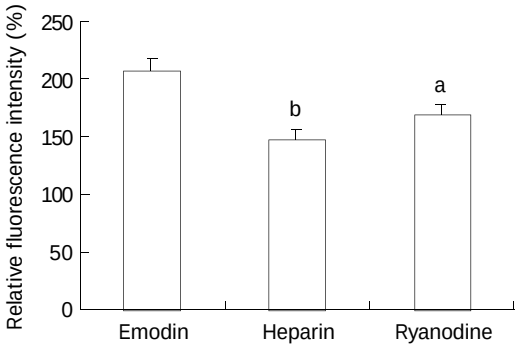

Figure 6 Effect of ryanodine and heparin on the change in $[Ca^{2+}]i$ induced by emodin. $n=15$ $^aP<0.05$ *vs* emodin group $^bP<0.01$ *vs* emodin group.

Because emodin-induced peak increase in $[Ca^{2+}]i$ was not affected by pretreatment with EGTA and nifedipine, the contribution of calcium release from the intracellular stores to the changes in $[Ca^{2+}]i$ in response to emodin was examined. Smooth muscle cells were pretreated for 10 min with ryanodine (10^{-5}M) to inhibit Ca^{2+} release from ryanodine-sensitive intracellular stores. Ryanodine markedly attenuated the peak increase in $[Ca^{2+}]i$ in response to emodin (Figure 5, $P<0.05$). In order to examine the role of IP_3 in emodin-induced increases in $[Ca^{2+}]i$, the effect of low molecular weight heparin, a specific IP_3 receptor antagonist was tested. Heparin did not diffuse across the plasma membrane, therefore, it was used in permeablized smooth muscle cells. In permeablized smooth muscle cells, the peak rise in $[Ca^{2+}]i$ induced by emodin was almost abolished by incubation with 10 μg/ml heparin (Figure 5).

DISCUSSION

The contractile effects of emodin on gastrointestinal smooth muscle have been described in several reports[8-10]. In this study, we have attempted to investigate the effects of emodin on circular smooth muscle cells of rat colon and to examine the mechanisms underlying its effects.

The result of this study showed that emodin had a direct contractile effect on smooth muscle cells freshly isolated from rat colon, as application of emodin resulted in a decrease in cell length. It was also found that exposure of smooth muscle cells to emodin induced an increase in $[Ca^{2+}]i$, and the rising in $[Ca^{2+}]i$ induced by emodin was a biphasic rise in $[Ca^{2+}]i$ consisting of a rapid, transient peak followed by a decline to sustained level that remained elevated than baseline. The involvement of calcium in emodin-induced contraction was in agreement with previous studies[9,10], reporting that emodin-induced contractions were related to calcium ion.

Calcium is believed to be the crucial signal for tension generation or shortening of smooth muscle cells[11-16]. The increase in $[Ca^{2+}]i$ induced by contractile agonists in smooth muscle cells is accompanied by Ca^{2+}/CaM-dependent activation of myosin light chain (MLC) kinase, leading to activation of myosin ATPase and cell contraction[14,17-19]. In these experiments, suppression of Ca^{2+}/CaM-dependent MLCK activity with ML-7 while maintaining Ca^{2+} mobilization partly inhibited emodin-induced cell contraction. This implies that Ca^{2+}/CaM-dependent MLCK signal pathway is involved in emodin-induced cell contraction.

Regulation of intracellular Ca^{2+} concentration ($[Ca^{2+}]i$) in smooth muscle cells involves multiple mechanisms[14,15,20]. Increases in $[Ca^{2+}]i$ can be resulted from either the transplasma membrane flux through plasma membrane Ca^{2+} channels or release of Ca^{2+} from intracellular stores, with a relative contribution from these two Ca^{2+} pools varying in different smooth muscle cells and in response to different stimuli[21-23]. The present study demonstrated that both Ca^{2+} influx and release of Ca^{2+} from intracellular sources contributed to the emodin-induced increase in $[Ca^{2+}]i$ in smooth muscle cells.

Removal of extracellular Ca^{2+} by EGTA solution caused a reduction of sustain phase of $[Ca^{2+}]i$ in response to emodin indicated extracellular Ca^{2+} contributed to the sustained elevation in $[Ca^{2+}]i$. Furthermore, compared with EGTA, blockade of L-type Ca^{2+} channel with nifedipine had no effect on the increase in $[Ca^{2+}]i$ induced by emodin. These results suggest that extracellular Ca^{2+} is essential for the sustain phase of $[Ca^{2+}]i$ and extracellular Ca^{2+} influx did not occur through L-type Ca^{2+} channel. These results also indicate that Ca^{2+} release from intracellular sources may be the main resources for the peak increases in $[Ca^{2+}]i$ induced by emodin.

Because pretreatment with EGTA and nifedipine had no effect on emodin-induced peak increase in $[Ca^{2+}]i$, it seemed likely that the portion of peak emodin-induced Ca^{2+} transient mainly depended on the calcium release from intracellular stores. The sarcoplasmic reticulum (SR) is the physiological intracellular source and sink of activator Ca^{2+} in smooth muscle cells[15,24]. The SR of smooth muscle is endowed with two different types of Ca^{2+} release channels, i.e. inositol 1, 4, 5-triphosphate receptors (IP_3Rs) and ryanodine receptors

(RyRs)[14,15,24-26]. Pretreating cells with ryanodine, a RyRs antagonist, attenuated but did not abolish the peak in $[Ca^{2+}]i$. In contrast, heparin, which inhibits the IP_3 binding to its receptor, almost abolished the peak component of the Ca^{2+} transient. These observations suggest that the residual Ca^{2+} peak observed in the presence of ryanodine is due to release of Ca^{2+} from IP_3-sensitive stores, and Ca^{2+} release through RyR receptors is possibly linked with the Ca^{2+}-induced Ca^{2+}-release (CICR). CICR means a process that a rise in $[Ca^{2+}]i$ resulted from extracellular Ca^{2+} influx or Ca^{2+} release from IP_3-sensitive store triggers further calcium release from RYR in the SR[14, 26-29]. Ryanodine receptors contain Ca^{2+} binding sites, allowing increased $[Ca^{2+}]i$ to initiate release from intracellular calcium stores[30,31]. CICR has been demonstrated to occur in a number of studies. On the basis of our findings, it appears to be operative in emodin-induced increase of $[Ca^{2+}]i$ in rat colonic smooth muscle cells.

Taken together, the results of this study indicate that emodin has a direct excitatory effect on circular smooth muscle cells from rat colon and its effect is mediated via Ca^{2+}/CaM-dependent MLCK signal pathway. The data suggest that the emodin-induced peak increases in $[Ca^{2+}]i$ primarily depend on Ca^{2+} release from IP_3 sensitive stores, which trigger Ca^{2+} release from ryanodine-sensitive stores through CICR mechanism. Additionally, Ca^{2+} influx from extracellular medium contributes to the sustained increase in $[Ca^{2+}]i$ observed in response to emodin.

ACKNOWLEDGE

We thank Professor Chang Chen for revising this article.

REFERENCES

1 **Liang JW**, Hsiu SL, Wu PP, Chao PD. Emodin pharmacokinetics in rabbits. *Planta Med* 1995; **61**: 406-408

2 **Xia Q**, Jiang JM, Gong X, Chen GY, Li L, Huang ZW. Experimental study of Tong Xia purgative method in ameliorating lung injury in acute necrotizing pancreatitis. *World J Gastroenterol* 2000; **6**: 115-118

3 **Chen H**, Wu X, Guan F. Protective effects of tongli gongxia herbs on gut barrier in rat with multiple organ dysfunction syndrome. *Zhongguo Zhongxiyi Jiehe Zazhi* 2000; **20**: 120-122

4 **You SY**, Wu XZ, Liu ML. Effects of dachengqi decoction on gut hormones and intestinal movement after cholecystectomy. *Zhongguo Zhongxiyi Jiehe Zazhi* 1994; **14**: 522-524

5 **Lee HZ**. Effects and mechanisms of emodin on cell death in human lung squamous cell carcinoma. *Br J Pharmacol* 2001; **134**: 11-20

6 **Lee HZ**. Protein kinase C involvement in aloe-emodin- and emodin-induced apoptosis in lung carcinoma cell. *Br J Pharmacol* 2001; **134**: 1093-1103

7 **Kuo YC**, Meng HC, Tsai WJ. Regulation of cell proliferation, inflammatory cytokine production and calcium mobilization in primary human T lymphocytes by emodin from Polygonum hypoleucum Ohwi. *Inflamm Res* 2001; **50**: 73-82

8 **Jin ZH**, Ma DL, Lin XZ. Study on effect of emodin on the isolated intestinal smooth muscle of guinea-pigs. *Zhongguo Zhongxiyi Jiehe Zazhi* 1994; **14**: 429-431

9 **Li JY**, Yang WX, Hu WW, Wang J, Jin ZG, Wang XY, Xu WS. Effects of emodin on the activity of K channel in guinea pig taenia coli smooth muscle cells. *Yaoxue Xuebao* 1998; **33**: 321-325

10 **Yang WX**, Wang J, Li JY, Yu Y, Xu WS. Characteristics of emodin evoked $[Ca^{2+}]i$ and inhibition of GDP in guinea pig taenia coli cells. *Shengwu Wuli Xuebao* 2001; **17**: 165-169

11 **Wang P**, Bitar KN. RhoA regulates sustained smooth muscle contraction through cytoskeletal reorganization of HSP27. *Am J Physiol* 1998; **275**(6Pt 1): 1454-1462

12 **Yamada H**, Strahler J, Welsh MJ, Bitar KN. Activation of MAP kinase and translocation with HSP27 in bombesin-induced contraction of rectosigmoid smooth muscle. *Am J Physiol* 1995; **269** (5Pt 1): 683-691

13 **Jacques D**, Sader S, El-Bizri N, Chouffani S, Hassan G, Shbaklo H. Neuropeptide Y induced increase of cytosolic and nuclear Ca^{2+} in heart and vascular smooth muscle cells. *Can J Physiol Pharmacol* 2000; **78**: 162-172

14 **Sanders KM**. Invited review: mechanisms of calcium handling in smooth muscles. *J Appl Physiol* 2001; **91**: 1438-1449

15 **Bolton TB**, Prestwich SA, Zholos AV, Gordienko DV. Excitation-contraction coupling in gastrointestinal and other smooth muscles. *Annu Rev Physiol* 1999; **61**: 85-115

16 **Makhlouf GM**, Murthy KS. Signal transduction in gastrointestinal smooth muscle. *Cell Signal* 1997; **9**: 269-276

17 **Sayeski PP**, Ali MS, Bernstein KE. The role of Ca^{2+} mobilization and heterotrimeric G protein activation in mediating tyrosine phosphorylation signaling patterns in vascular smooth muscle cells. *Mol Cell Biochem* 2000; **212**: 91-98

18 **Fan J**, Byron KL. Ca^{2+} signalling in rat vascular smooth muscle cells: a role for protein kinase C at physiological vasoconstrictor concentrations of vasopressin. *J Physiol* 2000; **524**(Pt 3): 821-831

19 **White C**, Mc Geown JG. Regulation of basal intracellular calcium concentration by the sarcoplasmic reticulum in myocytes from the rat gastric antrum. *J Physiol* 2000; **529**(Pt 2): 395-404

20 **Carl A**, Lee HK, Sanders KM. Regulation of ion channels in smooth muscles by calcium. *Am J Physiol* 1996; **271**(1Pt 1): 9-34

21 **McCarron JG**, Flynn ER, Bradley KN, Muir TC. Two Ca^{2+} entry pathways mediate $InsP_3$-sensitive store refilling in guinea-pig colonic smooth muscle. *J Physiol* 2000; **525**(Pt 1): 113-124

22 **Takeuchi M**, Watanabe J, Horiguchi S, Karibe A, Katoh H, Baba S, Shinozaki T, Miura M, Fukuchi M, Kagaya Y, Shirato K. Interaction between L-type Ca^{2+} channels and sarcoplasmic reticulum in the regulation of vascular tone in isolated rat small arteries. *J Cardiovasc Pharmacol* 2000; **36**: 548-554

23 **van Helden DF**, Imtiaz MS, Nurgaliyeva K, Von der Weid P, Dosen PJ. Role of calcium stores and membrane voltage in the generation of slow wave action potentials in guinea-pig gastric pylorus. *J Physiol* 2000; **524**(Pt 1): 245-265

24 **Flynn ER**, Bradley KN, Muir TC, McCarron JG. Functionally separate intracellular Ca^{2+} stores in smooth muscle. *J Biol Chem* 2001; **276**: 36411-36418

25 **Kotlikoff ML**, Wang YX, Xin HB, Ji G. Calcium release by ryanodine receptors in smooth muscle. *Novartis Found Symp* 2002; **246**: 108-119

26 **Ji G**, Barsotti RJ, Feldman ME, Kotlikoff MI. Stretch-induced calcium release in smooth muscle. *J Gen Physiol* 2002; **119**: 533-544

27 **Collier ML**, Ji G, Wang Y, Kotlikoff MI. Calcium-induced calcium release in smooth muscle: loose coupling between the action potential and calcium release. *J Gen Physiol* 2000; **115**: 653-662

28 **Morgan JM**, Gillespie JI. The modulation and characterisation of the Ca^{2+}-induced Ca^{2+} release mechanism in cultured human myometrial smooth muscle cells. *FEBS Lett* 1995; **369**: 295-300

29 **Henkel CC**, Asbun J, Ceballos G, del Carmen Castillo M, Castillo EF. Relationship between extra and intracellular sources of calcium and the contractile effect of thiopental in rat aorta. *Can J Physiol Pharmacol* 2001; **79**: 407-414

30 **Somlyo AP,** Somlyo AV. The sarcoplasmic reticulum: then and now. *Novartis Found Symp* 2002; **246**: 258-268

31 **Chambers P**, Neal DE, Gillespie JI. Ryanodine receptors in human bladder smooth muscle. *Exp Physiol* 1999; **84**: 41-46

Edited by Zhang JZ and Zhu LH

P.O.Box 2345, Beijing 100023,China
Fax: +86-10-85381893
E-mail: wjg@wjgnet.com www.wjgnet.com

World J Gastroenterol 2003;9(8):1808-1814
World Journal of Gastroenterology
 ISSN 1007-9327

• CLINICAL RESEARCH •

Relationship between telomerase activity and its subunit expression and inhibitory effect of antisense hTR on pancreatic carcinoma

Jia-Hua Zhou, Hong-Mei Zhang, Quan Chen, Dong-Dong Han, Fei Pei, Li-Shan Zhang, De-Tong Yang

Jia-Hua Zhou, Quan Chen, Dong-Dong Han, De-Tong Yang, Department of Biliary-pancreatic Surgery, Zhongda Hospital of Southeast University, Nanjing, Jiangsu Province, 210009, China
Hong-Mei Zhang, Li-Shan Zhang, Genetic Center, Southeast University, Nanjing, Jiangsu Province, 210009, China
Fei Pei, Department of General Surgery of Huangshi Central Hospital, Huangshi, Hubei Province, 435000, China
Supported by the Applied Basic Research Programs of Science and Technology Commission Foundation of Jiangsu Province, No BJ98080 (1998-2001)
Correspondence to: Jia-Hua Zhou, Department of Biliary-pancreatic Surgery, Zhongda Hospital Affiliated to Southeast University, 87 Dingjiaqiao, Nanjing 210009, Jiangsu Province, China. zhoujiahua@hotmail.com
Telephone: +86-25-3249268 **Fax:** +86-25-3272356
Received: 2002-10-08 **Accepted:** 2003-02-09

Abstract

AIM: To directly investigate the relationship between telomerase activity and its subunit expression and the inhibitory effect of antisense hTR on pancreatic carcinogenesis.

METHODS: We examined the telomerase activity and its subunit expression by cell culture, polymerase chain reaction (PCR), PCR-silver staining, PCR-ELISA, DNA sequencing, MTT and flow cytometry methods.

RESULTS: PCR-silver staining and PCR-ELISA methods had the same specificity and sensitivity as the TRAP method. Telomerase activity was detected in the extract of the 10^{th}, $20^{th}$and 30^{th} passages of P3 cells,while it was absent in fibroblasts. Furthermore, after the 30th generation, the proliferation period of fibroblast cells was significantly prolonged. Telomerase activity and hTERTmRNA were detected in two pancreatic carcinoma cell lines, but were found to be negative in human fibroblast cells. Telomerase activity and hTERTmRNA were tested in pancreatic carcinoma specimens of 24 cases. The telomerase activity was positive in 21 of the 24 cases (87.5 %), and the hTERTmRNA in 20 cases (83.3 %). In adjacent normal tissues positive rates were both 12.5 %. There was a significant difference between the two groups. This indicated a significant correlation between the expression level of telomerase activity and histologic differentiation, metastasis and advanced clinical stage of pancreatic carcinoma. Our findings showed that the expressions of hTR and TP1mRNA were not correlated with the activity of telomerase but the expression of hTERTmRNA was. After treatment with PS-ODNs, telomerase activity in P_3 cells weakened and the inhibiting effect became stronger with an increase in PS-ODNs concentration. There was a significant difference between different PS-ODN groups ($P<0.05$). Inhibition of telomerase activity occurred most significant with PS-ODN1.The results of the FCM test of pancreatic cancer P_3 cells showed an increase in the apoptotic rate with increasing PS-ODN1 and PS-ODN2 concentrations.

CONCLUSION: The expression of telomerase activity has a significant relationship to carcinogenesis. A strong correlation exists between telomerase activity and hTERTmRNA expression. The up-regulation of hTERTmRNA expression may play a critical role in human carcinogenesis. The expression of telomerase activity and its subunit level in pancreatic carcinoma significantly correlate with the clinical stage of pancreatic carcinoma and hence, may be helpful in its diagnosis and prognosis. The anti-hTR complementary to the template region of hTR is sufficient to inhibit P3 cell telomerase activity and cell proliferation *in vitro*, and can lead to a profound induction of programmed cell death.

Zhou JH, Zhang HM, Chen Q, Han DD, Pei F, Zhang LS, Yang DT. Relationship between telomerase activity and its subunit expression and inhibitory effect of antisense hTR on pancreatic carcinoma. *World J Gastroenterol* 2003; 9(8): 1808-1814
http://www.wjgnet.com/1007-9327/9/1808.asp

INTRODUCTION

Telomerase is a DNA-dependent RNA polymerase[1] carrying template features. It is different from reverse transcriptase, DNA polymerase of commonly pure proteins. The activated telomerase takes the 3' distal end of telomeres as the primer and its RNA component acts as the template. The protein component of telomerase regulates the catalytic activity in the synthesis of telomere repetitive sequence to maintain the telomere length. Human telomerase mainly consists of three subunits-human telomerase RNA (hTR), human telomerase-associated protein 1(TP_1) and human telomerase reverse transcriptase (hTERT). Telomerase activity has been found in most human tumor cells[2], while there is no evident expression in normal human tissues other than in germ cells, hemopoietic stem cells and cuticle basal cells[3,4]. This suggests that telomerase is a broad spectrum tumor marker[5-9]. It is recognized that activation of telomerase and stability of telomere length are necessary for tumor immortalization. However, it has been found that expression of hTERTmRNA is obviously related to telomerase activity. It is suggested that up-regulation of the expression level of hTERTmRNA is a key factor in the formation of tumor cells.

Human pancreatic cancer is one of the most frequent tumors. The present clinical treatment however has a low curative effect. The mortality rate of human pancreatic cancer is very high. Post-operative metastases are common and less than 3 % of patients have a survival rate of 5-years. In recent years, a close relationship has been found between telomerase and pancreatic cancer. By cell culture, PCR-silver staining, PCR-ELISA, RT-PCR, DNA sequencing technology, MTT and Flow cytometry methods, we have investigated the expression of telomerase activity and its subunits in pancreatic cancer cell line, fibroblasts, and in pancreatic cancer samples of 24 cases and their adjacent normal tissues. The purpose of this research was to explore the relationship between the biological behavior and clinico-pathological characteristics of human pancreatic cancer, as well as the inhibitory effects of hTR antisense oligonucleotide on pancreatic cancer cells.

MATERIALS AND METHODS

Cell lines and tissuse samples

In this study, the pancreatic cancer P_3 cells were provided by Peking Union Medical College Hospital, PaTu-8801 cells were provided by Shanghai Changhai Hospital, and the human skin fibroblasts were developed in the Zhongda Hospital. Cancer tissues and adjacent normal tissues from 24 patients with pancreatic cancer were provided and assayed by the Surgical Department of Zhongda Hospital Affiliated to Southeast University and Jiangsu Provincial People·s Hospital. These samples were frozen at -80 ℃ within 15 min after surgical removal and stored until use. Of the 24 patients, 13 were male and 12 female.Their age ranged between 55-74 years with an average of 63 years.

Cell culture

Culture of the pancreatic cancer P_3 cells and PaTu-8801 cells: P_3 cells and human skin fibroblasts were cultured in 1640 culture medium and PaTu-8801 cells in DMEM culture medium (high glucose content) with 10 % inactivated calf serum and all were put in 5 % CO_2 at 37 ℃ for generational culture at 100 % RH.

Telomerase assay

Telomerase extracts and assays of activity were done as TRAP method. Briefly frozen pancreatic tissue samples of approximately 200 mg were homogenized in 200 μl of lysis reagent containing 5 % CHPAS (3-(3-cholamidopropyl dimethyammonio)-1-propanesulfonate lysis buffer, Roche Co.). The cells obtained by cell culture were also treated with lysis reagent containing 5 % CHPAS (Roche Co.). After 30 min of incubation on ice,the lysates were centrifuged at 16 000×g (tissue) or 34 000×g (cell) for 20 min at 4 ℃, and the supernatants were rapidly frozen in liquid nitrogen and stored at -80 ℃ until use. In the extracts from frozen tissues, the concentration of protein was measured using the Coomassie brilliant blue method. BCA. Extracts of 293 cell line with telomerase activity were used as the standard, while extracts obtained by inactivation for 10 min at 94 ℃ or treated with RNase for 10 min at 37 ℃ were used as the negative control. For cell samples, aliquots corresponding to extracts derived from approximately 10^2, 10^3, 10^4, 10^5 cells were used for TRAP assay. Extracts of tissues containing 0.06, 0.6 and 6 μg of protein were used for TRAP assay. Each extract specimen was assayed in 25 μl reaction mixture (Roche Co assay kit containing dNTP, Taq enzyme, biotin tagged TS primer and CX primer) which was diluted to 50 μl with DEPC water solution. After 30 min incubation at 25 ℃ for telomerase-mediated extension of the TS primer, the reaction mixture was heated at 94 ℃ for 5 min and then subjected to 30 PCR cycles at 94 ℃ for 30 s, at 50 ℃ for 30 s and at 72 ℃ for 50 s and then extended for 10 min at 72 ℃. Firstly, the PCR product went through enzyme-linked immunosorbent assay (PCR-ELISA) containing DIG-labeled probes (Roche Co assay kit). After spectrophotometric determination, the absorbance value A(=A_{450}-A_{690}) was calculated. The result was positive if A >0.2. Secondly, the PCR product was electrophoresed on a 10 % polyacrylamide gel. The telomerase activity was positive if the specific band appeared. For each sample of pancreatic carcinoma tissue, the intensity of telomerase was graded according to the different contents of protein in the extract specimen. A sample intensity of telomerase was represented as (-) if the specimen containing 6 μg extracted protein was tested to be negative, or (+) if the specimen containing 6 μg extracted protein was tested positive. If both sample specimens containing 6 μg and 0.6 μg extracted protein were tested positive, while the specimen containing 0.06 μg extracted protein was tested to be negative, it was represented by (++), and (+++) if all three specimens containing 6 μg, 0.6 μg, and 0.06 μg extracted protein were tested positive[10].

Expression of the subunit of telomerase

Analysis of the expression of each telomerase subunit was performed by RT-PCR amplification[11-13]. hTERT mRAN was amplified by using the primer pair (145 bp): LT5 5' -CGGA AGAGTATCTGGAGCAA-3' , LT6 5' -GGATGAAGCGGA GTCTGGA-3' . TP1 mRAN was amplified by using the primer pair (340 bp), TP1.1 5' -TCAAGCCAAACCTGAATCTGAG-3' , TP1.2 5' -CCCCGAGTGAATCTTTCTACGC-3' . hTR was amplified by using the primer pair (134 bp): F3b 5' -TCTAACCCTAACTGAGAAGGGCGTAG-3' , R3c 5' -GTTTGCTCTAGAATGAACGGTGGAAG-3' . The efficiency of cDNA synthesis from each sample was estimated by PCR with glyceraldehyde-3-phosphate-dehydrogenase (GAPDH)-specific primers of (450 bp): K136 5' -CTCAGACACCATG GGGAAGGTGA-3' ,K137 5' -ATGATCTTGAGGCTG TTGTCATA-3' . cDNA was synthesized in 20 μl of reaction mixture containing 5×RT Buffer 4 μl, RNasin 0.5 μl, total RNA 1 μl, and MLV 0.8 μl with 1 μl random primers. The reaction mixture was incubated at 94 ℃ for 5 min before it was heated at 95 ℃ for 5 min to inactivate MLV. To amplify the cDNA 2 μl aliquots of the reversely-transcribed cDNA was subjected to 35 cycles of PCR in 50 μl containing 10×buffer (10 mM Tris-HCl (pH8.3), 25 mM $MgCl_2$, 500 mM KCl) 10 mM dNTP 1 μl, 25 mM $MgCl_2$ 2-3 μl, Taq enzyme 4 unit and 10 pM of specific primers 22 μ1. After heated at 94 ℃ for 5 min, each cycle consisted of de-naturation at 94 ℃ for 45 s, annealing at 56 ℃ for 45 s (hTERT) or at 61 ℃ for 45 s (hTR) or at 60 ℃ for 45 s (TP_1) and extension at 72 ℃ for 90 s and then extended at 72 ℃ for 10 min. PCR products were electrophoresed on 3 % agarose gel with ladder marker to determine the concentrations and purity of PCR amplified products. hTERTmRNA PCR products were sequenced (sent to Shanghai Biolottering Co, Ltd.).

Inhibitory effects of antisense hTR

Four nucleotides were synthesized as hTR template sequence (5' -CUAACCCUAAC-3') and modified by thiophosphoric acid. They were PS-ODN1: 5' -GTTAGG-3' (antisense), PS-ODN2: 5' -GTTAGGGTTAG-3' (antisense), PS-ODN3: 5' -CCTAAC-3' (pro-sense), and a PS-ODN4 with random sequence: 5' -AACTCGTAGTC-3' . After 5×10 P_3 cells and human fibroblasts were inoculated into culture bottles and replaced the old culture medium with a fresh one after 24-h-lasting cultivation, the cells stuck to the wall of bottle. The test group was arranged PS-ODN1, PS-ODN2, PS-ODN3, PS-ODN4 so that each had four concentrations, 3.16 μmol/L, 10 μmol/L, 31.6 μmol/L, and 100 μmo1/L. They were added into the culture bottles, respectively. Additional sets were the control groups which had no PS-ODN. The following tests were conducted when obvious change in cytomorphology was observed under the optical microscope. Firstly, P_3 and human fiber forming monolayer anchorage-dependent cells were digested. The suspended cells were cultured in RPMI 1640. After the suspended cell liquor was inoculated into a 96-cave culture board (100 μ1 per cave), 20 μ1 of freshly prepared 5 mg/ml MTT solution was added into each cave. This was incubated for 4 h at 37 ℃, the culture medium in the caves was discarded, and then dimethyl sulfoxide (DMSO) 150 μ1 was added into each cave to be shaken for 10 min to solve the crystal. The activity of succinic dehydrogenase (SDH) was determined according to the optical absorbance of the content in each cave at 540 μm in an enzyme-linked immunoassay analyzer. Secondly, after 2×10^6 P_3 cells were treated with each

of the different PS-ODNs, the activity of telomerase extracts was assayed according to the TRAP, PCR-ELISA and polyacrylamidedel gel (10 %) electrophoresis (PAGE). The telomerase extract of 293 cell line was taken as the positive control. The extract that was subjected to inactivation for 10 min at 94 ℃ or RNase treatment for 10 min at 37 ℃ was taken as the negative control. Finally, the single cell suspension was prepared by digesting anchorage-dependent cells after treatment with PS-ODN1 and PS-ODN2, respectively. It was cool-washed three times, and then centrifuged for 10 min at 2 000 rpm. After the supernatant was discarded and dried, precooled 95 % alcohol was added and the sample was placed into a refrigerator at 4 ℃ for 1 h, and then incubated with 10 μg/ml RNase at 4 ℃ for 3 h. The apoptotic rate and the cell cycle distribution of pancreatic cancer cells were analyzed by a flow cytometer (DB Corp. United States) after 1 ml propidium iodide comprehensive staining solution was added in an ice-bath for 15 min. Data were collected by Cellquest software and analyzed by Mmodift Lt software.

Statistic analysis

The data were processed by *t*-test and variance analysis. The *P* value was determined according to the *t* value, *F* value and FI value.

RESULTS

Cell culture

There were morphological changes in the fibroblasts (HE stain) of the 32nd generation, such as karyopyknosis, cytoplasmic concentration, and cell body shrinkage. No changes were found in P_3 cells. P_3 cells, and fibroblasts of the 10th, 20th, and 30th generations were used to detect the activity of telomerase in this test. All results were positive for P_3 cells, and negative for fibroblasts (Figure 1).

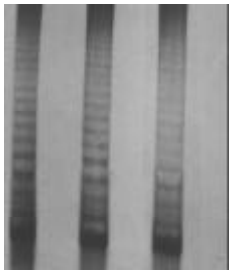

Figure 1 Telomerase activity of fibroblasts and P_3 cells of different generations (1, 3 and 5 were P_3 cells of the 10th, 20th, and 30th generations; 2, 4, and 6 were fibroblasts of the 10th, 20th, and 30th generations).

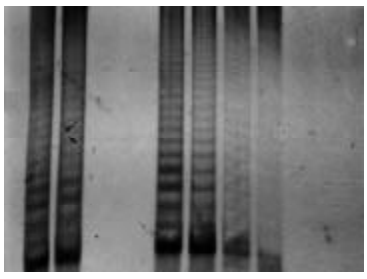

Figure 2 Specificity and sensitivity of telomerase activities in P3 cells (1, 293 cells as the positive control; 2,104 P_3 cells; 3, treated with RNase; 4, heat treated; 5, 6, 7, and 8 were 103, 102, 101, and 100 P_3 cells, respectively; 9, the lytic liquid).

Telomerase assay

The protein content was calculated from the sample extract, and standard curves were prepared by using the data. The protein contents in the sample extracts were determined by Coomassie brilliant blue method. PCR-silver staining method was used to detect the activities of telomerase in 10 cells or 1 μg protein extracted from a sample. PCR-ELISA method had a same sensitivity as PCR-silver staining (Figure 2).

The results were positive for the activity of telomerase in pancreatic cancer cells, and negative for fibroblasts. There were 21 cases whose telomerase activity was detected in the 24 pancreatic cancer tissues by PCR-ELISA or PCR silver staining. Four cases of them were (+++), 11 cases (++), and 6 cases (+). The rate of positive findings was 87.5 %. However, there were only 3 cases with telomerase activity (+) was found in adjacent normal tissues, with a positive rate of 12.5 % (Figure 3).

Figure 3a Telomerase activity of tumor and normal pancreas (T: tumor; N: normal).

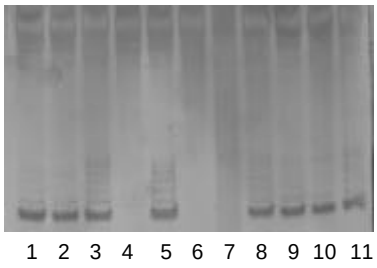

Figure 3b Semiquantitative telomerase activity of tumor and normal pancreas (1 2 3; 5 4 6; 9 10 11: T_{10}, T_{15} T_{18} 6 μg 0.6 μg 0.06 μg; 7: negative control, 8: positive control; T: tumor).

Detection of telomerase subunit

Pancreatic cancer cell P_3, and PaTu-8801 were taken as the positive control, while the fibroblast was taken as the negative control. There were 20 cases which expressed hTERTmRNA in cancer tissues of 24 cases, and 3 cases expressed hTERTmRNA in the adjacent normal tissues. 4 of 24 cases of cancer tissue did not express hTR and 3 cases of the adjacent normal tissues did not express hTR. Two cases tested were negative for TP_1 (Figure 4).

The cDNA sequencing of hTERTmRNA PCR products showed that there were 143 base groups that were significant sequences between the 51st and the 193rd base groups.The homology with hTERTcDNA reached 98.6 %, proving that the amplification products were the hTERTcDNA sequence amplified from hTERT.

Relationship between the expression of telomerase activities and its subunit with human pancreatic cancer, its biological behavior and clinico-pathological characteristics

Table 1 shows the relationship between telomerase activity

and tumor and adjacent normal tissue of pancreas.

Table 1 Telomerase activity of tumor and normal pancreas

	Cases	Telomerase activity	hTERTmRNA
Tumor	24	21[a]	20[b]
Normal	24	3	3

[a]P<0.01 (FI=28.82); [b]P<0.01 (FI=25.42).

There were significant differences in the expressions of telomerase activity and hTERTmRNA between pancreatic cancer tissues and adjacent normal tissues

Table 2 shows the relationship between telomerase activity and biological behavior of human pancreatic carcinoma.

Table 2 The relationship between telomerase activity and biological behavior of human pancreatic carcinoma

Biological behavior	Telomerase activity		
	–	+	AverageA (+)
Age	63.15±0.45	62.50±0.31	1.21±0.11
Sex			
Male	1	12	1.22±0.13
Female	2	9	1.15±0.44
Pathologic type			
Cystadenocarcinoma	1	1	1.19
Duct cell adenocystoma	2	19	1.13±0.39
Mucinous adenocystoma		1	1.22
Histologic differentiation			
Well-diff.	3	3	0.66±0.33[a]
Mod-diff.		10	1.10±0.16
Poorly-diff.		8	1.46±0.12
Invasion stage			
Non-invasive	1	3	0.86±0.31
Invasive	2	18	1.20±0.35
Lymphnode metastasis			
Absent	1	6	0.88±0.31[b]
Present	2	15	1.31±0.24
TNM stage			
I	1	1	1.19
II		5	0.81±0.35[c]
III	2	10	1.28±0.24
IV		5	1.34±0.12

[a]P<0.01 (F=26.06); [b]P<0.01 (t=3.22); [c]P<0.01 (F=9.31).

A correlation existed between the expression level of telomerase activity in pancreatic cancer tissues with histologic differentiation, presence of lymph node metastasis, and clinical TNM stage of the tumor (no significant difference between stages III and IV). However, in pancreatic cancer patients no correlation was found between the expression level of telomerase activities and age or sex of patients, pathologic category or tumor infiltration.

Table 3 shows the relationship between telomerase activity and telomerase subunit.

There was also an obvious correlation between expression of hTERT and telomerase activities in pancreatic cancer tissues, but no correlation was found between expressions of hTR and TPlmRNA and telomerase activities.

In 24 pancreatic cancer tissues and adjacent normal tissues, their hTR/GAPDH ratios were 0.592±0.056 and 0.510±0.059, respectively. No difference was found in the expression level of hTR.

Table 3 The relationship between telomerase activity and telomerase subunit

Telomerase activity	hTERT[a]		HTR[b]		TP1[c]	
	+	-	+	-	+	-
Tumor						
+	18	3	19	2	20	2
-	2	1	1	2	2	0
Normal						
+	1	2	3	0	3	0
-	1	20	18	3	19	2

[a]P>0.05 (χ^2=0.5); [b]P<0.01 (χ^2=13.76); [c]P<0.01(χ^2=15.70).

Inhibitory effects of antisense hTR

In the control groups, pancreatic cancer cells extended in polygon, showed large differences in their size and shape. The cells were more transparent, strong refractive, overlapped to grow after fully covering the bottom of the bottle and mitotic figures increased. After treatment with PS-ODN1 and PS-ODN2, morphologic changes of cells were obvious-refractiv, intercellular space became larger and the cells gradually became round, crenated, and fell off[14]. Occasionally, ballooning could be seen. When P_3 cells and human fibroblasts were treated with four PS-ODNs for reflecting the survival rate of cells, the results of SDH activity are shown in Table 4 and Table 5. There was a significant difference in the effects between the different PS-ODN groups (P<0.05). Along with an increase in concentrations of PS-ODN1 and PS-ODN2, the survival rate of cells significantly decreased. There was a significant difference between different concentrations in the same groups (P<0.05). No significant difference was found between PS-ODN1 and PS-ODN2. It was found that PS-ODN3 also might cause a decrease in SDH activity,but the decrease was less obvious than that of the former two. Inhibition of SDH activity occurred earliest with PS-ODN1. Comparison between different PS-ODNs and different concentrations of any PS-ODN (P<0.05) showed that the four PS-ODNs of any concentration had no significant effect on the survival rate of normal human fibroblasts.

Table 4 The viability of PS-ODNs treated P3 cells (%, $\bar{x}\pm s$)

PS-ODN	C1(3.16) V(%, $\bar{x}\pm s$)	C2(10) V(%, $\bar{x}\pm s$)	C3(31.6) V(%, $\bar{x}\pm s$)	C4(100) V(%, $\bar{x}\pm s$)
PS-ODN1	92.16±4.2	80.39±5.9	58.11±3.4	33.34±4.6
PS-ODN2	93.40±2.6	84.22±3.6	74.10±3.8	27.35±2.4
PS-ODN3	91.74±4.1	88.75±7.1	86.38±6.7	81.37±5.3
PS-ODN4	94.23±3.3	92.36±5.2	93.72±4.9	91.54±4.4

a.C is the concentration (unit). A is absorbance at 540 μm. V (%) is survival rate. V=$A_{CONTRAL\ GROUP}$*100 %.

Table 5 The viability of normal fibroblasts treated with PS-ODNs (%, $\bar{x}\pm s$)

PS-ODN	C1(3.16) V(%, $\bar{x}\pm s$)	C2(10) V(%, $\bar{x}\pm s$)	C3(31.6) V(%, $\bar{x}\pm s$)	C4(100) V(%, $\bar{x}\pm s$)
PS-ODN1	104.16±6.4	100.48±3.9	107.20±8.4	103.04±5.7
PS-ODN2	100.80±5.4	97.12±6.7	99.52±7.0	106.72±6.4
PS-ODN3	94.72±4.7	90.56±6.1	92.80±6.8	95.36±3.5
PS-ODN4	100.16±5.6	104.48±5.3	99.04±7.6	106.40±9.2

a.C is the concentration (unit). A is absorbance at 540 μm. V (%) is survival rate. V=$A_{CONTRAL\ GROUP}$*100 %.

After P_3 cells were treated by four PS-ODNs, their telomerase activity was detected using the PCR-ELISA method. The results showed that there was a significant difference between different PS-ODN groups ($P<0.05$). PS-ODN1 and PS-ODN2 showed similar results when different concentration groups were compared ($P<0.05$), suggesting that telomerase activity in P_3 cells weakened and the inhibiting effect became stronger with increasing concentration. There was no significant difference of telomerase activity between the different concentration groups of PS-ODN3 and PS-ODN4 ($P>0.05$) (Table 6). The results of quantitative tests of telomerase activity in PS-ODNs-treated P_3 cells by TRAP-PAGE silver staining method are shown in Figure 5. After treatment by PS-ODN1 and PS-ODN2, the telomerase activity in P_3 cells was positive. The brightness of the bands darkened with increasing PS-ODN1 and PS-ODN2 concentrations, and expression of the telomerase activity had a tendency to be depressed.

Table 6 Telomerase assay of PS-ODN treated P3 cells ($\bar{x}\pm s$)

PS-ODN	C0(0) B($\bar{x}\pm s$)	C1(3.16) B($\bar{x}\pm s$)	C2(10) B($\bar{x}\pm s$)	C3(31.6) B($\bar{x}\pm s$)	C4(100) B($\bar{x}\pm s$)
PS-ODN1	2.25±0.56	1.53±0.23	1.20±0.15	0.97±0.12	0.65±0.47
PS-ODN2	2.25±0.56	1.66±0.46	1.40±0.44	0.69±0.29	0.49±0.32
PS-ODN3	2.25±0.56	2.28±0.32	2.32±0.37	2.26±0.31	2.19±0.26
PS-ODN4	2.25±0.56	2.16±0.35	2.24±0.50	2.27±0.43	2.13±0.38

a.C0 (0 μmol/L) is the control group. B is telomerase activity.

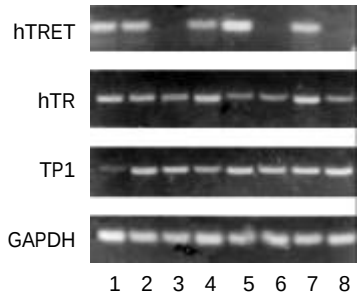

Figure 4 Telomerase subunit expression of pancreatic carcinoma (1: P3; 2: PaTu-8801; 3: fibroblast cell line; 4, 5, 7: tumor; 6, 8: normal).

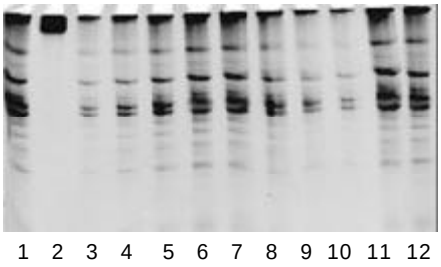

Figure 5 Telomerase activity after treated with PS-ODN in P3 cell line (1: positive control; 2: negative control; 3-6: 100 μmol/L, 31.60 μmol/L, 10 μmol/L, 3.16 μmol/L PS-ODN1 groups; 7-10: 3.16 μmol/L,10 μmol/L, 31.60 μmol/L, 100 μmol/L PS-ODN2 group; 11: 100 μmol/L PS-ODN3 group; 12: 100 μmol/L PS-ODN4 groups).

The FCM results of pancreatic cancer P_3 cells showed the apoptotic rate of cells increased along with increasing PS-ODN1 and PS-ODN2 concentrations. Fifty days or so after continuous treatment of the cells at 100 μM concentration of PS-ODN1 and PS-ODN2, the apoptotic rate of cells was 81.03 % and 70.75 %, respectively. The cycle distribution increased from 86.51 % and 83.89 % to 94.53 % and 95.39 % for cells in stage G_o/G_1, and reduced from 13.49 % and 16.11 % to 5.47 % and 2.11 % for cells in stage S, respectively (Figure 6).

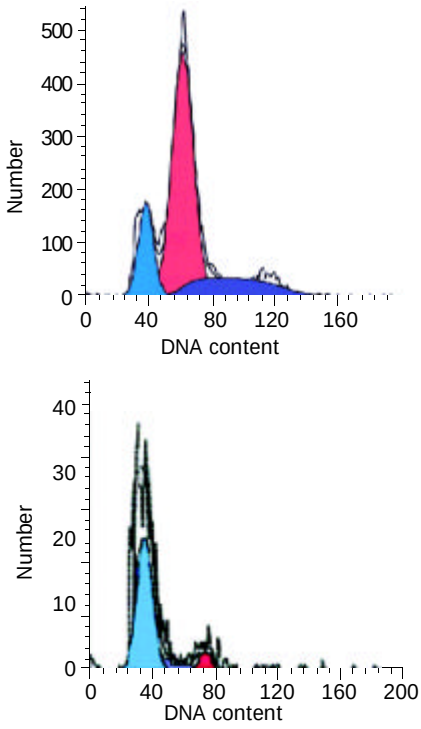

Figure 6 The apoptotic rate of P3 cells by the FCM test after treatment in P_3 cells with PS-ODN. A: PS-ODN1 10 μmol/L group; B: PS-ODN1 100 μmol/L group.

DISCUSSION

The activation of telomerase and maintenance of telomere length are essential for tumor cell immortalization. The positive rate of telomerase activity was 85-95 % in patients with pancreatic cancer, much higher than that in patients with benign pancreatic diseases[15-18]. Therefore, it can be deduced that there is a close link between telomerase activity and metastatic potential of pancreatic cancer cells[19].

The 10th, 20th, and 30th generations of cultured tumor cells and fibroblasts showed a significant difference in their telomerase activities. The results showed a positive telomerase activity for tumor cells, whereas it was absent in all generations of fibroblasts. After the 30th generation, the fibroblast cell proliferation period was obviously elongated, and part of the cells were found to have morphologic changes such as karyopyknosis, cytoplasmic concentration and cell-body shrinkage on HE stain. These findings indicate that telomerase is involved in immortalization of pancreatic cancer cells.

Hiyama *et al*[15]. reported positive telomerase activity was found in 43 cases. Among them, five cases were found to have a low level of telomerase activity expression in the adjacent normal tissues. In 24 pancreatic cancer samples, the positive rate of telomerase activity was 87.5 %, while there were 3 cases whose telomerase activity appeared in the adjacent normal tissue, a positive rate of 12.5 %. Of the three cases, one was proven to be infiltrated by tumor cells. The positive rate of hTERTmRNA in pancreatic cancer samples was 83.3 %, and 12.5 % in the adjacent normal tissue.

The results of this study support the theory that telomerase is involved in the formation of pancreatic cancer. It is a consensus that the prognosis is poor in patients with low differentiation and wide infiltration of human pancreatic cancer, i.e., those falling into the TNM stages III-IV of the

pancreatic cancer[20-22]. By statistic analysis, our data showed that there was a definite correlation between the expression level of telomerase activity in pancreatic cancer and histologic differentiation, presence of lymph node metastasis and TNM staging of the tumor. However, no significant correlation was found between it and age, sex of the subjects, pathologic category and degree of infiltration. Along with increasing expression level of telomerase, the tumor showed a higher lymph node metastasis. Therefore, the prognosis became much worse. We did not perform any post-operative follow-up studies.Tang *et al*[22] reported that patients with pancreatic endocrine neoplasm who were positive in telomerase expression usually had a shorter life expectancy than those who were negative in telomearse expression.

In the tumor cell line with positive telomerase expression, hTERTmRNA was found to have a higher expression level, whereas it was absent in normal tissues. In 21 cases of pancreatic cancer tissues with positive telomerase activity, hTERTmRNA was detected in 18 cases and only one case was found to be positive in the adjacent normal tissue which showed no telomerase activity.

Statistic analysis showed a significant correlation between hTERTmRNA and telomerase activity. Therefore, it may be thought that expression of hTERT is an important factor in governing telomerase activity[23, 24] and that up-regulation of hTERTmRNA expression may play an important role in the formation of pancreatic cancer. However hTERTmRNA was detected in two of the pancreatic cancer samples in which no telomerase activity was found. This may be explained by the following factors: (1) The expression level of each subunit or an equilibrium state between their expression levels determines the activity of telomerase; (2) Modification of the telomerase subunit after its transcription may have a regulating effect on the enzyme activity; (3) telomerase inhibitor existing in the cell extract reduces the activity of telomerase. Furthermore, there were 3 cases whose telomerase activity was detected, while the expression of hTERTmRNA showed negative results. There may be other factors to determine the activity of telomerase in this latter situation.

This study found that though the expression level of hTR in pancreatic cancer tissue was higher than that in adjacent normal tissue, it had no statistical significance. hTR itself cannot reflect the activity of telomerase. However, its function is essential for the activity of telomerase. This point is consistent with other studies[25-28].

It was found in our study that inhibition of the growth of P_3 cells by PS-ODN1 occurred the earliest. This was probably not only due to the smaller PS-ODN1 molecules entering cells, but also due to two important basic UC groups at the junction of the closed hTR templates. No significant effect was found on the survival rate of the P_3 cells in the random sequence group, while slight inhibition of P_3 cells growth was found in the pro-sense group. This could be explained as the pro-sense oligonucleotide competed against telomerase RNA in quantity and space, thus impeding the attachment of telomere with RNA template zone to a certain degree[29]. The results showed that inhibition of PS-ODN1 and PS-ODN2 on the growth of P_3 cells was dosage-dependent. This implies that after hTR template is closed, telomerase can no longer bring its activity into full play. Therefore it can be concluded that hTR is involved in the regulation of telomerase activity[30].

FCM results showed that the apoptotic rate of P_3 cells would increase along with increase of the concentrations of antisense oligonucleotide, at the same time, cells in G_0/G_1 stage increased in quantity while those in S stage decreased. This suggests that treatment with PS-ODN1 and PS-ODN2 may block the cells at G_0/G_1 stage and induce apoptosis.

In regard to the relationship between telomerase activity and cell cycle, it was thought[31] that the tolemerase activity was regulated in the cell cycle-leading mode. It was also thought that tolemerase should be activated at the DNA replication stage as tolemerase activity was essential to maintain tolemere. This activity is not required at the non- replication stage of the cell cycle. Telomerase has different activity at different stages of the cell cycle, its highest rate is at S stage, lowest at G_2/M stage, and almost no activity at G_0/G_1 stage. Our results support this point of view.

We simultaneously observed the influence of PS-ODNs on SDH activity and proliferation of normal human fibroblasts. The results showed that it had a significantly inhibitory effect on the metabolism and proliferation of cells. Therefore, it can be assumed that the effect of antisense hTR is cell-specific, and has no harmful action on normal cells.

Our study suggested that there was no correlation between the expression of TPlmRNA and telomerase activity in pancreatic cancer. However, the function of TP1 is still not clearly known, and it may be related to interaction with protein. TP1 may play a role in the interface between telomerase and telomere conjugated proteins. Modification after transcription of TPlmRNA may regulate the telomerase activity.

In conclusion, telomerase may be taken as a subsidiary parameter for the diagnosis and outcome of pancreatic cancer. For preoperative patients, detection of the telomerase activity may be conducted on blood, or pancreatic juice and duct cells taken from ERCP on fine needle aspiration specimens for early diagnosis[32-35]. Antisense oligonucleotide can reduce the activity of telomerase in pancreatic cancer P_3 cells, inhibit the growth of P_3 cells, promote changes in cell cycle and induce their apoptosis[36, 37].

REFERENCES

1 **Greider CW,** Blackburn EH. A telomeric sequence in the RNA of tetrahymena telomerase required for telomere repeat synthesis. *Nature* 1989; **337**: 331-337

2 **Kim NW,** Piatyszek MA, Prowse KR, Harley CB, West MD, Ho PL, Coviello GM, Wright WE, Weinrich SL, Shay JW. Specific association of human telomerase activity with immortal cells and cancer. *Science* 1994; **266**: 2011-2015

3 **Wan M,** Li WZ, Duggan BD, Felix JC, Zhao Y, Dubeau L. Telomerase activity in benign and malignant epithelial ovarian tumors. *J Natl Cancer Inst* 1997; **89**: 437-441

4 **Harle-Bachor C,** Boukamp P. Telomerase activity in the regenerative basal layer of the epidermis inhuman skin and in immortal and carcinoma-derived skin keratinocytes. *Proc Natl Acad Sci U S A* 1996; **93**: 6476-6481

5 **Wang J,** Liu X, Fang J. Expression and clinical significance of telomerase catalytic subunit gene in lung cancer and its correlations with genes related to drug resistance and apoptosis. *Zhonghua Zhongliu Zazhi* 1999; **21**: 350-353

6 **Zhang YL,** Zhang ZS, Wu BP, Zhou DY. Early diagnosis for colorectal cancer in China. *World J Gastroenterol* 2002; **8**: 21-25

7 **Shen ZY**, Xu LY, Li EM, Cai WJ, Chen MH, Shen J, Zeng Y. Telomere and telomerase in the initial stage of immortalization of esophageal epithelial cell. *World J Gastroenterol* 2002; **8**: 357-362

8 **Qin LX,** Tang ZY. The prognostic molecular markers in hepatocellular carcinoma. *World J Gastroenterol* 2002; **8**: 385-392

9 **Yao XX,** Yin L, Sun ZC. The expression of hTERT mRNA and cellular immunity in gastric cancer and precancerosis. *World J Gastroenterol* 2002; **8**: 586-590

10 **Kojima H,** Yokosuka O, Imazeki F, Saisho H, Omata M. Telomerase activity and telomere length in hepatocellular carcinoma and chronic liver disease. *Gastroenterology* 1997; **112**: 493-500

11 **Suzuki T,** Suzuki Y, Fujioka T. Expression of the catalytic subunit associated with telomerase gene in human urinary bladder cancer. *J Urol* 1999; **162**: 2217-2220

12 **Takakura M,** Kyo S, Kanaya T, Tanaka M, Inoue M. Expression of human telomerase subunits and correlation with telomerase

activity in cervical cancer. *Cancer Res* 1998; **58**: 1558-1561

13 **Lanham S,** Herbert A, Watt P. HPV detection and measurement of HPV-16,telomerase, and survivin transcripts in colposcopy clinic patients. *J Clin Pathol* 2001; **54**: 304-308

14 **Zhang FX,** Zhang XY, Fan DM, Deng ZY, Yan Y, Wu HP, Fan JJ. Antisense telomerase RNA induced human gastric cancer cell apoptosis. *World J Gastroenterol* 2000; **6**: 430-432

15 **Hiyama E,** Kodama T, Shinbara K, Iwao T, Itoh M, Hiyama K, Shay JW, Matsuura Y, Yokoyama T. Telomerase activity is detected in pancreatic cancer but not in benign tumors. *Cancer Res* 1997; **57**: 326-331

16 **Tsutsumi M,** Tsujiuchi T, Ishikawa O, Majima T, Yoshimoto M, Sasaki Y, Fukuda T, Oohigashi H, Konishi Y. Increased telomerase activities in human pancreatic duct adenocarcinomas. *Jpn J Cancer Res* 1997; **88**: 971-976

17 **Buchler P,** Conejo-Garcia JR, Lehmann G, Muller M, Emrich T, Reber HA, Buchler MW, Friess H. Real-time quantitative PCR of telomerase mRNA is useful for the differentiation of benign and malignant pancreatic disorders. *Pancreas* 2001; **22**: 331-340

18 **Iwao T**, Hiyama E, Yokoyama T, Tsuchida A, Hiyama K, Murakami Y, Shimamoto F, Shay JW, Kajiyama G. Telomerase activity for the preoperative diagnosis of pancreatic cancer. *J Natl Cancer Inst* 1997; **89**: 1621-1623

19 **Sato N,** Maehara N, Mizumoto K, Nagai E, Yasoshima T, Hirata K, Tanaka M. Telomerase activity of cultured human pancreatic carcinoma cell lines correlates with their potential for migration and invasion. *Cancer* 2001; **91**: 496-504

20 **Ohta K**, Kanamaru T, Morita Y, Hayashi Y, Ito H, Yamamoto M. Telomerase activity in hepatocellular carcinoma as a predictor of postoperative recurrence. *J Gastroenterol* 1997; **32**: 791-796

21 **Suda T,** Isokawa O, Aoyagi Y, Nomoto M, Tsukada K, Shimizu T, Suzuki Y, Naito A, Igarashi H, Yanagi M, Takahashi T, Asakura H. Quantitation of telomerase activity in hepatocellular carcinoma: a possible aid for a prediction of recurrent diseases in the remnant liver. *Hepatology* 1998; **27**: 402-406

22 **Tang SJ,** Dumot JA, Wang L, Memmesheimer C, Conwell DL, Zuccaro G, Goormastic M, Ormsby AH, Cowell J. Telomerase activity in pancreatic endocrine tumors. *Am J Gastroenterol* 2002; **97**: 1022-1030

23 **Meyerson M,** Counter CM, Eaton EN, Ellisen LW, Steiner P, Caddle SD, Ziaugra L, Beijersbergen RL, Davidoff MJ, Liu Q, Bacchetti S, Haber DA, Weinberg RA. HEST2, the putative human telomerase catalytic subunit gene, is up-regulated in tumor cells and during immortalization. *Cell* 1997; **90**: 785-795

24 **Nakamura TM,** Morin GB, Chapman KB, Weinrich SL, Andrews WH, Lingner J, Harley CB, Cech TR. Telomerase catalytic subunit homologs from fission yeast and human. *Science* 1997; **277**: 955-959

25 **Muller M**, Krause H, Heicappell R, Tischendorf J, Shay JW, Miller K. Comparison of human telomerase RNA and telomerase activity in urine for diagnosis of bladder cancer. *Clin Cancer Res* 1998; **4**: 1949-1954

26 **Kanaya T**, Kyo S, Takakura M, Ito H, Namiki M, Inoue M. hTERT is a critical determinant of telomerase activity in renal-cell carcinoma. *Int J Cancer* 1998; **78**: 539-543

27 **Kyo S**, Kanaya T, Takakura M, Tanaka M, Yamashita A, Inoue H, Inoue M. Expression of human telomerase subunits in ovarian malignant, borderline and benign tumors. *Int J Cancer* 1999; **80**: 804-809

28 **Harrington L**, McPhail T, Mar V, Zhou W, Oulton R, Bass MB, Arruda I, Robinson MO. A mammalian telomerase-associated protein. *Science* 1997; **275**: 973-977

29 **Yuan X**, Zhang B, Ying J, Wang H, Zhang H, Hou L, Wu B. Expression of antisense telomerase genes suppressing human cancer malignant phenotypes *Zhonghua Binglixue Zazhi* 1999; **28**: 356-360

30 **Teng L,** Chen S, Thomas JF. Stable expression of antisense hTR inhibits *in vitro* pancreatic cancer cell growth. *Chin Med J (Engl)* 2002; **115**: 1196-1200

31 **Zhu X**, Kumar R, Mandal M, Sharma N, Sharma HW, Dhingra U, Sokoloski JA, Hsiao R, Narayanan R. Cell cycle-dependent modulation of telomerase activity in tumor cells. *Proc Natl Acad Sci U S A* 1996; **93**: 6091-6095

32 **Inoue H,** Tsuchida A, Kawasaki Y, Fujimoto Y, Yamasaki S, Kajiyama G. Preoperative diagnosis of intraductal papillary-mucinous tumors of the pancreas with attention to telomerase activity. *Cancer* 2001; **91**: 35-41

33 **Myung SJ,** Kim MH, Kim YS, Kim HJ, Park ET, Yoo KS, Lim BC, Wan Seo D, Lee SK, Min YI, Kim JY. Telomerase activity in pure pancreatic juice for the diagnosis of pancreatic cancer may be complementary to K-ras mutation. *Gastrointest Endosc* 2000; **51**: 708-713

34 **Seki K**, Suda T, Aoyagi Y, Sugawara S, Natsui M, Motoyama H, Shirai Y, Sekine T, Kawai H, Mita Y, Waguri N, Kuroiwa T, Igarashi M, Asakura H. Diagnosis of pancreatic adenocarcinoma by detection of human telomerase reverse transcriptase messenger RNA in pancreatic juice with sample qualification. *Clin Cancer Res* 2001; **7**: 1976-1981

35 **Pearson AS**, Chiao P, Zhang L, Zhang W, Larry L, Katz RL, Evans DB, Abbruzzese JL. The detection of telomerase activity in patients with adenocarcinoma of the pancreas by fine needle aspiration. *Int J Oncol* 2000; **17**: 381-385

36 **Sato N,** Mizumoto K, Nagai E, Tanaka M. Telomerase as a new target for pancreatic cancer treatment. *J Hepatobiliary Pancreat Surg* 2002; **9**: 322-327

37 **Pirocanac EC**, Nassirpour R, Yang M, Wang J, Nardin SR, Gu J, Fang B, Moossa AR, Hoffman RM, Bouvet M. Bax-induction gene therapy of pancreatic cancer. *J Surg Res* 2002; **106**: 346-351

Edited by Lu HM and Wang XL

P.O.Box 2345, Beijing 100023,China
Fax: +86-10-85381893
E-mail: wjg@wjgnet.com www.wjgnet.com

World J Gastroenterol 2003;9(8):1815-1818
World Journal of Gastroenterology
 ISSN 1007-9327

• CLINICAL RESEARCH •

p53 protein expression and CA19.9 values in differential cytological diagnosis of pancreatic cancer complicated with chronic pancreatitis and chronic pancreatitis

De-Qing Mu, Guo-Feng Wang, Shu-You Peng

De-Qing Mu, Shu-You Peng, Department of Surgery, the Second Affiliated Hospital, Medical College of Zhe Jiang University, Hang Zhou 310009, Zhe Jiang Province, China
Guo-Feng Wang, Department of Pathology, the Second Affiliated Hospital, Medical College of Zhe Jiang University, Hang Zhou 310009, Zhe Jiang Province, China
Correspondence to: Dr. De-Qing Mu, Department of Surgery, the Second Affiliated Hospital, Medical College of Zhe Jiang University, Hangzhou 310009 Zhe jiang Province, China. samier-1969@163.com
Telephone: +86-0571-87783762
Received: 2003-01-11 **Accepted:** 2003-03-05

Abstract

AIM: To evaluate p53 protein overexpression and to measure serum CA19.9 concentrations in cytological diagnosis of patients with suspected pancreatic cancer.

METHODS: 24 patients with suspected pancreatic cancer due to chronic pancreatitis, had a pancreatic mass determined by imaging methods. The serum CA19.9 concentration was measured by solid phase radioimmunoassay. On laparotomy, puncture biopsy was performed, and specimens were divided into two parts for cytological diagnosis and detection of p53 protein.

RESULTS: Cytology offered a sensitivity of 0.63, a specificity of 1.00, and an accuracy of 0.63. p53 protein analysis offered a sensitivity of 0.44, a specificity of 1.00, and an accuracy of 0.73. CA19.9 offered a sensitivity of 0.44, a specificity of 0.80, and an accuracy of 0.67. The combined cytology and p53 protein analysis showed a sensitivity of 0.78, a specificity of 1.00, and an accuracy of 0.92. Cytology and CA19.9 showed a sensitivity of 0.67, a specificity of 0.80, an accuracy of 0.67. combined cytology and p53 protein analysis and CA19.9 showed a sensitivity of 0.78, a specificity of 0.80, and an accuracy of 0.79.

CONCLUSION: Superior to any single test, the combined approach is helpful for the differential diagnosis of pancreatic cancer complicated with chronic pancreatitis.The combined cytology and p53 protein analysis offers the best diagnostic efficacy.

Mu DQ, Wang GF, Peng SY. p53 protein expression and CA19.9 values in differential cytological diagnosis of pancreatic cancer complicated with chronic pancreatitis and chronic pancreatitis. *World J Gastroenterol* 2003; 9(8): 1815-1818
http://www.wjgnet.com/1007-9327/9/1815.asp

INTRODUCTION

The differential diagnosis of pancreatic cancer (PC) complicated with and chronic pancreatitis (CP) is difficult because of their common clinical symptoms and overlapping findings. Increased pancreatic adenocarcinoma risk in chronic pancreatitis patients has renewed the interest in early tumour diagnosis and in the differentiation of neoplastic and chronic inflammatory ductal changes[1, 2]. If a pancreatic mass is discovered by the imaging method, cytological examination is required to make a conclusive diagnosis. Owing to a large number of cases without a conclusive diagnosis[3], it would be worthy to diagnose it with other methods. Genomic alterations in p53 tumour-suppressor gene and overexpression of p53 protein are frequently found in pancreatic cancer, but rarely in chronic pancreatitis. An elevated serum CA19.9 concentrations is found in a high proportion of patients with pancreatic cancer and this is considered to be the standard serum marker for adenocarcinoma of the pancreas. In the current study, we retrospectively evaluated overexpression of p53 protein, serum CA19.9, and cytology in the diagnosis of pancreatic cancer.

MATERIALS AND METHODS

Materials

24 patients,19 men and 5 women, with a mean age 58.6 years, (range 41-69 years,) with jaundice, weight loss, and abdominal pain, underwent pancreatectomy in our hospital between January 1995 and December 2001 because of high suspicion of pancreatic cancer arising from chronic pancreatitis. Preoperatively, they were found to have a mass in the pancreas by CT and ERCP. 19 masses were located in pancreatic head, two in the body, and two in the tail, 1 with three foci.

Methods

CA19.9 determination The serum samples were stored at -20 ℃ for CA19.9 by solid phase radioimmunoassay. A value of 37 U/ml was the upper limit of normal.

Cytological examination Puncture biopsy of the pancreas was performed during laparotomy, and the specimen was divided into two parts: one part was used for making fresh smears, after papanicolaou staining. The presence of malignant cells and suspicious cells were examined under microscope (Figures 1-2). The other part was employed for immunohistochemical analysis.

Immunohistochemical analysis The sample was fixed in buffered formaldehyde and paraffin-embeded. Histological sections (5 μm) were prepared, mounted on poly-L-lysine-coated slides and dried for 12 to 24 h at 37 ℃. Immunohistochemistry was performed with the avidin-biotin complex (ABC) kit[4] using the monoclonal antibody which recognizes both mutant and wild-type p53.

The result was graded as either negative or positive. The specimen was considered to positive when >5 % of the tissure component was unequivocally immunoreactive in the appropriate cellular compartment (Figure 3).

Histological examination The resected specimens were fixed in 10 % formaldehyde and sliced into 5 mm sections and stained with hematoxylin-eosin. The presence or absence of cancer was microscopically determined.

Statistical analysis

Statistical analysis was performed with STATISTICA for Windows. Differences between the results of two groups were tested with one-sided *t* test. A *P* value <0.05 was considered statistically significant.

RESULTS

Histological diagnosis

9 patients were diagnosed as pancreatic cancer complicated with chronic pancreatitis, including carcinoma of the pancreas head in 6 cases; carcinoma of the body and/or tail of pancreas in 2 cases, multifocal cancer with three foci in 1 case. The other 15 patients were confirmed to be chronic pancreatitis, including 13 cases with inflammatory mass in the head of pancreas, and two cases with adenoma in the body and/or tail of pancreas.

To compare with histological diagnosis, cytology offered a conclusive diagnosis in 5 of 24 cases. The cytological report was not conclusive in 19 cases (9 cases with suspicious cells and 8 cases with insufficient material, and two cases without non-malignant cell) (Figures 1,2).

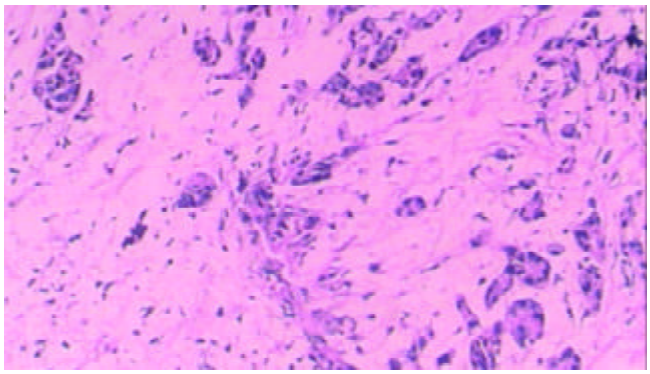

Figure 1 A little glandublar tissue and a large amount of fibrotic tissue.

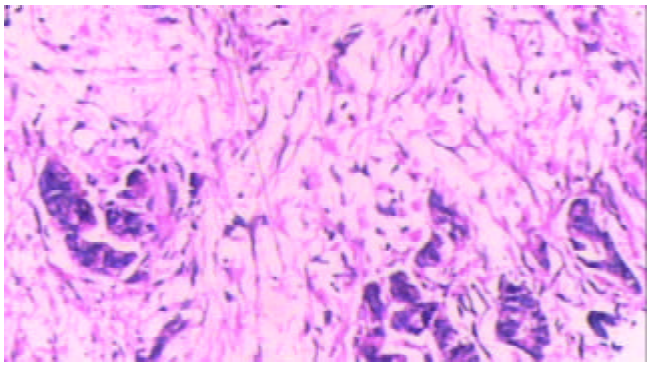

Figure 2 A few cancerous cells scattered in fibrotic gland tissue. (Papanicolaou staining, original magnification ×200).

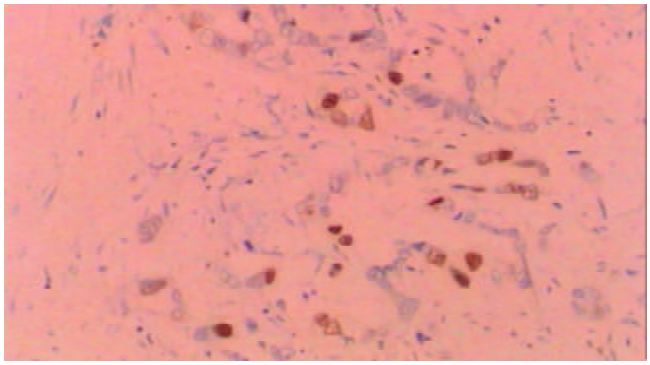

Figure 3 Yellow-brownly stained nuclei of p53 positive cells (ABC, original magnification ×400).

The presence of malignant cells in puncture samples was detected in 5 of 9 pancreatic cancer patients confirmed by histological examination. According to cytological diagnosis. The incidence of p53 protein overexpression and CA19.9 values ovre shown in Table 1.

Table 1 Patients with p53 protein overexpression and high serum CA19.9 with cytologically diagnosed pancreatic disease (*n*=24)

Histological diagnosis	Cytology				
	Patient *n*(%)	Malignant cells	Suspicious cells	Insufficient material	Non-malignant cells
Malignant diseases					
PC	9(37.5) p53(+)	2/5	1/1	1/1	0/2
	CA19.9≥37 U/ml	3/5	1/1	0/1	0/2
Benign disease					
IMH	13(54.2) p53(+)	0	0/5	0/4	0/4
	CA19.9≥37 U/ml	0	2/5	1/4	0/4
Adenoma	2(8.3)p53(+)	0	0/2	0	0
	CA19.9≥37 U/ml	0	0/2	0	0

PC: pancreatic cancer; IMH: inflammatory mass of the head of pancreas.

Table 2 Assay effectiveness in patients with pancreatic diseases (*n*=24)

Assay	Sensitivity TP/(TP+FN)	Specificity TN/(FP+TN)	Predictive value of positive test TP/(TP+FP)	Efficiency (TP+TN)/Total
Cytology alone	5/(5+3)=0.63	10/(0+10)=1.00	5/(5+0)=1.00	(5+10)/24=0.63
CA19.9>37 U/ml	4/(4+5)=0.44	12/(3+12)=0.80	4/(4+3)=0.57	(4+12)/24=0.67
P53(+)	4/(4+5)=0.44	15/(0+15)=1.00	4/(4+0)=1.00	(4+15)/24=0.79
Cytology+CA19.9	6/(6+3)=0.67	12/(12+3)=0.80	6/(6+3)=0.67	(6+12)/24=0.67
Cytology+P53	7/(7+2)=0.78	15/(15+0)=1.00	7/(7+0)=1.00	(7+15)/24=0.92
Cytology+P53+CA19.9	7/(7+2)=0.78	12(3+12)=0.80	7(7+3)=0.70	(7+12)/24=0.79

TP: true-positive; FN: false-negative; FP: false-positive; TN: true-negative.

p53 protein overexpression (shown by immunohistochemical staining) was positive in 4 of 9 patients with pancreatic cancer (Figure 3), and negative in the remaining 20 specimens. The combination of p53 protein overexpression and cytology offered a78 % sensitivity and a 100 % specificity.

Using the cut-off value of 37 U/ml as the normal upper limit, CA19.9 measurement identified 4 of 9 pancreatic carcinomas (range=41-480 U/ml). Additionally, high concentrations were also detected in 3 cases of chronic pancreatitis with a mass (range=210-1 200 U/ml). CA19.9 positivity in the chronic pancreatitis patient was related to common bile duct obstruction. The combined CA 19.9 and cytological assay showed a sensitivity of 67 % and a specificity of 80 %.

Combination of cytological analysis, P53 protein overexpression and CA19.9

Since all positive cytologies carried a final diagnosis of carcinoma, the main diagnostic contribution of p53 and CA19. 9 in the pancreatic cancer group was at the time when the cytology was suspicious or not contributory. Either test contributed to the final diagnosis of pancreatic adenocarcinoma in 4 out of 9 cases: in one case both were positive, in another case p53 protein showed overexpression but CA19.9 value was lower than 37 U/ml. None of the patients with chronic pancreatitis was positive for both markers. The sensitivity of the combined approach was 78 % with a specificity of 80 %. Both the sensitivity and efficiency of the combined approach (cytology, CA19.9, and p53 protein overexpression) were significantly higher than that of either test alone (P<0.01). Both the sensitivity and efficiency of combination of cytology and p53 were higher than that of combination of cytology, p53 and CA19.9 (P<0.05). Finally both the sensitivity and efficiency of the combined approach of cytology, p53 and CA19.9 were better than that of combination of cytology and CA19.9 (P<0.05) (Table 2).

DISCUSSION

Much effort has been devoted to achieve an optimum standard for conventional imaging procedures to increase the sensitivity and specificity of these diagnostic tools. Among which CT, ERCP are the mainstay for pancreatic cancer detection[5,6]. However, these morphologically oriented procedures, have an unsolved drawback ie, the inability to differentiate tumour tissue from pancreatic masses caused by chronic pancreatitis. Therefore, this has limited their application in patients with a suspected resectable mass for the decision of surgical exploration. FNA biopsy of the primary tumor has a significantly false negative rate due to the inflammatory response around the tumor, which accounts for the lower sensitivity[3]. According to a 1986 review, the average sensitivity was approximately 80 %[7]. A more recent, large, single-institution series reported a sensitivity of 72.5 %[8]. FNA-cytological distinction between chronic pancreatitis and pancreatic cancer is occasionally difficult because chronic pancreatitis can induce morphological changes similar to those seen in well differentiated adenocarcinoma[9]. This explains the equivocal results found in two kinds of pancreatic diseases, which can not be discriminated by clinical and imaging tests. In addition, the accuracy of cytology examination also depends on the quality and number of cells. The reported sensitivities of ERCP aspiration cytology, brush cytology, FNA biopsies, and forceps biopsies were in the range of 22 % to 71 %, and the use of multimethod samplings increased the sensitivity to 50-78 %[10]. Even with endoscopic ultrasonography-guided FNA biopsy, there were also false negative results[11]. Sometimes the accuracy of cytology might be damaged by poor staining or inadequate fixation[12]. The distinction between chronic pancreatitis and well-differentiated adenocarcinoma is difficult and it remains to find whether artificial intelligence algorithms can prove themselves useful in the cytologically differential diagnosis of carcinoma and chronic pancreatitis[9].

The greatest usefulness of carbohydrate antigen CA19.9 is its performance in detecting pancreatic cancer using a cutoff upper limit of 37 U/ml[13-16]. However, it can be confusing to interpret elevated concentrations of CA19.9, because the elevated concentration of CA19.9 used for the diagnosis of pancreatic cancer can also be seen in benign conditions such as pancreatitis[17-19], and conversely CA19.9 may be low in malignant conditions[20]. As shown in Table 1 and Table 2, the application of CA19-9 for differentiating cancer from chronic pancreatitis was disappointing in our study because of its low sensitivity and specificity, which were only 44 % and 80 %, similar to those reported by Okaga *et al*[21]. This may be explained by the elevation of CA19.9 in benign inflammatory conditions as well as in malignant diseases. According to Ker *et al*[22] CA19.9 is synthesized by normal biliary ductal cells. In benign biliary obstruction, epithelial cells will proliferate, and as a result, more CA19.9 may be secreted and leaks out into the bloodstream. The other mechanism concerning the false serum elevation of tumour markers in chronic pancreatitis has been shown to be a disturbed antigen polarity[23].

p53 gene abnormalities are considered to play an important role in the carcinogenesis of pancreatic cancer present in almost half of pancreatic cancer, but uncommon in chronic pancreatitis[24-26].

Studies on p53 abnormalities generally look for overexpression or persistence of the p53 protein, or for mutations in the genic sequence. Mutations of p53 gene lead to an accumulation of p53 protein reaching detectable concentrations by immunohistochemistry. In contrast, production of the wild type p53 gene is undetectable because of its short half-life. Thus there seems to be a good correlation between the overexpression of p53 protein and p53 gene mutations[27]. The p53 protein concentrations are correlated with percentage of p53 gene alterations[28,29]. In 40-60 % of pancreatic carcinomas, mutations of p53 gene and the increased accumulation of p53 protein have been shown by both direct sequencing and immunohistochemistry[30,31]. Both methods require tissue specimens. In comparison with cytology the, biggest advantage of gene analysis is no need to search for integrity or large number of cells. This method is sensitive enough to detect 3-30 mutant copies in the presence of 300 000 normal copies of the gene (which would be the equivalent to 0.01 ng of mutant DNA in 1 mcg of total DNA)[32]. In our series we found p53 protein overexpression in suspicious cells and insufficient materials.

In the current study, we analyzed the relative and combined contributions of the detection of p53 protein and CA19.9 concentration to the cytological diagnosis of pancreatic cancer when there was a clinical suspicion of pancreatic cancer corroborated by imaging diagnostic technique. In FNA samples, overexpressions were detected in 44 % of carcinoma. Fortunately no false-positives were detected even in the subset of chronic pancreatitis patients with a mass. Using a cut-off upper limit of 37 U/ml, the high CA19.9 concentrations were not strongly suggestive of pancreatic cancer. Although CA19. 9 is superior to any single markers elevated, it is not suitable for determining the nature of a pancreatic mass in patients with chronic pancreatitis. Similar results were also reported by other authors[33].

The combination of cytology and p53 offered the best diagnostic procedure. In four out of 9 patients with PC, the p53 protein overexpression contributed much to supporting the cytological diagnosis. Therefore, p53 protein overexpressions in FNAs are specific for pancreatic cancer, but CA19.9 values are not. Interestingly, none of the patients with chronic pancreatitis was positive for both markers,

suggesting that the combination of cytology and p53 might be useful in distinguishing PC and CP.

In conlusion, p53 protein analysis enhanced the diagnostic sensitivity of cytological evaluation in chronic pancreatitis patients with clinical suspicion of pancreatic cancer, especially in those with inconclusive cytological results such as the presence of suspicious cells or insufficient cellular material. In this case, p53 protein overexpression analysis offered a highly specific test although it was rarely employed as a clinical decision-making process.The previous clinical evidence also indicated the diagnostic benefit provided by p53 and other molecular marker analysis[34, 35], with an accumulation of more patients in such a study, there will be growing facilities for differentiating PC from CP.

REFERENCES

1 **Lowenfels AB**, Maisonneuve P, Cavallini G, Ammann RW, Lankisch PG, Andersen JR, Dimagno EP, Andren-Sandberg A, Domellof L. International pancreatitis study group. *N Engl J Med* 1993; **328**: 1433-1437

2 **Apple SK**, Hecht JR, Lewin DN, Jahromi SA, Grody WW, Nieberg RK. Immunohistochemical evaluation of k-ras,p53, and HER-2/neu expression in hyperplastic, dysplastic, and carcinomatous lesions of the pancreas: evidence for multistep carcinogenesis. *Hum Pathol* 1999; **30**: 123-129

3 **Robins DB**, Katz RL, Evans DB, Atkinson EN, Green L. Fine needle aspiration of the pancreas.In quest of accuracy. *Acta Cytol* 1995; **39**: 1-10

4 **Kawesha A**, Ghaneh P, Andren-Sandberg A, Ograed D, Skar R, Dawiskiba S, Evans JD, Campbell F, Lemoine N, Neoptolemos JP. K-ras oncogene subtype mutations are associated with survival but not expression of p53, p16(INK4A), p21(WAF-1), cyclin D1, erbB-2 and erbB-3 in resected pancreatic ductal adenocarcinoma. *Int J Cancer* 2000; **89**: 469-474

5 **Rosewicz S**, Wiedenmann B. Pancreatic carcinoma. *Lancet* 1997; **349**: 485-489

6 **Sheridan MB**, Ward J, Guthrie JA, Spencer JA, Craven CM, Wilson D, Guillou PJ, Robinson PJ. Dynamic contrast-enhanced MR imaging and dual-phase helical CT in the preoperative assessment of suspected pancreatic cancer: a comparative study with receiver operating characteristic analysis. *Am J Roentgenol* 1999; **173**: 583-590

7 **Bret PM**, Nicolet V, Labadie M. percutaneous fine-needle aspiration biopsy of the pancreas. *Diagn Cytopathol* 1986; **2**: 221-227

8 **Lerma E**, Musulen E, Cuatrecasas M, Martinez A, Montserrat E, Prat J. Fine needle aspiration cytology in pancreatic pathology. *Acta Cytol* 1996; **40**: 683-686

9 **Yeaton P**, Sears RJ, Ledent T, Salmon I, Kiss R, Decaestecker C. Discrimination between chronic pancreatitis and pancreatic adenocarcinoma using artificial intelligence-related algorithms based on image cytometry-generated variables. *Cytometry* 1998; **32**: 309-316

10 **Lee JG**, Leung J. Tissue sampling at ERCP in suspected pancreatic cancer. *Gastrointest Endosc Clin N Am* 1998; **8**: 221-235

11 **Gress F**, Gottlieb K, Sherman S, Lehman G. Endoscopic ultrasonography-guided fine-needle aspiration biopsy of suspected pancreatic cancer. *Ann Intern Med* 2001; **134**: 459-464

12 **Nakaizumi A**, Tatsuta M, Uehara H, Yamamoto R, Takenaka A, Kishigami Y, Takemura K, Kitamura T, Okuda S. Cytologic examination of pure pancreatic juice in the diagnosis of pancreatic carcinoma. The endoscopic retrograde intraductal catheter aspiration cytologic technique. *Cancer* 1992; **70**: 2610-2614

13 **Farini R**, Fabris C, Bonvicini P, Piccoli A, del Favero G, Venturini R, Panucci A, Naccarato R. CA 19-9 in the differential diagnosis between pancreatic cancer and chronic pancreatitis. *Eur J Cancer Clin Oncol* 1985; **21**: 429-432

14 **Steinberg WM**, Gelfand R, Anderson KK, Glenn J, Kurtzman SH, Sindelar WF, Toskes PP. Related Articles, Links Comparison of the sensitivity and specificity of the CA19-9 and carcinoembryonic antigen assays in detecting cancer of the pancreas. *Gastroenterology* 1986; **90**: 343-349

15 **Safi F**, Beger HG, Bittner R, Bucher M, Krautzberger W. CA19-9 and pancreatic adenocarcinoma. *Cancer* 1986; **57**: 779-783

16 **Kim HJ**, Kim MH, Myung SJ, Lim BC, Park ET, Yoo KS, Seo ISK, Min YI. A new strategy for the application of CA19-9 in the differentiation of pancreaticobiliary cancer: analysis using a receiver operating characteristic curve. *Am J Gastroenterol* 1999; **94**: 1941-1946

17 **Wakasugi H**, Funakoshi A, Iguchi H, Takase M, Inoue M, Ohshima A, Seo Y. Pancreatic carcinoma associated with chronic pancreatitis. *Intern Med* 1999; **38**: 951-956

18 **Uno K**, Azuma T, Nakajima M, Yasuda K, Hayakumo T, Mukai H, Sakai T, Kawai K. Clinical significance of cathepsin E in pancreatic juice in the diagnosis of pancreatic ductal adenocarcinoma. *J Gastroenterol Hepatol* 2000; **15**: 1333-1338

19 **Ridwelski K**, Meyer F, Fahlke J, Kasper U, Roessner A, Lippert H. Value of cytokeratin and CA19-9 antigen in immunohistological detection of disseminated tumor cells in lymph noodes in pancreas carcinoma. *Chirurg* 2001; **72**: 920-926

20 **Shimura T**, Tsutsumi S, Hosouchi Y, Kojima T, Kon Y, Yonezu M, Kuwano H. Clinical significance of soluble form of HLA class I molecule in Japanese patients with pancreatic cancer. *Hum Immunol* 2001; **62**: 615-619

21 **Okaga M**, Karasawa H, Kobayashi T, Satsukime N, Miki R. Effect of biliary tract obstruction and cholangitis on serum CA 19-9 levels. *Nippon Shokakibyo Gakkai Zasshi* 1985; **82**: 1418

22 **Ker CG**, Chen JS, Lee KT, Sheen PC, Wu CC. Assessment of serum and bile levels of CA19-9 and CA125 in cholangitis and bile duct carcinoma. *J Gastroenterol Hepatol* 1991; **6**: 505-508

23 **Satomura Y**, Sawabu N, Takemori Y, Ohta H, Watanabe H, Okai T, Watanbe K, Matsuno H, Konishi F. Expression of various sialyated carbohydrate antigens in malignant and nonmalignant pancreatic tissues. *Pancreas* 1991; **6**: 448-458

24 **Casey G**, Yamanaka Y, Friess H, Kobrin MS, Lopez ME, Buchler M, Beger HG, Korc M. p53 mutations are common in pancreatic cancer and are absent in chronic pancreatitis. *Cancer Lett* 1993; **69**: 151-160

25 **Tomaszewska R**, Karcz D, Stachura J. An immunohistochemical study of the expression of bcl-2 and p53 oncoproteins in pancreatic intraepithelial neoplasia and pancreatic cancer. *Int J Pancreatol* 1999; **26**: 163-171

26 **Yamaguchi K**, Chijiiwa K, Noshiro H, Torata N, Kinoshita M, Tanaka M. K-ras codon 12 point mutation and p53 mutation in pancreatic diseases. *Hepatogastroenterology* 1999; **46**: 2575-2581

27 **Boschman CR**, Stryker S, Reddy JK, Rao MS. Expression of p53 protein in precursor lesions and adenocarcinoma of human pancreas. *Am J Pathol* 1994; **145**: 1291-1295

28 **Luo JC,** Neugut AI, Garbowski G, Forde KA, Treat M, Smith S, Carney WP, Brandt-Rauf PW. Levels of p53 antigen in the plasma of patients with adenomas and carcinomas of the colon. *Cancer Lett* 1995; **91**: 235-240

29 **Fontanini G**, Vignati S, Bigini D, Merlo GR, Ribecchini A, Angeletti CA, Basolo F, Pingitore R, Bevilacqua G. Human non-small cell lung cancer: p53 protein accumulation is an early event and persists during metastatic progression. *J Pathol* 1994; **174**: 23-31

30 **Barton CM**, Staddon SL, Hughes CM, Hall PA, O'Sullivan C, Kloppel G, Theis B, Russel RC, Neoptolemos J, Williamson RC. Abnormalities of the p53 tumour suppressor gene in human pancreatic cancer. *Br J Cancer* 1992; **64**: 1076-1082

31 **Scarpa A**, Capelli P, Mukai K, Zamboni G, Oda T, Iacono C, Hirohashi S. Pancreatic adenocarcinomas frequently show p53 gene mutations. *Am J Pathol* 1993; **142**: 1534-1543

32 **Tada M**, Omata M, Kawai S, Saisho H, Ohto M, Saiki RK, Sninsky JJ. Detection of ras gene mutations in pancreatic juice and peripheral blood of patients with pancreatic adenocarcinoma. *Cancer Res* 1993; **53**: 2472-2474

33 **Wakasugi H**, Funakoshi A, Iguchi H, Takase M, Inoue M, Oshima A, Seo Y. Pancreatic carcinoma associated with chronic pancreatitis. *Intern Med* 1999; **38**: 951-956

34 **Pellegata NS**, Sessa F, Renault B, Bonato M, Leone BE, Solcia E, Ranzani GN. K-ras and p53 gene mutations in pancreatic cancer: ductal and nonductal tumors progress through different genetic lesions. *Cancer Res* 1994; **54**: 1556-1560

35 **Yamaguchi Y**, Watanabe H, Yrdiran S, Ohtsubo K, Motoo Y, Okai T, Sawabu N. Detection of mutations of p53 tumor suppressor gene in pancreatic juice and its application to diagnosis of patients with pancreatic cancer: comparson with k-ras mutations. *Clin Cancer Res* 1999; **5**: 1147-1153

Edited by Lu HM and Wang XL

P.O.Box 2345, Beijing 100023,China
Fax: +86-10-85381893
E-mail: wjg@wjgnet.com www.wjgnet.com

World J Gastroenterol 2003;9(8):1819-1823
World Journal of Gastroenterology
 ISSN 1007-9327

• CLINICAL RESEARCH •

Pancreatic cancer mortality in China (1991-2000)

Li Wang, Gong-Huan Yang, Xing-Hua Lu, Zheng-Jing Huang, Hui Li

Li Wang, Hui Li, Department of Epidemiology, School of Basic Medical Sciences, PUMC, Institute of Basic Medical Sciences, CAMS, Beijing, 100005, China
Gong-Huan Yang, Zheng-Jing Huang, Institute of Epidemiology and Microbiology, Center for Disease Control and Prevention of China, Beijing, 100050, China
Xing-Hua Lu, Department of Internal Medicine, Peking Union Hospital, Beijing, 100730, China
Supported by the Ministry of Public Health, No. 20010102
Correspondence to: Li Wang, Graduate School of Peking Union Medical College, 9 Dongdan 3 Tiao, Beijing, 100730, China. wangli0528@vip.sina.com
Telephone: +86-10- 65237943 **Fax**: +86-10-65284767
Received: 2003-03-02 **Accepted:** 2003-03-29

Abstract

AIM: To describe the mortality rate of pancreatic cancer and its distribution in China during the period of 1991-2000.

METHODS: Based on the data of demography and death collected through China's Disease Surveillance Point System (DSPS) over the period of 1991-2000, the distribution of death rate of pancreatic cancer was described in terms of age group, gender, calendar year, rural/urban residence and administrative district.

RESULTS: A total of 1 619 death cases attributed to pancreatic cancer (975 men and 644 women) were reported by DSPS during 1991-2000. The reported, adjusted and age-standardized mortality rates increased from 1.46, 1.75, and 2.18 per 100 000 populations in 1991 to 2.38, 3.06, and 3.26 per 100 000 populations in 2000. The majority (69.62 %) of the deaths of pancreatic cancer were seen in the age group of 60 years and older. The mortality rate was higher in men than in women, but the male to female death rate ratios decreased during the 10 years. Our data also showed that the death rate of pancreatic cancer in urban areas was about 2-4 fold higher than that in rural areas, and in Northeast and East China, the death rates were higher than those in the other 5 administrative districts.

CONCLUSION: The death rate due to pancreatic cancer was rising during the period of 1991-2000 and the peak mortality of pancreatic cancer might arrive in China.

Wang L, Yang GH, Lu XH, Huang ZJ, Li H. Pancreatic cancer mortality in China (1991-2000). *World J Gastroenterol* 2003; 9 (8): 1819-1823

http://www.wjgnet.com/1007-9327/9/1819.asp

INTRODUCTION

Pancreatic cancer is one of the most formidable malignant tumors worldwide. It is difficult to diagnose at early stage, unresectable at the time of diagnosis with extremely poor survival rate due to its inaccessible location, proximity to other vital organs, and inherently aggressive pattern of growth[1,2]. The death to incidence ratio of pancreatic cancer is approximately 0.98-0.99:1[3,10]. With more than 27 000 people died from pancreatic cancer each year, it is the fourth leading cause of cancer death in the United States[4]. Some sporadic reports have shown that the mortality rates of pancreatic cancer in China have increased constantly over the last decades[5-7]. But there is little descriptive documentation countrywide on its epidemiology. By analyzing the death data from China's Disease Surveillance Point System (DSPS), we presented the first report on the mortality from pancreatic cancer and its distribution among the surveillance population during the period of 1991-2000 in China.

MATERIALS AND METHODS

Materials

All mortality data were collected from the population who resided in 145 DSPs (Disease Surveillance Points) of China. The DSPS was originated in the beginning of 1980s for the surveillance of morbidity and mortality, and the present system was established in 1989. DSPs were selected from an official list of all neighborhoods in urban areas and villages in rural areas using stratified multistage sampling. The strata was involved in geographic areas (urban or rural status: within the rural areas, stratification into 4 levels based on indicators of mortality and socioeconomic status). In 1989, 145 surveillance points with a total population of around 10 million under surveillance (Table 1) were chosen, and scattered in 31 provinces, autonomous regions, or municipalities in China. Comparisons among the DSP population and the whole population over the country showed no significant differences in terms of socioeconomic conditions, population constitution, and health status. Such comparisons were made annually[8].

The obtained information related to death in China was based on the causes of death reported by qualified physicians on medical death certificates. The underlying causes of death were ascertained following the procedures specified by the World Health Organization in the (Manual of the International Statistical Classification of Diseases, Injuries, and Causes of Death), ninth revision (ICD-9). If the death causes of the deceased were either uncertain, or out of accord with the classification standards or could not be coded with ICD-9, the registry staff would clarify and/or justify the causes of death through interviewing the relatives of the patient or consulting his or her physicians.

Evaluation on data quality

Since the beginning of the disease surveillance, the National Center of DSPs had developed a series of quality control and evaluation system to examine data quality from DSPs every year, to assure that the surveillance data over the period of 1991-2000 were reliable and valuable for estimating the mortality of surveillance population. The quality of the data was evaluated as follows: (1) The demographic data and distribution of population by age and gender were credible and suitable for a denominator for calculating the rates since the United Nations Integrated Index of Population[9] fluctuates between 15 and 20. (2) The cases with uncertain death causes accounted for around 5 % of all death cases. (3) Three types of medical evidences from medical records or files were used for

Table 1 Population distribution by age group in DSPs during 1991-2000 in China (10 000)[a]

Age group	1991	1992	1993	1994	1995	1996	1997	1998	1999	2000
0-	18.52	15.74	13.84	13.56	11.47	11.60	12.00	10.40	9.92	10.17
1-	72.69	66.59	64.06	64.94	57.60	60.96	61.20	52.76	49.51	50.16
5-	88.94	83.27	79.72	83.66	76.27	80.52	82.40	70.60	66.62	69.51
10-	91.70	87.86	81.64	83.12	75.32	79.54	87.59	73.59	73.60	79.71
15-	106.24	96.25	90.63	94.48	82.97	90.43	94.27	81.45	78.51	83.92
20-	105.41	101.42	97.64	101.40	88.72	95.43	98.82	83.81	81.04	83.31
25-	99.66	98.06	93.77	95.82	86.55	92.23	97.02	83.60	81.07	83.60
30-	82.29	80.92	77.13	81.59	75.30	82.17	84.81	73.89	73.50	76.26
35-	77.87	77.00	75.00	76.67	68.58	73.37	76.82	68.56	67.84	70.99
40-	60.53	61.85	60.06	63.28	60.86	65.06	67.89	61.70	59.62	60.93
45-	48.19	48.48	47.51	50.14	47.67	51.95	54.45	50.14	49.87	52.72
50-	44.32	43.93	42.62	44.74	41.93	44.51	46.30	41.76	41.83	44.05
55-	40.80	40.08	39.46	40.59	37.76	40.99	41.62	37.14	37.10	38.55
60-	33.19	32.92	32.91	33.93	31.45	34.80	35.64	32.22	31.98	33.01
65-	25.73	25.45	25.94	26.65	24.50	27.56	28.54	26.10	25.93	27.17
70-	17.85	18.32	18.31	19.16	17.60	19.66	19.82	18.13	18.18	18.95
75-	11.18	11.64	11.73	12.33	11.24	12.21	12.39	11.25	11.28	11.86
80-	5.92	6.33	6.14	6.64	5.86	6.77	6.66	6.09	6.35	6.55
85+	2.81	2.59	2.90	3.08	3.17	3.67	3.38	3.13	3.30	3.51
Total	1033.84	998.70	961.01	995.78	904.82	973.43	1011.62	886.32	867.05	904.93

[a]Population of the surveillance points with poor quality deleted.

the diagnosis and classification of the causes of death, including autopsy or biopsy, laboratory or radiology tests (clinical diagnosis), and inference after death (without certain documentation from biopsy or radiology test, but making highly suspicious diagnosis in terms of clinical symptoms, signs and some laboratory tests). Cases of pancreatic cancer, diagnosed using pathological test and clinical test, accounted for 31.56 % and 64.13 % respectively, the remaining (4.31 %) was determined by inference diagnosis. The percentage of cases diagnosed at different levels of hospitals was as follows: 92 % by hospitals of county grade and above (36.4 % by provincial grade and 29.1 % by municipal grade). This showed that the diagnosed death causes were credible and could be used for data analysis. (4) Validation was undertaken through periodic under-reporting surveys. A stratified three-stage cluster sampling design was adopted by each DSP to obtain the under-reporting rate. The overall under-reporting rate for mortality fluctuated between 12.25 % and 22.46 %.

Analysis methods

Based on the surveillance data from the DSPs during the period of 1991-2000, the distribution of death rate of pancreatic cancer was described by age group, gender, calendar year, rural/urban residence and administrative district. The reported death rate was expressed as the reported number of deaths of pancreatic cancer per 100 000 populations per year. The adjusted death rate was calculated with the formula, reported death rate/(1-under-reporting rate) and the age-standardized rate was calculated with the indirect method in terms of World Standard Population (*http://www3.who.int/whosis/discussion_papers/htm/paper31.htm)*. All analyses were conducted using software EPI 2000.

RESULTS

During 1991-2000, 504 604 death cases were reported in DSPs population. The reported death rate fluctuated between 507.67 and 546.60 per 100 000 populations in 1991-2000. The adjusted death rate remained relatively stable in 1991-1997 and increased gradually after 1997. But the age-standardized death rate decreased slightly during the 10 years.

Table 2 Mortality rate of pancreatic cancer during 1991-2000 in China (1/100 000)

Year	Death number	Reported death rate	Adjusted death rate	Age-standardized death rate	Deaths due to tumor (%)[a]
1991	151	1.46	1.75	2.18	1.83
1992	139	1.39	1.60	1.92	1.66
1993	129	1.34	1.54	1.80	1.51
1994	142	1.43	1.63	1.90	1.69
1995	145	1.60	1.85	2.12	1.79
1996	161	1.65	1.91	2.14	1.75
1997	168	1.66	1.92	2.18	1.86
1998	183	2.06	2.66	2.92	2.10
1999	186	2.16	2.78	2.96	2.23
2000	215	2.38	3.06	3.26	2.26

[a]Calculated by reported death rate.

Eighty six thousand five hundred and fifty six patients died from tumor in the 10 years, accounting for 17.15 % of total death cases reported in DSPs population. The reported, adjusted and age-standardized death rate for tumor increased from 79.86, 95.57 and 118.74 per 100 000 in 1991 to 104.91, 135.30 and 145.63 in 2000 respectively, with a steady increase on average of 3.08 %, 3.94 % and 2.29 % per year. Tumor contributed 15.65 % of all deaths in 1991, and 19.23 % in 2000. Tumor ranked the third of death cause in all death cases during 1991-1998, and went up to the second rank in 1999-2000.

One thousand six hundred and nineteen deaths were attributed to pancreatic cancer during the 10 years, accounting for 1.87 % of all deaths due to tumors. The reported, adjusted and age-standardized mortality rate increased by 5.53 %, 6.41 % and 4.57 % annually, from 1.46, 1.75, 2.18 per 100 000 populations in 1991 to 2.38, 3.06, and 3.26 per 100 000 populations in 2000. Pancreatic cancer accounted for 1.83 %

of all deaths due to tumor in 1991 and 2.26 % in 2000, with the 6-8th rank for men and the 9-10th for women. The details and the time trend are shown in Table 2.

The death rate of pancreatic cancer was closely related to age. The majority (69.62 %) of the deaths of pancreatic cancer were seen in the age group of 60 years and more, while fewer cases (3.95 %) were found among people aged less than 40 years. Table 3 also shows the changing trend of annual mortality in all age groups during the 10 years. The annual mortality rates in the 10 years fluctuated around 2 per 100 000 populations in the age group of 45 to 54 years, but the rates were higher than 10 per 100 000 populations in the group aged 65 to 84 years, approximately 5-fold difference between these groups. Around 2-fold increase was found in the mortality in the last few years compared with that at the beginning of 1990' s in people aged over 65 years.

Table 3 Reported death rate of pancreatic cancer by age during 1991-2000 in China (1 / 100 000)

Age group	1991	1992	1993	1994	1995	1996	1997	1998	1999	2000
0-	0.00	0.00	0.00	0.00	0.00	0.00	0.00	0.00	0.00	0.00
15-	0.19	0.00	0.05	0.00	0.06	0.00	0.05	0.00	0.00	0.00
25-	0.22	0.11	0.00	0.11	0.12	0.06	0.16	0.19	0.26	0.06
35-	0.51	0.14	0.89	0.64	0.46	0.36	0.41	1.15	0.63	0.53
45-	2.70	2.06	2.44	0.95	1.45	1.76	2.38	2.50	2.84	1.65
55-	6.49	6.71	4.01	6.58	6.94	6.73	6.99	6.78	6.37	7.27
65-	9.18	10.74	9.49	9.17	9.98	11.86	11.17	13.11	16.55	18.87
75-	10.53	10.01	11.76	14.23	18.13	13.17	11.03	18.45	16.45	23.36
85+	17.82	7.74	6.89	13.01	6.32	16.36	14.79	15.98	9.08	17.10
Total	1.46	1.39	1.34	1.43	1.60	1.65	1.66	2.06	2.15	2.37

Of all the reported death cases of pancreatic cancer between 1991 and 2000, 975 were diagnosed in men and 644 in women. The mortality rates of pancreatic cancer by gender are presented in Table 4. The data showed that all the reported, adjusted and age-standardized rates in males increased during the 10 years, from 1.86, 2.23, and 2.94 per 100 000 populations in 1991 to 2.70, 3.48, and 3.87 per 100 000 populations in 2000, with an increase on average of 4.23 %, 5.07 % and 3.10 % per year respectively. All these rates in female increased from 1.05, 1.25, and 1.49 to 2.04, 2.63 and 2.68 per 100 000 populations, with an annual average increase of 7.66 %, 8.61 % and 6.74 %. The male to female standardized death rate ratios decreased from 1.97 in 1991 to 1.44 in 2000.

The distribution of pancreatic cancer differed among the administrative districts (Table 5). The reported death rates in Northeast and East China were higher than those in the other 5 districts. After adjusted by the under-reporting rates for different districts, the rates of Northeast and East China were still higher than the latter (Figure 1).

Table 5 Reported death rate of pancreatic cancer by the administrative district of DSPs, China, 1991-2000 (1 / 100 000)

Year	North China	Northeast China	East China	Central China	South China	Northwest China	Southwest China
1991	2.22	1.23	2.52	0.85	1.26	1.28	1.14
1992	1.43	2.43	2.10	0.86	0.90	1.93	1.15
1993	2.01	0.70	2.75	0.95	0.74	0.76	0.71
1994	1.27	3.18	2.62	1.13	0.60	0.88	0.92
1995	1.67	3.30	3.33	1.01	0.73	0.91	1.08
1996	1.68	3.37	3.34	1.27	1.07	0.67	0.78
1997	2.08	3.39	3.01	0.96	0.89	1.17	1.37
1998	1.80	4.26	4.04	1.31	0.51	1.61	1.85
1999	1.83	4.72	5.51	1.28	0.89	1.29	1.15
2000	1.55	6.96	4.31	1.26	1.48	0.73	1.79

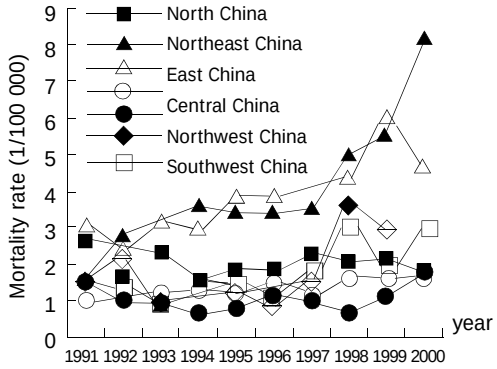

Figure 1 The adjusted mortality rate of pancreatic cancer by different districts, China, 1991-2000.

The distribution of pancreatic cancer was variable among rural and urban areas as well. The reported mortality rates in the urban areas were much higher than those in the rural areas. After adjusted by the differential under-reporting rates, the adjusted rates in the urban areas were still higher than those in the rural areas. And the death rates of pancreatic cancer displayed an increasing trend for both rural and urban areas during the period of 1991-2000 (Table 6). In 1991 the reported death rate of pancreatic cancer was 3.37 per 100 000 populations in the urban areas and 0.91 in the rural areas, and the adjusted death rates were 3.97 and 1.09, respectively. In 2000, the correspondent rates were 5.53 and 1.54, 7.32 and

Table 4 Mortality rate of pancreatic cancer by gender during 1991-2000 in China (1 / 100 000)

Year	Male				Female			
	Death number	Reported death rate	Adjusted death rate	Age-standardized rate	Death number	Reported death rate	Adjusted death rate	Age-standardized rate
1991	98	1.86	2.23	2.94	53	1.05	1.25	1.49
1992	97	1.90	2.19	2.77	42	0.86	0.99	1.13
1993	81	1.66	1.90	2.36	48	1.02	1.17	1.29
1994	79	1.56	1.78	2.24	63	1.29	1.47	1.62
1995	94	2.04	2.36	2.87	51	1.15	1.33	1.44
1996	90	1.82	2.10	2.47	71	1.48	1.72	1.85
1997	98	1.89	2.20	2.61	70	1.41	1.63	1.76
1998	106	2.34	3.02	3.45	77	1.77	2.28	2.40
1999	108	2.44	3.15	3.57	78	1.83	2.36	2.40
2000	124	2.70	3.48	3.87	91	2.04	2.63	2.68

1.97, respectively. Between 1991 and 2000, the reported and adjusted death rates increased by 5.02 % and 7.03 % per year in the urban areas and 6.02 % and 6.80 % in the rural areas, respectively.

Table 6 Mortality rate of pancreatic cancer by areas during 1991-2000 in China (1/100 000)

Year	Reported death rate			Adjusted death rate		
	Urban	Rural	Ratio of urban to rural	Urban	Rural	Ratio of urban to rural
1991	3.37	0.91	3.70	3.97	1.09	3.64
1992	3.00	0.92	3.26	3.37	1.06	3.18
1993	3.25	0.81	4.01	3.65	0.93	3.93
1994	3.50	0.84	4.17	3.84	0.96	4.00
1995	3.63	0.99	3.67	4.28	1.14	3.75
1996	4.12	0.88	4.68	4.86	1.01	4.81
1997	3.80	1.02	3.73	4.47	1.18	3.79
1998	3.77	1.56	2.42	4.99	2.00	2.50
1999	3.89	1.61	2.42	5.15	2.07	2.49
2000	5.53	1.54	3.59	7.32	1.97	3.72

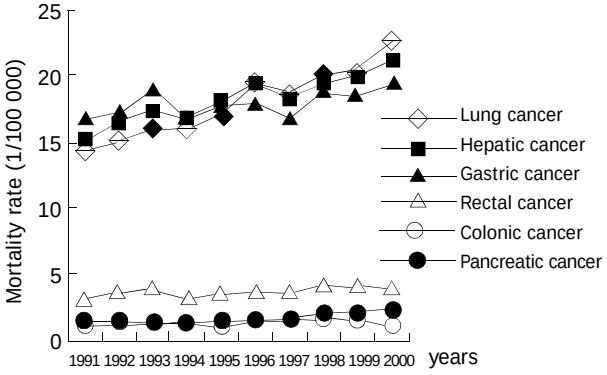

Figure 2 The trend of reported mortality of pancreatic cancer and some major cancers in DSP, China, 1991-2000.

Figure 2 shows the dynamic trend of mortality rate of pancreatic cancer and other common tumors. The increasing trend of pancreatic cancer paralleled the slight variation seen in rectal and colonic cancer, while the death rates of hepatic, stomach and lung cancers changed more remarkablely.

DISCUSSION

Our data analysis was performed based on the data of demography and death, collected through DSPs over the period from 1991 to 2000. The DSPS data were of good representative ness due to their selection by probability sampling and their rigorous management[8] and therefore the results derived from surveillance population can be inferred to health status of national population. The assessment of indicators used for data quality evaluation, including the United Nations Integrated Index on Population, the proportion of cases with uncertain death cause, the diagnosis evidence of pancreatic cancer and the under-reporting rate, demonstrates that these data are reliable and the mortality rate of pancreatic cancer derived from the DSPs data might be used to estimate the death level over the whole community. However, the mortality rates reported in this study might be lower in view of the impact of technology development in the diagnosis of pancreatic cancer and its nonspecific clinical symptoms.

Pancreatic cancer may be one of the diseases that are correlated with industrialization. Reports from the studies on the mortality of pancreatic cancer worldwide in 1990 suggested that majority deaths (66 %) occurred in developed countries[10]. WHO reported[11] the age-standardized mortality rates of pancreatic cancer in Western developed countries such as the United States, the United Kingdom, Australia, and Japan, ranged from 6 to 8 per 100 000 in males, and 4 to 6 in females, which were about 2-4 times higher than that in China (about 2 to 3 per 100 000 in males and 1 to 3 in females) in the same period. But in these countries, the mortality rate of pancreatic cancer, both in males and females, have leveled off and even dropped by the end of last century. And in some Asian countries, such as South Korea and Singapore, the age-standardized rates of pancreatic cancer are also higher than those in China, even though not reaching the peak yet[11]. In addition, we have seen a rapid increasing of death rates of pancreatic cancer in China, particularly among those aged over 65 years in the recent decade. The reported, adjusted and age-standardized death rates of pancreatic cancer have increased by 62.33 %, 74.86 % and 49.54 % respectively. This is, to some extent, explained by the improved diagnosis and cancer death registration since pancreatic cancer is difficult to be diagnosed and classified[31], but it is also probably attributed to the increased risk factors associated with industrialization, such as diet- and smoking-related factors as well as life-style changes[21,22]. At present, little is known about the etiology of pancreatic cancer. Cigarette smoking is the only firmly established factor[17, 25-28], with a 1. 2- to 3.1-fold increase in risk. Smoking, however, cannot by itself totally explain the increasing trends. There is less certainty concerning the risks associated with a range of dietary factors. Some studies have reported an increased risk with higher consumption of meat, protein and cholesterol and lower consumption of fruits and vegetables[27-30].

The role of life-style and dietary factors[27-30] in the etiology of pancreatic cancer is also supported by the higher mortality rates observed in the urban areas. Of course, the higher rates in the urban areas could be partly attributed to the improved diagnosis. Also our data showed that the death rates of pancreatic cancer were not identical in different administrative districts. The mortality rate was considerably higher in Northeast and East China than that in the other 5 districts, and the reasons led to this difference need to be discussed further, but a partial reason might be associated with higher level of industrialization and urbanization in these areas.

The mortality rate of pancreatic cancer was strongly related to age in our study. Our study indicated that the majority of death cases of pancreatic cancer occurred in the age group of 60 years or older, and the patients aged less than 45 years only accounted for 3.95 %, almost the same as the results in other studies[12-17]. Similar to the other studies[11,14,18-20], our data have also found the gender difference between male and female. And the mortality from pancreatic cancer in males was higher than that in females, but the male to female mortality rate ratio showed a decreased trend in the period of 1991-2000.

Our study indicated that the increasing trend of mortality rate of pancreatic cancer paralleled that of rectal cancer. And other studies have also shown that there are remarkable similarities between the increased incidence of pancreas cancer and breast cancer in women and prostate cancer in men, and bowel cancer in both sexes over approximately the same period[23,24]. Dietary- and smoking- factors as the common risk factors may be relevant to the similarly increased trends of breast[33], prostate[32], bowel[34] and pancreatic cancers.

It is suggested that with the entry into an aging society and urbanization in China, the peak mortality of pancreatic cancer arrive soon in the next few decades. Therefore, it is crucial to carry out further studies on the etiology of pancreatic cancer and set up screening indicators earlier to reduce the number of deaths from pancreatic cancer.

REFERENCES

1 **Warshaw AL,** Fernandez-del Castillo C. Pancreatic carcinoma. *N Engl J Med* 1992; **326:** 455-465
2 **Williamson RC.** Pancreatic cancer: the greatest oncological challenge. *Br Med J* 1988; **296**: 445-446
3 **Devesa SS,** Blot WJ, Stone BJ, Miller BA, Tarone RE, Fraumeni JF Jr. Recent cancer trends in the United States. *J Natl Cancer Inst* 1995; **87**: 175-182
4 **Greenlee RT**, Murray T, Bolden S, Wingo PA. Cancer statistics, 2000. *CA Cancer J Clin* 2000; **50**: 7-33
5 **Qian MF**, Wang XH, Ma XY, Lei TH, Yao KY. Aresearch on the epidemiologic trend and mortality with cancer in Jiashan County. *Zhongguo zhongliu* 2001; **10:** 381-383
6 **Tan YD**, Jin YS, Lu XJ, Zhu YH. The change of death spectrum for major malignancies in Xiaoshan from 1970s to 1990s. *Zhejiang Zhongliu* 2000; **6:** 128-129
7 **Men BY**, Li SY, Wang Y, Gao HY, Zhang WL, Wang F, Liu L. A comparison between the results of cancer mortalities in 1972-1975 and in 1992-1994 in a rural areas of Shanxi proivince. *Zhonghua Liuxing Bingxue Zazhi* 1997; **33**: 5-8
8 **Yang GH**, Zhen XW, Zen G, Wang LS, Chen YL, Chen AP, Huang ZJ, Ge WM. Selection of DSP points in the second stage and their presentation. *Zhonghua Liuxing Bingxue Zazhi* 1992; **13**: 197-201
9 Department of Control Disease of MOPH, Chinese Academy of Preventive Medicine. A series of reports on Chinese disease surveillance: 1995 annual report on Chinese disease surveillance. *Beijing, China: People's Medical Publishing House* 1997: 9
10 **Pisani P,** Parkin DM, Bray F, Ferlay J. Estimates of the worldwide mortality from 25 cancers in 1990. *Int J Cancer* 1999; **83**: 18-29
11 **Worldwide cancer mortality statistics**. [cited 2002-06]. Available form: URL: http / / www-depdb.iarc.fr / who / menu.htm.
12 **Lillemoe KD,** Yeo CJ, Cameron JL. Pancreatic cancer: state-of-the-art care. *CA Cancer J Clin* 2000; **50**: 241-268
13 **Tan HP,** Smith J, Garberoglio CA. Pancreatic adenocarcinoma: an update. *J Am Coll Surg* 1996; **183**: 164-184
14 **Oomi K,** Amano M. The epidemiology of pancreatic disease in Japan. *Pancreas* 1998; **16**: 233-237
15 **Lillemoe KD**. Pancreatic disease in the elderly patient. *Surg Clin North Am* 1994; **74:** 317-344
16 **Hedberg M,** Anderson H, Borgstrom A, Janzon L, Larsson SA. Rising incidence of pancreatic carcinoma in middle-aged and older women-time trends 1961-90 in the city of Malmo, Sweden. *Br J Cancer* 1996; **73:** 843-846
17 **Nilsen TI,** Vatten LJ. A prospective study of lifestyle factors and the risk of pancreatic cancer in nord-trondelag, Norway. *Cancer Causes and Control* 2000; **11:** 645-652
18 **Niederhuber JE,** Brennan MF, Menck HR. The national cancer data base report on pancreatic cancer. *Cancer* 1995; **76**: 1671-1677
19 **Zheng T,** Holford TR, Ward BA, McKay L, Flannery J, Boyle P. Time trend in pancreatic cancer incidence in Connecticut, 1935-1990. *Int J Cancer* 1995; **61**: 622-627
20 **Karlson BM,** Ekbom A, Josefsson S, McLaughlin JK, Fraumeni JF Jr, Nyren O. The risk of pancreatic cancer following pancreatitis: an association due to confounding? *Gastroenterology* 1997; **113:** 587-592
21 Chinese Academy of Preventive Medicine, Dept. of Disease Control of Ministry of Health, P. R. China, Chinese Association of Smoking or Health, Office of Committee of the National Patriotic Health Campaign. Smoking and health in China, 1996 national prevalence survey of smoking pattern. *Beijing, China: China Science and Technology Press* 1997: 2-4
22 **Yang GH**. The transition of health mode and the control strategy on chronic disease in China. *Zhongguo Manxingbing Yufang yu Kongzhi* 2001; **9**: 145-148
23 **Stephens FO.** The increased incidence of cancer of the pancreas: is there a missing dietary factor? Can it be reversed? *Aust N Z J Surg* 1999; **69:** 331-335
24 **Jin F,** Devesa SS, Zheng W, Blot WJ, Fraumeni JF Jr, Gao YT. Cancer incidence trends in urban Shanghai, 1972-1989. *Int J Cancer* 1993; **53**: 764-770
25 **Coughlin SS,** Calle EE, Patel AV, Thun MJ. Predictors of pancreatic cancer mortality among a large cohort of united states adults. *Cancer Causes Control* 2000; **11:** 915-923
26 **Chiu BC,** Lynch CF, Cerhan JR, Cantor KP. Cigarette smoking and risk of bladder, pancreas, kidney and colorectal cancers in Iowa. *Ann Epidemiol* 2001; **11:** 28-37
27 **Stolzenberg-Solomon RZ,** Pietinen P, Barrett MJ, Taylor PR, Virtamo J, Albanes D. Dietary and other methyl-group availability factors and pancreatic cancer risks in a cohort of male smokers. *Am J Epidemiol* 2001; **153**: 680-687
28 **Baghurst PA,** McMichael AJ, Slavotinek AH, Baghurst KI, Boyle P, Walker AM. A case-control study of diet and cancer of the pancreas. *Am J Epidemiol* 1991; **134**: 167-179
29 **Farrow DC, Davis S.** Diet and the risk of pancreatic cancer in men. *Am J Epidemiol* 1990; **132**: 423-431
30 **Norell SE,** Ahlbom A, Erwald R, Jacobson G, Lindberg-Navier I, Olin R, Tornberg B, Wiechel KL. Diet and pancreatic cancer: a case-control study. *Am J Epidemiol* 1986; **124**: 894-902
31 **La Vecchia C,** Lucchini F, Negri E, Boyle P, Maisonneuve P, Levi F. Trends in cancer mortality in Europe, 1955-1989: I, Digestive sites. *Eur J Cancer* 1992; **28:** 132-235
32 **Shirai T,** Asamoto M, Takahashi S, Imaida K. Diet and prostate cancer. *Toxicology* 2002; **181-182**: 89-94
33 **Wolff MS,** Britton JA, Wilson VP. Environmental risk factors for breast cancer among African-American women. *Cancer* 2003; **97** (Suppl): 289-310
34 **Tiemersma EW,** Kampman E, Bueno de Mesquita HB, Bunschoten A, van Schothorst EM, Kok FJ, Kromhout D. Meat consumption, cigarette smoking, and genetic susceptibility in the etiology of colorectal cancer: results from a Dutch prospective study. *Cancer Causes Control* 2002; **13**: 383-393

Edited by Yuan HT and Wang XL

P.O.Box 2345, Beijing 100023,China
Fax: +86-10-85381893
E-mail: wjg@wjgnet.com www.wjgnet.com

World J Gastroenterol 2003;9(8):1824-1827
World Journal of Gastroenterology
 ISSN 1007-9327

• CLINICAL RESEARCH •

Influence of acute hyperglycemia in human sepsis on inflammatory cytokine and counterregulatory hormone concentrations

Wen-Kui Yu, Wei-Qin Li, Ning Li, Jie-Shou Li

Wen-Kui Yu, Wei-Qin Li, Ning Li, Jie-Shou Li, Medical College of Nanjing University, Research Institute of General Surgery, Jinling Hospital, Nanjing 210002, Jiangsu Province, China
Supported by the Key Project of the Tenth-Five-year plan Foundation of PLA, No. 01Z011
Correspondence to: Wen-Kui Yu, Research Institute of General Surgery, Jinling Hospital, 305 Zhongshan East Road, Nanjing 210002, Jiangsu Province, China. yudrnj@163.com
Telephone: +86-25-4826808 Ext 58067
Received: 2002-12-28 **Accepted:** 2003-02-16

Abstract

AIM: In human sepsis, a prominent component of the hypermetabolite is impaired glucose tolerance (IGT) and hyperglycemia. Elevations in plasma glucose concentration impair immune function by altering cytokine production from macrophages. We assessed the role of glucose in the regulation of circulating levels of insulin, glucagon, cortisol, IL-6 and TNF-α in human sepsis with normal or impaired glucose tolerance.

METHODS: According to the results of intravenous glucose tolerance test, forty patients were classified into two groups: control group (n=20) and IGT group (n=20). Plasma glucose levels were acutely raised in two groups and maintained at 15 mmol/L for 3 hours. Plasma insulin, glucagon and cortisol levels were measured by radioimmunoassay, the levels of TNF-α and IL-6 were detected by ELISA.

RESULTS: In IGT group, the fasting concentrations of plasma glucose, insulin, glucagon, cortisol, IL-6 and TNF-α levels were significantly higher than those in control group (P<0.05). During clamp, the control group had a higher average amount of dextrose infusion than the IGT group (P<0.01). In control group, plasma insulin levels rose from a basal value to a peak at an hour (P<0.05) and maintained at high levels. Plasma glucagon levels descended from a basal value to the lowest level within an hour (P<0.01) and low levels were maintained throughout the clamp. In IGT group, plasma insulin was more significantly elevated (P<0.01), and plasma glucagon levels were not significantly declined. Plasma cortisol levels were not significantly changed in two groups. In control group, plasma IL-6 and TNF-α levels rose (P<0.01) within 2 hours of the clamp and returned to basal values at 3 hours. In IGT group, increased levels of plasma cytokine lasted longer than in control group (3 hours *vs*. 2 hours, P<0.05), and the cytokine peaks of IGT group were higher (P<0.05) than those of control group.

CONCLUSION: Acute hyperglycemia pricks up hyperinsulinemia and increases circulating cytokine concentrations and these effects are more pronounced in sepsis with IGT. This suggests a potential modulation of immunoinflammatory responses in human sepsis by hyperglycemia.

Yu WK, Li WQ, Li N, Li JS. Influence of acute hyperglycemia in human sepsis on inflammatory cytokine and counterregulatory hormone concentrations. *World J Gastroenterol* 2003; 9(8): 1824-1827
http://www.wjgnet.com/1007-9327/9/1824.asp

INTRODUCTION

Severe human sepsis is associated with hypermetabolic stress response, and affects protein, carbohydrate and lipid metabolism throughout the body[1-7]. A prominent component of hypermetabolic stress response is hyperglycemia and impaired glucose tolerance (IGT). The mechanisms of stress hyperglycemia are well known[8]. Counterreglulatory hormone and excess cytokine result in insulin resistance, and many hospitalized patients are insulin deficient for a variety of reasons (e.g. old age, pancreatitis, hypothermia, hypoxemia). Excess dextrose infusion is an often-overlooked contributor to hyperglycemia[9].

The harm of acute hyperglycemia in stress response patients has been demonstrated in several clinical and experimental conditions[10-12]. An increased susceptibility to infections in the presence of hyperglycemia has long been known in patients with diabetes[10,11,13]. And recent investigations have demonstrated that elevations in plasma glucose concentration impair immune function by altering cytokine production from macrophages, diminishing lymphocyte proliferation, and depressing intracellular bactericidal activity of leukocytes[14-17]. Furthermore, in the issue of circulation, Esposito K. argued hyperglycemia acutely increased circulating cytokine concentrations, and this effect was more pronounced in group with IGT[18]. But former researches focused on normal human being, diabetes or critically ill patients, etc. and rarely concentrated on severe human sepsis.

The present study was to test whether circulating levels of hormones and cytokines are regulated by glucose levels in sepsis, and to measure serum insulin, glucagon, cortisol, TNF-α, and IL-6 concentrations during acute hyperglycemia in septic patients with normal or impaired glucose tolerance (IGT).

MATERIALS AND METHODS

Subjects

The subjects of this study were the patients admitted from January 5 to November 1, 2002 to the medical SICU of Jinling Hospital in Nanjing. Forty patients (23 men, 17 women) with a mean (s.d.) age of 52.2 (15.6) years with abdominal or pelvic sepsis were studied. Patients with diabetes mellitus, trauma, human immunodeficiency virus disease, end-stage renal disease, end-stage hepatic disease, the patients receiving immunosuppressive agents were excluded. Forty patients were divided into two groups according to normal (control group, n=20) or impaired (IGT group, n=20) glucose tolerance (Table 1). The patients' glucose tolerance was assessed by intravenous glucose tolerance test (IVGTT). After an overnight fast each patient underwent IVGTT: a 50 % glucose solution (glucose 0.5 gm/kg of body weight) was injected into the femoral vein

for 2 minutes. Patients in IGT group had a 2-hour plasma glucose value between 7.7 mmol/L and 11 mmol/L, and the control group had normal glucose tolerance (2-hour plasma glucose value below 7.7 mmol/L). Informed consent was obtained from all participating patients or their surrogates.

Severity of sepsis and underlying diagnosis

Sepsis was defined by the American College of Chest Physicians-Society of Critical Care Medicine consensus statement by an identifiable site of infection and evidence of a systemic inflammatory response manifested by at least three of the following criteria: (1) temperature, >38 ℃ or <36 ℃; (2) heart rate, >90 beats per minute; (3) respiratory rate, >20 breaths per minute; (4) white blood cell count, >12 000/mm^3 or <4 000/mm^3[19]. Patients meeting enrollment criteria were entered within 24 h. The cause of sepsis was severe acute pancreatitis (n=11), colorectal anastomotic dehiscence (n=9), perforated diverticular disease (n=9), gastroduodenal perforation (n=7), gallbladder perforation (n=3) and spontaneous splenic abscess (n=1). Sepsis severity was scored using the method of Elebute and Stoner[20]. This scoring procedure takes into account the site of infection, bacteriology, body temperature, secondary effects (e.g. jaundice) and various haematological and biochemical variables, such as white cell count and plasma albumin concentration.

Study protocol

After 12-hour fast overnight, the patients were placed in a supine comfortable position with the sickroom temperature between 20 ℃ and 24 ℃. Intravenous lines were inserted into a large antecubital vein of one arm for infusions and into a dorsal vein of the contralateral arm for blood sampling. Patency was preserved in a slow saline infusion (0.9 % NaCl). After withdrawal of baseline blood samples, plasma glucose concentrations were acutely raised with a bolus injection of 0.25 g/kg glucose followed by a varying 30 % glucose infusion to achieve steady-state plasma glucose concentrations of about 15 mmol/L for 180 minutes.

Analysis

Samples for analysis of plasma glucose were collected in tubes containing a trace of sodium fluoride. Plasma glucose was determined according to the glucose oxidase method with an autoanalyzer (Beckman Instruments). Serum samples for measuring hormone and cytokine level were stored at -80 ℃ until assay. Commercially available kits were used for radioimmunoassay of plasma insulin, glucagon and cortisol concentrations. Serum concentrations of TNF-α, IL-6 were determined in duplicate with commercially available kits (R&D Systems). Dilution curves of serum samples were parallel to those of standard. Intra-assay and interassay coefficients of variation were 3.8 % and 5.8 % for TNF-α, 2.8 % and 3.3 % for IL-6.

Statistical analysis

Results were given as mean ±SD. One-way ANOVA was used to compare baseline data, followed by Scheffé's test for pairwise comparisons. Multiple comparison tests were made with ANOVA, followed by post hoc analysis (Student-Newman-Keuls test) to locate the significant difference indicated by ANOVA. A value of P<0.05 was considered statistically significant. Data were analysed using Statistical Package for the Social Sciences computer software (SPSS 11.0).

RESULTS

During the 7-month study period 46 patients were collected, however analysis was limited to 40 patients with complete and available data. IGT group had higher admission severity scores than control group (APACHE Ⅱ, 10 (7-15) *vs*. 7 (4-10), sepsis score, 13 (8-19) *vs*. 8 (6-13); P<0.05). In IGT group, the levels of fasting plasma glucose, insulin, glucagon, cortisol, IL-6 and TNF-α levels were significantly higher than those in control group (Table 1). During the clamp, plasma glucose became stabilized at 15 mmol/L with oscillations not exceeding 5 % of the prefixed value. The control group had a higher average amount of dextrose infusion than IGT group (0.68±0.31 g/kg *vs*. 0.42±0.16 g/kg; P<0.01).

Table 1 Details of control and IGT groups

Variable	Control group (n=20)	IGT subject (n=20)
Age, y	41±4	42±6
Sex, M/F, n	13/7	12/8
Body mass index, kg/m2	21.11±1.22	20.12±1.43
Plasma glucose, mmol/L	5.22±0.89	7.23±0.73[a]
Plasma insulin, pmol/L	72.00±14.83	82.95±10.23[a]
Plasma glucagon, pmol/L	80.75±12.98	90.90±15.54[a]
Plasma cortisol, mmol/L	0.68±0.11	0.79±0.12[b]
IL-6, pg/ml	3.18±0.64	3.63±0.43[a]
TNF-α, pg/ml	4.66±0.70	5.99±0.76[b]
APACHE Ⅱ score	7(4-10)	10(7-15)[a]
Sepsis score	10(8-16)	15(10-25)[a]

All data were the mean (s.d.), except APACHE Ⅱ score and sepsis score which were the median (range). APACHE, acute physiology and chronic health evaluation. [a]P<0.05 *vs*. control group. [b]P<0.01 *vs* control group.

Counterregulatory hormone

During the clamp, plasma insulin levels increased from a basal level of 72.00±14.83 pmol/L to a peak of 83.40±14.29pmol/L within one hour (P<0.05) and maintained at high levels in control group. Whereas, plasma insulin levels increased more significantly in IGT group (P<0.01) (Figure 1). In control group, plasma glucagon levels decreased from a basal value of 80.75±12.98 pmol/L to the lowest level of 74.70±11.40 pmol/L within an hour (P<0.01) and low levels maintained, and was not significantly declined in IGT group during the entire observation period (Figure 2). Plasma cortisol was not significantly changed in two groups (Figure 3).

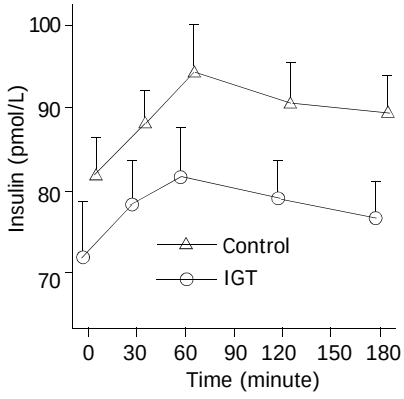

Figure 1 Circulation insulin levels during hyperglycemia clamps in 20 patients of control group (○-○) and in 20 patients of IGT group (△-△). Mean ± S.E.M. in human sepsis. Plasma insulin levels rose from a basal value to a peak within an hour (P<0.01) and high levels maintained in two groups.

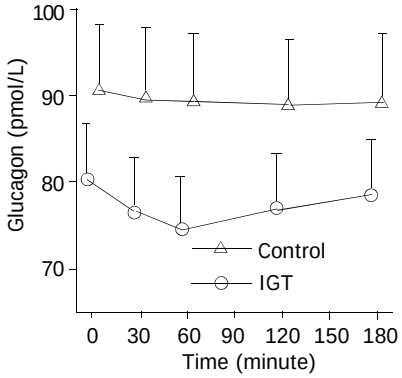

Figure 2 Circulation glucagon levels during hyperglycemia clamps in 20 patients of control group (○-○) and in 20 patients of IGT group (△-△). Mean ± S.E.M. in human sepsis. In control group, plasma glucagon levels decreased from a basal value to the lowest level within half an hour (P<0.01) and a low level maintained, and was not significantly declined in IGT group in the entire observation period.

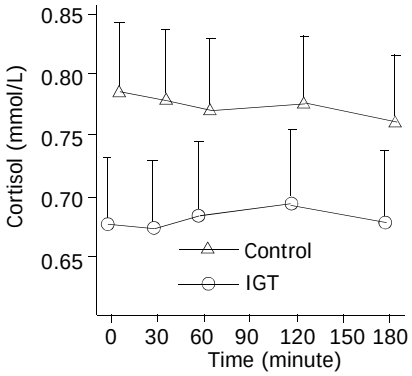

Figure 3 Circulation cortisol levels during hyperglycemia clamps in 20 patients of control group (○-○) and in 20 patients of IGT group (△-△). Mean ± S.E.M. in human sepsis. There were no significant changes in two groups.

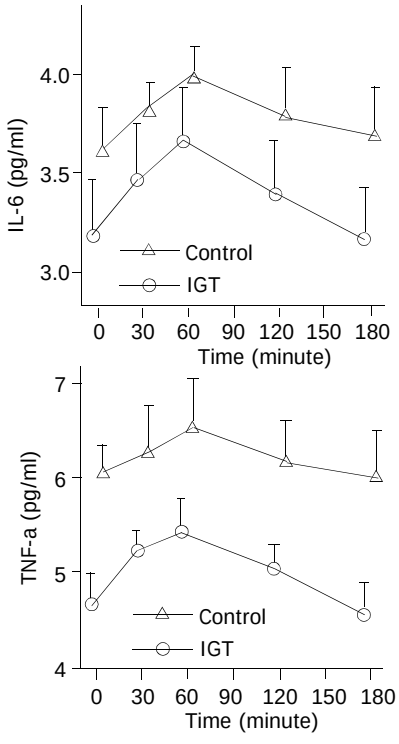

Figure 4 Circulation IL-6, TNF-α levels during hyperglycemia clamps in 20 patients of control group (○-○) and in 20 patients of IGT group (△-△). Mean ± S.E.M. in human sepsis. In two groups, plasma IL-6, TNF-α levels rose from a basal value to a peak within 1 hour (P<0.01). In IGT group, increased level of plasma TNF-α, IL-6 during the clamping lasted longer than in control group (3 hours *vs*. 2 hours; P<0.05).

Inflammatory cytokine

In control group, plasma IL-6 levels increased from a basal value of 3.18±0.64 pg/mL to a peak of 3.67±0.57 pg/mL within 1 hour (P<0.01) and returned to basal level at 3 hours. Fasting plasma TNF-α levels were 4.66±0.70 pg/mL, they peaked at 1 hour (5.4±0.64 pg/mL, P<0.01), and returned to baseline at 3 hours. In IGT group, increased levels of plasma cytokine during the clamp lasted longer than in control group (3 hours *vs*. 2 hours; P<0.05) (Figure 4, 5).

DISCUSSION

In this study, we found that IGT group had higher admission severity scores than control group, and had high plasma concentrations of counterregulatory hormones and inflammatory cytokines. During the clamp, IGT group had a less average amount of dextrose infusion than control group. In IGT patients, a short term of hyperglycemia after glucose infusion failed to adjust the plasma concentration of counterregulatory hormones to maintain glucose homeostasis. Acute hyperglycemia in control and in IGT patients induced an increase in plasma IL-6, TNF-α concentrations and insulin levels, and the effect was amplified by IGT group. These results indicate that hyperglycemia in human sepsis with IGT is more easy to be revoked, and plays a potential modulation role in immunoinflammatory responses.

The mechanisms for "stress IGT" are well known. Human sepsis is accompanied by a marked increase in plasma concentration of counterregulatory hormones, i.e. glucagons, epinephrine, cortisol and growth hormone that affect glucose homeostasis. These hormones can lead to significant reductions in insulin sensitivity through poorly understood mechanisms likely related to alterations in insulin signal pathway[21]. Counterregulatory hormones also enhance lipolysis and level of free fatty acids (FFA) which may contribute additional defects to the defective insulin action. Cytokine, TNF-α and IL-6 may exert their influence indirectly by stimulating counterregulatory hormone secretion and by direct action themselves[22-24]. TNF-α and IL-6 individually and synergistically increase net glucose flux through resistance to insulin actions in muscle and liver via poorly understood post-receptor mechanisms[25]. Hepatic insulin resistance leads to ongoing glucose production even in hyperglycemia[26]. Peripheral insulin resistance decreases sketetal muscle glucose uptake and reduces glucose clearance, which leads to the development of IGT and even hyperglycemia.

After glucose infusion, in normal group, glucagon and glucose concentrations reduced by host insulin were sufficient and inhibited hepatic gluconeogenesis and glycogenolysis and prevented glucose production[27]. In contrast, in IGT group, glucose infusion failed to suppress endogenous glucose production despite accompanying hyperinsulinemia. Using stable isotopes, it was demonstrated that hepatic glucose production was -150 % of the normal resting post-absorptive values of healthy subjects in spite of provision of total parenteral nutrition with dextrose at rates exceeding the basal energy expenditure[28].

Glucose-based nutrition in septic patients may cause marked hyperinsulinemia due to peripheral insulin resistance[29]. Hyperinsulinemia associated with glucose-based nutrition in sepsis might augment proinflammatory cytokine production and stress response in septic patients[30]. The present findings

also demonstrated that acute hyperglycemia affected concentration of plasma cytokines in human sepsis, and this effect was more pronounced in IGT patients. *In vitro* studies using supraphysiological glucose concentration (>22 mmol/l) showed an increase in TNF-α and IL-6 secretion from healthy human mononuclear cells[31]. Furthermore, increased synthesis of TNF-α has been reported both in rat uterine cells cultured *in vitro* with increasing concentrations of glucose[32] and in placental tissue explants from women with gestational diabetes incubated with high glucose (25 mmol/l)[33]. Human monocytes produced by IL-6 in healthy volunteers increased during 24-hour incubation in high-glucose medium[34]. These findings are in accordance with our observations *in vivo*, suggesting a potential modulation of immunoinflammatory response by carbohydrates.

In summary, IGT in sepsis is associated with marked changes in plasma concentrations of counterregulatory hormones and inflammatory cytokines, and these changes partially account for the fact that IGT easily develops acute hyperglycemia during glucose infusion. Acute hyperglycemia pricks up hyperinsulinemia and increases circulating cytokine concentrations. This suggests a potential role of hyperglycemia in inflammatory responses in human sepsis.

REFERENCES

1 **Wu XN**. Current concept of pathogenesis of severe acute pancreatitis. *World J Gastroenterol* 2000; **6**: 32-36
2 **Netea MG**, Van der Meer JW, Kullberg BJ. Sepsis-theory and therapies. *N Engl J Med* 2003; **348**: 1600-1602
3 **Han DW**. Intestinal endotoxemia as a pathogenetic mechanism in liver failure. *World J Gastroenterol* 2002; **8**: 961-965
4 **Douglas RG**, Shaw JH. Metabolic response to sepsis and trauma. *Br J Surg* 1989; **76**: 115
5 **Wray CJ**, Mammen JM, Hasselgren PO. Catabolic response to stress and potential benefits of nutrition support. *Nutrition* 2002; **18**: 971-977
6 **Wu XN**. Treatment revisited and factors affecting prognosis of severe acute pancreatitis. *World J Gastroenterol* 2000; **6**: 663-665
7 **Chen QP**. Enteral nutrition and acute pancreatitis. *World J Gastroenterol* 2001; **7**: 185-192
8 **Mesotten D**, Van Den Berghe G. Clinical potential of insulin therapy in critically ill patients. *Drugs* 2003; **63**: 625-636
9 **Hirsch IB**. In-patient hyperglycemia-are we ready to treat it yet? *J Clin Endocrinol Metab* 2002; **87**: 975-977
10 **Beckman JA**, Goldfine AB, Gordon MB, Creager MA. Ascorbate restores endothelium-dependent vasodilation impaired by acute hyperglycemia in humans. *Circulation* 2001; **103**: 1618-1623
11 **Mizock BA**. Alterations in fuel metabolism in critical illness: hyperglycaemia. *Best Pract Res Clin Endocrinol Metab* 2001; **15**: 553-551
12 **Vasa FR**, Molitch ME. Endocrine problems in the chronically critically ill patient. *Clin Chest Med* 2001; **22**: 193-208
13 **Alexiewicz JM**, Kumar D, Smogorzewski M, Massry SG. Elevated cytosolic calcium and impaired proliferation of B lymphocytes in type II diabetes mellitus. *Am J Kidney Dis* 1997; **30**: 98-104
14 **Losser MR**, Bernard C, Beaudeux JL, Pison C, Payen D. Glucose modulates hemodynamic, metabolic, and inflammatory responses to lipopolysaccharide in rabbits. *J Appl Physiol* 1997; **83**: 1566-1574
15 **Reinhold D**, Anosorge S, Scheeicher ED. Elevated glucose levels stimulate transforming growth factor-beta 1 (TGF-beta 1), suppress interleukin IL-2, IL-6 and IL-10 Production and DNA synthesis in peripheral blood mononuclear cells. *Horm Metab Res* 1996; **28**: 267-270
16 **Gregory R**, McElveen J, Tattersall RB, Todd I. The effects of 3-hydroxybutyrate and glucose on human T cell responses to Candida albicans. *FEMS Immunol Med Microbiol* 1993; **7**: 315-320
17 **Moises RS**, Heidenreich KA. Glucose regulates expression of Gi-proteins in cultured BC3H-1 myocytes. *Biochem Biophys Res Commun* 1992; **182**: 1193-1200
18 **Esposito K**, Nappo F, Marfella R, Giugliano G, Giugliano F, Ciotola M, Quagliaro L, Ceriello A, Giugliano D. Inflammatory cytokine concentrations are acutely increased by hyperglycemia in humans: role of oxidative stress. *Circulation* 2002; **106**: 2067-2072
19 American College of Chest Physicians / Society of Critical Care Medicine Consensus Conference: definitions for sepsis and organ failure and guidelines for the use of innovative therapies in sepsis. *Crit Care Med* 1992; **20**: 864-874
20 **Elebute EA**, Stoner HB. The grading of sepsis. *BR J Surg* 1983; **70**: 29-31
21 **Shamoon H**, Hendler R, Sherwin RS. Altered responsiveness to cortisol, eipinephrine and glucagon in insulin-infused juvenile-onset diabetes A mechanism for diabetic instability. *Diabetes* 1980; **29**: 284-291
22 **Zhang GL**, Wang YH, Teng HL, Lin ZB. Effects of aminoguanidine on nitric oxide production induced by inflammatory cytokines and endotoxin in cultured rat hepatocytes. *World J Gastroenterol* 2001; **7**: 331-334
23 **Webber J.** Abnormalities in glucose metabolism and their relevance to nutrition support in the critically ill. *Curr Opin Clin Nutr Metb Care* 1998; **1**: 191-194
24 **Wang P**, Li N, Li JS, Li WQ. The role of endotoxin, TNF-α, and IL-6 in inducing the state of growth hormone insensitivity. *World J Gastroenterol* 2002; **8**: 531-536
25 **Chang HR**, Bistrian B. The role of cytokines in the catabolic consequences of infection and injury. *J Parenter Enteral Nutr* 1998; **22**: 156-166
26 **Wolfe RR**. Substrate utilization / insulin resistance in sepsis / trauma. *Balliere's Clin Endocrinol Metab* 1997; **11**: 645-657
27 **Rizza RA**, Mandarino LJ, Gerich JE. Dose-response characteristics for effects of insulin on production and utilization of glucose in man. *Am J Physiol* 1981; **240**: E630-E639
28 **Tappy L**, Schwarz JM, Schneiter P, Cayeux C, Revelly JP, Fagerquist CK, Jequier E, Chiolero R. Effects of isoenergetic glucose-based or lipid-based parenteral nutrition on glucose metabolism, de novo lipogenesis, and respiratory gas exchanges in critically ill patients. *Crit Care Med* 1998; **26**: 860-867
29 **Saeed M**, Carlson GL, Little RA, Irving MH. Selective impairment of glucose storage in human sepsis. *Br J Surg* 1999; **86**: 813-821
30 **Soop M**, Duxbury H, Agwunobi AO, Gibson SM, Hopkins SJ, Childs C, Cooper RG, Maycock P, LittLe RA, Carlson GL. Euglycemic hyperinsulinemia augments the cytokine and endocrine responses to endotoxin in humans. *Am J Physiol Endocrinol Metab* 2002; **282**: E1276-E1285
31 **Morohoshi M**, Fujisawa K, Uchimura I, Numano F. Glucose-dependent interleukin 6 and necrosis factor production by human peripheral blood monocytes in vitro. *Diabetes* 1996; **45**: 954-959
32 **Pampfer S**, Vanderheyden I, De Hertogh R. Increased synthesis of tumor necrosis factor-alpha in uterine explants from pregnant diabetic rats and in primary cultures of uterine cells in high glucose. *Diabetes* 1997; **46**: 1214-1224
33 **Coughlan MT**, oliva K, Georgiou HM, Permezel JM, Rice GE. Glucose-induced release of tumor necrosis factor-alpha from human placental and adipose tissues in gestational diabetes mellitus. *Diabet Med* 2001; **18**: 921-927
34 **Morohoshi M**, Fujisawa K, Uchimura I, Numano F. The effect of glucose and advanced glycosylation end products on IL-6 production by human monocytes. *Ann N Y Acad Sci* 1995; **748**: 562-570

Edited by Ren SY and Wang XL

P.O.Box 2345, Beijing 100023,China
Fax: +86-10-85381893
E-mail: wjg@wjgnet.com www.wjgnet.com

World J Gastroenterol 2003;9(8):1828-1831
World Journal of Gastroenterology
 ISSN 1007-9327

• CLINICAL RESEARCH •

Percentage of peak-to-peak pulsatility of portal blood flow can predict right-sided congestive heart failure

Jui-Ting Hu, Sien-Sing Yang, Yun-Chih Lai, Cheng-Yen Shih, Cheng-Wen Chang

Jui-Ting Hu, Yun-Chih Lai, Cheng-Yen Shih, Liver Unit, Cathay General Hospital, Taipei, Taiwan
Sien-Sing Yang, Liver Unit, Cathay General Hospital, Taipei and Medical Faculty, China Medical College, Taichung, Taiwan
Cheng-Wen Chang, Department of Cardiology, Cathay General Hospital, Taipei, Taiwan
Correspondence to: Sien-Sing Yang, MD., Liver Unit, Cathay General Hospital, 280, Jen-Ai Road, Sec. 4, Taipei 106, Taiwan yangss@cgh.org.tw
Telephone: +886-2-2708-2121 Ext 3123 **Fax:** +886-2-2707-4949
Received: 2003-03-28 **Accepted:** 2003-04-24

Abstract

AIM: To study the change of portal blood flow for the prediction of the status of right-sided heart failure by using non-invasive way.

METHODS: We studied 20 patients with rheumatic and atherosclerotic heart diseases. All the patients had constant systemic blood pressure and body weight 1 week prior to the study. Cardiac index (CI), left ventricular end-diastolic pressure (LVEDP), mean aortic pressure (AOP), pulmonary wedge pressure (PWP), mean pulmonary arterial pressure (PAP), mean right atrial pressure (RAP), right ventricular end-diastolic pressure (RVEDP) were recorded during cardiac catheterization. Ten patients with RAP <10 mmHg were classified as Group 1. The remaining 10 patients with RAP ⩾10 mmHg were classified as Group 2. Portal blood velocity profiles were studied using an ultrasonic Doppler within 12 h after cardiac catheterization.

RESULTS: CI, AOP, and LVEDP had no difference between two groups. Patients in Group 1 had normal PWP (14.6±7.3 mmHg), PAP (25.0±8.2 mmHg), RAP (4.7±2.4 mmHg), and RVEDP (6.4±2.7 mmHg). Patients in Group 2 had increased PWP (29.9±9.3 mmHg), PAP (46.3±13.2 mmHg), RAP (17.5±5.7 mmHg), and RVEDP (18.3±5.6 mmHg) (P<0.001). Mean values of maximum portal blood velocity (Vmax), mean portal blood velocity (Vmean), cross-sectional area (Area) and portal blood flow volume (PBF) had no difference between 2 groups. All the patients in Group 1 had a continuous antegrade portal flow with a mean percentage of peak-to-peak pulsatility (PP) 27.0±8.9 % (range: 17-40 %). All the patients in Group 2 had pulsatile portal flow with a mean PP 86.6±45.6 (range: 43-194 %). One patient had a transient stagnant and three patients had a transient hepatofugal portal flow, which occurred mainly during the ventricular systole. Vmax, Vmean and PBF had a positive correlation with CO (P<0.001) but not with AOP, LVEDP, PWP, PAP, RAP, and RVEDP. PP showed a good correlation (P<0.001) with PWP, PAP, RAP, and RVEDP but not with CI, AOP, and LVEDP. All the patients with PP >40 % had a right-sided heart failure with a RAP=10 mmHg.

CONCLUSION: The measurement of PP change is a simple and non-invasive way to identify patients with right heart failure.

Hu JT, Yang SS, Lai YC, Shih CY, Chang CW. Percentage of peak-to-peak pulsatility of portal blood flow can predict right-sided congestive heart failure. *World J Gastroenterol* 2003; 9 (8): 1828-1831
http://www.wjgnet.com/1007-9327/9/1828.asp

INTRODUCTION

Hepatic artery and portal vein contribute to the hepatic blood inflow. In cirrhotic patients, oral nitroglycerin can reduce portal blood flow due to systemic hypotension[1-4]. Congestive heart failure, systemic hypotension and the use of hypotensive agents can decrease cardiac output. The reduced cardiac out put and systemic hypotension can decrease the portal inflow volume. Marked reduction of hepatic inflow may cause ischemic hepatitis. Patients with cardiopulmonary diseases may develop ischemic hepatitis with abnormal serum ALT levels[5,6].

On the other hand, right-sided congestive heart failure can result in the increase of pressure in inferior vena cava and hepatic veins[6,7]. The liver in passive "backward" congestion status can develop hepatomegaly and synchronous pulsation, and the liver histology shows engorged and dilated terminal hepatic veins, atrophy of hepatocytes and eventually cardiac cirrhosis. The high pressure of the hepatic veins can transmit through the liver to result in post-sinusoidal portal hypertension and cardiac ascites. The diameter of portal vein has been proved to correlate with right atrial pressure[8]. Thus, right-sided heart failure can affect portal vein flow patterns.

The role of heart function in portal blood flow remains uncertain. Therefore, we studied the changes of portal blood flow in patients with different degree of right-sided heart failure using non-invasive ultrasonic Dopper[5,8-11].

MATERIALS AND METHODS

We studied the portal blood velocity profiles in 20 patients (9 males, 11 females, mean age: 49±16 years) who underwent cardiac and/or Swan-Ganz catheterizations for cardiovascular disorders (16 rheumatic heart disease cases, 4 atherosclerotic heart disease cases) to compare the portal profiles of 20 healthy volunteers. Although all the patients took medications affecting the hemodynamics such as isosorbide dinitrate and furosemide, their systemic blood pressure and body weight were constant for at least 1 week prior to the study. Patients with fever, infection, and shock were excluded. All the patients had no past history of liver disease, alcoholism or other metabolic disorders such as chronic renal failure or diabetes mellitus. None underwent transfusion or under cardiac inotropic agents. All the patients had an abdominal sonographic examination excluding chronic liver disease or splenomegaly. Patients with severe dyspnea were excluded if they were not able to remain on supine position for the study of ultrasonic Doppler.

Cardiac profiles including cardiac index (CI), left ventricular end-diastolic pressure (LVEDP), mean aortic pressure (AOP), pulmonary wedge pressure (PW), mean pulmonary arterial

pressure (PAP), mean right atrial pressure (RAP), right ventricular end-diastolic pressure (RVEDP) were recorded during the cardiac and Swan-Ganz catheterizations. Ten patients with PAP <10 mmHg (range: 1-7 mmHg) without right heart failure were classified as Group 1. The other 10 patients with right heart failure and RAP=10 mmHg (range: 10-28 mmHg) were classified as Group 2.

We studied the portal profiles using an ultrasonic Doppler composed of a real-time mechanical sector scanner and a 3.5 mHz pulsed Doppler flowmeter (Aloka Echo Camera Model SSD-650, Tokyo) within 12 h after cardiac catheterization. After more than 8 h fasting, portal profiles were measured in supine position for more than 30 min. Portal blood flow was measured from the main portal vein with the patient in expiratory apnea. We located the cursor in the main portal vein at a site just entering or immediately after entering the liver and opened the gate of cursor as wide as possible to include the inner diameter of the main portal vein. We corrected the flow angle formed by the directions of ultrasonic beam and the portal blood flow below 55 degree to minimize the variation caused by the angle of insonation. The Doppler signal could be viewed on the screen and heard through a build-in speaker. Portal blood flow was measured by the same physician to avoid inter-observer variations[12].

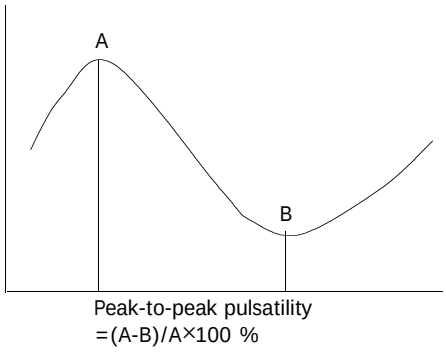

Figure 1 Mean portal blood velocity (Vmean) was calculated (cm/s) by the equation of "Vmean=0.57×maximum portal blood velocity (Vmax)".

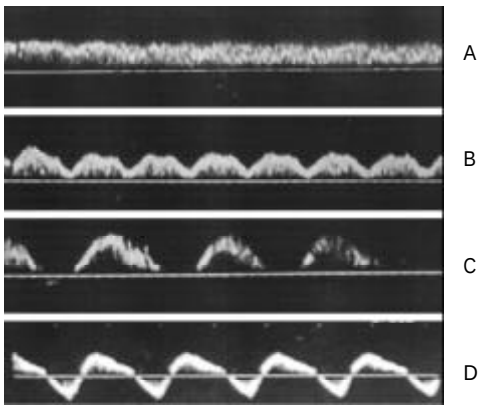

Figure 2 Representative waveform of portal blood flow from patients with normal (A; PP: 17 %), transiently reduced (B; PP: 60 %), stagnant (C; PP: 100 %) or retrograde (D; PP: 194 %) portal blood flow.

For each measurement, at least 3 reproducible patterns were made to calculate the mean maximum portal blood velocity (Vmax) over a period of 4 seconds to ensure the measurement accuracy. Mean portal blood velocity (Vmean) was calculated (cm/s) by the equation of "Vmean=0.57×Vmax" as described by Moriyasu *et al* (Figure 1)[13]. Cross-sectional area (Area) was also recorded (cm^2) at the site of main portal vein where portal blood velocity was measured. The direction of portal blood velocity, antegrade or retrograde, was also measured. Positive signal above the zero velocity indicated the flow toward the transducer and vice versa. Portal blood flow volume (PBF) was obtained (ml/min) by the equation "PBF=Area×Vmean ×60"[12,13]. The percentage of peak-to-peak pulsatility (PP) was calculated by the equation of PP=(maximum-minimum)/maximum frequency shift (Figure 1)[5,10,12]. The waveforms were classified as continuous (PP=40 %; Figure 2A), decreased (PP 41-99 %; Figure 2B), stagnant (PP=100 %; Figure 2C), and retrograde (PP >100 %; Figure 2D).

The study protocol was reviewed and approved by the Institutional Review Committee under the guidelines of the 1975 Declaration of Helsinki. Statistical analysis was performed using Student's *t*-test and linear regression as appropriate.

RESULTS

The clinical and biochemical data are shown in Table 1. All the controls had normal blood chemistries. All the patients had normal serum bilirubin, and prothrombin time. The mean serum albumin levels were lower in Group 1 (3.9±0.7 g/dL, $P<0.02$) and Group 2 (3.7±0.5 g/dL, $P<0.01$) than Controls. The serum ALT levels were all less than two times of the upper normal limit. Group 2 patients (35±20 IU/L) had a higher mean serum ALT activity than that of the controls (24±6 IU/L, $P<0.05$) but not statistically different from that of Group 1 (23±8 IU/L). Group 2 (59±29 IU/L) had a higher mean AST level than those of Group 1 (31±11 IU/L, $P=0.004$) and controls (21±6 IU/L, $P<0.001$). The higher serum AST activities, were supposed to be related to ischemic hepatitis. The other clinical and biochemical data between Group 1 and 2 showed no statistical difference.

Table 1 Clinical and biochemical data of patients with congestive heart failure ($\bar{x}\pm s$)

	Control	Group 1	Group 2
Gender (M/F)	10/10	4/6	5/5
Age (y)	46±12	50±13	47±19
Total protein (g/dL)	7.5±0.6	7.1±0.8	6.9±1.1
Albumin (g/dL)	4.3±0.2	3.9±0.7	3.7±0.5
Total serum bilirubin (mg/dL)	0.9±0.4	1.3±0.8	1.4±0.8
AST (IU/L)	21±6	31±11	59±29
ALT (IU/L)	24±6	23±8	35±20
Prolonged prothrombin time (s)	-	1.1±0.9	1.4±0.8

The CI [3.0±1.4 L/(min· m^2); range: 2.3-8.6 L/(min· m^2) *vs* 2.4±0.5 L/(min· m^2); range: 2.8-4.2 L/(min· m^2)], AOP (87.8±11.7 mmHg; range: 65-100 mmHg *vs* 87.6±16.5 mmHg; range: 65-115 mmHg), and LVEDP (12.2±9.3 mmHg; range: 4-40 mmHg *vs* 22.8±13.0 mmHg; range: 10-40 mmHg) were not statistically different between Group 1 and 2 (Table 2). All the Group 1 patients had normal PWP (mean: 14.6±7.3 mmHg; range: 5-40 mmHg), PAP (mean: 25.0±8.2 mmHg; range: 16-48 mmHg), RAP (mean: 4.7±2.4 mmHg; range: 1-10 mmHg), and RVEDP (mean: 6.4±2.7 mmHg; range: 4-14 mmHg). All the group 2 patients had abnormally higher PWP (mean: 29.9±9.3 mmHg; range: 13-38 mmHg), PAP (mean: 46.3±13.2 mmHg; range: 25-65 mmHg), RAP (mean: 17.5±5.7 mmHg; range: 12-28 mmHg), and RVEDP (mean: 18.3±5.6 mmHg; range: 9-26 mmHg) than those of Group 1 patients ($P<0.001$).

Table 2 Cardiac profiles in patients with congestive heart failure [$\bar{x}\pm s$, (n)]

	Group 1	Group2
CI [L/(min· m²)]	3.0±1.4 (6)	2.4±0.5 (7)
AOP (mmHg)	87.8±11.7 (9)	87.6±16.5 (8)
LVEDP (mmHg)	12.2±9.3(10)	22.8±13.0(9)
PWP (mmHg)	14.6±7.3(9)	29.9±9.3[a] (9)
PAP (mmHg)	25.0±8.2(10)	46.3±13.2[a] (9)
RAP (mmHg)	4.7±2.4(10)	17.5±5.7[a] (10)
RVEDP (mmHg)	6.4±2.7(10)	18.3±5.6[a] (10)

[a]P<0.001 *vs* group 1.

The mean values of Vmax (24.5±4.9 cm/s; range: 17-33 cm/s *vs* 21.5±6.1 cm/s; range: 16-33 cm/s), Vmean (14.0±2.9 cm/s; range: 9.7-18.8 cm/s *vs*12.3±3.5 cm/s; range: 8.6-13.7 mmHg), area (0.80±0.17 cm²; range: 0.64-1.13 cm² *vs* 0.94±0.18 cm²; range: 0.79-1.33 cm²) and PBF (678±239 ml/min; range: 373-1120 ml/min *vs* 684±191 ml/min; range: 432-922 ml/min) between Group 1 and 2 did not show any statistical difference (Table 3). All the 10 patients in Group 1 had a continuous antegrade portal flow with a mean PP 27.0±8.9 % (range: 17-40 %). The mean PP of the remaining 10 patients in Group 2 was 86.6±45.6 % (range: 43-194 %); all the patients had a pulsatile portal blood flow with PP >40 %. 6, 1 and 3 patients had transiently reduced, stagnant, and hepatofugal portal blood flow, respectively. The transiently reduced, stagnant and retrograde flow occurred mainly immediately after the corresponding ventricular systole. Different from earlier reports, we have observed that the decreased or reversed portal blood flow did not occur during ventricular systole in 3 patients with ventricular premature depolarizations or atrial fibrillation (Figure 3).

Table 3 Portal profiles in patients with congestive heart failure ($\bar{x}\pm s$)

	Control (n=20)	Group1 (n=10)	Group2 (n=10)
Vmax (cm/s)	20.1±3.1	24.5±4.9	21.5±6.1
Vmean (cm/s)	11.2±1.9	14.0±2.9	12.3±3.5
Area (cm²)	1.01±0.20	0.80±0.17	0.94±0.18
PBF (ml/min)	685±136	678±239	684±191
PP (%)	23.3±6.3	27.0±8.9	86.6±45.6[a]

[a]P<0.001 *vs* control and group 1.

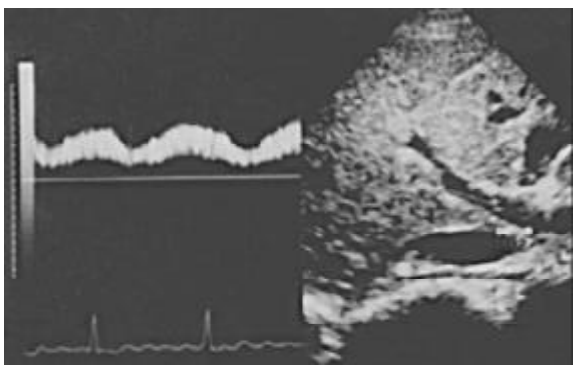

Figure 3 Occurrence of reduced portal blood flow immediately after ventricular systole.

By using linear correlation, Vmax, Vmean and PBF had a positive correlation with CI (P<0.001) but not with AOP, LVEDP, PWP, PAP, RAP, and RVEDP. PP showed a good correlation with PWP, PAP, RAP, and RVEDP (P<0.001) but did not show any correlation with CI, AOP, and LVEDP. PP had no correlation with Vmax, Vmean and PBF.

DISCUSSION

In the present study, all the 10 patients with RA=10 mmHg had a PP>40 %. On the contrary, all the patients with RAP <10 mmHg had a PP 40 % or less. It suggested these patients developed transiently reduced, stagnant or hepatofugal portal blood flow. 4 (36 %) of the patients with RAP=10 mmHg had a retrograde portal blood flow with a PP >100 %. Therefore, the portal blood flow can be retrograde during severe right heart failure[13]. Furthermore, RAP, PWP and RVEDP have a good correlation with PP. Thus, the waveforms of portal blood flow correlate well with right heart function[14]. Therefore, the measurement of PP change is a simple and non-invasive way to identify patients with right heart failure[9,15].

In the present study, AOP did not correlate with PP and "estimated" PBF[12,13,16]. Actually, all the patients had preserved AOP and only 1 patient whose AOP was 2.3 L/(min· m²) with RAP< 10 mmHg had AOP less than 2.6 L/(min· m²). Thus, right heart failure rather than reduced CI is responsible for PP changes[5,17-19]. Furthermore, "estimated" portal inflow showed no difference between patients with high and low RAP. Since the portal inflow can be transiently reduced, stagnant or hepatofugal during severe right heart failure, the "actual" portal inflow volume should be lower than the "estimated" volume[20]. As a consequence, the "estimated" volume does not represent the "actual" portal inflow volume. Hence, the correlation among "actual" PBF, AOP and RAP warrants further study.

Portal blood flow contributes to 90 % of blood flow and 50 % of oxygen supply of the liver. Therefore, portal inflow plays an important role in the delivery of oxygen to the liver[16]. It has been well known that cirrhosis with portal hypertension can result in reduced PP[16,21,22]. However, the volume of portal inflow varies due to the occurrence of collaterals or the presence of portal hypertension. In alcoholic cirrhosis, oral nitroglycerin can cause systemic hypotension to reduce portal inflow[1-4,22,23]. In the present study, all the patients did not experience systemic hypotension. Therefore, their transiently reduced, stagnant or hepatofugal portal blood flow was not likely to be related to systemic hypotension[15,24].

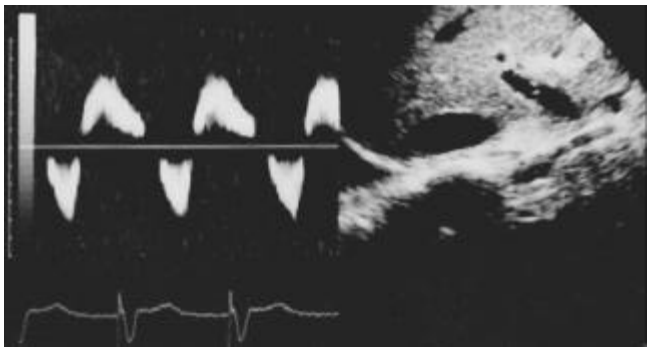

Figure 4 The occurrence of transient hepatofugal portal blood flow immediately after ventricular systole.

In the present study, the occurrence of transiently reduced (Figure 3), stagnant or hepatofugal (Figure 4) portal blood flow was immediately after ventricular systole[14,24,25]. The increased PP in those patients with RAP=10 mmHg suggests that the portal inflow is transiently reduced immediately after ventricular systole. The occurrence of transiently stagnant or hepatofugal portal blood flow may impair the delivery of

oxygen to the liver. It is well known that left heart failure and systemic hypotension can decrease hepatic inflow to cause ischemic hepatitis with a higher AST level[15,26]. However, it is not uncommon that some patients with heart failure have both abnormally higher serum ALT and LDH levels even without systemic hypotension clinically[5,6,24]. Thus, the occurrence of transiently reduced, stagnant or hepatofugal portal blood flow may in part explain the relatively higher AST levels in those patients with RAP=10 mmHg than those <10 mmHg.

ACKNOWLEDGMENT

A part of the present data was presented at the VIII World Congress of Ultrasound in Medicine and Biology, Buenos Aires, 1997, Ultrasound in Medicine and Biology 1997;23:22.

REFERENCES

1 **Yang SS**, Ralls PW, Korula J. The effect of oral nitroglycerin on portal vein flow. *J Chin Gastroenterol* 1991; **13**: 173-177
2 **Nagy I,** Szilvassy Z. Tolerance to nitroglycerin in rats with experimental liver cirrhosis: an *in vitro* study on aortic rings. *Hepatology* 1998; **1:** 71
3 **Garcia-Taso G,** Groszmann RJ. Portal hemodynamic during nitroglycerin administration in cirrhotic patients. *J hepatol* 1987; **7:** 805-809
4 **Gibson PR,** Mclean AJ, Dudley FJ. The hypotensive effect of oral nitroglycerin on portal venous pressure in patients with cirrhotic portal hypertension. *J Gastroenterol Hepatol* 1986; **1:** 201-206
5 **Yang SS,** Wu CH, Chen TK, Lee CL, Lai YC, Chen DS. Portal blood flow in acute hepatitis with and without ascites: A noninvasive measurement using ultrasonic Doppler. *J Gastroenterol Hepatol* 1995; **10:** 36-41
6 **Pannen BH.** New insights into the regulation of hepatic blood flow after ischemia and reperfusion. *Anesth Analg* 2002; **94:** 1448-1457
7 **Shen B,** Younossi ZM, Dolmatch B, Newman JS, Henderson JM, Ong JP, Gramlich T, Yamani M. Patent ductus venosus in an adult presenting as pulmonary hypertension, right-sided heart failure, and portosystemic encephalopathy. *Am J Med* 2001; **110:** 657-660
8 **Catalano D,** Caruso G, DiFazzio S, Carpinteri G, Scalisin N, Trovato GM. Portal vein pulsatility ratio and heart failure J. *Clin Ultrasound* 1998; **26:** 27-31
9 **Tang SS,** Shimizu T, Kishimoto R, Kodama Y, Miyasaka K. Analysis of portal venous waveform after living related liver transplantation with pulsed Doppler ultrasound. *Clin Transplant* 2001; **15:** 380-387
10 **Koslin DB,** Mulligan SA, Berland LL. Duplex assessment of the portal venous system. *Semin Ultrasound CT MR* 1992; **13:** 22-33
11 **Bolondi L,** Gaiani S, Barbara L. Accuracy and reproducibility of portal flow measurement by Doppler US. *J hepatol* 1991; **13:** 269-273
12 **Sabba C,** Weltin GG, Cicchetti DV, Ferraioli G, Taylor KJ, Nakamura T, Moriyasu F, Groszmann RJ. Observer variability in echo-Doppler measurements of portal flow in cirrhotic patients and normal volunteers. *Gastroenterology* 1990; **98:** 1603-1611
13 **Moriyasu F,** Nishida O, Ban N, Nakamura T, Miura K, Sakai M, Miyake T, Uchino H. Measurement of portal vascular resistance in patients with portal hypertension. *Gastroenterology* 1986; **90:** 710-717
14 **Rengo C,** Brevetti G, Sorrentino G, D'Amato T, Imparato M, Vitale DF, Acanfora D, Rengo F. Portal vein pulsatility ratio provides a measure of right heart function in chronic heart failure. *Ultrasound Med Biol* 1998; **24:** 327-332
15 **Hosoki T,** Arisawa J, Marukawa T, Tokunaga K, Kuroda C, Kozuka T, Nakano S. Portal blood flow in congestive heart failure: pulsed duplex sonographic findings. *Radiology* 1990; **174:** 733
16 **Valla D,** Flejou JF, Lebrec D, Bernuau J, Rueff B, Salzmann JL, Benhamou JP. Portal hypertension and ascites in acute hepatitis: clinical, hemodynamic and histological correlations. *Hepatology* 1989; **10:** 482-487
17 **Moriyasu F,** Nishida O, Ban N, Nakamura T, Miura K, Sakai M, Uchino H, Miyake T. "Congestion index" of the portal vein. *AJR Am J Roentgenol* 1986; **146:** 735-739
18 **Bihari DJ,** Gimson AE, Williams R. Cardiovascular, pulmonary and renal complications of fulminant hepatic failure. *Semin Liver Dis* 1986; **6:** 119-128
19 **Sherlock S.** Vasodilatation associated with hepatocellular disease: Relation to functional organ failure. *Gut* 1990; **31:** 365-367
20 **Lebrec D**. Pharmacological treatment of portal hypertension: presnt and future. *J Hepatology* 1998; **28:** 896-907
21 **Chiu KW,** Changchien CS, Liaw YF, Yang SS. Albumin gradient and portal vein velocity in severe viral hepatitis patients complicated with ascites. *Hepatogastroenterology* 2000; **47:** 1700-1702
22 **Ozaki CF,** Anderson JC, Liebeman RP, Rikker LF. Duplex ultrasonography as a noninvasive technique for assessing portal hemodynamics. *Am J Surg* 1988; **155:** 70-75
23 **Bosch J,** Garcia-Pagan JC. Complication of cirrhosis. I. Portal Hypertension. *J Hepatol* 2000; **32:** 141-156
24 **Wachsberg RH,** Needleman L, Wilson DJ. Portal vein pulsatility in normal and cirrhotic adults without cardiac disease. *J Clin Ultrasound* 1995; **23:** 33
25 **Abu-Yousef MM,** Milam SG, Faner RM. Pulsatile portal vein flow: a sign of tricuspid regurgitation on duplex Doppler sonography. *AJR Am J Roentgenol* 1990; **155:** 785
26 **Taourel P,** Blanc P, Dauzat M, Chabre M, Pradel J, Gallix B, Larrey D, Bruel JM. Doppler study of mesenteric, hepatic, and portal circulation in alcoholic cirrhosis: relationship between quantitative Doppler measurements and the severity of portal hypertensive and hepatic failure. *Hepatology* 1998; **28:** 932-936

Edited by Xu XQ and Wang XL

P.O.Box 2345, Beijing 100023,China
Fax: +86-10-85381893
E-mail: wjg@wjgnet.com www.wjgnet.com

World J Gastroenterol 2003;9(8):1832-1833
World Journal of Gastroenterology
 ISSN 1007-9327

• BRIEF REPORTS •

Efficacy of saccharomyces boulardii with antibiotics in acute amoebiasis

Fariborz Mansour-Ghanaei, Najaf Dehbashi, Kamyar Yazdanparast, Afshin Shafaghi

Fariborz Mansour-Ghanaei, Afshin Shafaghi, Gastrointestinal and Liver Diseases Research Center, Guilan University of Medical Sciences, Rasht, Iran
Najaf Dehbashi, Department of Gastroenterology, Shiraz University of Medical Sciences, Shiraz, Iran
Kamyar Yazdanparast, Department of Microbiology, Shiraz University of Medical Sciences, Shiraz, Iran
Correspondence to: Professor Fariborz Mansour-Ghanaei, Gastrointestinal and Liver Diseases Research Center, Guilan University of Medical Sciences, Sardar-e-jangle Ave, Razi Hospital, Rasht 41448-95655, Iran. ghanaei@gums.ac.ir
Telephone: +98-131-5535116 **Fax:** +98-131-2232514
Received: 2003-04-12 **Accepted:** 2003-05-24

Abstract

AIM: To compare the efficacy of antibiotics therapy alone with antibiotics and saccharomyces boulardii in treatment of acute amebiasis.

METHODS: In a double blind, random clinical trial on patients with acute intestinal amoebiasis, 57 adult patients with acute amoebiasis, diagnosed with clinical manifestations (acute mucous bloody diarrhea) and amebic trophozoites engulfing RBCs found in stool were enrolled in the study. Regimen 1 included metronidazole (750 mg Tid) and iodoquinol (630 mg Tid) for 10 days. Regimen 2 contained capsules of lyophilized saccharomyces boulardii (250 mg Tid) orally in addition to regimen 1. Patients were re-examined at two and four weeks after the treatment, and stool examination was performed at the end of week 4. Student's *t*-test, χ^2 and McNemar's tests were used for statistical analysis.

RESULTS: Three patients refused to participate. The other 54 patients were randomized to receive either regimen 1 or regimen 2 (Groups 1 and 2 respectively, each with 27 patients). The two groups were similar regarding their age, sex and clinical manifestations. In Group 1, diarrhea lasted 48.0±18.5 hours and in Group 2, 12.0±3.7 hours ($P<0.0001$). In Group 1, the durations of fever and abdominal pain were 24.0±8.8 and 24.0±7.3 hours and in Group 2 they were 12.0±5.3 and 12.0±3.2 hours, respectively ($P<0.001$). Duration of headache was similar in both groups. At week 4, amebic cysts were detected in 5 cases (18.5 %) of Group 1 but in none of the Group 2 ($P<0.02$).

CONCLUSION: Adding saccharomyces boulardii to antibiotics in the treatment of acute amebiasis seems to decrease the duration of clinical symptoms and cyst passage.

Mansour-Ghanaei F, Dehbashi N, Yazdanparast K, Shafaghi A. Efficacy of saccharomyces boulardii with antibiotics in acute amoebiasis. *World J Gastroenterol* 2003; 9(8): 1832-1833
http://www.wjgnet.com/1007-9327/9/1832.asp

INTRODUCTION

Intestinal amoebiasis is caused by the protozoan entamoeba histolytica. This organism feeds on the intestinal contents without any invasion to human tissue. It occasionally invades the intestinal wall and causes dysentery. It may also spread from the bowel to the liver and other organs and cause abscess in these organs. In addition, it may persist as cysts in the intestine and the patients become long-term cyst carriers, most of whom remain asymptomatic[1,2].

In most cases, the organism is avirulent but it may become virulent under different circumstances like immune suppression, malnutrition and alterations in intestinal flora[3,4].

Entamoeba histolytica is common all over the world but is more virulent in areas with low hygienic standards and in tropical and subtropical regions[1].

A luminal amebicide achieving high concentrations in the intestine like iodoquinol, paromomycin or diloxanide furoate is usually used to treat cysts. Tissue amebicides with high concentrations in the blood like the nitroimidazoles (especially metronidazole) are the cornerstone of treatment of invasive amoebiasis[5].

Saccharomyces boulardii is saprophytic, thermophylic yeast, which is found growing applications in the prevention and treatment of human septic enteritis[6,7]. The optimal temperature for this yeast to grow is 37 ℃. The gastric juice has no effect on it and it grows all along the gastrointestinal tract. It is used clinically as an oral lyophilized preparation[8]. No significant side effects have been reported with its consumption[9-11].

We assessed the effects of adding saccharomyces boulardii to the standard treatment for invasive amoebiasis.

To compare the routine treatment by means of metronidazole and iodoquinol with metronidazole, iodoquinol and saccharomyces boulardii in the treatment of acute amoebiasis, we performed this study on 57 patients at Shahid Beheshti Educational and Therapeutic Center in Shiraz during one-year period from March 21, 1995 to March 21, 1996.

MATERIALS AND METHODS

Patients with acute amebic dysentery who consented to participate were enrolled. The diagnosis was made according to compatible clinical presentations (acute mucous bloody diarrhea, fever and abdominal pain) and presence of amoeba trophozoite engulfing RBCs in diarrheal stool. Pregnant females, those on maintenance of hemodialysis, steroids or chemotherapy were excluded. The patients were then randomized to receive either metronidazole 750 mg and iodoquinol 650 mg thrice a day for 10 days (Group 1) or the same medication plus lyophilized saccharomyces boulardii (Ultra-levure®, Bio codex, Montrougo, France) 250 mg orally thrice a day (Group 2).

The patients were followed up at two and four weeks. At each visit in addition to recording patients' symptoms and possible adverse effects, pill count was performed. At the end of week 4, another stool examination (fresh spread and floatation) was done. Student's *t*-test, Chi-square and McNemar's tests were used for statistical analysis.

RESULTS

57 consenting patients were randomized (29 in Group 1 and 28 in Group 2). Two patients from Group 1 and one from Group

2 were excluded because of non-compliance. There were 12 (44.4 %) females in Group 1 and 10 (37 %) females in Group 2. Mean age was 29.3 years in Group 1 and 30.8 years in Group 2. Table 1 shows frequency of clinical findings in both groups. The two groups were comparable regarding their clinical presentations, too.

Table 1 Clinical manifestations in two therapeutic groups

	Regimen 1	Regimen 2	*P*
Diarrhea	27 (100 %)	27 (100%)	-
Fever	6 (22.2 %)	7 (26%)	N.S
Abdominal pain	19 (70.4 %)	22 (81.5%)	N.S
Headache	20 (74.1 %)	18 (66.7%)	N.S

N.S=Not significant.

As shown in Table 2, adding saccharomyces boulardii to the usual treatment of acute amebic dysentery decreased the mean duration of diarrhea to almost 25 % ($P<0.0001$) and the duration of abdominal pain and fever to almost half ($P<0.001$). Headache lasted almost equally in the two groups.

Table 2 Time of recovery from main clinical findings

	Regimen 1 (h)	Regimen 2 (h)	*P*
Diarrhea	48.0±18.5	12.0±3.7	<0.0001
Fever	24.0±8.8	12.0±5.3	<0.001
Abdominal pain	24.0±7.3	12.0±3.2	<0.001
Headache	24.0±8.6	24.0±7.9	N.S

N.S=not significant.

Amebic cysts were found in stool specimens of 5 patients (18.5 %) in group 1 and none in group 2 at week 4 ($P<0.02$, Table 3).

Table 3 Amebic cyst carriers in the fourth week after the treatment

	Regimen 1	Regimen 2
Cyst absent	22 (81.5 %)	27 (100 %)
Cyst present	5 (18.5 %)	0 (0 %)

DISCUSSION

Saccharomyces boulardii is a saprophytic yeast which is recommended for the prevention and treatment of septic enteritis[6,7] especially diarrhea caused by clostridium difficile[8,12,13]. It can also reduce the incidence of traveler' s diarrhea[12] and prevent the occurrence of diarrhea in acutely ill patients fed by nasogastric tube[14, 15]. Other diseases in which saccharomyces boulardii has been achieved some success include antibiotic associated colitis[11, 16] and Crohn' s disease[9]. Considering its inhibitory activity on enteropathogens and its anti-diarrheal characteristics, it has also been used in children with diarrhea[17]. Saccharomyces boulardii has been shown to have trophical effects on the small intestine in healthy human volunteers[18].

The exact mechanism by which this yeast prevents or improves diarrhea is still unclear. Saccharomyces boulardii may cause its trophic effect on the small intestine by releasing spermine and spermidine[6]. This yeast can hinder the cholera toxin excretion in the jejunum of mice.

Our data showed that co-administration of lyophilized saccharomyces boulardii with conventional treatment for acute amebic colitis significantly decreased the duration of symptoms and chances of cyst carriers after 4 weeks. This may be due to its potential to restore the beneficial normal flora of the gut, although the precise mechanism of the action remains to be elucidated. Considering the lack of any reported adverse reactions to this product, if our results are reproduced by other investigators, then lyophilized saccharomyces boulardii would be a very useful addition to the treatment of acute amebic dysentery.

ACKNOWLEDGMENT

We would like to thank Dr. Amirhossein Bagherzadeh, the member of Gastrointestinal & Liver Diseases Research Center, Guilan University of Medical Sciences, for his help in preparing and reviewing this manuscript.

REFERENCES

1 **Nanda R,** Baveja U, Anand BS. Entamoeba Histolytica cyst passers: clinical features and outcome in untreated subjects. *Lancet* 1984; **2:**301-303
2 **Lai SW,** Lin HC, Lin CC. Clinical analysis of a dysentery outbreak in Taichung, Taiwan .*Chung Hua Min Kuo Hsiao Erh Ko I Hsueh Hui Tsa Chih* 2000; **41:** 18-21
3 **Lewis EA,** Antia AU. Amoebic colitis. *Trop Med Hyg* 1969; **112:**633-638
4 **Neal RA.** Pathogenesis of amoebiasis. *Gut* 1971; **12:** 482-486
5 **Reed SL.** Amebiasis and infection with free- living amebas. In: Braunwald E, eds. Harrison's principles of internal medicine. *New york: McGraw-Hill* 2001: 1199-1203
6 **Buts JP,** De-Keyser N, De-Raedemaeker L. Saccharomyces boulardii enhances rat intestinal enzyme expression by endoluminal release of polyamines. *Pediatr Res* 1994; **36:** 522-527
7 **Muller J,** Remus N, Harms KH. Mycoserological study of the treatment of paediatric cystic fibrosis patients with saccharomyces boulardii. *Mycoses* 1995; **38:**119-123
8 **Corthier G,** Dubos F, Ducluzeau R. Prevention of C difficile induced mortality in gnotobiotic mice by Saccharomyces boulardii. *Can J Microbiol* 1986; **32:** 894-896
9 **Plein K,** Hotz J. Therapeutic effects of saccharomyces boulardii on mild residual symptoms in a stable phase of Crohn's disease with special respect to chronic diarrhea- a pilot study. *Z Gastroenterol* 1993; **31:** 129-134
10 **Kollaritsch H,** Holst H, Grobara P, Wiedermann G. Prevention of traveler's diarrhea with saccharomyces boulardii. Results of a placebo controlled double - blind study. *Fortschr Med* 1993; **111:** 152-156
11 **McFarland LV,** Surawicz CM, Greenberg RN. A randomized placebo - controlled trial of saccharomyces boulardii in combination with standard antibiotics for clostridium difficile disease. *JAMA* 1994; **271:** 1913-1918
12 **Pothoulakis C,** Kelly CP, Joshi MA. Saccharomyces boulardii in inhibits clostridium difficile toxin A binding and enterotoxicity in rat ileum. *Gastroenterology* 1993; **104:** 1108-1115
13 **Castagliuolo I,** LaMont JT, Nikulasson ST, Pothoulakis C**.** Saccharomyces boulardii protease inhibits clostridium difficile toxin A effects in rat ileum. *Infect Immun* 1996; **64:** 5225-5232
14 **Bleichner G,** Blehaut H, Mentec H, Moyse D. Saccharomyces boulardii prevents diarrhea in critically ill tube-fed patients. A multicenter randomized double- blind placebo - controlled trial. *Intensive Care Med* 1997; **23:** 517-523
15 **Surawicz CM,** Elmer GW, Speelman P. Prevention of antibiotic-associated diarrhea by saccharomyces boulardii: A prospective study. *Gastroenterology* 1989; **96:** 981-988
16 **McFarland LV,** Surawicz CM, Greenberg RN, Elmer GW. Prevention of β- Lactam - associated diarrhea by saccharomyces boulardii compared with placebo. *Am J Gastroenterol* 1995; **90:** 439-448
17 **Saavedra J.** Probiotics and infectious diarrhea. *Am J Gastroenterol* 2000; **95:** S16-S18
18 **Jahn HU,** Ullrich R, Schneider T, Liehr RM, Schieferdecker HL, Holst H, Zeitz M. Immunological and trophical effects of saccharomyces boulardii on the small intestine in healthy human volunteers. *Digestion* 1996; **57:** 95-104

Edited by Xu XQ

P.O.Box 2345, Beijing 100023,China
Fax: +86-10-85381893
E-mail: wjg@wjgnet.com www.wjgnet.com

World J Gastroenterol 2003;9(8):1834-1835
World Journal of Gastroenterology
 ISSN 1007-9327

• BRIEF REPORTS •

Prevalence of amebiasis in inflammatory bowel disease in Turkey

Sebnem Ustun, Hande Dagci, Umit Aksoy, Yuksel Guruz, Galip Ersoz

Sebnem Ustun, Department of Gastroenterology, School of Medicine, University of Ege, 35100, Bornova, Izmir, Turkey
Hande Dagci, Department of Parasitology, School of Medicine, University of Ege, 35100, Bornova, Izmir, Turkey
Umit Aksoy, Department of Parasitology, School of Medicine, University of Dokuz Eylul, Izmir, Turkey
Yuksel Guruz, Department of Parasitology, School of Medicine, University of Ege, 35100, Bornova, Izmir, Turkey
Galip Ersoz, Department of Gastroenterology, School of Medicine, University of Ege, 35100, Bornova, Izmir, Turkey
Correspondence to: Sebnem Ustun, Department of Gastroenterology, School of Medicine, University of Ege, 35100, Bornova, Izmir, Turkey. sustun@med.ege.edu.tr
Telephone: +90-232-3881969
Received: 2003-03-28 **Accepted:** 2003-04-20

Abstract

AIM: To explore the prevalence of amebiasis in inflammatory bowel disease (IBD) in Turkey.

METHODS: In this study, amoeba prevalence in 160 cases of IBD, 130 of ulcerative colitis and 30 of Crohn's disease were investigated in fresh faeces by means of wet mount+Lugol's iodine staining, modified formol ethyl acetate and trichrome staining methods and to compare the diagnostic accuracy of wet mount+Lugol's iodine staining, modified formol ethyl acetate and trichrome staining methods in the diagnosis of *Entamoeba histolytica (E. histolytica)*/ *Entamoeba dispar (E. dispar).*

RESULTS: *E. histolytica/E. dispar* cysts and trophozoites were found in 14 (8.75 %) of a total of 160 cases, 13 (10.0 %) of the 130 patients with ulcerative colitis and 1 (3.3 %) of the 30 patients with Crohn's disease. As for the 105 patients in the control group who had not any gastrointestinal complaints, 2 (1.90 %) patients were found to have *E. histolytica* /*E. dispar* cysts in their faeces. Parasite prevalence in the patient group was determined to be significantly higher than that in the control group (Fischer's Exact Test, $P<0.05$). When the three methods of determining parasites were compared with one another, the most effective one was found to be trichrome staining method (Kruskal-Wallis Test, $P<0.01$).

CONCLUSION: Consequently, amoeba infections in IBD cases have a greater prevalence compared to the normal population. The trichrome staining method is more effective for the detection of *E. histolytica* /*E. dispar* than the wet mount+Lugol's iodine staining, modified formol ethyl acetate methods.

Ustun S, Dagci H, Aksoy U, Guruz Y, Ersoz G. Prevalence of amebiasis in inflammatory bowel disease in Turkey. *World J Gastroenterol* 2003; 9(8): 1834-1835
http://www.wjgnet.com/1007-9327/9/1834.asp

INTRODUCTION

Amebiasis, which affects nearly 500 million people in the world, is more prevalent in developing countries in particular[1]. It is difficult to distinguish IBD from colitis associated with amoeba according to both symptomatic and endoscopic appearance of the colon. It is not even possible to establish a differential diagnosis by means of microscopic examination. Sometimes IBD can co-exist with amebiasis. This, of course, leads to confusion in the diagnosis and treatment of the disease[2].

This study was planned to consider amoeba in the cases diagnosed as IBD in the gastroenterology clinic and to compare the accuracy of wet mount + Lugol's iodine staining, modified formol ethyl acetate and trichrome staining methods in the diagnosis of *E. histolytica/E. dispar*.

MATERIALS AND METHODS

160 people who were diagnosed as IBD by endoscopic, histopathologic, radiologic and laboratory examinations at our clinic were included in this study which was carried out between January 2000 and June 2001. Of all the cases, 130 were diagnosed as ulcerative colitis and 30 as Crohn's disease. 105 people of even age and sex distribution who had not any gastrointestinal complaints and reported to the district health centre with other complaints were assessed as the control group. Fresh faeces samples taken from these people were examined immediately using the wet mount+Lugol's iodine staining, modified formol ethyl acetate and trichrome staining methods.

Fisher's exact test was applied to the groups (ulcerative colitis, Crohn's disease and control) for a comparison of amoeba frequency among them. The assessment of wet mount+Lugol's iodine staining, modified formol ethyl acetate methods used in the diagnosis of *E. histolytica/E. dispar*, was conducted by calculation of sensitivity, specificity, negative predictive value, positive predictive value and rate of accuracy.

RESULTS

In our study in which the prevalence of *E. histolytica/E. dispar* in IBD was investigated, we found *E. histolytica/E. dispar* cysts and trophozoits in 14 (8.75 %) of the 160 IBD cases. *E. histolytica/E. dispar* cysts and/or trophozoits were also determined in 13 (10.0 %) of the 130 patients with ulcerative colitis and 1 (3.3 %) of the 30 Crohn's disease patients (Table 1). Frequency of *E. histolytica/E. dispar* in patients with IBD was significantly higher than that in the control group (Fisher's exact test, $P<0.05$). When the groups of patients with IBD were compared with the control group separately, the frequency of *E. histolytica/E. dispar* in patients with ulcerative colitis was significantly higher than that in the control group. For Crohn's disease, on the other hand, it was not significantly different from the control group. A comparison between the patients with ulcerative colitis and those with Crohn's disease revealed that *E. histolytica/E. dispar* were more significantly frequent in the patients with ulcerative colitis (Fisher's exact test, $P<0.05$). When the three methods of determining parasites were compared with one another, the most effective one was found to be trichrome staining method as can be seen in Table 1 (Kruskal-Wallis test, $P<0.01$). The sensitivity of wet

mount+Lugol' s iodine staining, modified formol ethyl acetate methods was found to be quite low as compared to the trichrome staining method (36 %, 64 %, respectively) (Table 2).

Table 1 Number and methods for determination of *E. histolytica* determined in cases with IBD diagnosis and control group

	Wet mount ± Lugol's iodine staining	Modified formol ethyl acetate	Trichrome staining method	Total (none of parasite / patient)
Ulcerative colitis	5*(%3.84)	8*(%6.15)	13*(%10.0)	13 / 130
Crohn's disease	-	1*(%3.33)	1*(%3.33)	1 / 30
Control group	1*(%0.95)	2*(%1.90)	2*(%1.90)	2 / 105

*The parasite was determined by more than one method (+).

Table 2 Comparison of wet mount+Lugol's iodine, modified formol ethyl acetate methods with trichrome staining method

	Modified formol ethyl acetate (%)	Wet mount+Lugol's iodine staining (%)
Sensitivity	64	36
Specificity	99	98
False negatives	36	64
False positives	0.1	0.1
Positive predictive value	90	63
Negative predictive value	97	95
Rate of accuracy	97	93

DISCUSSION

Few studies have been performed in Turkey on this particular subject. In a study they carried out in the Province of Istanbul between April 1994 and July 1995. Bayramicli *et al*[3] explored the presence of amebiasis in 19 patients being investigated with a preliminary diagnosis of ulcerative colitis and found *E. histolytica* in 69 % of the cases. In a study they carried out in the Province of Antalya to determine the rate of amebiasis in 43 patients with ulcerative colitis. Suleymanlar *et al*[4] found *E. histolytica* cysts and trophozoites in 22 (54 %) of the patients. These values are higher than those we have found. The reason for this is the fact that the incidence of *E. histolytica/E. dispar* has been diminishing in Turkey in recent years.

Prokopowicz *et al*[5] determined 5 cases of amebiasis (4.85 %) among 103 patients with ulcerative colitis and claimed that this rate was significant in the treatment of chronic ulcerative colitis patients. We have obtained a higher rate than that of Prokopowicz in our study in which we found *E. histolytica/E. dispar* cysts and trophozoites in 13 (10.0 %) of 130 patients with ulcerative colitis**.** This was due to the environmental factors as high temperature and humidity, which are effective in and around Izmir, as well as lower immune resistance against the infection in addition to poorer hygiene. Chan *et al*[6] presented three cases with ulcerative colitis and *E. histolytica* infection and mentioned the problems to be faced during treatment.

In conclusion, amoeba infection in IBD cases, especially in patients with ulcerative colitis is more prevalent compared to the normal population. A differential diagnosis is extremely important for IBD and amebiasis cases. Therefore, we believe that *E. histolytica/E. dispar* must be explored in the faeces before planning a diagnostic scheme for cases diagnosed as IBD. In addition, the sensitivity of wet mount+Lugol' s iodine staining and modified formol ethyl acetate methods was found to be low in this study. Therefore, we think it would be necessary to use the trichrome staining method in the investigation of *E. histolytica/E. dispar* in patients with IBD diagnosis.

REFERENCES

1 **Andersen PL**. Amebiasis. *Ugeskr Laeger* 2000; **162:** 1537-1541
2 **Hansen LH,** Lund C. Amebiasis-a differential diagnosis from inflammatory bowel disease. *Ugeskr Laeger* 1998; **160:** 5514-5515
3 **Bayramicli OU,** Dalay R, Konuksal F, Kilic G, Akbayir N, Ovunc O. Ulseratif kolitle amebiasisin birlikteligi. *Turk J Gastroenterol* 1997; **8:** 94-96
4 **Süleymanlar I,** Atilgan S, Ertugrul C, Isitan F. Ulseratif kolit ve intestinal amebiasis birlikteligi ve tedavide karsilasilan sorunlar. *Gastroenteroloji* 1996; **7:** 22
5 **Prokopowicz D,** Zagorski K, Kramarz P. Amoebiasis-a problem in patients with ulcerative colitis. *Wiad Lek* 1994; **47:** 248-251
6 **Chan KL,** Sung JY, Hsu R, Liew CT. The association of the amoebic colitis and chronic ulcerative colitis. *Singapore Med J* 1995; **36:** 303-305

Edited by Xu XQ and Wang XL

P.O.Box 2345, Beijing 100023,China
Fax: +86-10-85381893
E-mail: wjg@wjgnet.com www.wjgnet.com

World J Gastroenterol 2003;9(8):1836-1839
World Journal of Gastroenterology
 ISSN 1007-9327

• BRIEF REPORTS •

Meta analysis of propranolol effects on gastrointestinal hemorrhage in cirrhotic patients

Jin-Wei Cheng, Liang Zhu, Ming-Jun Gu, Zhe-Ming Song

Jin-Wei Cheng, Liang Zhu, Zhe-Ming Song, Department of Gastroenterology, Changzheng Hospital, Second Military Medical University, Shanghai 200003, China
Ming-Jun Gu, Department of Endocrinology, Changzheng Hospital, Second Military Medical University, Shanghai 200003, China
Supported by the National Natural Science Foundation of China, No. 19872074
Correspondence to: Dr. Liang Zhu, Department of General Medicine, Changzheng Hospital, Second Military Medical University, Shanghai 200003, China. jinnwave@sohu.com
Telephone: +86-21-63610109 Ext 73181 **Fax:** +86-21-63520020
Received: 2002-12-24 **Accepted:** 2003-02-24

Abstract

AIM: To assess the effects of propranolol as compared with placebo on gastrointestinal hemorrhage and total mortality in cirrhotic patients by using meta analysis of 20 published randomized clinical trials.

METHODS: A meta analysis of published randomized clinical trials was designed. Published articles were selected for study based on a computerized MEDLINE and a manual search of the bibliographies of relevant articles. Data from 20 relevant studies fulfilling the inclusion criteria were retrieved by means of computerized and manual search. The reported data were extracted on the basis of the intention-to-treat principle, and treatment effects were measured as risk differences between propranolol and placebo. Pooled estimates were computed according to a random-effects model. We evaluated the pooled efficacy of propranolol on the risk of gastrointestinal hemorrhage and the total mortality.

RESULTS: A total of 1 859 patients were included in 20 trials, 931 in the propranolol groups and 928 as controls. Among the 652 patients with upper gastrointestinal tract hemorrhage, 261 patients were treated with propranolol, and 396 patients were treated with placebo or non-treated. Pooled risk differences of gastrointestinal hemorrhage were -18 % [95 % CI, -25 %, -10 %] in all trials, -11 % [95 % CI, -21 %, -1 %] in primary prevention trials, and -25 % [95 % CI, -39 %, -10 %] in secondary prevention trials. A total of 440 patients died, 188 in propranolol groups and 252 in control groups. Pooled risk differences of total death were -7 % [95 % CI, -12 %, -3 %] in all trials, -9 % [95 % CI, -18 %, -1 %] in primary prevention trials, and -5 % [95 % CI, -9 %, -1 %] in secondary prevention trials.

CONCLUSION: Propranolol can markedly reduce the risks of both primary and recurrent gastrointestinal hemorrhage, and also the total mortality.

Cheng JW, Zhu L, Gu MJ, Song ZM. Meta analysis of propranolol effects on gastrointestinal hemorrhage in cirrhotic patients. *World J Gastroenterol* 2003; 9(8): 1836-1839
http://www.wjgnet.com/1007-9327/9/1836.asp

INTRODUCTION

Gastrointestinal hemorrhage due to portal hypertension is a leading cause of death in patients with cirrhosis. The first episode of bleeding is fatal in 40 % to 50 % of such patients and two-thirds die within 1 year. It has been shown that treatment with propranolol can reduce portal venous pressure[1], portal blood flow[2] and superior portosystemic collateral blood flow[3] and its efficacy on preventing gastrointestinal hemorrhage has been assessed in many randomized clinical trials. Some trials have been primary, in which the drug was used to prevent hemorrhage in patients who have not bled, some have been secondary with the drug used to prevent rebleeding. Numerous primary and secondary prevention studies concluded that propranolol treatment decreased the incidence of gastrointestinal hemorrhage. Thus far, however, randomized clinical trials usually included small sample sizes and showed conflicting results, which hindered researchers drawing conclusions from the trials.

In meta analysis each treated group is compared with controls from the same study, and the treatment effect is combined across all studies, to provide information both about the presence of any significant effect and about its size. We have made extensive efforts to find all relevant studies by means of computerized and manual search. Then we combined all the studies including primary and secondary, to assess the effectiveness of propranolol as compared with placebo on the prevention of gastrointestinal hemorrhage.

MATERIALS AND METHODS

This meta analysis was performed according to a protocol determined before the study, and the widely accepted methodological recommendations[4-6]. Measurement of treatment effectiveness was determined on the basis of primary or recurrent gastrointestinal hemorrhage, and mortality.

Selection of trials

Studies that fulfilled the following criteria were included in the present meta analysis: (a) propranolol was compared with placebo; (b) patients were randomly assigned to the treatment regimen, and studies were prospective; (c) patients with cirrhosis of liver were included; (d) outcomes of primary or recurrent bleeding, and death were assessed; (e) results were published as abstracts or full reports.

Study identification

Pertinent studies were retrieved from MEDLINE database by using the search terms "propranolol", "cirrhosis" and "gastrointestinal hemorrhage" and by limiting the search to reports of clinical trials and studies with human patients. In addition, a manual search was performed by checking the reference lists from articles or reviews to identify studies not yet included in MEDLINE database. When the results of a single study were reported in more than one publication, only the most recent and complete data were included in the meta-analysis. Finally, twenty randomized clinical trials that fulfilled the criteria were identified, fifteen were published in full form[7-21], and five in abstract form[22-26].

Data extraction

Data from each randomized clinical trial were extracted by two independent reviewers (Jin-Wei Cheng, Liang Zhu). For each study and each type of treatment, the following data were extracted: number of patients, and number of each outcome. Numeric discrepancies between the two independent data extractions were resolved after discussion.

Statistical methods

All comparisons were performed according to the randomly assigned treatment (intended-treatment analysis). Because of different clinical characteristics among study groups, and varying sample sizes, we assumed that heterogeneity was present even not statistically significant, and we decided to combine data by using a random-effects model to achieve more conservative estimates[27].

For all the outcomes, the pooled estimates were computed with the method of DerSimonian and Laird[27]. Summary point estimates and 95 % confidence interval (CI) were reported. Risk differences less than zero denoted an advantage for propranolol. Those more than zero denoted an advantage for placebo. 95 % CIs of risk differences not including 0 denoted a statistically significant advantage.

RESULTS

All trials

A total of 1 859 patients were included in the twenty trials, 931 in the propranolol groups and 928 as controls.

Table 1 Point estimates and 95 % CIs of the risk difference of gastrointestinal hemorrhage

	Prapranolol group		Control group		Risk difference and its 95 % CI (%)
	Total	Bled	Total	Bled	
Primary prevention					
Pascal (1984)	34	1	35	9	-23 [-38, -7]
Mills (1987)	38	19	43	33	-27 [-47, -6]
Pascal (1987)	118	20	112	30	-10 [-20, 1]
Italian (1988)	85	16	89	27	-12 [-24, 1]
Strauss (1988)	20	4	16	4	-5 [-33, 23]
Colman (1990)	23	8	25	2	27 [5, 49]
Andreani (1990)	43	2	41	13	-27 [-43,-11]
Conn (1991)	51	4	51	14	-20 [-34, -5]
Prova (1991)	68	23	72	19	7 [-8, 23]
Subtotal	480	97	484	151	-11 [-21, -1]
Overall effect			*Z*=-2.15	*P*=0.03	
Secondary prevention					
Burroughs (1983)	26	14	22	13	-5 [-33, 23]
Lebrec (1984)	38	6	36	23	-48 [-68,-29]
Cerbelaud (1986)	42	17	42	33	-38 [-57,-19]
Villeneuve (1986)	42	32	37	30	-5 [-23, 13]
Queuniet (1987)	51	29	48	31	-8 [-27, 11]
Marbet (1988)	10	2	10	9	-70 [-101,-39]
Colombo (1989)	32	8	30	14	-22 [-45, 2]
Sheen (1989)	18	8	18	15	-39 [-68,-10]
Garden (1990)	38	20	43	36	-31 [-50,-12]
Colman (1990)	26	9	26	13	-15 [-42, 11]
Perez-Ayuso (1991)	26	16	28	24	-24 [-47, -1]
Calès (1999)	102	3	104	4	-1 [-6, 4]
Subtotal	451	164	444	245	-25 [-39,-10]
Overall effect			*Z*=-3.34	*P*=0.0008	
All trials					
Total	931	261	928	396	-18 [-25, -10]
Overall effect			*Z*=-4.38	*P*=0.00001	

In the 20 trials, among the 652 patients with upper gastrointestinal tract hemorrhage, 261 were treated with propranolol, and 396 were treated with placebo or not treated. The overall weighted bleeding rate was 31 % for propranolol and 48 % for controls. The pooled risk difference was -18 % [95 % CI, -25 %, -10 %], and the reduction had statistical significance (Z=-4.38, P<0.001, Table 1).

A total of 440 patients died, 188 in propranolol groups and 252 in control groups. The overall weighted bleeding rate was 17 % after propranolol treatment and 24 % after placebo treatment. The pooled risk difference was -7 % [95 % CI, -12 %, -3 %], and the reduction due to propranolol also was statistically significant (Z=-3.44, P<0.001, Table 2).

In ten trials, the overall weighted rate of death due to bleeding was 6 % in propranolol groups and 12 % in controls. The pooled risk difference was -5 % [95 % CI, -9 %, -2 %] (Z=-3.12, P=0.002).

Table 2 Point estimates and 95 % CIs of the risk difference of death

	Prapranolol group		Control group		Risk difference and its 95 % CI (%)
	Total	Death	Total	Death	
Primary prevention					
Pascal (1984)	34	1	35	13	-34 [-51, -17]
Mills (1987)	38	15	43	19	-5 [-26, 17]
Pascal (1987)	118	25	112	40	-15 [-26, -3]
Italian (1988)	85	30	89	22	11 [-3, 24]
Strauss (1988)	20	7	16	7	-9 [-41, 23]
Colman (1990)	23	6	25	7	-2 [-27, 23]
Andreani (1990)	43	13	41	18	-14 [-34, 7]
Conn (1991)	51	8	51	11	-6 [-21, 9]
Prova (1991)	68	7	72	14	-9 [-21, 3]
Subtotal	480	112	484	151	-9 [-18, -1]
Overall effect			*Z*=-2.11	*P*=0.03	
Secondary prevention					
Burroughs (1983)	26	4	22	5	-7 [-30, 15]
Lebrec (1984)	38	3	36	8	-14 [-30, 2]
Cerbelaud (1986)	42	5	42	12	-17 [-33, 0]
Villeneuve (1986)	42	19	37	14	7 [-14, 29]
Queuniet (1987)	51	12	48	13	-4 [-21, 14]
Marbet (1988)	10	1	10	3	-20 [-54, 14]
Colombo (1989)	32	4	30	7	-11 [-30, 8]
Sheen (1989)	18	0	18	2	-11 [-28, 6]
Garden (1990)	38	14	43	19	-7 [-29, 14]
Colman (1990)	26	1	26	1	0 [-10, 10]
Perez-Ayuso (1991)	26	4	28	7	-10 [-31, 12]
Calès (1999)	102	9	104	10	-1 [-9, 7]
Subtotal	451	76	444	101	-5 [-9, -1]
Overall effect			*Z*=-2.26	*P*=0.02	
All trials					
Total	931	188	928	252	-7 [-12, -3]
Overall effect			*Z*=-3.44	*P*=0.0006	

Primary prevention

There were 964 patients in the nine primary prevention trials. Of the total 480 patients treated with propranolol, 97 patients bled from upper gastrointestinal tract, the overall weighted rate was 20 %. And 112 patients died, the overall weighted rate was 22 %. In the control groups (484 patients), the overall weighted rate of bleeding was 31 % (151 patients), and that of death was 31 % (151 patients).

The pooled risk difference of bleeding was -11 % [95 %CI, -21 %, -1 %], and that of death was -9 % [95 % CI, -18 %, -1 %]. Both of the reduction due to propranolol had statistical

significance (Table 1, Table 2).

Death due to bleeding was reported in 5 primary prevention trials, the overall weighted rate was 6 % in propranolol groups and 10 % in controls. The pooled risk difference was -4 % [95 % CI, -8 %, 0 %] (Z=-2.06, P=0.04).

Secondary prevention

Among the 895 patients in the twelve secondary prevention trials, 451 were treated with propranolol and 444 were treated with placebo.

The number of patients with bleeding was 164 in propranolol groups and 245 in control groups, the overall weighted rate was 39 % and 63 % respectively. The pooled risk difference of hemorrhage was -25 % [95 % CI, -39 %, -10 %], which had statistical significance (Z=-3.34, P<0.001, Table 1).

In all secondary prevention trials, the total number of patients died after propranolol treatment was 76, and 101 in controls. The overall weighted rate of death was 13 % and 20 % respectively. The pooled risk difference of death was -5 % [95% CI, -9 %, -1 %], and the reduction was statistically significant (Z=-2.26, P=0.02, Table 2).

In 5 recurrent prevention trials, the overall weighted rate of death due to bleeding was 6 % after propranolol treatment and 15 % in controls. The pooled risk difference was -8 % [95% CI, -15 %, -2 %] (Z=-2.53, P=0.01).

DISCUSSION

Propranolol reduces portal pressure, portal blood flow, and superior portosystemic collateral blood flow, so it can reduce the variceal pressure to prevent upper gastrointestinal hemorrhage[1-3]. However, reduction of the risk of gastrointestinal bleeding could not be replicated in some trials[7, 19, 21]. In the present meta analysis, we reviewed 20 randomized clinical trials to assess the efficacy of propranolol on gastrointestinal hemorrhage. The overall results showed that propranolol significantly reduced the risk of upper gastrointestinal tract bleeding, with a same effect on survival.

The beneficial effect of propranolol on both first and recurrent gastrointestinal hemorrhage was observed in all but six of the trials. The average rate of gastrointestinal hemorrhage was 28 % in patients treated with propranolol, but 43 % in controls, suggesting that this interventional therapy is highly effective on prevention of upper gastrointestinal tract bleeding. The results also demonstrated the efficacy of propranolol on preventing the first episode or recurrence of upper gastrointestinal tract bleeding in patients with cirrhosis. In the six trials, propranolol used to prevent variceal bleeding was proved to be ineffective, four were published in full form[7,10,19,21], and two in abstract form[25, 26].

The results of this meta analysis showed that propranolol significantly affected survival in all trials, primary prevention trials, or secondary trials. The average mortality was 20 % in patients treated with propranolol, but 27 % in controls. The reduction in total mortality was consistent with a limited effect on death due to bleeding. Other causes of death, including liver failure, sepsis, and the development of hepatocellular carcinoma, were not affected by propranolol.

Although the beta-blockade effect of propranolol can decrease hepatic blood flow, which may in turn induce deterioration of liver function in cirrhotic patients, but hepatic decompensation has been rarely encountered in patients treated with propranolol. In addition, other adverse effects of propranolol such as hypotension (3.6 %), heart failure (2.2 %), arrhythmia (1.4 %), bronchial spasm (2.7 %), dizziness (2.0 %), asthenia (3.4 %) etc were rarely encountered.

Endoscopic sclerotherapy is a conventional treatment for reducing the risk of recurrent bleeding, and long-term survival may also improve[28-33]. Another meta analysis which we conducted showed that the average recurrent bleeding rate was 42 % after endoscopic sclerotherapy, but was only 36 % in propranolol groups, and 55 % in control group in our present meta analysis. A randomized clinical trial suggested that the efficacy of combined sclerotherapy and propranolol on the primary prevention of hemorrhage in cirrhotic patients with varices was the same as propranolol alone[34]. In other words, endoscopic sclerotherapy did not consistently improve survival. Sclerotherapy, like propranolol, is associated with a low incidence of side-effects, but side effects such as esophageal perforation, may be life-threatening. The technique also is more time demanding on both physicians and patients.

In conclusion, the results of this meta analysis of the existing controlled trials show that propranolol is an effective means of reducing both the incidence of bleeding from upper gastrointestinal tract and the total mortality, and has the advantage of being safe and cost-effective. The combined data indicate that propranolol reduces the risk of bleeding or rebleeding by about 20 %, in both primary and secondary prevention and it also reduces mortality. The primary prevention trials, which included patients with obvious varices at high risk of bleeding, clearly show a beneficial effect. Based upon the analysis we would recommend a long-term treatment of gastrointestinal hemorrhage with propranolol. However, for many patients with portal hypertension without obvious varices, large prospective multicenter trials are indicated to determine the preventive benefit of propranolol. Further comparative trials of propranolol versus sclerotherapy are required to identify which is superior for secondary prevention of gastrointestinal hemorrhage.

REFERENCES

1 **Luca A**, Garcia-Pagan JC, Feu F, Lopez-Talavera JC, Fernandez M, Bru C, Bosch J, Rodes J. Noninvasive measurement of femoral blood flow and portal pressure response to propranolol in patients with cirrhosis. *Hepatology* 1995; **21**: 83-88

2 **Albillos A**, Perez-Paramo M, Cacho G, Iborra J, Calleja JL, Millan I, Munoz J, Rossi I, Escartin P. Accuracy of portal and forearm blood flow measurements in the assessment of the portal pressure response to propranolol. *J Hepatol* 1997; **27**: 496-504

3 **Escorsell A**, Bordas JM, Feu F, Garcia-Pagan JC, Gines A, Bosch J, Rodes J. Endoscopic assessment of variceal volume and wall tension in cirrhotic patients: effects of pharmacological therapy. *Gastroenterology* 1997; **113**: 1640-1646

4 **Egger M**, Smith GD, Phillips AN. Meta-analysis: principles and procedures. *BMJ* 1997; **315**: 1533-1537

5 **Egger M**, Smith GD. Meta-Analysis. Potentials and promise. *BMJ* 1997; **315**: 1371-1374

6 **Pogue J**, Yusuf S. Overcoming the limitations of current meta-analysis of randomised controlled trials. *Lancet* 1998; **351**: 47-52

7 **Burroughs AK**, Jenkins WJ, Sherlock S, Dunk A, Walt RP, Osuafor TO, Mackie S, Dick R. Controlled trial of propranolol for the prevention of recurrent variceal hemorrhage in patients with cirrhosis. *N Engl J Med* 1983; **309**: 1539-1542

8 **Lebrec D**, Poynard T, Bernuau J, Bercoff E, Nouel O, Capron JP, Poupon R, Bouvry M, Rueff B, Benhamou JP. A randomized controlled study of propranolol for prevention of recurrent gastrointestinal bleeding in patients with cirrhosis: a final report. *Hepatology* 1984; **4**: 355-358

9 **Villeneuve JP**, Pomier-Layrargues G, Infante-Rivard C, Willems B, Huet PM, Marleau D, Viallet A. Propranolol for the prevention of recurrent variceal hemorrhage: a controlled trial. *Hepatology* 1986; **6**: 1239-1243

10 **Queuniet AM**, Czernichow P, Lerebours E, Ducrotte P, Tranvouez JL, Colin R. Controlled study of propranolol in the prevention of recurrent hemorrhage in cirrhotic patients. *Gastroenterol Clin Biol* 1987; **11**: 41-47

11 **Pascal JP**, Cales P. Propranolol in the prevention of first upper gastrointestinal tract hemorrhage in patients with cirrhosis of the liver and esophageal varices. *N Engl J Med* 1987; **317**: 856-861

12 **The Italian Multicenter Project for Propranolol in Prevention of Bleeding**. Propranolol for prophylaxis of bleeding in cirrhotic patients with large varices: a multicenter, randomized clinical trial. *Hepatology* 1988; **8**: 1-5

13 **Marbet UA**, Straumann A, Gyr KE, Beglinger C, Schaub N, Bogtlin J, Loosli J, Kiowski W, Ritz R, Stalder GA. Reduction in early recurrence of variceal bleeding by propranolol. *Scand J Gastroenterol* 1988; **23**: 369-374

14 **Colombo M**, de Franchis R, Tommasini M, Sangiovanni A, Dioguardi N. Beta-blockade prevents recurrent gastrointestinal bleeding in well-compensated patients with alcoholic cirrhosis: a multicenter randomized controlled trial. *Hepatology* 1989; **9**: 433-438

15 **Sheen IS**, Chen TY, Liaw YF. Randomized controlled study of propranolol for prevention of recurrent esophageal varices bleeding in patients with cirrhosis. *Liver* 1989; **9**: 1-5

16 **Garden OJ**, Mills PR, Birnie GG, Murray GD, Carter DC. Propranolol in the prevention of recurrent variceal hemorrhage in cirrhotic patients. A controlled trial. *Gastroenterology* 1990; **98**: 185-190

17 **Andreani T**, Poupon RE, Balkau BJ, Trinchet JC, Grange JD, Peigney N, Beaugrand M, Poupon R. Preventive therapy of first gastrointestinal bleeding in patients with cirrhosis: results of a controlled trial comparing propranolol, endoscopic sclerotherapy and placebo. *Hepatology* 1990; **12**: 1413-1419

18 **Conn HO**, Grace ND, Bosch J, Groszmann RJ, Rodes J, Wright SC, Matloff DS, Garcia-Tsao G, Fisher RL, Navasa M, Drewniak SJ, Atterbury CE, Bordas JM, Lerner E, Bramante C. Propranolol in the prevention of the first hemorrhage from esophagogastric varices: A multicenter, randomized clinical trial. The Boston-New Haven-Barcelona Portal Hypertension Study Group. *Hepatology* 1991; **13**: 902-912

19 **The PROVA Study Group**. Prophylaxis of first hemorrhage from esophageal varices by sclerotherapy, propranolol or both in cirrhotic patients: a randomized multicenter trial. *Hepatology* 1991; **14**: 1016-1024

20 **Perez-Ayuso RM**, Pique JM, Bosch J, Panes J, Gonzalez A, Perez R, Rigau J, Quintero E, Valderrama R, Viver J, Esteban R, Rodrigo L, Bordas JM, Rodes J. Propranolol in prevention of recurrent bleeding from severe portal hypertensive gastropathy in cirrhosis. *Lancet* 1991; **337**: 1431-1434

21 **Cales P**, Oberti F, Payen JL, Naveau S, Guyader D, Blanc P, Abergel A, Bichard P, Raymond JM, Canva-Delcambre V, Vetter D, Valla D, Beauchant M, Hadengue A, Champigneulle B, Pascal JP, Poynard T, Lebrec D. Lack of effect of propranolol in the prevention of large oesophageal varices in patients with cirrhosis: a randomized trial. French-Speaking Club for the Study of Portal Hypertension. *Eur J Gastroenterol Hepatol* 1999; **11**: 741-745

22 **Pascal JP**. Prophylactic treatment of variceal bleeding in cirrhotic patients with propranolol: a multicentric randomized study. *Hepatology* 1984; **4**: 1092

23 **Cerbelaud P**, Lavignolle A, Perrin D, Jutel P, Beaujard E, Colomb P, Le Bodic L. Propranolol et prevention des recidives de rupture de varice oesophagienne du cirrhotique. *Gastroenterol Clin Biologique* 1986; **10**: 18

24 **Mills PR**, Garden OJ, Birnie GG, Carter DC. Propranolol in the prevention of further variceal hemorrhage in cirrhosis. *Gastroenterology* 1987; **92**: 1755

25 **Strauss E**, de Sa MFG, Albano A, Lacet CMC, Leite MO, Maffei RA. A randomized controlled trial for the prevention of the first upper gastrointestinal bleeding due to portal hypertension in cirrhosis: sclerotherapy or propranolol versus control groups. *Hepatology* 1988; **8**: 1395

26 **Colman J**, Jones P, Finch C, Dudley F. Propranolol in the prevention of variceal haemorrhage in alcoholic cirrhotic patients. *Hepatology* 1990; **12**: 851

27 **Der Simonian R**, Laird N. Meta-analysis in clinical trials. *Control Clin Trials* 1986; **7**: 177-188

28 **de la Pena J**, Rivero M, Sanchez E, Fabrega E, Crespo J, Pons-Romero F. Variceal ligation compared with endoscopic sclerotherapy for variceal hemorrhage: prospective randomized trial. *Gastrointest Endosc* 1999; **49**: 417-423

29 **Umehara M**, Onda M, Tajiri T, Toba M, Yoshida H, Yamashita K. Sclerotherapy plus ligation versus ligation for the treatment of esophageal varices: a prospective randomized study. *Gastrointest Endosc* 1999; **50**: 7-12

30 **Masci E**, Stigliano R, Mariani A, Bertoni G, Baroncini D, Cennamo V, Micheletti G, Casetti T, Tansini P, Buscarini E, Ranzato R, Norberto L. Prospective multicenter randomized trial comparing banding ligation with sclerotherapy of esophageal varices. *Hepatogastroenterology* 1999; **46**: 1769-1773

31 **Hou MC**, Lin HC, Kuo BI, Lee FY, Chang FY, Lee SD. The rebleeding course and long-term outcome of esophageal variceal hemorrhage after ligation: comparison with sclerotherapy. *Scand J Gastroenterol* 1999; **34**: 1071-1076

32 **Hata Y**, Hamada E, Takahashi M, Ota S, Ogura K, Shiina S, Okamoto M, Okudaira T, Teratani T, Maeda S, Koike Y, Sato S, Obi S, Tanaka T, Kawabe T, Shiratori Y, Kawase T, Nomura M, Omata M. Endoscopic variceal ligation is a sufficient procedure for the treatment of oesophageal varices in patients with hepatitis C liver cirrhosis: comparison with injection sclerotherapy. *J Gastroenterol Hepatol* 1999; **14**: 236-240

33 **Gotoh Y**, Iwakiri R, Sakata Y, Koyama T, Noda T, Matsunaga C, Ogata SI, Ishibashi S, Sakata H, Tsunada S, Fujimoto K. Evaluation of endoscopic variceal ligation in prophylactic therapy for bleeding of oesophageal varices: a prospective, controlled trial compared with endoscopic injection sclerotherapy. *J Gastroenterol Hepatol* 1999; **14**: 241-244

34 **Avgerinos A**, Armonis A, Manolakopoulos S, Rekoumis G, Argirakis G, Viazis N, Vlachogiannakos J, Adamopoulos A, Kanaghinis T, Raptis SA. Endoscopic sclerotherapy plus propranolol versus propranolol alone in the primary prevention of bleeding in high risk cirrhotic patients with esophageal varices: a prospective multicenter randomized trial. *Gastrointest Endosc* 2000; **51**: 652-658

Edited by Xu JY and Wang XL

P.O.Box 2345, Beijing 100023,China
Fax: +86-10-85381893
E-mail: wjg@wjgnet.com www.wjgnet.com

World J Gastroenterol 2003;9(8):1840-1843
World Journal of Gastroenterology
 ISSN 1007-9327

• BRIEF REPORTS •

Inhibition of hepatitis B virus by a novel L-nucleoside, b-L-D4A and related analogues

Jin-Ming Wu, Ju-Sheng Lin, Na Xie, Kuo-Huan Liang

Jin-Ming Wu, Ju-Sheng Lin, Na Xie, Kuo-Huan Liang, Institute of liver diseases, Tongji Medical College, Huazhong University of Science and Technology, Wuhan 430030, China
Jin-Ming Wu, Department of Digestive Medicine, the First Affiliated Hospital, Wenzhou Medical College, Wenzhou 325000, Zhejiang Province, China
Supported by National Natural Science Foundation of China, No. 39970858
Correspondence to: Dr. Ju-Sheng Lin, Institute of Liver Diseases, Tongji Medical College, Huazhong University of Science and Technology, Wuhan430030, Hubei Province, China. linjusheng2001@163.net
Telephone: +86-27-83662578
Received: 2003-01-04 **Accepted:** 2003-02-17

Abstract

AIM: To explore the inhibition of β-L-D4A on hepatitis B virus (HBV) in 2.2.15 cells derived from HepG2 cells transfected with HBV genome.

METHODS: 2.2.15 cells were plated at a density of 5×10^4 per well in 12-well tissue culture plates, and treated with various concentrations of β-L-D4A for 6 days. In the end, 5 μl of medium was used for the estimation of HBsAg and HBeAg, the other medium was processed to obtain virions by a polyethlene glycol precipitation method. At the same time, intracellular DNA was also extracted and digested with HindIII. Both DNAs were subjected to Southern blot, hybridized with a ^{32}P-labeled HBV probe and autoradiographed. Intensity of the autoradiographic bands was quantitated by densitometric scans of computer and ED_{50} was calculated. Then Hybond-N membrane was washed and rehybridized with a ^{32}P-labeled mtDNA-specific probe, and effect of β-L-D4A on mitochondrial DNA was studied. 2.2.15 cells were also seeded in 24-well tissue culture plates, and cytotoxicity with different concentrations was examined by MTT method. ID_{50} was calculated. Structure-activity relationships between D2A and D4A were also studied as above.

RESULTS: Autoradiographic bands were similar between supernatant and intracellular HBV DNA. Episomal HBV DNA was inhibited in a dose-dependent manner. ED_{50} was 0.2 μM. HBsAg or HBeAg was not apparently decreased, and inhibition of mitochondrial DNA was not obvious. The experiment of cytotoxicity gained ID_{50} at 200 μM.

CONCLUSION: β-L-D4A possesses potent inhibitory effects on the replication of HBV *in vitro* with little cytotoxicity and mitochondrial toxicity, TI value is 1000. It is expected to be developed as a new clinically anti-HBV drug.

Wu JM, Lin JS, Xie N, Liang KH. Inhibition of hepatitis B virus by a novel L-nucleoside, β-L-D4A and related analogues. *World J Gastroenterol* 2003; 9(8): 1840-1843
http://www.wjgnet.com/1007-9327/9/1840.asp

INTRODUCTION

Like interferon, nucleoside analogues have become the focus of investigations of anti-HBV drugs[1]. However, most anti-HBV nucleoside analogues tested to date have at best only transient and limited effects in a small percentage of the general population of HBV-infected individuals and exist moderately to seriously side effects[2,3]. Vidarabine, ribavirin, acyclovir, ganciclovir, famciclovir, fialuridine, etc. have not been used widely. In recent years, considerable interest has been focused on the use of 2', 3'-dideoxynucleosides (DDNs) for the treatment of chronic HBV infection[4]. DDNs are phosphorylated to triphosphate in cells, which in turn specifically inhibits the viral polymerase, terminates the elongation of HBV DNA, showing potent anti-HBV activities with relatively low cellular toxicities[5].

Lamivudine as one of DDNs has been used widely in clinic, and has a rapidly potent anti- HBV effect, but there is a rebound of HBV DNA after treatment, and drug resistance and viral mutants may appear after a long-term treatment with lamivudine[6]. Thus it is important to search for more effective agents against HBV, even with an improved therapeutic index. In this report, 2', 3'-didehydro-2', 3'-dideoxyadenine (β-L-D4A), a novel L-Nucleoside was demonstrated to effectively block the production of HBV in 2.2.15 cells *in vitro*. Mitochondrial effects and cytotoxicity were also investigated to evaluate the potential use of these compounds in treatment of HBV infection.

MATERIALS AND METHODS

Compounds and agents

β-L-D4A was synthesized by ourselves with the help of Pharmaceutic College of Wuhan University and identified by infrared, mass spectra, nuclear-magnetic resonance. Lamivudine, ddC' D-D4A, L-D2A, D-D2A were provided by Professor Cheng YC (School of Medicine, Yale University, New Haven, CT). All compounds were dissolved in phosphate-buffered saline (pH 7.4).

Determination of anti-HBV activity in 2.2.15 cells

2.2.15 cells (clonal cells derived from hepG2 cells that were transfected with a plasmid containing HBV DNA) that could secrete heptitis B virions, kindly provided by Prof. Cheng, were incubated in DMEM medium with 10 % (vol/vol) fetal bovine serum, 100 IU/mL penicillin and 100 μg/mL streptomycin at 37 ℃ in a moist atomosphere containing 5 % CO_2/95 % air. The cells were inoculated at a density of 5×10^4/ml per well in 12-well tissue culture plates. The compounds studied were added to the medium 3 days after the inoculation. The cells were grown in the presence of drugs for 9 days with changes of medium every 3 days. On the 12th day, the culture medium was havested. An aliquot of the culture medium (5 μl) was used for estimation of HBV surface antigen (HBsAg) and HBV e antigen (HBeAg). The remaining medium was processed to obtain virions by a polyethylene glycol precipitation method[7]. The viral DNA recovered from the secreted particles was subjected to Southern blot analysis. Cellular DNA was isolated according to the standard protocols. Inhibition of viral DNA replication was determined by comparison of the viral DNA from drug-treated

and nontreated cultures. The level of inhibition was determined by hybridization of the blots to an HBV-specific probe followed by autoradiography. Quantitation of the autoradiographs was performed by density scanning with a computer software.

Effect of b-L-D4A on mitochondrial DNA

Since some of the nucleosides used in the treatment of HBV, such as FIAU[8], could affect liver function, especially mitochondrial function, a detailed analysis of the effect of β-L-D4A on mitochondrial DNA synthesis was carried out. 2.2.15 cells were cultured as above and after 24 h in culture, treatment with the compounds was initiated. β-L-D4A was added at concentrations of 0.4 μM and 10 μM in DMEM. Cultures treated with 0.4 μM 2' 3' -dideoxycytidine (ddC) were maintained in parallel as positive controls for damage of mitochondrial DNA. Blank control was also set. Cellular DNA was isolated according to the standard protocols and digested with restriction enzyme BamH I. Hybridizations and detection of the mitochodrial DNA were done according to the laboratory manual of molecular cloning. The probe was cytochrome oxidase III DNA labeled by ^{32}pdCTP.

Cytotoxicity

Cells were inoculated at a density of 5×10^3/ml per well in 24-well tissue culture plates. After 24 h in culture, the cells were treated with various concentrations of β-L-D4A in DMEM for 3 days. Then 3-(4, 5-dimethylthiazol-2-yl)-2, 5-diphenyltetrazolium bromide (MTT) assays were performed using the cell titer kit™ (Promega) following the standard procedure with the following exceptions. At the time points described as illustrations, 15 μl MTT reagent was added per well, allowed to incubate for 30 minutes, after which 130 μl stop/lysis buffer was added. Plates were sealed with Parafilm™ and left overnight at room temperature to allow solubilization of the formazan salt product. Absorbance was measured at 750 nm and 570 nm using a Thermomax (Molecular Devices, San Jose, CA), or a cytoFluor microplate reader (PE Biosystems, Foster City, CA). The data were normalized (A570-A750 nm) and the mean absorbance (5 wells/concentration) was plotted against drug concentration. The ID_{50} values were calculated as described above.

Determination of effects of b-L-D4A on HBsAg and HBeAg

HBsAg and HBeAg in the culture medium were determined according to the protocols supplied by the manufacturer. Essentially, the culture medium was appropriately diluted with phosphate-buffered saline and absorbed on the surface of plates coated by antibody to HBsAg or HBeAg. After an incubation period, the plates were washed and incubated in orthophenylene diamine. After a 30-min incubation, the reaction was terminated by adding 1N sufuric acid. The A_{490} of the final reaction was read. Appropriate positivity and negativity were assayed along with the samples.

RESULTS

Structure-activity relationships

The 2.2.15 cell line was used to evaluate the antiviral activities of ddA analogues: D-D4A, L-D2A, D-D2A (Structures are shown in Figure 1). The antiviral effects were measured by an analysis of extracellular HBV DNA. The experiment revealed that the inhibition of HBV DNA was more strong by L-isomer than by D-isomer and much more notable by L-D4A than by L-D2A (Figure 2).

Dosage-activity relationships

Inhibition of HBV DNA replication by β-L-D4A was evident as demonstrated by the amount of DNA obtained from the secreted viral particles as well as from the intracellular episomal particles. Concentrations of β-L-D4A ranging from 0.08 μM to 10 μM produced a dose-dependent inhibition (Figure 3). The intensity of autoradiographic bands for extracellular HBV DNA was quantitated by densitometric scans of computer and ED_{50} was calculated at 0.2 μM(Figure 4). Analysis of the intracellular episomal HBV DNA reflected similar trends in inhibition (Figure 5).

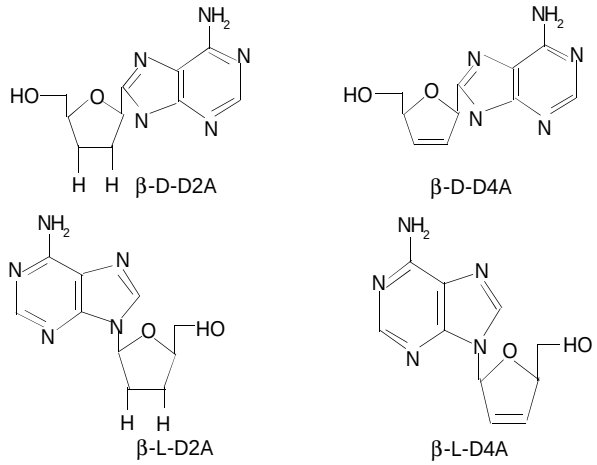

Figure 1 Structures of β-L-D4A and analogues.

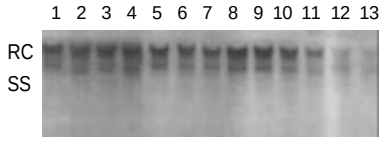

Figure 2 Inhibition of isomers of D4A and D2A on HBV DNA replication in supernatant. Lane 1 as negative control; lanes 2, 3, 4 as D-D2A at 2 μM, 4 μM and 8 μM, respectively; lanes 5, 6, 7 as L-D2A at 2 μM, 4 μM and 8 μM, respectively; lanes 8, 9, 10 as D-D4A at 2 μM, 4 μM and 8 μM, respectively; lanes 11, 12, 13 as L-D4A at 2 μM, 4 μM and 8 μM, respectively. RC: relaxed circular HBV DNA; SS: single-stranded HBV DNA.

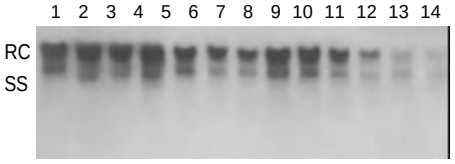

Figure 3 Inhibition on replication of extracellular HBV DNA by β-L-D4A. lanes 1, 2 as negative control; lanes 3, 4 as lamivudine at 1 μM; lanes 5, 6 as β-L-D4A at 10 μM; lanes 7, 8 as β-L-D4A at 2 μM; lanes 9, 10 as β-L-D4A at 0.4 μM; lanes 11, 12 as β-L-D4A at 0.08 μM; lanes 13, 14 as blank control ($HepaG_2$). RC: relaxed circular HBV DNA; SS: single-stranded HBV DNA.

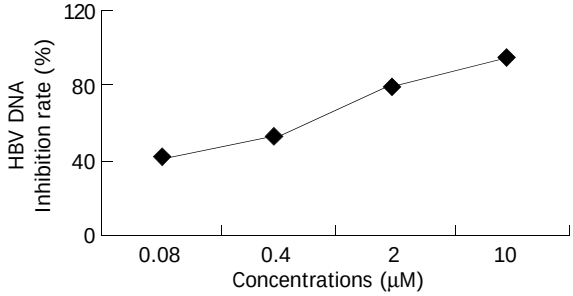

Figure 4 Inhibition on replication of extracellular HBV DNA by β-L-D4A.

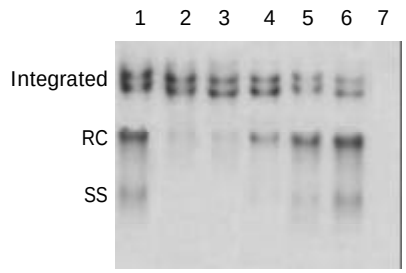

Figure 5 Inhibition on replication of intracellular HBV DNA by β-L-D4A. lane 1 as negative control; lane 2 as lamivudine at 1 μM; lane 3 as β-L-D4A at 10 μM; lane 4 as β-L-D4A at 2 μM; lane 5 as β-L-D4A at 0.4 μM; lane 6 as β-L-D4A at 0.08; lane 7 as blank control (HepaG2). RC: relaxed circular HBV DNA; SS: single-stranded HBV DNA.

Effect of b-L-D4A on mitochondrial DNA

Hybridization of intracellular DNA to a cytochrome oxidase III was done to evaluate the effect of β-L-D4A on mitochondrial DNA. Mitochondrial DNA levels treated with 0.4 μM and 10 μM β-L-D4A were nearly similar to the blank control, but were obviously lower for ddC at 0.4 μM (Figure 6).

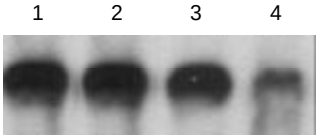

Figure 6 Toxicity of mitochondrial DNA. lane 1 as blank control; lane 2 as β-L-D4A at 0.4 μM; lane 3 as β-L-D4A at 10 μM; lane 4 as ddC at 0.4 μM.

Cytotoxicity of b-L-D4A

β-L-D4A did not show evident toxicity to 2.2.15 cells even at a concentration of 10 μM, but at high concentrations it had cytotoxicity, with 50 % inhibitory concentration (ID_{50}) of 200 μM, The data are shown in Table 1 and Figure 7.

Table 1 Effect-dosage relationship of inhibition of cell growth by β-L-D4A

Dosage (μM)	*n*	A value ($\bar{x}$±*s*)	Inhibition rate (%)
50	3	0.84±0.22	22.3
100	3	0.75±0.16	36.0
150	3	0.73±0.12	37.2
200	3	0.67±0.21	50.4
250	3	0.53±0.15	73.5
300	3	0.43±0.25	89.2
0	3	2.01±0.23	0

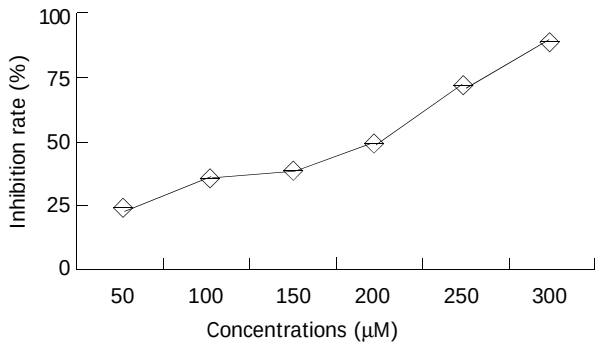

Figure 7 Effect of β-L-D4A on cell growth curve.

Effects of b-L-D4A on HBsAg and HBeAg

Measurements of the levels of viral surface antigen and e antigen from the media of cultures treated with β-L-D4A revealed that β-L-D4A had no significant inhibitory effect on HBsAg and HBeAg at low concentrations, but had marked effect of reducing HBsAg and HBeAg at 2 μM and 10 μM, significantly different from the blank group ($P<0.05$ or $P<0.01$, respectively) (Shown in Table 2).

Table 2 Effect-dosage relationship of inhibition of HBsAg and HBeAg by β-L-D4A

Dosage(μM)	*n*	HBsAg		HBeAg	
		P / N value ($\bar{x}$±*s*)	Inhibition rate(%)	P / N value ($\bar{x}$±*s*)	Inhibition rate (%)
0.08	3	2.96±0.18	13.7	4.98±0.23	5.5
0.4	3	2.84±0.22	22.3	4.97±0.15	5.7
2	3	2.75±0.16[a]	36.0	4.88±0.25	9.4
10	3	2.73±0.12[a]	37.2	4.02±0.33[b]	37.5
Blank	3	3.09±0.21	0	5.27±0.27	0

[a]$P<0.05$; [b]$P<0.01$ *vs* blank control.

DISCUSSION

One rational approach to the development of drugs for the treatment of HBV infection in patients is to identify those compounds that specifically inhibit HBV DNA replication[9,10]. Since deoxynucleoside analogues were found to be effective on a variety of viruses, several compounds have been tested *in vitro* and *in vivo* against hepadnaviruses[9-12]. The selectivity of these compounds against HBV in general is assessed by their relative potency against HBV versus cellular toxicity[13-16]. Cytotoxicity studies are usually conducted by growth retardation assays that measure cell growth in the presence of compounds tested for three or four generations[17]. This growth retardation assay could not, however, detect delayed cytotoxicity of deoxynucleoside analogues such as ddC that have an effect on cellular mtDNA synthesis. Since mitochondria play an important role in organ function, it was hypothesized that the delayed toxicity as shown by peripheral neuropathy (e.g., observed in patients treated with ddC analogs) could be due to decreases in mtDNA[18]. In this study, in addition to assessing their anti-HBV activities, compounds were examined for their effects on 4-day cell growth and on mtDNA.

Deoxynucleosides such as D2A and D4A can exist as (+)- or (-)- enatiomers. From the results we got, we could see that (-)-isomers were superior to (+)-isomers, and β-L-D4A was the most potent inhibitor of HBV replication in 2.2.15 cells, which could almost completely block HBV DNA replication at a concentration of 4 μM. However, (+) -isomers were almost inactive against HBV replication when tested up to 8 μM, mechanism of which might be in that the compounds could be deaminated intracellularly to the inactive analogues as reported before[19].

β-L-D4A was the most potent inhibitor of HBV replication in 2.2.15 cells from our results. No effects on mtDNA were observed. Cell growth retardation with the administration of β-L-D4A at low concentrations was not evident, but at high concentrations, β-L-D4A began to show cytotoxicity in a dose-dependent manner with 50 % inhibitory concentration (ID_{50}) of 200 μM. Since β-L-D4A does not inhibit mtDNA synthesis at concentrations that inhibit virus production, the delayed toxicity, such as peripheral neuropathy, associated with the treatment of ddC[20] may not occur. In addition, β-L-D4A is not toxic to proliferting cells at concentrations that completely block the synthesis of HBV virion, suggesting that acute bone

marrow toxicity may not be a concern. The study on dosage-activity relationships showed that β-L-D4A could inhibit HBV DNA replication in a markedly dose-dependent manner with 50 % inhibitory concentration (ED_{50}) of 0.2 μM. As the therapeutic index (TI value) was equal to ID_{50}/ ED_{50}, we got the TI value of β-L-D4A at 1 000. TI of lamivudine was 750 as reported in another article[21]. Therefore β-L-D4A like lamivudine possesses potent anti-HBV replication effect and has a higher TI value. In addition to that, β-L-D4A shows inhibition of expression of HBV antigens at high concentrations, indicating that β-L-D4A may be able to decrease the levels of HBsAg and HBeAg with a long term use.

About the mechanism of action of β-L-D4A, we think it is likely the inhibition of viral DNA polymerase, chain-termination resulted from incorporation into elongated DNA strand, or both. The mechanism needs to be further explored.

On the basis of the study of nucleoside analogs against HIV, human immunodeficiency virus resistant to ddC is not cross resistant to the thymidine analog zidovudine[22]. This permits the possibility of HBV treatment with β-L-D4A in the event of resistance to cytosine analogs as lamivudine. Furthermore, possibilities of a combined therapy of β-L-D4A and lamivudine for HBV can be explored.

REFERENCES

1 **Bridges EG,** Cheng YC. Use of novel beta-L(-)-nucleoside analogues for treatment and prevention of chronic hepatitis B virus infection and hepatocellular carcinoma. *Prog Liver Dis* 1995; **13**: 231-245

2 **Freiman JS**, Mc Caughan GW. Current limitations to nucleoside analogue therapy for chronic hepatitis B virus infection in the liver transplant and non-transplant settings. *J Gastroenterol Hepatol* 2000; **15**: 227-229

3 **Pan-Zhou XR**, Cui L, Zhou XJ, Sommadossi JP, Darley-Usmar VM. Differential effects of antiretroviral nucleoside analogs on mitochondrial function in HepG2 cells. *Antimicrob Agents Chemother* 2000; **44**: 496-503

4 **Van Draanen NA,** Tisdale M, Parry NR, Jansen R, Dornsife RE, Tuttle JV, Averett DR, Koszalka GW. Influence of stereochemistry on antiviral activities and resistance profiles of dideoxycytidine nucleosides. *Antimicrob Agents Chemother* 1994; **38**: 868-871

5 **Zoulim F.** Therapy of chronic hepatitis B virus infection: inhibition of the viral polymerase and other antiviral strategies. *Antiviral Res* 1999; **44**: 1-30

6 **Lai CL,** Yuen MF. Profound suppression of hepatitis B virus replication with lamivudine. *J Med Virol* 2000; **61**: 367-373

7 **Hawkins AE,** Zuckerman MA, Briggs M, Gilson RJ, Goldstone AH, Brink NS, Tedder RS. Hepatitis B nucleotide sequence analysis: linking an outbreak of acute hepatitis B to contamination of a cryopreservation tank. *J Virol Methods* 1996; **60**: 81-88

8 **Tennant BC,** Baldwin BH, Graham LA, Ascenzi MA, Hornbuckle WE, Rowland PH, Tochkov IA, Yeager AE, Erb HN, Colacino JM, Lopez C, Engelhardt JA, Bowsher RR, Richardson FC, Lewis W, Cote PJ, Korba BE, Gerin JL. Antiviral activity and toxicity of fialuridine in the woodchuck model of hepatitis B virus infection. *Hepatology* 1998; **28**: 179-191

9 **Chu CK,** Boudinot FD, Peek SF, Hong JH, Choi Y, Korba BE, Gerin JL, Cote PJ, Tennant BC, Cheng YC. Preclinical investigation of L-FMAU as an anti-hepatitis B virus agent. *Antivir Ther* 1998;**3** (Suppl 3): 113-121

10 **Colacino JM.** Mechanisms for the anti-hepatitis B virus activity and mitochondrial toxicity of fialuridine (FIAU). *Antiviral Res* 1996; **29**: 125-139

11 **Lin JS,** Kira T, Gullen E, Choi Y, Qu F, Chu CK, Cheng YC. Structure-activity relationships of L-dioxolane uracil nucleosides as anti-Epstein Barr virus agents. *J Med Chem* 1999; **42**: 2212-2217

12 **Ma T,** Pai SB, Zhu YL, Lin JS, Shanmuganathan K, Du J, Wang C, Kim H, Newton MG, Cheng YC, Chu CK. Structure-activity relationships of 1-(2-Deoxy-2-fluoro-beta-L-arabinofuranosyl) pyrimidine nucleosides as anti-hepatitis B virus agents. *J Med Chem* 1996; **39**: 2835-2843

13 **Kotra LP,** Xiang Y, Newton MG, Schinazi RF, Cheng YC, Chu CK. Structure-activity relationships of 2'-deoxy-2', 2'-difluoro-L-erythro-pentofuranosyl nucleosides. *J Med Chem* 1997; **40**: 3635-3644

14 **Qiu YL,** Ptak RG, Breitenbach JM, Lin JS, Cheng YC, Kern ER, Drach JC, Zemlicka J**.** (Z)- and (E)-2-(hydroxymethylcyclopropylidene)-methylpurines and pyrimidines as antiviral agents. *Antivir Chem Chemother* 1998; **9**: 341-352

15 **Qiu YL,** Ksebati MB, Ptak RG, Fan BY, Breitenbach JM, Lin JS, Cheng YC, Kern ER, Drach JC, Zemlicka J**.** (Z)- and (E)-2-((hydroxymethyl) cyclopropylidene) methyladenine and -guanine. New nucleoside analogues with a broad-spectrum antiviral activity. *J Med Chem* 1998; **41**: 10-23

16 **Du J,** Surzhykov S, Lin JS, Newton MG, Cheng YC, Schinazi RF, Chu CK**.** Synthesis, anti-human immunodeficiency virus and anti-hepatitis B virus activities of novel oxaselenolane nucleosides. *J Med Chem* 1997; **40**: 2991-2993

17 **Lu X,** Gong S, Monks A, Zaharevitz D, Moscow JA. Correlation of nucleoside and nucleobase transporter gene expression with anti-metabolite drug cytotoxicity. *J Exp Ther Oncol* 2002; **2**: 200-212

18 **Hostetler KY,** Korba BE, Sridhar CN, Gardner MF. Antiviral activity of phosphatidyl-dideoxycytidine in hepatitis B-infected cells and enhanced hepatic uptake in mice. *Antiviral Res* 1994; **24**: 59-67

19 **Gudmundsson KS,** Tidwell J, Lippa N, Koszalka GW, van Draanen N, Ptak RG, Drach JC, Townsend LB. Synthesis and antiviral evaluation of halogenated beta-D- and -L-erythrofuranosylbenzimidazoles. *J Med Chem* 2000; **43**: 2464-2472

20 **Dalakas MC,** Semino-Mora C, Leon-Monzon M**.** Mitochondrial alterations with mitochondrial DNA depletion in the nerves of AIDS patients with peripheral neuropathy induced by 2'3'-dideoxycytidine (ddC). *Lab Invest* 2001; **81**: 1537-1544

21 **Leung N.** Liver disease-significant improvement with lamivudine. *J Med Virol* 2000; **61**: 380-385

22 **Descamps D,** Flandre P, Joly V, Meiffredy V, Peytavin G, Izopet J, Tamalet C, Zeng AF, Harel M, Lastere S, Aboulker JP, Yeni P, Brun-Vezinet F. Effect of zidovudine resistance mutations on virologic response to treatment with zidovudine or stavudine, each in combination with lamivudine and indinavir. *J Acquir Immune Defic Syndr* 2002; **31**: 464-471

Edited by Xu XQ and Wang XL

P.O.Box 2345, Beijing 100023,China
Fax: +86-10-85381893
E-mail: wjg@wjgnet.com www.wjgnet.com

World J Gastroenterol 2003;9(8):1844-1847
World Journal of Gastroenterology
 ISSN 1007-9327

• BRIEF REPORTS •

Generation and characterization of transgenic mice expressing tamoxifen-inducible cre-fusion protein specifically in mouse liver

Huan-Zhang Zhu, Jian-Quan Chen, Guo-Xiang Cheng, Jing-Lun Xue

Huan-Zhang Zhu, Istitute of Pathology, Southwest Hospital, Third Military Medical University, Chongqing 400038, China
Jian-Quan Chen, Guo-Xiang Cheng, Shanghai Transgenic Research Center, Shanghai 201203, China
Huan-Zhang Zhu, Jing-Lun Xue, State Key Laboratory of Genetic Engineering, Institute of Genetics, School of Life Sciences, Fudan University, Shanghai 200433, Chian
Supported by the National Natural Science Foundation of China No.30070380
Correspondence to: Jing-Lun Xue, State Key Laboratory of Genetic Engineering, Institute of Genetics, School of Life Sciences, Fudan University, Shanghai 200433,Chian. jlxue@fudan.ac.cn or Guo-Xiang Cheng, Shanghai Transgenic Research Center, Shanghai 201203, China. chenggx@cngenon.com
Telephone: +86-21-65642424
Received: 2003-01-04 **Accepted:** 2003-02-24

Abstract

AIM: To establish transgenic mice expressing tamoxifen-inducible Cre-ERt recombinase specifically in the liver and to provide an efficient animal model for studying gene function in the liver and creating various mouse models mimicking human diseases.

METHODS: Alb-Cre-ERt transgenic mice were produced by microinjecting the construct with Cre-ERt fusion gene of DNA fragments into fertilized eggs derived from inbred C57BL/6 strain. Transgenic mice were identified by using PCR and Southern blotting. Expression of Cre-ERt fusion gene was analyzed in the liver, kidney, brain and lung from F1 generation transgenic mice at 8 weeks of age by reverse transcription (RT)-PCR.

RESULTS: Four hundred and fourteen fertilized eggs of C57 BL/6 mice were microinjected with recombinant Alb-Cre-ERt DNA fragments, and 312 survival eggs injected were transferred to the oviducts of 12 pseudopregnant recipient mice, 6 of 12 recipient mice became pregnant and gave birth to 44 offsprings. Of the 44 offsprings, two males and one female carried the hybrid Cre-ERt fusion gene. Three mice were determined as founders, and were back crossed to set up F1 generations with other inbred C57BL/6 mice. Transmission of Cre-ERt fusion gene in F1 offspring followed Mendelian rules. The expression of Cre-ERt mRNA was detected only in the liver of F1 offspring from two of three founder mice.

CONCLUSION: Transgenic mice expressing tamoxifen-inducible Cre-ERt recombinase under control of the liver-specific promoter are preliminary established.

Zhu HZ, Chen JQ, Cheng GX, Xue JL. Generation and characterization of transgenic mice expressing tamoxifen-inducible cre-fusion protein specifically in mouse liver. *World J Gastroenterol* 2003; 9(8): 1844-1847
http://www.wjgnet.com/1007-9327/9/1844.asp

INTRODUCTION

The liver plays a central role in regulation of carbohydrate, lipid, and urea metabolism as well as in production of most plasma proteins and detoxification of exogenous chemicals. The ability to create defined genetic modifications *in vitro* and *in vivo* provides a promising way to understand relevant functions of numerous hepatic genes in health and disease. Ligand-dependent chimeric Cre recombinases are powerful tools to induce specific DNA rearragements in cultured cells and mice[1-3]. To introduce defined genetic modifications in a temporally controlled manner in the liver, an alternative approach is to establish transgenic mice expressing tamoxifen-inducible Cre recombinase under control of the liver specific promoter. To this end, we constructed the fusion gene of Cre and the ligand binding domain (LBD) of a mutated human estrogen receptor (ER) that recognizes anti-estrogen 4-hydroxytamoxifen (4-OHT), Cre-ERt , under control of a liver-specific regulatory sequence from the mouse albumin gene. By using microinjection technology, two transgenic mice lines expressing Cre-ERt only in the liver were finally obtained.

MATERIALS AND METHODS

Materials

Restriction enzymes and other reagents Enzymes *Eco*RI, *Sma*I, *Sac*II *Hin*dIII, *Bam*HI, *Bgl* I, T4 DNA ligase, dNTP, Taq DNA polymerase, MMLV reverse transcriptase, etc, were purchased from NEB, Sangon and Sigma companies, respectively.
Mice C57BL/6, ICR mice (clean animal) were purchased from Laboratory Animal Center, Shanghai, China.

Methods

Construction of recombinant plasmid Construction of the Alb-Cre-ERt (Figure 1) was performed according to Sambrook *et al*[4]. In brief, a 0.6 Kb *Sma*I-*Sac*II fragment containing CMV promoter from plasmid pCMV-Cre-ERt (kindly provided by Prof. Chambon P) was replaced with a 2.3 Kb *Sac*II-*Eco*RV fragment containing albumin enhancer and promoter (alb e/p) from p2335A (kindly provided by Prof. Palmiter). Identity of the constructs was confirmed by restriction enzyme mapping and DNA sequence analysis.

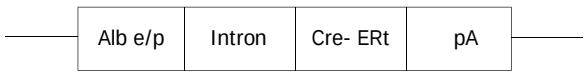

Figure 1 Structure of alb-Cre-ERt expression vector. The DNA fragments contained albumin gene promoter/enhancer (alb e/p), rabbit β-globin intron, fusion gene of Cre-ERt, and polyadenylation site (pA).

Production of transgenic mice Transgenic mice were generated by standard methods[5]. In brief, the transgene construct was linearized using *Bgl* l. The fragment was gel-purified with QIAGEN Kit. After diluted to 1 μg/ml final concentration in microinjection buffer, DNA was microinjected into the male pronucleus of fertilized C57BL/

6 mice oocytes. Then injected eggs were transplanted into the oviduct of pseudopregnant mice. Operated mice got pregnant and gave birth. Selected mice were bred with wild-type animals to establish transgenic lines that were maintained at heterozygosity.

Detection of transgenic integration Genomic DNA was extraction from transgenic mice tails (about 1-1.5 cm) at 4 weeks of age. Total DNA was extracted with the method described by Sambrook[4].

PCR assay The primers were designed on Cre gene sequence and synthesized by Cybersyn Biotechnology Company. The sequence of primers for PCR was as follows: the 5' primer for Cre was 5' -ATC CGA AAA GAA AAC GTT GA-3' and the 3' primer was 5' -ATC CAG GTT ACG GAT ATA G T-3' . The PCR reaction condition contained 2 μl of 10×PCR Buffer, 0.4 μl of 25 mM Mg^{2+}, 1 μl of 15 mM dNTP, 1 μl of 10 pmol each of primer, 2u of Taq DNA polymerase, 1 μg sample DNA. A 20 μl total reaction volume was obtained by adding sterile water, the reaction procedure of PCR was: beginning at 95 ℃ for 5 min, then 30 cycles at 94 ℃ denature for 30 s, annealing at 58 ℃ for 40 s and extension at 72 ℃ for 40 s, final extension at 72 ℃ for 10 min. 1.8 % agarose gel was prepared and 10 μl PCR products was loaded in the gel, then electrophoresed at 80 voltage for 40 min, the result of electrophoresis was observed.

Southern blot analysis Southern-blotting analysis was performed with the following standard procedures[4]: 10 μg tail DNA was digested with *Eco*RI and separated by electrophoresis on a 0.6 % agarose gel, and transferred onto a nylon membrane (Boehringer Mannheim). The nylon membrane was prehybridized for 5 h at 42 ℃ and hybridized overnight with a probe from a 0.7 kb *Bam*HI-*Xho*I Cre fragment that was a random primer labeled using α-32P dCTP (Amersham Pharmacia Biotech Inc). Bands were detected by X-ray film after 6 days of exposure.

Detection of Cre-ERt mRNA synthesis in mice The level of Cre-ERt mRNA was estimated by RT-PCR. Total RNA was isolated from F1 generation of 4 weeks old mouse tissues (liver, kidney, brain and lung) by Sambrooks method[4]. The upstream primer was 5' -CAGAACCTGAAGATGTTCG-3' and downstream was 5' -GGATCATCAGCTACACCAG-3' , resulting in a 505 bp fragment of the Cre-ERt cDNA. First stranded cDNA was synthesized as follows: The reverse transcriptase reactions contained 1 μg RNA, 5 μl of 10×PCR Buffer, 3 μl of 15 mM dNTP, 1 μl of RNasin (80 u/μl), 2 μl 10 pmol upstream primer, 1 μl MMLV(200 u). A 50 μl total reaction volume was obtained by adding sterile DEPC treated water. Reaction conditions were at 48 ℃ for 45 min for reverse transcription. The products of reverse transcriptase reactions were used directly in PCR reactions, adding 2 u Taq DNA polymerase, 3 μl of 10 pmol upstream/downstream primers, respectively. PCR denaturation was at 96 ℃ for 2 min, then for 35 cycles of reaction (denaturation at 94 ℃ for 30 s, annealing at 62 ℃ for 40 s, extension at 72 ℃ for 40 s, and a final extension at 72 ℃ for 7 min).

RESULTS

Identity of constructs

The *Sma*I-*Sac*II (blunted) fragment containing Cre-ERt of plasmid pCMV-Cre-ERt was isolated; the *Sac*II (blunted)-*Eco*RV fragment containing albumin enhancer and promoter (alb e/p) of p2335A were isolated, respectively. The two individual fragments were ligated to generate palb-Cre-ERt. The identity of palb-Cre-ERt was confirmed by restriction enzyme mapping (Figure 2) and DNA sequence analysis (data not shown), indicating that the albumin enhancer and promoter were correctly inserted and linked.

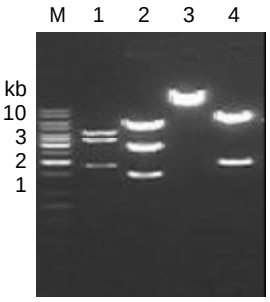

Figure 2 Identification of palb-Cre-ERt recombinant. M: GeneRuler 1 kb DNA Laddar, 1: recombinant-*Hin*dIII, 2: recombinant-*Sca*I, 3: recombinant-*Eco*RV, 4:Vector-*Hin*dIII.

Establishment of Cre-ERt transgenic mice

Recombinant Cre-ERt DNA fragment was microinjected into the male pronucleus of the 414 fertilized eggs of C57 BL/6 mice, and 312 survival eggs injected were transferred to the oviducts of 12 pseudopregnant recipient mice, 6 of 12 recipient mice became pregnant and gave birth to 44 offspring mice. The survial rate and birth rate of zygotes were 75 % (312/414) and 14 % (44/312), respectively. DNA extracted from tails of 44 offspring mice was screened by PCR assay and Southern blot analysis (Figure 3). The results showed that three mice carried the Cre-ERt gene. Three mice(two male, one female) were determined as founders. Total integration rate and efficiency of transgene were 6 % (3/44) and 0.7 % (3/414), respectively.

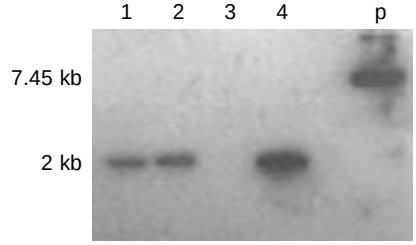

Figure 3 A part of mice was screened by Southern blot analysis. P: positive plasmid, 1,2,4: positive mice(2kb), 3: negative mice.

Stable transgenic mice of Cre-ERt

The founders were back crossed to set up F1 offsprings with other inbred C57BL/6 mice or transgenic littermates, respectively. All offsprings were screened by PCR (Figure 4), indicating that the integrated Cre-ERt gene was stably transmitted to subsequent generations (Table 1).

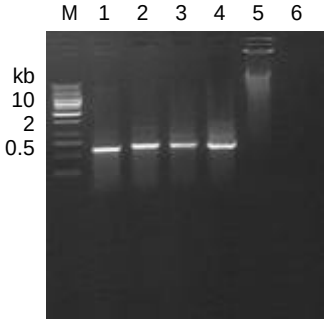

Figure 4 Electrophoresis analysis of PCR products amplified from DNA obtained from F1 mice tail tissues. Lanes 1-4 (transgenic mice) : positive bands (600 bp), lane 5: normal mouse (negative control), lane 6: blank control, M: Generuler of 1Kb DNA landar.

Table 1 Transmission rate of Alb Cre-ERt transgene to offspring

Founder line	Sex	No. of littermates	No. of offsprings	No. of transgenic mice	Ratio (%)
1	M	3	12	5	41.6
2	M	4	18	8	44.4
3	F	2	9	5	55.5

Expression of Cre-ERt gene in F1 mice

We performed RT-PCR to examine whether Cre-ERt transgene expressed only in liver tissues of F1 mice of transgenic mice lineages. The RT-PCR product (505 bp) was detected only in the liver of two of three transgenic mouse lineage (Figure 5).

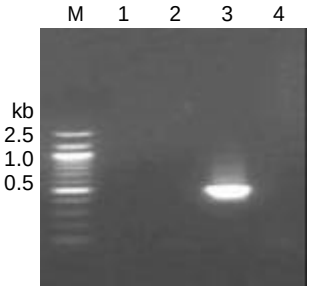

Figure 5 Electrophoresis analysis of RT-PCR products from transgenic mice. Lane 1: kidney tissue, lane 2: brain tissue, lane 3: liver (505 bp), lane 4: lung, M: Generuler of 100 bp DNA laddar.

DISCUSSION

By using transgenic mice carrying Cre recombinase under the control of a liver-specific promoter, the spatial window of gene modification can be strictly fixed to the liver. More recently, the generation and characterization of transgenic mice carrying Cre recombinase under the control of constitutive liver-specific promoters have been described[5-8]. These investigators used the constructs in which either mouse albumin regulation elements and α-fetoprotein enhancers or promoters and upstream enhancers of rat albumin gene were used to drive the Cre recombinase expression. These lines, AlfpCre, AlbCre, and Albumin-cre, allowed precise targeting of gene modifications in the liver. Nevertheless, the time of recombination remained strictly dependent on the promoter activity in these transgenic mice. In AlfpCre mice, Cre was shown to be constitutively active shortly after the appearance of the liver bud. Using the AlfpCre mice, mutagenesis of hepatic genes that serves essential functions during development could result in embryonic lethality, thus precluding analysis of their putative functions at subsequent stages. As for the temporal control of Cre expression in the liver, it was possible by using adenoviruses carrying the Cre transgene[9-11]. However, the immune response led to elimination of infected cells and could have deleterious effects on the general health status of mice[12]. An alternative approach for the temporal regulation of Cre activity is to create chimeric Cre fused to mutated ligand-binding domains of steroid hormone receptors which are insensitive to the endogenous ligands but still responsive to synthetic drugs. At present, tamoxifen-inducible Cre recombination can be achieved in many tissues of Cre-ERt transgenic adult mice and in developing mouse embryo as well as in cultured cells[13-18]. By combining the use of liver-specific promoters driving the expression of Cre and a ligand-activated Cre, gene modifications could be achieved in the liver at selected time points. Tannour-Louet *et al.*[19] established transgenic mice expressing tamoxifen-inducible Cre-mer recombinase under the control of the transthyretin promoter (TTR-Cre ind), the result showed a high recombination efficiency in the fetal and adult liver after treatment with 4-OHT. Imai *et al.*[20] established transgenic mice expressing tamoxifen-inducible Cre-ERt recombinase under control of the human 1-antitrypsin promoter, the result showed a low recombination efficiency, making it useful only to produce genetic chimeras which are not suitable for hepatic gene inactivation. In this study, the promoter and upstream enhancer of the mouse albumin gene were used to drive tamoxifen-inducible Cre-ERt recombinase expression for producing transgenic mice. After injecting the construct into oocytes, two lines expressing Cre-ERt in the liver, but not in other tested organs, were finally obtained. The results demonstrated that the promoter and upstream enhancer of the mouse albumin gene were liver-specific expression.

When the transgene results from random integration of a DNA fragment injected into a fertilized egg' s pronucleus, its level of expression in the resulting transgenic animal varied and depended upon certain factors, such as integration site, transgene cope number, genetic background of mouse, promoter/enhancer of fusion gene, etc. In this study, we only got two transgenic mice lines expressing Cre-ERt in the liver from three founder mice. The result was consistent with that of Imai *et al.*[20] in which three of 20 transgenic founder animals expressed Cre-ERt in the liver. These results indicate that not every transgenic founder mouse expresses Cre recombinase effectively, the chromosomal integration site may affect the expression pattern of transgenes.

Taken together, we have produced transgenic mice expressing Cre-ERt gene specific in the liver. This work will certainly permit a better understanding of hepatic gene functions and establish various mouse models mimicking human diseases.

ACKNOWLEDGEMENT

We thank Prof. Chambon P of Universite Louis Pasteur for providing plasmid pCMV Cre-ERt, Prof. Palmiter of University of Washington for plasmid p2335A, Prof. Orkin SH of Howard Hughes Medical Institute for Rosa26 reporter mice. This work was also supported by the Postdoctoral Foundation of China.

REFERENCES

1 **Rossant J**, McMahon A. "Cre"-ating mouse mutants- a meeting review on conditional mouse genetics. *Genes Dev* 1999; **13**: 142-145
2 **Le Y**, Sauer B. Conditional gene knockout using Cre recombinase. *Mol Biotechnol* 2001; **17**: 269-275
3 **Metzger D**, Chambon P. Site- and time-specific gene targeting in the mouse. *Mehods* 2001; **24**: 71-80
4 **Sambrook J**, Fritsch EF, Maniatis T. "Molecular Cloning: A Laboratory Manual," 2nd ed. *Cold Spring Harbor Laboratory Press, Cold Spring Harbor, New York* 1989: 9.31-9.61
5 **Hogan B**, Costantini f, Lacy E. Manipulating the mouse embryo: A laboratory manual. *Cold Spring Harbour, Cold Spring Harbor Laboratory, New York* 1980: 116-188
6 **Kellendonk C**, Opherk C, Anlag K, Schutz G, Tronche F. Hepatocyte- specific expression of Cre recombinase. *Genesis* 2000; **26**: 151-153
7 **Postic C,** Magnuson MA. DNA excision in liver by an albumin-Cre transgene occurs progressively with age. *Genesis* 2000; **26**: 149-150
8 **Yakar S**, Liu JL, Stannard B, Butler A, Accili D, Sauer B, LeRoith D. Normal growth and development in the absence of hepatic insulin- like growth factor I. *Proc Natl Acad Sci U S A* 1999; **96**: 7324-7329
9 **Wang Y**, Krushel LA, Edelman GM. Targeted DNA recombination *in vivo* using an adenovirus carrying the cre recombinase gene. *Proc Natl Acad Sci U S A* 1996; **93**: 3932-3936
10 **Rohlmann A**, Gotthardt M, Willnow TE, Hammer RE, Herz J. Sustained somatic gene inactivation by viral transfer of Cre recombinase. *Nat Biotechnol* 1996; **14**: 1562-1565

11 **Okuyama T**, Fujino M, Li XK, Funeshima N, Kosuga M, Saito I, Suzuki S, Yamada M. Efficient Fas-ligand gene expression in rodent liver after intravenous injection of a recombinant adenovirus by the use of a Cre-mediated switching system. *Gene Ther* 1998; **5**: 1047-1053
12 **Akagi K**, Sandig V, Vooijs M, Van Der Valk M, Giovannini M, Strauss M, Berns A. Cre-mediated somatic site-specific recombination in mice. *Nucleic Acids Res* 1997; **25**: 1766-1773
13 **Hayashi S**, McMahon AP. Efficient recombination in diverse tissues by a tamoxifen-inducible form of Cre: a tool for temporally regulated gene activation/inactivation in the mouse. *Dev Biol* 2002; **15**: 305-318
14 **Zheng B**, Zhang Z, Black CM, de Crombrugghe B, Denton CP. Ligand-dependent genetic recombination in fibroblasts: a potentially powerful technique for investigating gene function in fibrosis. *Am J Pathol* 2002; **160**: 1609-1611
15 **Vallier L**, Mancip J, Markossian S, Lukaszewicz A, Dehay C, Metzger D, Chambon p, Samarut J, Savatie P. An efficient system for conditional gene expression in embryonic stem cells and in their *in vitro* and *in vivo* differentiated derivatives. *Proc Natl Acad Sci U S A* 2001; **98**: 2467-2472
16 **Brocard J,** Warot X, Wendling O, Messaddeq N, Vonesch JL, Chambon P, Metzger D. Spatio-temporally controlled site-specific somatic mutagenesis in the mouse. *Proc Natl Acad Sci U S A* 1997; **94**: 14559-14563
17 **Li M**, Indra AK, Warot X, Brocard J, Messddeq N, Kato S, Metzger D, Chambon P. Skin abnormalities generated by temporally controlled RXRα mutations in mouse epidermis. *Nature* 2000; **407**: 633-636
18 **Utomo AR**, Nikitin AY, Lee WH. Temporal, spatial, and cell type-specific control of Cre-mediated DNA recombination in transgenic mice. *Nat Biotechnol* 1999; **17**: 1091-1096
19 **Tannour-Louet M**, Porteu A, Vaulont S, Kahn A, Vasseur-Cognet M. A tamoxifen-inducible chimeric Cre recombinase specifically effective in the fetal and adult mouse liver. *Hepatology* 2002; **35**: 1072-1081
20 **Imai T**, Chambon P, Metzger D. Inducible site-specific somatic mutagenesis in mouse hepatocytes. *Genesis* 2000; **26**: 147-148

Edited by Xu XQ and Wang XL

P.O.Box 2345, Beijing 100023,China
Fax: +86-10-85381893
E-mail: wjg@wjgnet.com www.wjgnet.com

World J Gastroenterol 2003;9(8):1848-1852
World Journal of Gastroenterology
 ISSN 1007-9327

• BRIEF REPORTS •

Concurrent hyperglycemia does not influence the long-term prognosis of unresectable hepatocellular carcinomas

Xiao-Ping Li, Zhen Chen, Zhi-Qiang Meng, Wen-Xia Huang, Lu-Ming Liu

Xiao-Ping Li, Zhen Chen, Zhi-Qiang Meng, Wen-Xia Huang, Lu-Ming Liu, Department of Liver Neoplasms, Cancer Hospital, Fudan University, Shanghai 200032, China
Correspondence to: Xiao-Ping Li, Department of Liver Neoplasms, Cancer Hospital, Fudan University, Shanghai 200032, China. lxpmy@sohu.com
Telephone: +86-021-64175590-1308
Received: 2003-03-04 **Accepted:** 2003-04-01

Abstract

AIM: The association has been established between the disorder of carbohydrate metabolism and liver cancer. However, little is known regarding the impact of concurrent hyperglycemia on prognosis of hepatocellular carcinoma (HCC). The present study aimed at solving this problem.

METHODS: A total of 225 patients included in this study, were admitted from January 1998 to December 2001 for an unresectable HCC proven by histological and imaging examinations. Most of the patients received interventional treatment, radiation and biotherapy. Response was evaluated by computerized tomography (CT) scan conducted 4-6 weeks following completion of the treatment, and then every 3 months. Survival was calculated from the beginning of treatment using the Kaplan-Meier method. Pretreatment, treatment and follow-up variables with possible prognostic significance were analyzed. A stepwise multivariate analysis was performed using the Cox regression model, and a prognostic index was obtained.

RESULTS: No differences were observed in survival parameters between the patients with and without hyperglycemia, median survival times of the patients were being 26±3.46 months and 29.5±2.04 months, respectively, and the 3-year survival rate was 8.36 % and 9.62 %, respectively. The univariate analysis indicated that there were several survival-associated variables including serum AFP level, clinical stage, Child-Pugh grade, method of treatment, size and number of tumor nodule (s). However, only the clinical stage, Child-Pugh grade and the treatment procedure were proved to be independent prognostic factors in the multivariate analysis.

CONCLUSION: This study indicates that hyperglycemia does not influence the long-term prognosis of HCC, and concurrent hyperglycemia should not be considered as an unfavorable prognostic factor during the treatment of patients with HCC.

Li XP, Chen Z, Meng ZQ, Huang WX, Liu LM. Concurrent hyperglycemia does not influence the long-term prognosis of unresectable hepatocellular carcinomas. *World J Gastroenterol* 2003; 9(8): 1848-1852
http://www.wjgnet.com/1007-9327/9/1848.asp

INTRODUCTION

Hepatocellular carcinoma (HCC) is the most common cancer of human liver in the world[1]. Its increasing incidence and mortality have been observed in China and some other countries. Both case-control and cohort studies have associated chronic viral hepatitis with its development[2,3]. The majority (60-80 %) of HCCs are found in livers with cirrhosis, frequently in a macronodular type in Southeast Asia and causally linked with chronic infection of hepatitis B virus (HBV) or hepatitis C virus (HCV)[3].

A large body of evidences have demonstrated that chronic liver diseases are associated with an increased incidence of glucose intolerance and diabetes[4-7]. The glucose intolerance is one of the most frequent complications in patients with HCC. Hypoglycemia is often considered as a paraneoplastic syndrome of HCC. The incidence of hyperglycemia or diabetes, however, is also increasing[8-10], accounting for 5-15 % of cases with HCC. Hyperglycemia and HCC may be found simultaneously. In some patients, HCC occurs following hyperglycemia[11]. In fact, diabetes mellitus (DM) has been considered as a risk factor for HCC development in addition to other well known factors[11-13]. In clinical views, hyperglycemia may need specific pharmacological treatment, dietary restrictions, or both procedures. It appears logical to regard hyperglycemia as an unfavorable factor during the prognosis evaluation of HCC, but this remains unsettled. A Japanese group has described the long-term impact of diabetes mellitus on the prognosis of HCC after resection[14]. Much more HCCs, however, are found at advanced stages in this country, and hence cannot be resected. For this reason, we conducted the study to evaluate the possible impact of concurrent hyperglycemia on the peri-treatment outcome and long-term survival in a large series of consecutive patients with unresectable HCCs.

MATERIALS AND METHODS

The survey involved 230 HCC patients consecutively admitted from January 1998 to December 2001. In 2002, all the clinical records of these patients were retrospectively examined, and the following clinical and laboratory indices were collected, including the values of AST, ALT, alkaline phosphatase (AP), γ-glutamyl-transpeptidase (γ-GT), prothrombin time (PT), serum bilirubin, serum proteins, albumin, γ-globulins, platelet number and glucose control. Of these, 225 cases with a complete clinical record were included. They were comprised of 180 males and 45 females, and their ages ranged from 32 to 76 years (mean ±SD, 53.19±12 years). A diagnosis of HCC was made by the ultrasound-guided transcutaneously fine-needle aspiration and subsequently by cytological examinations in 184 cases, and for the other cases the diagnosis was made by a combined consideration of the history, physical examinations, α-fetoprotein (AFP) levels and noninvasive imaging procedures. Indications for HBV and HCV infection were found in 125 and 15 patients, respectively.

Of the 225 patients examined, 28 had hyperglycemia, as determined with the concentration of plasma glucose exceeding 6.8 mmol/L in at least 2 fasting samples for each case or with the active treatment with insulin or oral hypoglycemic drugs necessary to control blood glucose levels. No consideration was given to those who had slight alternations in glucose

metabolism, such as impaired glucose tolerance demonstrated through an oral glucose tolerance test according to the criteria of World Health Organization[15,16], and those who had no evidence of glycosuria, because the test was performed in about 20 % of cases. Of the 28 hyperglycemic patients, 8 had overt diabetes mellitus when admitted to our department, and 20 had hyperglycemia identified after the diagnosis of HCC. The clinical and laboratory data are listed in Table 1.

As treatment for HCC, 146 patients received transcatheter arterial chemoembolization (TACE), 20 received radiotherapy only, 30 were treated by TACE and local radiotherapy, 14 by percutaneous ethanol injection therapy (PEIT), 162 received biotherapy.

TACE was performed with infusion of Fluorouracil or 5-FUDR (1.0 g), cisplatin (40-60 mg), followed by chemoembolization with a mixture of iodized oil and doxorubicin (40-60 mg) or mitomycin (10-20 mg), or with gelatin-sponge particles for the embolization. Radiotherapy was performed using a Co^{60} or 18-MV linear accelerator[17]. CT scan was performed to determine the radiation fields, and then whole or partial liver irradiation was conducted using the moving-strip technique or local radiotherapy covering tumors with generous margins (2-3 cm). The irradiation dose was 40-50 Gy daily in 1.8 fractions. During the treatment, the patients were monitored weekly with a complete blood count and liver function tests. For the concurrent hyperglycemia, one patient used dietary therapy, 13 received insulin therapy, and 6 took hypoglycemic drugs.

Effects of the treatments were evaluated based on serial CT scans 4-6 weeks following completion of the therapies and then every one to three months. The complete disappearance of the tumor was regarded as complete remission (CR), a decrease of over 50 % in tumor size as partial remission (PR), a decrease of less than 50 % or no change as stable disease (SD), and progression as progressive disease (PD). The response rate was calculated for CR or PR, and the SD cases were considered as non-responsive. Survival was estimated from the starting date of treatment according to the Kaplan-Meier method.

After the procedures as described above, the outcome of patients was investigated by visiting their families. Follow-up was carried out for all the subjects regularly for more than 6 months, with a median follow-up period of 25 months. The follow-up program included measurement of serum AFP and ultrasonography or CT scan every 3 months. The patients with recurrence were managed with various therapeutic methods including TACE, PEIT and/or biotherapy.

Statistical analysis

The data collected were presented as mean ± standard deviation. Continuous laboratory values were clustered to obtain two samples of approximately equal size. Statistical comparison between groups was performed using the χ^2 test with the Yates' correction for nominal data, and the Student's *t* test for numerical data.Kaplan -Meier survival plots were built to evaluate the prognostic values of individual indices, and compared using the log rank test. The same method was used for univariate analysis of survival. The univariate analysis was also carried out with age, sex, etiology and liver function parameters measured at the beginning of observation to establish their predictive value for survival. Baseline variables included in the univariate analysis were also analyzed by multivariate analysis using the step-wise forward Cox regression model to assess their predictive value with respect to survival. To check proportionality of risk factors with time, we plotted the log of cumulative hazards against time, demonstrating parallel behaviors in the two groups of patients separately with low- and high-risk values of selected prognostic covariates. All statistical analyses were computerized using the softpackage SPSS 10.0 (SPSS Inc., Chicago, Illinois). $P<0.05$ was considered statistically significant.

RESULTS

Hyperglycemia was found in 28 of the 225 patients when they were admitted. No difference in other clinical or laboratory indices was present between the groups with and without detectable hyperglycemia at the time (Table 1). Hyperglycemia was treated by insulin alone in 13, by oral hypoglycemic agents in 9, by diet therapy in 2, and by a combination of insulin and oral hypoglycemic agents in 4 patients. Table 1 shows a comparison of the clinicopathological data between hyperglycemic and non-hyperglycemic patients under the treatment for HCC.

The mean age of hyperglycemic patients was higher than that of non-hyperglycemic patients, but the difference was not significant. The two groups were comparable regarding their pathological factors such as size of the largest tumor nodules, number of tumor nodules, clinical stage and Child-Pugh grade. No significant difference was found between these two groups in other laboratory data such as total bilirubin, platelet count, prothrombin time and initial treatment.

Table 1 Clinicopathological data of hyperglycemic and non-hyperglycemic patients with HCC

Variables	With hyperglycemia (*n*=28)	Wthout hyperglycemia (*n*=197)
Age (year)	55±1.99	51.91±1.08
HBsAg(+/-)	15/13	110/87
Cirrhosis (+/-)	20/8	133/64
Gender (male/female)	23/5	157/40
Laboratory data		
ALT (U/L)	48.91±10.41	39.82±11.21
PT (s)	12.24±0.20	12.67±0.23
Albumin (g/L)	39.63±6.35	35.81±7.86
Total bilirubin (μmmol/L)	12.32±7.15	13.54±8.97
Platelet count ($\times10^9$/L)	158.41±18.14	155.75±7.37
TNM stage (I/II/III/IVa/IVb)[a]	0/3/12/5/8	0/32/76/48/41
Child-Pugh grades (A/B/C)	22/5/1	165/30/2
Sizes of the largest tumor (cm)	3.80±6.30	3.50±6.75
Initial treatment (TACE/radiotherapy/TACE+radiotherapy/PEI/biotherapy)	18/3/5/3/15	128/17/15/11/147

[a]The criteria for TNM classification were based on the criteria of UICC(1987).

During the follow up, 73 patients, 10 with and 63 without hyperglycemia, died of the hyperglycemic complications or from liver-related causes. Intrahepatic spreading was observed in 10 of them, and extrahepatic metastases occurred in 12 of the patients. Among them, 4 were complicated with lung metastases, 2 with bone metastases, 5 with para-aortic lymph node metastases, 1 with lung and bone metastases, 1 with lung and brain metastases and 1 with bone and para-aortic lymph node metastases. All of these patients received treatments according to their liver function status.

Response rates were calculated for the groups with and without hyperglycemia, which were 21.4 % and 20 %, respectively. The difference was not significant ($P>0.05$; Table 2).

Table 2 Comparison of treatment responses between the groups with (HG) and without hyperglycemia (Non-HG)

Groups	Response rate	CR (%)	PR(%)	NC(%)	PD(%)
HG	21.4(6/28)	7.1(2/28)	14.3(4/28)	53.6(15/28)	25.0(7/28)
Non-HG	23.4(46/197)	8.1(16/197)	15.2(30/197)	48.2(95/197)	28.4(56/197)
P values	0.821	0.858	0.896	0.596	0.706

The one-, two- and three-year survival rate was 51 %, 31 % and 8 % respectively for the hyperglycemia group, and was 60 %, 30 % and 10 %, respectively for the group without detectable hyperglycemia. Median survival times of these two groups were 26.0±3.5 months and 29.5±2.0 months, respectively. Figure 1 shows the overall cumulative survival after treatment.

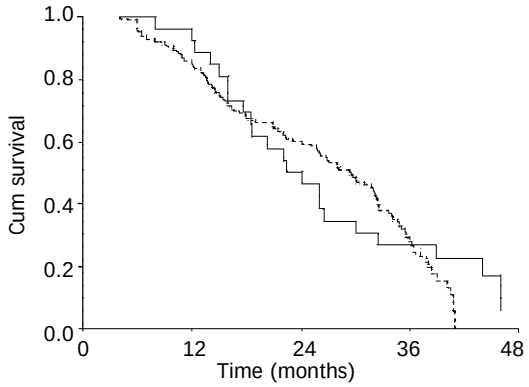

Figure 1 Kaplan-Meier survival curves for HCC patients with (green) and without hyperglycemia (red).

The incidence of complications included in this survey is shown in Table 3. The post-embolization syndrome consisted of abdominal pain, fever apparently unrelated to the tumor, and, slight or severe nausea, was seen in almost all the patients. Narcotics, anti-emetics and acetaminophen were given to relieve the symptoms. The main complications of TACE and radiotherapy included hepatic insufficiency or infarction, tumor rupture, upper gastrointestinal tract (GI) bleeding. Slight increase in serum bilirubin (n=20), elevation of serum transaminase (n=45), ascites (n=14), leukopenia (n=46) and thrombocytopaenia (n=15) were also seen during the therapies. These side effects were transient or easily controlled with medications in most cases. Two patients died of acute hepatic failure immediately after TACE, five died of hepatic encephalopathy and 2 died of severe GI bleeding. Thirty patients without hyperglycemia showed TACE- or radiotherapy-related complications, while ten with hyperglycemia showed complications after treatment and the symptoms were more severe. There was a significant difference between these two groups in the occurrence of complications.

Table 3 Incidence of complications during follow-up

Complication	With hyperglycemia		Without hyperglycemia		*P* value
	I-II	III-IV	I-II	III-IV	
Leucopoenia	6	8	22	10	0.000
Erythrocytopenia	5	1	16	2	0.049
Thrombocytopenia	2	1	10	2	0.359
Reaction of GI system	3	0	12	0	0.359
Impairment of liver function	5	1	13	0	0.008
Impairment of renal function	1	0	2	0	0.270

The univariate analysis showed that AFP level, clinical stage, Child-Pugh grade, treatment procedure, size of tumor and number of tumor nodules were independent factors predicting survival for all patients, but hyperglycemia was not. The effects of possible prognostic factors are shown in Table 4.

The Cox proportional hazards model showed that clinical stage, Child-Pugh grade and treatment procedure employed were independent factors predicting survival (Table 5). The 3-year survival rate was 1 % for Stage T4 cases and 15 % for others. The patients with T4 disease had a significantly shorter survival (P=0.0049). When the survival rates were compared according to Child-Pugh grade, patients of grade A survived significantly longer than those of grade B or C. The 3-year survival rate was 11.1 % and 0 %, respectively. The treatment procedure employed also had similar impacts on the survival. The 3-year survival rate for patients treated with TACE alone, radiotherapy alone and radiotherapy combined with TACE was 8 %, 4 % and 25 %, respectively (P=0.0042).

Table 4 Association between various clinical parameters after treatment and the survival

Clinical status		*n*	Cumulative survival rate (%)			Median survival (± SE, months)	*P* value
			1-year	2-year	3-year		
Overall		225	58.5	30.6	9.4	28.0±1.40	
Age (year)	<60	130	59.4	27.4	9.1	28.1±2.37	
	⩾60	95	57.3	35.4	9.7	26.8±2.60	0.815
HBV	Negative	100	61.8	31.2	9.69	29.3±2.01	
	Positive	125	54.4	29.9	8.97	26.1±3.63	0.876
AFP	<400	129	66.1	34.4	10.9	30.0±2.38	
(ng/ml)	⩾400	96	47.8	25.4	6.9	22.2±4.05	0.001
Hyperglycemia	Negative	28	51.1	30.7	8.36	26.0±3.46	
	Positive	197	59.7	30.5	9.62	29.5±2.04	0.231
Tumor	<6 cm	124	67.4	38.1	12.1	31.7±1.99	
size (cm)	⩾6 cm	101	47.0	19.9	5.42	21.0±3.55	0.028
Number of	Solitary	152	67.6	34.7	10.4	29.3±1.40	
tumors	Multiple	73	52.0	21.3	7.1	25.8±4.73	0.041
Child pugh	A	187	65.1	34.7	11.1	31.0±1.65	
	B or C	38	28.4	9.5	0	12.1±2.49	0.002
Clinical	Non-T4 disease	121	69.5	39.3	15.3	32.1±1.13	
stage	T4 disease	104	44.6	18.6	1.43	20.9±2.17	0.018
Method of	TACE	181	56.4	27.1	8.48	26.8±1.43	
treatment	Radiotherapy	23	58.3	29.2	4.17	32.6±9.85	
	TACE+ radiotherapy	21	77.8	63.0	25.2	37.8±6.62	0.0001

Table 5 Significant factors predicting survival tested by the Cox proportional hazards model

Variable	Coefficient	SE	Coefficient/ SE	*P* value
Clinical stage	0.8014	0.2695	2.9737	0.0019
Child-Pugh grade	0.3275	0.0657	4.9574	0.0001
Method of treatment	1.2144	0.3672	3.3072	0.0005

DISCUSSION

It is not surprising that many interactions exist between the liver and endocrine system demonstrated by some clinical and laboratory parameters. Liver diseases can result in endocrine disorders, and some endocrine disorders may affect the liver[18]. The role of the liver in glucose homeostasis is important. The regulation of hepatic glucose uptake involves a complex interaction of neural and hormonal mechanisms. HCC is often complicated with cirrhosis, and carbohydrate intolerance is seen in approximately 50 % of patients with

cirrhosis. The carbohydrate intolerance is most likely due to profound biochemical and physiologic derangements concurrent with advanced liver diseases, including portal-systemic shunting of glucose, elevated glucagon or growth hormone level, peripheral and/or hepatic resistance to insulin, malnutrition, elevated level of free fatty acids and hypokinemia[19,20]. Therefore, hyperglycemia or diabetes mellitus is often seen in HCC patients. Relatively mild hypoglycemia occurs in rapidly growing HCC among Chinese patients as a part of an end-stage illness[18], but their definite association remains lack of unequivocal evidences.

Accumulated data have associated diabetes with an increased risk for primary liver cancer[21-25]. One possible mechanism might be the proposed growth-stimulating and/or apoptosis-suppressing effects of insulin. This is particularly true for the tissues harboring preneoplastic or neoplastic lesions[26]. We observed that 68 % (153/225) of HCCs occurred in the liver with cirrhosis, and 8 of the patients had known diabetes mellitus before the diagnosis of HCC. Based on our observations, however, it is not clear whether cirrhosis and HCC were the causes or consequence of hyperglycemia and diabetes mellitus, or these two groups of disorders were merely clinically concurrent rather than causally linked.

To date, the knowledge is limited about the treatment of HCC complicated with hyperglycemia. Diabetes mellitus is regarded as an unfavorable factor in determining surgical resection for HCC patients[27-29]. Hepatic operation and anesthesia may have profound metabolic effects, potentially exacerbating the preexisting diabetes by insulin deficiency, its reduced secretion or insensitivity. This may diminish phagocyte functions, and thus impairs the resistance to infection and delays wound healing. Diabetes may also result in some cardiovascular diseases, neuropathy and nephropathy. All these factors will increase the morbidity and mortality of surgical procedures. Diabetes mellitus has been reported to be the only independent risk factor for liver failure after major hepatic resection of HCC patients with a low remnant liver volume. Ikeda *et al*[14] reported 342 hepatectomies for HCCs, the 10-year survival rate was 12.6 % and 24.6 % for diabetic and non-diabetic patients, respectively. Thus, diabetes mellitus complicated with hepatocellular carcinoma was proposed to be a high-risk condition for the higher morbidity and a shorter survival after operation. However, this notion was not approved by several recent observations carried out in Hong Kong[29], Japan[30,31] and Taiwan[27].

The impact of diabetes mellitus on the function of the liver with end-stage diseases remains obscure. Toyoda *et al*. pointed out that the presence of diabetes mellitus didn' t necessarily correlate with the severity of cirrhosis. In the present study, most of the cases of hyperglycemia did not show any symptom of diabetes, and might be simply regarded as carbohydrate intolerance, a subclinical stage to overt diabetes mellitus. Therefore, the influence of hyperglycemia on liver functions is not obvious, as indicated by the data we presented here. On the other hand, non-surgical treatments, as employed in this study, may help to reserve hepatic intracellular energy during the treatment and achieve a better peri-operational outcome, compared to those more stressful surgical procedures. Our data also showed that concurrent hyperglycemia did not significantly influence the overall survival of HCC patients after non-surgical treatment. Certainly, patients with hyperglycemia and HCC are a heterogeneous group, which is partly linked to a genetic alteration, and patients with the so-called hepatogenous hyperglycemia, are mainly associated with the acquired insulin resistance. These two conditions may have different metabolic abnormalities and possible different outcomes.

Our study was partly retrospective, and only a small number of patients underwent an oral glucose tolerance test during hospitalization, so we could not say some patients with hyperglycemia were diabetes. The prevalence of hyperglycemia in this series was higher than that reported in several previous studies. On the other hand, fasting glucose and detailed data about the treatments were available for most cases. In this survey, it was difficult to clearly identify these subgroups. Approximately 50 % of the patients had hyperglycemia before the diagnosis of HCC, whereas patients with hyperglycemia superimposed on cirrhosis were more likely to have hepatogenous hyperglycemia. Gentilini *et al*.[32] held that distinction as to either cirhhosis or diabetes occurring first did not substantially help classify patients. Carefully prospective studies are needed to answer this question.

Tumor stage was confirmed as an independent prognostic factor in our series. Patients who had non-T4 diseases survived significantly longer than those with T4 diseases. This is in agreement with a previous study[33], so we need to detect and treat liver cancer earlier[34,35]. Recently, many articles reported that combined TACE and radiotherapy might significantly increase survival rate[17,33,36].Cheng *et al*.[33]reported that the 2-year survival rate was 13 % and 55 % for patients treated with radiotherapy alone and with combined TACE and radiotherapy (P=0.0003), respectively. Our studies also confirmed this. We are currently using three dimensional conformal radiotherapy (3-DCRT) and applying the dose-volume model for every patient. With the advances in treatment planning, local radiotherapy can be more safely delivered and further studies are required to elucidate the efficacy of these regiments.

In summary, our data suggest that hyperglycemia does not significantly influence the long-term prognosis of patients who receive the proper non-surgical treatment. The T4 disease is associated with an unfavorable pognosis. Patients with Child-Pugh grade B or C have a higher risk. Further studies are needed to evaluate the impact of hyperglycemia on patients with HCC.

REFERENCES

1 **Chan AO**, Yuen MF, Hui CK, Tso WK, Lai CL. A prospective study regarding the complications of transcatheter intraarterial lipiodol chemoembolization in patients with hepatocellular carcinoma. *Cancer* 2002; **94**: 1747-1752

2 **Takano S**, Yokosuka O, Imazaki F, Tagawa M, Omata M. Incidence of hepatocellular carcinoma in chronic hepatitis B and C: A prospective study of 251 patients. *Hepatology* 1995; **21**: 650-655

3 **Hadziyannis S**, Tabor E, Kaklamani E, Tzonou A, Stuver S, Tassopoulos N, Mueller N, Trichopoulos D. A case-control study of hepatitis B and C virus infections in the etiology of hepatocellular carcinoma. *Int J Cancer* 1995; **60**: 627-631

4 **Kingston ME**, Ali MA, Atiyeh M, Donnelly RJ. Diabetes mellitus in chronic active hepatitis and cirrhosis. *Gastroenterology* 1984; **87**: 688-694

5 **Hadziyannis S**, Karamanos B. Diabetes mellitus and chronic hepatitis C virus infection. *Hepatology* 1999; **29**: 604-605

6 **Caronia S**, Taylor K, Pagliaro L, Carr C, Palazzo U, Petrik J, O'Rahilly S, Shore S, Tom BD, Alexander GJ. Further evidence for an association between non-insulin-dependent diabetes mellitus and chronic hepatitis C virus infection. *Hepatology* 1999; **30**: 1059-1063

7 **Petit JM**, Bour JB, Galland-Jos C, Minello A, Verges B, Guiguet M, Brun JM, Hillon P. Risk factors for diabetes mellitus and early insulin resistance in chronic hepatitis C. *J Hepatology* 2001; **35**: 279-283

8 **Nelson R**, Persky V, Davis F, Becker E. Excess risk of primary liver cancer in patients with diabetes mellitus. *J Natl Cancer Inst* 1997; **89**: 327-328

9 **Czyzyk A**, Szczepanik Z. Diabetes mellitus and cancer. *Eur J Intern Med* 2000; **11**: 245-252

10 **Petrides AS**, Vogt C, Schulze-Berge D, Matthews D, Strohmeyer G. Pathogenesis of glucose intolerance and diabetes mellitus in cirrhosis. *Hepatology* 1994; **19**: 616-627

11 **Fujino Y**, Mizoue T, Tokui N, Yoshimura T. Prospective study of

diabetes mellitus and liver cancer in Japan. *Diabetes Metab Res Rev* 2001; **17**: 374-379

12 **La Vecchia C**, Negri E, Franceschi S, D'Avanzo B, Boyle P. A case-control study of diabetes mellitus and cancer risk. *Br J Cancer* 1994; **70**: 950-953

13 **El-Serag HB**, Richardson PA, Everhart JE. The role of diabetes in hepatocellular carcinoma: a case-control study among United States Veterans. *Am J Gastroenterol* 2001; **96**: 2462-2467

14 **Ikeda Y**, Shimada M, Hasegawa H, Gion T, Kajiyama K, Shirabe K, Yanaga K, Takenaka K, Sugimachi K. Prognosis of hepatocellular carcinoma with diabetes mellitus after hepatic resection. *Hepatology* 1998; **27**: 1567-1571

15 **American Diabetes Association**. Report of the expert committee on the diagnosis and classification of diabetes mellitus. *Diabetes Care* 2003; **26**: S5-20

16 **Fajans SS**. Classification and diagnosis of diabetes. In: *Ellenberg and Rifkin's diabetes mellitus*. 5th .New York: *McGraw-Hill* 2000:369

17 **Guo WJ**, Yu EX. Evaluation of combined therapy with chemoembolization and irradiation for large hepatocellular carcinoma. *Br J Radiol* 2000; **73**: 1091-1097

18 **Marks JB**, Skyler JS. The liver and the endocrine system. In: *Schiff's diseaseas of the liver*. Vol 1. 8th. Philadelphia: *Lippincott-Raven* 1998: 479-481

19 **Holstein A**, Hinze S, Thiessen E, Plaschke A, Egberts EH. Clinical implications of hepatogenous diabetes in liver cirrhosis. *J Gastroenterol Hepatol* 2002; **17**: 677-681

20 **Yeh CN**, Chen MF, Lee WC, Jeng LB. Prognostic factors of hepatic resection for hepatocellular carcinoma with cirrhosis: univariate and multivariate analysis. *J Surg Oncol* 2001; **81**: 195-202

21 **Deans C**, Leslie P. Hepatocellular carcinoma. *Lancet* 1999; **354**: 253-254

22 **LaVecchia C**, Negri E, Decarli A, Franceschi S. Diabetes mellitus and the risk of primary liver cancer. *Int J Cancer* 1997; **73**: 204-207

23 **Braga C**, LaVecchia C, Negri E, Franceschi S. Attributable risks for hepatocellular carcinoma in northern Italy. *Eur J Cancer* 1997; **33**: 629-634

24 **Adami HO**, Chow WH, Nyren O, Berne C, Linet MS, Ekbom A, Wolk A, McLaughlin JK, Fraumeni JF Jr. Excess risk of primary liver cancer in patients with diabetes mellitus. *J Natl Cancer Inst* 1996; **88**: 1472-1477

25 **Wideroff L**, Gridley G, Mellemkjaer L, Chow WH, Linet M, Keehn S, Borch-Johnsen K, Olsen JH. Cancer incidence in a population-based cohort of patients hospitalized with diabetes mellitus in Denmark. *J Natl Cancer Inst* 1997; **89**: 1360-1365

26 **Yu MC**, Tong MJ, Govindarajan S, Henderson BE. Nonviral risk factors for hepatocellular carcinoma in a low-risk population, the non-Asians of Los Angeles County, California. *J Natl Cancer Inst* 1991; **83**: 1820-1826

27 **Chen MF**, Jeng LB, Lee WC. Surgical results in patients with hepatitis virus-related hepatocellular carcinoma in Taiwan. *World J Surg* 2002; **26**: 742-747

28 **Shimada M**, Takenaka K, Fujiwara Y, Gion T, Shirabe K, Yanaga K, Sugimachi K. Risk factors linked to postoperative morbidity in patients with hepatocellular carcinoma. *Br J Surg* 1998; **85**:195-198

29 **Poon RT**, Fan ST, Wong J. Does diabetes mellitus influence the perioperative outcome or long term prognosis after resection of hepatocellular carcinoma? *Am J Gastroenterol* 2002; **97**: 1480-1488

30 **Toyoda H**, Kumada T, Nakano S, Takeda I, Sugiyama K, Kiriyama S, Tanikawa M, Sone Y, Hisanaga Y. Impact of diabetes mellitus on the prognosis of patients with hepatocellular carcinoma. *Cancer* 2001; **91**: 957-963

31 **Nagasue N**, Yamanoi A, El-Assal ON, Ohmori H, Tachibana M, Kimoto T, Kohno H. Major compared with limited hepatic resection for hepatocellular carcinoma without underlying cirrhosis: A retrospective analysis. *Eur J Surg* 1999; **165**: 638-646

32 **Gentilini P**, Laffi G, La Villa G, Romanelli RG, Buzzelli G, Casini-Raggi V, Melani L, Mazzanti R, Riccardi D, Pinzani M, Zignego AL. Long course and prognostic factors of virus-induced cirrhosis of the liver. *Am J Gastroenterol* 1997; **92**: 66-72

33 **Cheng JC**, Chuang VP, Cheng SH, Huang AT, Lin YM, Cheng TI, Yang PS, You DL, Jian JJ, Tsai SY, Sung JL, Horng CF. Local radiotherapy with or without transcatheter arterial chemoembolization for patients with unresectable hepatocellular carcinoma. *Int J Radiat Oncol Biol Phys* 2000; **47**: 435-442

34 **Li L**, Wu PH, Mo YX, Lin HG, Zheng L, Li JQ, Lu LX, Ruan CM, Chen L. CT arterial portography and CT hepatic artetiography in detection of micro liver cancer. *World J Gastroenterol* 1999; **5**: 225-227

35 **Sithnamsuwan P**, Piratvisuth T, Tanomkiat W, Apakupakui N, Tongyoo S. Review of 336 patients with hepatocellular carcinoma at Songkianagarind hospital. *World J Gastroenterol* 2000; **6**: 339-343

36 **Chia-Hsien Cheng J**, Chuang VP, Cheng SH, Lin YM, Cheng TI, Yang PS, Jian JJ, You DL, Horng CF, Huang AT. Unresectable hepatocellular carcinoma treated with radiotherapy and/or chemoembolization. *Int J Cancer* 2001; **96**: 243-252

Edited by Su Q and Wang XL

P.O.Box 2345, Beijing 100023,China
Fax: +86-10-85381893
E-mail: wjg@wjgnet.com www.wjgnet.com

World J Gastroenterol 2003;9(8):1853-1855
World Journal of Gastroenterology
 ISSN 1007-9327

• BRIEF REPORTS •

Expression of class I MHC molecule, HSP70 and TAP in human hepatocellular carcinoma

Xiao-Ling Deng, Wei Chen, Mei-Ying Cai, Da-Peng Wei

Xiao-Ling Deng, Wei Chen, Mei-Ying Cai, Da-Peng Wei, Immunology Department, West China Medical Center of Sichuan University, Chengdu 610044, Sichuan Province, China
Supported by the National Natural Science Foundation of China, No. 30070855
Correspondence to: Da-Peng Wei, Immunology Department, West China Medical Center of Sichuan University, Chengdu 610044, Sichuan Province, China. dengxiaoling@163.com
Telephone: +86-28-85501259
Received: 2002-12-22 **Accepted:** 2003-01-18

Abstract

AIM: To demonstrate whether class I MHC molecule, transporter associated with antigen processing (TAP), and heat-shock proteion70 (HSP70) expressed in liver cancer cells before the design and construction of CTL vaccine against hepatocellular carcinoma (HCC).

METHODS: We studied 30 HCC specimens by labeled streptavidin biotin (LSAB) method of immunohistochemistry.

RESULTS: The results showed that the majority of HCC cells investigated naturally expressed class I MHC and TAP, which were different from other tumor cells. Furthermore, we found that HSP70 expressed not only in cellular cytoplasm, but also on the cell surface in HCC.

CONCLUSION: Our findings indicate that our understanding about immune escape mechanisms employed by HCC cells may be further improved. It is important to design and construct CTL vaccine against HCC.

Deng XL, Chen W, Cai MY, Wei DP. Expression of class I MHC molecule, HSP70 and TAP in human hepatocellular carcinoma. *World J Gastroenterol* 2003; 9(8): 1853-1855
http://www.wjgnet.com/1007-9327/9/1853.asp

INTRODUCTION

It is commonly accepted that tumor rejection is mediated by lymphocytes, and most notably, by cytotoxic T lymphocytes (CTL). The recognization of a tumor cell by CTL is regulated by interactions between T-cell receptor and antigenic peptide -MHC complex. TAP, HSP70 and class I MHC molecule are important components in endogenous processing of peptides through the MHC class I pathway. Among many proteins that contribute to MHC class I assembly, TAP complex is one of the most important components. It translocates endogenously processed peptides from cytosol into ER for binding to class I MHC, resulting in surface presentation of these complexes to CTL. Most of the studies described the defect of endogenous processing function in tumors such as melanomas, cervical carcinomas, and renal cell carcinomas[1-3]. These findings suggest that TAP down-regulation might represent an important mechanism for immune escape of malignant cells in tumors. Another importantly associated presentation protein is heat-shock proteion70 (HSP70). HSP70 has long been known to be located in the cytoplasm, where it performs chaperoning function. Recent studies have also indicated that conditional over-expression of HSP70 in target cells enhances the susceptibility to CTL[4]. Moreover, HSP70 may enhance TAP function[5]. Therefore, there is an increasing realization that expression of these molecules on tumor cell surface may potentially affect CTL-mediated recognition.

HCC is one of the most malignant cancers. However, to date most of the studies that described expressions of class I MHC, TAP, and HSP70 were carried out with cell lines[6]. Limited information is available about these molecules in HCC tumor tissues. Nevertheless, it is important to demonstrate whether these molecules can also be expressed in HCC *in vivo* before the design and construction of CTL vaccine against HCC.

MATERIALS AND METHODS

Human tissues

Thirty pathological samples were obtained from surgically resected tissues of HCC patients in West China Medical Center of Sichuan University. The specimens were frozen immediately in liquid nitrogen. Cryostat sections (4 μm) were prepared and stored at -70 ℃. Pathological diagnoses were made based on routinely processed HE sections.

Main reagents

Mouse anti-human HLA-ABC (DAKO Corp., working dilutions 1:100), rabbit anti-human TAP (Chemicon International, Inc., working dilutions 1:1 000), mouse anti-human HSP70 (DAKO Corp., working dilutions 1:50), biotin labeled goat anti-mouse IgG and goat anti-rabbit IgG, HRP-labeled streptavidin and avidin biotin blocking system were all purchased from Beijing Zhongshan Corp.

Immunohistochemistry

The frozen sections were fixed in cold acetone for 10 min. 3 % H_2O_2 containing methanol was added to block endogenous peroxidase. Fixed sections were incubated with normal goat serum for blocking and subsequently with mAb (HLA-ABC, TAP and HSP70 respectively) or PBS as control at 37 ℃ for 2 h, then washed with PBS. After incubation with biotin labeled goat anti-mouse IgG or goat anti-rabbit IgG for 30 min at 37 ℃, and washed as before, HRP-labeled streptavidin was added. The following incubation and washing were exactly the same as above. Finally, freshly prepared substrate DAB was added for color development. The reaction was stopped with tap water rinse and then counterstained with hematoxylin and mounted for examination.

RESULTS

Expression of class I MHC molecule

Strongly positive staining of class I MHC molecule was presented in all cases of HCC. The staining was mainly located

on the membrane of the liver cancer cells, in the cytoplasm, and the perinuclear area. The staining showed granular pattern (Figure 1).

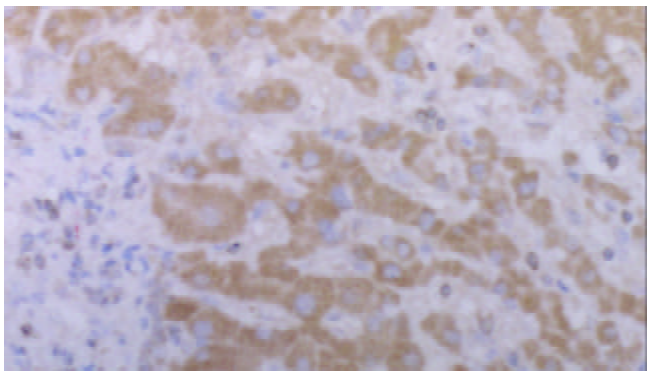

Figure 1 Displayed class I MHC molecule in hepatocellular carcinoma (×180).

The positive staining was mainly located on the membrane of the liver cancer cells. Some of the cells showed positive staining in the cytoplasm and the perinuclear area.

HSP70 expression

Tumor cells as well as adjacent non-neoplastic hepatocytes displayed intense and extensive positive staining. The staining was uniform throughout the specimen. The cytoplasmic staining showed granular pattern. The membranous staining displayed linear pattern, which made the interface between cells very clear (Figure 2).

Staining was typically uniform throughout the specimen. The cytoplasmic staining showed granular pattern. The membranous staining displayed linear pattern, which made the border between cells very clear.

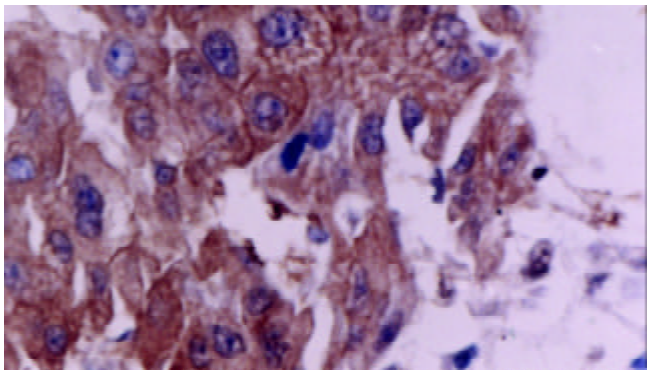

Figure 2 Hepatocellular carcinoma stained for HSP70 (×350).

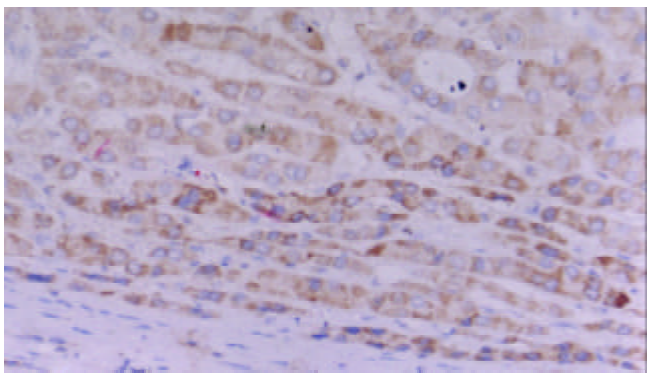

Figure 3 Hepatocellular carcinoma stained for TAP (×100).

TAP expression

Positive staining for TAP was present in 29 of 30 cases. The staining was located in the cytoplasm and the perinuclear area. It showed granular intracytoplasmic pattern accompanied by variable staining intensity. Faint or negative staining was observed within sinusoids (Figure 3).

It showed granular intracytoplasmic pattern accompanied by variable staining intensity. Hepatocytes beside the sinusoid were more intensely stained than cells in the central tissues.

DISCUSSION

In this study we examined the expressions of class I MHC, TAP, and HSP70 in 30 HCC samples by immunohistochemical methods. The results showed that the majority of HCC investigated naturally expressed TAP, which was different from other tumors. This is consistent with the results of several other groups. Kurokohchi *et al*[6] examined TAP mRNA and HLA antigen in seven HCC cell lines. They found that only one HCC cell line (HuH-7) had low expression of HLA-B and C and TAP mRNA. All the other lines expressed high levels of both TAP mRNA and HLA. They speculated posttranscriptional events or failure to transport and load peptides for MHC might allow HCC cells to escape from CTL. Whereas our results suggested HCC cells with the expression of TAP might be more susceptible to host immunity. Recently, Alimonti *et al*[7] reported that TAP expression provided a general method for improving the recognition of malignant cells. They transfected TAP gene into the TAP^- cell line and introduced it into tumor-burdened individuals. The result showed that TAP could improve tumor cell immunogenicity and host survival. This would be of a potential significance for the tumors with deficiency in components of antigen-processing molecules. However, Seliger *et al*[8,9] identified the structural alterations of TAP in the MHC class I antigen-processing pathway in melanoma after analyzing the sequence of TAP. The possibility of structural transformation of TAP in HCC cells could not be excluded and needs to be further studied.

As our understanding of the molecular aspects of the class I processing pathway has been improved, there is an increasing realization that expression of class I MHC antigen on cell surface is crucial for recognition by CTL. It is well established that many tumors escape T cell recognition by loss or down regulation of class I molecule expression on the surface of tumor cells. Previous reports described a correlation between HLA loss and TAP gene defects in some tumors[10]. So we also analyzed the expression of class I MHC on the surface of hepatocytes in HCC. Our investigation showed that most liver cancer cells in HCC tissues had strong class I MHC antigen expression. This is consistent with the results of several other groups[6,11]. The possible mechanism for the appearance of class I MHC antigen on hepatocytes remains controversial. One of the possibilities is that the expression of class I MHC antigen on HCC cells is related with viral infection. Sung *et al*[12] found that HCC patients were infected by HBV. Zhou *et al*[13] suggested cytokines such as γ-interferon released by T lymphocytes infiltrated in HCC tissues might be contributed to the expression of class I MHC molecules. The other possibility is that malignant transformation in HCC is characterized by expression of class I MHC molecules[11]. Although the underlying molecular mechanism is not well understood, the expression of class I MHC antigen on HCC cells may influence the behavior of tumor cells and has a significant effect on the reactivity of host immune system against HCC cells.

Earlier work suggested that HSP70 was shown to accumulate in the cytoplasm and the perinuclear area by cellular stress, such as non-lethal heat shock. In this study, we demonstrated

that HSP70 expressed not only in cytoplasm, but also on the surface of cells in HCC. Most members of the HSP families do not possess signal peptides. So it is still unclear how these proteins are transported to the cell membrane. Morimoto *et al*[14] postulated that some HSP might be transported to the cell surface via autoregulatory mechanism like in normal cells. Our results indicate that HSP70 may be transported to the cell surface after binding to MHC molecules. The main reason of this speculation is that class I MHC is found on the membrane of HCC cells. HSP70 is known to have strong protein-binding capacities. Therefore, it is reasonable to suggest that MHC class I may be the best candidate. It is interesting that cell-surface localization of HSP70 may make it possible to increase the immunogenicity of HCC cells. Many evidences have shown that HSPs expressing on affected cell types is recognized by the immune system[15]. Binder *et al*[16] recently identified HSP-chaperoned peptides introduced into cytosol were quite efficient as compared with free peptides. They even suggested that HSP70 was involved not only in the afferent end of this process by chaperoning partially or fully unfolded polypeptide chains, but also in chaperoning the resulting antigenic peptides to the TAP complex. These evidences indicate that HSP70 expressing on the surface of cells may be potentially promising target molecules for the immunotherapy of HCC.

On the whole, our data suggest that HCC cells express TAP, HSP70, and class I MHC. The results indicate that the mechanism of HCC cellular escape should be re-evaluated. Especially when designing immunotherapeutic strategies for HCC, it is very important to consider the potential problems associated with the ability of tumor cells to present target epitopes for immune recognition. Moreover, it needs to stress that tumor progression is dependent on multiple factors. Several scenarios have been proposed to be responsible for tumor immune-escape mechanisms, including production of suppressive cytokines by tumor cells, and expression of Fas ligand on tumor cells[17]. A recent study from Chai *et al*[18] suggested that T cell-expressed CD80 had a regulatory function and played a key role in the induction of T cell unresponsiveness by co-stimulation-deficient antigen presentation. So elucidation of the immune deficiency against cancer progression has been a difficult task because no single mechanism can explain the complicated cancer-host immune interactions. It is important to determine a more appropriate approach of combining different strategies to control the outgrowth of HCC cells.

REFERENCES

1 **Seliger B**, Ritz U, Abele R, Bock M, Tampe R, Sutter G, Drexler I, Huber C, Ferrone S. Immune escape of melanoma: first evidence of structural alterations in two distinct components of the MHC class I antigen processing pathway. *Cancer Res* 2001; **61:** 8647-8650

2 **Ritz U**, Momburg F, Pilch H, Huber C, Maeurer MJ, Seliger B. Deficient expression of components of the MHC class I antigen processing machinery in human cervical carcinoma. *Int J Oncol* 2001; **19**: 1211-1220

3 **Dovhey SE**, Ghosh NS, Wright KL. Loss of interferon-gamma inducibility of TAP1 and LMP2 in a renal cell carcinoma cell line. *Cancer Res* 2000; **60**: 5789-5796

4 **Dressel R**, Lubbers M, Walter L, Herr W, Gunther E. Enhanced susceptibility to cytotoxic T lymphocytes without increase of MHC class. I antigen expression after conditional overexpression of heat shock protein 70 in target cells. *Eur J Immunol* 1999; **29:** 3925-3935

5 **Chen D**, Androlewicz MJ. Heat shock protein 70 moderately enhances peptide binding and transport by the transporter associated with antigen processing. *Immunol Lett* 2001; **75:** 143-148

6 **Kurokohchi K**, Carrington M, Mann DL, Simonis TB, Alexander-Miller MA, Feinstone SM, Akatsuka T, Berzofsky JA. Expression of HLA class I molecules and the transporter associated with antigen processing in hepatocellular carcinoma. *Hepatology* 1996; **23:** 1181-1188

7 **Alimonti J**, Zhang QJ, Gabathuler R, Reid G, Chen SS, Jefferies WA. TAP expression provides a general method for improving the recognition of malignant cells *in vivo*. *Nat Biotechnol* 2000; **18:** 515-520

8 **Seliger B**, Ritz U, Abele R, Bock M, Tampe R, Sutter G, Drexler I, Huber C, Ferrone S.Immune escape of melanoma: first evidence of structural alterations in two distinct components of the MHC class I antigen processing pathway. *Cancer Res* 2001; **61:** 8647-8650

9 **Seliger B**, Bock M, Ritz U, Huber C. High frequency of a non-functional TAP1/LMP2 promoter polymorphism in human tumors. *Int J Oncol* 2002; **20:** 349-353

10 **Cromme FV**, Airey J, Heemels MT, Ploegh HL, Keating PJ, Stern PL, Meijer CJ, Walboomers JM. Loss of transporter protein, encoded by the TAP-1 gene, is highly correlated with loss of HLA expression in cervical carcinomas. *J Exp Med* 1994; **179:** 335-340

11 **Paterson AC**, Sciot R, Kew MC, Callea F, Dusheiko GM, Desmet VJ. HLA expression in human hepatocellular carcinoma. *Br J Cancer* 1988; **57:** 369-373

12 **Sung CH**, Hu CP, Hsu HC, Ng AK, Chou CK, Ting LP, Su TS, Han SH, Chang CM. Expression of class I and class II major histocompatibility antigens on human hepatocellular carcinoma. *J Clin Invest* 1989; **83:** 421-429

13 **Zhou DX**, Taraboulos A, Ou JH, Yen TS. Activation of class I major histocompatibility complex gene expression by hepatitis B virus. *J Virol* 1990; **64:** 4025-4028

14 **Morimoto RI**. Cells in stress: transcriptional activation of heat shock genes. *Science* 1993; **259:** 1409-1410

15 **Schueller G**, Paolini P, Friedl J, Stift A, Dubsky P, Bachleitner-Hofmann T, Jakesz R, Gnant M. Heat treatment of hepatocellular carcinoma cells: increased levels of heat shock proteins 70 and 90 correlate with cellular necrosis. *Anticancer Res* 2001; **21:** 295-300

16 **Binder RJ**, Blachere NE, Srivastava PK. Heat shock protein-chaperoned peptides but not free peptides introduced into the cytosol are presented efficiently by major histocompatibility complex I molecules. *J Biol Chem* 2001; **276:** 17163-17171

17 **Restifo NP**. Not so Fas: Re-evaluating the mechanisms of immune privilege and tumor escape. *Nat Med* 2000; **6:** 493-495

18 **Chai JG**, Vendetti S, Amofah E, Dyson J, Lechler R. CD152 ligation by CD80 on T cells is required for the induction of unresponsiveness by costimulation- deficient antigen presentation. *J Immunol* 2000; **65:** 3037-3042

Edited by Xu JY and Wang XL

P.O.Box 2345, Beijing 100023,China
Fax: +86-10-85381893
E-mail: wjg@wjgnet.com www.wjgnet.com

World J Gastroenterol 2003;9(8):1856-1858
World Journal of Gastroenterology
 ISSN 1007-9327

• BRIEF REPORTS •

Diagnosis and treatment of hepatic angiomyolipoma in 26 cases

Ning Ren, Lun-Xiu Qin, Zhao-You Tang, Zhi-Quan Wu, Jia Fan

Ning Ren, Lun-Xiu Qin, Zhao-You Tang, Zhi-Quan Wu, Jia Fan, Liver Cancer Institute and Zhongshan Hospital, Fudan University, Shanghai 200032, China
Correspondence to: Ning Ren, Liver Cancer Institute and Zhongshan Hospital, Fudan University, Shanghai 200032, China. ningren@zshospital.com
Telephone: +86-21-64041990-3078 **Fax:** +86-21-64037181
Received: 2003-03-12 **Accepted:** 2003-04-11

Abstract

AIM: To summarize the experience of the diagnosis and treatment of hepatic angiomyolipoma (HAML).

METHODS: The clinical, imaging and pathological features, and treatment strategies of 26 patients with HAML treated at the authors' institute between October 1998 and January 2003 were retrospectively analyzed. All the patients received liver resection and were followed up till the study. Immunohistochemical assays were performed with a panel of antibodies.

RESULTS: There was an obvious female predominance (21:5), and most of the patients (18/26) had no symptoms. Heterogeneous high echo was found in ultrasonography and punctiform or filiform vascular distribution pattern was found in color Doppler-sonography in most of the lesions (21/26). All of the 5 lesions further enhanced with Levovist showed early and prolonged enhancement. At contrast-enhanced spiral CT, the soft-tissue components of 24 lesions were markedly enhanced in the arterial phase and 18 lesions remained enhanced in the portal venous phase. MRI was performed in 9 patients, and showed hypointensity or hyperintensity on T1-weighted images and heterogeneous hyperintensity on T2-weighted images. Histopathologically, all lesions were composed of adipose tissues, smooth muscle and blood vessels with different proportions. Most lesions showed positive immunohistochemical staining for HMB45 (26/26), A103 (24/26) and SMA (24/26). All of the 26 patients showed a benign course with no sign of recurrence.

CONCLUSION: Preoperative radiological diagnosis of HAML is possible. The demonstration of intratumoral fat and central vessels is helpful in the diagnosis. HMB45, A103 and SMA are promising markers for pathologic diagnosis of HAML, and surgical resection is effective for the treatment of HAML.

Ren N, Qin LX, Tang ZY, Wu ZQ, Fan J. Diagnosis and treatment of hepatic angiomyolipoma in 26 cases. *World J Gastroenterol* 2003; 9(8): 1856-1858
http://www.wjgnet.com/1007-9327/9/1856.asp

INTRODUCTION

Hepatic angiomyolipoma (HAML) is a rare benign mesenchymal neoplasm of the liver. Since its first description by Ishak in 1976[1], not more than 200 cases have been reported in the English literatures[2-7]. However, with recent progress in imaging diagnostic techniques, the reported cases of HAML are increasing in number, and the significance of accurate diagnosis is becoming more important clinically. The purpose of this study was to investigate the clinical, imaging and pathological features of HAML and to summarize our experience in the diagnosis and treatment of this disease.

MATERIALS AND METHODS

Patients and clinical data

Twenty-six patients with HAML were surgically treated in Liver Cancer Institute of Fudan University from October 1998 to January 2003. There was a marked female predominance (21/26) and the mean age was 44.3 with a range of 31 to 64 years. Most of the patients (18/26) had no symptoms and were detected incidentally by medical check-up. Seven of 26 patients had symptoms caused by tumor oppression and one patient had slight fever as a chief complaint. The average tumor size at detection was 6.1 cm ranging from 1.5 to 15 cm. None of them was found complicated with a diagnosis of tuberous sclerosis and renal AML. Concomitant hepatic hemangioma was found in one patient. None of them had the history of hepatitis virus infection. Serum alpha-fetoprotein (AFP) levels were all within normal limits.

Imaging examinations

All of the patients underwent ultrasonography, color Doppler-sonography and computer tomography (CT) examinations. Nine patients also received magnetic resonance imaging (MRI) examination.

Treatment and follow-up

Limited partial liver resections were performed in 19 patients, left lateral lobectomy in 4, left hemihepatectomy in 2, and right hemihepatectomy in 1. All the patients have been followed up till the study.

Pathological and immunochemical assays

Routine histopathological examination with hematoxylin and eosin staining was performed. Immunohistochemical studies were performed by the EnVision™ method using a panel of antibodies (HMB45, A103, smoothmuscle actin, S100, Vimentin and CK8) in all of the tumor tissues.

RESULTS

Imaging features

Most lesions (21/26) showed heterogeneous high echo in ultrasonography, and punctiform or filiform vascular distribution pattern in color Doppler-sonography. Five lesions were further enhanced with Levovist, and all of them were found to have early and prolonged enhancement.

In contrast-enhanced spiral CT examination, the soft-tissue components of 24 lesions were markedly enhanced in the arterial phase, and 18 lesions remained enhanced in the portal venous phase.

MRI was performed in 9 patients, hypointensity or hyperintensity was found on T1-weighted images and heterogeneous hyperintensity on T2-weighted images.

Histopathological and immunochemical characteristics

The tumors were well circumscribed but no obvious capsule could be found. The non-tumorous liver parenchyma was normal, and no cirrhosis was found. All tumors were composed of adipose tissues, smooth muscle and blood vessels in different proportions. In immunohistochemical studies, most tumors were positive for HMB45 (26/26), A103 (24/26), SMA (24/26), S100 (20/26) and Vimentin (16/26), but negative for CK8 (22/26).

Treatment and prognosis

All of the 26 patients received hepatectomy. Six patients were followed-up for more than one year and finally decided to receive operation because of the enlargement of the lesions. All the patients have been followed up since their surgical resection. No recurrence was found in any patient during the follow-up period.

DISCUSSION

Angiomyolipoma, which occurs relatively frequent in kidney, is a rare benign mesenchymal neoplasm of the liver. The tumor size of HAML at the first diagnosis is variable, ranging from 0.1 cm to ⩾36 cm. Clinically, most of the patients have no symptoms and are detected incidentally by medical check-ups. Patients with large tumors usually have some symptoms caused by tumor compression. The diagnosis of HAML before operation mainly depends on imaging examination.

According to our experience, typical performance of HAML is a smoothly contoured heterogeneous high echo lesion, with a well-defined border separating it from adjacent normal hepatic tissues by ultrasonography and punctiform or filiform vascular distribution pattern by color Doppler-sonography. In further enhanced imaging with Levovist, the tumor showed early and prolonged enhancement. The lesions appeared as hypodense, and adipose dense could be found in pre-contrast CT scans. In the arterial phase, the soft-tissue components of the lesions were markedly enhanced and central vessels could be found. In the portal venous phase, the lesions remained in enhancement[8]. As reported, the adipose fraction of HAML varied from 5 % to 90 %, so adipose signals could be found on MRI in most lesions. Sakamoto *et al*.[9] described MRI studies showing extensive enhancement on gadolinium-enhanced images. In addition, fat could be seen with great sensitivity on T1-weighted images as high-signal intensity. However, HAML showed various patterns of imaging features, because the relative proportions of vessels, muscle and fat varied widely from tumor to tumor. So, although diagnosis may be suggested by imaging methods, histological confirmation remains mandatory.

Histopathologically, in our study, most tumors were well-circumscribed, but not encapsulated. The lesions were composed of adipose tissue, smooth muscle and blood vessels in different proportions. The tissue components in the tumor were highly variable from case to case, and even between different areas of the same mass. According to the line of differentiation and predominance of tissue components, Tsui *et al*.[6] subcategorized the tumors into mixed, lipomatous (⩾ 70 % fat), myomatous (⩽ 10 % fat), and angiomatous types. We found that the mixed type was the most common category which comprised sheets of epithelioid muscle cells admixed with islands of adipocytes, abnormal vessels, and frequently, hematopoietic cells. Some authors advocated to diagnose HAML by fine-needle aspiration (FNA)[10], for the presence of adipocytes was a clue to the diagnosis. However, adipose tissue might be a minute fraction of HAML, in which FNA diagnosis may be difficult. So we think that immunohistochemical examination may be the only authoritative method to diagnose HAML. According to our results, all the 26 tumors were positive for HMB45, the staining was intense, granular, and concentrated in tumor cell perinuclear cytoplasm. For A103, 24 tumors showed strongly and diffusely granular cytoplasmic staining in the majority of myoid cells, the staining in the other two was only focal. Smooth muscle actin (SMA) staining was weak to moderate in epithelioid cells and strong in spindle cells in 24 tumors. So HMB45, A103 and SMA are promising markers in pathologic diagnosis of HAML.

Exclusion of hepatocellular carcinoma (HCC) is the most important issue in the diagnosis of HAML, because both kinds of the lesions show similar imaging characteristics, including rich blood flow detected in Doppler-sonography, early enhancement in CT contrast scan, etc. Most of the patients with HAML had no histories of hepatitis virus infection or negative for hepatitis marker, and had no liver cirrhosis, and AFP level was normal, which might be helpful in the differential diagnosis. In CT contrast scan, there are also differences in the peak time and duration of enhancement between HAML and HCC. Ahmadi *et al*.[11] reported that HAML showed early and prolonged enhancement (>4 min) with delayed peak enhancement at 40-80 seconds, as opposed to HCC which had peak enhancement at 10 seconds and absent or minimally delayed enhancement. Further more, differentiation from HCC with fatty metamorphosis can also be made based on the angiomyolipomas prolonged tumor enhancement (>6 min) relative to HCC. Fat suppression MRI was also reported to be successful in distinguishing HAML from HCC[12].

HAML is a benign lesion and often grows slowly without any clinical symptom, so conservative treatment with close follow-up is recommended after diagnosis. For the rarity of the cases most of which are diagnosed by pathology after operation, there has been no report about culture doubling time or growth velocity of HAML yet. In this series, one patient was followed up for five years before operation, the tumor increased from 4 cm to 10 cm in size. Another one was followed up for thirteen years before operation, the size of tumor increased from 1.5 cm to 5 cm.

Spontaneous rupture, later recurrence and vascular invasion of HAML have been reported[13-15]. So surgery may be recommended for patients with symptoms, for patients in whom diagnostic imaging can not exclude malignancy, and for patients in whom the tumor enlarges obviously in short time or shows extrahepatic growth and has a risk of spontaneous rupture. All our cases received hepatectomy and have been followed up till the study for a period between 1 month and 52 months, no mortality and serious morbidity were found in these patients. Follow-up information of the 26 cases showed a benign course with no signs of recurrences. So surgical resection is safe and effective for the treatment of HAML.

REFERENCES

1 **Bakhotmah MA**, Yamasaki S. Hepatic angiomyolipoma. *HPB Surg* 1994; **8**: 133-137
2 **Ji Y**, Zhu X, Xu J, Zhou J, Tan Y, Wang J, Fan J, Zhou Y. Hepatic angiomyolipoma: a clinicopathologic study of 10 cases. *Chin Med J* 2001; **114**: 280-285
3 **Yeh CN**, Chen MF, Hung CF, Chen TC, Chao TC. Angiomyolipoma of the liver. *J Surg Oncol* 2001; **77**: 195-200
4 **Barnard M**, Lajoie G. Angiomyolipoma: immunohistochemical and ultrastructural study of 14 cases. *Ultrastruct Pathol* 2001; **25**: 21-29
5 **Sajima** S, Kinoshita H, Okuda K, Saito N, Hashino K, Sugimoto R, Eriguchi N, Aoyagi S. Angiomyolipoma of the liver-a case report and review of 48 cases reported in Japan. *Kurume Med J* 1999; **46**: 127-131
6 **Tsui WM**, Colombari R, Portmann BC, Bonetti F, Thung SN,

Ferrell LD, Nakanuma Y, Snover DC, Bioulac-Sage P, Dhillon AP. Hepatic angiomyolipoma: a clinicopathologic study of 30 cases and delineation of unusual morphologic variants. *Am J Surg Pathol* 1999; **23**: 34-48

7 **Nonomura A**, Mizukami Y, Kadoya M. Angiomyolipoma of the liver: a collective review. *J Gastroenterol* 1994; **29**: 95-105

8 **Yan F**, Zeng M, Zhou K, Shi W, Zheng W, Da R, Fan J, Ji Y. Hepatic angiomyolipoma: various appearances on two-phase contrast scanning of spiral CT. *Eur J Radiol* 2002; **41**: 12-18

9 **Sakamoto Y**, Inoue K, Ohtomo K, Mori M, Makuuchi M. Magnetic resonance imaging of an angiomyolipoma of the liver. *Abdom Imaging* 1998; **23**: 158-160

10 **Messiaen T,** Lefebvre C, Van Beers B, Sempoux C, Cosyns JP, Geubel A. Hepatic angiomyo(myelo)lipoma: difficulties in radiological diagnosis and interest of fine needle aspiration biopsy. *Liver* 1996; **16**: 338-341

11 **Ahmadi T**, Itai Y, Takahashi M, Onaya H, Kobayashi T, Tanaka YO, Matsuzaki Y, Tanaka N, Okada Y. Angiomyolipoma of the liver: significance of CT and MR dynamic study. *Abdom Imaging* 1998; **23**: 520-526

12 **Hooper LD**, Mergo PJ, Ros PR. Multiple hepatorenal angiomyolipomas: diagnosis with fat suppression, gadolinium-enhanced MRI. *Abdom Imaging* 1994; **19**: 549-551

13 **Guidi G**, Catalano O, Rotondo A. Spontaneous rupture of a hepatic angiomyolipoma: CT findings and literature review. *Eur Radiol* 1997; **7**: 335-337

14 **Croquet V**, Pilette C, Aube C, Bouju B, Oberti F, Cervi C, Arnaud JP, Rousselet MC, Boyer J, Cales P. Late recurrence of a hepatic angiomyolipoma. *Eur J Gastroenterol Hepatol* 2000; **12**: 579-582

15 **Dalle I**, Sciot R, de Vos R, Aerts R, van Damme B, Desmet V, Roskams T. Malignant angiomyolipoma of the liver: a hitherto unreported variant. *Histopathology* 2000; **36**: 443-450

Edited by Ma JY

P.O.Box 2345, Beijing 100023,China
Fax: +86-10-85381893
E-mail: wjg@wjgnet.com www.wjgnet.com

World J Gastroenterol 2003;9(8):1859-1862
World Journal of Gastroenterology
 ISSN 1007-9327

• BRIEF REPORTS •

Expression of telomerase activity and oxidative stress in human hepatocellular carcinoma with cirrhosis

Dao-Yong Liu, Zhi-Hai Peng, Guo-Qiang Qiu, Chong-Zhi Zhou

Dao-Yong Liu, Department of General Surgery, Shanghai No.5 People' s Hospital, Shanghai 200240, China
Zhi-Hai Peng, Guo-Qiang Qiu, Chong-Zhi Zhou, Department of General Surgery, Shanghai First People' s Hospital, Shanghai 200080, China
Supported by Science and Technology Foundation of Shanghai, No. 984119001
Correspondence to: Dr. Zhi-Hai Peng, Department of General Surgery, Shanghai First People' s Hospital, 85 Wujin Road, Shanghai 200080, China. pengpzhb@online.sh.cn
Received: 2003-03-04 **Accepted:** 2003-05-11

Abstract

AIM: To study the expression and significance of telomerase activity and oxidative stress in hepatocellular carcinoma (HCC) with cirrhosis.

METHODS: In this study, TRAP-ELISA assay was used to determine telomerase activity in 21 cases of HCC as well as in 23 cases of hepatic cirrhosis. Malondialdehyde (MDA), glutathione S-transferase (GST) and total anti-oxidative capacity (T-AOC) were also examined in the same samples with human MDA, GST and T-AOC kits.

RESULTS: Eighteen of 21 cases of HCC were found to have increased telomerase activity, whereas only three of the 23 non-cancerous cirrhotic samples were found to have weak telomerase activity, and the difference was significant ($P<0.001$). No significant difference in telomerase activity was detected according to different tumor size, tumor stage, histological grade, HBsAg, contents of albumin, bilirubin, ALT, AFP, r-GT and platelet. There were significant differences between HCC and cirrhosis in the expression of MDA, GST and T-AOC respectively. Telomerase activity correlated positively with the content of MDA ($P<0.05$).

CONCLUSION: Telomerase activation is the early event of carcinogenesis, which is not correlated with clinicopathological factors of HCC. The dysfunction of the anti-oxidative system is closely correlated with the progression from cirrhosis to hepatocellular carcinoma. Oxidative stress may contribute partly to telomerase activation.

Liu DY, Peng ZH, Qiu GQ, Zhou CZ. Expression of telomerase activity and oxidative stress in human hepatocellular carcinoma with cirrhosis. *World J Gastroenterol* 2003; 9(8): 1859-1862
http://www.wjgnet.com/1007-9327/9/1859.asp

INTRODUCTION

Telomeres correspond to the ends of eukaryotic chromosomes and are specialized structures containing unique (TTAGGG)n repeats[1]. Telomeres protect the chromosomes from DNA degradation, end to end fusions, rearrangements, and chromosome loss[2]. Because cellular DNA polymerases cannot replicate the 5' end of the linear DNA molecule, the number of telomere repeats decreases (by 50-200 nucleotides/cell division) during aging of normal somatic cells. Shortening of telomeres may control the proliferative capacity of normal cells[3]. Telomerase, a ribonucleicacid-protein complex, adds hexameric repeats of 5'-TTAGGG-3' to the end of telomeres to compensate for the progressive loss[4]. Although normal somatic cells do not express telomerase, immortalized cells such as tumor cells express this enzyme[5]. More recently, HeLa cells transfected with an antisense human telomerase were found to lose telomeric DNA and to die after 23 to 26 doublings[6]. Pertersen *et al*. found that the rate of shortening of telomere restriction fragments in human fibroblasts could be accelerated significantly by oxidative stress[7]. Importantly, after treatment of cells with short single stranded telomeric G-rich DNA fragments, glioblastoma cells recovered from the arrest and showed enhanced telomerase activity and elongated telomeres[8].

However, the mechanisms of activation and regulation of telomerase have not been establishednd. Cell line data indicate that a telomere length-dependent mechanism is the major pathway. On the other hand, normal lymphocytes up-regulate telomerase activity upon antigen and mitogen stimulation *in vitro* and *in vivo*. This indicates that telomere length-dependent mechanisms may be important or specific to different cell types for regulation of telomerase activation[9]. Only a few studies have specifically examined the relationship between telomerase activity in tumors and the status of oxidative stress. Our data implied that genetic defects in HCC facilitated the reactivation of telomerase activity, a process that might be associated with the increased expression of oxidative stress.

MATERIALS AND METHODS

Sample collection and processing

All 21 HCC specimens were sampled from patients who had undergone curative hepatectomy. Patients who had received radiotherapy or chemotherapy before operation were excluded. Liver cirrhosis tissues were obtained from those who had received hepatic biopsy in the operation for hypersplenia. Informed consent was obtained from all patients for subsequent use of their resected tissues. These specimens were immediately dissected into small pieces under aseptic condition within half an hour after removed, snap frozen in liquid nitrogen and stored at -80 ℃ until extracts for telomerase activity analysis and determination of oxidative stress.

Telomerase assay

Frozen tissue samples (100 μg) were homogenized in 500 μL of freshly made ice-cold lysis buffer. After 30 min incubation on ice, the lysate was centrifuged for 20 min at 16 000 g, and the supernatant was transferred to fresh tubes and used as tissue extracts for the telomerase assay. The protein concentrations were determined. Telomerase activity was assayed by the TRAP-ELISA kit, a polymerase chain reaction (PCR)-based on an improved version of the original method described by Kim *et al*[10]. In brief, aliquots of tissue extract containing 40 μg protein were added to 50 μL reaction mixtures containing

0.1 μg substrate oligonucleotide (TS) primer, TSK (internal control) template. The reaction mixtures were incubated at 25 ℃ for 20 min and then amplified for 33 cycles of PCR at 94 ℃ for 30 s, at 50 ℃ for 30 s, and at 72 ℃ for 90 s, then preserved at 4 ℃ for ELISA reaction process. 5 μg PCR product was taken for ELISA reaction. The value at A450 was read within 30 min. Telomerase activity equaled A450 for experimental well minus A450 for control well. The strength of telomerase activity was defined as follows: ++, >0.4; +, >0.2; -, <0.2.

MDA, GST and T-AOC determination

Frozen tissue samples (100 mg) were homogenized in 1.0 mL, the homogenized samples were centrifuged for 15 min at 3 000 r/min, and the supernatant was transferred to fresh tubes. After the protein concentrations were determined, MDA, GST and T-AOC were assayed with human MDA, GST and T-AOC kit (Jiancheng Biological Technical Institute, Nanjing, China).

Statistics analysis

Contingency table methods were used to analyze the univariate association between telomerase activity and clinicopathological data (age, sex, tumor grade, tumor size, and liver status). Significance was confirmed by Fisher's exact test. The association between telomerase activity and oxidative stress was investigated by Pearson correlation analysis test. All calculations were performed using the SPSS version 10.0 statistical software package, and the results were considered statistically significant at $P<0.05$.

RESULTS

Telomerase activity in HCC and hepatic cirrhosis

Telomerase positive cells were used as a positive control for assessing telomerase activity in clinical specimens. We measured telomerase activity in surgically resected specimens from 21 cases of HCC and 23 cases of liver cirrhotic tissue. Telomerase activity was detected in 18 of the 21 HCC specimens (85.7 %), but it was detected only in 3 of 23 samples of liver cirrhosis (13.4 %). There was a significant difference in telomerase activity between HCC and hepatic cirrhosis ($P<0.001$). There was no significant difference in telomerase activity in regard to different tumor size, tumor stage, histological grade, HBsAg, contents of albumin, bilirubin, ALT, AFP, r-GT and platelet (Table 1).

Table 1 Relationship between telomerase activity and clinicopathologic factors in HCC

	Telomerase activity		
	High	Low or loss	*P* value
Tumor size (cm)	7.7±3.5	7.1±3.6	0.664
Tumor grade (high / low)	9 / 4	4 / 4	0.245
Tumor stage (early / advanced)	6 / 7	3 / 5	0.327
ALT (normal / abnormal)	9 / 2	6 / 4	0.212
Bilirubin (normal / elevated)	9 / 2	9 / 1	0.414
Platelet (normal / decreased)	9 / 2	7 / 3	0.324
HbsAg (positive / negetive)	6 / 5	7 / 3	0.272
AFP (>400U / <400U)	7 / 5	5 / 5	0.309
Albumin (g / L)	39.2±5.6	39.3±4.2	0.946
Globulin (g / L)	28.6±5.3	26.8±6.5	0.423
γ-GT(U)	115.2±98.7	108.9±69.5	0.814

Expression of MDA, GST and T-AOC in HCC and hepatic cirrhosis

The content of MDA was 84.76±26.98 nM/ml in HCC, while it was 49.49±23.03 nM/ml in hepatic cirrhosis, and the difference was significant between them ($P<0.001$). Nevertheless, the contents of GST and T-AOC were lower in HCC than those in hepatic cirrhosis ($P<0.001$).

Table 2 Expression of MDA, GST and T-AOC ($\bar{x}\pm s$)

	HCC	Cirrhosis	*P* value
MDA (nM / ml)	84.76±26.98	49.49±23.03	<0.001
GST (U / mg)	8.18±5.59	18.70±5.20	<0.001
T-AOC (U / mg)	0.257±0.241	0.689±0.302	<0.001

Telomerase activity and content of MDA

The relationship between telomerase activity and oxidative stress was investigated by Pearson correlation analysis. Tumor specimes with a higher level of MDA expressed increased telomerase activity ($r=0.496$, $P<0.05$).

DISCUSSION

HCC is the most common solid tumor worldwide, being responsible for more than 1 million deaths annually, especially in Eastern Asia and South Africa[11], which ranks eighth in frequency among cancers in the world[12]. It is one of the few human cancers in which an underlying etiology can be identified in most cases, and has a background of chronic inflammatory liver disease caused by viral infection that induces cirrhosis[13]. However, it is not clear how these disorder results in HCC. The reactivation of telomerase activity may play a significant role in hepatocarcinogenesis.

Telomerase is a ribonucleoprotein complex[14] that is thought to add telomeric repeats onto the ends of chromosomes during the replicative phase of the cell cycle. Telomeres have classically been regarded as a simple linear structure, possibly capped by specific proteins. However, this simple structural view was challenged. Recent data have shown that the structure of human telomeres might be more complicated than originally thought[15]. Three different mechanisms were currently thought to contribute to telomere shortening: the so-called end replication problem, the C-strand degradation model and single-strand damage[16]. Both the end replication problem and the C-strand degradation model of telomere shortening do not take into account the possibility that the shortening rate of telomeres depends on external influences, especially oxidative stress-dependent DNA damage. von Zglonicki *et al* demonstrated that the telomere shortening rate could be either accelerated or decelerated by a modification of the amount of oxidative stress[17].

Recently, a highly sensitive PCR based TRAP assay for measuring telomerase activity that also includes an improved method of detergent lysis has been developed[10]. This assay allows more uniform extraction of telomerase from a small number of cells than conventional techniques, in which telomerase first synthesizes extension products that then serve as templates for PCR amplification. The simplicity and increased sensitivity of this assay have resulted in a dramatic increase in the investigation of telomerase expression. In this study, telomerase activity was positive in 18 of 21 HCC specimens (85.7 %), which suggested that telomerase activation was a universal event in human hepatocellular carcinoma. However, undetectable telomerase activity has been reported by others in about 10 % of tumors samples[18,19]. Some immortal cell lines without detectable telomerase activity have been described that were characterized by long and heterogenous telomeres[20,21]. These observations might indicate the presence of a telomerase-independent mechanism for telomere length maintenance in these tumors.

It is well documented that telomerase activity is detectable in the majority of cancers but rarely in normal somatic tissue. Some studies have demonstrated that some types of somatic cells express low levels of telomerase activity[22-24]. In particular physiologically regenerating somatic cells, such as hematopoietic cells, epithelial cells of skin or intestine, and endometrial cells, have been shown low levels of telomerase activity. In this study, low telomerase activity was detected in 3 of 23 cirrhotic specimens. One possible explanation for this finding was that these cirrhotic tissue samples may also contained probable cancer cell, infiltration of lymphoid cells, or dysplasia cells. Finally, demographic and clinical information of patients, such as tumor size, tumor stage, histological grade, HBsAg, albumin, bilirubin, ALT, AFP, r-GT and platelet were not correlated with the telomerase activity.

Many lines of evidence indicate that telomerase is reversibly regulated[25]. Resting lymphocytes express little telomerase activity, but stimulation of specific antigen receptors on the cell plasma membrane markedly increases telomerase activity[26-29]. High-level sun light exposure of normal human skins results in an increased incidence of telomerase activation[30]. Human hematopoietic cells with γ-rays[31], or human carcinoma cell lines with X-rays[32] induce the activation of telomerase. Activated telomerase in cancer cells is repressed when the cells leaves the cell cycle and become quiescent[33-37]. Nevertheless, the mechanisms of telomerase regulation, such as its suppression in normal human somatic cells and activation in neoplastic cells, are far from established.

Telomeres are believed to protect the ends of chromosomes against exonuclease and ligases, to prevent the activation of DNA-damage checkpoints, and to counteract loss of terminal DNA-segments that occurs when linear DNA is replicated[2,38,39]. Oikawa *et al* demonstrated that oxidative stress induced DNA damage at the 5' site of 5' -GGG-3' in the telomere sequence, and the telomeric G triplet was especially sensitive to cleavage by oxidative damage[40,41]. Moreover, it was shown that oxidative stress increased the frequency of S1 nuclease-sensitive sites, especially in telomeres[42,43]. However, it was unknown whether oxidative stress was associated with the telomerase activity in human tissue specimens. In this study, the expression of malondialdehyde, glutathione S-transferase and total anti-oxidative capacity were examined in the same samples. There were higher levels of the expression of glutathione S-transferase and total anti-oxidative capacity in hepatic cirrhosis specimens, while enhanced expression of malondialdehyde was found in HCC specimens. The difference between HCC and hepatic cirrhosis was significant (P<0.05). These findings suggested that the dysfunction of the anti-oxidative system was closely correlated with the progression from hepatic cirrhosis to hepatocellular carcinoma. Other studies also showed that HCC patients with higher anti-oxidative capacity levels survived longer after hepatectomy[44].

Henle *et al*. found that the telomeric G triplet was especially sensitive to cleavage by oxidative damage. In MRC-5 fibroblasts and U87 glioblastoma cells, oxidative stress-mediated production of single-strand damage in telomeres was concomitant to cell cycle arrest. This response can be modeled by treatment of cells with short single stranded telomeric G-rich DNA fragments. Recovery from it is accompanied by up-regulation of telomerase activity and elongation of telomeres[45]. The gene transcription of TERT is an essential rate-limiting step in telomerase activation and may be subjected to multiple levels of control and regulated by different factors in different cellular contexts[46]. In the present study we found that telomerase activity correlated positively with the content of MDA (P<0.05). One possible explanation for this observation was that telomere shortening might be accelerated by oxidative stress when telomere reached critical length, which caused the gene transcription of TERT, and telomerase was activated. Buchkovich *et al*[47] first demonstrated that in primary human leukocytes stimulated with phytohemagglutinin, telomerase activity was increased by more than 10-fold as naturally quiescent cells entered the cell cycle. In an animal model, treatment with an antagonist of growth hormone-releasing hormone dramatically decreased telomerase activity in xenografted U-87-MG human glioblastoma cells[46]. Their research was the first demonstration of a signaling pathway in normal cells that regulated telomerase, and paved the way for experimental analysis of "upstream" regulators. The possibility of a relationship between upstream regulators and oxidative stress is an important issue for future experimental studies on control of telomerase activity.

Although tumor cells have a much shorter telomere length, telomeres shorten with rates between 15 and 76 bp/PD in different culture. Too much time[48] is needed to reach the critical length of telomeres in tumor cells. However, oxidative stress may increase the rate of telomere shortening by the site-specific DNA damage in the telomere sequence. Thus, combination treatment[7] of oxidative stress and telomerase inhibitor in cancer cells will accelerate greatly the telomere shortening. Telomeres might shorten quickly to the point which is no longer able to divide.

REFERENCES

1 **Blackburn EH.** Structure and function of telomeres. *Nature* 1991; **350**: 569-573
2 **de Lange T.** Activation of telomerase in a human tumor. *Proc Natl Acad Sci U S A* 1994; **91**: 2882-2885
3 **Harley CB**, Futcher AB, Greider CW. Telomeres shorten during ageing of human fibroblasts. *Nature* 1990; **345**: 458-460
4 **Greider CW**, Blackburn EH. Identification of a specific telomere terminal transferase activity in Tetrahymena extracts. *Cell* 1985; **43**: 405-413
5 **Chiu CP**, Dragowska W, Kim NW, Vaziri H, Yui J, Thomas TE, Harley CB, Lansdorp PM. Differential expression of telomerase activity in hematopoietic progenitors from adult human bone marrow. *Stem Cells* 1996; **14**: 239-248
6 **Feng J**, Funk WD, Wang SS, Weinrich SL, Avilion AA, Chiu CP, Adams RR, Chang E, Allsopp RC, Yu J. The RNA component of human telomerase. *Science* 1995; **269**: 1236-1241
7 **Petersen S**, Saretzki G, von Zglinicki T. Preferential accumulation of single-stranded regions in telomeres of human fibroblasts. *Exp Cell Res* 1998; **239**: 152-160
8 **Saretzki G**, Sitte N, Merkel U, Wurm RE, von Zglinicki T. T e - lomere shortening triggers a p53-dependent cell cycle arrest via accumulation of G-rich single stranded DNA fragments. *Oncogene* 1999; **18**: 5148-5158
9 **Norrback KF**, Dahlenborg K, Carlsson R, Roos G. Telomerase activation in normal B lymphocytes and non-Hodgkin's lymphomas. *Blood* 1996; **88**: 222-229
10 **Kim NW,** Piatyszek MA, Prowse KR, Harley CB, West MD, Ho PL, Coviello GM, Wright WE, Weinrich SL, Shay JW. Specific association of human telomerase activity with immortal cells and cancer. *Science* 1994; **266**: 2011-2015
11 **Qin LX,** Tang ZY. The prognostic significance of clinical and pathological features in hepatocellular carcinoma. *World J Gastroenterol* 2002; **8**: 193-199
12 **Tang ZY.** Hepatocellular carcinoma-cause, treatment and metastasis. *World J Gastroenterol* 2001; **7**: 445-454
13 **Schafer DF**, Sorrell MF. Hepatocellular carcinoma. *Lancet* 1999; **353**: 1253-1257
14 **Meyne J**, Ratliff RL, Moyzis RK. Conservation of the human telomere sequence (TTAGGG)n among vertebrates. *Proc Natl Acad Sci U S A* 1989; **86**: 7049-7053
15 **Griffith JD**, Comeau L, Rosenfield S, Stansel RM, Bianchi A, Moss H, de Lange T. Mammalian telomeres end in a large duplex loop. *Cell* 1999; **97**: 503-514
16 **von Zglinicki T**. Role of oxidative stress in telomere length regulation and replicative senescence. *Ann N Y Acad Sci* 2000; **908**:

99-110
17 **von Zglinicki T**, Pilger R, Sitte N. Accumulation of single-strand breaks is the major cause of telomere shortening in human fibroblasts. *Free Radic Biol Med* 2000; **28**: 64-74
18 **Hsieh HF**, Harn HJ, Chiu SC, Liu YC, Lui WY, Ho LI. Telomerase activity correlates with cell cycle regulators in human hepatocellular carcinoma. *Liver* 2000; **20**: 143-151
19 **Shoji Y**, Yoshinaga K, Inoue A, Iwasaki A, Sugihara K. Quantification of telomerase activity in sporadic colorectal carcinoma: association with tumor growth and venous invasion. *Cancer* 2000; **88**: 1304-1309
20 **Rogan EM**, Bryan TM, Hukku B, Maclean K, Chang AC, Moy EL, Englezou A, Warneford SG, Dalla-Pozza L, Reddel RR. Alterations in p53 and p16INK4 expression and telomere length during spontaneous immortalization of Li-Fraumeni syndrome fibroblasts. *Mol Cell Biol* 1995; **15**: 4745-4753
21 **Strahl C**, Blackburn EH. Effects of reverse transcriptase inhibitors on telomere length and telomerase activity in two immortalized human cell lines. *Mol Cell Biol* 1996; **16**: 53-65
22 **Hiyama K**, Hirai Y, Kyoizumi S, Akiyama M, Hiyama E, Piatyszek MA, Shay JW, Ishioka S, Yamakido M. Activation of telomerase in human lymphocytes and hematopoietic progenitor cells. *J Immunol* 1995; **155**: 3711-3715
23 **Yasumoto S**, Kunimura C, Kikuchi K, Tahara H, Ohji H, Yamamoto H, Ide T, Utakoji T. Telomerase activity in normal human epithelial cells. *Oncogene* 1996; **13**: 433-439
24 **Kyo S**, Takakura M, Kohama T, Inoue M. Telomerase activity in human endometrium. *Cancer Res* 1997; **57**: 610-614
25 **Liu JP**. Studies of the molecular mechanisms in the regulation of telomerase activity. *FASEB J* 1999; **13**: 2091-2104
26 **Igarashi H**, Sakaguchi N. Telomerase activity is induced in human peripheral B lymphocytes by the stimulation to antigen receptor. *Blood* 1997; **89**: 1299-1307
27 **Hu BT**, Lee SC, Marin E, Ryan DH, Insel RA. Telomerase is upregulated in human germinal center B cells *in vivo* and can be re-expressed in memory B cells activated *in vitro*. *J Immunol* 1997; **159**: 1068-1071
28 **Hathcock KS**, Weng NP, Merica R, Jenkins MK, Hodes R. Cutting edge: antigen-dependent regulation of telomerase activity in murine T cells. *J Immunol* 1998; **160**: 5702-5706
29 **Weng NP**, Hathcock KS, Hodes RJ. Regulation of telomere length and telomerase in T and B cells: a mechanism for maintaining replicative potential. *Immunity* 1998; **9**: 151-157
30 **Ueda M**, Ouhtit A, Bito T, Nakazawa K, Lubbe J, Ichihashi M, Yamasaki H, Nakazawa H. Evidence for UV-associated activation of telomerase in human skin. *Cancer Res* 1997; **57**: 370-374
31 **Leteurtre F**, Li X, Gluckman E, Carosella ED. Telomerase activity during the cell cycle and in gamma-irradiated hematopoietic cells. *Leukemia* 1997; **11**: 1681-1689
32 **Hyeon Joo O**, Hande MP, Lansdorp PM, Natarajan AT. Induction of telomerase activity and chromosome aberrations in human tumour cell lines following X-irradiation. *Mutat Res* 1998; **401**: 121-131
33 **Sharma HW**, Sokoloski JA, Perez JR, Maltese JY, Sartorelli AC, Stein CA, Nichols G, Khaled Z, Telang NT, Narayanan R. Differentiation of immortal cells inhibits telomerase activity. *Proc Natl Acad Sci U S A* 1995; **92**: 12343-12346
34 **Holt SE**, Wright WE, Shay JW. Regulation of telomerase activity in immortal cell lines. *Mol Cell Biol* 1996; **16**: 2932-2939
35 **Bestilny LJ**, Brown CB, Miura Y, Robertson LD, Riabowol KT. Selective inhibition of telomerase activity during terminal differentiation of immortal cell lines. *Cancer Res* 1996; **56**: 3796-37802
36 **Xu D**, Gruber A, Peterson C, Pisa P. Supression of telomerase activity in HL60 cells after treatment with differentiating agents. *Leukemia* 1996; **10**: 1354-1357
37 **Savoysky E**, Yoshida K, Ohtomo T, Yamaguchi Y, Akamatsu K, Yamazaki T, Yoshida S, Tsuchiya M. Down-regulation of telomerase activity is an early event in the differentiation of HL60 cells. *Biochem Biophys Res Commun* 1996; **226**: 329-334
38 **Morin GB**. Is telomerase a universal cancer target? *J Natl Cancer Inst* 1995; **87**: 859-861
39 **Sharma HW**, Maltese JY, Zhu X, Kaiser HE, Narayanan R. Telomeres, telomerase and cancer: is the magic bullet real? *Anticancer Res* 1996; **16**: 511-515
40 **Oikawa S**, Kawanishi S. Site-specific DNA damage at GGG sequence by oxidative stress may accelerate telomere shortening. *FEBS Lett* 1999; **453**: 365-368
41 **Henle ES**, Han Z, Tang N, Rai P, Luo Y, Linn S. Sequence-specific DNA cleavage by Fe2+-mediated fenton reactions has possible biological implications. *J Biol Chem* 1999; **274**: 962-971
42 **von Zglinicki T**, Saretzki G, Docke W, Lotze C. Mild hyperoxia shortens telomeres and inhibits proliferation of fibroblasts: a model for senescence? *Exp Cell Res* 1995; **220**: 186-193
43 **Sitte N**, Saretzki G, von Zglinicki T. Accelerated telomere shortening in fibroblasts after extended periods of confluency. *Free Radic Biol Med* 1998; **24**: 885-893
44 **Lin MT**, Wang MY, Liaw KY, Lee PH, Chien SF, Tsai JS, Lin-Shiau SY. Superoxide dismutase in hepatocellular carcinoma affects patient prognosis. *Hepatogastroenterology* 2001; **48**: 1102-1105
45 **Wick M**, Zubov D, Hagen G. Genomic organization and promoter characterization of the gene encoding the human telomerase reverse transcriptase (hTERT). *Gene* 1999; **232**: 97-106
46 **Kiaris H**, Schally AV. Decrease in telomerase activity in U-87MG human glioblastomas after treatment with an antagonist of growth hormone-releasing hormone. *Proc Natl Acad Sci U S A* 1999; **96**: 226-231
47 **Buchkovich KJ**, Greider CW. Telomerase regulation during entry into the cell cycle in normal human T cells. *Mol Biol Cell* 1996; **7**: 1443-1454
48 **Kondo S**, Tanaka Y, Kondo Y, Hitomi M, Barnett GH, Ishizaka Y, Liu J, Haqqi T, Nishiyama A, Villeponteau B, Cowell JK, Barna BP. Antisense telomerase treatment: induction of two distinct pathways, apoptosis and differentiation. *FASEB J* 1998; **12**: 801-811

Edited by Zhang JZ

P.O.Box 2345, Beijing 100023,China
Fax: +86-10-85381893
E-mail: wjg@wjgnet.com www.wjgnet.com

World J Gastroenterol 2003;9(8):1863-1865
World Journal of Gastroenterology
 ISSN 1007-9327

• BRIEF REPORTS •

Relationship between nuclear morphometry, DNA content and resectability of pancreatic cancer

Yin-Cheng He, Wei Peng, Jian-Guo Qiao, Jun Cao, Ji-Wei Chen

Yin-Cheng He, Jian-Guo Qiao, Jun Cao, Ji-Wei Chen, Department of General Surgery, Zhongnan Hospital, Wuhan University, Wuhan 430071, Hubei Province, China
Wei Peng, Medical College, Jingmen Technical College, Jingmen 448000, Hubei Province, China
Correspondence to: Dr. Yin-Cheng He, Department of General Surgery, Zhongnan Hospital, Wuhan University, Wuhan 430071, Hubei Province, China. w030508h@public.wh.hb.cn
Telephone: +86-27-67812963
Received: 2003-05-11 **Accepted:** 2003-06-04

Abstract

AIM: To investigate the association of nuclear morphometry and DNA content with resectability of pancreatic cancer.

METHODS: A total of 36 patients with pancreatic adenocarcinoma were divided into resectable group and unresectable group. The nuclear morphometry and DNA contents of tumor cells were analyzed by IBAS autoimagine analyzer from paraffin-embedded materials. Localization size, histological type and grade, and clinical stage of the tumor were evaluated. Factors influencing resectability of pancreatic cancer were investigated using stepwise regression analysis.

RESULTS: Statistical significance was found in nuclear DNA content (integrated optical density, IOD) of tumor cells (1.64±0.41 *vs* 2.96±0.55), DNA ploidy, ages (46.5±5.3 years *vs* 58.6±0.7 years) and tumor volumes (298.1±101.5 cm^3 *vs* 634.7±512.5 cm^3) in both groups ($P<0.05$), and no difference was found in the nuclear morphometry ($P>0.05$). The rates of diploid/tetraploid and aneuploid were 66.7 % and 33.3 % in resectable group respectively, and 38.9 % and 62.1 % in unresectable group, respectively ($P<0.05$). IOD (X_{12}), ploidy status (X_{13}) and clinical stage (X_3) were radical resectable indicators with statistical significance. The regression equation for resectability was $Y=-9.2053+3.5428X_{12}+2.5390X_{13}-2.3001X_3$ ($RR=0.8780$, $P<0.01$).

CONCLUSION: There is a high correlation between resectability of pancreatic cancers and their DNA contents, DNA ploidy status and clinical stage.

He YC, Peng W, Qiao JG, Cao J, Chen JW. Relationship between nuclear morphometry, DNA content and resectability of pancreatic cancer. *World J Gastroenterol* 2003; 9(8): 1863-1865
http://www.wjgnet.com/1007-9327/9/1863.asp

INTRODUCTION

Pancreatic cancer is a highly malignant tumor, and has the most dismal prognosis among abdominal malignancies[1-6]. The overall five-year survival for all the patients is only 0.4 %. Patients who undergo radical resection have five-year survival rates between 10-24 %[1,3,4]. The traditional approach to patients has been surgical procedure, but approximately 10 % to 20 % of cancers of the pancreatic head, body and tail can be resected for potential cure[7-9]. The reason is the topographical peculiarities of the pancreas and the biological aggressiveness are involved. Recent results indicated that there was a relation between DNA ploidy, DNA content of tumor cell nuclei and the biological behaviour of tumors[10-15]. The present study was to investigate the effect of the clinical characteristics, nuclear morphometry and DNA contents of pancreatic cancer on its resectability.

MATERIALS AND METHODS

Patients and group

A total of 36 patients with pancreatic carcinoma were enrolled in this study. There were 20 men and 16 women with a mean age of 52.7±8.4 years (range 32-72 years). They were followed up from 1999 to December 2002. No patient had received preoperative chemotherapy and radiotherapy. The patients were divided into: resectable group and unresectable group (18 patients per group). In resectable group, 15 patients underwent radical resection with Whipple' s procedure, 2 splenopancreatectomy and 1 total pancreatectomy. In unresectable group, palliative bypass of the biliary tree and/or the duodenum was performed in 14 patients and biopsy in 4 patients. Criteria for unresectability included definite liver metastases, tumor spread to the whole pancreas proved by needle biopsy on operation, obstruction or invasion of the portal or mesenteric veins, and/or tumor encasement of the celiac or superior mesenteric arteries. Localization size, histological type, histological grade, and clinical stage of the tumor were evaluated for each patient.

Preparation of sections

From paraffin blocks, areas with high contents of neoplastic parenchymal cells were selected. Sections about 50 to 100 μm thick were cut from these parts and deparaffinized. The two 5 μm slides were preparated, one was stained with hematoxylin and eosin for confirmation of the presence of pancreatic cancer cells in the 50 μm sections, the other was stained with Feulgen method for DNA measurement.

Feulgen reaction

The cell nuclei were stained by the classic Feulgen reaction. The sections were deparaffinized and washed with distilled water. Cells were hydrolyzed (1 N HCl at 25 ℃ for 2-3 minutes, 1N HCl at 60 ℃ for 10-12 minutes, 1 N HCl at 25 ℃ for 2-3 minutes) and washed with distilled water again, then stained with Schiff ' s reagents for 80 minutes at room temperature, treated with freshly prepared sulfurous acid rinse 3 times (3-6 minutes), and washed in running tap water for 10 minutes. After dehydration, sections were coverslipped for DNA analysis.

Image analysis

Morphological characteristics and nuclear DNA content of tumor cells were measured by IBAS image analyzer (Kontron Company, Germany). The light was a halogen lamp (12V, 100W). Measurements were made using an interferential filter centered at 546 nm. Lymphocytes admixed with the tumor cells on the sections were used as internal control cells in the

procedure. At least 100 structurally identified neoplastic cell nuclei, selected at random on three different areas, were analyzed in each specimen. The structural identification was based on conventional cytodiagnostic criteria such as nuclear shape and chromatin texture. Morphological characteristics [nuclear areas, perimeter (μm), length of minor axis (μm), length of major axis (μm), form factor (FF)] and nuclear DNA content of tumor cells (integrated optical density, IOD) were analyzed. FF was calculated using the following equation: $FF= 4\pi A/P^2$. Where A is nuclear areas (μm^2), and *P* is nuclear perimeter (μm).

DNA ploidy

The same investigator made all measurements with no previous knowledge of coded clinical data. The DNA histograms were divided into three groups[16]. Type A with one stemline within the diploid region (1.5-2.5 C) and a G_2 fraction in the tetraploid region, type B with one stemline in the tetraploid region (3.5-4.5 C) and a G_2 fraction in the octoploid region, independent of the presence of a diploid stemlione, and type C with a stemline outside the diploid/ tetraploid region or a mosaic pattern.

Statistical analysis

All the data were input into a microcomputer, and statistical evaluation was carried out using the SPSS 10.0 statistical package. Differences between the mean values were analyzed for significance using the Student' s *t* test. Fisher' s exact probability test (two tailed) was used to assess the constituent ratio between two groups because of N of valid cases <40. To establish a relation between independent variables (X_1-X_{13}, Table 1) and dependent variables (Y, resectabiliry), stepwise regression analysis was used. The difference was considered significant when *P* value was less than 0.05.

RESULTS

Histological examination

The 36 cases consisted of 33 ductal adenocarcinoma, 1 acinus cell carcinoma, 1 mucinous carcinoma, and 1 adenosquamous carcinoma.

Nuclear morphometry and DNA contents

Nuclear morphometry and DNA contents are shown in Table 1. Statistical significance was found in IOD, ages and tumor volumes between resectable group and unsectable group ($P<0.05$). No difference was found in the nuclear morphometry of tumor cells when resectable group with unsectable group were compared ($P>0.05$, Table 1).

Nuclear DNA content of tumor cells (IOD) versus *clinical pathologic parametesr*

Relationships between IOD and clinical pathologic characteristics are presented in Table 1. Except for clinical stage (correlation coefficient $r=0.683$, $P<0.05$), no statistically significant relationship was found between IOD and age ($r=0.201$, $P>0.05$), tumor cell sources ($r=0.209$), histological grade ($r=0.167$), site ($r=0.235$), size ($r=0.312$), nuclear areas ($r=0.184$), perimeter ($r=0.085$), minor axis ($r=0.202$), major axis ($r=0.206$) and form factor ($r=0.149$).

Correlation analysis of resectability

Relationships between resectability and clinical pathologic characteristics were analyzed using Pearson correlation analysis. Correlation coefficients "*r*" are listed in Table 1. Age, clinical stage, site, size, IOD and ploidy status were covariates independently associated with resectability of pancreatic cancer.

Table 1 Relationship between DNA contents, clinical characteristics and resectability

Variable Factor		Resectable group	Unresectable group	Correlation coefficient (*r*)
X_1	Age (years)	46.5±5.3	58.6±0.7[a]	0.536[b]
X_2	Tumor cells (*n*)			0.387
	Ductal	17(94%)	16(89%)	
	Other	1(6%)	2(11%)	
X_3	Clinical stage (*n*)[c]			0.605[b]
	Stage I	9(50%)	0(0%)[a]	
	Stage II	8(44%)	3(17%)	
	Stage III	1(6%)	11(61%)[a]	
	Stage IV	0(0%)	4(22%)	
X_4	Histological grade (*n*)			0.394
	Kloppel I	5(28%)	3(17%)	
	Kloppel II	6(33%)	9(50%)	
	Kloppel III	7(39%)	6(33%)	
X_5	Site (n)[c]			-0.545[b]
	Head of pancreas	16(89%)	10(56%)[a]	
	Other	2(11%)	8(44%)[a]	
X_6	Size (cm^3)	298.1±101.5	634.7±512.5[a]	0.575[b]
X_7	Nuclear areas (μm^2)	33.37±8.42	34.74±6.93	0.478
X_8	Perimeter (μm)	24.90±4.02	25.60±3.02	0.367
X_9	Minor axis (μm)	5.56±0.68	5.67±0.57	0.482
X_{10}	Major axis (μm)	8.31±1.10	8.56±0.93	0.434
X_{11}	Form factor	0.75±0.05	0.70±0.06	0.376
X_{12}	IOD	1.64±0.41	2.96±0.55[a]	0.787[b]
X_{13}	DNA ploidy (*n*)			0.735[b]
	Diploid / tetraploid	12(67%)	7(39%)[a]	
	Aneuploid	6(33%)	11(61%)[a]	

[a]$P<0.05$, *vs* resectable group, [b]$P<0.05$, *T* test, [c]$P<0.05$, resectable group *vs* unresectable group

Stepwise regression analysis of resectability

Resectability predictors were evaluated in a stepwise regression model. In this model, stepwise regression analysis demonstrated that IOD (X_{12}), ploidy status (X_{13}) and clinical stage (X_3) were statistically significant resectable indicators after backward elimination ($F=2.80$). The regression equation for resectability was $Y=-9.2053+3.5428X_{12}+2.5390X_{13}-2.3001X_3$ ($RR=0.8780$, $P<0.01$). IOD remained to be the most important predictor, ploidy status was th second important one, followed by clinical stage according to variable *F* values.

DISCUSSION

The prognosis of pancreatic cancer though remarkable diagnosis and therapeutic advances, have led many surgeons to question whether patients with pancreatic cancer should be submitted to radical surgery[17-20]. Nevertheless, the only chance for longterm survival and cure is undoubtedly related to the feasibility of radical surgery. Therefore, many surgeons have investigated the resectability of pancreatic cancer. Although the biologic behavior and location of the tumor are the most common predictors reliable factors that may predict resectability before laparotomy are waiting to be found[21-26].

DNA aneuploidy is one of the markers of malignant tumour cells. Aneuploidy DNA pattern may be related to the development of distant organ metastases, invasion and prognosis[27-29]. Weger *et al*[16] investigated the relationship between DNA ploidy status and resectability of pancreatic cancer, in which 77 cases were studied by automatic DNA image cytometry, and the authors found that the radical resectable rates of diploid, tetraploid and aneuploid tumors were 87.5 %, 48.6 % and 25.9 % respectively. Joensuu *et al* found that only 3 of 15 resected pancreatic cancers had

aneuploid DNA content, whereas 35 of 47 nonresected pancreatic cancers had aneuploid, and the patients with diploid tumors lived longer than patients with aneupoid cancers. These findings suggested that the biological behavior of tumor could influence life span and resectability[30], which was in agreement with our study. Nuclear morphometry (nuclear area, perimeter, length of minor axis, length of major axis and form factor) was not significant between resectable group and unresectable group (P>0.05), but the tumor cellular DNA contents and ploidies in resectable group were different from those in unresectable group (P<0.05). It is suggested that there may be some difference between both groups at molecular levels, despite no difference was found in nuclear morphometry. Table 1 shows that the rates of diploid/tetraploid and aneuploid were 66.7 % and 33.3 % in resectable group, and 38.9 % and 62.1 % in unresectable group, respectively (P<0.05). The resectable rate of aneuploid tumor was lower than that of diploid/tetraploid. Compared with diploid cells, metabolism of the aneuploid cells was significantly accelerated, and the tumor cells underwent more rapid differentiation and proliferation, and had higher levels of DNA synthesis, accompanied by high DNA contents and DNA ploidy levels. According to our findings, there was a high correction between resectability of tumors and their quantitative DNA contents, DNA ploidy status. That is to say, radical or palliative resection of tumors is principally determined by DNA contents and ploidy status of tumor nuclei. Tumor tissue could be easily obtained in most cases by ultrasound guided percutaneous fine needle aspiration biopsy before operation[31]. Therefore, DNA image analysis for aspirated cellular materials may provide important preoperative information, and may help surgeons plan for radical or palliative procedure. We are convinced that the clinical application of preoperative imaging techniques and DNA measurements as a guide to select patients for surgical resection will become mature in the near future.

REFERENCES

1 **Li YJ**, Ji XR. Relationship between expression of E-cadherin-catenin complex and clinicopathologic characteristics of pancreatic cancer. *World J Gastroenterol* 2003; **9**: 368-372
2 **Postier RG**, Lerner MR, Lightfoot SA, Vannarath R, Lane MM, Hanas JS, Brackett DJ. DNA ploidy and markovian analysis of neoplastic progression in experimental pancreatic cancer. *J Histochem Cytochem* 2003; **51**: 303-309
3 Zheng M, Liu LX, Zhu AL, Qi SY, Jiang HC, Xiao ZY. K-ras gene mutation in the diagnosis of ultrasound guided fine-needle biopsy of pancreatic masses. *World J Gastroenterol* 2003; **9**: 188-191
4 **Shankar A**, Russell RC. Recent advances in the surgical treatment of pancreatic cancer. *World J Gastroenterol* 2001; **7**: 622-626
5 Yoshida T, Matsumoto T, Sasaki A, Morii Y, Aramaki M, Kitano S. Prognostic factors after pancreatoduodenectomy with extended lymphadenectomy for distal bile duct cancer. *Arch Surg* 2002; **137**: 69-73
6 **Wagman R**, Grann A. Adjuvant therapy for pancreatic cancer: current treatment approaches and future challenges. *Surg Clin North Am* 2001; **81**: 667-681
7 **Gebhardt C**, Meyer W, Reichel M, Wunsch PH. Prognostic factors in the operative treatment of ductal pancreatic carcinoma. *Langenbecks Arch Surg* 2000; **385**: 14-20
8 **Warshaw AL**, Gu ZY, Wittenberg J, Waltman AC. Preoperative staging and assessment of resectability of pancreatic cancer. *Arch Surg* 1990; **125**: 230-233
9 **Durup Scheel-Hincke J**, Mortensen MB, Qvist N, Hovendal CP. TNM staging and assessment of resectability of pancreatic cancer by laparoscopic ultrasonography. *Surg Endosc* 1999; **13**: 967-971
10 **Bazan V**, Migliavacca M, Zanna I, Tubiolo C, Corsale S, Calo V, Amato A, Cammareri P, Latteri F, Grassi N, Fulfaro F, Porcasi R, Morello V, Nuara RB, Dardanoni G, Salerno S, Valerio MR, Dusonchet L, Gerbino A, Gebbia N, Tomasino RM, Russo A. DNA ploidy and S-phase fraction, but not p53 or NM23-H1 expression, predict outcome in colorectal cancer patients. Result of a 5-year prospective study. *J Cancer Res Clin Oncol* 2002; **128**: 650-658
11 **Berczi C**, Bocsi J, Bartha I, Math J, Balazs G. Prognostic value of DNA ploidy status in patients with rectal cancer. *Anticancer Res* 2002; **22**: 3737-3741
12 **El-Rayes BF**, Maciorowski Z, Pietraszkiewicz H, Ensley JF. Comparison of DNA content parameters in paired, fresh tissue pretreatment biopsies and surgical resections from squamous cell carcinoma of the head and neck. *Otolaryngol Head Neck Surg* 2003; **128**: 169-177
13 **Sugai T**, Uesugi N, Nakamura S, Habano W, Jiao YF, Noro A, Takahashi H, Akasaka I, Higuchi T. Evolution of DNA ploidy state and DNA index in colorectal adenomas and carcinomas using the crypt isolation technique: New hypothesis in colorectal tumorigenesis. *Pathol Int* 2003; **53**: 154-162
14 **Tsutsui S**, Ohno S, Murakami S, Kataoka A, Kinoshita J, Hachitanda Y. Prognostic significance of the combination of biological parameters in breast cancer. *Surg Today* 2003; **33**: 151-154
15 **Huang JJ**, Yeo CJ, Sohn T, Lillemoe KD, Sauter PK, Coleman J, Hruban RH, Cameron JL. Quality of life and outcomes after pancreaticoduodenectomy. *Ann Surg* 2000; **6**: 890-898
16 **Weger AR**, Glaser KS, Schwab G, Oefner D, Bodner E, Auer GU, Mikuz G. Quantitative nuclear DNA content in fine needle aspirates of pancreatic cancer. *Gut* 1991; **32**: 325-328
17 **Sohn TA**, Yeo CJ, Cameron JL, Koniaris L, Kaushal S, Abrams RA, Sauter PK, Coleman J, Hruban RH, Lillemoe KD. Resected adenocarcinoma of the pancreas-616 patients: results, outcomes and prognostic indicators. *J Gastrointest Surg* 2000; **4**: 567-579
18 **Liu B**, Staren E, Iwamura T, Appert H, Howard J. Effects of Taxotere on invasive potential and multidrug resistance phenotype in pancreatic carcinoma cell line SUIT-2. *World J Gastroenterol* 2001; **7**: 143-148
19 **Zhang LJ**, Chen KN, Xu GW, Xing HP, Shi XT. Congenital expression of mdr-1 gene in tissues of carcinoma and its relation with pathomorphology and prognosis. *World J Gastroenterol* 1999; **5**: 53-56
20 **Guo XZ**, Friess H, Shao XD, Liu MP, Xia YT, Xu JH, Buchler MW. KAI1 gene is differently expressed in papillary and pancreatic cancer: influence on metastasis. *World J Gastroenterol* 2000; **6**: 866-871
21 **G House M**, Campbell K, D Schulick R, Leach S, J Yeo C, Horton K, Fishman E, L Cameron J, D Lillemoe K. PANCREAS Surgery 123. Predicting Resectability of Periampullary Tumors With 3-Dimensional Computed Tomography. *J Gastrointest Surg* 2003; **7**: 296
22 **Catalano C**, Laghi A, Fraioli F, Pediconi F, Napoli A, Danti M, Reitano I, Passariello R. Pancreatic carcinoma: the role of high-resolution multislice spiral CT in the diagnosis and assessment of resectability. *Eur Radiol* 2003; **13**: 149-156
23 Saftoiu A, Ciurea T. The role of imaging for the evaluation of pancreatic cancer resectability. *Rom J Gastroenterol* 2002; **11**: 78-79
24 **John TG**, Wright A, Allan PL, Redhead DN, Paterson-Brown S, Carter DC, Garden OJ. Laparoscopy with laparoscopic ultrasonography in the TNM staging of pancreatic carcinoma. *World J Surg* 1999; **23**: 870-881
25 **Lim JE**, Chien MW, Earle CC. Prognostic factors following curative resection for pancreatic adenocarcinoma: a population-based, linked database analysis of 396 patients. *Ann Surg* 2003; **237**: 74-85
26 **Merchant NB**, Conlon KC, Saigo P, Dougherty E, Brennan MF. Positive peritoneal cytology predicts unresectability of pancreatic adenocarcinoma. *J Am Coll Surg* 1999; **188**: 421-426
27 **Xu L**, Zhang SM, Wang YP, Zhao FK, Wu DY, Xin Y. Relationship between DNA ploidy,expression of ki-67 antigen and gastric cancer metastasis. *World J Gastroenterol* 1999; **5**: 10-11
28 **Alanen KA**, Joensuu H, Klemi PJ, Marin S, Alavaikko M, Nevalainen TJ. DNA ploidy in pancreatic neuroendocrine tumors. *Am J Clin Pathol* 1990; **93**: 784-788
29 **Alanen KA**, Joensuu H, Klemi PJ, Marin S, Alavaikko M, Nevalainen TJ. DNA ploidy in pancreatic neuroendocrine tumors. *Am J Clin Pathol* 1990; **93**: 784-788
30 **Joensuu H**, Alanen KA, Klemi PJ. Doubts on "curative" resecti on of pancreatic cancer. *Lancet* 1989; **1**: 953-954
31 **Williams DB**, Sahai AV, Aabakken L, Penman ID, van Velse A, Webb J, Wilson M, Hoffman BJ, Hawes RH. Endoscopic ultrasound guided fine needle aspiration biopsy: a large single centre experience. *Gut* 1999; **44**: 720-726

Edited by Zhang JZ and Wang XL

P.O.Box 2345, Beijing 100023,China
Fax: +86-10-85381893
E-mail: wjg@wjgnet.com www.wjgnet.com

World J Gastroenterol 2003;9(8):1866-1870
World Journal of Gastroenterology
 ISSN 1007-9327

• BRIEF REPORTS •

Early protective effect of ischemic preconditioning on small intestinal graft in rats

Shu-Feng Wang, Guo-Wei Li

Shu-Feng Wang, Department of General Surgery, First Hospital, Xi' an Jiaotong University, Xi' an 710061, Shannxi Province, China
Guo-Wei Li, Department of General Surgery, Second Hospital, Xi' an Jiaotong University, Xi' an 710004, Shannxi Province, China
Supported by The National Natural Science Foundation of China, No.30271275
Correspondence to: Dr. Shu-Feng Wang, Department of General Surgery, First Hospital, Xi' an Jiaotong University, Xi' an 710061, Shannxi Province, China. dawnwsf@sina.com
Telephone: +86-29-5271909
Received: 2003-01-18 **Accepted:** 2003-03-10

Abstract

AIM: To investigate the early protective effect of ischemic preconditioning on small intestinal graft in rats.

METHODS: SD rats were randomly divided into the following groups: sham operation group (S group, *n*=6), small bowel transplantation group (SBT group, *n*=12), ischemic preconditioning plus small bowel transplantation group (ISBT group, *n*=12). Heterotopic SBT was performed with a technique modified from that described by Monchik *et al*.When the graft was revascularized successfully and reperfused for 1 h, samples were obtained from the different groups. Laminin was analyzed with immunohistochemical staining. Quantitative analysis of laminin positive signals was performed using image acquiring analysis system. Apoptotic epithelia of small intestinal graft were detected by the TdT-mediated dUTP nick end labeling method. The morphological change of epithelial basement membrane was observed by transmission electron microscopy.

RESULTS: The mean optical density value of laminin positive signals was 39.52±2.60, 13.53±0.44, 25.40±1.79, respectively, in S, SBT and ISBT groups. The average optical density value of laminin positive products in SBT group was sharply lower than that in S group ($P<0.05$). However, the mean optical density value of laminin positive products in ISBT group was significantly higher than that in SBT group ($P<0.05$). The apoptotic index (AI) in S, SBT and ISBT group was 2.2±0.83,30.8±3.2, 13.2±2.86, respectively. The AI in SBT group was significantly higher than that in S group ($P<0.05$), and AI in ISBT group was sharply lower than that in SBT group ($P<0.05$). On transmission electron microscopy, the epithelial basement membrane in S group stayed normal, but in SBT group it became disrupted and collapsed, even disappeared. The lesion of epithelial basement membrane in ISBT group was slighter compared with that in SBT group.

CONCLUSION: Ischemic preconditioning has an early protective effect on epithelial cells and extracellur matrix of small intestinal graft. Inhibition of epithelial cell apoptosis may be one of the mechanisms of ischemic preconditioning.

Wang SF, Li GW. Early protective effect of ischemic preconditioning on small intestinal graft in rats. *World J Gastroenterol* 2003; 9(8): 1866-1870
http://www.wjgnet.com/1007-9327/9/1866.asp

INTRODUCTION

Small bowel transplantation (SBT) has been advocated as the preferred therapy for patients with irreversible intestinal failures such as short bowel syndrome[1-6]. In recent years, although potent immunosuppressive agents have been used, rejection rate of small intestinal grafts still amounts to 50 %[7]. Primary graft rejection and reperfusion damage involved in loss of small intestine function after transplantation are still the major obstacle to SBT[8-10]. Postischemic reperfusion damage, a nonspecific injury, may enhance graft immunogenicity and is likely to play an important role in the development of early specific and late rejection-related events, and threatens graft function and graft survival[11]. Therefore, it has important clinical significance for SBT if reperfusion injury of the graft could be ameliorated or prevented.

Studies have indicated that ischemic preconditioning can alleviate reperfusion injury of tissues or organs. Ischemic preconditioning (IPC) refers to a phenomenon in which a tissue is rendered resistant to the deleterious effects of prolonged ischemia and reperfusion by prior exposure to brief periods of vascular occlusion[12]. With regard to organ transplantation, the beneficial effect of IPC has been previously described in transplantation procedures involving in ameliorating heart preservation injury and liver reperfusion damage[13,14], but its protective capacity against reperfusion injury in small bowel transplantation has not completely defined. Lately, Sola *et al*[15]. have shown that the release of lactate dehydrogenase (marker of cell injury) decreases markedly during small intestinal graft preservation and reperfusion, and morphological change of graft improves greatly, after IPC was carried out. Extracelluar matrix is the early target of reperfusion injury[16]. Epithelial cell apoptosis of small intestinal graft is the major mode of cell death[17]. But no study has covered the effect of IPC on them. So this study was to investigate the protective effect of ischemic preconditioning on epithelial cells and extracelluar matrix of intestinal graft in rats.

MATERIALS AND METHODS

Animal preparation

Healthy male Sprague-Dawley (SD) rats, weighing 280±20 g, provided by Medical Experiment Animal Center, Xi' an Jiaotong University, were housed in standard animal facilities and fed with commercially available rat chow and tap water *ad libitum* for 1 week before test to acclimatize the laboratory. They were maintained on a 12 h light/dark cycle.

Experimental design

SD rats were used as donors and recipients. They were randomly divided into the following groups: (1) sham operation group (S group, *n*=6), in which animals were only subjected

to anesthesia and laparotomy; (2) heterotopic segmental small bowel transplantation group (SBT group, *n*=12), in which the donor and recipient were paired according to the similar body weight; (3) IPC plus SBT group (ISBT group, *n*=12). IPC was carried out before the graft was harvested. Namely, the superior mesenteric artery was occluded for 10 min with a microsurgical atraumatic vascular clamp, then it was released, and the graft was reperfused for 10 min. The following surgical procedures were the same as SBT group.

Heterotopic small bowel transplantation

Heterotopic SBT was performed with a technique modified from that described by Monchik and others scholars[18-21]. All animals were fasted for 12 h, but had free access to water before operation. They were anesthetized with pentobarbital sodium solution (2 %, 35 mg/kg) intraperitoneally. After perfused *in situ* with cold lactated Ring' s solution, the small intestine 5 cm distal to the Treitz ligament was harvested from donor rat with a vascular pedicle including portal vein (PV) and aorta segment with superior mesenteric artery, and stored at 4 ℃ in lactated Ringer' s solution for 1 h. After left nephrectomy, left renal vein and abdominal aorta of the recipient were isolated. The graft was revascularized by end-to-side anastomosis between donor aorta and recipient aorta using continuous 9-0 non-traumatic nylon suture and end-to-end anastomosis between donor PV and the left renal vein of the recipient using a cuff technique. The recipient' s own intestine was left intact. During transplantation, mean warm ischemia time of graft was 25-30 min, and the longest did not exceed 40 min[22].

Immuohistochemical staining and evaluation

When the graft was revascularized successfully and reperfused for 1 h, samples were obtained from the different groups. Specimens were fixed in 4 % paraformaldehyde, embeded in paraffin, sliced 4 μm thick, and stained by the SP methods. A polyclonal antirat laminin antibody (Boster Biotech, Wuhan, China) was used at concentration of 1:100. DAB was used for visualization. For negative control, the slides were treated with PBS instead of primary antibody.

Laminin is one of the major components of epithelial basement membrane. It was regarded as positive signals when epithelial basement membrane became brownish yellow. Quantitative analysis of positive products was performed using image acquiring analysis system (Leica QWin500CW, Germany). The image system randomly selected five visual fields per slice to measure the optical density value, using the average value as the mean optical density.

Detection of cell apoptosis

Apoptosis was detected on sections from paraformaldehyde-fixed and paraffin-embedded blocks by the terminal deoxynucleotidyl-transferase (TdTase) mediated d-UTP-biotin nick end labeling (TUNEL) method[23]. Apoptosis assay with a detection kit from Bochinger Mannheim Germany, conformed to the manufacturer' s protocol strictly. The nuclei of apoptotic cells were stained brown as detected under light microscope, and apoptotic cells were quantified by calculating the apoptotic index (apoptotic cells/10 high-power fields)[24]. Negative control was designed by PBS instead of TdTase.

Transmission electron microscopy

For transmission electron microscopy, intestinal fragments of approximately 2 mm^3 obtained from different groups, were fixed in 2.5 % glutaraldehyde for 3 h, rinsed in PBS, then postfixed in 1 % osmium tetroxide for 2 h. Samples were dehydrated in graded alcohols, and embedded in Epon 812, cut on an ultramicrotome and stained with uranyl acetate and lead citrate. Ultrathin sections were viewed using transmission electron microscopy (Hitachi H-600).

Statistical analysis

Data were expressed as mean ± standard error of the mean. One-way analysis of variance (ANOVA) was used for multiple comparisons with Student Newman Keylls (SNK) test. Significant difference was assumed when $P<0.05$.

RESULTS

Quantitative analysis of laminin expression in different groups

As seen from Table 1, the mean optical density value of laminin positive products in SBT group was sharply lower than that in S group ($P<0.05$). However, after IPC was carried out, the mean optical density value of positive products in ISBT group was higher, compared with that in SBT group ($P<0.05$). It indicated that IPC had a protective effect on the basement membrane, one of the components of extracelluar matrix.

Table 1 Expression of laminin in different groups

Group	*n*	Mean optical density value
S	6	39.52±2.60
SBT	6	13.53±0.44[a]
ISBT	6	25.40±1.79[b]

[a]$P<0.05$ *vs* S group q=29.87, [b]$P<0.05$ *vs* SBT group q=13.64.

Cell apoptosis in different groups

As shown in Figure 1 and Table 2 in S group, apoptotic epithelial cells at villus tip were found only occasionally. However, after the graft underwent 60 min of cold ischemia and 60 min of warm reperfusion, many apoptotic cells appeared at villus tip of the graft in SBT group, The AI in SBT groups was significantly higher than that in S group ($P<0.05$), but the number of apoptotic cells at villus tip of the graft decreased sharply after transient IPC was carried out. The AI in ISBT group was sharply lower than that in SBT group ($P<0.05$). It showed that the mechanism of IPC was also involved in inhibition of epithelial cell apoptosis induced by ischemia and reperfusion in small intestinal graft.

Table 2 AI of epithelial cells of small intestinal graft in different groups

Group	*n*	AI
S	6	2.2±0.83
SBT	6	30.8±3.2[a]
ISBT	6	13.2±2.86[b]

[a]$P<0.05$ *vs* S group q=25.33 [b]$P<0.05$ *vs* SBT group q=15.59.

Morphological analysis of epithelial basement membrane

Under light microscope, epithelial basement membrane was stained brownish yellow in S, SBT and ISBT groups, but there was an obvious difference in the structure of epithelial basement membrane. Basement membrane in S group showed line-shaped continuous normal structure, however, it became disrupted and collapsed, even disappeared in SBT group. The lesion of basement membrane in ISBT group was slighter compared with that in SBT group. Under transmission electron microscope, the morphological change of epithelial basement membrane was the same as that under light microscopy (Figure 2).

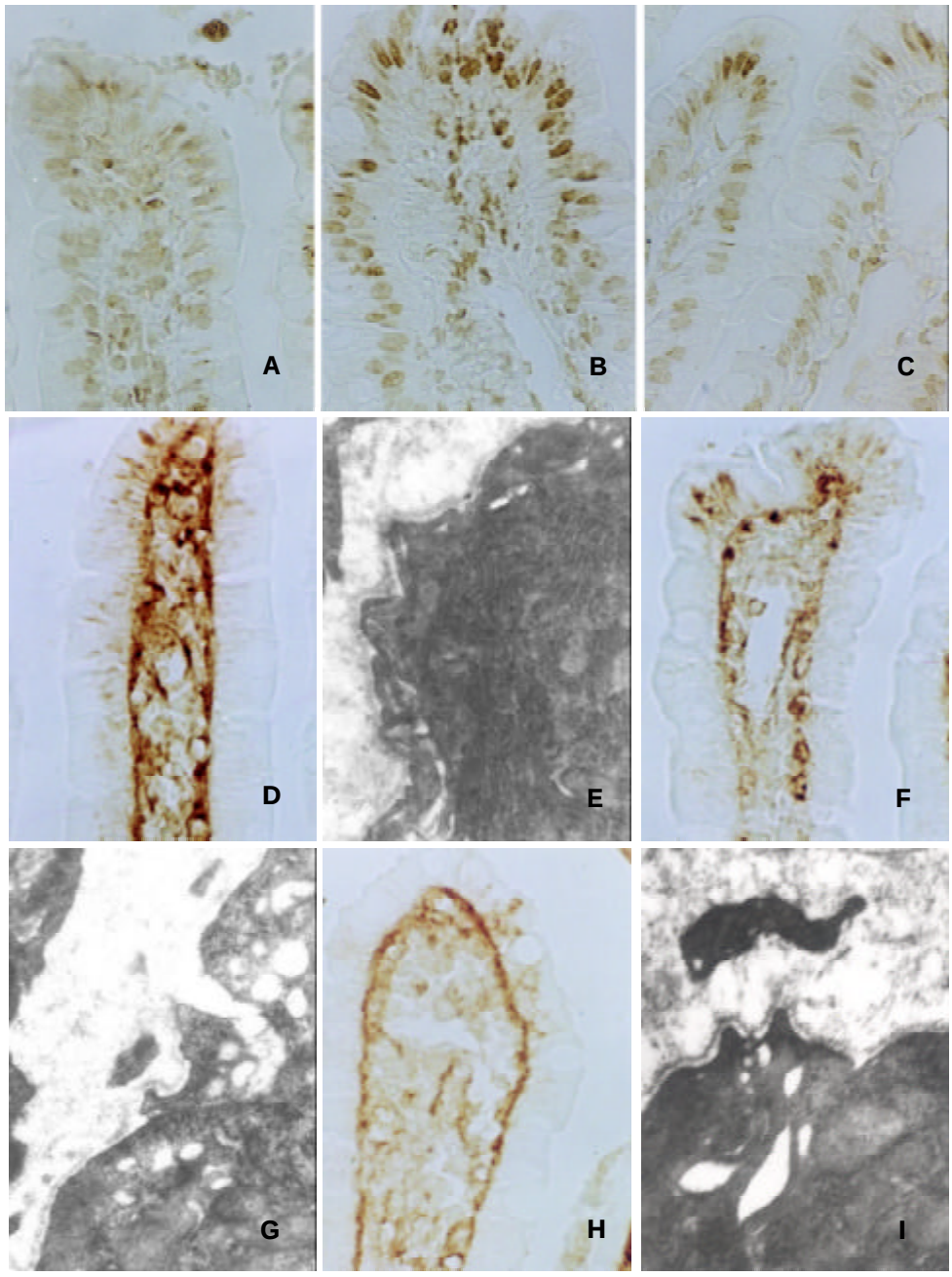

Figure 1 Light micrographs of apoptotic cells detected by TUNEL method (original magnification ×400). A: In S group, TUNEL signals were only observed accidentally at villi tip. B: In SBT group, many TUNEL signals appeared at villi tip of the graft. C: In ISBT group, after IPC was carried out, TUNEL signals decreased significantly at villi tip of the graft.

Figure 2 Light and electron micrographs (LM and EM) of morphological change of epithelial basement membrane (BM) (LM, original magnification ×400, EM, original magnification ×20 000). D and E: In S group, BM showed line-shaped, continuous normal structure. F and G: In SBT group, BM became disrupted and collapsed, even disappeared. H and I: In ISBT group, after IPC was function carried out, the lesion of BM was slighter, compared with that in SBT group.

DISCUSSION

Available evidences indicate that the small intestinal mucosa is susceptible to postischemic reperfusion, 15 minutes of ischemia alone could induce detectable mucosal injury, and reperfusion exacerbates the mucosal injury[25]. Under physiological conditions, the gut shows a remarkable rate of turnover, and a rapid regeneration of the epithelial layer has also been reported after intestinal hypoxia/reperfusion. Taguchi *et al*. have found that 15 minutes of ischemia and 1 h reperfusion could result in increase of the expression of proliferation cell nuclear antigen (PCNA) in small intestine[26]. PCNA, a kind of nuclear protein that produces or expresses in proliferative cells, is a significant cell-regulated nuclear protein for DNA-polymerase δ. So PCNA is a marker for proliferative cells[27-29]. The increase of small intestinal PCNA expression after 1 h reperfusion indicates that the repair process of epithelia is initiated by ischemia and reperfusion. In order to discover the deleterious effect of reperfusion and protective effect of IPC, respectively, on epithelia and extracelluar matrix of the small intestinal graft, and to prevent influence on graft due to the recovery of epithelia during reperfusion, the present study was designed to obtain specimens from different groups 1 h after reperfusion when the vascular anastomosis had finished.

The protective effect of IPC was first described in heart[30], and many comprehensive studies on IPC indicated that it could be divided into two major classes. One is the early phase of protection that appears 1-3 h after IPC, and the other is the late phase of protection that appears 24 h after IPC (the second

window of protection). Lately, this protective effect has been also demonstrated in the small intestine[31]. Although the effects of IPC on small intestine are not completely understood, several studies suggested that they were involved in transient increase of nitric oxide synthesis, activation of K_{ATP} channel, release of calcitonin gene-related peptide and endogenous opioid peptides, and inhibition of P-selectin expression in small intestine[32-36]. Apoptosis regulates many physiological and pathological processes. The influence of IPC on cell apoptosis in small bowel graft is not well known. Apoptosis is a major mode of epithelial death and peaks at 60 min during reperfusion period, in comparison, necrosis was relatively minor[37,38]. Therefore, loss of intestinal epithelia is a consequence of apoptosis during reperfusion. In the present experiment, apoptotic epithelial cells at villus tip were found accidentally in S group. Under physiological circumstances, apoptosis was reported to be an important mechanism of epithelial cell renewal. However, in SBT group after the graft underwent 60 min of cold ischemia and 60 min of warm reperfusion, many apoptotic cells appeared at villus tip of the graft. Compared with S group, the number of apoptotic cells was significantly higher. It indicated that apoptosis was initiated by ischemia and reperfusion in the graft. But in ISBT group, after transient IPC was carried out, the number of apoptotic cells at villus tip of the graft decreased sharply, in comparison with that in SBT group. It suggests that the mechanism of IPC may also involve the inhibition of epithelial cell apoptosis induced by ischemia and reperfusion in small intestinal graft.

Extracelluar matrix proteins provide structural support and maintenance, and also modulate a number of cell functions such as repair and immunity[39]. Laminin, an active glycoprotein with many biological functions, is one of the most abundant components of epithelial basement membrane[40]. It may play an important role in regulating cell-cell interactions, cell migration and differentiation. Laminin can be produced by epithelial and endothelial cells. In the present study, after laminin expression was evaluated by immunohistochemical staining and analyzed by quantitative analysis system, it was found that intestinal epithelial basement membrane in S group appeared line-shaped continuous structure, but it became decomposed and disrupted, even disappeared in SBT group. Compared with the average optical density value of laminin positive expression signals in S group, it was significantly lower in SBT group. Hence, it proved again that epithelial basement membrane was an early target of reperfusion injury. The small bowel contains a large reservoir of mediators, such as reactive oxygen radicals, various protease and cytokines, as well as adhesion molecules[41]. During reperfusion, laminin regulates polymorphonuclear cells to adhere and migrate to epithelial villus, and it is reactive oxygen radicals and various proteases released from polymorphonuclear cells that decompose epithelial basement membrane, meanwhile reperfusion injury damages the ability of epithelial cells to produce laminin. So, more damage and less production result in the collapse of epithelial basement membrane. In accordance with immunohistochemical results, under transmission electron microscopy, intestinal epithelial basement membrane in S group kept normal, but it showed disruption, even disappeared in SBT group. After IPC, the morphological change of epithelial basement membrane in ISBT group improved greatly, and the mean optical density value of laminin positive expression signals became higher, compared with that in SBT group. Under transmission electron microscope, the reperfusion injury degree of basement membrane in ISBT group was slighter than that in SBT group. It indicates strongly that IPC has protective effects on extracelluar matrix of small intestinal graft, and the beneficial effect may appear at early phase after IPC.

In summary, the present study demonstrates that ischemic preconditioning has an early protective effect on epithelial cells and extracelluar matrix of small intestinal graft. Inhibition of epithelial cell apoptosis initiated by reperfusion may be one of the mechanisms of IPC. With regard to organ transplantation, IPC may have a substantial impact on clinical practice. Alleviation of reperfusion injury of graft by IPC can enhance the function grafts and prolong their survival.

REFERENCES

1 **Platell CF**, Coster J, McCauley RD, Hall JC. The management of patients with the short bowel syndrome. *World J Gastroenterol* 2002; **8**: 13-20
2 **Kato T**, Ruiz P, Thompson JF, Eskind LB, Weppler D, Khan FA, Pinna AD, Nery JR, Tzakis AG. Intestinal and multivisceral transplantation. *World J Surg* 2002; **26**: 226-237
3 **Park BK**. Intestinal transplantation in pediatric patients. *Prog Transplant* 2002; **12**: 97-113
4 **Kaufman SS**. Small bowel transplantation: selection criteria, operative techniques, advances in specific immunosuppression, prognosis. *Curr Opin Pediatr* 2001; **13**: 425-428
5 **Dionigi P**, Alessiani M, Ferrazi A. Irreversible intestinal failure, nutrition support, and small bowel transplantation. *Nutrition* 2001; **17**: 747-750
6 **Reyes J**. Intestinal transplantation for children with short bowel syndrome. *Semin Pediatr Surg* 2001; **10**: 99-104
7 **Ghanekar A,** Grant D. Small bowel transplantation. *Curr Opin Crit Care* 2001; **7**: 133-137
8 **Farmer DG**, Amersi F, Shen XD, Gao F, Anselmo D, Ma J, Dry S, McDiarmid SV, Shaw G, Busuttil RW, Kupiec-Weglinski J. Improved survival through the reduction of ischemia-reperfusion injury after rat intestinal transplantation using selective P-selectin blockade with P-selectin glycoprotein ligand-Ig. *Transplant Proc* 2002; **34**: 985
9 **Guo WH**, Chan KL, Fung PP, Chan KW, Tam PK. Nitric oxide protects segmental intestinal grafts from ischemia and reperfasion injury. *Transplant Proc* 2000; **32**: 1297-1298
10 **Carey HV**, Mangino MJ, Southard JH. Changes in gut function during hibernation: implications for bowel transplantation and surgery. *Gut* 2001; **49**: 459-461
11 **Massberg S**, Messmer K. The nature of ischemia / reperfusion injury. *Transplant Proc* 1998; **30**: 4217-4223
12 **Sola A**, Rosello-Catafau J, Alfaro V, Pesquero J, Palacios L, Gelpi E, Hotter G. Modification of glyceraldehyde-3-phosphate dehydrogenase in response to nitric oxide in intestinal preconditioning. *Transplantation* 1999; **67**: 1446-1452
13 **Karck M**, Rahmanian P, Haverich A. Ischemic preconditioning enhances donor heart preservation. *Transplantation* 1996; **62**: 17-22
14 **Yin DP**, Sankary HN, Chong AS, Ma LL, Shen J, Foster P, Williams JW. Protective effect of ischemic preconditioning on liver preservation-reperfusion injury in rats. *Transplantation* 1998; **66**: 152-157
15 **Sola A**, De Oca J, Gonzalez R, Prats N, Rosello-Catafau J, Gelpi E, Jaurrieta E, Hotter G. Protective effect of ischemic preconditioning on cold preservation and reperfusion injury associated with rat intestinal transplantation. *Ann Surg* 2001; **234**: 98-106
16 **Mueller AR**, Platz KP, Heckert C, Hausler M, Guckelberger O, Schuppan D, Lobeck H, Neuhaus P. Extracellular matrix: an early target of preservation / reperfusion injury and acute rejection after small bowel transplantation. *Transplant Proc* 1998; **30**: 2569-2571
17 **Shah KA**, Shurey S, Green CJ. Characterization of apoptosis in intestinal ischaemia-reperfusion injury - a light and electron microscopic study. *Int J Exp Pathol* 1997; **78**: 355-363
18 **Monchik GJ**, Russell PS. Transplantation of small bowel in the rat: technical and immunological considerations. *Surgery* 1971; **70**: 693-702
19 **Wu XT**, Li JS, Zhao XF, Zhuang W, Feng XL. Modified techniques of heterotopic total small intestinal transplantation in rats. *World J Gastroenterol* 2002; **8**: 758-762
20 **Li YX**, Li JS, Li N. Improved technique of vascular anastomosis for small intestinal transplantation in rats. *World J Gastroenterol* 2000; **6**: 259-262

21 **Li YX**, Li JS, Li N. Surgical technique for intestinal transplantation in rats. *Huaren Xiaohua Zazhi* 1998; **6**: 667-669

22 **Giele HP**, Heel KA, Storrie A, McCauley RD, Hall JC. Warm ischaemia time in a model for small bowel transplantation. *Microsurgery* 1996; **17**: 438-443

23 **Wu MY**, Liang YR, Wu XY, Zhuang CX. Relationship between Egr-1 gene expression and apoptosis in esophageal carcinoma and precancerous lesions. *World J Gastroenterol* 2002; **8**: 971-975

24 **Farber A**, Connors JP, Friedlander RM, Wagner RJ, Powell RJ, Cronenwett JL. A specific inhibitor of apoptosis decreases tissue injury after intestinal ischemia-reperfusion in mice. *J Vasc Surg* 1999; **30**: 752-760

25 **Noda T**, Iwakiri R, Fujimoto K, Matsuo S, Aw TY. Programmed cell death induced by ischemia-reperfusion in rat intestinal mucosa. *Am J Physiol* 1998; **274**: G270-276

26 **Taguchi T**, Shima Y, Nakao M, Fujii Y, Tajiri T, Ogita K, Suita S. Activation of immediate early genes in relation to proliferation and apoptosis of enterocytes after ischemia-reperfusion injury of small intestine. *Transplant Proc* 2002; **34**: 983

27 **Zhao ZQ**, Liu FL, Zhang L. Expressions of C-fos PCNA and Bax in intestine after ischemia and in dogs. *Shijie Huaren Xiahua Zazhi* 2001; **9**: 1021-1026

28 **Luo YQ**, Ma LS, Zhao YL, Wu KC, Pan BR, Zhang XY. Expression of proliferating cell nuclear antigen in polyps from large intestine. *World J Gastroenterol* 1999; **5**: 160-164

29 **Prelich G**, Tan CK, Kostura M, Mathews MB, So AG, Downey KM, Stillman B. Functional identity of proliferating cell nuclear antigen and a DNA polymerase-delta auxiliary protein. *Nature* 1987; **326**: 517-520

30 **Murry CE**, Jennings RB, Reimer KA. Preconditioning with ischemia: a delay of lethal cell injury in ischemic myocardium. *Circulation* 1986; **74**: 1124-1136

31 **Aksoyek S**, Cinel I, Avlan D, Cinel L, Ozturk C, Gurbuz P, Nayci A, Oral U. Intestinal ischemic preconditioning protects the intestine and reduces bacterial translocation. *Shock* 2002; **18**: 476-480

32 **Vlasov TD**, Smirnov DA, Nutfullina GM. Preconditioning of the small intestine to ischemia in rats. *Neurosci Behav Physiol* 2002; **32**: 449-453

33 **Yang SP**, Hao YB, Wu YX, Dun W, Shen LH, Zhang Y. Ischemic preconditioning mediated by activation of KATP channels in rat small intestine. *Zhongguo Yaoli Xuebao* 1999; **20**: 341-344

34 **Dun Y**, Hao YB, Wu YX, Zhang Y, Zhao RR. Protective effects of nitroglycerin-induced preconditioning mediated by calcitonin gene-related peptide in rat small intestine. *Eur J Pharmacol* 2001; **430**: 317-324

35 **Zhang Y**, Wu YX, Hao YB, Dun Y, Yang SP. Role of endogenous opioid peptides in protection of ischemic preconditioning in rat small intestine. *Life Sci* 2001; **68**: 1013-1019

36 **Davis JM**, Gute DC, Jones S, Krsmanovic A, Korthuis RJ. Ischemic preconditioning prevents postischemic P-selectin expression in the rat small intestine. *Am J Physiol* 1999; **277**: H2476-2481

37 **Ikeda H**, Suzuki Y, Suzuki M, Koike M, Tamura J, Tong J, Nomura M, Itoh G. Apoptosis is a major mode of cell death caused by ischaemia and ischaemia / reperfusion injury to the rat intestinal epithelium. *Gut* 1998; **42**: 530-537

38 **Fukuyama K**, Iwakiri R, Noda T, Kojima M, Utsumi H, Tsunada S, Sakata H, Ootani A, Fujimoto K. Apoptosis induced by ischemia-reperfusion and fasting in gastric mucosa compared to small intestinal mucosa in rats. *Dig Dis Sci* 2001; **46**: 545-549

39 **Fujisaki** S, Kimizuka K, Park E, Tomita R, Fukuzawa M, Matsumoto K. Immunohistochemical analysis in the extracellular matrix during acute rejection of small bowel grafts in rats. *Transplant Proc* 2000; **32**: 1316-1317

40 **Liu CQ**, Ye JX, Jin B. Components of the extracelluarr matrix. *Shijie Huaren Xiaohua Zazhi* 2002; **10**: 53-54

41 **Mueller AR**, Platz KP, Heckert C, Hausler M, Schuppan D, Lobeck H, Neuhaus P. Differentiation between preservation reperfusion injury and acute rejection after small bowel transplantation. *Transplant Proc* 1998; **30**: 2657-2659

Edited by Zhang JZ and Wang XL

P.O.Box 2345, Beijing 100023,China
Fax: +86-10-85381893
E-mail: wjg@wjgnet.com www.wjgnet.com

World J Gastroenterol 2003;9(8):1871-1873
World Journal of Gastroenterology
 ISSN 1007-9327

• BRIEF REPORTS •

Outcome of gallbladder preservation in surgical management of primary bile duct stones

Ming-Guo Tian, Wei-Jin Shi, Xin-Yuan Wen, Hai-Wen Yu, Jing-Shan Huo, Dong-Feng Zhou

Ming-Guo Tian, Xin-Yuan Wen, Hai-Wen Yu, Jing-Shan Huo, Dong-Feng Zhou, Department of Hepatobiliary Surgery, Affiliated Hospital of Jining Medical College, Jining 272129, Shandong Province, China
Wei-Jin Shi, Department of General Surgery, Ren Ji Hospital of Shanghai Second Medical University, Shanghai 200001, China
Correspondence to: Dr. Ming-Guo Tian, Department of Hepatobiliary Surgery, Affiliated Hospital of Jining Medical College, Jining City 272129, Shandong Province, China. tian88@hotmail.com
Telephone: +86-537-2903270 **Fax:** +86-537-2213030
Received: 2003-02-25 **Accepted:** 2003-03-29

Abstract

AIM: To evaluate the methods and outcome of gallbladder preservation in surgical treatment of primary bile duct stones.

METHODS: Thirty-five patients with primary bile duct stones and intact gallbladders received stone extraction by two operative approaches, 23 done through the intrahepatic duct stump (RBD-IDS, the RBD-IDS group) after partial hepatectomy and 12 through the hepatic parenchyma by retrograde puncture (RBD-RP, the RBD-RP group). The gallbladders were preserved and the common bile duct (CBD) incisions were primarily closed. The patients were examined postoperatively by direct cholangiography and followed up by ultrasonography once every six months.

RESULTS: In the RBD-IDS group, residual bile duct stones were found in three patients, which were cleared by a combination of fibrocholedochoscopic extraction and lithotripsy through the drainage tracts. The tubes were removed on postoperative day 22 (range: 16-42 days). In the RBD-RP group, one patient developed hemobilia and was cured by conservative therapy. The tubes were removed on postoperative day 8 (range: 7-11 days). Postoperative cholangiography showed that all the gallbladders were well opacified, contractile and smooth. During 54 (range: 6-120 months) months of follow-up, six patients had mildly thickened cholecystic walls without related symptoms and further changes, two underwent laparotomies because of adhesive intestinal obstruction and gastric cancer respectively, three died of cardiopulmonary diseases. No stones were found in all the preserved gallbladders.

CONCLUSION: The intact gallbladders preserved after surgical extraction of primary bile duct stones will not develop gallstones. Retrograde biliary drainage is an optimal approach for gallbladder preservation.

Tian MG, Shi WJ, Wen XY, Yu HW, Huo JS, Zhou DF. Outcome of gallbladder preservation in surgical management of primary bile duct stones. *World J Gastroenterol* 2003; 9(8): 1871-1873
http://www.wjgnet.com/1007-9327/9/1871.asp

INTRODUCTION

The gallbladder is important for digestion. Cholecystectomy can give rise to postoperative symptoms such as flatulent dyspepsia, abdominal pain, distention, heart burn, obstipation and diarrhea[1-5], and may lead to increase of incidence of carcinoma of the proximal colon[6]. Many patients with primary bile duct stones do not have stones in the gallbladders. However, as T-tube drainage after common bile duct (CBD) exploration may cause adhesion and subsequent cholecystitis and stone formation, these intact gallbladders are often concomitantly resected. Since 1991, we have adopted retrograde biliary drainage instead of T-tube drainage for primary bile duct stones. Thirty-five intact gallbladders have been thus preserved.

MATERIALS AND METHODS

Patients

Thirty-five patients with primary bile duct stones and intact gallbladders received retrograde biliary drainage (RBD) between December 1991 and December 2001. The age of the patients ranged from 29 to 70 (mean 44) years. Preoperative diagnosis was made by ultrasonography and in some cases by a combination with percutaneous transhepatic cholangiography (PTC). During the operation, the gallbladders were normal in appearance and no stones and lesions were found by intraoperative ultrasonography (IOUS). Stones extracted from the bile ducts had the typical features of pigment stones with brown color and soft quality. Stone distribution and the operation methods are shown in Table 1. Postoperatively, all the patients were routinely examined by direct cholangiography and followed up once every six months by ultrasonography. The follow-up duration ranged from 6 to 120 (mean 54 months) months.

Table 1 Stone distribution and operation methods

Stone distribution	Cases	Operation methods	Cases
Left hepatic	11	RBD-IDS&II, III segmentectomy	15
Extrahepatic	8	RBD-RP	12
Intra-and extrahepatic	8	RBD-IDS & left hepatectomy	6
Bilateral hepatic	7	RBD-IDS & III segmentectomy	1
Segment VII	1	RBD-IDS & VII segmentectomy	1
Total	35	Total	35

Notes: RBD-RP: retrograde biliary drainage by retrograde puncture, RBD-IDS: retrograde biliary drainage through intrahepatic duct stump.

Methods

RBD through intrahepatic duct stump (RBD-IDS) After partial hepatectomy for intrahepatic bile duct stones, biliary tract exploration was done by fibrocholedochoscopy through the intrahepatic bile duct stump. The CBD was incised in the patient with big concurrent extrahepatic bile duct stones which could not be extracted retrogradely. The RBD tube was placed through the hepatic duct stump and the CBD incision was closed primarily. In case of suspected residual stones, the RBD

tube was sheathed by a tube of larger bore from the abdominal wall to the lumen of the stump.

RBD by retrograde puncture (RBD-RP) After CBD exploration and stone clearance, a guide sheath was inserted into the right hepatic duct, with the tip as deep in the duct as possible. The direction was regulated with IOUS to avoid injury of large blood vessels. An 8Fr cannula fitting over a matching stylet was inserted through the guide sheath and pushed forward until the tip came out of the liver. From the other end, an 8Fr Silastic drainage tube was inserted over the guide wire which was introduced through the cannula. When the tip of the drainage tube emerged in the CBD incision, the guide wire, retrograde cannula and guide sheath were retracted together. The end of the drainage tube was brought out of the abdominal wall subcostally. The CBD incision was primarily closed. Intraoperative cholangiography was done to rule out residual stones in some suspected cases.

RESULTS

In the RBD-IDS group, postoperative drainage of bile was 340-780 ml/d (mean 440±140 ml/d). The drainage tubes were removed on postoperative day 16-42 (mean 22 days). Residual stones were found in three cases. After four weeks, stone extraction started through the tracts with the help of fibrocholedochoscope and ultrasonic lithotriptor. All patients had the stones cleared after 2-5 sessions of extraction. In the RBD-RP group, postoperative drainage of bile was 150-800 ml/d (mean 520±210 ml/d). Bile drainage was interrupted intermittently in two patients owing to blockage of the tubes and it resumed to draining after flushing with normal saline. The drainage tubes were removed on postoperative day 7-11 (mean 8 days). Hemobilia occurred in one earlier treated patient. She recovered soon after conservative therapy. No tube dislocation or residual stones occurred in this series.

Postoperative cholangiography of both methods showed that the extrahepatic bile ducts had no stricture at the sites of CBD incisions. The preserved gallbladders were well opacified, contractile and smooth (Figure 1). During the follow-up, six patients were found to have rough and mildly thickened cholecystic walls at 12-36 months after operation. However, these patients had no related symptoms and no further changes afterwards. Two patients underwent laparotomies because of adhesive intestinal obstruction and gastric cancer, respectively. Three died of cardiopulmonary diseases. No stones occurred in the preserved gallbladders.

Figure 1 Direct cholangiogram showed that the preserved gallbladder was well opacified and contractile.

DISCUSSION

A high recurrent rate of gallbladder stone after successful extracorporeal shock wave lithotripsy and dissolution has been documented by many reports[7-11]. However, the gallbladders after endoscopic sphincterotomy for common bile duct calculi rarely formed stones[12-14]. One explanation for the difference of the results is that sphincterotomy decreases fasting volume of the gallbladder and increases its contraction ability[15, 16]. Another is that the primary bile duct pigment stone is different from the cholecystic cholesterol one in both epidemiology[17-21] and pathogenesis[22-26]. It is therefore generally considered that both kinds of stones are different diseases[26]. The results of this study also showed that the gallbladders preserved during operation of the patients with primary bile duct stones had no tendency to form stones. As most gallbladders of the patients with primary intrahepatic bile duct stones are not affected, concomitant cholecystectomy during surgical extraction of stones or liver resection in these patients seems unjustified.

T-tube drainage after choledochostomy or after liver resection is a conventional method for primary bile duct stones. However, many reports in recent decades have demonstrated the problems it brought about[27,28]. The long tube-bearing not only results in inconvenience, but also causes pathological changes of the CBD[29]. T-tube tract can also adhere to the gallbladder and impair its function. Therefore, intact gallbladder is often concomitantly resected during these operations. In recent years, several alternatives to T-tube drainage have been reported[30-33]. However, preservation of the gallbladder during surgical management of primary bile duct stones and its long-term outcome have not been reported yet. After retrograde biliary drainage, the function of the gallbladder will not be impaired by tube stimulation or tube induced local adhesion because the gallbladder does not contact the drainage tube. This study also demonstrated that both methods had respective advantages over T-tube placement in residual stone management and the duration of tube-bearing.

Therefore, we conclude that retrograde biliary drainage is an optimal method for preservation of gallbladder during surgical management of primary bile duct stones.

REFERENCES

1 **Ure BM**, Troidl H, Spangenberger W, Lefering R, Dietrich A, Eypasch EP, Neugebauer E. Long-term results after laparoscopic cholecystectomy. *Br J Surg* 1995; **82**: 267-270

2 **Sand J**, Pakkala S, Nordback I. Twenty to thirty year follow-up after cholecystectomy. *Hepatogastroenterology* 1996; **43**: 534-537

3 **Ros E**, Zambon D. Postcholecystectomy symptoms. A prospective study of gall stone patients before and two years after surgery. *Gut* 1987; **28**: 1500-1504

4 **McNamara DA**, O'Donohoe MK, Horgan PG, Tanner WA, Keane FB. Symptoms of esophageal reflux are more common following laparoscopic cholecystectomy than in a control population. *Ir J Med Sci* 1998; **167**: 11-13

5 **Carrilho-Ribeiro L**, Serra D, Pinto-Correia A, Velosa J, De Moura MC. Quality of life after cholecystectomy and after successful lithotripsy for gallbladder stones: a matched-pairs comparison. *Eur J Gastroenterol Hepatol* 2002; **14**: 741-744

6 **Alley PG**, Lee SP. The increased risk of proximal colonic cancer after cholecystectomy. *Dis Colon Rectum* 1983; **26**: 522-524

7 **Pelletier G**, Raymond JM, Capdeville R, Mosnier H, Caroli-Bosc FX. Gallstone recurrence after successful lithotripsy. *J Hepatol* 1995; **23**: 420-423

8 **Plauletzki J**, Holl J, Sackmann M, Neubrand M, Klueppelberg U, Sauerbruch J, Paumgartner G. Gallstone recurrence after direct contact dissolution with methyl tert-butyl ether. *Dig Dis Sci* 1995; **40**: 1775-1781

9 **Benes J**, Chmel J, Blazek O, Marecek Z. Extracorporeal shock wave lithotripsy of gallstones with oral dissolution: results in course of ten years in czech republic in correlation to indication criteria. *Sb Lek* 2001; **102**: 17-22

10 **Chen P**, Wang BS, He LQ. Multifactorial analysis of recurrence of cholecy stolithiasis in Shanghai area. *World J Gastroenterol* 1999; **5**: 31-33

11 **Janssen J**, Johanns W, Weickert U, Rahmatian M, Greiner L. Long-term results after successful extracorporeal gallstone lithotripsy: outcome of the first 120 stone-free patients. *Scand J Gastroenterol* 2001; **36**: 314-317

12 **Kwon SK**, Lee BS, Kim NJ, Lee HY, Chae HB, Youn SJ, Park SM. Is cholecystectomy necessary after ERCP for bile duct stones in patients with gallbladder in situ? *Korean J Intern Med* 2001; **16**: 254-259

13 **Benattar JM**, Caroli-Bosc FX, Harris AG, Dumas R, Delmont J. Endoscopic sphincterotomy for common bile duct calculi in patients without stones in the gallbladder. *Dig Dis Sci* 1993; **38**: 2225-2227

14 **Tanaka M**, Ikeda S, Yoshimoto H, Matsumoto S. The long term fate of the gallbladder after endoscopic sphincterotomy. *Am J Surg* 1987; **154**: 505-509

15 **Sugiyama M**, Atomi Y. Long term effects of endoscopic sphincterotomy on gall bladder motility. *Gut* 1996; **39**: 856-859

16 **Sharma BC**, Agarwal DK, Baijal SS, Negi TS, Choudhuri G, Saraswat VA. Effect of endoscopic sphincterotomy on gall bladder bile lithogenicity and motility. *Gut* 1998; **42**: 288-292

17 **Kawai M**, Iwahashi M, Uchiyama K, Ochiai M, Tanimura H, Yamaue H. Gram-positive cocci are associated with the formation of completely pure cholesterol stones. *Am J Gastroenterol* 2002; **97**: 83-88

18 **Lee DK**, Tarr PI, Haigh WG, Lee SP. Bacterial DNA in mixed cholesterol gallstones. *Am J Gastroenterol* 1999; **94**: 3502-3506

19 **Ko CW**, Lee SP. Gallstone formation: local factors. *Gastroenteral Clin North Am* 1999; **28**: 99-115

20 **Sandstad O**, Osnes T, Skar V, Urdal P, Osnes M. Structure and composition of common bile duct stones in relation to duodenal diverticula, gastric resection, cholecystectomy and infection. *Digestion* 2000; **61**: 181-188

21 **Makino I**, Chijiiwa K, Higashijima H, Nakahara S, Kishinaka M, Kuroki S, Mibu R. Rapid cholesterol nucleation time and cholesterol gall stone formation after subtotal or total colectomy in humans. *Gut* 1994; **35**: 1760-1764

22 **Donovan JM**. Physical and metabolic factors in gallstone pathogenesis. *Gastroenterol Clin North Am* 1999; **28**: 75-97

23 **Higashijima H**, Ichimiya H, Nakano T, Yamashita H, Kuroki S, Satoh H, Chijiiwa K, Tanaka M. Deconjugation of bilirubin accelerates coprecipitation of cholesterol, fattyacids, and mucin in human bile - *in vitro* study. *J Gastroenterol* 1996; **31**: 828-835

24 **Diehl AK**, Schwesinger WH, Holleman DR Jr, Chapman JB, Kurtin WE. Clinical correlates of gallstone composition: distinguishing pigment from cholesterol stones. *Am J Gastroenterol* 1995; **90**: 967-972

25 **Ho KJ**, Lin XZ, Yu SC, Chen JS, Wu CZ. Cholelithiasis in Taiwan: Gallstone characteristics, surgical incidence, bile lipid composition, and role of beta-glucuronidase. *Dig Dis Sci* 1995; **40**: 1963-1973

26 **Sarli L**, Gafa M, Bonilauti E, Longinotti E, Carreras F, Pietra N, Peracchia A. Pigment vs. cholesterol microlithiasis: comparison of clinical features, bacteriology, stone and gallbladder composition. *Hepatogastroenterology* 1989; **36**: 156-159

27 **Wills VL**, Gibson K, Karihaloot C, Jorgensen JO. Complications of biliary T-tube after choledochotomy. *ANZ J Surg* 2002; **72**: 177-180

28 **Corbett CR**, Fyfe NC, Nicholls RJ, Jackson BT. Bile peritonitis after removal of T-tubes from the common bile duct. *Br J Surg* 1986; **73**: 641-643

29 **Lee SH,** Burhenne HJ. Extrahepatic bile duct angulation by T-tube: the elbow sign. *Gastrointest Radiol* 1991; **16**: 157-158

30 **Zhi QH**. New development of biliary surgery in China. *World J Gastroenterol* 2000; **6**: 187-192

31 **Tsunoda T**, Kusano T, Furukawa M, Eto T, Tsuchiya R. Common bile duct exploration--primary closure of the duct with retrograde transhepatic biliary drainage. *Jpn J Surg* 1991; **21**: 162-166

32 **Tian MG**, Wen XY, Liu ZY, Cao HX, Li H. Operative percutaneous transhepatic biliary catheterization by retrograde puncture. *Zhongguo Putong Waike Zazhi* 1995; **4**: 91-93

33 **Goseki N**, Methaste A, Gen T, Ito K, Endo M. Extraperitoneal retrograde transhepatic biliary drainage for common bile duct exploration for prevention of tube dislodgement and its earlier removal. *Dig Surg* 1998; **15**: 12-14

Edited by Xu XQ

P.O.Box 2345, Beijing 100023,China
Fax: +86-10-85381893
E-mail: wjg@wjgnet.com www.wjgnet.com

World J Gastroenterol 2003;9(8):1874-1877
World Journal of Gastroenterology
 ISSN 1007-9327

• BRIEF REPORTS •

Effects of neurotrophins on gastrointestinal myoelectric activities of rats

Ning-Li Chai, Lei Dong, Zong-Fang Li, Ke-Xin Du, Jian-Hua Wang, Li-Kun Yan, Xi-Lin Dong

Ning-Li Chai, Lei Dong, Xi-Lin Dong, Department of Digestion, Second Affiliated Hospital, Xi' an Jiaotong University, Xi' an 710004, Shaanxi Province, China
Zong-Fang Li, Department of General Surgery, Second Affiliated Hospital, Xi' an Jiaotong University, Xi' an 710004, Shaanxi Province, China
Ke-Xin Du, Functional Center of Medical School, Xi' an Jiaotong University, Xi' an 710061, Shaanxi Province, China
Jian-Hua Wang, Li-Kun Yan, Department of General Surgery, Shaanxi Provincial People' s Hospital, Xi' an 710068, Shaanxi Province, China
Supported by the National Natural Science Foundation of China, No. 30170414
Correspondence to: Lei Dong, Department of Digestion, Second Affiliated Hospital, Xi' an Jiaotong University, Xi' an 710004, Shaanxi Province, China. csxlily@ hotmail.com
Telephone: +86-29-8024005 **Fax:** +86-29-7231758
Received: 2003-01-18 **Accepted:** 2003-03-10

Abstract

AIM: To observe the effects of mouse nerve growth factor (NGF), rat recombinant brain derived neurotrophic factor (rm-BDNF) and recombinant human neurotrophin-3 (rh-NT-3) on the gastrointestinal motility and the migrating myoelectric complex (MMC) in rat.

METHODS: A randomized, double-blinded, placebo-controlled experiment was performed. 5-7 days after we chronically implanted four or five bipolar silver electrodes on the stomach, duodenum, jejunum and colon, 21 experimental rats were coded and divided into 3 groups and injected NGF, rm-BDNF, rh-NT-3 or placebo respectively via tail vein at a dose of 20 $\mu g \cdot kg^{-1}$. The gastrointestinal myoelectrical activity was recorded 2 hours before and after the test substance infusions in these consciously fasting rats.

RESULTS: The neurotrophins-induced pattern of activity was characterized by enhanced spiking activity of different amplitudes at all recording sites, especially in the colon. In the gastric antrum and intestine, only rh-NT-3 had increased effects on the demographic characteristics of electrical activities ($P<0.05$), but did not affect the intervals of MMCs. In the colon, all the three kinds of neurotrophins could significantly increase the frequency, amplitude and duration levels of spike bursts, and also rh-NT-3 could prolong the intervals of MMC in the transverse colon (25±11 min *vs* 19±6 min, $P<0.05$). In the distal colon rh-NT-3 could evoke phase III-like activity and disrupt the MMC pattern, which was replaced by a continuously long spike bursts (LSB) and irregular spike activity (ISA) for 48±6 min.

CONCLUSION: Exogenous neurotrophic factors can stimulate gut myoelectric activities in rats.

Chai NL, Dong L, Li ZF, Du KX, Wang JH, Yan LK, Dong XL. Effects of neurotrophins on gastrointestinal myoelectric activities of rats. *World J Gastroenterol* 2003; 9(8): 1874-1877
http://www.wjgnet.com/1007-9327/9/1874.asp

INTRODUCTION

Many basic studies have shown that neurotrophins play fundamental roles in the differentiation, survival and maintenance of peripheral and central neurons[1-5] and have suggested the possible use of neurotrophins as therapeutic tools for degenerative neuronal disorders[6]. Neurotrophic factors comprise nerve growth factor (NGF), brain-derived neurotrophic factor (BDNF), neurotrophin-3 (NT-3), NT-4/5, and NT-6[7-9]. These factors signal their effects through specific tyrosine-kinase (trk) receptors[10,11]. In addition to the high sequence homology of neurotrophins, neurotrophic factors including NT-3, BDNF and NGF are also highly conserved across species (mouse, rat and human)[13].

In a clinical study of patients with a variety of neurologic disorders treated with rh-NT-3 or recombinant human BDNF (rh-BDNF), they were found to have alterations of bowel function, and a dose-related tendency to increasing frequency of stools or having "diarrhea"[14]. Studies also have proved that exogenous neurotrophic factors stimulate gut motility and accelerate colonic transit in health and constipation[14]. This suggests that the action of rh-NT-3 and rh-BDNF on the gastrointestinal tract parallels their effect on the central nervous system. Review of the clinical reports suggested an increased frequency of bowel movements with less impressive effects on stool consistency[15], but the mechanism is unclear so far.

All the conclusions of previous studies lead to the hypothesis that neurotrophins alter bowel motor function, leading to increased frequency of bowel movements. In order to assess the action of neurotrophins on gut motility, in the present study we injected respectively NGF, rm-BDNF and rh-NT-3 via tail vein and registered the electrical activities with chronically implanted electrodes in fasting rats.

MATERIALS AND METHODS

Animal preparation

21 healthy Sprague-Dawley (SD) rats, weighing 250-300 (mean 276±17) g, 15 male and 6 female, individually housed, fed on chow pellets and water *ad libitum*, were used for these experiments. After fasted for 24 h, the rats were intraperitoneally anesthetized with sodium pentobarbital 30 $mg \cdot kg^{-1}$ (ip) A segment of the small intestine was exposed through a midline incision. Four or five bipolar insulated silver electrodes made by teflon-coated wire (0.5 mm in outer diameter, 20 cm in length) were implanted into the muscular layer of the bowel with a needle as a trocar. 1 mm of the wire was exposed near the implanted end, and the interval between pairs of electrodes should be 2.0-3.0 mm. The electrodes were placed on the gastric antrum at 5 mm proximal to the pylorus, on the duodenum and jejunum respectively at 5 cm and 20 cm distal to the pylorus, and on the transverse colon 5 cm distal to the ileocaecal junction. Among the 21 experimental animals, 9 were implanted electrodes on the distal colon 10 cm distal to the ileocaecal junction at the same time. The bundled electrode wires were grasped by the clamp through a silastic tube (2.4 mm in diameter), which then passed

through the subcutaneous tunnel from the abdominal incision to the back of the shoulder exit. Following surgery, the rats were individually housed, and allowed 5 to 7 days to recover from the surgery.

Motility recordings

The animals were fasted for 8 h with free access to water. The experiments were performed in conscious rats. The electromyographic (EMG) recordings were monitored by using a polygraph (Biolap98, Chengdu, China), with time constant set at 0.01 s, gain set at 1 000, the filtering at lower and higher frequencies set at 0.3 Hz and 100 Hz, respectively. The amplitudes of contractions were recorded in microvolts and the paper speed was 5 cm· h^{-1}.

Experimental procedure

A randomized, double-blinded, placebo-controlled experiment was performed. The rats were coded and divided into 3 groups, 7 animals in each group. On each experimental day, at the beginning of the experiments, the gastrointestinal myoelectrical activity was recorded for 2 h for each rat, and during this period at least 3 MMCs appeared. Then, the test substances were infused through the tail vein. The substances were dissolved immediately before use in normal saline. In each group, 2 rats were placed as control that received placebo (vehicle), 0.2 mL saline containing 250 μg bovine serum albumin (BSA, Sigma), the other 5 received 0.2 ml saline containing neurotrophins at a dose of 20 μg· kg^{-1}. Of them, 3 were placed electrodes on the distal colon as well. The three groups were injected them NGF (Sigma), rm-BDNF (Sigma) and rh-NT-3 (Sigma), respectively. After tail vein injection, the gastrointestinal myoelectrical activity of the rats was continuously recorded at least for 2 h. The codes of rats were not released (sealed) for analysis until all the EMG recordings and the entire data set for statistical studies were completed.

Statistical analysis

The results were expressed as $\bar{x}\pm s$ unless otherwise stated. Student' s *t* test was used to compare the different paired values before and after the test substance administration in the 3 groups. It was considered to be statistically significant when $P<0.05$.

RESULTS

Gastrointestinal myoelectrical activity during fasting

About 1 week later, among the 93 pairs of electrodes, 2 pairs implanted on the gastric antrum failed possibly due to the their slipping off, the other 91 pairs continued to function until the study was completed. A typical pattern of myoelectrical activity in the fasting state was observed in all rats (Figure 1, Table 1). Of the totally 238 activity fronts recorded in fasting rats under control, we observed that 199 (80 %) started in the duodenum.

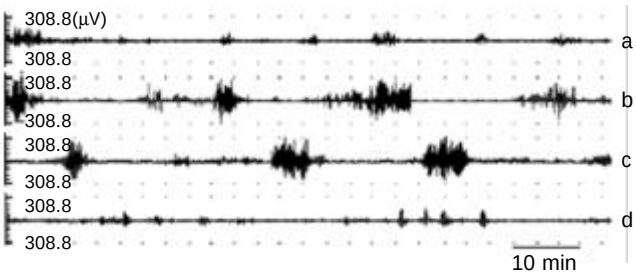

Figure 1 Electrical activity recorded directly from four electrode sites on the gastric antrum (a) at 5 mm proximal to the pylorus, on the duodenum (b) and jejunum (c) respectively at 5 cm and 20 cm distal to the pylorus, and on the transverse colon (d) at 5 cm distal to the ileocaecal junction in one fasting rat.

The antral myoelectrical activity was characterized by the presence of spike bursts, superimposed at 34.5 % of the

Table 1 Effects of neurotrophins (20 μg· kg^{-1}) on gut myoelectric activity profiles 2 h before and 1 h after administration. ($\bar{x}\pm s$)

Parameter	Site	*n*	NGF treatment		rm-BDNF treatment		rh-NT-3 treatment		Placebo treatment	
			Before	After	Before	After	Before	After	Before	After
	Antrum	5	1.6±0.5	1.6±0.5	1.6±0.5	1.6±0.5	1.6±0.5	1.8±0.6[a]	1.6±0.5	1.6±0.5
Frequency of	Duodenum	5	16.2±5.4	17.5±5.8	15.9±5.2	17.2±5.9	16.3±5.6	20.1±9.3[a]	16.3±5.4	16.5±5.6
spike bursts	Jejunum	5	12.1±2.8	13.5±3.4	11.9±2.6	13.2±3.7	12.2±2.7	16.5±7.1[a]	12.5±2.9	12.4±2.8
(min^{-1})	Transverse colon	5	0.6±0.1	0.8±0.1[a]	0.6±0.1	0.8±0.1[a]	0.6±0.1	0.9±0.2[b]	0.6±0.1	0.6±0.1
	Distal colon*	3	0.5±0.1	0.7±0.1[a]	0.5±0.1	0.7±0.1[a]	0.5±0.1	0.9±0.2[b]		
	Antrum	5	180.2±18.6	182.3±19.1	181.3±17.9	182.5±20.4	180.6±17.9	185.2±22.1[a]	180.9±18.8	180.4±18.9
Amplitude of	Duodenum	5	306.5±73.6	308.8±72.7	306.7±72.9	308.4±72.4	306.5±72.7	314.6±81.8[a]	305.6±74.2	306.2±74.5
spike bursts	Jejunum	5	295.8±87.2	297.4±88.5	296.5±88.1	298.6±89.3	295.6±86.7	313.8±98.3[b]	296.8±87.3	295.8±88.5
(μV)	Transverse colon	5	138.7±32.1	142.5±35.9[a]	139.4±33.4	145.5±38.8[a]	139.5±33.3	160.3±47.5[b]	137.9±31.8	139.1±32.5
	Distal colon*	3	142.9±29.9	163.5±40.1[a]	141.2±27.3	160.5±37.4[a]	142.6±29.1	173.4±35.4[b]		
	Antrum	5	4.8±1.1	4.8±1.2	4.7±1.2	4.9±1.3	4.8±1.2	4.9±1.5	4.8±1.2	4.8±1.2
Duration of	Duodenum	5	6.5±2.7	6.6±3.1	6.5±2.8	6.6±3.2	6.5±2.8	11.5±6.8[a]	6.5±2.8	6.5±2.7
spike bursts	Jejunum	5	6.7±3.1	6.8±3.2	6.7±3.1	6.9±3.4	6.8±3.2	12.9±8.3[a]	6.8±3.2	6.8±3.2
(s)	Transverse colon	5	9.3±2.2	14.3±6.2[a]	9.3±2.2	13.5±7.2[a]	9.3±2.3	15.3±7.5[a]	9.3±2.2	9.3±2.3
	Distal colon*	3	12.7±2.7	17.8±3.8[a]	12.7±2.7	19.7±4.7[a]	12.7±2.8	46.2±7.3[b]		
	Antrum	5	10.1±3.1	11.3±4.0	10.2±3.4	11.3±4.3	10.1±3.1	12.3±6.2	10.3±3.3	10.2±3.1
Intervals	Duodenum	5	15.3±5.4	16.9±6.1	16.1±5.5	17.2±6.2	15.5±5.5	17.3±7.5	15.6±5.5	15.6±5.2
of MMC	Jejunum	5	16.8±5.8	18.2±7.4	17.1±5.9	18.9±7.6	16.8±5.8	19.1±9.1	16.4±5.6	16.4±5.6
(min)	Transverse colon	5	18.4±6.0	19.7±6.1	19.3±6.1	21.0±7.5	18.9±6.0	25.1±11.1[a]	19.2±6.2	19.7±6.3
	Distal colon*	3	19.7±4.1	22.2±8.0	20.8±5.3	23.5±8.4	19.9±4.2	-		

[a]$P<0.05$, [b]$P<0.01$ *vs* before, * There were 3 among 5 experimental rats in the three groups placed bipolar electrodes at distal colon.

rhythmic oscillatory potentials corresponding to the slow wave rhythm. In fasting rats, the pattern of spike bursts of the small intestine was organized into cyclic MMCs that occurred at regular 15.6±5.4 min intervals and were propagated from the duodenum to the jejunum at 2 to 3 cm· min^{-1}. Each MMC was a cycle consisting of four phases: a period of silence (slow wave), namely phase I lasting 7.3±0.8 min, which was followed sequentially by a period of ISA (irregular spike activity), namely phase II lasting 4.1±0.9 min, and phase III of intense RSA (regular spike activity) lasting 3.6±1.1 min. Phase IV was the last period from the end of phase III to the start of phase I lasting 0.9±0.3 min. The intervals between the MMCs were measured from the end of one activity before to the end of the next one.

The pattern of colonic myoelectrical activity was characterized by randomly occurring spike bursts at a frequency of 0.6±0.07 per minute in the transverse colon and 0.5±0.09 per minute in the distal colon.

Effects of neurotrophins on the gastrointestinal and colon myoelectric activity

The effect of neurotrophins on the gastrointestinal motility was established within 2 to 4 min after commencement of the infusion. The neurotrophin-induced pattern of activity was characterized by enhanced spiking activity of different amplitudes at all recording sites, especially at the colon, which continued about 50±8 min and gradually returned to normal complexes. There was no significant difference in demographic characteristics before and after placebo treatment. Table 1 summarizes the effect of neurotrophins on the different electromyographic parameters before and after treatment.

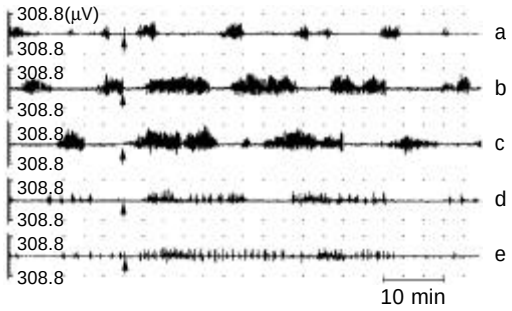

Figure 2 The effects of rh-NT-3 on the myoelectric activities respectively recorded from gastric antrum (a), duodenum (b), jejunum (c), transverse colon (d), and distal colon (e) in one case. The arrows indicated the time point of rh-NT-3 injection via tail vein at a dose of 20 μg·kg^{-1}.

In the gastric antrum and intestine of fasting rats, administration of 20 μg· kg^{-1} mouse NGF and rm-BDNF didn' t significantly increase electrical activities (P>0.05), whereas intravenous infusion of 20 μg· kg^{-1} rh-NT-3 could increase the frequency, amplitude and duration of spike bursts (P<0.05, Table 1), but did not affect the intervals of MMCs (Figure 2).

In the colon, treatment with mouse NGF and rm-BDNF prolonged the duration as well as increased the frequency and amplitude of spike bursts (P<0.05, Table 1) without alterations of MMC intervals. In the transverse colon, rh-NT-3 not only significantly increased the electrical activities, but also prolonged the intervals of MMC (25±11 min *vs* 19±6 min, P<0.05) (Figure 2). The distal colon electromyogram recordings in 3 cases implanted bipolar electrodes on the distal colon, showed that rh-NT-3 could evoke phase III-like activity and disrupt the MMC pattern that were replaced by a continuous long spike bursts (LSB) and irregular spike activity (ISA) for 48±6 min (Figure 2).

DISCUSSION

Previous studies showed that rm-BDNF and rh-NT-3 caused diarrhea in a dose-related manner[15] and that exogenous neurotrophic factors accelerated colonic transit and increased stool frequency in humans[14]. The present studies were carried out to evaluate comparatively the effects of NGF, rm-BDNF and rh-NT-3 on the gastrointestinal myoelectric activity in fasting rats. The study firstly showed that neurotrophin-induced pattern of activity was characterized by enhanced spiking activity of different amplitudes at all recording sites, especially in the colon. The MMCs were firstly described in the small intestine of fasting dogs and its presence was observed in several species, including rats. In the present studies, MMC was also observed in fasting rats and found that in gastric antrum and intestine, only rh-NT-3 had enhanced effects on demographic characteristics of electrical activities (P<0.05), but did not affect the intervals of MMCs. In the colon, not only all the three kinds of neurotrophins infusion could significantly increase the frequency, amplitude and duration of spike bursts, but also rh-NT-3 could prolong the intervals of MMC in the transverse colon (25±11 min *vs* 19±6 min, P<0.05), and in the distal colon, rh-NT-3 could evoke phase III-like activity and disrupt the MMC pattern, which was replaced by continuous LSB and ISA for 48±6 min. Thus the present results indicate that exogenous neurotrophic factors can stimulate gut myoelectric activity in rats. The recording of myoelectrical activity by means of chronically implanted electrodes in rats is a suitable experimental animal model to investigate the mechanism of action of neurotrophins on intestinal motility.

Our conclusion is consistent with the previous ones. Probably it can contribute to the explanation of the mechanisms of the rapid onset of diarrhea in clinical trials with these neurotrophins, that neurotrophins lead to increases of bowel motor, as a result the gastrointestinal contents are transmitted too quickly, leading to diarrhea for the water having not been fully absorbed.

Two mechanisms mediating the actions of neurotrophins on neuromuscular function are considered: trophic effects or a direct effect on neurotransmission[22]. The neurotrophins have long-term trophic actions, including prolongation of survival and speeding up phenotypic maturation of many types of neurons[16-19]. These functions are mediated by the Trk family of tyrosine kinase receptors[20-23]. Modulation of neurotransmission has been shown by acute or short-lived effects of neurotrophins[24,25]. For example, BDNF modulates neurotransmitter synthesis, increases neuronal excitability, and provides long-term synaptic potentiation of neurons[26], and it has been reported that NT-3 stimulates the expression of SP and neurotrophins, enhances not only synthesis but also storage of acetylcholine (Ach) in cultured septal neurons[27]. The time of the onset of effects on bowel movements with exogenous r-metHuBDNF and r-merHuNT-3 suggested direct actions on the neuromuscular apparatus or a very rapid trophic or regenerative effect on gut neuromuscular function. The other study suggested that the mechanism of rh-NT-3 excitation of colonic muscle involved increased noncholinergic contractility and decreased NANC neurotransmission with reduction in number of nitric oxide synthase (NOS) neurons. The abundance of BDNF protein in certain internal organs suggests that this neurotrophin may regulate the function of adult visceral sensory and motor neurons.

We are not quite clear why different enhancements of neurotrophins accelerating gut transition in the stomach, duodeno-jejunum and colon are possibly associated with the receptors of different neurotrophin distribution in gastrointestinal tract. Decreased trk C expression may reflect developmental abnormalities in Hirschsprung' s disease and idiopathic slow-transit constipation (STC)[28]. Further studies are needed to elucidate the precise mechanism by which neurotrophins

influence smooth muscle contractility and/or enteric nerve functions in the human gastrointestinal tract.

Gut motility disorder is common in clinical practice[29-33], and its suitable treatment should be studied[34-38]. In this respect, our data indicate that neurotrophins are the promising agents capable of modifying transit in the entire gastrointestinal tract and may provide novel treatments for patients with disturbed gut motility, such as Hirschspnmg' s disease[28, 39].

REFERENCES

1 **Shao Y,** Akmentin W, Toledo-Aral JJ, Rosenbaum J, Valdez G, Cabot JB, Hilbush BS, Halegoua S. Pincher, a pinocytic chaperone for nerve growth factor/TrkA signaling endosomes. *J Cell Biol* 2002; **157:** 679-691

2 **Chiabrando GA,** Sanchez MC, Skornicka EL, Koo PH. Low-density lipoprotein receptor-related protein mediates in PC12 cell cultures the inhibition of nerve growth factor-promoted neurite outgrowth by pregnancy zone protein and alpha2-macroglobulin. *J Neurosci Res* 2002; **70:** 57-64

3 **Groth R,** Aanonsen L. Spinal brain-derived neurotrophic factor (BDNF) produces hyperalgesia in normal mice while antisense directed against either BDNF or trkB, prevent inflammation-induced hyperalgesia. *Pain* 2002; **100:** 171-181

4 **Mizoguchi Y,** Monji A, Nabekura J. Brain-derived neurotrophic factor induces long-lasting Ca^{2+}-activated K^+ currents in rat visual cortex neurons. *Eur J Neurosci* 2002; **16:** 1417-1424

5 **Bartlett SE,** Reynolds AJ, Weible M, Hendry IA. Phosphatidylinositol kinase enzymes regulate the retrograde axonal transport of NT-3 and NT-4 in sympathetic and sensory neurons. *J Neurosci Res* 2002; **68:** 169-175

6 **Alberch J,** Perez-Navarro E, Canals JM. Neuroprotection by neurotrophins and GDNF family members in the excitotoxic model of Huntington's disease. *Brain Res Bull* 2002; **57:** 817-822

7 **Stucky C,** Shin JB, Lewin GR. Neurotrophin-4: a survival factor for adult sensory neurons. *Curr Biol* 2002; **12:** 1401-1404

8 **Caleo M,** Menna E, Chierzi S, Cenni MC, Maffei L. Brain-derived neurotrophic factor is an anterograde survival factor in the rat visual system. *Curr Biol* 2000; **10:** 1155-1161

9 **von Bartheld CS,** Wang X, Butowt R. Anterograde axonal transport, transcytosis, and recycling of neurotrophic factors: the concept of trophic currencies in neural networks. *Mol Neurobiol* 2001; **24:** 1-28

10 **Schneider MB,** Standop J, Ulrich A, Wittel U, Friess H, Andren-Sandberg A, Pour PM. Expression of nerve growth factors in pancreatic neural tissue and pancreatic cancer. *J Histochem Cytochem* 2001; **49:** 1205-1210

11 **Shinoda M,** Hidaka M, Lindqvist E, Soderstrom S, Matsumae M, Oi S, Sato O, Tsugane R, Ebendal T, Olson L. NGF, NT-3 and Trk C mRNAs, but not TrkA mRNA, are upregulated in the paraventricular structures in experimental hydrocephalus. *Childs Nerv Syst* 2001; **17:** 704-712

12 **Ricci A,** Greco S, Mariotta S, Felici L, Bronzetti E, Cavazzana A, Cardillo G, Amenta F, Bisetti A, Barbolini G. Neurotrophins and neurotrophin receptors in human lung cancer. *Am J Respir Cell Mol Biol* 2001; **25:** 439-446

13 **Mukai J,** Hachiya T, Shoji-Hoshino S, Kimura MT, Nadano D, Suvanto P, Hanaoka T, Li Y, Irie S, Greene LA, Sato TA. NADE, a p75NTR-associated cell death executor, is involved in signal transduction mediated by the common neurotrophin receptor p75NTR. *J Biol Chem* 2000; **275:** 17566-17570

14 **Coulie B,** Szarka LA, Camilleri M, Burton DD, McKinzie S, Stambler N, Cedarbaum JM. Recombinant human neurotrophic factors accelerate colonic transit and relieve constipation in humans. *Gastroenterology* 2000; **119:** 41-50

15 **The BDNF Study Group.** A controlled trial of recombinant methionyl human BDNF in ALS: The BDNF study Group (phase III). *Neurology* 1999; **52:** 1427-1433

16 **Ciccolini F,** Svendsen CN. Neurotrophin responsiveness is differentially regulated in neurons and precursors isolated from the developing striatum. *J Mol Neurosci* 2001; **17:** 25-33

17 **Guarino N,** Yoneda A, Shima H, Puri P. Selective neurotrophin deficiency in infantile hypertrophic pyloric stenosis. *J Pediatr Surg* 2001; **36:** 1280-1284

18 **Ip FC,** Cheung J, Ip NY. The expression profiles of neurotrophins and their receptors in rat and chicken tissues during development. *Neurosci Lett* 2001; **301:** 107-110

19 **Carr MJ,** Hunter DD, Undem BJ. Neurotrophins and asthma. *Curr Opin Pulm Med* 2001; **7:** 1-7

20 **Roux PP,** Barker PA. Neurotrophin signaling through the p75 neurotrophin receptor. *Prog Neurobiol* 2002; **67:** 203-233

21 **Wiesmann C,** de Vos AM. Nerve growth factor: structure and function. *Cell Mol Life Sci* 2001; **58:** 748-759

22 **Galter D,** Unsicker K. Brain-derived neurotrophic factor and trkB are essential for cAMP-mediated induction of the serotonergic neuronal phenotype. *J Neurosci Res* 2000; **61:** 295-301

23 **Ichinose T,** Snider WD. Differential effects of TrkC isoforms on sensory axon outgrowth. *J Neurosci Res* 2000; **59:** 365-371

24 **Skup M,** Dwornik A, Macias M, Sulejczak D, Wiater M, Czarkowska-Bauch J. Long-term locomotor training up-regulates TrkB(FL) receptor-like proteins, brain-derived neurotrophic factor, and neurotrophin 4 with different topographies of expression in oligodendroglia and neurons in the spinal cord. *Exp Neurol* 2002; **176:** 289-307

25 **Heppenstall PA,** Lewin GR. BDNF but not NT-4 is required for normal flexion reflex plasticity and function. *Proc Natl Acad Sci U S A* 2001; **98:** 8107-8112

26 **Baldelli P,** Novara M, Carabelli V, Hernandez-Guijo JM, Carbone E. BDNF up-regulates evoked GABAergic transmission in developing hippocampus by potentiating presynaptic N- and P/Q-type Ca2+ channels signalling. *Eur J Neurosci* 2002; **16:** 2297-2310

27 **Malcangio M,** Ramer MS, Boucher TJ, McMahon SB. Intrathecally injected neurotrophins and the release of substance P from the rat isolated spinal cord. *Eur J Neurosci* 2000; **12:** 139-144

28 **Facer P,** Knowles CH, Thomas PK, Tam PK, Williams NS, Anand P. Decreased tyrosine kinase C expression may reflect developmental abnormalities in Hirschsprung's disease and idiopathic slow-transit constipation. *Br J Surg* 2001; **88:** 545-552

29 **Yang M,** Fang DC, Long QL, Sui JF, Li QW, Sun NX. Effects of gastric pacing on the gastric myoelectrical activity of a canine model of gastric motor disorders. *Shijie Huaren Xiaohua Zazhi* 2002; **10:** 1152-1156

30 **Platell CFE,** Coster J, McCauley RD, Hall JC. The management of patients with the short bowel syndrome. *World J Gastroenterol* 2002; **8:** 13-20

31 **Zhou X,** Li YX, Li N, Li JS. Effect of bowel rehabilitative therapy on structural adaptation of remnant small intestine: animal experiment. *World J Gastroenterol* 2001; **7:** 66-73

32 **Xie DP,** Chen LB, Liu CY, Liu JZ, Liu KJ. Effect of oxytocin on contraction of rabbit proximal colon *in vitro*. *World J Gastroenterol* 2003; **9:** 165-168

33 **Xie DP,** Li W, Qu SY, Zheng TZ, Yang YL, Ding YH, Wei YL, Chen LB. Effect of areca on contraction of colonic muscle strips in rats. *World J Gastroenterol* 2002; **8:** 350-352

34 **Liu CY,** Chen LB, Liu PY, Xie DP, Wang PS. Effects of progesterone on gastric emptying and intestinal transit in male rats. *World J Gastroenterol* 2002; **8:** 338-341

35 **Wang X,** Zhong YX, Zhang ZY, Lu J, Lan M, Miao JY, Guo XG, Shi YQ, Zhao YQ, Ding J, Wu KC, Pan BR, Fan DM. Effect of L-NAME on nitric oxide and gastrointestinal motility alterations in cirrhotic rats. *World J Gastroenterol* 2002; **8:** 328-332

36 **Peng X,** Feng JB, Yan H, Zhao Y, Wang SL. Distribution of nitric oxide synthase in stomach myenteric plexus of rats. *World J Gastroenterol* 2001; **7:** 852-854

37 **Wang X,** Zhong YX, Lan M, Zhang ZY, Shi YQ, Lu J, Ding J, Wu KC, Jin JP, Pan BR, Fan DM. Screening and identification of proteins mediating senna induced gastrointestinal motility enhancement in mouse colon. *World J Gastroenterol* 2002; **8:** 162-167

38 **Wang X,** Lan M, Wu HP, Shi YQ, Lu J, Ding J, Wu KC, Jin JP, Fan DM. Direct effect of croton oil on intestinal epithelial cells and colonic smooth muscle cells. *World J Gastroenterol* 2002; **8:** 103-107

39 **Camilleri M,** Lee JS, Viramontes B, Bharucha AE, Tangalos EG. Insights into the pathophysiology and mechanisms of constipation, irritable bowel syndrome, and diverticulosis in older people. *J Am Geriatr Soc* 2000; **48:** 1142-1150

Edited by Xu XQ, Wang XL and Zhu LH

P.O.Box 2345, Beijing 100023,China
Fax: +86-10-85381893
E-mail: wjg@wjgnet.com www.wjgnet.com

World J Gastroenterol 2003;9(8):1878-1880
World Journal of Gastroenterology
 ISSN 1007-9327

• BRIEF REPORTS •

Intestinal permeability in patients after surgical trauma and effect of enteral nutrition versus parenteral nutrition

Xiao-Hua Jiang, Ning Li, Jie-Shou Li

Xiao-Hua Jiang, Ning Li, Jie-Shou Li, Research Institute of General Surgery, Medical School of Nanjing University, Nanjing 210002, Jiangsu Province, China
Correspondence to: Xiao-Hua Jiang, Research Institute of General Surgery, Medical School of Nanjing University, Nanjing 210002, Jiangsu Province, China. dr_jxh@163.com
Telephone: +86-25-3593192 **Fax:** +86-25-4803956
Received: 2003-03-04 **Accepted:** 2003-04-03

Abstract

AIM: To study the intestinal permeability (IP) following stress of abdominal operation and the different effects on IP of enteral nutrition (EN) and parenteral nutrition (PN).

METHODS: Forty patients undergoing abdominal surgery were randomized into EN group and PN group. Each group received nutritional support of the same nitrogen and calorie from postoperative day (POD) 3 to POD 11. On the day before operation (POD-1), POD 7 and POD 12, 10 g of lactulose and 5 g of mannitol were given orally, and urine was collected for 6 hours. Urine excretion ratios of lactulose and mannitol (L/M) were measured.

RESULTS: L/M ratios of EN group on POD-1, POD 7 and POD 12 were 0.026±0.017, 0.059±0.026, 0.027±0.017, respectively, and those of PN group were 0.025±0.013, 0.080±0.032, 0.047±0.021, respectively. Patients of both groups had elevated L/M ratios on POD 7 *vs*. POD-1. However the ratio returned toward control level in EN group by POD 12. In contrast, PN group still had elevated L/M ratios on POD 12.

CONCLUSION: L/M ratio increases for a period of time after surgical trauma and the loss of gut mucosal integrity can be reversed by substitution of enteral nutrition.

Jiang XH, Li N, Li JS. Intestinal permeability in patients after surgical trauma and effect of enteral nutrition versus parenteral nutrition. *World J Gastroenterol* 2003; 9(8): 1878-1880
http://www.wjgnet.com/1007-9327/9/1878.asp

INTRODUCTION

Apart from the major function for digestion and absorption of nutrients, intestine also acts as "a central organ of stress". In many pathological conditions such as severe trauma, operation, chemotherapy and acute severe pancreatitis, intestine is a barrier to prevent microorganisms and toxins in the lumen from spreading to distant tissues and organs.

Nutritional support has been used in clinical care for more than forty years. Total parenteral nutrition (TPN) is the form of nutritional support most suitable to patients with gut failure, in which it is lifesaving[1]. However, studies have found that TNP has many disadvantages, such as gut barrier dysfunction and bacterial translocation. Enteral nutrition may not have these disadvantages[2-4].

Many studies have demonstrated that intestinal permeability (IP) can reflect gut barrier function[5,6]. When the integrity of gut mucosal barrier is damaged, increased intestinal permeability may occur. The excretion ratio of L/M of urine has been used to measure intestinal permeability[7]. However, few studies have directly compared the effect of EN versus PN on intestinal permeability after surgical trauma. Therefore, the present study was to observe intestinal permeability following operation and to investigate the different effects of enteral nutrition and parenteral nutrition on IP.

MATERIALS AND METHODS

Patients

A prospective and randomized study was designed. Forty patients with digestive tract tumor were enrolled. All the patients had normal liver and kidney functions but no metabolic diseases. Informed consent was obtained from all the patients preoperatively.

All the patients were randomized intraoperatively after complete resection of tumor. The groups were defined as follows. EN group: Patients received enteral nutrition via jejunostomy tube or nasojejunal tube starting from POD 3. All the tubes were placed approximately 20 cm distal to the ligament of Treitz. PN group: Patients received total parenteral nutrition via central venous catheter starting from POD 3. Control group: It consisted of twenty healthy volunteers. All controls underwent an overnight fast and took the test solution orally.

Nutrition

All the patients of the two groups received isonitrogenous (0.1728 g/Kg/d) and isocaloric (30 Kcal/Kg/d) nutritional support starting from POD 3. The aim of enteral or parenteral nutrition was to meet 50 % of nutritional requirements according to the protocol and GI tolerance of the patient on POD3, 75 % on the next day and 100 % on POD5.

EN group: Patients received Isosource (Novartis Corp, Switzerland) fluid polymeric formulation containing 14 % protein, 29 % fat, 57 % carbohydrate calories. Nutrient solution was given at a steady speed.

PN group: Patients received total parenteral nutrition. Amino acids, fat, glucose and minerals were mixed and infused steadily.

Lactulose/mannitol test

Intestinal permeability was performed on POD-1, POD7 and POD12. All the patients fasted for at least 6 hours and their bladders were emptied before the test. The test solution consisted of 10 g of lactulose and 5 g of mannitol in a total volume of 50 mL with osmotic pressure 1 200 mOsm/L. The solution was given via the jejunostomy tubes or by nasojejunal or oral routes. The urine volume was collected for the subsequent 6 hours. One hour after the test started, the patients were encouraged to drink. After 2 h, liberal intake of food was allowed. The urine volume was recorded, and 10-mL portion was frozen and stored at -80 ℃.

Analysis

Urinary lactulose and mannitol were assayed using high-

pressure liquid chromatography (HPLC) as described by Willems D and colleagues[8]. Calibration was performed on a daily basis with authentic standards at multiple concentrations, and the experimental standards were diluted so that the areas of all peaks fell within the calibration range. Fractional excretions (lactulose and mannitol) and L/M ratios were calculated. Fractional excretion was defined as the fraction of the gavaged dose recovered in the urine sample, and L/M ratio was a ratio of fractional excretions (lactulose-mannitol).

Statistical analysis

Statistical analysis was performed using analysis of variance (ANOVA) when comparing mean L/M ratios within groups and by an independent *t* test for differences between groups and *vs* control. Enumeration data were analyzed by χ^2 square test. Differences were considered significant when $P<0.05$, and obviously significant when $P<0.01$. All values were expressed as means ±SD.

RESULTS

Patients ' general data

From April 2000 to July 2001, forty patients with digestive tract tumors were randomized to receive enteral nutrition or total parenteral nutrition. Preoperative and procedure related data for the two groups are listed in Table 1.

Table 1 Comparison of preoperative and procedure related data between experimental groups

	EN group	PN group
Age (y)	50.8±14.9	53.1±15.6
Sex (M / F)	13 / 7	11 / 9
Weight (Kg)	60.0±6.8	61.3±12.3
Cancer of stomach	15	11
Cancer of colon	5	9
Complete gastrectomy	7	5
Partial gastrectomy	8	6
Left hemicolectomy	4	5
Right hemicolectomy	1	4

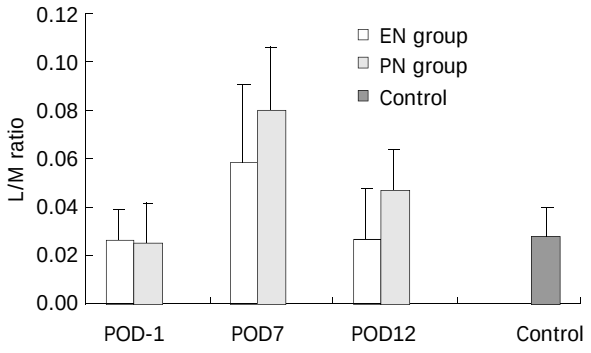

Figure 1 Mean ratio of recovered lactulose to mannitol (L / M) in the urine. A significant elevated ratio was seen on POD7 *vs* that on POD-1 in both groups ($P<0.01$). Significant decreases in the ratio were seen in both groups on POD12 *vs* POD7 ($P<0.01$). The L / M ratio of EN group was significantly lower than PN group on POD7 ($P<0.05$) and on POD12 ($P<0.01$).

Intestinal permeability

Figure 1 depicts the mean L/M ratios for all groups. On POD-1, there were no significant differences in EN group (0.026±0.017) and PN group (0.025±0.013) *vs* control (0.028±0.012) ($P>0.05$). Also there was no significant difference in EN group *vs* PN group ($P>0.05$). On POD7, there was one-fold to two-fold increase in the L/M ratios in both EN group (0.059±0.026) and PN group (0.080±0.032) *vs* that on POD-1 ($P<0.01$). However, there was a significant difference between PN group and EN group ($P<0.05$). On POD12, there was a significant difference in L/M ratios in both EN group and PN group *vs.* that on POD7 ($P<0.01$). However, there was a decreasing trend in L/M ratio in EN group (0.027±0.017) *vs.* that on POD-1 ($P>0.05$), while there was a significant difference in PN group (0.047±0.021) *vs.* that on POD-1 ($P<0.01$). There was a significant difference between PN group and EN group on POD12 ($P<0.01$).

DISCUSSION

Small intestinal permeability has been used to quantify the damage of gut mucosal barrier[9,10]. Intestinal permeability changes have been detected by oral administration of probes such as ^{51}Cr-EDTA, sucrose, lactulose, cellobiose, and polyethylene glycol[11-14]. The measurement of urinary excretion of nonmetabolized sugars has been widely used as a noninvasive method to assess mucosal integrity of the small bowel[15-17]. Monosaccharides such as mannitol and L-rhamnose pass through the transcellular routes of aqueous pores, reflecting the degree of absorption of small molecules (0.65 nm). Disaccharides, including lactulose and cellobiose, pass through the intercellular junctional complexes and extrusion zones at the villous tips, reflecting the permeability of large molecules (0.93 nm). The permeabilities of mono- and disaccharides are usually compared and expressed as an excretion ratio such as lactulose/mannitol or lactulose/L-rhamnose in urine samples. Lactulose and mannitol represent ideal compounds for measuring differential sugar absorption because they have a negligible affinity for the monosaccharide transport system and are passively absorbed and not metabolized before urine excretion. Intraindividual differences in gastric emptying, small intestinal transit, and urinary excretion are therefore eliminated[5-7,16].

Several enzymatic, colorimetric, and thin-layer chromatographic methods have been developed for the determination of lactulose and mannitol[5,6]. However, most of them are time-consuming and do not allow a simultaneous assay of both sugars. More recently, gas chromatographic and HPLC procedures have been proposed to overcome these problems[8,18]. Data from our study suggested that HPLC was a good method of measuring lactulose and mannitol. Our data also showed that L/M ratios could reflect intestinal permeability.

Sepsis, systemic inflammatory response and trauma in both animal and human are associated with gut mucosal damage and dysfunction[19-21]. Gut dysfunction is a common problem, resulting in loss of gut mucosal barrier selectivity, increased permeability to various hydrophilic solutes and translocation of bacterial products into the circulation, which may then further increase the inflammatory response in distant organs, leading to multiple organ dysfunction and death[22]. As a result, many authors considered the gut as an "engine" that drived sepsis. One possible contributory mechanism to endotoxin-induced gut mucosal damage was the increased apoptosis[11]. Inflammatory mediators enhanced apoptosis in a large number of cell lines. In intact animals, increased cardiac and hepatic apoptosis during sepsis might contribute to sepsis-related dysfunction of those organs. Thus paracellular tight junction may be injured and intestinal permeability increases. Our study showed an increased permeability after the stress of surgical trauma.

Nowadays nutritional support has become a routine therapy method. In the stress condition, proper nutritional support may provide necessary nutrients, reduce clinical complications and

promote patients' recovery from illness[3]. Total parenteral nutrition (TPN) provides significant benefits to surgical patients. However, there are still many complications. The effects of total parenteral nutrition on the gastrointestinal tract include decreasing brush-border hydrolase and nutrient-transporter activity, increasing mucosal permeability, and decreasing microvillus height[23-25]. Thus TPN is complicated by bacterial translocation (BT). Enteral nutrition after stress can maintain immunocompetence, and promote wound healing. Furthermore, it is considered that enteral nutrition can maintain gut barrier integrity, reduce septic complications[26] and the risk of death of critical care patients[3, 27]. In our study, we used L/M ratio as a marker to reflect gut mucosal barrier. On POD7, L/M ratios in both EN group and PN group were elevated, but L/M ratio of EN group was significantly lower than that of PN group. And on POD12, L/M ratio of EN group returned to the level of POD-1, while L/M ratio of PN group was still higher than that of POD-1 and EN group.

It is concluded that L/M ratio increases in a period of time after surgical trauma and institution of enteral nutrition can reverse the loss of gut mucosal integrity.

REFERENCES

1 **Jeejeebhoy KN**. Total parenteral nutrition: potion or poison? *Am J Clin Nutr* 2001; **74**: 160-163
2 **Windsor AC**, Kanwar S, Li AG, Barnes E, Guthrie JA, Spark JI, Welsh F, Guillou PJ, Reynolds JV. Compared with parenteral nutrition, enteral feeding attenuates the acute phase response and improves disease severity in acute pancreatitis. *Gut* 1998; **42**: 431-435
3 **Minard G**, Kudsk KA. Nutritional support and infection: does the route matter? *World J Surg* 1998; **22**: 213-219
4 **Zhu L**, Yang ZC, Li A, Cheng DC. Protective effect of early enteral feeding on postburn impairment of liver function and its mechanism in rats. *World J Gastroenterol* 2000; **6**: 79-83
5 **Travis S**, Menzies I. Intestinal permeability: functional assessment and significance. *Clin Sci* 1992; **82**: 471-488
6 **Bjarnason I**, MacPherson A, Hollander D. Intestinal permeability: an overview. *Gastroenterology* 1995; **108**: 1566-1581
7 **Barboza Junior MS**, Silva TM, Guerrant RL, Lima AA. Measurement of intestinal permeability using mannitol and lactulose in children with diarrheal diseases. *Braz J Med Biol Res.* 1999; **32**: 1499-1504
8 **Willems D**, Cadranel S, Jacobs W. Measurement of urinary sugars by HPLC in the estimation of intestinal permeability: evaluation in pediatric clinical practice. *Clin Chem* 1993; **39**: 888-890
9 **Meddings JB**, Gibbons I. Discrimination of site-specific alterations in gastrointestinal permeability in the rat. *Gastroentology* 1998; **114**: 83-92
10 **Wu CT**, Huang XC, Li ZL. Intestinal mucosal permeability increase and intestinal bacterial translocation. *Shijie Huaren Xiaohua Zazhi* 1999; **7**: 605-606
11 **Uil JJ**, van Elburg RM, van Overbeek FM, Mulder CJ, VanBerge-Henegouwen GP, Heymans HS. Clinical implications of the sugar absorption test: intestinal permeability test to assess mucosal barrier function. *Scand J Gastroenterol Suppl* 1997; **223**: 70-78
12 **Fink MP**. Gastrointestinal mucosal injury in experimental models of shock, trauma, and sepsis. *Crit Care Med* 1991; **19**: 627-641
13 **Smecuol E**, Bai JC, Sugai E, Vazquez H, Niveloni S, Pedreira S, Maurino E, Meddings J. Acute gastrointestinal permeability responses to different non-steroidal anti-inflammatory drugs. *Gut* 2001; **49**: 650-655
14 **Blomquist L**, Bark T, Hedenborg G, Norman A. Evaluation of the lactulose / mannitol and 51Cr-ethylenediaminetetraacetic acid / 14C-mannitol methods for intestinal permeability. *Scand J Gastroenterol* 1997; **32**: 805-812
15 **Smecuol E**, Bai JC, Vazquez H, Kogan Z, Cabanne A, Niveloni S, Pedreira S, Boerr L, Maurino E, Meddings JB. Gastrointestinal permeability in celiac disease. *Gastroenterology* 1997; **112**: 1129-1136
16 **Dong HL**. Intestinal permeability test and its clinical significance. *Shijie Huaren Xiaohua Zazhi* 2000; **8**: 562-563
17 **Tibble JA**, Bjarnason I. Non-invasive investigation of inflammatory bowel disease. *World J Gastroenterol* 2001; **7**: 460-465
18 **Smecuol E**, Bai JC, Sugai E, Vazquez H, Niveloni S, Pedreira S, Maurino E, Meddings J. Acute gastrointestinal permeability responses to different non-steroidal anti-inflammatory drugs. *Gut* 2001; **49**: 650-655
19 **Deitch EA**. Intestinal permeability is increased in burn patients shortly after injury. *Surgery* 1990; **107**: 411-416
20 **Wang W**, Smail N, Wang P, Chaudry IH. Increased gut permeability after hemorrhage is associated with upregulation of local and systemic IL-6. *J Surg Res* 1998; **79**: 39-46
21 **Sun XQ**, Fu XB, Zhang R, Lu Y, Deng Q, Jiang XG, Sheng ZY. Relationship between plasma D(-)-lactate and intestinal damage after severe injuries in rats. *World J Gastroenterol* 2001; **7**: 555-558
22 **Peng YZ**, Yuan ZQ, Xiao GX. Effects of early enteral feeding on the prevention of enterogenic infection in severely burned patients. *Burns* 2001; **27**: 145-149
23 **Li J**, Langkamp-Henken B, Suzuki K, Stahlgren LH. Glutamine prevents parenteral nutrition-induced increases in intestinal permeability. *J Parenter Enteral Nutr* 1994; **18**: 303-307
24 **Helton WS**. The pathophysiologic significance of alterations in intestinal permeability induced by total parenteral nutrition and glutamine. *J Parenter Enteral Nutr* 1994; **18**: 289-290
25 **Illig KA**, Ryan CK, Hardy DJ, Rhodes J, Locke W, Sax HC. Total parenteral nutrition-induced changes in gut mucosal function: atrophy alone is not the issue. *Surgery* 1992; **112**: 631-637
26 **Braunschweig CL**, Levy P, Sheean PM, Wang X. Enteral compared with parenteral nutrition: a meta-analysis. *Am J Clin Nutr* 2001; **74**: 534-542
27 **Omura K**, Hirano K, Kanehira E, Kaito K, Tamura M, Nishida S, Kawakami K, Watanabe Y. Small amount of low-residue diet with parenteral nutrition can prevent decreases in intestinal mucosal integrity. *Ann Surg* 2000; **231**: 112-118

Edited by Zhao P and Wang XL

P.O.Box 2345, Beijing 100023,China
Fax: +86-10-85381893
E-mail: wjg@wjgnet.com www.wjgnet.com

World J Gastroenterol 2003;9(8):1881-1883
World Journal of Gastroenterology
 ISSN 1007-9327

• BRIEF REPORTS •

Single-dose daclizumab induction therapy in patients with liver transplantation

Lu-Nan Yan, Wei Wang, Bo Li, Shi-Chun Lu, Tian-Fu Wen, Qi-Yuan Lin, Yong Zeng, Nan-Sheng Cheng, Ji-Chun Zhao, Yue-Meng Dai

Lu-Nan Yan, Wei Wang, Bo Li, Shi-Chun Lu, Tian-Fu Wen, Qi-Yuan Lin, Yong Zeng, Nan-Sheng Cheng, Ji-Chun Zhao, Yue-Meng Dai, Liver Transplantation Center, West China Hospital, Sichuan University, Chengdu 610041, Sichuan Province, China
Correspondence to: Dr. Lu-Nan Yan, Department of Surgery, West China Hospital, Sichuan University, Chengdu 610041, Sichuan Province, China. yanlunan@hotmail.com
Telephone: +86-28-85422072 **Fax:** +86-28-85423724
Received: 2002-06-20 **Accepted:** 2002-10-17

Abstract

AIM: To investigate the efficacy and safety of a single-dose daclizumab induction therapy in orthotopic liver transplantation (OLTx).

METHODS: A retrospective study was made for 54 cases of OLTx in recent three years. The daclizumab group consisted of 23 cases of OLTx who received single-dose of 2 mg/kg intravenously after postoperative 24 hours. The control group consisted of the remaining 31 patients. Additional immunosuppressors included steroids, mycomphenolate mofetil, facrolimus or microemulsion cyclosporine used in all patients. Meta-statistical analysis was made for general data, incidence of acute rejection and infection, postoperative clinical course, complications and prognosis between two groups.

RESULTS: Pretransplant demographies were not significantly different between two groups. In the induction group there were significantly less acute rejection episodes (5 of 23, 21.74 %) than those in the control group (12 of 31, 38.71 %), which were proved by pathologic diagnosis ($P<0.05$). The incidence of infection at the early stage was not significantly different between two groups.

CONCLUSION: Induction therapy with single-dose of daclizumab is safe and effective and appears to be able to reduce the incidence of acute rejection.

Yan LN, Wang W, Li B, Lu SC, Wen TF, Lin QY, Zeng Y, Cheng NS, Zhao JC, Dai YM. Single-dose daclizumab induction therapy in patients with liver transplantation. *World J Gastroenterol* 2003; 9(8): 1881-1883
http://www.wjgnet.com/1007-9327/9/1881.asp

INTRODUCTION

One of the key elements for successful liver transplantation is to effectively prevent acute rejection in patients with liver transplantation. Even the routine immunosuppressants such as azathioprin (AZA), cyclosporin (CSA), mycomphenolate mofetil (MMF) and tacrolinous (FK506)were used, the acute rejection rate in liver transplantation was still as high as 30-40 %[1-3]. Daclizumab, a humanized form of murine monoclonal antibody, has been recently shown to be able to decrease the acute rejection in liver transplanted recipients[4-7].

In this retrospective study, whether daclizumab induction therapy was effective and safe in orthotopic liver transplantation (OLTx) was evaluated.

MATERIALS AND METHODS

General data

We retrospectively reviewed the results of 54 consecutive OLTx performed from February, 1999 to January, 2002 at the West China Hospital in Sichuan University. There were 44 males and 10 females,their age ranged from 11 to 68 years old (average 38.98 years old). 42 patients had benign hepatic diseases, 29 had cirrhosis due to hepatitis B, 2 had diffusive intrahepatic stones with liver cirrhosis, 1 had alcoholic cirrhosis, 1 had polycystic liver with cirrhosis, 2 had Budd-Chari' s syndrome, 3 had unibobar carolis syndrome, 1 had alcoholic cirrhosis and 3 had alveolar echinococcosis. 12 patients had hepatocellular carcinoma. According to the Child' s classification, 39 of the 54 patients were grade A, 2 were grade B and 13 were grade C. According to the classification of the united network of organ share (UNOS), 14 were grade I, 40 were grade II.

Among them, 14 cases were performed emergency liver transplantation because of acute hepatic failure with severe jundice (total bilirubin 129-676 nmol/L), large volume of ascites (2 500-11 000 ml) or severe coagulopathy, and 4 cases had hepatic enphacelopathy. 23 patients received induction therapy with daclizumab and 31 patients were managed with conventional immunosuppression (non induction). In the control group (non-induction), oral cyclosporin was administered at a dosage of 6-10 mg/kg/day, starting within 24 hours before the operation. Dosage adjustments were based on achieving servm level of CSA between 200 ng and 300 ng/dL. Patients received methylprednisolone during surgery 200 mg intravenously, which was decreased by 40 mg daily over a period of 5 days. On postoperative day 5, patients started to administer prednisone at 20 mg/day. MMF was administered at a dosage of 0.75 g, twice daily.

In the induction group, daclizumab was given 2 mg/kg intravenously within the postoperative 24 hours, cyclosporin, steroid and MMF were identical to the control group.

Tacrolimas was used in patients with CSA toxicity and occasionally as the primary therapy.

Diagnosis of rejection

Rejection was suspected by biochemical evidence of deteriorating liver function and/or clinical signs. Pathological examimation was done in all patients suspected of rejection. The patients in both groups received methyprednisolone every day for the treatment of acute rejection at 500 mg intravenously for 3 days.

Concomitant therapy

The patients in both groups received losec for prophylaxis of stress ulcer (40 mg, intravenously, daily). Cephaloxin was used for postoperative infection prophylaxis. HBV-DNA positive patients were given lamivudine (100 mg, orally, daily). The

patients accompanied by suspected virus infection were treated with acyclovir (800 mg, orally twice daily) or ganciclovir (5 mg/kg , intravenously twice daily).

Liver transplantation

Operative procedures were performed according to standard surgical techniques, and all grafts were perfused with the University of Wisconsin solution[8]. Veno-venous bypass was used in all cases. Buct-to-duct over a T-tube biliary anastomosis or choledochojejunostomy was performed.

Statistical analysis

All the patients received a minimum follow-up for 60 days. Values of the descriptive variables between groups were compared with a nonparainetric wilcoxon rank sum test. Chi-square test or Fisher exact test was used to evaluate the data of the independent groups.

RESULTS

Survival rate

The general data of patients in this study are shown in Table 1, which were similar in two groups.

Table 1 General data in two groups

	Induction group (n=23)	Non-induction group (n=31)
Average age(yr)	39.17(19-68)	38.76(11-57)
Male / female	21 / 2	23 / 8
Indication with		
Liver cirrhosis	15	18
Liver cancer	6	6
Other	2	7
UNOS classification		
Grade I	5	10
Grade II	18	21
Child classification		
Grade A	4	9
Grade B	2	0
Grade C	17	22
Blood type		
ABO-identical	14	23
ABO-compatible	9	8

The 1-, 3-, and 6-month survival rate in patients receiving the induction therapy with daclizumab was 91.3 %, 86.9 % and 86.9 %, respectively *vs* 90.0 %, 83.9 % and 83.9 %, respectively for patients not receiving induction therapy (P>0.05). There was a significant difference between two groups. Six months after the transplantation, 20 of the 23 patients with daclizumab induction were still alive. Deaths occurred in this group were due to the following rensons: complications of intercereberal bleeding (1case), heart failure (1case) and pulmonary infection (1case). In the non induction group, 26 of 31 patients surrived for 6 months. Deaths occurred in this group were due to the following rensons: complications of intracerebral bleeding (1case), pulmonary fungus infection (2case), MOF(1case) and recurrent of cancer (1case).

No patients in either group developed primary dysfunction or died of blood vessel complications.

Complications

Complications especially infection were less in the induction group than those in the non induction group, without significant difference (Table 2).

Table 2 Postoperative complications in two groups

	Induction (n=23)	Non-induction (n=31)
Intraperitoneal bleeding	1	3
Ascite infection	0	1
Stress ulcer bleeding	1	3
Stress ulcer perforation	0	1
Pulmonary infection	5	11
Heart failure	1	3
Biliary leakage	1	3
Chronic oral ulcer	2	3
Bowel fungal infection	1	2
Intracerebral bleeding	1	3
Total	13	32

Rejection

Overall, in the first month, acute rejection occurred less in patients of the daclizumab induction group than that in the non-induction group(21.74 % *vs* 38.71 %, P<0.05). None in either group had acute rejection after the first month and occurred chronic rejection during the first 6 months. None in the induction group and one patient in the noninduction group had OKT_3 added to their immunosuppression for intractable rejection.

Tolerance of daclizumab

None in the daclizumab group required reduction of their dose or cessation of daclizumab for side effects. Daclizumab was well tolerated without apparently clinical or biochemical toxicity.

DISCUSSION

In the recent 30-40 years, with the development of organ transplantation biology, many immunosuppressive agents have been introduced to reduce the incidence of acute rejection[9-12]. The introduction of azathioprine (AZA) was in 1960s by Starzl. Cyclosporin A has (CSA) achieved long-term survival rade since early 1980s[13-17], and occurrenc of tacrolimus (FK506)[18-22] and mycomphenolate mofetil (MMF)[23-27] has prolonged the long-term survival. In spite of these major advances in liver transplantation, there are a number of problems associated with its use. For example, the incidence of acute rejection is still as high as 30-40 %[1].

Thus, the next advance that is required in immunosuppression in recipients with liver transplantation is an agent that can either decrease the rejection without increase of toxicity or decrease toxicity with maintenance of effective immunosuppression.

Daclizumab, a humanized anti-IL-2R a-chain (CD25) antibody, is a new immunosuppressant, its proposed actions include blockade of signaling *via* the high-affinity IL-2R, down-modulation of CD25, depletion of CD25+ cells, and interaction with its FC fragments and FCRs on activated T cells[28, 29]. Induction therapy with daclizumab has been shown effective in preventing acute rejection in kidney transplantation patients[30-32]. Routine use of antibody induction therapy in liver transplantation has not gained widespread acceptance[1].

This study explored the results of adding daclizumab to conventional immunosuppressive therapy in 23 liver recipients with liver transplantation compared to the results in 31 control recipients. It was found that adding daclizumab appeared to be able to decrease the incidence of acute rejection from 38.71 % to 21.74 % without any apparent toxicity or opportunistic infections.

In this study, a different dosing schedule for daclizumab was used. Ciancio *et al* reported their dosing schedule was that daclizumab (1 mg/kg) was given on the day of surgery and every other week for a total of 5 doses[31]. Devin' s schedule

was that the first dose (2 mg/kg) was given before organ engraftment and the second dose (1 mg/kg) was given on postoperative day 5[1]. Both results suggest the efficacy of their dosing schedule. Our dosage of daclizumab was smaller than that in other transplant centers, but we still found that daclizumab appeared to be able to reduce the incidence of acute rejection singnificantly without apparent toxicity and was well tolerated. In conclusion, the induction therapy with single-dose of daclizumab is safe and effective.

REFERENCES

1 **Eckhoff DE**, Mcguire B, Sellers M, Contreras J, Frenette L, Young C, Hudson S, Bynon JS. The safety and efficacy of a two-dose daclizumab (zenapax) induction therapy in liver transplant recipients. *Transplantation* 2000; **69**: 1867-1872

2 **Kwekkeboom J**, Zondervan PE, Kuijpers MA, Tilanus HW, Metselaar HJ. Fine-needle aspiration cytology in the diagnosis of acute rejection after liver transplantation. *Br J Surg* 2003; **90**:246-247

3 **Ramji A**, Yoshida EM, Bain VG, Kneteman NM, Scudamore CH, Ma MM, Steinbrecher UP, Gutfreund KS, Erb SR, Partovi N, Chung SW, Shapiro J, Wong WW. Late acute rejection after liver transplantation: the Western Canada experience. *Liver Transpl* 2002; **8**: 945-951

4 **Levy GA.** Neoral is superior to FK506 in liver transplantation. *Transplant Proc* 1998; **30**: 1812-1815

5 **Niemeyer G**, Koch M, Light S, Kuse ER, Nashan B. Long-term safety, tolerability and efficacy of daclizumab (zenapax) in a two-dose regimen in liver transplant recipients. *Am J Transplant* 2002; **2**: 454-460

6 **Carswell CI,** Plosker GL, Wagstaff AJ. Daclizumab: a review of its use in the management of organ transplantation. *Biodrugs* 2001; **15**: 745-773

7 **Koch M,** Niemeyer G, Patel I, Light S, Nashan B. Pharmacokinetics, pharmacodynamics, and immunodynamics of daclizumab in a two-dose regimen in liver transplantation. *Transplantation* 2002; **73**: 1640-1646

8 **Yan LN,** Li B, Lu SC, Jin LR, Wen TF, Wu XD, Jia QB, Zhou Y, Wu YT. Orthotopic liver transplantation: a report of 15 cases. *Zhonghua Qiguan Yizhi Zazhi* 2000; **21**: 275-277

9 **Ankersmit HJ**, Roth G, Zuckermann A, Moser B, Obermaier R, Taghavi S, Brunner M, Wieselthaler G, Lanzenberger M, Ullrich R, Laufer G, Grimm M, Wolner E. Rapamycin as rescue therapy in a patient supported by biventricular assist device to heart transplantation with consecutive ongoing rejection. *Am J Transplant* 2003; **3**: 231-234

10 **Rose ML**, Smith J, Dureau G, Keogh A, Kobashigowa J. Mycophenolate mofetil decreases antibody production after cardiac transplantation. *J Heart Lung Transplant* 2002; **21**: 282-285

11 **Calmus Y,** Scheele JR, Gonzalez-Pinto I, Jaurrieta EJ, Klar E, Pageaux GP, Scudamore CH, Cuervas-Mons V, Metselaar HJ, Prestele H, Girault D. Immunoprophylaxis with basiliximab, a chimeric anti-interleukin-2 receptor monoclonal antibody, in combination with azathioprine-containing triple therapy in liver transplant recipients. *Liver Transpl* 2002; **8**: 123-131

12 **Agha IA**, Rueda J, Alvarez A, Singer GG, Miller BW, Flavin K, Lowell JA, Shenoy S, Howard TK, Ramachandran V, Irish W, Schnitzle MA, Brennan DC. Short course induction immunosuppression with thymoglobulin for renal transplant recipients. *Transplantation* 2002; **73**: 473-475

13 **Calne RY,** Rolles K, White DJ, Thiru S, Evans DB, Mcmaster P, Dunn DC, Graddock GN, Henderson RG, Aziz S, Lewis P. Cyclosporin A initially as the only immunosuppressant in 34 recipients of cadaveric organs: 32 kidneys, 2 pancreases, and 2 livers. *Lancet*, 1979; **2**: 1033-1036

14 **Lerut JP**, Ciccarelli O, Mauel E, Gheerardhyn R, Talpe S, Sempoux C, Laterre PF, Roggen FM, Van Leeuw V, Otte JB, Gianello P. Adult liver transplantation and steroid-azathioprine withdrawal in Cyclosporine (Sandimmun)-based immunosuppression - 5 year results of a prospective study. *Transpl Int* 2001; **14**: 420-428

15 **Venkiteswaran K**, Sgoutas DS, Santanam N, Neylan JF. Tacrolimus, Cyclosporine and plasma lipoproteins in renal transplant recipients. *Transpl Int* 2001; **14**: 405-410

16 **Gonwa TA**, Hricik DE, Brinker K, Grinyo JM, Schena FP. Sirolimus Renal Function Study Group Improved renal function in sirolimus-treated renal transplant patients after early Cyclosporine elimination. *Transplantation* 2002; **74**: 1560-1567

17 **Meier-Kriesche HU**, Kaplan B. Cyclosporine microemulsion and tacrolimus are associated with decreased chronic allograft failure and improved long-term graft survival as compared with sandimmune. *Am J Transplant* 2002; **2**: 100-104

18 **Fung JJ,** Todo S, Tzakis A, Demetris A, Jain A, Abu-Elmaged K, Alessiani M, Starzl TE. Conversion of liver allograft recipients from Cyclosporine to FK506-based immunosuppression: benefits and pitfalls. *Transplant Proc* 1991; **23**(1Pt 1): 14-21

19 **Kato T,** Sato Y, Kurasaki I, Yamamoto S, Hirano K, Nakatsuka H, Kobayashi T, Kameyama H, Watanabe T, Hatakeyama K. FK506 may suppress liver injury during the early period following living-related liver transplantation. *Transplant Proc* 2003; **35**: 79

20 **Chen JW**, Pehlivan M, Gunson BK, Buckels JA, McMaster P, Mayer D. Ten-year results of a randomised prospective study of FK506 versus Cyclosporine in management of primary orthotopic liver transplantation. *Transplant Proc* 2002; **34**: 1507-1510

21 **Ahmad SM**, Stegman Z, Fructhman S, Asbell PA. Successful treatment of acute ocular graft-versus-host disease with tacrolimus (FK506). *Cornea* 2002; **21**: 432-433

22 **Vincenti F**, Jensik SC, Filo RS, Miller J, Pirsch J. A long-term comparison of tacrolimus (FK506) and Cyclosporine in kidney transplantation: evidence for improved allograft survival at five years. *Transplantation* 2002; **73**: 775-782

23 **Lebranchu Y**, Bridoux F, Buchler M, Le Meur Y, Etienne I, Toupance O, Hurault de Ligny B, Touchard G, Moulin B, Le Pogamp P, Reigneau O, Guignard M, Rifle G. Immunoprophylaxis with basiliximab compared with antithymocyte globulin in renal transplant patients receiving MMF-containing triple therapy. *Am J Transplant* 2002; **2**: 48-56

24 **Boggi U**, Vistoli F, Coppelli A, Marchetti P, Rizzo G, Mosca F. Use of basiliximab in conjunction with either Neora / MMF / steroids or Prograf / MMF / steroids in simultaneous pancreas-kidney transplantation. *Transplant Proc* 2001; **33**: 3201-3202

25 **Ciancio G**, Burke GW, Miller J. Current treatment practice in immunosuppression. *Expert Opin Pharmacother* 2000; **1**: 1307-1330

26 **Mouly-Bandini A**. A new immunosuppressor: CellCept. *Presse Med* 2001; **30**: 66-67

27 **Wu MJ**, Shu KH, Cheng CH, Chen CH, Lian JD. MMF-based regimen in maintenance therapy after kidney transplantation. *Transplant Proc* 2000; **32**: 1748-1750

28 **Van Assche G**, Dalle I, Noman M, Aerden I, Swijsen C, Asnong K, Maes B, Ceuppens J, Geboes K, Rutgeerts P. A pilot study on the use of the humanized anti-interleukin-2 receptor antibody daclizumab in active ulcerative colitis. *Am J Gastroenterol* 2003; **98**: 369-376

29 **Krueger JG**, Walters IB, Miyazawa M, Gilleaudeau P, Hakimi J, Light S, Sherr A, Gottlieb AB. Successful *in vivo* blockade of CD25 (high-affinity interleukin 2 receptor) on T cells by administration of humanized anti-Tac antibody to patients with psoriasis. *J Am Acad Dermatol* 2000; **43**: 448-458

30 **Light JA**, Sasaki TM, Ghasemian R, Barhyte DY, Fowlkes DL. Daclizumab induction / tacrolimus sparing: a randomized prospective trial in renal transplantation. *Clin Transplant* 2002; **16** (Suppl 7): 30-33

31 **Ciancio G,** Burke GW, Suzart K, Mattiazzi A, Rosen A, Zilleruello G, Abitbol C, Montane B, Miller J. Effect of daclizumab, tacrolimus, and mycophenolate mofetil in pediatric first renal transplant recipients. *Transplant Proc* 2002; **34**: 1944-1945

32 **Vincenti F**, Kirkman R, Light S, Bumgardner G, Pescovitz M, Halloran P, Neylan J, Wilkinson A, Ekberg H, Gaston R, Backman L, Burdick J. Interleukin-2-receptor blockade with daclizumab to prevent acute rejection in renal transplantation. *N Engl J Med* 1998; **338**: 161-165

Edited by Xu XQ and Wang XL